UNIVERSITÄT
ZU KÖLN

*The Cologne Prehistory Series*

# BARMAKY: EPIGRAVETTIAN IN VOLHYNIA

Edited by Victor Chabai and Andreas Maier

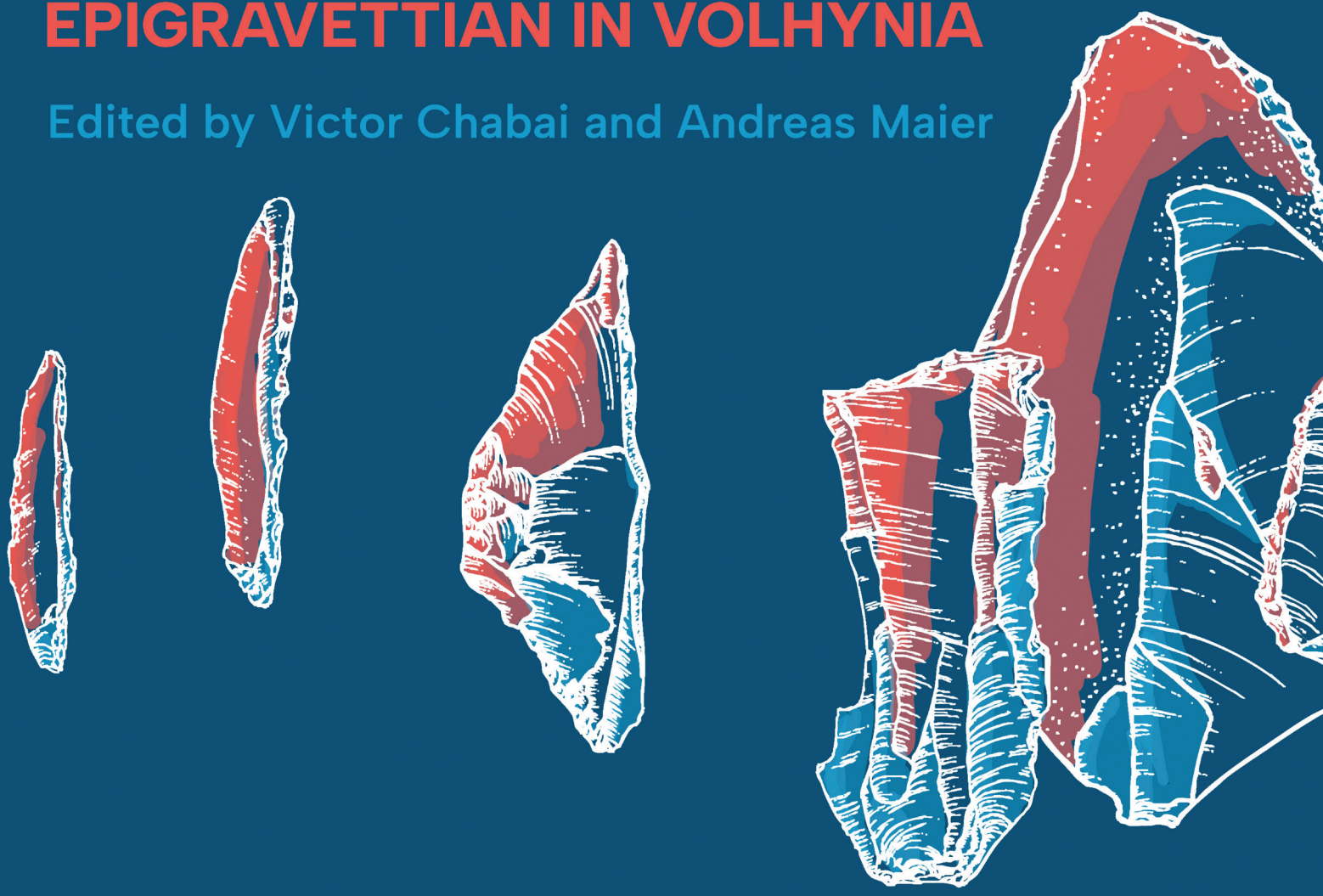

INSTITUTE FOR PREHISTORIC ARCHAEOLOGY

The Cologne Prehistory Series

# BARMAKY: EPIGRAVETTIAN IN VOLHYNIA

July 2025

409 pages, 221 figures, 128 tables

Realised in the framework of the project:

Between east and west. Social networks and environmental conditions before, during, and after the Last Glacial Maximum in Volhynia (western Ukraine)

DFG project number: 392605832

Cover and Layout: Anja Duwe and Florian Sauer
Typesetting: Anja Rüschmann
Editing: Victor Chabai and Andreas Maier

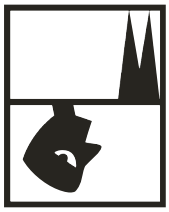

INSTITUT FÜR UR- UND FRÜHGESCHICHTE

# BARMAKY:
# EPIGRAVETTIAN IN VOLHYNIA

Edited by: Victor Chabai and Andreas Maier

July 2025

# TABLE OF CONTENTS


| | | |
|---|---|---|
| **Preface** | | 1 |
| **Chapter 1** | **History of investigations at the site of Barmaky**<br>*Diana Dudnyk* | 2 |
| **Chapter 2** | **Barmaky: setting, lithological & archaeological sequences, structures**<br>*Victor Chabai* | 27 |
| **Chapter 3** | **Radiocarbon dating of Barmaky and the wider chronological context of the Mid Dnieper Epigravettian**<br>*Andreas Maier* | 66 |
| **Chapter 4** | **Barmaky: molluscs (Gastropoda)**<br>*Stefan Meng* | 71 |
| **Chapter 5** | **The animal remains of Barmaky, excavations of 2018–2020 and 1990**<br>*Kerstin Pasda* | 73 |
| **Chapter 6** | **Stable isotope analyses of the faunal assemblage**<br>*Lilian Reiss, Kerstin Pasda, Christoph Mayr, Andreas Maier* | 130 |
| **Chapter 7** | **Lithic raw materials**<br>*Michael Brandl* | 139 |
| **Chapter 8** | **Barmaky: lithic artefacts**<br>*Victor Chabai & Diana Dudnyk* | 141 |
| **Chapter 9** | **Barmaky: artefacts from organic materials & adornments**<br>*Dmytro Stupak, Victor Chabai, Andrei Veselsky & Volodymyr Hrytsenko* | 293 |
| **Chapter 10** | **Site function of Barmaky: raw material transport and faunal exploitation**<br>*Victor Chabai, Kerstin Pasda, Diana Dudnyk & Andreas Maier* | 313 |
| **Chapter 11** | **Eastern Europe after the Last Glacial Maximum and the origin of Epigravettian industries north of 50° latitude**<br>*Victor Chabai, Andreas Maier & Diana Dudnyk* | 324 |
| **Bibliography** | | 385 |
| **Contributors** | | 409 |

# PREFACE

Despite the relatively long history of investigations of Palaeolithic sites in the eastern part of Volhynia, a comprehensive archaeological and environmental analysis was conspicuously missing. About one hundred years ago, the materials from the pioneering excavations by Ludwik Sawicki at the site of Gorodok were published in preliminary fashion, initiating long debates regarding their chronological position and cultural affiliation. Subsequent investigations by Myhailo Ostrovskyi, Volodymyr Savych, Evgen Lupenko, and Dmytro Nuzhnyi focused on artefact descriptions and the definition of taxonomic cultural units. Meanwhile, Valery Piasetsky presented an extensive analysis of the site's topography and geology, but paid little attention to artefacts (Chapter 1).

To date, the here-presented site of Barmaky, dated to roughly 19 ka and thus shortly after the Last Glacial Maximum, is certainly among the most important sites to understand the Palaeolithic settlement processes in the region. Its importance results from the decent preservation of lithic and organic materials, as well as its geographical position at the western fringe of the high-density site cluster of the mid-Dnieper basin, closest to the neighbouring site cluster in the Dniester basin to the south. The book at hand unites the results of archaeological and environmental analyses carried out on recently and previously excavated material from Barmaky in a comprehensive way. It comprises information on the accumulation of the lithological and archaeological sequence (Chapter 2), age estimates of the cultural deposits (Chapter 3), the mollusc as well as mammal and bird assemblages (Chapters 4 and 5), food web reconstructions based on isotope analyses of faunal remains (Chapter 6), lithic raw materials (Chapter 7), and extensive studies on lithic and organic artefacts as well as fossil shells (Chapters 8 and 9). Against this background, we out forward inferences about the subsistence strategy of hunter-gatherers at Barmaky (Chapter 10) and explore the potential role of Barmaky during the earliest resettlement of the periglacial landscapes of the Eastern European Plain north of 50° latitude after the Last Glacial Maximum and in the wider chorological context (Chapter 11).

Since the start of this project in 2018, not everything that was initially been planned could be done. During the last five years, the COVID pandemic and Russian missiles have affected field- and lab-work alike, for instance by hampering the transportation of both samples and specialists between countries and labs. Nevertheless, thanks to the immense personal commitment of the people excavating and analysing the artefacts and those writing up the results, we are eventually able to present our findings.

Special thanks go to all excavators and authors, Yuri Oliynyk for sample transportation, Valeria Telizhenko for artefacts illustration, Anja Rüschmann for the layout of this book, and Thorsten Uthmeier for the power bank, which has significantly increased the working time for this volume during the long hours without electricity. We are also grateful to the DFG, which funded our work within the project *"Between East and West. Social networks and environmental conditions before, during and after Last Glacial Maximum in Volhynia, Western Ukraine"* (DFG-392605832) and granted flexible support in the face of the various adversities.

*Victor Chabai and Andreas Maier*

# HISTORY OF INVESTIGATIONS AT THE SITE OF BARMAKY

1

DIANA DUDNYK

## INTRODUCTION

Palaeolithic research in the Volhynian Upland began with the discovery of several sites near the village of Horodok between 1909 and the 1920th (Sawicki 1927a, 1927b, 1933). Although the artefact collections have been lost since decades, Horodok II has repeatedly been interpreted as analogous to sites in the Dnieper Basin from the "Magdalenian-period", such as Kyrylivska, Dobranichivka, Buhorok – Pushkari IX, Chulativ I, Chulativ II, Mizyn, and Gintsy. Some researchers have also classified it as part of the Mizyn-Pavlovian culture (Savych 1975: 113; Bibikov 1981: 79-86).

In the 1930th, M. I. Ostrovskyi discovered the multi-layered sites of Lypa VIII, Lypa VI, and Myrohoshcha I, which were later grouped into a local taxonomic unit called the "Lypa culture" (Ostrovskyi, Grigoriev 1966). However, V. P. Savych, who studied Lypa I and Lypa VI in the 1960th, did not support the concept of a distinct "Lypa local culture". Instead, he suggested that these assemblages reflect a chronological sequence, ranging from the final phase of the "Aurignacian-Solutrean" to the "Late Magdalenian" (Savych 1975). Recently, O. S. Sytnyk has argued that the term "Lypa culture" proposed by G. P. Grigoriev is inappropriate, as its definition was based on collections from different periods and contained nonhomogeneous materials from redeposited sediments, making it an unreliable taxonomic unit (Sytnyk 2010).

The local geologist Valeriy Piasetsky initiated the most productive phase of Volhynian Palaeolithic research in the 1980th. Over nearly two decades of exploration, he discovered numerous Palaeolithic sites, including Barmaky (Rivne site), Zhorniv, Ivanychi, Hriadky, and Zbytenka (Piasetsky 1999; 2009).

Piasetsky discovered the site of Barmaky near Rivne in 1980 during an examination of a valley near the Barmatskyi Stream. On the surface, he identified non-patinated flint artefacts and fragments of animal bones. In 1981, a first trench was excavated near the find spot on the right side of the valley (Fig. 1-1). Trench 1 measured 4×4 m and artefacts were found in the 0,4 m thick "main loess" and partly within or beneath the modern soil (Lupenko 1983: 1).

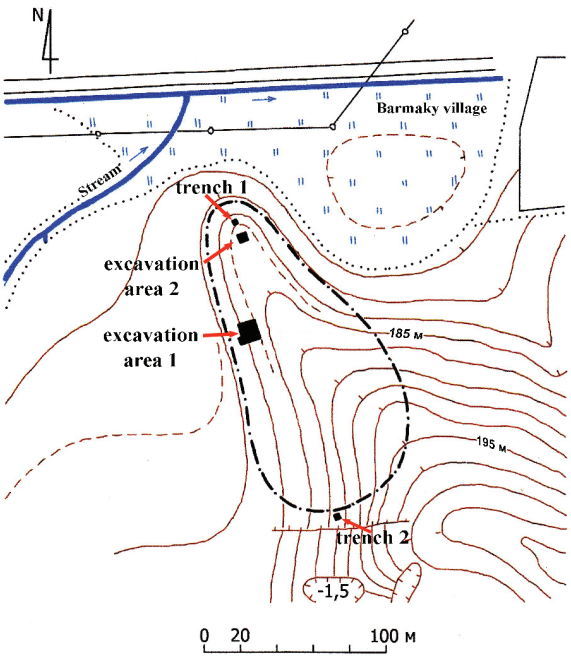


Fig. 1-1. Barmaky, topographical plan with tranches of 1980 and 1982, excavation areas of 1982 and 1990, and the protected zone (shown as a dotted line), redrawn from Piasetsky and Samoliuk 1990.

The loess layer lies above a chalk base. Excavation of the trench yielded three scapulae, a limb bone, fragments of a mammoth skull, several flint flakes and tools, and fossilised shells from Sarmatian deposit with artificial perforations (Piasetsky 2009: 130–131). However, this excavation has not been documented.

In 1982, Piasetsky excavated a second trench roughly 150 m to the south, beyond the surface scatter of flint artefacts (Fig. 1–1). Trench 2 had a depth of 1.7 m, with the stratigraphic sequence of geological layers described as follows:

1. Holocene soil – 0–0.4 m;
2. Brown loam (subsoil) – 0.4–1.1 m;
3. Buried grey soil, described as "heavily cryoturbated" – 1.1–1.2/1.3 m;
4. Pale yellow loess, non-striated – 1.3–1.7 m.

In 1982, Evgen Lupenko conducted the first large-scale field research at the site of Barmaky (Lupenko 1983). In 1990, Piasetsky resumed excavations (Piasetsky, Samoliuk 1990). In 2002–2005 and 2007, Dmytro Nuzhnyi carried out further investigations (Nuzhnyi 2003; Nuzhnyi et al. 2004; 2005; 2006). From 2018 to 2020, the Volhynian Palaeolithic Expedition, led by Victor Chabai, continued excavation at the site (Chabai et al. 2019a; 2020a; 2021). This complex investigation was conducted within the DFG project *"Between East and West. Social networks and environmental conditions before, during and after Last Glacial Maximum in Volhynia, Western Ukraine".*

## The 1982 field campaign

Lupenko's research aimed to clarify the stratigraphic situation of the cultural layer, its chronological position relative to other Upper Palaeolithic sites, and the characteristics of the flint and fauna assemblages. The excavation covered an area of 64 m² and was conducted using a grid of square meters, with numbers indicating an east-west orientation and letters representing a north-south alignment (Fig. 1–2, *1*; 1–3, *1*). Artefact depths were measured from the surface, and some finds were recorded on a plan at a 1:20 scale (Lupenko 1983). Sieving of sediments did not take place.

According to Lupenko, seven lithological layers make up the stratigraphic sequence of the site (Fig. 1–4):

1. Modern soil – 0.00–0.25 m
2. Light yellow silty-loess, non-striated – 0.25–0.90 m
3. Grey silty-loess – 0.90–1.00 m
4. Yellow silty-loess, with sandy layers – 1.00–1.25 m
5. Yellowish brown silty-loess – 1.25–2.45 m
6. Dark brown silty-loess with animal burrows (krotovinas) – 2.45–2.55 m
7. Dark brown silty-loess with layers of chalk deposits – 2.55–3.25 m

### *Spatial structure of the find layer*

The archaeological material was found in the second lithological layer with a sediment thickness of 0.65 m (Fig. 1–4). Lupenko documented a spatially structure distribution of finds with three distinct clusters of artefacts and faunal remains, differing in thickness, composition, quantity, depth, and state of preservation. Additionally, the archaeological level exhibited an inclination towards the southwest, corresponding to the slope of the modern surface. The cultural level contained flint artefacts, faunal remains, fossil shells, ochre and amber fragments.

The first find cluster, located in squares 10К, 11КЛ, and 12КЛ, exhibits an elongated outline oriented south-north. It predominantly consists of flint artefacts, including cores, tools, blades, flakes, chunks, and a few bones (Fig. 1–5).

The second cluster, situated in squares 13Ж3 and 14Ж3, is characterised by a lower density of artefacts compared to the first cluster, but also includes cores, tools, blades, flakes, faunal remains, and even fossil shells (Fig. 1–5). In addition, a hammer on reindeer antler and a fragment of a schematised female figurine on a mammoth tusk were found (Figs 1–6; 1–7).

The third cluster, found in squares 12ОПР and 13ОПР, features again a diverse assemblage of flint artefacts (cores, tools, blades, and flakes), fossil shells, mammoth tusks and their fragments, and numerous bones from mammoths and other animals (Fig. 1–5).

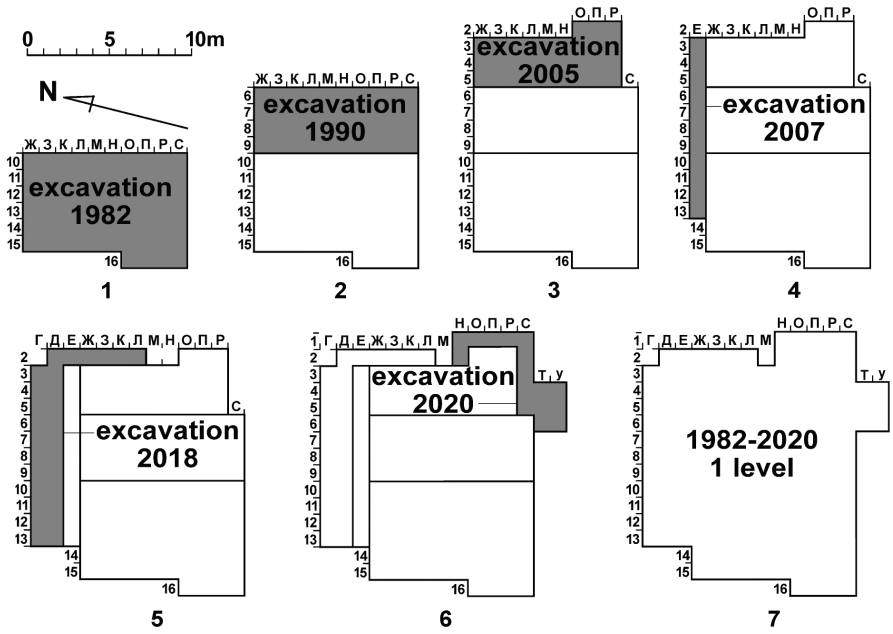


Fig. 1–2. Barmaky, the 1st (upper) archaeological level: excavation plans by field seasons.

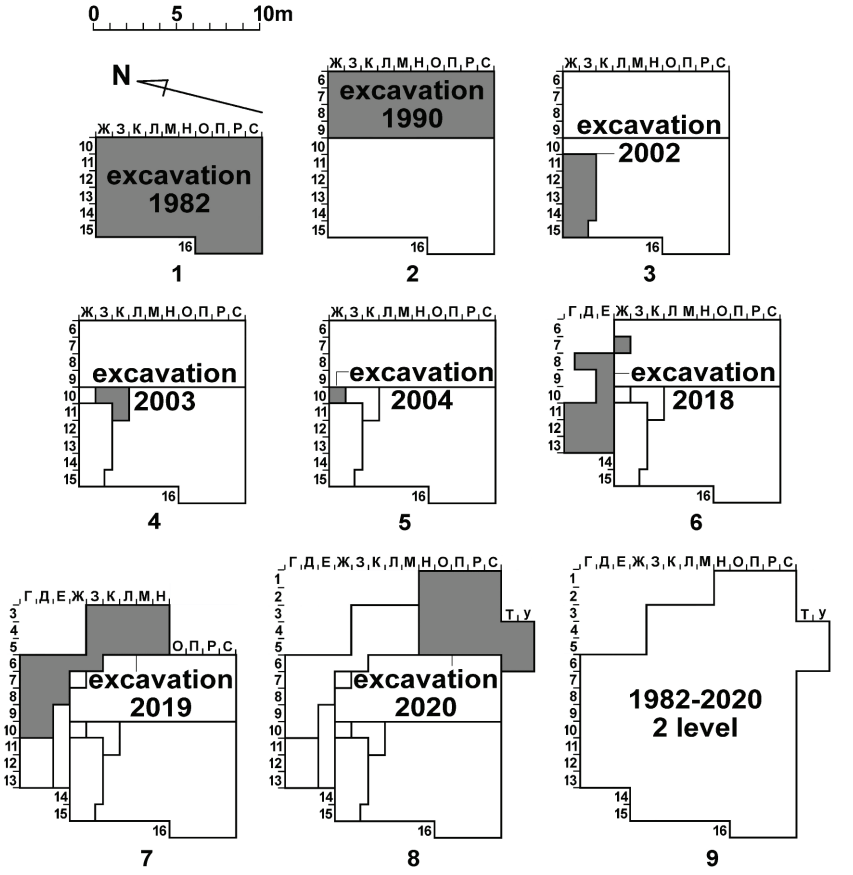


Fig. 1–3. Barmaky, the 2nd (lower) archaeological level: excavation plans by field seasons.

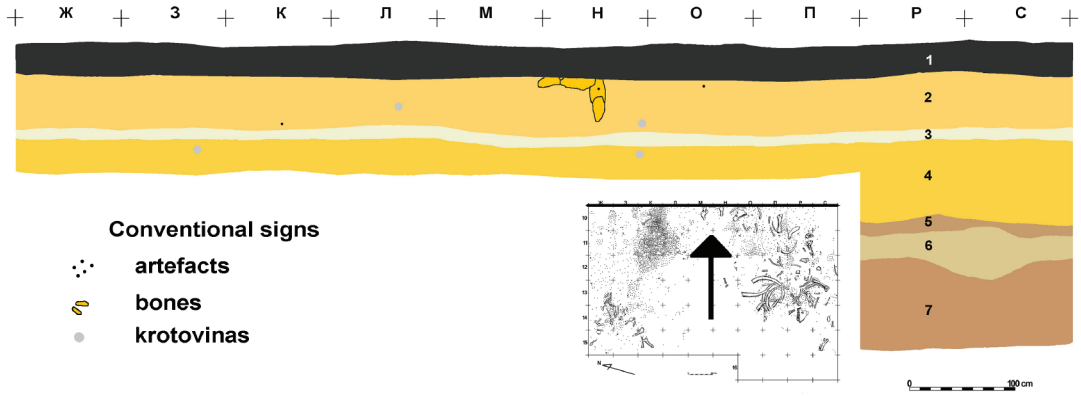


Fig. 1-4. Barmaky: the stratigraphic section along the squares line 9Ж-С/10Ж-С, redrawn from Lupenko 1983.

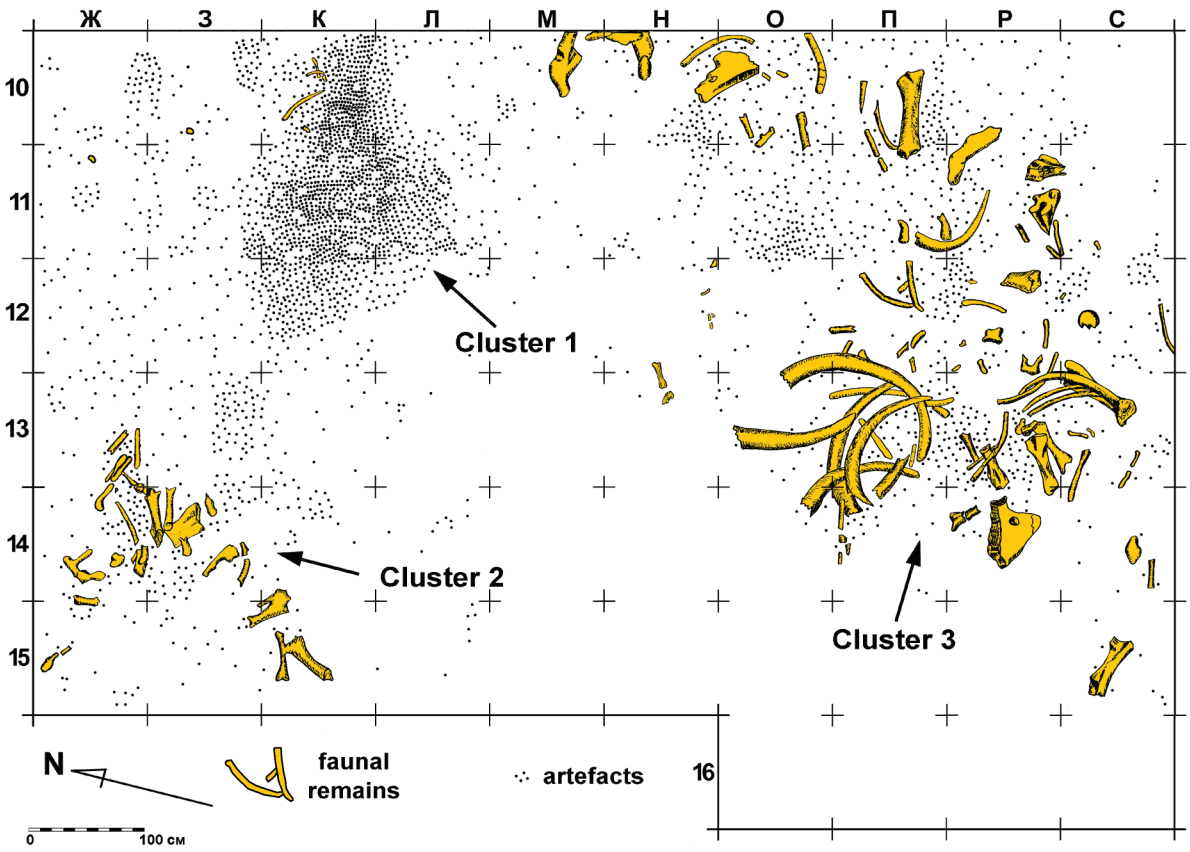


Fig. 1-5. Barmaky, 1982: excavation plan, redrawn from Lupenko 1983.

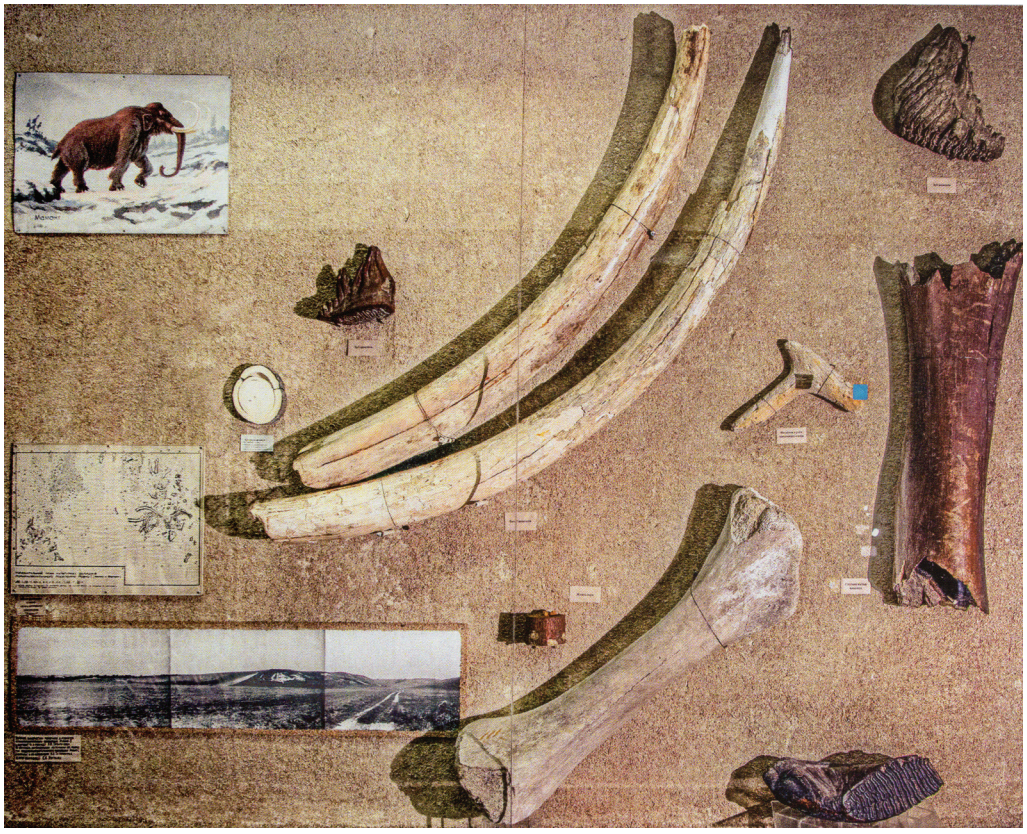

Fig. 1–6. Barmaky: a “hammer” made on the reindeer antler, after Pryshchepa 2021.

Fig. 1–7. Barmaky: a female figurine made on the mammoth tusk, after Pryshchepa 2021.

No evidence of a fireplace was observed at the site (Lupenko 1983). However, the presence of cores at various stages of utilisation, primary blades and flakes with traces of cortex, numerous chunks, as well as finished and unfinished tools led Lupenko to suggest that the three clusters represent areas of specific activities, where flint and bone processing took place (Lupenko 1983: 8).

### *Lithic artefacts*

Lupenko noted that flint artefacts from the site were made from local raw material sourced from the Turonian chalk deposits. Outcrops of this flint are found approximately 150–300 m south of the site. The lithic assemblage from the 1982 excavations amounted to 4860 pieces.

According to Lupenko, many artefacts have a limestone cortex, while patina was observed on only 0.35% of the pieces. Excluding chips, core-like pieces make up about 2%; tools account for more than 8%. Flakes predominate, with lamellar *debitage* making up a third of the collection. Among the technical *debitage*, Lupenko identified core tablets, which accounted for less than 0.5% of the total assemblage (Table 1-1).

"Prismatic" cores predominate among the core-like pieces. About a quarter are described as "amorphous". Cores labelled "close to disc-shaped", "irregular prismatic", "flattened unilaterally, and "turtle-like" occur as single specimens (Table 1-2). The largest category, "prismatic" unidirectional cores, comprised 60%, while bidirectional cores account for 40%. E. Lupenko observed examples with opposite and adjacent striking platforms among the bidirectional cores, categorised as "symmetrical" or "offset" and provided a summary metrical description: the lengths range from 2.5 cm to 10 cm, and most cores are 6–8 cm long (Lupenko 1983: 10). They differ in design, and some show more distinct traces of the preparation of the striking surface.

Most of the tools are made on blades and fragments of blades, with some are manufactured on cores and flakes. Lamellar *debitage* ranged in length from 4.5 to 8.1 cm. Most have "regular" shapes, "correct" dorsal scar patterns and straight profiles. Some blades show signs of use, such as scratched, blunted, or polished edges. Burins dominate the toolkit with around 60% (Table 1-3), among which those on truncated blades predominate. Angel burins comprise about a third, dihedral ones about a quarter, and single specimens are reported for "dihedral-angel", "multi-faceted", and "beak-like" (Table 1-4). Truncated pieces – "blades with the oblique terminal end" in the terminology of Lupenko – make up more than 9%. End-scrapers, all simple end-scrapers except for one double specimen, account for 8% of the tools. Almost 7% are microliths, while points and retouched pieces – "blades and their fragments with retouching along the edge" according to Lupenko – amount to 5%, respectively. Borer-perforators, "scraper-like" tools, notched pieces and combined tools make up 1%, respectively, and "cutters", "core-like" tools and "tips with lateral notch" all occur in shares below 1% (Lupenko 1983: 13; Table 1-3).

Lupenko saw the assemblages of Yeliseevychi, Mizyn, Kostenki IV, Lypa I and Lypa VI, Chulativ I, and Suponevo as providing the closest typological analogies to the assemblage from Barmaky, particularly for end-scrapers and burins, and attributed it to the "Early Magdalenian period" (Lupenko 1983: 5–17).

### *Other artefacts*

Lupenko found 35 specimens of fossil shells, most exhibiting artificial holes, which he attributed to Cerithium vulgatem Brug and Mactra. Given their concentrations in clusters 2 and 3, Lupenko suggested that they likely have been components of two necklaces rather than individual pendants, and highlighted that similar perforated shells are characteristic of many Upper Palaeolithic sites, including Mizyn (Lupenko 1983: 2, 20).

The figurine made on a mammoth tusk is damaged, with the preserved part showing a cutter groove, which appears to be part of an ornamental pattern (Piasetsky, Samoliuk 1990: 12).

Similar anthropomorphic statuettes have been discovered during the excavations at Mizyn. Shovkoplias proposed referring to these artefacts as female figurines (Shovkoplias 1965: 217–236). Iakovleva suggests categorising these figurines into four distinct types of anthropomorphic sculptures made

| Lithics | | 1982 season | | 1990 season | | | | 2002–2005 seasons | | | |
|---|---|---|---|---|---|---|---|---|---|---|---|
| | | | | level 1 | | level 2 | | level 1 | | level 2 | |
| | | n | % | n | % | n | % | n | % | n | % |
| core-like pieces | cores & pre-cores | 56 | 1,15 | 1 | 1,01 | 76 | 0,63 | – | 1,16 | 116 | 0,39 |
| | "core-like chunks" | 17 | 0,35 | – | – | 51 | 0,42 | 1 | | – | – |
| tools | | 297 | 6,11 | 3 | 3,03 | 491 | 4,05 | 13 | 15,12 | 550 | 1,87 |
| flakes | | 1976 | 40,66 | 29 | 29,29 | 2056 | 16,97 | 45 | 52,33 | 3373 | 11,45 |
| lamellar *debitage* | blades | | | 21 | 21,21 | 1440 | 11,89 | | | 1290 | 4,38 |
| | bladelets | 1068 | 21,98 | 3 | 3,03 | 716 | 5,91 | 27 | 31,40 | 1229 | 4,17 |
| | micro-blades | | | – | – | 68 | 0,56 | | | 642 | 2,18 |
| technical *debitage* | core tablets | 13 | 0,27 | – | – | – | – | – | – | – | – |
| | "thick *debitage*" | – | – | 5 | 5,05 | 231 | 1,91 | – | – | – | – |
| | crested pieces | – | – | 1 | 1,01 | 109 | 0,90 | – | – | – | – |
| burin spalls | | – | – | 2 | 2,02 | 678 | 5,60 | – | – | 657 | 2,23 |
| truncation spalls | | – | – | – | – | – | – | – | – | 112 | 0,38 |
| unidentifiable *debitage* | | – | – | – | – | – | – | – | – | 1464 | 4,97 |
| chips | | 1433 | 29,49 | 34 | 34,34 | 5990 | 49,45 | – | – | 19986 | 67,87 |
| chunks | | – | – | – | – | 207 | 1,71 | – | – | 28 | 0,10 |
| | **Total:** | **4860** | **100,00** | **99** | **100,00** | **12113** | **100,00** | **86** | **100,00** | **29447** | **100,00** |

Table 1-1. Barmaky: lithic assemblages, by field campaigns and levels: after Lupenko 1983; Piasetsky, Samoliuk 1990; Nuzhnyi 2003; Nuzhnyi et al. 2004; 2005; 2006; the level 2 calculations of 2002–2005 assemblage are after V. Chabai and D. Dudnyk.

on mammoth tusks (Iakovleva 2013: 84-96), attributing the figurine from Barmaky to the second type: a highly schematised female body carved in round form from a mammoth tusk (Iakovleva 2016: 9).

## *Faunal remains*

During the 1982 surveys, 208 faunal remains were uncovered and 180 identified to species level (Lupenko 1983: 19). According to the MNIs, mammoth dominates together with hare, while fox, red deer and reindeer are three times less common. Bear, wolf, horse, and an unspecified carnivore are represented with a single individual, respectively (Table 1-5). The presence of red deer within the faunal assemblage is particularly striking. This species typically inhabits temperate forests or forest steppe environments, which contrasts sharply with the periglacial conditions assumed for the occupation of the site during the "Early Magdalenian period".

## *Conclusions*

Based on the analysis of the site`s topography, stratigraphy, flint assemblage, organic artefacts, and faunal complex, Lupenko proposed the following conclusions:

1. The site is located on an ancient slope of the Rivne loess plateau near flint outcrops, and represents a long-term Upper Palaeolithic settlement.
2. The single cultural level is embedded in diluvial yellow silty-loess, shows an inclination to the southwest, and is spatially structured by three clusters of artefacts and faunal remains representing distinct areas of activities.
3. Flint artefacts were produced on-site from "prismatic" cores. The typological and statistical characteristics of the tools are consistent with "Early Magdalenian" assemblages in the Rivne region (Horodok II, Lypa I and Lypa VI), the Middle Dnieper (Yeliseevychi, Mizyn, Dobranichivka, Suponevo, Chulativ I, II), and the Don basins (Kostenki IV).

| | | 2002–2005 seasons | | 1990 season | 1982 season |
|---|---|---|---|---|---|
| | **Core-like pieces** | **level 1** | **level 2** | **level 1** | **level 2** |
| unidirectional | unidirectional, cylindrical | – | 1 | 46 | 21 |
| | unidirectional, sub-cylindrical | – | 7 | | |
| | unidirectional, narrow flaking surface | 1 | 36 | | |
| | unidirectional, flattened | – | 4 | | |
| | unidirectional, bi-lateral, narrow flaking surface | – | 10 | | |
| | unidirectional, unidentifiable | – | 1 | | |
| bidirectional | bidirectional, sub-cylindrical | | 6 | 28 | 14 |
| | bidirectional, narrow flaking surface | – | 12 | | |
| | bidirectional, flattened | – | 1 | | |
| | bidirectional-adjacent, sub-cylindrical | – | 3 | | |
| | bidirectional-adjacent, narrow flaking surface | – | 2 | | |
| | bidirectional-adjacent, flattened | – | 1 | | |
| | bidirectional-alternate, narrow flaking surface | – | 5 | | |
| | bidirectional-bi-lateral-alternate, narrow flaking surface | – | 1 | | |
| | bidirectional, perpendicular-adjacent, sub-cylindrical | – | 1 | | |
| | bidirectional, perpendicular-adjacent, narrow flaking surface | – | 1 | | |
| multidirectional, sub-cylindrical | | – | 4 | – | – |
| multidirectional / "amorphous" | | – | – | 2 | 13 |
| "close to disc-shaped" | | – | – | – | 3 |
| "irregular prismatic" | | – | – | – | 3 |
| "flattened unilateral" | | – | – | – | 1 |
| "tortoise-like" | | – | – | – | 1 |
| unidentifiable, narrow flaking surface | | – | 15 | – | – |
| unidentifiable (core fragments) | | – | 5 | 51 | 17 |
| | **Total:** | **1** | **116** | **127** | **73** |

Table 1-2. Barmaky: number of cores, by field campaigns and levels: after Lupenko 1983; Piasetsky, Samoliuk 1990; Nuzhnyi 2003; Nuzhnyi et al. 2004; 2005; 2006; the level 2 calculations of 2002–2005 assemblage are after V. Chabai and D. Dudnyk.

4. Organic artefacts include a hammer crafted from deer antlers and a female statuette carved from a mammoth tusk. Fossil shells with artificial holes were interpreted as remnants of necklaces.
5. Mammoth remains dominate the faunal assemblage, with a minimum number of 6 individuals and a total number of 113 identified bones.

Lupenko claimed that the artefact-bearing lithological layer was more than 0.6 m thick, with the artefacts unevenly distributed both horizontally and vertically (Fig. 1-4). However, the reasons for the unequal vertical distribution within the cultural level remain unclear. Despite excavating the largest area of the site across all research seasons, Lupenko recovered 2.5 times fewer flint artefacts compared to the collection obtained by Piasetsky in the following season (Fig. 1-5) (Table 1-1). This discrepancy raises an important question: Did Lupenko investigate a peripheral area of the site, or could his research methods have lacked diligence?

Lupenko suggests that the concentrations of artefacts and faunal remains represent workshops for bone and tusk processing. However, neither the spatial nor the quantitative analysis of the material remains from these clusters is

| | 1982 season | | 1990 season | | | | 2002–2005 seasons | | | |
|---|---|---|---|---|---|---|---|---|---|---|
| | | | level 1 | | level 2 | | level 1 | | level 2 | |
| **Tools** | **n** | **%** | **n** | **%** | **n** | **%** | **n** | **%** | **n** | **%** |
| end-scrapers | 25 | 8,42 | 1 | 33,33 | 30 | 6,11 | 2 | 15,38 | 11 | 2,00 |
| burins | 175 | 58,92 | 2 | 66,67 | 357 | 72,71 | 7 | 53,85 | 231 | 42,00 |
| truncated pieces | 28 | 9,43 | – | – | 50 | 10,18 | 1 | 7,69 | 90 | 16,36 |
| denticulates | – | – | – | – | – | – | – | – | 1 | 0,18 |
| borer-perforators | 3 | 1,01 | – | – | 5 | 1,02 | – | – | 13 | 2,36 |
| points | 15 | 5,05 | – | – | 1 | 0,20 | – | – | 2 | 0,36 |
| raclette | – | – | – | – | – | – | – | – | 2 | 0,36 |
| combined tools | 4 | 1,35 | – | – | 8 | 1,63 | – | – | 2 | 0,36 |
| microliths | 20 | 6,73 | – | – | 21 | 4,28 | – | – | 81 | 14,73 |
| retouched pieces | 15 | 5,05 | – | – | 7 | 1,43 | 2 | 15,38 | 86 | 15,64 |
| thinned pieces | – | – | – | – | – | – | – | – | 1 | 0,18 |
| bifacial | – | – | – | – | – | – | 1 | 7,69 | – | – |
| notched | 3 | 1,01 | – | – | – | – | – | – | – | – |
| "cutters" | 2 | 0,67 | – | – | – | – | – | – | – | – |
| "core-like" tools | 2 | 0,67 | – | – | – | – | – | – | – | – |
| "scraper-like" tools | 3 | 1,01 | – | – | – | – | – | – | – | – |
| "tips with lateral noth" | 2 | 0,67 | – | – | – | – | – | – | – | – |
| "choppers" | – | – | – | – | 6 | 1,22 | – | – | – | – |
| "blades with symmetrical terminal notch" | – | – | – | – | 5 | 1,02 | – | – | – | – |
| unidentifiable | – | – | – | – | 1 | 0,20 | – | – | 30 | 5,45 |
| **Total:** | **297** | **100,00** | **3** | **100,00** | **491** | **100,00** | **13** | **100,00** | **550** | **100,00** |

Table 1-3. Barmaky: tools, by field campaigns and levels: after Lupenko 1983; Piasetsky, Samoliuk 1990; Nuzhnyi 2003; Nuzhnyi et al. 2004; 2005; 2006; the level 2 calculations of 2002–2005 assemblage are after V. Chabai and D. Dudnyk.

| | 1982 season | | 1990 season | | 2002–2005 seasons | | | |
|---|---|---|---|---|---|---|---|---|
| | | | level 2 | | level 1 | | level 2 | |
| **Burins** | **n** | **%** | **n** | **%** | **n** | **%** | **n** | **%** |
| on truncated pieces | 76 | 43,43 | 214 | 59,94 | 1 | 14,29 | 130 | 56,28 |
| angle | 54 | 30,86 | 34 | 9,52 | 3 | 42,86 | 42 | 18,18 |
| dihedral | 40 | 22,86 | 67 | 18,77 | 3 | 42,86 | 25 | 10,82 |
| "dihedral-angle" | 2 | 1,14 | – | – | – | – | – | – |
| "beak-like" | 1 | 0,57 | – | – | – | – | – | – |
| "multifaceted" | 2 | 1,14 | – | – | – | – | – | – |
| transversal | – | – | 2 | 0,56 | – | – | 2 | 0,87 |
| combined | – | – | 40 | 11,20 | – | – | 29 | 12,55 |
| unidentifiable | – | – | – | – | – | – | 3 | 1,30 |
| **Total:** | **175** | **100,00** | **357** | **100,00** | **7** | **100,00** | **231** | **100,00** |

Table 1-4. Barmaky: burins, by field campaigns and levels: after Lupenko 1983; Piasetsky, Samoliuk 1990; Nuzhnyi 2003; Nuzhnyi et al. 2004; 2005; 2006; the level 2 calculations of 2002–2005 assemblage are after V. Chabai and D. Dudnyk.

provided to support this claim. Lupenko also links these workshops to the relative proximity of the flint outcrop as well as evidence of on-site core reduction and tool production. However, the available data are insufficient and provoke several critical questions: Which clusters reflect the production of stone tools, and which are specialised in bone and tusk processing? What are the characteristics of the flint assemblages found in these workshops?

Based on his analysis of the flint collection, Lupenko stresses close parallels to the assemblage of Lypa IV, which, according to Savych (1975: 67), is dated to the "Early Magdalenian", approximately 17 kyr BP, with reference to the 5th layer of Molodovo V. Consequently, Lupenko has assigned the site of Barmaky also to the "Early Magdalenian period".

Eventually, these studies left several key questions unanswered:

1. What are the characteristics of the accumulation of lithological and archaeological deposits?
2. What is the time frame for the accumulation of the cultural deposit?
3. What are the detailed characteristics of the faunal remains?
4. Which typological and technological features characterise the lithic industry?
5. What models can be proposed for the exploitation of the lithic raw materials and faunal resources?
6. And what is the appropriate taxonomic attribution of the Barmaky assemblage within its broader context?

## The 1990 field campaign

In 1990, Piasetsky conducted excavations at Barmaky to define the boundaries of the occupation surface and to examine its geological and archaeological characteristics, resulting in a topographical plan at a scale of 1:2000 with a delineation of the site's protection zone (Fig. 1-1). Two excavation areas were investigated. Excavation area 1 expanded Lupenko's area to 40 m² (Fig. 1-2, *2*; 1-3, *2*). Excavation area 2, measuring 16 m², was located approximately 40 meters to the north (Fig. 1-1). The location of each artefact was documented on a plan at a scale of 1:20, with the depth of each find recorded using the Baltic altitude system. Sieving did not take place.

### *Lithology*

The stratigraphic sequence of excavation area 1 consists of four lithological layers (Fig. 1-8; 1-9):

1. Holocene soil, "chernozem" – 0.2-0.3 m
2. Pale yellow loose silty-loess – 1.1-1.4 m
3. The coloured part of the cultural level (cluster 6) – 0.2-0.3 m
4. Striated yellow silty-loess – the studied thickness reaches 1.1 m

The stratigraphic sequence of excavation area 2 consists of three lithological layers (Piasetsky 2009: 13-14):

1. Holocene soil – thickness not specified.
2. Silty-loess sediments of the "Prycherno morski horizon" – thickness not specified.
3. Chalk deposits – thickness not specified.

The lithological layers 2 and 4 of area 1 were attributed to the Prychernomoski and Bug horizons, respectively (Piasetsky, Samoliuk 1990: 10; Piasetsky 2009: 131, 147), based on the Veklich chronostratigraphic scheme (Veklich 1983). Piasetsky estimated the age of the "Prychernomorski horizon" to approximately 25-10 kyr BP. He also correlated a buried soil within this horizon, which could only be observed in trench 2, to the Lasko Interstadial, around 17-16 kyr BP (Piasetsky 2009: 147), although the exact ages of both the "Prychernomorski horizon" and the Lasko Interstadial have not yet been established for Ukraine, as Piasetsky acknowledges (Piasetsky, Samoliuk 1990: 5; Piasetsky 2009: 26-27, 131-132, 147, 174).

### *Archaeological levels*

Piasetsky identified two archaeological levels in excavation area 1. The first level was located in the upper part of lithological layer 2, just beneath the Holocene soil, while the second level was found in lithological layers 2 and 3, in contact with lithological layer 4 (Fig. 1-8; 1-9), both levels with an inclination towards the north-west. The distribution of the cultural re-

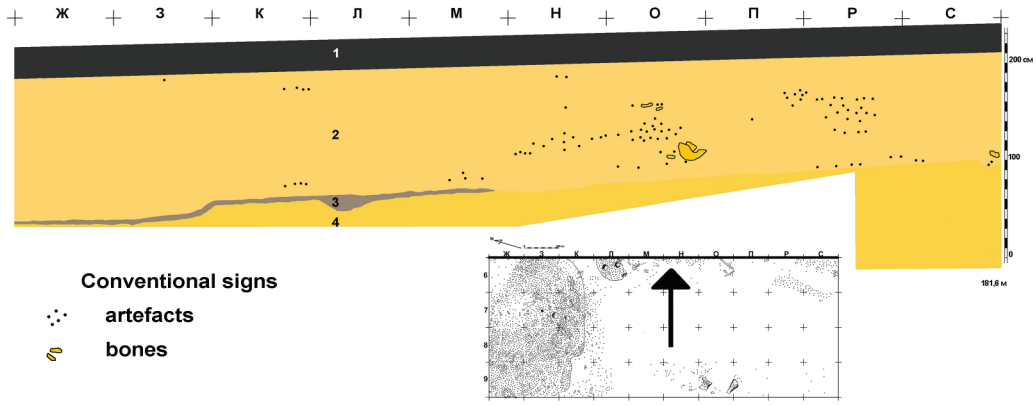


Fig. 1-8. Barmaky: the stratigraphic section along the squares line 5Ж-С/6Ж-С, redrawn from Piasetsky and Samoliuk 1990.

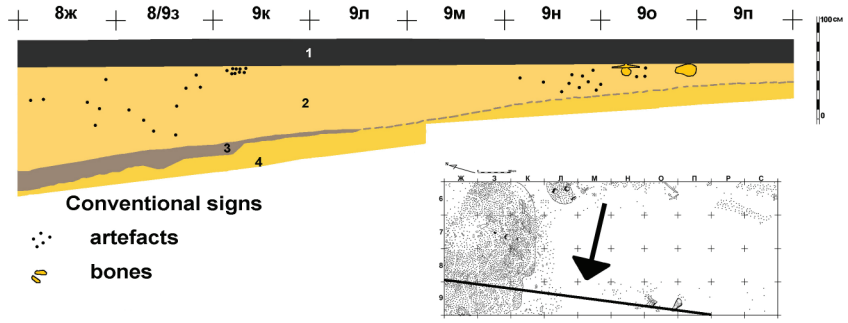


Fig. 1-9. Barmaky: the stratigraphic section along the lines on squares 8-9Ж-П, redrawn from Piasetsky, Samoliuk 1990.

mains is marked by the presence of six artefact clusters (Fig. 1-10; 1-11), clusters 1 and 3-6 in level 2 and cluster 2 in level 1. Here, lithological layer 3 is present in and around cluster 6, distinguished from lithological layer 2 solely by the colour of the sediments.

Piasetsky reports that the 171 flint artefacts, most of the patinated, and 2 horse teeth of the first archaeological level were unevenly distributed within lithological layer 2 across squares 6З-К, 6М-О, 6Р, 7Ж-З, 7Л, 8Ж-М, and 9Ж-Л, with no dominant position or orientation (Fig. 1-11). Cluster 2, located in square 9К, was recorded and subjected to a typological and statistical analysis (Table 1-1). In the second archaeological level, cluster 1 is a continuation of cluster 3, which Lupenko first identified in 1982. It is located in sq. 9М-П and consists of flint artefacts (Table 6), a siltstone retoucher, and faunal remains, including a scapula, a mammoth femur, and a processed mammoth tusk. Piasetsky observed a notably high percentage of lamellar *debitage* in cluster 1 compared to the other clusters (Table 1-6). All tools in this assemblage were identified as burins (Table 1-7).
Cluster 3 (sq. 6РС and 7РС) consists of flint artefacts (Tables 1-6, 1-7), fossil shells, ochre, and amber fragments. The presence of burin spalls led Piasetsky to interpret cluster 3 as part of a tool production workshop.

Cluster 4 is located in sq. 6М-О. It consists of flint artefacts (Tables 1-6, 1-7) and faunal remains, including bone fragments, the tooth and skull of a young mammoth and mammoth ribs. The skull lies outside the excavation area, in squares 5О and 6О, and has been preserved for future research.

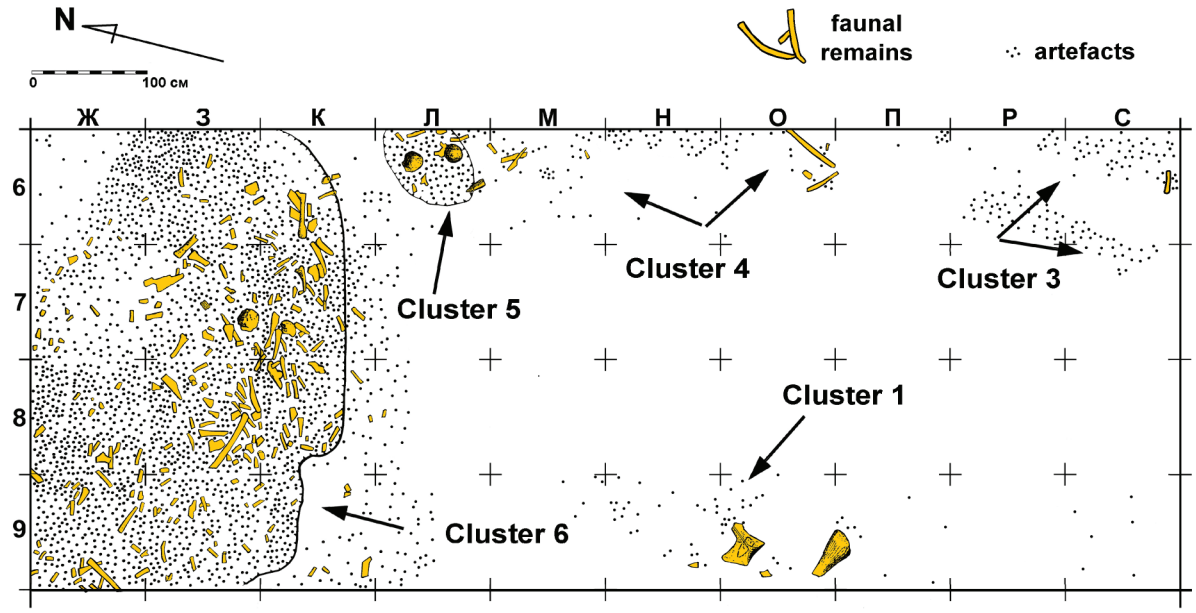


Fig. 1–10. Barmaky, the 2nd (lower) archaeological level: plan, redrawn from Piasetsky and Samoliuk 1990.

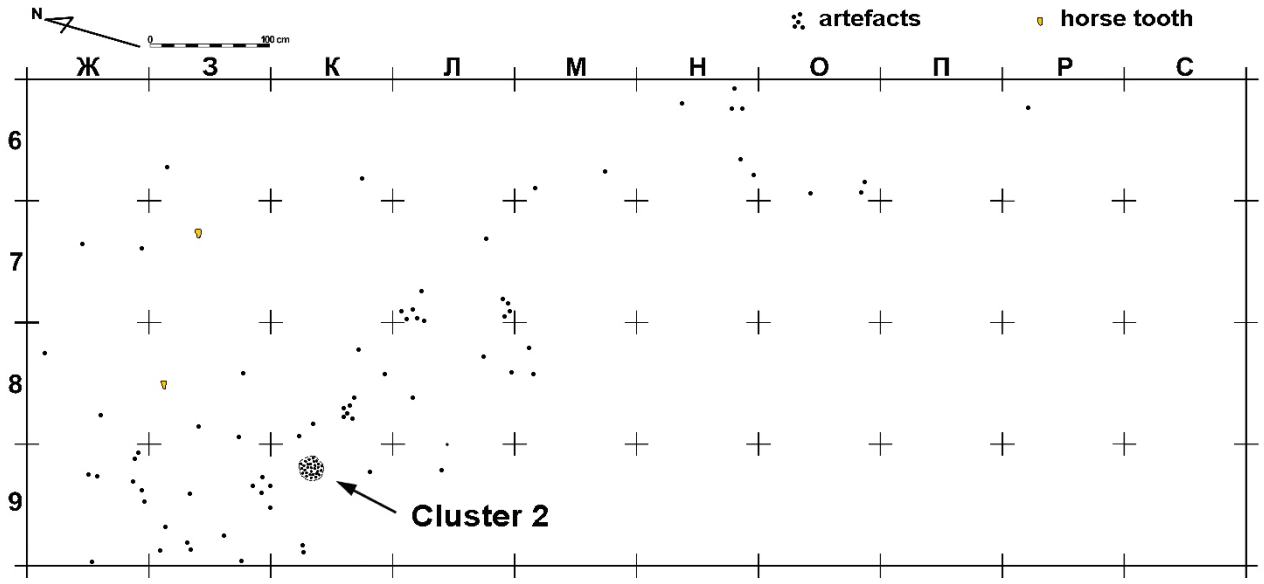


Fig. 1–11. Barmaky, the 1st (upper) archaeological level: plan, redrawn from Piasetsky and Samoliuk 1990.

| | 1982 season | | 2003 season | |
|---|---|---|---|---|
| **Species** | **NISP** | **MNI** | **NISP** | **MNI** |
| *Mammuthus primigenius* | 113 | 6 | 157 | 2 |
| *Bison priscus* | – | – | – | – |
| *Equus ferus* | 5 | 1 | – | – |
| *Rangifer tarandus* | 8 | 2 | – | – |
| *Canis lupus* | 5 | 1 | – | – |
| *Vulpes vulpes* | 7 | 2 | – | – |
| *Vulpes lagopus* | – | – | 20 | 2 |
| *Gulo gulo* | – | – | 6 | 1 |
| *Ursus arctos* | 3 | 1 | – | – |
| *Lepus* | 14 | 6 | – | – |
| *Cervus elaphus* | 22 | 3 | – | – |
| Carnivora unidentifiable | 3 | 1 | – | – |
| **Total:** | **180** | **23** | **183** | **5** |

Table 1-5. Barmaky: fauna, by field campaigns: after Lupenko 1983; Nuzhnyi et al. 2004; the definition of 1982 assemblage was made by M. Boguslavych; the 2003 assemblage was defined by S. Pean. NISP: Number of identified specimens; MNI: minimum number of individuals.

Cluster 5 is a continuation of cluster 4 in sq. 6Л, with patches of brownish-reddish ochre-stained sediment, featuring a shallow, 0.2 m deep pit. Cluster 5 is characterised by the presence of flint artefacts (Tables 1-6, 1-7) and faunal remains, including fragments of tubular bones, mammoth femoral epiphyses, a fragment of reindeer antler, and lower and upper jaws of arctic fox. The presence of a fragment of amber is also noteworthy.

Cluster 6 is located in sq. 6Ж-К, 7Ж-К, 8Ж-К, 9Ж-К and represents a shallow depression, up to 0.4 m deep, with an irregular bottom relief. The depression decreases in depth toward the north-western direction and is characterised by ochre-coloured sediments. Cluster 6 accumulated at the contact of lithological layers 2 and 4 (Fig. 1-8; 1-9) and contains five times more flint artefacts than the entirety of all other clusters (Tables 1-6, 1-7). The artefacts are distributed unevenly, ranging from 87 flint artefacts in sq. 6Ж to 1743 in sq. 7К. Cluster 6 contains many faunal remains, especially fragments of ribs. Arctic fox jaws are also found. Many bones were found arranged in anatomical order. Additionally, fossil shells, fragments of amber, and a processed tusk were found. Piasetsky suggested that cluster 6 likely extends beneath the lower boundary of the 1982 excavation (Piasetsky, Samoliuk 1990: 6-10) and interprets it as the remains of a deepened "dwelling-workshop" (Piasetsky 1997: 155; Piasetsky, Samoliuk 1990: 6-10; Piasetsky 2009: 135), which he attributed without further explanation to the summer season (Piasetsky 1997: 155).

In excavation area 2, Piasetsky uncovered flint artefacts, faunal remains and a fragment of amber (Fig. 1-12). This area is characterised by a low density of artefacts within the archaeological level. Unlike excavation area 1, the artefacts and faunal remains here do not form any visible clusters (Piasetsky, Samoliuk 1990: 13-14).

## *Flint artefacts*

The flint artefact assemblage from the first archaeological level of the excavation area 1 comprises 171 specimens, of which only 99 from Cluster 2 were analysed (Table 1-1). Many artefacts are patinated, but those for which a raw material determination was possible were all made from local raw materials. There is a single unidirectional core-like object. Chips, flakes, and blades dominate the assemblage, while bladelets, crested pieces, and burin spalls are represented by only a single specimen each (Table 1-6). Tools comprise one end-scraper and two burins on truncated pieces (Table 1-7).

The flint artefacts from archaeological level 2 are made from local raw materials, not patinated. In addition, Piasetsky found amber and minerals, such as fine-grained light grey sandstone, siltstone (used as retoucher), ochre, and basalt. All of these minerals originate from the Goryn River valley (Piasetsky, Samoliuk 1990: 11-12).

The flint assemblage from archaeological level 2 includes 12213 artefacts (Table 1-1). Cores and core-like pieces account for about 1% of the assemblage. Here, unidirectional cores predominate, followed by bidirectional cores (Table 1-2). Piasetsky argued that cores were used to produce lamellar blanks. With almost 50%, chips make up the majority of the assemblage, while flakes accounted for 17% (Table 1-1). Piasetsky divided the lamellar *debitage* according to the width of blanks into blades (> 1.2 cm), bladelets (< 1.2 cm) and micro-blades (< 0.7 cm) (Piasetsky, Samoliuk 1990: table 2).

| | level 1 | | | | level 2 | | | | | | | |
|---|---|---|---|---|---|---|---|---|---|---|---|---|
| | cluster 2 | | cluster 1 | | cluster 3 | | cluster 4 | | cluster 5 | | cluster 6 | |
| **Lithics** | **n** | **%** | **n** | **%** | **n** | **%** | **n** | **%** | **n** | **%** | **n** | **%** |
| cores | 1 | 1,01 | 4 | 4,04 | – | – | 3 | 0,47 | 5 | 0,62 | 64 | 0,63 |
| "core-like chunks" | – | – | 3 | 3,03 | 2 | 0,48 | – | – | 1 | 0,12 | 45 | 0,44 |
| tools | 3 | 3,03 | 13 | 13,13 | 2 | 0,48 | 9 | 1,41 | 12 | 1,48 | 464 | 4,57 |
| flakes | 29 | 29,29 | 11 | 11,11 | 68 | 16,27 | 102 | 15,94 | 127 | 15,64 | 1748 | 17,22 |
| blades | 21 | 21,21 | 44 | 44,44 | 43 | 10,29 | 62 | 9,69 | 46 | 5,67 | 1245 | 12,26 |
| bladelets | 3 | 3,03 | 8 | 8,08 | 34 | 8,13 | 27 | 4,22 | 34 | 4,19 | 613 | 6,04 |
| micro-blades | – | – | – | – | 2 | 0,48 | – | – | 3 | 0,37 | 63 | 0,62 |
| "thick *debitage*" | 5 | 5,05 | 2 | 2,02 | 6 | 1,44 | 3 | 0,47 | 6 | 0,74 | 214 | 2,11 |
| crested pieces | 1 | 1,01 | 1 | 1,01 | 3 | 0,72 | 1 | 0,16 | 4 | 0,49 | 100 | 0,98 |
| burin spalls | 2 | 2,02 | 3 | 3,03 | 15 | 3,59 | 20 | 3,13 | 20 | 2,46 | 620 | 6,11 |
| chips | 34 | 34,34 | 8 | 8,08 | 238 | 56,94 | 410 | 64,06 | 538 | 66,26 | 4796 | 47,24 |
| chunks | – | – | 2 | 2,02 | 5 | 1,20 | 3 | 0,47 | 16 | 1,97 | 181 | 1,78 |
| **Total:** | **99** | **100,00** | **99** | **100,00** | **418** | **100,00** | **640** | **100,00** | **812** | **100,00** | **10153** | **100,00** |

Table 1-6. Barmaky, 1990 field campaign, by levels and clusters: lithics after Piasetsky and Samoliuk 1990.

| | level 1 | | | | level 2 | | | | | | | |
|---|---|---|---|---|---|---|---|---|---|---|---|---|
| | cluster 2 | | cluster 1 | | cluster 3 | | cluster 4 | | cluster 5 | | cluster 6 | |
| **Tools** | **n** | **%** | **n** | **%** | **n** | **%** | **n** | **%** | **n** | **%** | **n** | **%** |
| end-scrapers | 1 | 33,33 | – | – | – | – | 1 | 11,11 | 1 | 8,33 | 28 | 6,03 |
| burins | 2 | 66,67 | 13 | 100 | 2 | 100 | 6 | 66,67 | 9 | 75,00 | 335 | 72,20 |
| truncated pieces | – | – | – | – | – | – | – | – | 1 | 8,33 | 49 | 10,56 |
| borer-perforators | – | – | – | – | – | – | – | – | – | – | 5 | 1,08 |
| points | – | – | – | – | – | – | – | – | – | – | 1 | 0,22 |
| combined tools | – | – | – | – | – | – | – | – | – | – | 9 | 1,94 |
| microliths | – | – | – | – | – | – | 2 | 22,22 | – | – | 19 | 4,09 |
| retouched pieces | – | – | – | – | – | – | – | – | – | – | 7 | 1,51 |
| "choppers" | – | – | – | – | – | – | – | – | – | – | 6 | 1,29 |
| "blades with terminal notch" | – | – | – | – | – | – | – | – | 1 | 8,33 | 4 | 0,86 |
| unidentifiable | – | – | – | – | – | – | – | – | – | – | 1 | 0,22 |
| **Total:** | **3** | **100,00** | **13** | **100** | **2** | **100** | **9** | **100,00** | **12** | **100,00** | **464** | **100,00** |

Table 1-7. Barmaky, 1990 field campaign, by levels and clusters: tools after Piasetsky and Samoliuk 1990.

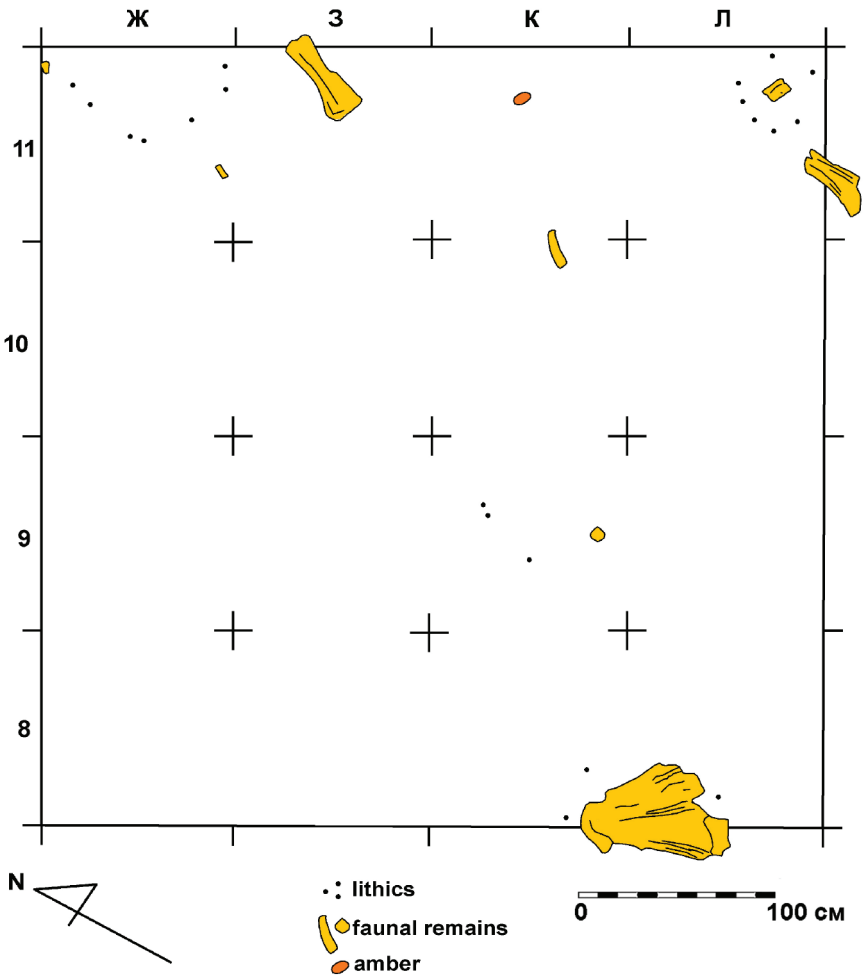


Fig. 1–12. Barmaky, excavation area 2: plan, redrawn from Piasetsky and Samoliuk 1990.

Lamellar *debitage* is quantitatively dominant over flakes (Table 1–1), with blades being most numerous, bladelets being half as common as blades, and micro-blades occurring rarely (Table 1–1). Burin spalls are common (Table 1–1). Piasetsky further distinguished "thick *debitage*" (nearly 4% of the assemblage, esse) and crested pieces (almost 2%, esse).

Tools comprise about 8% of the assemblage in essential accounts (Table 1–1). Most of the tools are made from lamellar blanks. Scrapers on wide blades account for 6%. Burins dominate the assemblage with more than 70% (Tables 1–3, 1–7). Here, burins on truncated pieces prevail, while angel, dihedral and combined burins make up only a small proportion. Transversal "Suponevo" burins, according to Piasetsky, are asso present (Table 1–4). Truncated pieces are the second most numerous tool category. Microliths make up only about 4% of the toolkit. A few borer-perforators, points, "blades with the symmetrical notch at the terminal end", chopping tools, combined tools, and retouched pieces occur (Tables 1–3, 1–7).

In excavation area 2, flint finds are not numerous. They are made from local raw materials and are not patinated. The assemblage consists of two tools (an end-scraper and a burin), six chips, four flakes, and one "massive longitudinal *debitage* from cores" (Piasetsky, Samoliuk 1990: 14).

### *Other artefacts and finds*

During the 1990 excavation, two fragments of a processed mammoth tusk and a tusk blade were uncovered. Approximately 200 specimens of fossil shells were found in excavation area 1, most of which have an artificially made hole. A large number of shells originated from cluster 6, the "dwelling-workshop". The fossil shells were analysed by V. Prysiazhniuk from the Institute of Geological Sciences of the National Academy of Sciences of Ukraine. Most specimens belong to *Nassa (Duplicata) corbiana Orb.* and *Nassa supirabile Koles.* Specimens with an artificial hole are most common among these shells. There are fewer shells of *Gibbula sulcatopodolika Koles*, only 4 of which have an artificial hole. *Venerupis (Pelititapes) tricuspis Eichw.* is also present. All fossil shells are local and originate from the Lower Middle Sarmatian Miocene deposits (Piasetsky 1997: 159). Piasetsky later noted that the genus name *Nassa* should be updated to *Dorsanum* from the family *Buccinidae* (Piasetsky 2009: 143). Until analysed by Dr K. Pasda 2018 at the Rivne Regional Museum, the faunal remains from the 1990 assemblage had not been studied (see Chapter 5, this volume).

## Piasetsky's conclusions

Piasetsky offered the following conclusions and observations:

1. Archaeological materials from both excavations were found in silty-loess sediments of the so-called "Prychernomoski horizon". The cultural level likely formed after 16 uncal kyr BP (Piasetsky 2009: 147).
2. Excavation areas 1 and 2 uncovered different parts of the settlement, separated by a natural depression (Piasetsky, Samoliuk 1990: 13-14).
3. Excavation area 1 revealed two archaeological levels that differ in depth, distribution, and density of finds, as well as in the composition of faunal remains. Excavation area 2 revealed a single archaeological level with a low density of finds.
4. A single cluster of finds was found in the upper archaeological level of the excavation area 1, and five clusters were identified in the lower level. Clusters 3 and 6 have been identified as the remains of workshops. In addition, cluster 6, was identified as a deepened "dwelling-workshop" that likely functioned during the summer season (Piasetsky 1997: 155). The "dwelling-workshop" may extend beneath the 1982 excavation area.
5. The lithic assemblages from both excavation areas are most similar to the assemblages from Mizyn (Piasetsky 1997: 160-161; Nuzhnyi, Piasetsky 2003: 70-73; Piasetsky 2009: 144-146).
6. Most of the fossilised shells belong to the genus *Dorsanum* from the *Buccinidae* family and are of local Miocene origin (Piasetsky 2009: 143). Specimens with an artificial hole prevail among these species. Piasetsky disputes the identification of the shells discovered in 1982 as *Cerithium vulgatem* (Piasetsky, Samoliuk 1990: 13). This species is considerably younger and is thought to originate from the Black Sea region.
7. Flint raw materials were processed on-site (Piasetsky, Samoliuk 1990: 10).
8. Different hunter-gatherer groups periodically occupied the site for short periods (Piasetsky, Samoliuk 1990: 5, 9).
9. A part of the Mizyn population migrated to the Volhynian Upland (Piasetsky 1997: 160-161; Piasetsky 2009: 28, 144-147).

Piasetsky argues that the site's geo-archaeological characteristics are more complicated than Lupenko initially suggested. He demonstrated that the archaeological materials were distributed across two distinct levels, with evidence indicating that the lower level likely extends beneath the 1982 excavation area. However, the origin of the upper level remains unclear.

In contrast to Lupenko, Piasetsky identified distinct classes of lamellar *debitage*: blades, bladelets, and micro-blades. He also identified burin spalls as a separate artefact category, constituting a significant portion of the assemblage. According to Piasetsky, the high number of burin spalls reflects the intensive production of burins and their likely use in processing bone, tusk, and, possibly, wood. The low number of microliths and small artefacts, such as chips and micro-blades, is likely due to the absence of water sieving during the excavation rather than reflecting specific econom-

ic activities in the excavated area. Sadly, 7377 artefacts were officially removed from the museum collection and discarded (Piasetsky, Samoliuk 1990: 15).

The numerous burin spalls in clusters 3 and 6 are the only evidence to support Piasetsky conclusion about the presence of workshops in the settlement. Piasetsky interpreted cluster 6 as the remains of a deepened "dwelling-workshop". However, either were structural elements of a dwelling identified, nor did Piasetsky present arguments to validate his claim that the "dwelling-workshop" was used during the summer season, nor did he present sections corroborating his suggestion that the different stratigraphic positions of the clusters reflect periodic visits by hunters.

Piasetsky identified technological and typological similarities between the flint artefacts from the Barmaky and Mizyn, including "prismatic" core reduction, burins on truncated blades, end-scrapers on blades, obliquely truncated blades and combined tools (end-scrapers combined with burins on truncated blades). He concluded that Barmaky postdates the occupation at Mizyn, probably representing a westward migration from the Desna River basin to the region of Rivne (Piasetsky 1997: 160–161; Piasetsky 2009: 28, 144–147).

Given Piasetsky's conclusions, it was necessary to clarify:

1. the geo-archaeological characteristics of the accumulation of archaeological deposits,
2. the technological and typological characteristics of the lithic assemblage,
3. the modes of raw material and fauna exploitation, and
4. the absolute chronology of the archaeological deposits at the site.

## The 2002–2007 field campaigns

During 2002–2005 and again in 2007, Nuzhnyi conducted field and laboratory research at the site (Fig. 1-2, *3, 4*; 1-3, *3, 4, 5*). The primary objective of the 2002–2004 excavations was to investigate the deepened-dwelling workshop discovered by Piasetsky in 1990. For this purpose, a trench 5 m long and 2 m wide was excavated along the northern wall of the 1982 excavation in squares 11Ж3, 12Ж3, 13Ж3, 14Ж3, 15Ж, and partly of 153. In 2003, the excavations were continued in squares 103К, 113 and partly in 11К. In 2004, excavations expanded to square 10Ж. The 2005 research aimed to determine the characteristics of the upper archaeological level. For this purpose, a 21 m² excavation was carried out in squares 3Ж–Р, 4Ж–Р, 5Ж–Р and 2ОПР (Fig. 1-13). In 2007, an 11 m long and 1 m wide trench was excavated along lines 3–13Е to clarify the vertical and horizontal characteristics of both the upper and lower archaeological levels (Fig. 1-2, *4*).

Nuzhnyi conducted excavations using the square grid system initially introduced by Lupenko. In areas previously excavated in 1982 and 1990, the Baltic Height System was applied as proposed by Piasetsky. In 2005, while investigating a new area of the site, depths were determined using a datum point, a concrete monument – Barmaky site protective marker installed at the top of the cape (Nuzhnyi 2003; Nuzhnyi et al. 2004, 2005, 2006). The artefacts and faunal remains of the first (upper) archaeological level were recorded on a 1:20 scale plan. Excavated sediments were washed through a 4 × 4 mm mesh sieve to reveal the smallest finds (Nuzhnyi et al. 2006). All second (lower) archaeological level finds were recorded on a 1:10 scale plan. A separate plan was created for faunal remains, the tusk products and the colour boundaries of the cultural deposits. The surface of the archaeological level was measured and marked on the plan after artefacts were removed. To ensure the detection of the smallest artefacts and bone fragments, sediments from this level were washed through a 1.5 mm mesh sieve (Nuzhnyi 2003).

The stratigraphic sequence consists of three lithological layers (Fig. 1-14; 1-15):

1. Holocene topsoil.
2. Yellow silty-loess sediments.
3. The cultural level is intensely ochre-coloured, particularly in the area of the deepened dwelling-workshop.

The upper level was directly beneath the ploughing layer within yellow silty-loess sediments at 25 to 50 cm depth from the present-day surface. No artefact clusters were observed at this level. Due to the activity of digging animals and other natural processes, materials were vertically displaced within a

range of 30–40 cm. The archaeological levels "converged" southward (Nuzhnyi et al. 2006: 15). Sterile sediments separating the upper and lower levels measured 30–40 cm in thickness (Nuzhnyi 2015: 163).

According to Nuzhnyi's observations, the lower archaeological level was located within the third lithological layer, at a depth of 1.2–1.4 m from the present-day surface, with a thickness of 10 cm. The archaeological level contained an object intensely coloured with red ochre, which Piasetsky interpreted as a dwelling-workshop (Nuzhnyi 2003: 7–8; Nuzhnyi et al. 2005: 4; Nuzhnyi 2015: 163–165, 210).

The dwelling-workshop was oval, measuring approximately 7 m in diameter in cross-section, extending west to east. It was a depression up to 30 cm deep, featuring sloping edges and a wavy bottom. The cultural level within the dwelling was filled up to 15 cm thick (Nuzhnyi 2003: 7–8, Nuzhnyi et al. 2005: 4). This level was intensely coloured with red ochre and underlain by whitish silty-loess. However, whitish silty-loess was not mentioned in the stratigraphic description of the studied area (Nuzhnyi 2003: 5).

The artefacts of the cultural level are represented by chaotically arranged faunal remains, a large number of flint artefacts, fossil shells, tusk fragments with processing traces, bone charcoal, small nodules of amber and accumulations of red ochre (Fig. 1–16). Nuzhnyi attributed the uneven distribution of material remains to partial destruction caused by natural factors, such as erosion by water streams (Nuzhnyi 2003: 7–8). However, no evidence of erosion in the form of sediment sorting was observed. Nuzhnyi suggested that a 10–15 cm deep trench, likely intended for water drainage, surrounded the dwelling. This trench was located on the southeast side of the dwelling and extended downslope towards the valley (Nuzhnyi et al. 2004: 18). However, this trench has not been documented.

In 2003, a bone sample from the lower archaeological level (?) of the site was radiocarbon dated in a Kyiv laboratory as 14300 ± 250 years BP (KI-11087). However, Nuzhnyi questioned the accuracy of this date, arguing that it was too young. He suggested that the sample had been buried for a prolonged period beneath the backfill sediments from the 1982 excavation, allowing modern organic infiltration that potentially affected the dating results (Nuzhnyi et al. 2004: 27; Nuzhnyi 2015: 161, 210).

The flint artefacts were made exclusively from local raw materials. Nuzhnyi analysed flint artefacts from 1982–2002. Excluding the smallest artefacts (chips), the assemblage comprises 21300 pieces (Nuzhnyi 2015: 167). According

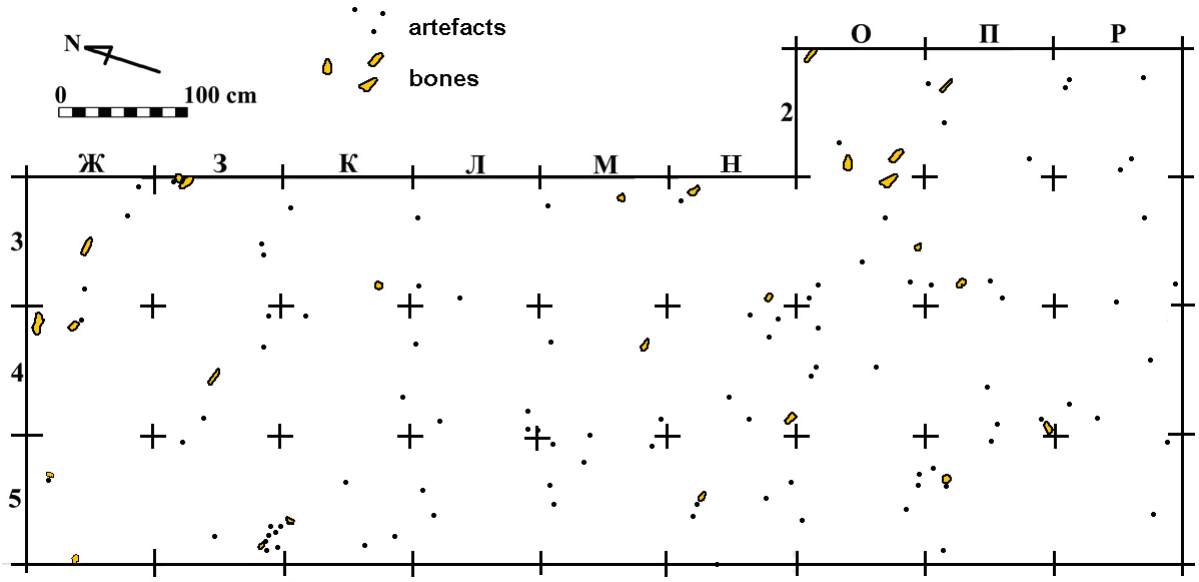


Fig. 1–13. Barmaky, the 1st (upper) archaeological level: plan, redrawn from Nuzhnyi et al. 2006.

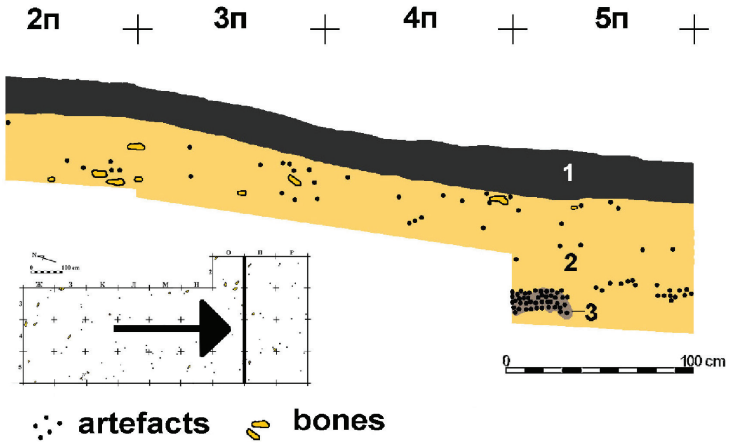


Fig. 1-14. Barmaky: the stratigraphic section along the squares line 2-5О/2-5П, redrawn from Nuzhnyi et al. 2006.

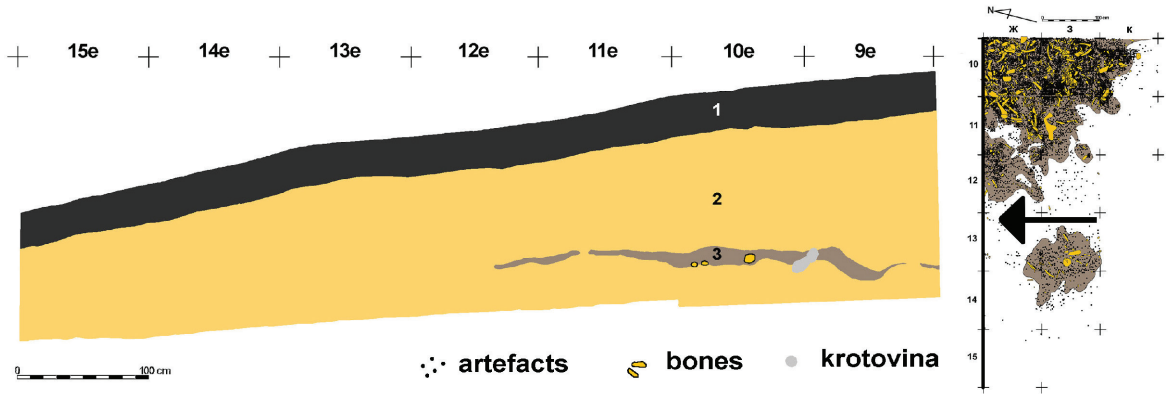


Fig. 1-15. Barmaky: the stratigraphic section along the squares line 9-15Е/9-15Ж, redrawn from Nuzhnyi et al. 2004; 2005.

to Chabai's and Dudnyk's calculations, the flint assemblage of the 2002-2004 collection from the second archaeological level comprises 29447 items. This is almost twice the number recorded from the 1982 and 1990 collections.
The flint assemblage from the upper level consists of 86 specimens (Table 1-1). More than half are flakes. Lamellar *debitage* is about one-third, and tools are 15.12%. A fragment of a unidirectional narrow flaking surface core represents core-like pieces (Table 1-2).

The toolkit from the upper level consists of seven burins, two end-scrapers, one truncated piece, two retouched pieces and one bifacial piece (Table 1-3). Based on the analysis of this assemblage and the first level artefacts studied by Piasetsky in 1990, Nuzhnyi concluded that the artefacts from the upper layer do not differ technologically and typologically from those of the lower level, with one exception. The bifacial tool likely belongs to a later period (Nuzhnyi 2015: 209).

The lower level assemblage from the 2002-2004 excavations primarily comprises chips – 67.87% (Table 1-1). Excluding chips, chunks and unidentifiable *debitage*, core-like pieces make up 1.46% of the assemblage, tools – 6.90%, flakes – 42.33%, lamellar *debitage* – 39.67%, burin spalls – 8.24% and truncation spalls – 1.41%.

The core-like pieces of the second archaeological level are predominantly unidirectional, with 59 specimens recorded (Table 1-2). Most of these have a narrow flaking surface – 46

specimens, ten of which are bilateral. Additionally, there are seven sub-cylindrical specimens, four flattened, one cylindrical, and one unidentifiable unidirectional core-like piece. The assemblage also includes 33 bidirectional core-like pieces, with the predominant type being narrow flaking surface – 21 specimens. Among them, five are alternate, two adjacent, one bilateral-alternate and one perpendicular-adjacent. Ten bidirectional core-like pieces belong to the sub-cylindrical type, two of which are adjacent, and one is perpendicular-adjacent. Two bidirectional core-like pieces belong to the flattened type, one of which is adjacent. Additionally, 4 multidirectional sub-cylindrical core-like pieces and 20 unidentifiable core-like pieces were recorded. Among the unidentifiable specimens, 15 belong to the narrow flaking surface type.

The toolkit is predominantly composed of burins – 42%, truncated pieces – 16.36%, and microliths – 14.73% (Table 1-3). Approximately 2% consists of end-scrapers and borer-perforators. One piece is classified as a denticulate, and one as a thinned piece. Points, *raclette*, and combined tools are represented by a few pieces. Retouched pieces make up 15.64%, while unidentifiable tools account for 5.45%.

Most burins were made on truncated pieces – 56.28% (Table 1-4). Angle burins account for 18.18%, while dihedral burins make up 10.82%. Two burins are transversal. Combined burins constitute 12.55%. Three burins are unidentifiable.

On the upper level, two fossil *Dorsanum sp.* shells and one unidentified species were found (Nuzhnyi 2015: 209). The assemblage of Miocene fossil shell pendants from the lower level is significantly larger, consisting of complete specimens with artificial holes and fragmented pieces. A total of 368 specimens were recovered in 2002-2005 field seasons, including 136 with perforations (see Chapter 9). According to Prysiazhniuk, the shells belong to two species: *Dorsanum sp.* and *Trochidae sp.*, the latter being highly fragmented due to their fragility. Shells with artificial holes are most commonly found among *Dorsanum sp.* (Nuzhnyi 2015: 208).

Organic artefacts were found exclusively in the lower level and are represented by mammoth tusk products (see Chapter 9). These include ten fragments of spindle-shaped points, five fragments of a herring-like ornamental bracelet, a pendant with an interception (dumbbell-shaped beads), and 29 fragments of the processed tusk, four of which are needle fragments (Nuzhnyi 2003: 15; Nuzhnyi et al. 2004: 22; Nuzhnyi et al. 2005: 8). A schematic mammoth figurine made of marl was also found among the mobile art objects (Nuzhnyi 2015: 208).

Based on the 2003 assemblage, the faunal analysis was conducted by Stephane Pean (National Museum of Natural History, France). The collection is dominated by mammoth remains, accounting for more than 80% (NISP) and represented by two individuals. Except for the tusks, these remains exhibit high bone

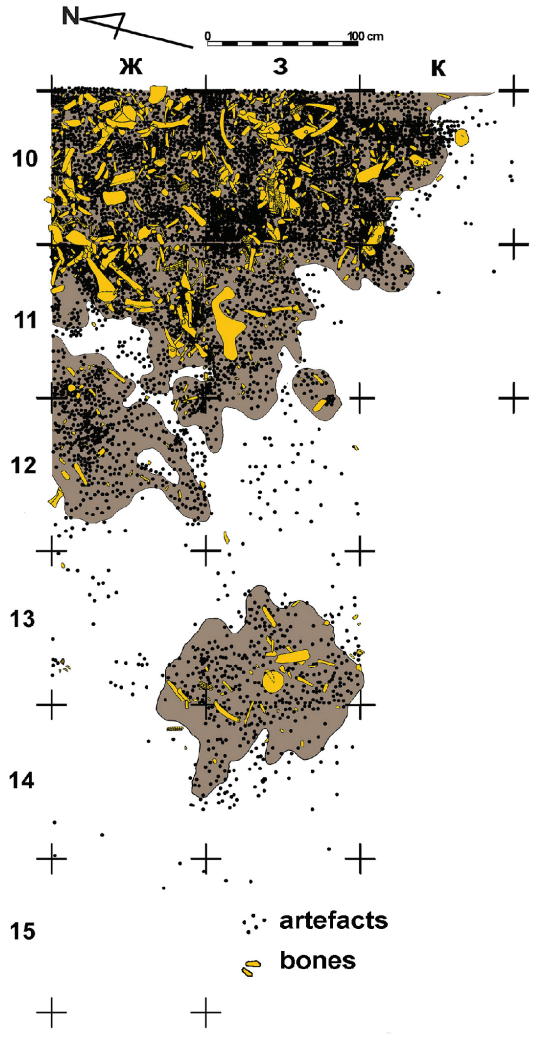


Fig. 1-16. Barmaky, the 2nd (lower) archaeological level: the combined plan of 2002, 2003 and 2004 field season, redrawn from Nuzhnyi et al. 2004; 2005.

fragmentation and a complete absence of cranial bones. The assemblage includes two arctic fox individuals, with limb bones found in anatomical order, and a single wolverine individual, represented by six bones (Table 1–5). Thus, Nuzhnyi suggested the following interpretation of the site:

1. The upper level is probably redeposited, as its flint assemblage shares similar technical and typological characteristics with the lower level.
2. The dwelling-workshop extends north and northwest beyond the 1982 and 1990 excavations and is surrounded by a trench on the north side.
3. The chaotic distribution of material remains is probably caused by natural factors.
4. The Barmaky and Mizyn flint assemblages belong to the Mizyn type of the Epigravettian industry.
5. The Barmaky site was likely occupied during the warm season, as indicated by the absence of mammoth bone dwellings and the site's topographical conditions (Nuzhnyi 2015: 412–424).
6. The radiocarbon date of 14300±250 BP (Ki-11087) obtained in the Kyiv laboratory is unlikely to be reliable due to the conditions of the sample origin (Nuzhnyi et al. 2004: 27; Nuzhnyi 2015: 161, 210).

Nuzhnyi's excavation methods and archaeological material analyses differed significantly from those of his predecessors. One key distinction was the sieving of sediments, which influenced both the total number and typological composition of the artefact assemblage, particularly affecting the microliths (Tables 1–4). Additionally, the archaeological material from the second archaeological level was meticulously recorded on a 1:10 scale plan. Due to the large number of flint artefacts, faunal remains and organic material, products were documented separately. For the first time, radiocarbon dating was conducted on the lower level of the site. However, the stratigraphic origin of the sample remains uncertain, raising concerns about the reliability of the results.

Although Nuzhnyi obtained a collection of artefacts over four field seasons (2002–2005), his interpretation of the technical and typological features of the industry is based on the analysis of collections from 1982, 1990, 2002, and 2005 (Nuzhnyi 2015: 162–210). However, only the 2002 and 2005 collections originate from excavations conducted with an appropriate methodological approach, ensuring higher data reliability.

Nuzhnyi suggested that a trench fence the dwelling (?), but this feature is not shown on the plan or sections. He found no direct evidence supporting Piasetsky's hypothesis regarding the existence of a dwelling-workshop. As a result, in his publications, he refers to the feature with cautious terminology, using phrases such as "depression or pit (dwelling?)", "depression or dwelling (?)" and "probably deepened dwelling structure" (Nuzhnyi 2003: 7–8; Nuzhnyi et al. 2005: 4; Nuzhnyi 2015: 163–165, 210).

Nuzhnyi argued that the flint complex is characterised by "prismatic" reduction and that tools made on "blades" dominate. However, he did not provide specific characteristic features of the "prismatic" reduction. Additionally, he used the term "blades" to refer to all lamellar *debitage* without distinguishing between blades, bladelets, and micro-blades. He noted, however, that the length and width of the Barmaky "blades" are "significantly larger" than those from other Epigravettian sites (Nuzhnyi 2015: 166).

Nuzhnyi identified several unique characteristics of the flint industry at Barmaky and Mizyn: the predominance of unidirectional cores; among microliths, the dominance of microgravette points on bladelets, distinguished by straight-backed forms with obliquely truncated or retouched bases; and the prevalence of burins on obliquely truncated pieces. Additionally, he noted a large number of truncated pieces with various truncation types, the presence of end-scrapers with proximal oblique truncation, and combined tools, particularly end-scraper and burin on truncation combinations. Another distinctive feature is the lateral retouching observed on burins and end-scrapers (Nuzhnyi 2015: 169–200, 208–209).

Nuzhnyi also noted similarities in mammoth tusk artefacts between Barmaky and Mizyn, such as spindle-shaped points and herring-like ornamental bracelets (Nuzhnyi 2015: 207–208). Additionally, as at Mizyn, a large number of fossil shell pendants were found at Barmaky (Nuzhnyi 2015: 209).

Nuzhnyi suggested that the Barmaky settlement was occupied during the warm season, arguing that its dwelling structure differs from the mammoth bone dwellings at Mizyn, which are supposed to reflect the cold season (Nuzhnyi 2015: 424). Additionally, the high percentage of microliths in the tool assemblage and macroscopic damage indicative of intensive hunting activity may further support the hypothesis of warm seasonal occupation (Nuzhnyi, Stupak 2001).

Despite extensive research, several key questions remain unanswered:

1. Geo-archaeological characteristics of sediment and cultural deposit accumulation.
2. The presence or absence of a dwelling-workshop remains.
3. Radiocarbon age of the site.
4. Technological and typological features of the lithic assemblage.
5. Models of exploitation of flint raw materials and faunal resources.

## The 2018–2020 field campaigns

From 2018 to 2020, the Barmaky site was investigated by the Volhynian Palaeolithic Expedition of the Institute of Archaeology of the National Academy of Sciences of Ukraine, led by Victor Chabai. This research was conducted as part of the international Ukrainian-German archaeological project: *"Between East and West. Social networks and environmental conditions before, during, and after the Last Glacial Maximum in Volhynia, Western Ukraine"*, DFG-392605832. Excavations were conducted during three field seasons, each lasting three months. The primary objectives were to clarify the geo-archaeological characteristics of the cultural deposits, to obtain a series of geological and faunal samples to illuscidate the chronology, the environmental context, and the subsistence strategies, and to collect an artefact assemblage for detailed technological and typological analysis (Chabai et al. 2019a; 2019b; 2020a; 2021).

The expedition was attended by staff (Fig. 1-17) of the Institute of Archaeology of the National Academy of Sciences of Ukraine (Dr. Victor Chabai, Dr. Dmytro Stupak, Dr. Pavlo Vasyliev, Dr. Oksana Votiakova, junior researches Andrey Veselsky, Diana Dudnyk and Maria Vasylieva, Institute Deputy Director for General Affairs Yuriy Oliynyk); Institute of Prehistoric Archaeology, Friedrich-Alexander-Universität Erlangen-Nürnberg (Dr. Andreas Maier, Dr. Kerstin Pasda, students Olivia Kaiser and Rajit Yoganantam); Dr. rer. nat. Stefan Meng and Dipl. Geogr. Axel Heise from the University of Greifswald; senior researcher Ivan Khoptynets from State Scientific Centre for Protection of Cultural Heritage from Technogenic Disasters; survey consultant Vitaliy Tkach from Dubno district Natural History Museum; survey consultant Oleksandr Pozikhovsky from Rivne and Ostrog districts Historical Museums; senior scientist Olga Lozovska; volunteers Yuriy Lytvyn, Kateryna Zinchuk, Grit Müller, Victoria Kaliuzhna, and Yuriy Nemchenko.

Each year, a wooden frame shed with a plastic roof was constructed over the excavation area, protecting it from weather conditions and preventing the exposed cultural layer from being affected by atmospheric phenomena. At the end of each field season, the walls and floor of the excavation were protected using plastic sheeting, wooden boards, and sediments to ensure preservation until the next field season.

A spatial reference grid warranted consistency in spatial recording. Excavation of the cultural deposits was conducted according to lithological layers and their angles, ensuring precise stratigraphic control. For depth measurements, the datum point of Nuzhnyi's was used.

Depth measurements were taken using a LaserXZ-24 optical level. Excavation of the cultural deposits was conducted manually using wooden and metal tools (Fig. 1-18). All artefacts and faunal remains identified during excavation were recorded in a field diary, including the number and name of the find, the distance from the north and west walls of the square, and the depth from the reference point. Artefact type, position (horizontal, oblique, vertical) and orientation (north-south, east-west) were also noted for each artefact.

A separate numbering system was used for each square, beginning with No. 1. Artefacts, ochre samples, marl/chalk, quartzite/sandstone fragments and charcoal were numbered separately from faunal remains. Distribution plans for archaeological materials were created using QGIS v.3.4.4 and Adobe Photoshop CC 2018.

Faunal remains, sections, and site plans were graphically recorded on millimetre paper. Faunal remains were drawn at a 1:10 scale, preserving their actual contours. To graphically represent the second cultural layer's topography, the floor depth was measured every 5 cm (400 points for 1m2). A 3D surface model was created using Golden Software Surfer v.15. Photographs were taken with a NIKON D90 digital camera at 300 dpi/inch resolution.

When necessary, bones and tusks were fixed at the site and in the field laboratory with Paraloid B-72 glue to prevent damage. All sediments from the cultural layer were bagged and washed in the field laboratory using a 1 mm mesh sieve to recover small artefacts, bone fragments, microfauna, and malacofauna. Approximately 24 tonnes of sediment were processed. All archaeological material was cleaned of sediment, washed, labelled and inventoried in the field laboratory.

To thoroughly investigate the questionable dwelling structure reported by Piasetsky, an excavation was conducted during the 2018 and 2019 field seasons on squares 3-13Г, 2-13Д, 2-13Е, 2-5Ж, 2-53, 2-5К, 2-5Л, covering a total area of 51 m² (Fig. 1-2, *5*; 1-3, *6*). The first (upper) archaeological level was thoroughly investigated over 18 m², in squares 8-13Г, 8-13Д, 8-13Е and partially over 33 m², in squares 3-7Г, 2-7Д, 2-7Е, 2-5Ж, 2-53, 2-5К, 2-5Л (Fig. 1-2, *5*). The second archaeological level was thoroughly investigated over 13.5 m², in squares 8Г, 8Д, 8Е, 9Е, 10Е, 11Г, 11Д, 11Е, 12Г, 12Д, 12Е, 13Г, 13Д, 13Е (Fig. 1-3, *6*) (Chabai et al. 2019a).

One of the main objectives of the 2019 field season was to study the role of cryoturbation processes in the accumulation of the site's cultural deposits. To achieve this, excavation was conducted in squares 10Г, 10Д, 9Г, 9Д, 8Г, 8Д, 8Е, 7Г, 7Д, 7Е, 7Ж, 6Г, 6Д, 6Е, 6Ж, 63, 53,

Fig. 1-17. Participants of the Volhynian Palaeolithic Expedition, 2018. From left to right are standing: Dmytro Stupak, Yuriy Oliynyk, Victor Chabai, Andreas Maier, Rajit Yoganantam; sitting: Andrey Veselsky, Diana Dudnyk, Maria Vasylieva, Katerына Zinchuk, Yuriy Lytvyn and Oksana Votiakova.

5К, 5Л, 5М, 5Н, 43, 4К, 4Л, 4М, 4Н, 33, 3К, 3Л, 3М, 3Н, covering a total area of 31 m² of the lower level. This included squares 8Д, 8Е, 7Ж, 6Ж, and 63, which had been partially excavated during the 2018 and 1990 field seasons (Fig. 1-3, *7*). The upper level in these squares was investigated in previous years (Chabai et al. 2020a).

During the 2020 field season, both the first and second cultural layers were fully investigated in squares 1Н, 1О, 1П, 1Р, 1С, 2Н, 2О, 2П, 2Р, 2С, 3Н, 3О, 3П, 3Р, 3С, 4Н, 4О, 4П, 4Р, 4С, 4Т, 4У, 5Н, 5О, 5П, 5Р, 5С, 5Т, 5У, 6Т, 6У (Fig. 1-2, *6*; 1-3, *8*). Additionally, 1.5 m² of the second cultural level was excavated in the eastern parts of squares 6Н, 6О, 6П, 6Р, 6С and the southern part of square 6С, which had not been fully excavated in 1990. The presence of cultural deposits in these squares was due to the non-vertical walls of the 1990 excavation. During the 2020 field season, the first level was excavated over 31 m² and the second level over 32.5 m² (Chabai et al. 2021). By the end of the 2020 field season, the total excavation area reached 189 m², of which the first level covered 189 m² and the second level – 171 m² (Fig. 1-2, *7*; 1-3, *9*).

## CONCLUSION

The study of the site of Barmaky is crucial for understanding the human occupation of the Volhynian Upland during the Upper Palaeolithic. Lupenko, Piasetsky, and Nuzhnyi excavated a significant part of the settlement between 1981 and 2007. Two archaeological levels have been identified, the techno-typological characteristics of the lithic industry have been analysed, and probable production zones have been identified. The materials obtained during these investigations indicate technological and cultural similarities between the assemblages of Barmaky and Mizyn, suggesting cultural connections and possible migration events between these regions.

Fig. 1-18. Barmaky, 2018, the 2nd archaeological level: excavation of squares 10Е and 11Д. From left to right are Olivia Kaiser, Andrey Veselsky, Diana Dudnyk and Dmytro Stupak.

However, an analysis of previous research methods has revealed several key issues. The main shortcomings include limited stratigraphic analysis, insufficient chronological control, and non-optimal methods of material collection. The lack of detailed consideration of geoarchaeological processes, particularly cryoturbation and erosion, complicates the reconstruction of stratigraphic contexts. Sediments were not systematically sieved during early excavations, resulting in the partial loss of small artefacts, such as microliths, micro-blades and burin spalls. The faunal remains have been studied partly and research has only been conducted on the 1982 and 2003 assemblages. In addition, the interpretation of the settlement structures needs to be revised, as the hypothesis of a "summer workshop dwelling" remains unconfirmed. To address these challenges, the investigations reported in this book focus on:

1. Geo-archaeological analyses to evaluate the impact of natural and anthropogenic factors on cultural deposits accumulation
2. Establishing a reliable chronological framework for the observed stratigraphic units
3. Archaeozoological analyses to determine patterns of faunal exploitation and seasonality
4. Environmental studies to reconstruct the ecological situation during the time of occupation
5. Lithic analyses to clarify raw materials procurement and exploitation strategies, the technological and typological characteristics of the assemblage, and its relation to the Mizyn industry
6. Analyses of the adornments and organic artefacts to identify their stylistic and technological characteristics
7. Inference of Barmaky's site function and position in the subsistence patterns of the Epigravettian in the periglacial zone of Eastern Europe.

# BARMAKY: SETTING, LITHOLOGICAL & ARCHAEOLOGICAL SEQUENCES, STRUCTURES

# 2

V. CHABAI

## SETTING

The site of Barmaky (50°37.700'N; 26°17.579'E) is situated in the eastern suburb of Rivne, on the western slope of the cape of a small hill, whose top is about 10 m above the valley of Barmatsky Creek (Fig. 2-1, *2*). In a broader geographical context, Barmaky is situated within the loess plateau of the Volhynian-Lublin Upland, which is a hilly plain with several erosional cuts (Fig. 2-1, *1*). Barmatsky Creek is a right tributary of the Ustia River, itself being a left tributary of the Goryn River which belongs to the drainage system of the Middle Dnieper basin. Silty-loess sediments with a maximum thickness of up to 3 m cover the hills of Barmatsky Creek. Turonian chalk containing flint nodules underlies the silty-loess deposits. The left bank of Barmatsky Creek is gently sloping; the right bank is relatively steep, formed by several capes, and featuring a number of erosional channels often yielding flint nodules (Fig. 2-1, *2*; 2-2, *1*). The closest of such flint outcrops is about 150–300 m south of the site of Barmaky (Fig. 2-2, *3*). The site of Barmaky and the flint outcrop are located on the high right bank of Barmatsky Creek. The Barmatsky Creek is a modern time artificial channel that dries the swamp between Rivne City and Barmaky village. That is, several decades ago, the Barmaky site was situated on the cape partly surrounded by the swamp.

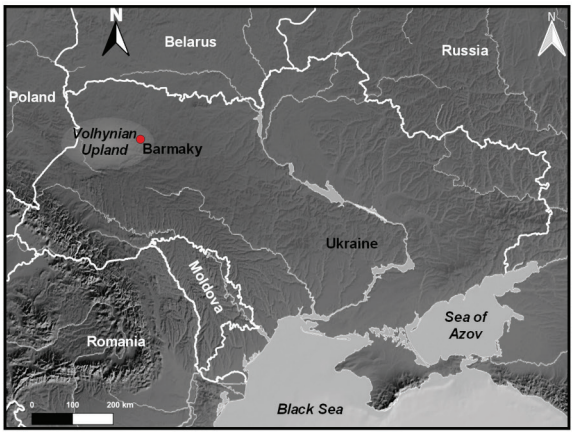


1

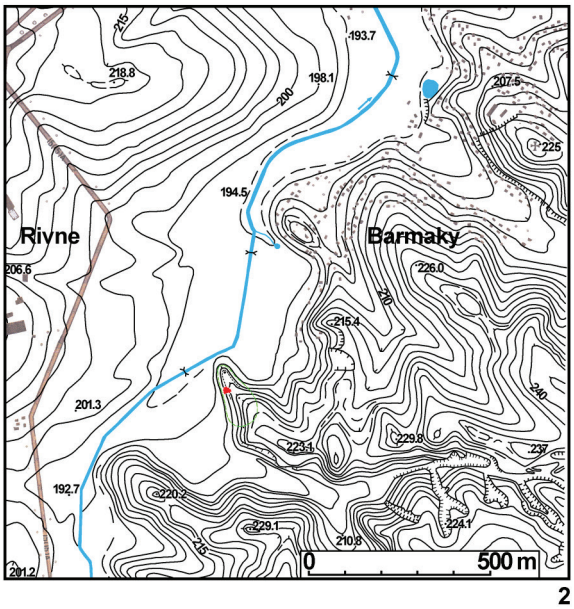


2

Fig. 2-1. Barmaky: 1 – location of the site in Eastern Europe; 2 – topographic map of the site, the red dot shows location of the excavation area.

## THE EXCAVATION: STRATEGY AND CONDUCT

The Barmaky cape was studied by the main excavation area (1982–2020) and the number of sondages (Fig. 2–2, *1, 2*). The proposed excavation strategy of the first two seasons aimed at the continuation of the previously unfinished excavations of "deepened dwelling" and pit 1 by V. Piasetsky and D. Nuzhnyi (see Chapter 1, this volume). Therefore, square lines "Г", "Д", and "Е" were chosen for investigation. At the end of the 1990 field campaign, pit 2 was only partly studied. During the third season, the square lines from "Н" until "У" were thus excavated. Overall, 72 square meters were studied during the three field campaigns between 2018 and 2020 (Fig. 2–2, *2*).

To protect the excavation area from rain, a wooden carcass with a plastic roof was built (Fig. 2–3, *3*). The excavations followed a one-square-meter grid system and datum point of the coordinate system established during the previous campaign to warrant consistency. A 3D coordinate system is used to document all visible lithic pieces in each square. All fauna remains were mapped at a scale of 1:10. The same scale was employed for drawings of artificial structures and lithological sections. If necessary, the fauna remains were treated with Paraloid B–72 in the field laboratory for preservation. During the three field campaigns, 3 months each, water sieving through a 1 mm sieve was conducted for more than 20 tons of sediments from cultural deposits (Fig. 2–3, *1*). After each field campaign, the walls and floor of the excavated area were conserved by plastic, wooden constructions and back dirt (Fig. 2–3, *2*).

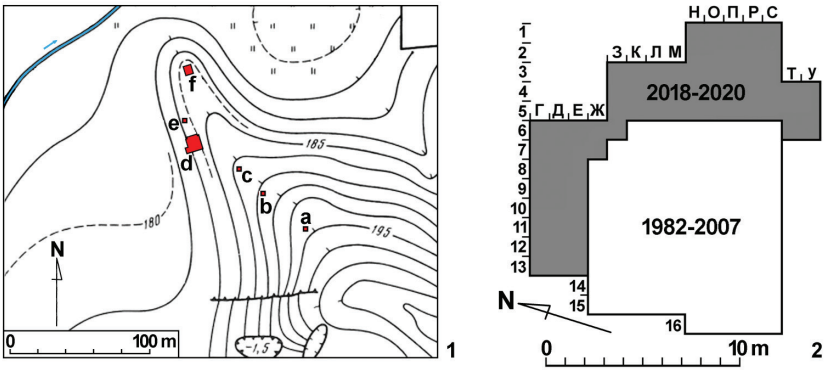

Fig. 2–2. Barmaky:
1 – topographic map of Barmaky cape, showing the sondages and excavation area (a – sondage 1; b – sondage 2, c – sondage 3, d – 1982–2020 excavation area, e – sondage 4, f – sondage of the 1990 field campaign);
2 – plan of the 1982–2020 excavation area;
3 – site and flint outcrop, blue roof covers the excavation area, the whitish eroded slope is the flint outcrop.

Fig. 2-3. Barmaky: 1 –water sieving of sediments by Rajit Yoganantam; 2 – site conservation process; 3 –roof building process.

## THE LITHOLOGICAL LAYERS

The lithological and cultural stratigraphy was studied in the 1982-2020 excavation area and sondages 1-4. No information is available from the 1990 sondage.

The stratigraphic sequence in the 1982-2020 excavation area comprises a maximum of 2.5 m of sediment, subdivided into 12 lithological layers (Fig. 2-4—2-11). Most of the layers show an inclination angle of about 3° in east-west direction, thus matching the gradient and direction of the modern slope. An important feature that has heavily affected the Pleistocene deposits and caused post-depositional movements is a large depression consisting of several channels, which formed when a larger polygonal permafrost structure melted during the postglacial warming process.

**Layers 1 and 1a** – *chernozem* intensively grey/black colour (10B, 2.5/1) soil with pronounced traces of modern agricultural digging activity (1a) and bioturbation processes; the thickness is up to 0.4 m (Fig. 2-4—2-9).

**Layer 2** – grey colour (N, 4/) Holocene soil with pronounced traces of bioturbation processes; loose sediment structure; the upper boundary is clear; the thickness is up to 0.6 m (Fig. 2-4—2-7; 2-9).

**Layer 3** – greyish brown (7.5YR, 5/2) loose silty-loess; spread over the entire excavated area; contains carbonate concretions – *beloglazka* and animal burrows – *krotovinas*; in the western part of the excavated area, the sediments of layer 3 fill a permafrost depression; the upper boundary is gradual; this lithological layer is recognised in all of the studied sections; the thickness of lithological layer 3 varies from 0.1 up to 0.9 m (Fig. 2-4—2-11).

**Layer 4** – light brown (7.5YR, 6/4) compact silty-loess; found in the western part of the excavated area as several separated lenses; both upper and lower boundaries are clear; often the lenses of layer 4 are truncated by permafrost depression channel fillings or constitute the upper part of such fillings; the maximum length and thickness of each lens is up to 1.0 and 0.25 m, respectively (Fig. 2-4—2-6; 2-8—2-10).

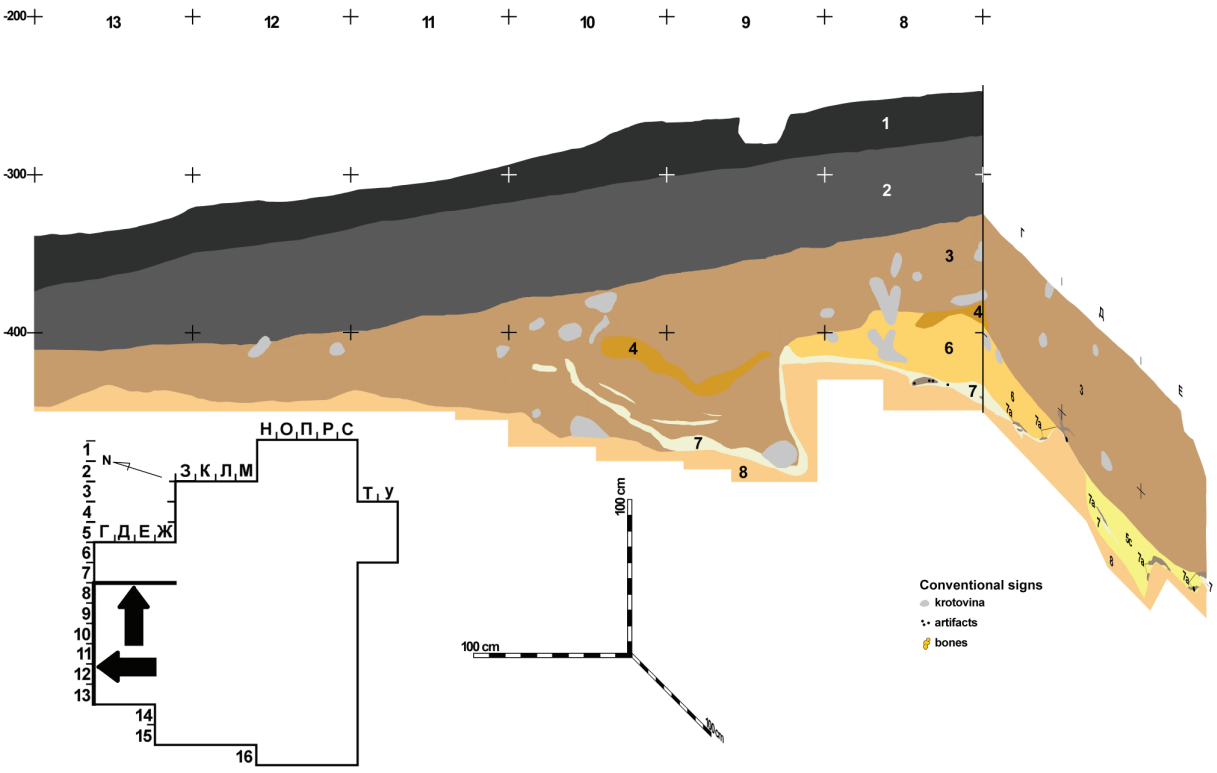


Fig. 2-4. Barmaky: stratigraphic sections along square lines В/Г and 7/8, cabinet projection.

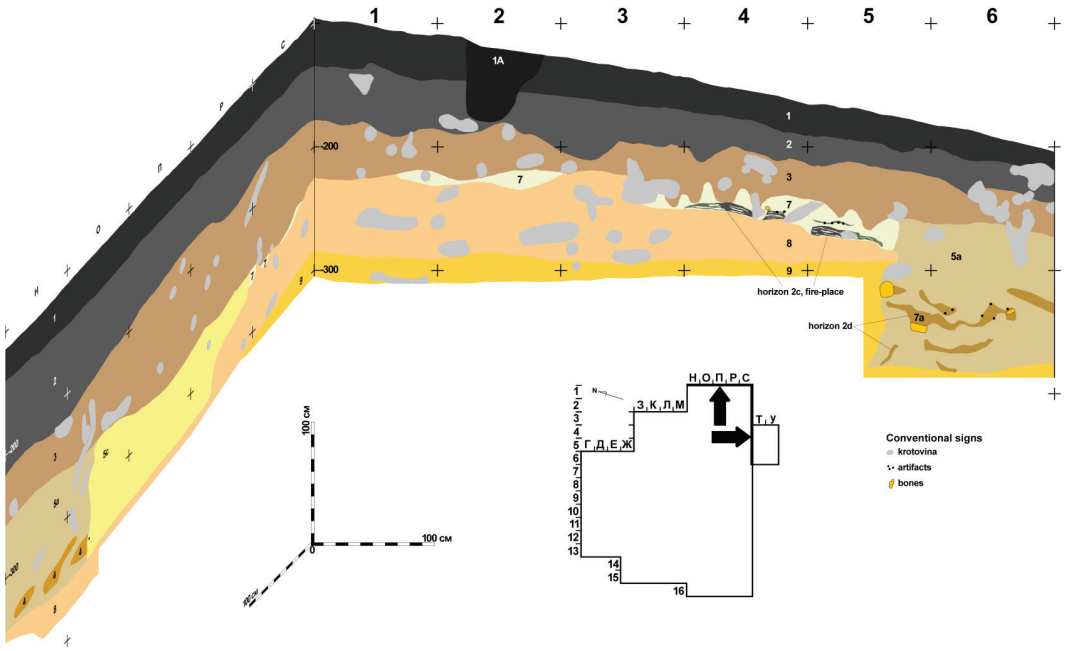


Fig. 2-5. Barmaky: stratigraphic sections along square lines С/Т and 0/1, cabinet projection.

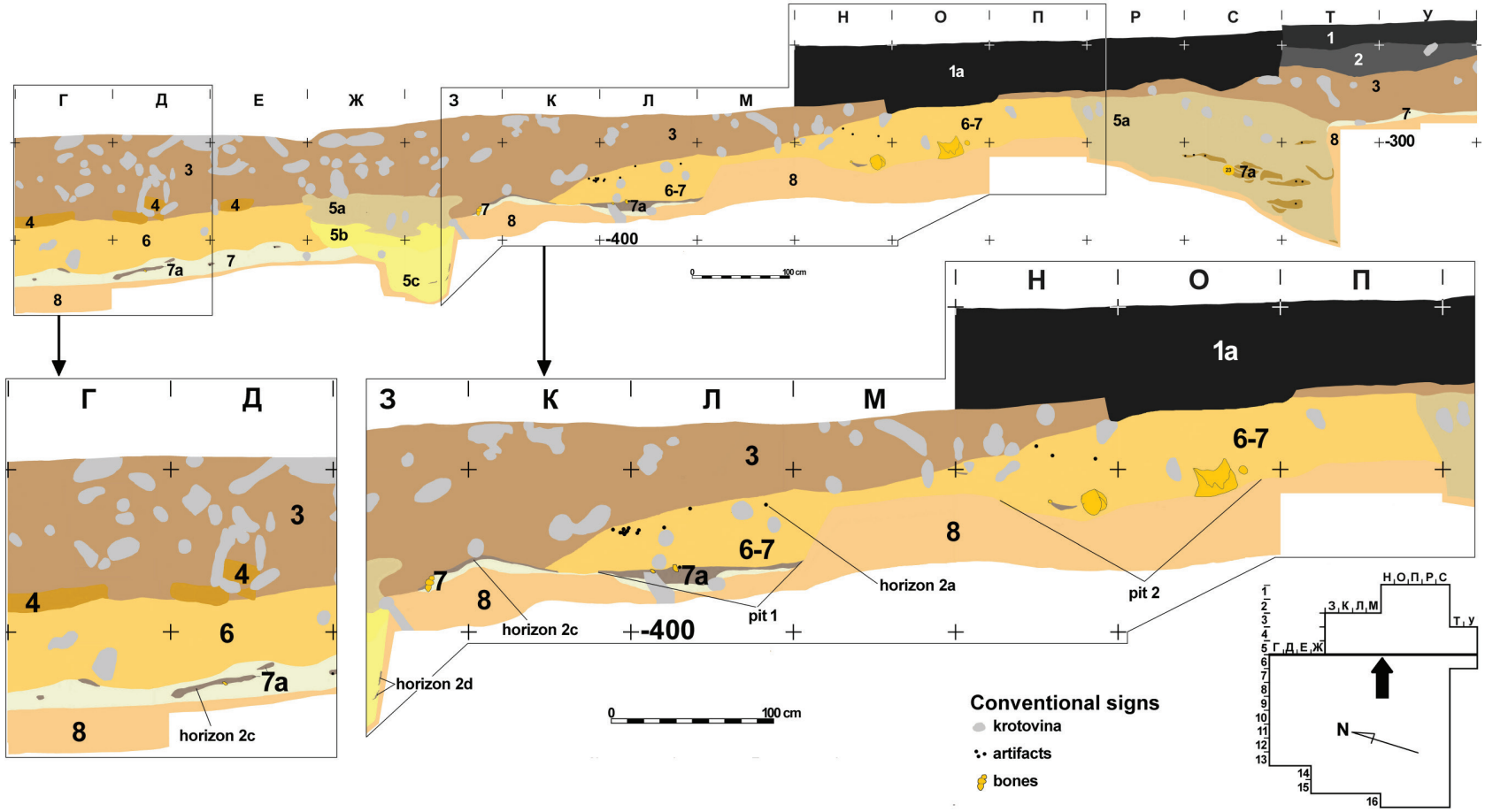


Fig. 2-6. Barmaky: stratigraphic section along square line 5/6.

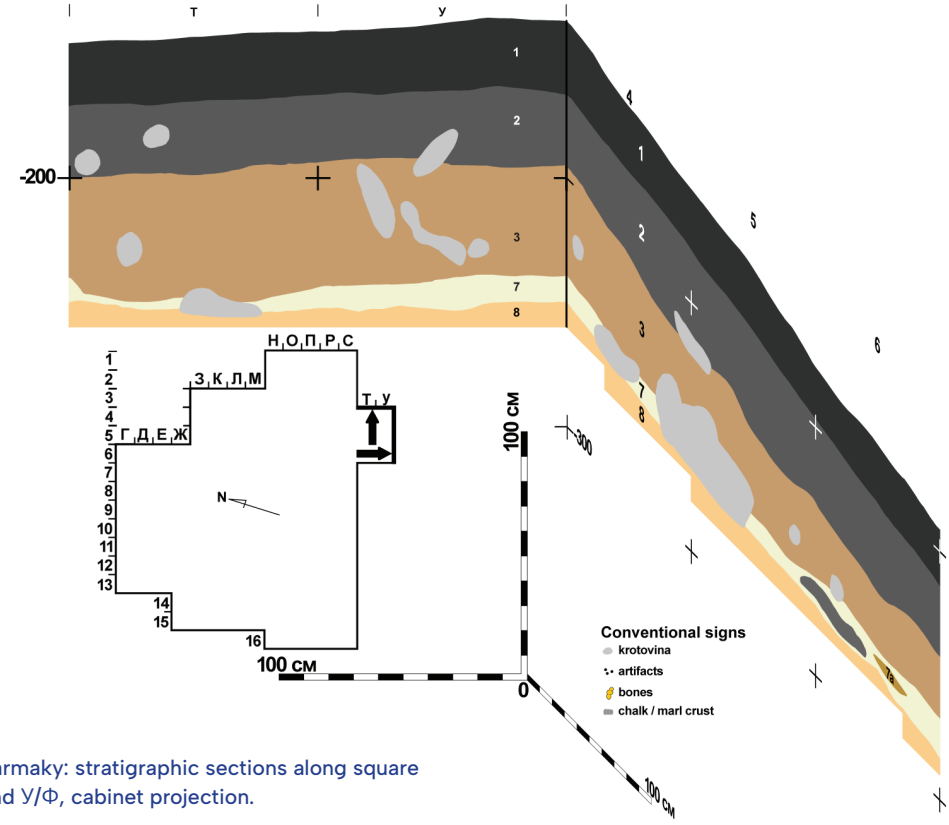


Fig. 2–7. Barmaky: stratigraphic sections along square lines 3/4 and У/Ф, cabinet projection.

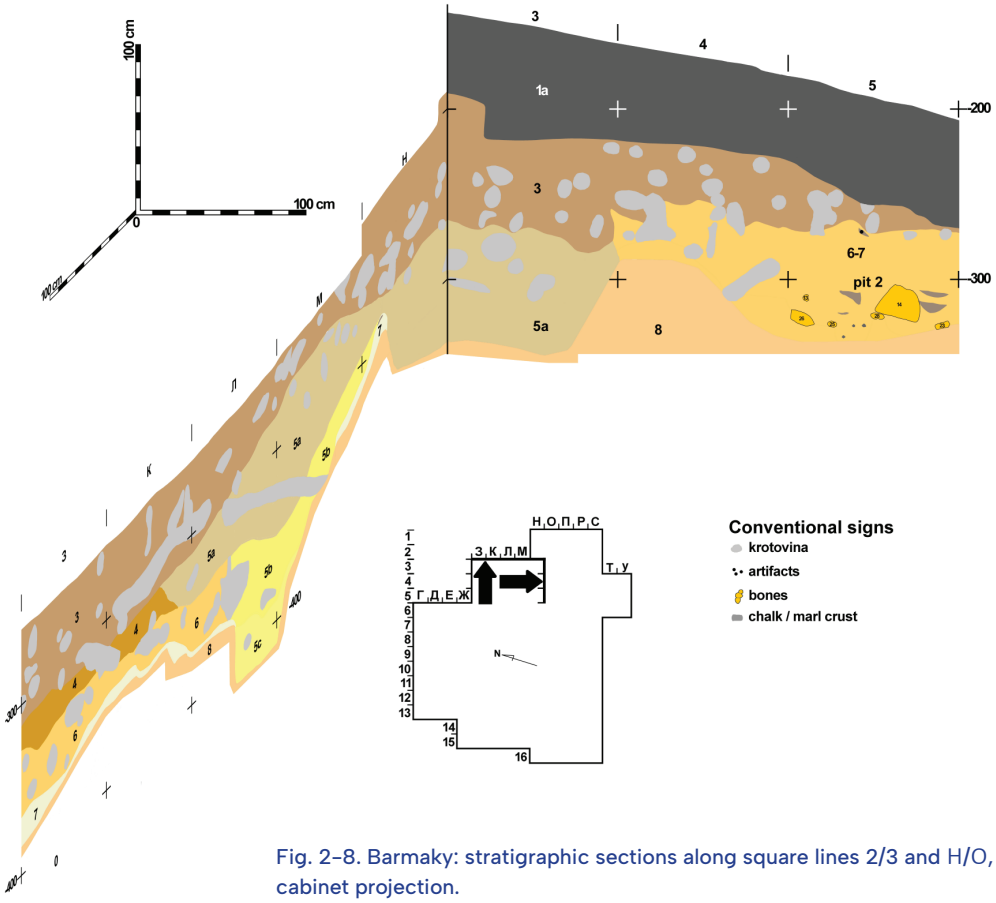


Fig. 2–8. Barmaky: stratigraphic sections along square lines 2/3 and Н/О, cabinet projection.

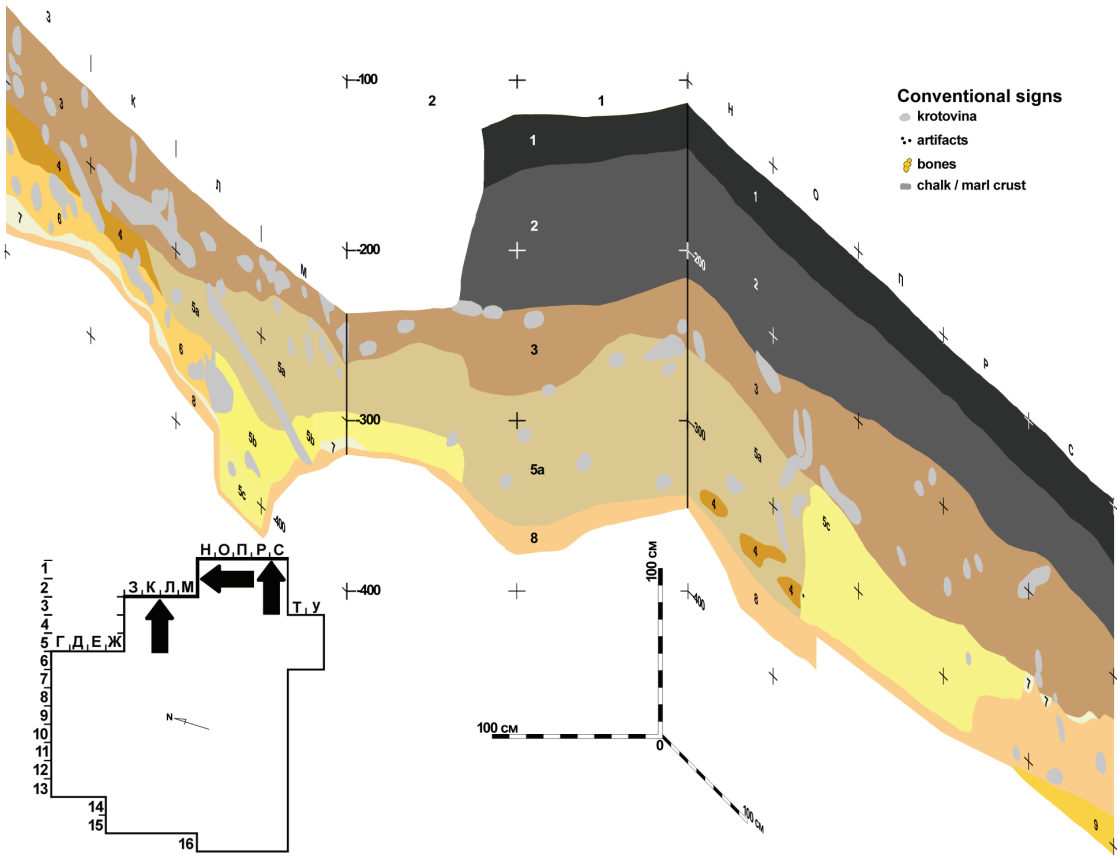


Fig. 2–9. Barmaky: stratigraphic sections along square lines 0/1, М/Н, and 2/3, cabinet projection.

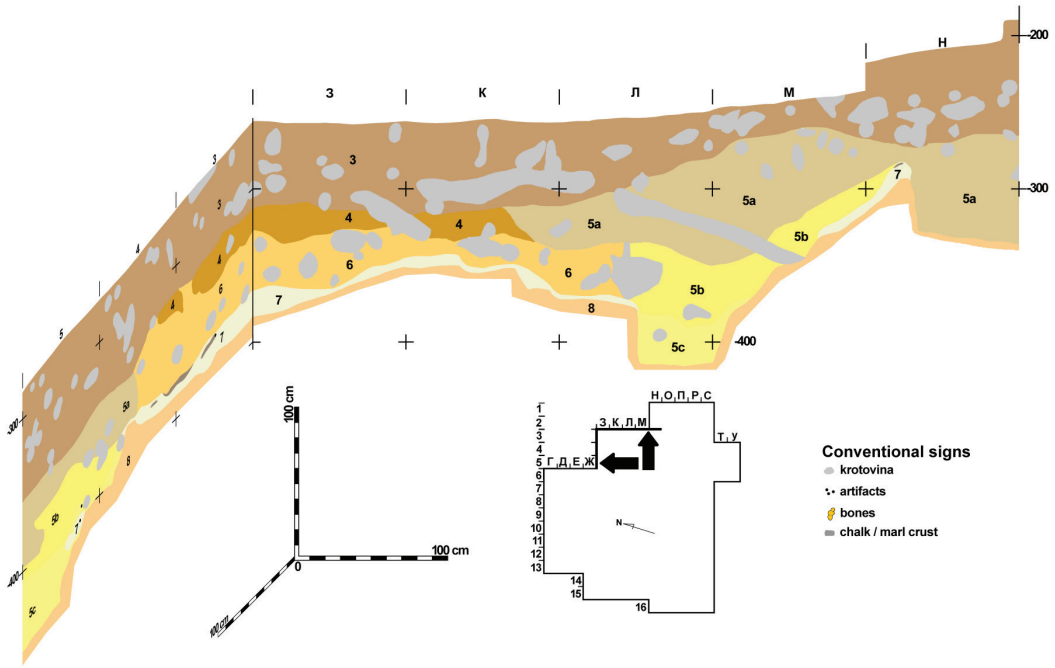


Fig. 2–10. Barmaky: stratigraphic sections along square lines 2/3 and Ж/З, cabinet projection.

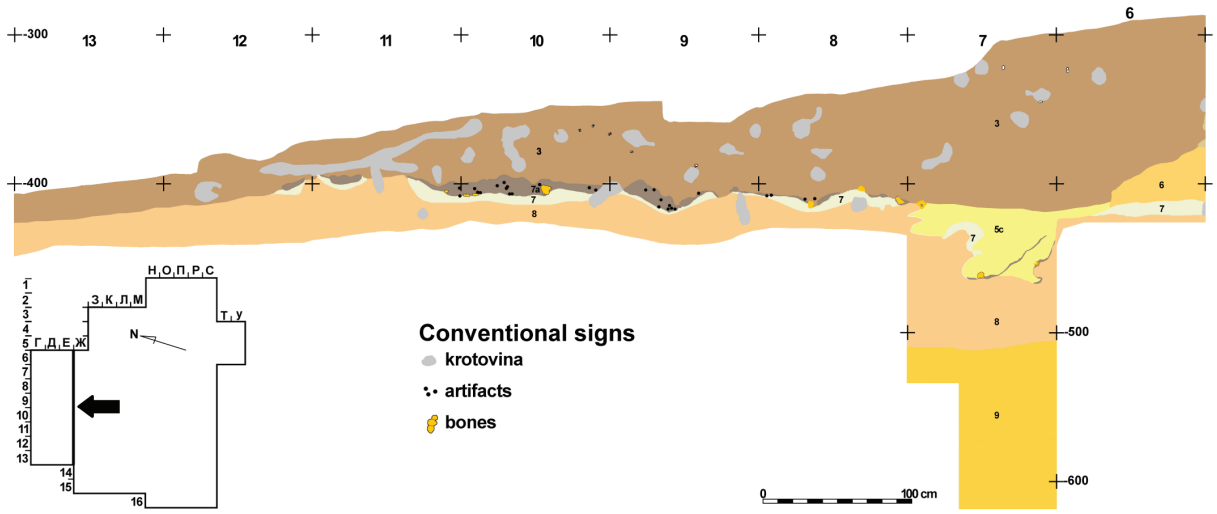


Fig. 2-11. Barmaky: stratigraphic section along square lines Е/Ж.

**Layers 5a, 5b, and 5c** – light greyish 5a (2.5Y, 7/2), yellowish 5b (2.5Y, 7/4), and light-yellowish 5c (2.5Y, 6/4) silty-loess sediments; striated and loose sediment structures; clumpy when dry; represent the filling of permafrost depression channels; the upper boundaries are gradual; the lower boundary is clear; the maximum thickness found in the eastern part of the excavated area in the section along the line of squares С/Т is up to 1.4 m; the difference in colour between layers 5a, 5b, and 5c reflect the local condition of depression channels filling; it is impossible to establish the order of layers 5a, 5b, and 5c accumulation, since these lenses with bones and artefacts originated separately in the sediments of the permafrost depression except for the westernmost part, where they are absent (Fig. 2-4—2-6; 2-8; 2-9—2-13); the studied depression channels are part of a bigger polygonal permafrost system.

**Layer 6** – dark yellow (10YR, 6/6) silty-loess; compact; spread over the entire excavated area, except the westernmost and easternmost square lines; contains carbonate concretions – *beloglazka*; the upper boundaries in contact with lithological layers 3 and 4 are gradual and clear, respectively; on squares 6Е, 7Д, 8Г, 8Д, and 9Г, lithological layer 6 is truncated by the fillings of erosional depression channels (layers 3, 5a, 5b, 5c); on squares 3М, 3Н, 4Л, 4М, 4Н, 4О, 5К, 5Л, 5М, 5Н, 5О, 5П, 6К, 6Л, 6Н, 6О, and 6П, this layer was probably removed by past anthropogenic activity; the maximum thickness is up to 0.57 m (Fig. 2-4; 2-6; 2-8—2-11).

**Layer 6-7** – yellow (10YR, 8/6) silty-loess sediments; loose; found in the eastern part of the excavated area on squares 3М, 3Н, 4Л, 4М, 4Н, 4О, 5К, 5Л, 5М, 5Н, 5О, 5П, 6К, 6Л, 6Н, 6О, and 6П, above and around pits 1 and 2; contains bone fragments, flint artefacts, and lenses of brownish sediments; the upper boundaries in contact with lithological layers 1 and 3 are clear and gradual, respectively; the lower boundary with the lithological layers 8, 7, and 7a are clear; the northern and southern parts of lithological layer 6-7 are truncated by the filling of the permafrost depression channels; the western part was excavated in 1990; the available profiles exhibit a mound-like sections of this lithological layer; the maximum thickness is about 0.6 m (Fig. 2-6; 2-8; 2-14).

**Layer 7** – whitish (7.5YR, 7/1) silty-loess sediment; discontinuously spread nearly all over the excavated area; compact; truncated by fillings of permafrost depression; constitute the filling of permafrost depression channels; the upper and lower boundaries are wavy and clear; the maximum thickness is about 0.25 m (Fig. 2-4—2-11).

**Layer 7a** – brownish (7.5YR, 3/3) silty loess in the western area and greyish (10YR, 5/2) silty loess in the eastern area; compact; found inside and sometimes above the whitish sediments of lithological layer 7 and in the filling of permafrost depression channels and pit 2; in channels and pit 2, the sediments of 7a accumulated as small, thin, often vertically located lenses of

brown silty loess; contain flint artefacts, faunal remains, burnt material, lenses of chalk/marl crust, ochre pieces, and powder, as well as thin whitish/yellowish lenses of solifluction origin (Fig. 2-15, *1*); the upper and lower boundaries are both wavy and clear; truncated by fillings of the permafrost depression channels; the maximum thickness is about 0.15 m; the deposits of 7a were covered by the chalk/marl crust in the squares 4К, 4Л, 4М, 5Л, 5М, 5У, 6У (Fig. 2-4—2-8; 2-10—2-15); lithological layer 7a is the *coloured* part of lithological layer 7.

**Layer 8** – pale-yellow (2.5Y, 8/3) silty-loess; spread all over the excavated area; compact; striated; the upper boundary is clear; the maximum thickness is about 0.7 m; the upper and lower boundaries on square lines 1, 2, 3, 4, and partly 5 are more or less horizontal, while on the square lines 6 through 13, the boundaries of layer 8 exhibit an inclination angle of 3-4° (Fig. 2-4—2-14).

**Layer 9** – pale-yellow (2.5Y, 8/3) silty-loess; spread all over the excavated area; compact; intensively striated; the upper boundary is unclear; the studied thickness is more than 1.8 m (Fig. 2-5; 2-9; 2-11).

The stratigraphic sequences in sondages 1-4 are not as complex as in the 1982-2020 excavation area. The Holocene sediments are represented by equivalents of layers 1 and 2 in the main excavation area. The Pleistocene sediments are recognised as dark yellow (10YR, 6/6) silty-loess, which is supposed to be the analogy of the lithological layer 6 from the 1982-2020 excavation area (Fig. 2-16, *1*). No archaeological material was found in sondages 1 and 2. One bone fragment originates from sondage 3. About 20 bone fragments and 419 flint artefacts formed the vertically and horizontally compact lens on squares L-32 and L-33 in sondage 4 (Fig. 2-16, *2*) (Vasyliev et al. 2019: 6-9). The archaeological material from sondages 3 and 4 is associated with the deposits of lithological layer 6.

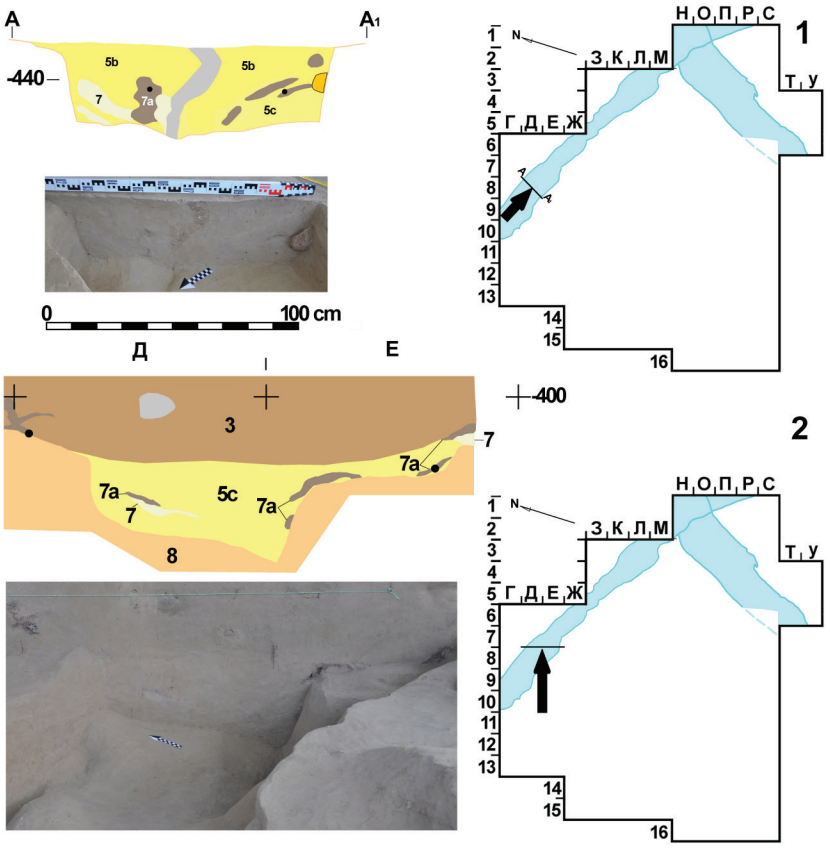


Fig. 2-12. Barmaky, permafrost depression channels:
1 – square 8Д, section;
2 – section along square line 7/8.

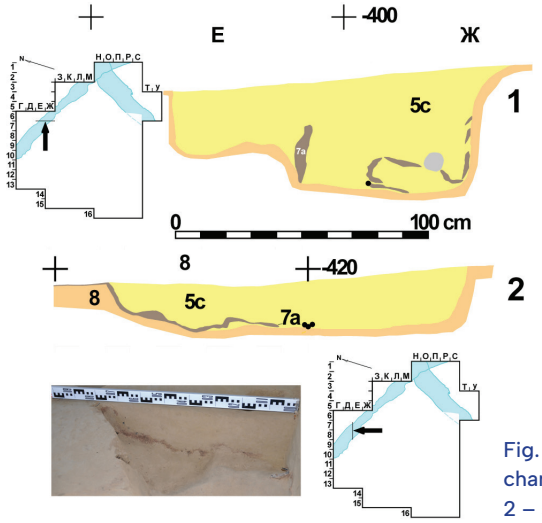


Fig. 2-13. Barmaky, permafrost depression channels: 1 – section along square line 6/7; 2 – section along square line Д/Е.

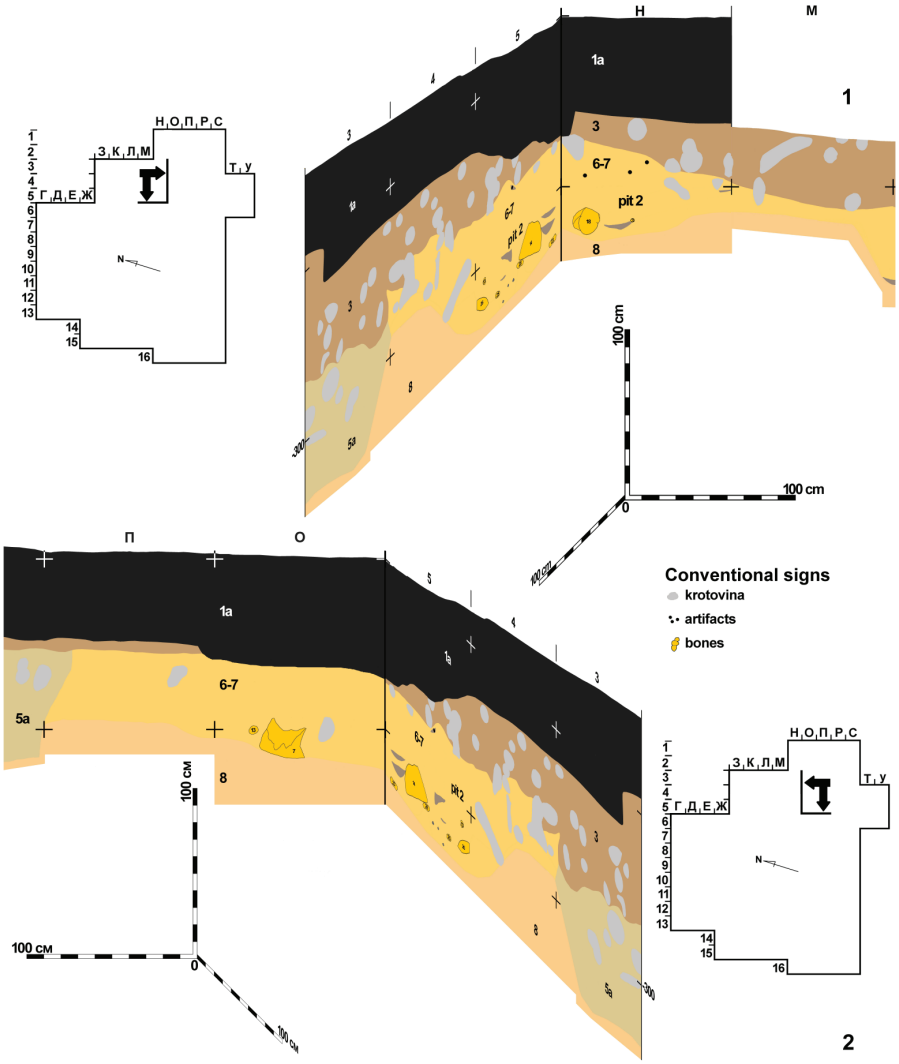


Fig. 2-14. Barmaky, pit 2, stratigraphic sections along square lines 5/6 and Н/О, cabinet projections: 1 –view from the north; 2 –view from the south.

1

2

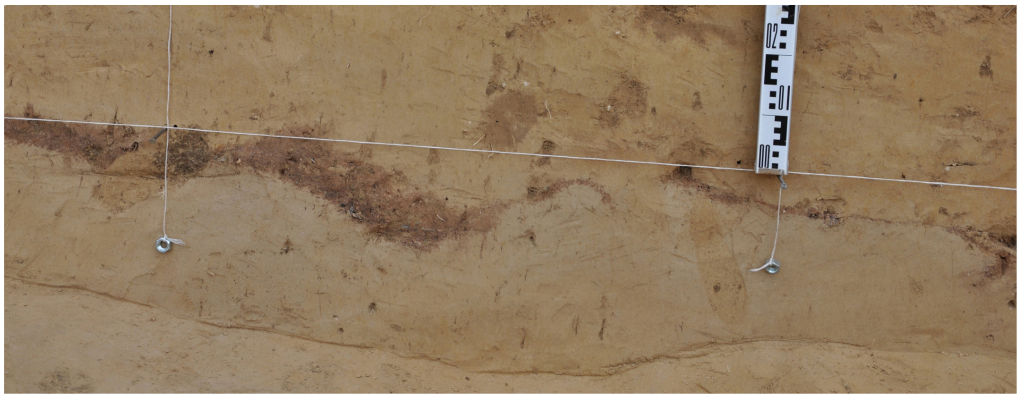

3

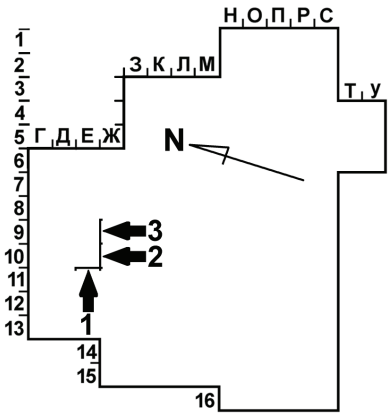


Fig. 2–15. Barmaky, lithological layer 7a:
1 – section along square line 10Е/11Е;
2 – section along square line 10Е/10Ж;
3 – section along square line 9Е/9Ж.

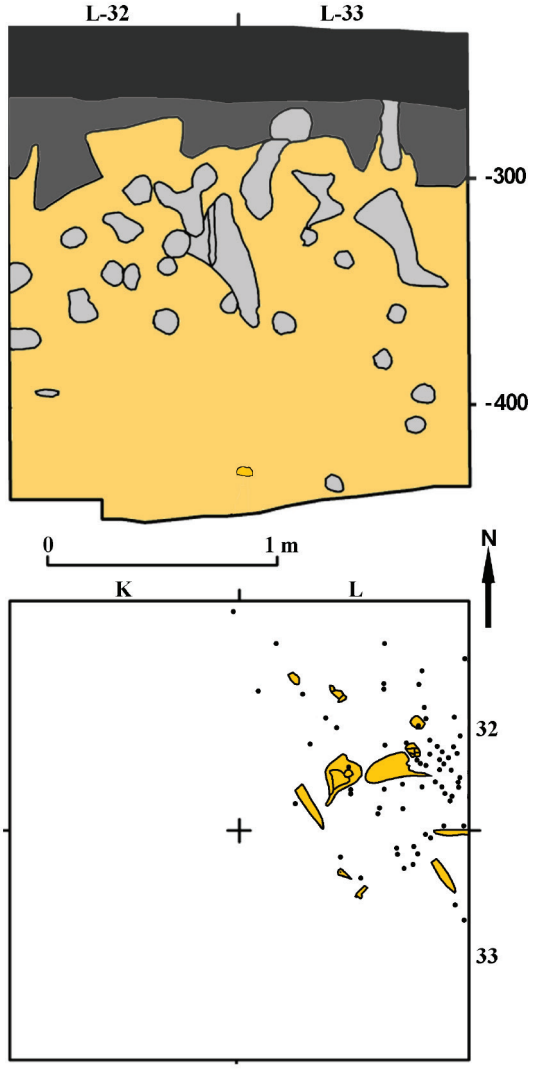


Fig. 2-16. Barmaky, sondage 4: 1 – section along the square line L/M; 2 – plan of archaeological horizon.

## THE ARCHAEOLOGICAL SEQUENCE

The artefacts of the 1st archaeological level originate from the 3rd lithological layer. Archaeological level 2 is subdivided into several horizons: 2a, 2a1, 2b, 2c, and 2d. Horizon 2a was found in the deposits of lithological layer 6–7. The finds from the marl crust, which is accumulated on lithological layer 7, were defined as archaeological horizon 2b. The finds from lithological layers 7 and 7a compose the material of archaeological horizon 2c. The material from permafrost depression channels (lithological layers 5a, 5b, 5c) was labelled as archaeological horizon 2d.

The analysis of the lithological inclination angles suggests that the occupations of Barmaky, level 2, accumulated both at the top (squares 1H–1C, 2H–2C, 3M–3C, 4Л–4У, 5К–5У) and the upper slope (square lines 6–13) of the hill (Fig. 2-2, *2*).

**Archaeological level 1** contains a small number of flint artefacts and a few bone fragments, which originate from lithological layer 3. There are two separate concentrations of archaeological material. The eastern concentration originates from squares 3P, 4C, and 5C (Fig. 2-17). It contains no bones and the artefacts amount to about 40 pieces (see Chapter 6). The artefacts are distributed relatively compactly on a horizontal surface of less than one square meter. Their dominant position and orientation were not recorded. The difference between the depths of neighbouring pieces constitutes no more than 6 cm. It cannot be excluded that the eastern concentration of level 1 is indeed the upper part of the underlying level 2. Alternatively, roots might have caused the relocation of sediments from lithological layer 3 into the lower deposits.

The western concentration of flint artefacts was studied on square lines 7–13 (Fig. 2-18). The maximum difference in depth of neighbouring artefacts reaches up to 0.6 m. In the western area, layer 1 was excavated by four artificial horizons with no sterile sediments between them. About seven hundred artefacts and a few bones originate from the western concentration of level 1. About five hundred artefacts were found in the lowest artificial horizon, in contact with lithological layer 7a (see Chapter 9). They do not form compact horizontal lenses, but are rather evenly distributed over the entire thickness of the 3 lithological layer. There is no dominant orientation of artefacts, but vertical and oblique positions prevail over horizontally placed pieces. In squares 8E and 12E, the artefacts of level 1 originate from clearly visible krotovinas. The western concentration of artefacts thus accumulated in lithological layer 3 likely as a result of a partial destruction of the artefact-bearing lithological layer 7 by both erosion and bioturbation processes, resulting in horizontal and vertical transportation and redeposition of artefacts and eventually the formation of level 1.

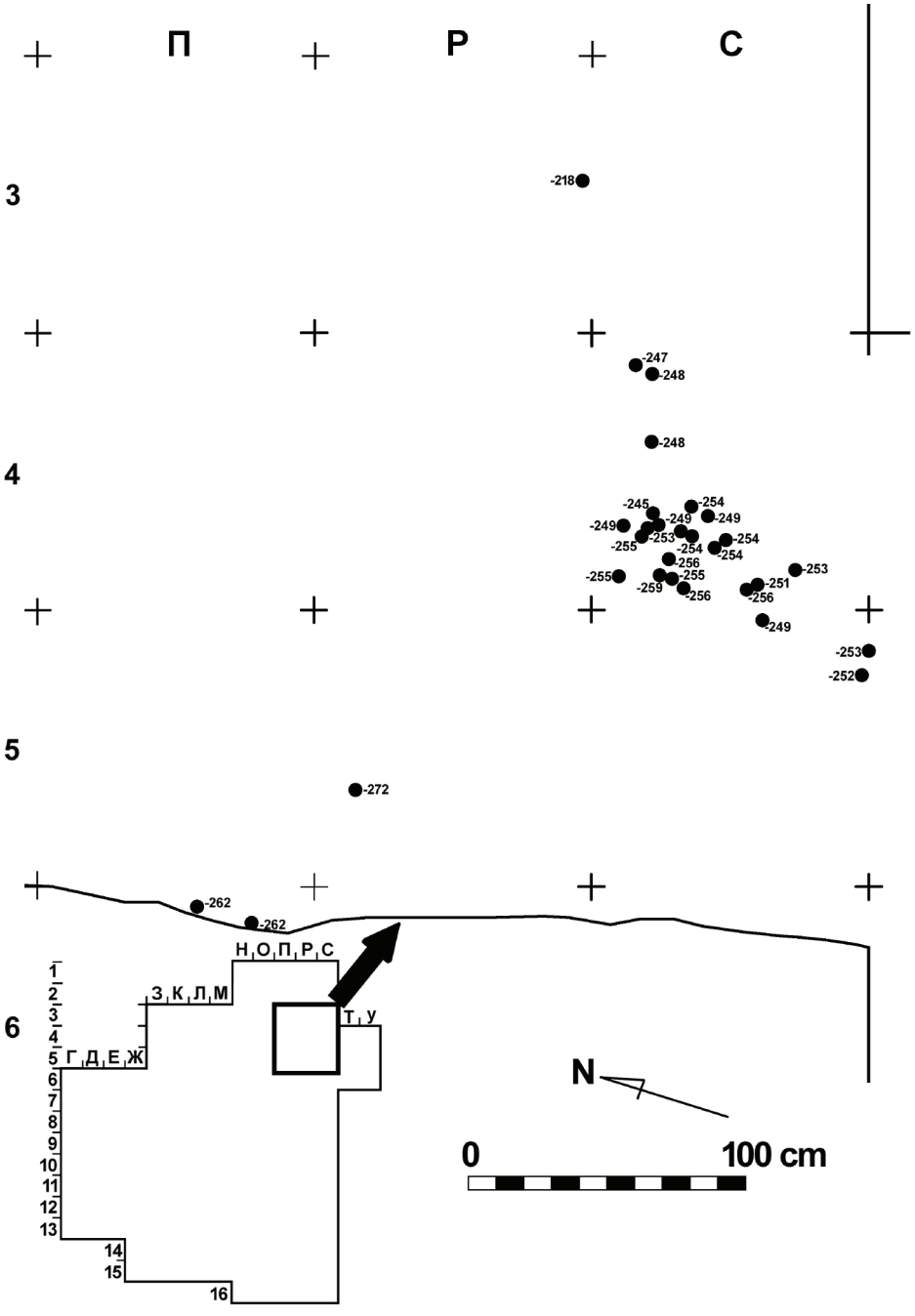


Fig. 2–17. Barmaky, eastern area, level 1: distribution of artefacts.

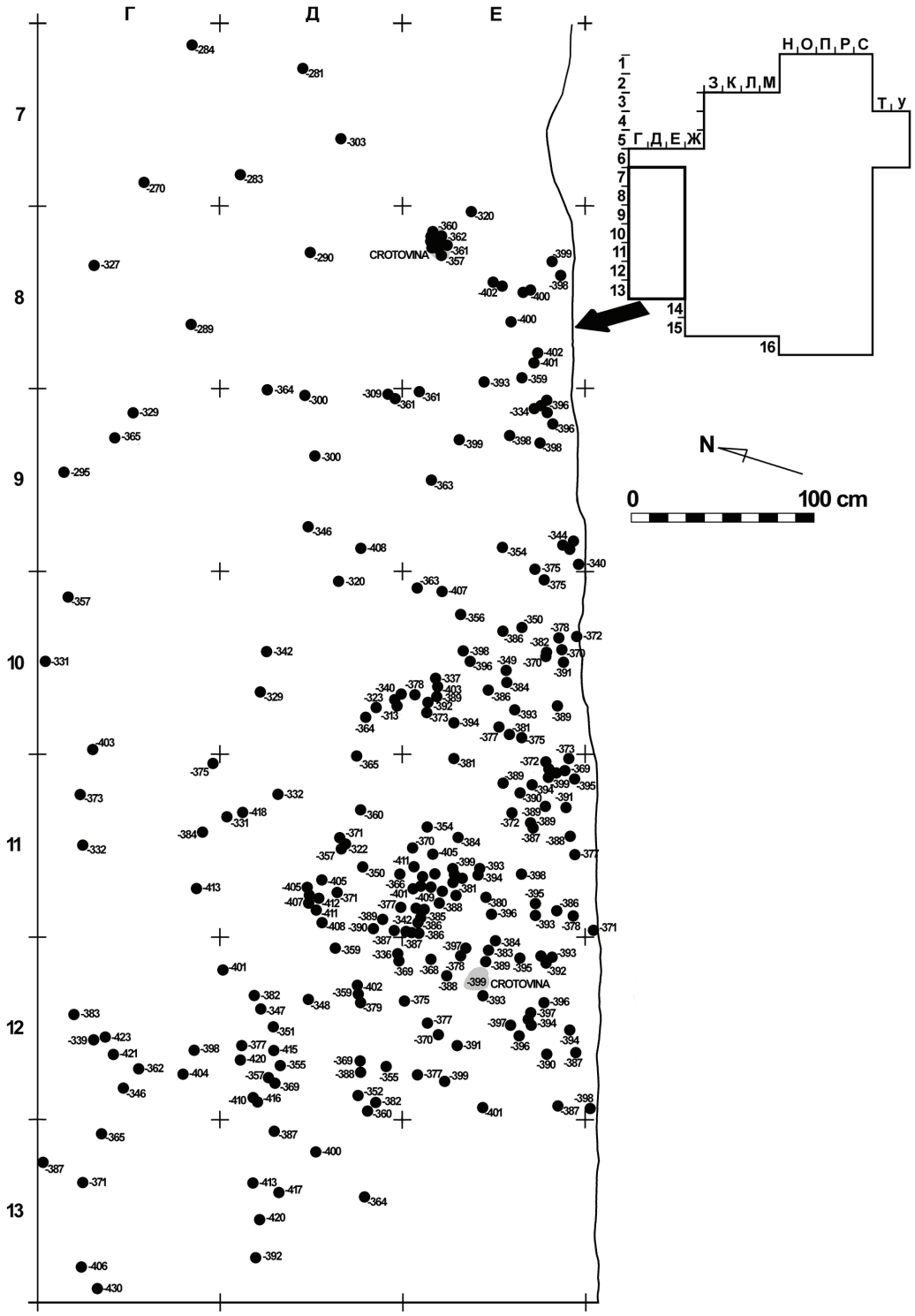


Fig. 2–18. Barmaky, western area, level 1: distribution of artefacts.

**The archaeological horizon 2a** as well as the sediments of lithological layer 6–7 are found on a limited area above and around pits 1 and 2, that is, at about 17 m2, in squares 3М, 3Н, 4Л, 4М, 4Н, 4О, 5К, 5Л, 5М, 5Н, 5О, 5П, 6К, 6Л, 6Н, 6О, 6П.

6,637 flint artefacts, 55 bone fragments, 6 perforated shells, one bone needle, small pieces of ochre, chalk/marl, and sandstone originate from horizon 2a. The main concentrations of bones and artefacts from horizon 2a are situated strictly above pit 2 (Fig. 2–19, *1, 3*). Conspicuously, layer 6–7 shows a dome-like depositional structure (Fig. 2–6; 2–8; 2–14). More than half of the artefacts originate from squares 4Н, 5Н, and 5О. The largest variations of artefact depths (0.49–0.28 m) are found in squares 4О, 5О, 6Н, and 6О, which are associated with the supposed centre of the mound. The obliquely positioned and north–south oriented artefacts are dominant (Tables 2–1; 2–2; Fig. 2–20, *1, 2*). The same is true for bone positions and orientations (Tables 2–3; 2–4; Fig. 2–19, *1*). The ochre concentrations and bones in anatomical order were not recognised. A few burnt flint artefacts do not form clear vertical and horizontal concentrations. The burnt bones are absent.

There is possible evidence for the construction of a kind of cover over the deepened pit structures, namely the topography of the site with the dome-like cross-section of the lithological layer 6–7 and the position of artefacts above pit 2. The presence of artefacts, bone fragments, and brownish lenses within layer 6–7 suggests that cultural deposits were already present before pit 2 was dug, and the absence of lithological layers 6, 7, and 7a around pit 2 suggests that its immediate surrounding was the main source of sediments for the mentioned cover.

Most likely, the archaeological layer 1 defined by V. Piasetsky in 1990 is horizon 2a of the last field campaigns (see Chapter 1, this volume).

**The archaeological horizon 2a1** takes the form of a 1.5 m² wide and 0.1 m thick, vertically and horizontally compact lens of flint artefacts directly above pit 1 in squares 5К, 5Л, 6К, 6Л. This lens is separated by 0.1–0.15 m thick sterile sediments from both the above and below deposited finds of horizons 2a and 2c, respectively (Fig. 2–21, *3*). No bones but 229 lithic artefacts originate from this horizon. Nearly all of them were found on squares 5Л and 6Л. Obliquely positioned artefacts prevail over vertical and horizontal ones (Table 2–1; Fig. 2–21, *1*). The north–south orientation of artefacts is dominant (Table 2–2; Fig. 2–21, *2*). The small number of artefacts, however, limits the significance of this observation.

**The archaeological horizon 2ab** is unites finds from cleaning the cracks in the chalk/marl crust in squares 4Л, 4М, 5Л, and 5М and comprises 1 bladelet fragment, 4 pieces of unidentifiable débitage, and 123 chips.

**The archaeological horizon 2b** is composed of two concentrations of chalk/marl crust of probably anthropogenic origin. The largest concentration was found in squares 4К, 4Л, 4М, 5Л, and 5М (Fig. 2–22, *1*). It directly underlies the deposits of lithological layer 6–7 – archaeological horizon 2a – and overlies the brownish deposits of lithological layer 7a – archaeological horizon 2c – (Fig. 2–22, *3*). The stratigraphic relation between archaeological horizons 2a1 and 2b is unclear because of a lack of direct contact. Due to the post-depositional permafrost degradation process, the chalk/marl crust was partly affected by vertical translocation (Fig. 2–22, *2*). Five bone fragments and 276 flint artefacts originate from this crust with a dominantly north–south orientation and oblique position (Tables 2–1—2–4).

The second chalk/marl crust is found in squares 5У and 6У in the deposits of lithological layer 7 (Fig. 2–23, *1, 3*). A direct connection between this crust and the coloured sediments of lithological layer 7a was not observed (Fig. 2–23, *2*). No lithic artefacts or fauna are related to the crust on squares 5У and 6У.

**The archaeological horizon 2c** accumulated in lithological layer 7a, which is the brownish/greyish lens inside lithological layer 7. Lithological layer 7a has been documented in two spatially distinct areas in the western (35 m2) and eastern (19 m2) parts of the site. The colour in the western area is more brownish, while in the eastern area, it is more greyish. The border between these two areas roughly runs through squares 3М, 4М, and 5М (Fig. 2–24). Unfortunately, due to the post-depositional cryoturbation processes and, probably, due to the anthropogenic digging activity during the

| | 2a | 2a1 | 2b | 2c, WA | 2c, pit 1, WA | 2d, WA | 2c, EA | 2c, EA, ash | 2c, EA, hearth | 2d, EA | pit 2 |
|---|---|---|---|---|---|---|---|---|---|---|---|
| Vertical | 17,42 | 24,44 | 20,69 | 19,97 | 5,29 | 30,38 | 16,44 | 8,89 | 7,66 | 19,37 | 17,62 |
| Horizontal | 32,16 | 31,11 | 13,79 | 34,71 | 62,50 | 14,59 | 24,83 | 37,78 | 31,75 | 13,67 | 23,14 |
| Oblique | 50,42 | 44,45 | 65,52 | 45,32 | 32,21 | 55,03 | 58,73 | 53,33 | 60,59 | 66,96 | 59,24 |
| **TOTAL:** | 100,00 | 100,00 | 100,00 | 100,00 | 100,00 | 100,00 | 100,00 | 100,00 | 100,00 | 100,00 | 100,00 |

Table 2–1. Barmaky, level 2, by horizons and objects: artefact positions, as percentages.

| | 2a | 2a1 | 2b | 2c, WA | 2c, pit 1, WA | 2d, WA | 2c, EA | 2c, EA, ash | 2c, EA, hearth | 2d, EA | pit 2 |
|---|---|---|---|---|---|---|---|---|---|---|---|
| NS | 61,11 | 76,92 | 29,41 | 45,50 | 59,46 | 45,27 | 50,00 | 51,82 | 46,26 | 56,12 | 44,90 |
| EW | 38,89 | 23,08 | 70,59 | 54,50 | 40,54 | 54,73 | 50,00 | 48,18 | 53,74 | 43,88 | 55,10 |
| **TOTAL:** | 100,00 | 100,00 | 100,00 | 100,00 | 100,00 | 100,00 | 100,00 | 100,00 | 100,00 | 100,00 | 100,00 |

Table 2–2. Barmaky, level 2, by horizons and objects: artefact orientations, as percentages.

| | 2a | 2b | 2c, WA | 2c, pit 1, WA | 2d, WA | 2c, EA | 2c, ash, EA | 2c, hearth, EA | 2d, EA | pit 2 |
|---|---|---|---|---|---|---|---|---|---|---|
| Vertical | 11,11 | – | 5,14 | 3,23 | 13,12 | 11,11 | – | 5,56 | 5,19 | 4,40 |
| Horizontal | 38,89 | 20,00 | 50,00 | 61,29 | 19,38 | 33,33 | 37,50 | 38,88 | 18,19 | 36,26 |
| Oblique | 50,00 | 80,00 | 44,86 | 35,48 | 67,50 | 55,56 | 62,50 | 55,56 | 76,62 | 59,34 |
| **TOTAL:** | 100,00 | 100,00 | 100,00 | 100,00 | 100,00 | 100,00 | 100,00 | 100,00 | 100,00 | 100,00 |

Table 2–3. Barmaky, level 2, by horizons and objects: faunal remains positions, as percentages.

| | 2a | 2b | 2c, WA | 2c, pit 1, WA | 2d, WA | 2c, EA | 2c, ash, EA | 2c, hearth, EA | 2d, EA | pit 2 |
|---|---|---|---|---|---|---|---|---|---|---|
| NS | 60,00 | 60,00 | 39,62 | 56,00 | 42,61 | 80,00 | 73,68 | 50,00 | 57,50 | 43,75 |
| EW | 40,00 | 40,00 | 60,38 | 44,00 | 57,39 | 20,00 | 26,32 | 50,00 | 42,50 | 56,25 |
| **TOTAL:** | 100,00 | 100,00 | 100,00 | 100,00 | 100,00 | 100,00 | 100,00 | 100,00 | 100,00 | 100,00 |

Table 2–4. Barmaky, level 2, by horizons and objects: faunal remains orientations, as percentages.

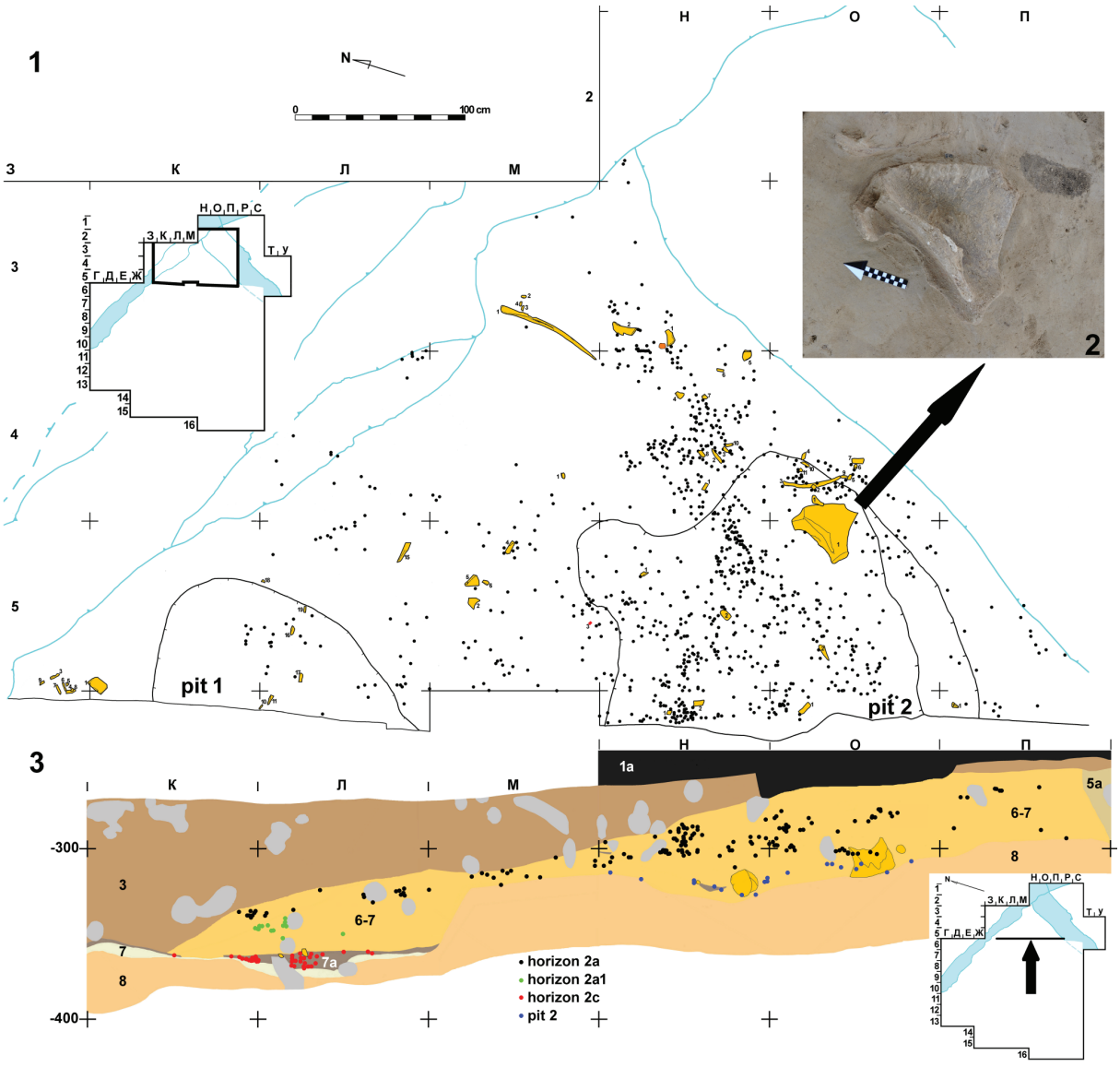


Fig. 2-19. Barmaky, archaeological horizon 2a: 1 – distribution of artefacts and bones; 2 – mammoth scapula on squares 4O and 5O; 3 – profile along square line 5/6 showing the vertical distribution of artefacts of the archaeological horizons 2a, 2a1, 2c, and pit 2.

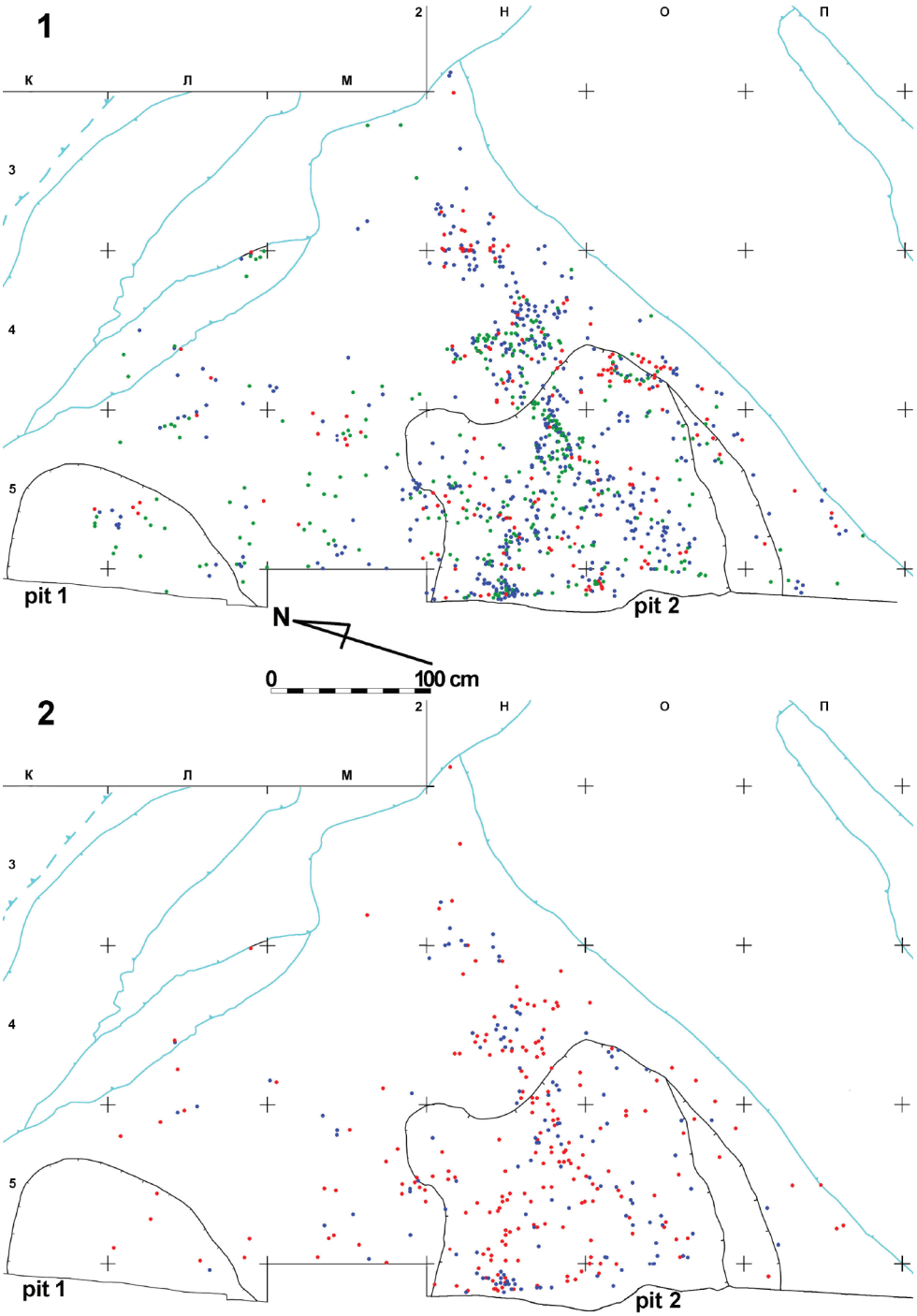


Fig. 2–20. Barmaky, archaeological horizon 2a: 1 –position of artefacts, green dots – horizontal, red dots – vertical, blue dots – oblique; 2 – orientation of artefacts, red dots – north–south, blue dots – east–west.

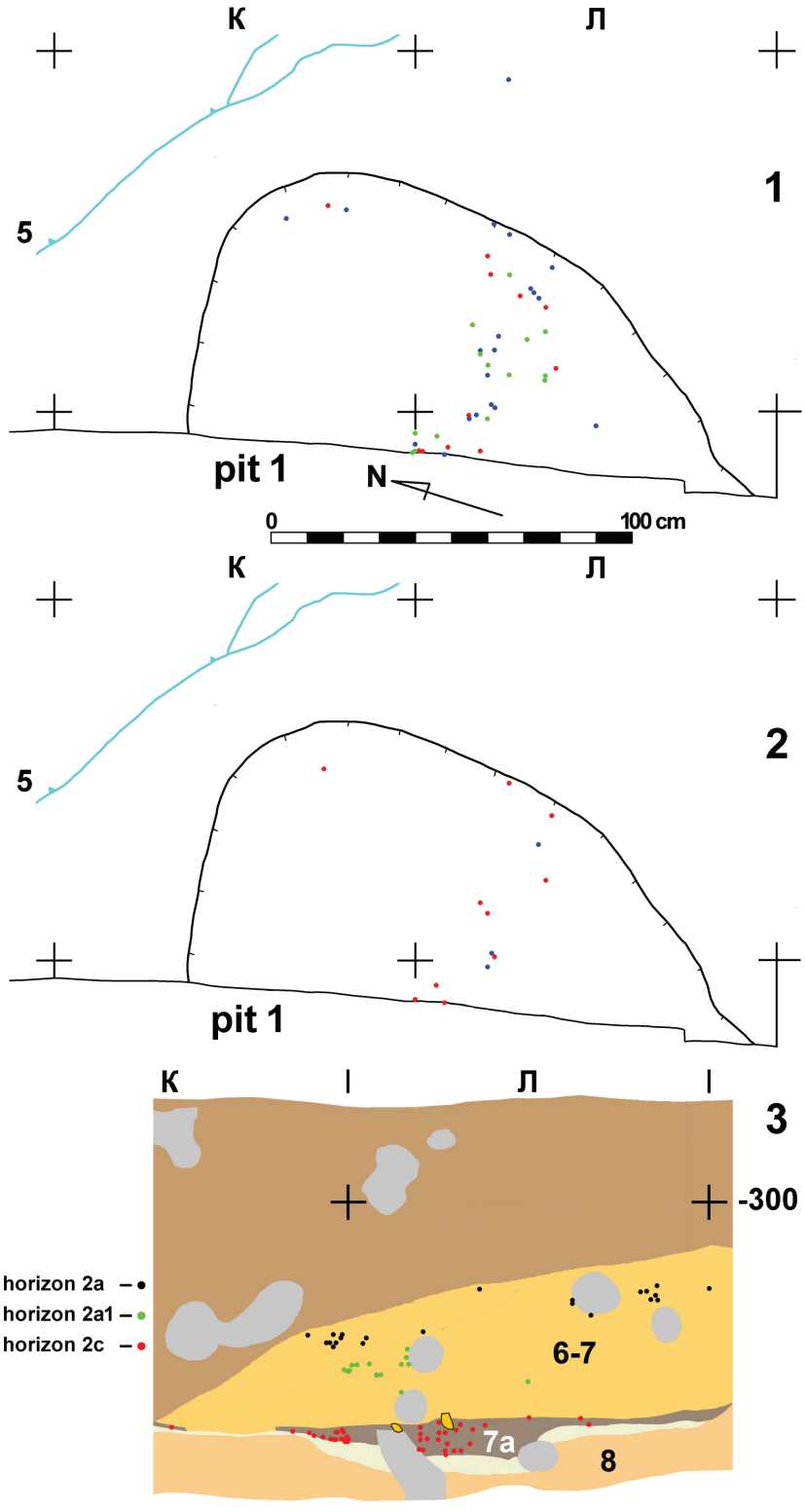


Fig. 2–21. Barmaky, archaeological horizon 2a1: 1 – position of artefacts, green dots – horizontal, red dots – vertical, blue dots – oblique; 2 – orientation of artefacts, red dots – north–south, blue dots – east–west; 3 – stratigraphic position of archaeological horizons 2a, 2a1, and 2c in pit 1.

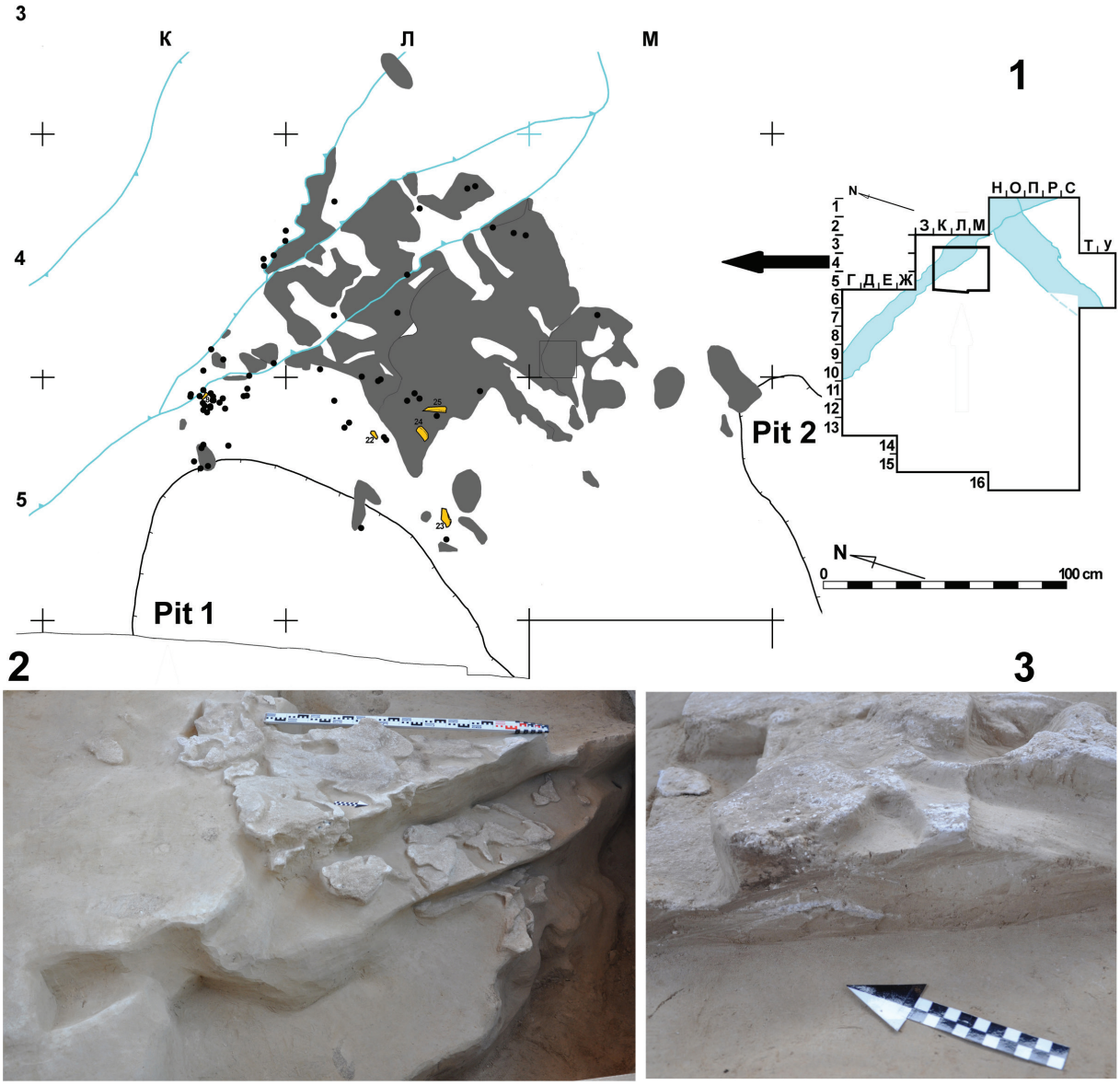


Fig. 2–22. Barmaky, archaeological horizon 2b, squares 4К, 4Л, 4М, 5Л, 5М: 1 – chalk/marl crust and association with its flint and faunal materials; 2 – chalk/ marl crust, partly vertically translocated into a permafrost depression channel; 3 – section on square line 4М/5М showing the chalk/marl crust and underlying brownish sediments of lithological layer 7a.

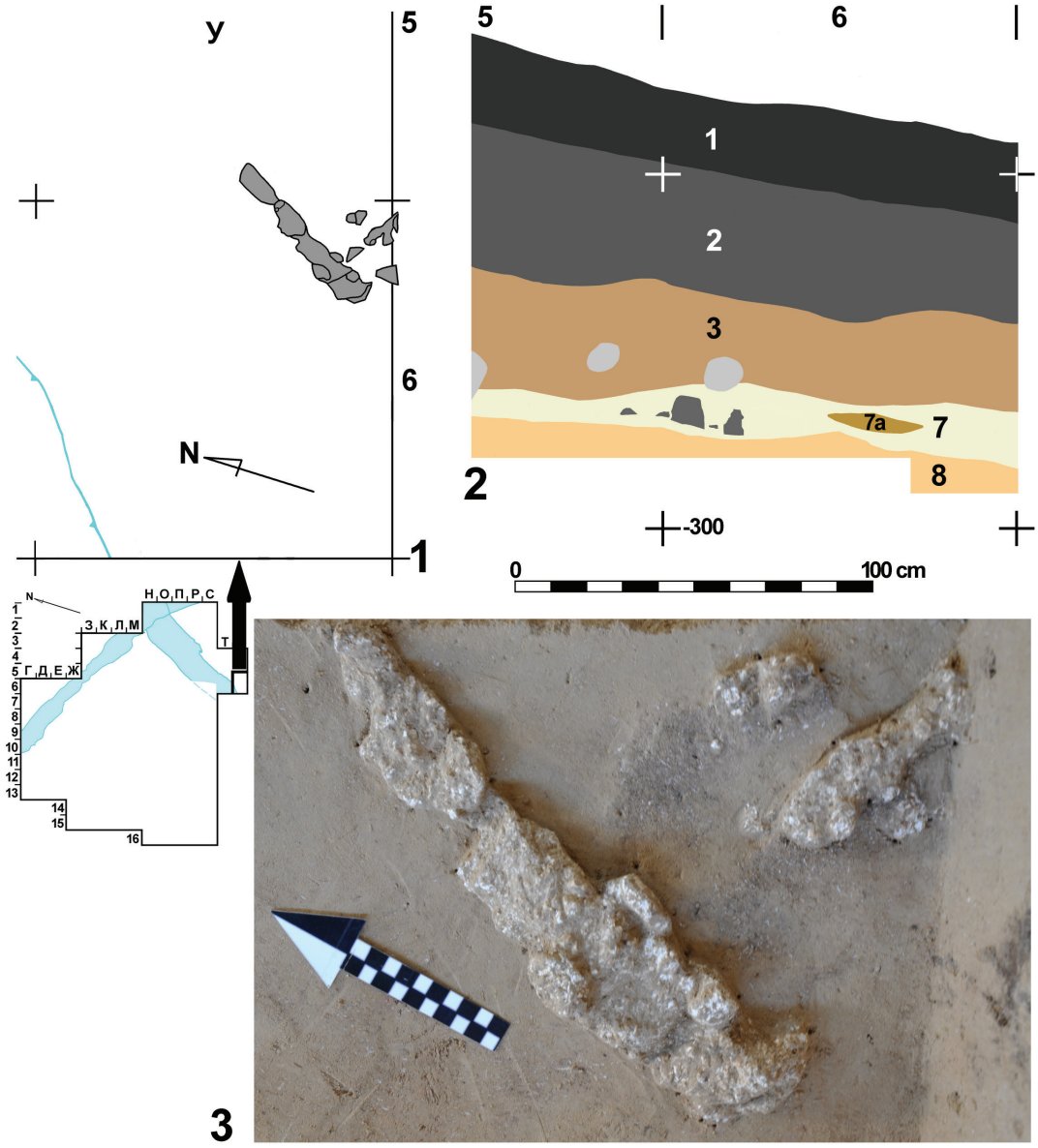


Fig. 2-23. Barmaky, archaeological horizon 2b, squares 5У and 6У: 1 – chalk/marl crust; 2 – section along the square line 5У/5Ф, 6У/6Ф showing the stratigraphic position of the chalk/marl crust; 3 – view of the chalk/marl crust.

formation of the site, direct stratigraphic contact between the two areas was not found. These areas are characterised by both continuous and patchy distribution of brownish/greyish sediments of layer 7a and whitish sediments of layer 7. The same is true for the depositional characteristics of archaeological horizon 2c. Its surface is wavy and truncated by permafrost depression channels. In addition, solifluction processes affected the deposits of horizon 2c (Fig. 2-15, *1*). The thickness of archaeological horizon 2c is up to 0.12 m (Fig. 2-15, *2, 3*).

A hearth surrounded by ashy sediment is found in the eastern area, while pit 1 relates to the western area. Despite the presence of a hearth, there is no evidence of intensive use of fire in the rest of the site and burnt materials are relatively rare. The few burnt flint artefacts and bones are of brownish colours and the surfaces are without visible traces of fire destruction. Most pieces of burnt material originate from those squares which also have the largest concentrations of unburnt lithics and bones.

The number of artefacts in the western and eastern areas of horizon 2c comprise 71,326 and 4,317 pieces, respectively (see Chapter 6), while the number of bone fragments amounts to 521 in the west and 52 in the east. The number of artefacts in the most densely packed squares (sq. 9E) is up to 14,000 items. In the western area, four worked tusks, 9 ochre pieces, 21 pieces of chalk/marl, and 199 perforated and non-perforated fossil marine shells, add to the finds of horizon 2c. In the eastern area, additional finds are 3 pieces of chalk/marl and 1 perforated fossil marine shell, and all originate from the ashy zone and hearth.

The deposits of horizon 2c covered the floor of pit 1 (Fig. 2-6). Thin coloured lenses of its cultural deposits were translocated down into the permafrost depression channels and are also found in the cover of pit 2. Around pit 2, however, deposits of horizon 2c were not found (Fig. 2-6; 2-14). It is probable, that 2c deposits, as well as lithological layers 7 and 7a, were removed during the construction of the cover of pit 2.

The inclination angles of horizon 2c vary in the range of 3-7°. The oblique position of artefacts and nearly equal representation of north-south and east-west oriented pieces are most characteristic for all areas and structures of horizon 2c (Table 2-1; 2-2; Fig. 2-25—2-28). The assemblage from pit 1, however, is an exception. Here, the lithic artefacts are mainly characterised by a horizontal position and north-south orientation (Tables 2-1; 2-2). In the western area, horizontally positioned bones prevail, while vertical orientation is uncommon (Table 2-3). In the western area, an east-west orientation prevails over a north-south orientation, while the latter is dominant among the bones from pit 1 (Table 2-4; Fig. 2-24). In the eastern area, including the ash and hearth zones, obliquely positioned bones dominate (Table 2-3) together with a north-south orientation, except for the hearth area (Table 2-4; Fig. 2-24). The latter comprises 16 bones, which are equally subdivided between north-south and east-west orientations.

It needs to be stressed that despite the cryogenic processes, the net movement of objects in terms of both distance and quantity, was quite low. This is demonstrated by several cases of ochre powder concentrations and bones in anatomical order, indicating a plastic deformation of the find horizon rather than stronger erosional events (Fig. 2-29; 2-30, *1*).

**The archaeological horizon 2d** found in the permafrost depression channels (lithological layers 5a, 5b, 5c) contains numerous flint artefacts, faunal remains, parts of chalk/marl crust of 2b horizon, and brownish to yellow-greyish lenses of 2c horizon (Fig. 2-4—2-6; 2-8—2-13). There are three channels: two on the western part and one on the eastern part of the excavated area (Fig. 2-24).

The eastern channel was studied on a length of 7.2 m on the following squares: 1H, 1O, 2H, 2O, 2П, 3H, 3O, 3П, 3P, 4O, 4П, 4P, 4C, 5П, 5P, 5C, 5T, 6P, 6C, 6T, 6У. Its maximum width is 1.95 m and its maximum depth is 1.2 m. The eastern channel exhibits straight and sometimes stepped walls and a relatively horizontal floor (Fig. 2-5; 2-6; 2-9). The cultural deposits in the shape of thin dark-coloured lenses were observed both in vertical and horizontal positions. The vertical lenses with bones and artefacts were found near the channel's walls, while the horizontal lenses were exposed on the floor of the channel (Fig. 2-30, *2*; 2-31; 2-32). The bones in anatomical order were studied on the floor of the depression channel (Fig. 2-30, *2*; 2-31, *1*). In addition, the number of dark-coloured lenses with bones and artefacts lies in different inclination angles and dif-

ferent depths inside the lithological layer 5a – i.e. the deposits of the depression channels. The latter might be evidence of repeated translocation of cultural deposits in the depression channel (Fig. 2-5).

The lithic artefact assemblage of the eastern channel consists of 42,466 items. In addition, 1 piece of ochre, 91 small to medium-sized chalk/marl fragments, and 21 perforated fossil marine shells originate from the eastern permafrost depression. The fauna assemblage consists of 233 fragments. Two-thirds of the lithic artefacts exhibit an oblique position. Nearly equal proportions are observed for horizontal and vertical positions (Table 2-1; Fig. 2-27) as well as north-south and east-west orientations (Table 2-2; Fig. 2-28) which is also true for bones (Tables 2-3; 2-4; Fig. 2-24).

The western channel has been studied on a length of 13.5 m, a width of 1.1 m, and a depth of 0.2-0.6 m. It is situated on the following squares: 1Н, 1О, 2Н, 3К, 3Л, 3М, 43, 4К, 4Л, 53, 6Е, 6Ж, 7Д, 7Е, 8Г, 8Д, 9Г, 9Д, 10Г. The western and eastern permafrost depression channels converge in squares 1Н, 1О, 2Н, and 2О almost at a right angle (Fig. 2-9; 2-24). The shapes of the walls of the channel are both vertical and stepped; the floor is horizontal and rounded. The positions of the dark-coloured lenses of artefacts and bones are the same as in the above-described eastern channel. In the westernmost part of the excavation area, the permafrost depression channels do not contain the sediments of lithological layers 5a, 5b, and 5c. In that area, the sediments of lithological layers 3, 4, and 7 represent the filling of the permafrost depression channel (Fig. 2-4). The numbers of both lithic artefacts and bones in the depression and neighbouring areas of horizon 2c are comparable.

The westernmost channel is found in squares 33, 3К, 43, 4К, 53, 6Г, 6Д, 6Е, 7Г, 7Д, 8Г, and partly 9Г, in close proximity and parallel to the above-described permafrost depression. It is studied at 4.2 m length, 2.6 m width, and 0.29 m depth (Fig. 2-24). The deposits of this feature (lithological layer 6) differ from the other channels. Therefore, it may not be a "real" depression channel, but a wavy surface depression of archaeological horizon 2c.

21,946 flint artefacts, 2 ochre pieces, 6 chalk/marl fragments, 58 perforated and non-perforated fossil marine shells, and 160 bones represent the assemblage of both western channels. Obliquely positioned and east-west oriented pieces dominate among the lithic and faunal remains (Tables 2-1—2-4; Fig. 2-24—2-26).

Despite the assumed stratigraphic sequence of lithological layers 5a, 5b, and 5c, the order of appearance in the eastern and western channels is not clear (Fig. 2-5; 2-9). The origin of the dark-coloured lenses, however, relates to the cultural deposits of horizon 2c.

**Pit 2** was parcelled out as a separate archaeological unit. The infill consists of sediments of geological layer 6-7, supposedly of anthropogenic origin. The lenses of coloured sediments, probably the remains of the removed lithological layer 7a, were found throughout the entire thickness of lithological layer 6-7. It is clear that lithological layer 6-7 have accumulated above layers 7 and 7a on the square lines К, Л, and, partly, М. The stratigraphic position of layer 6-7 relative to the sediments of lithological layers 7 and 7a (archaeological horizon 2c) on the square lines of П, Р, С, Т, and У, in contrast, is unclear, because of the eastern channel permafrost depression. The filling of pit 2 yielded 5,289 flint artefacts, 1 piece of amber, 1 piece of ochre, 1 piece of sandstone, 28 fragments of chalk/marl, 6 perforated marine shells, and 91 bone fragments. Obliquely positioned and east-west oriented objects dominate (Table 2-1—2-4).

Despite the fact that material of archaeological horizon 2a and the filling of pit 2 are connected to lithological layer 6-7, they were distinguished as different archaeological events. The reason for this separation is the presence of sterile sediments between the upper part of lithological layer 6-7, which is above the pit, and its lower part, which is inside the pit 2 (Fig. 2-19, *3*). The lowermost elevation of a mammoth scapula found on top of the mound-like structure above pit 2 is at -270 cm; the uppermost elevation of the ribs and bones inside pit 2 is at -302 cm. The thickness of sterile sediments between the lowest artefacts from horizon 2a and the uppermost artefacts from pit 2 varies from 6 to 12 cm. Sterile sediments are usually

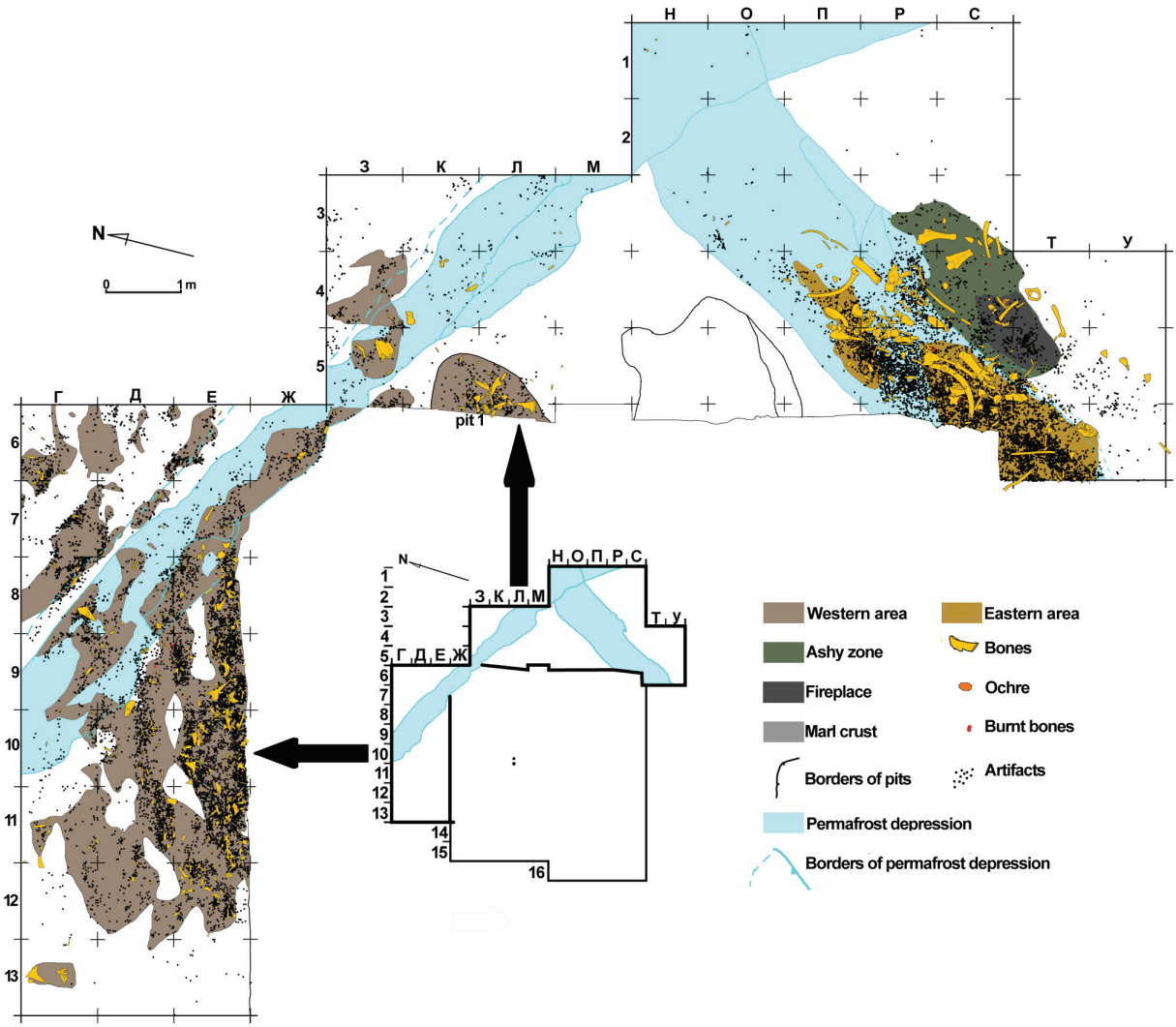


Fig. 2-24. Barmaky, plan of archaeological horizons 2c and 2d.

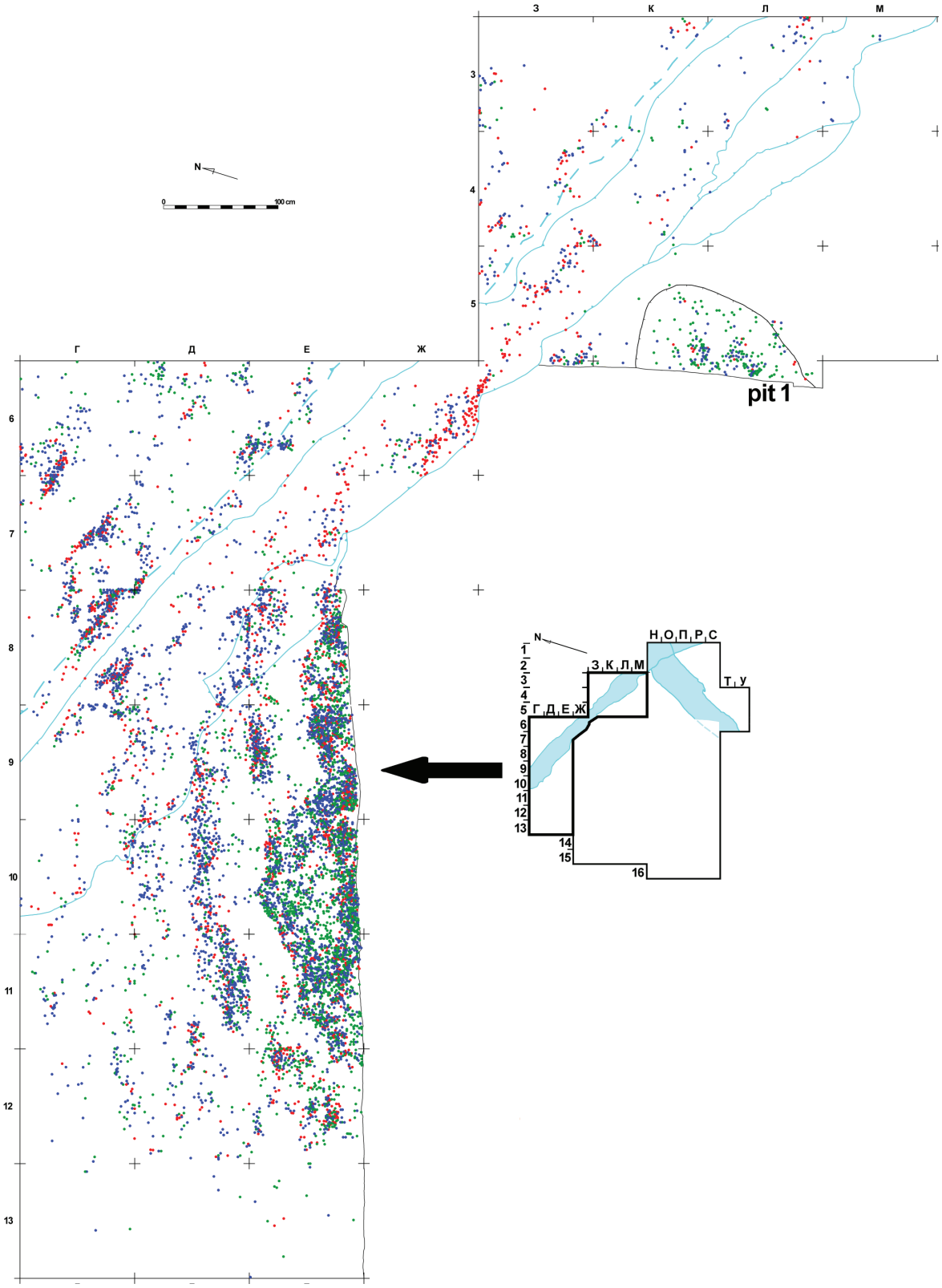


Fig. 2–25. Barmaky, western area, archaeological horizons 2c and 2d: position of artefacts, green dots – horizontal, red dots – vertical, blue dots – oblique.

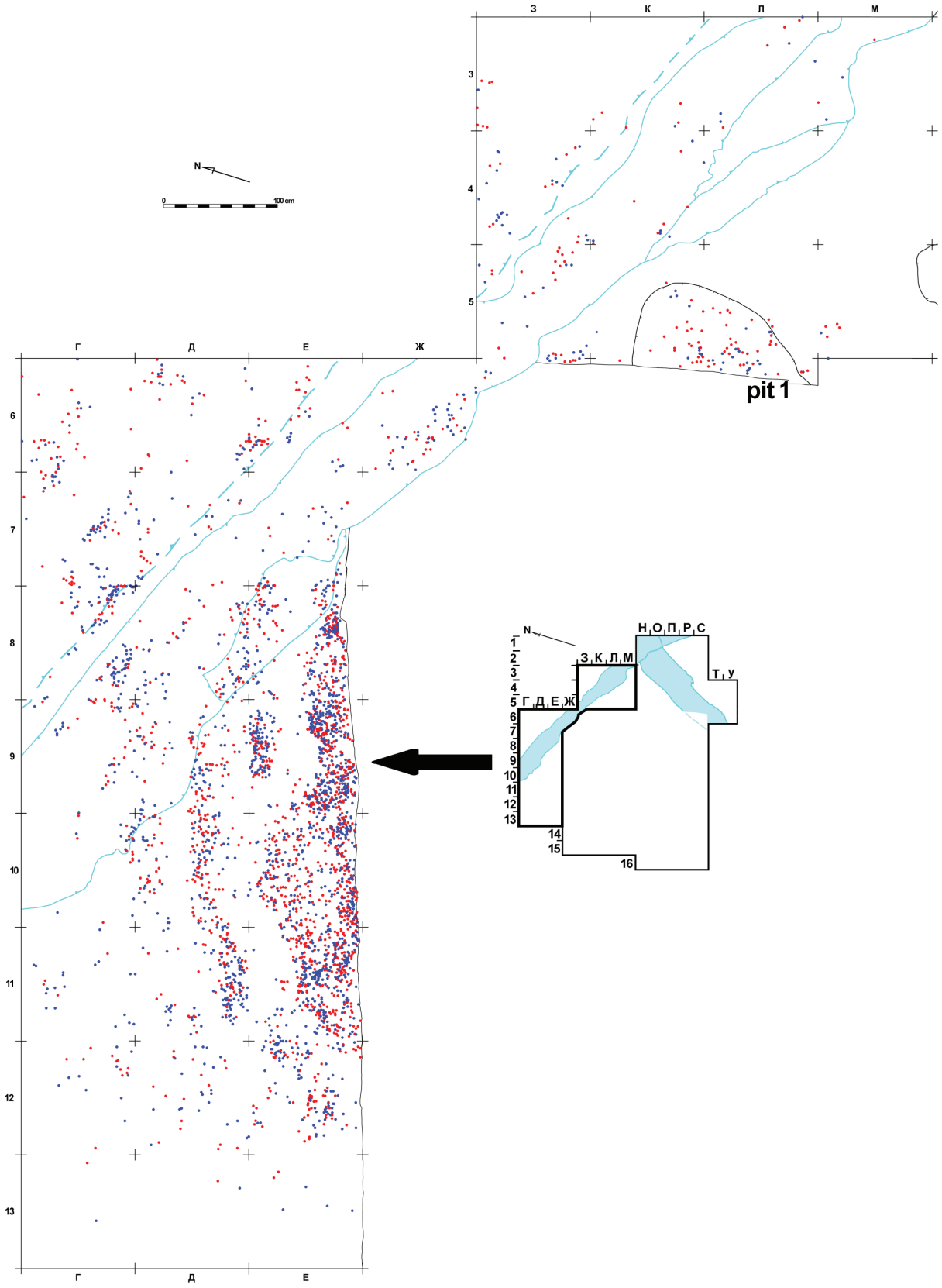


Fig. 2–26. Barmaky, western area, archaeological horizons 2c and 2d: orientation of artefacts, red dots – north–south, blue dots – east–west.

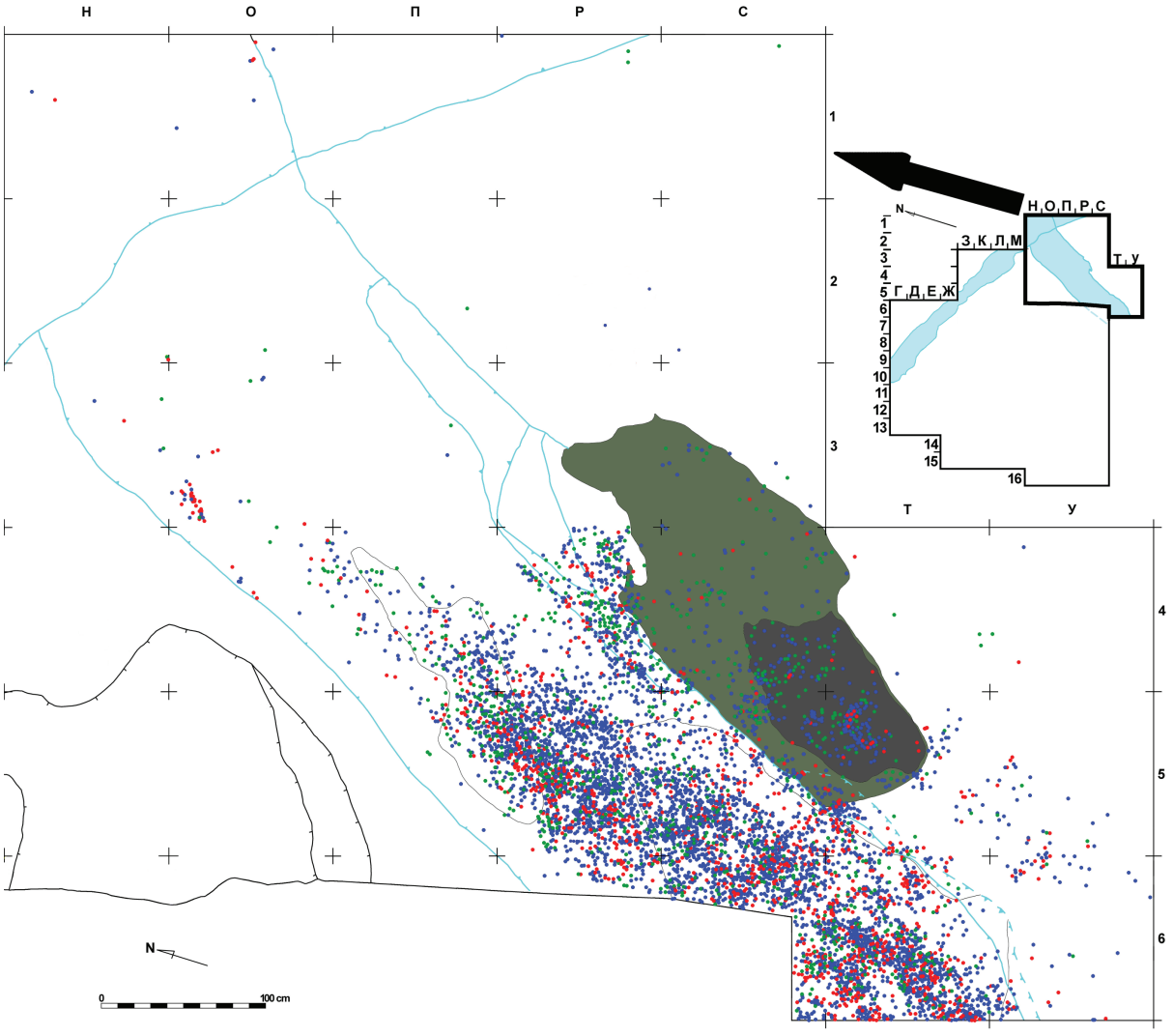


Fig. 2–27. Barmaky, eastern area, archaeological horizons 2c and 2d: position of artefacts, green dots – horizontal, red dots – vertical, blue dots – oblique.

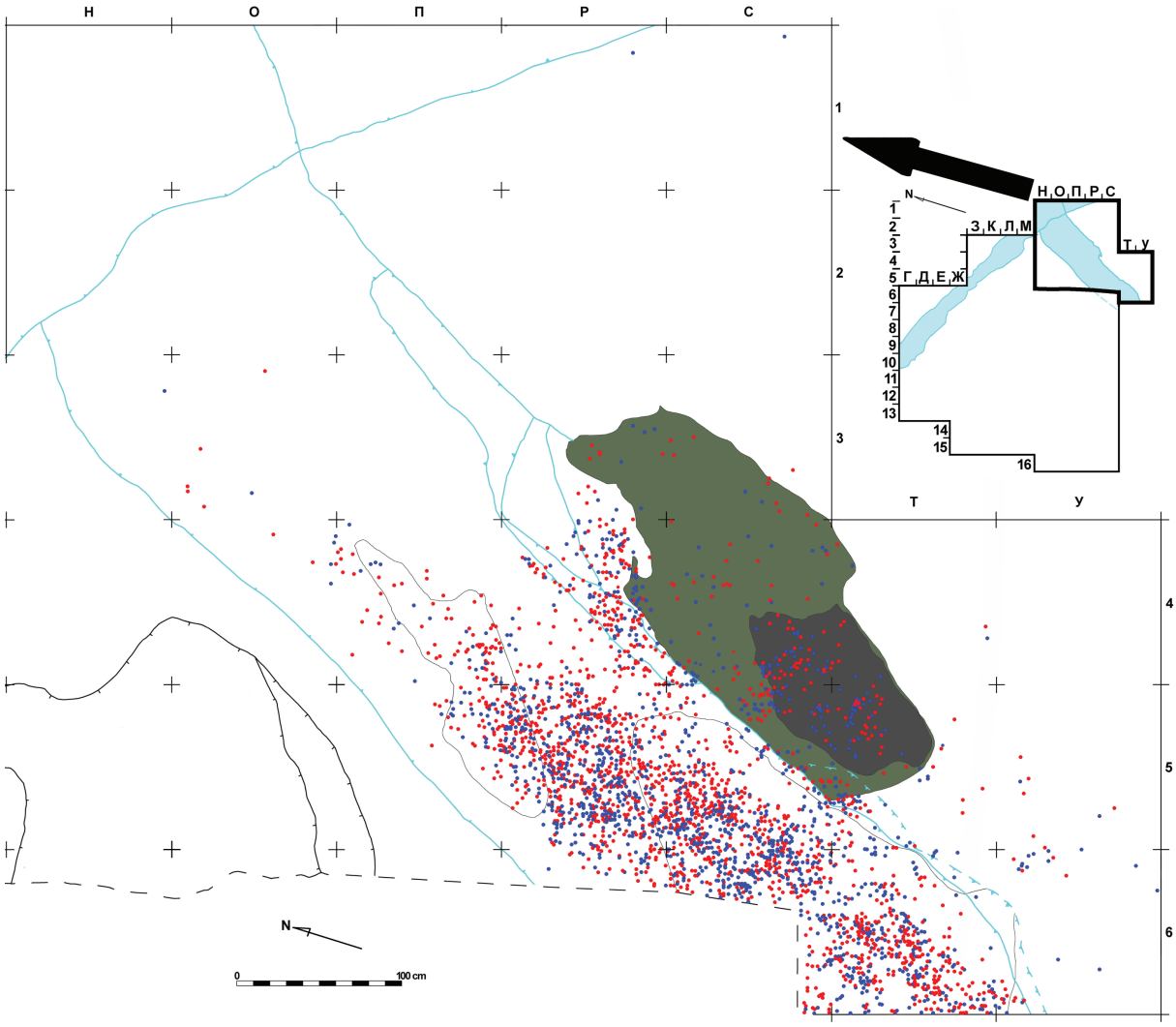


Fig. 2–28. Barmaky, eastern area, archaeological horizons 2c and 2d: orientation of artefacts, red dots – north–south, blue dots – east–west.

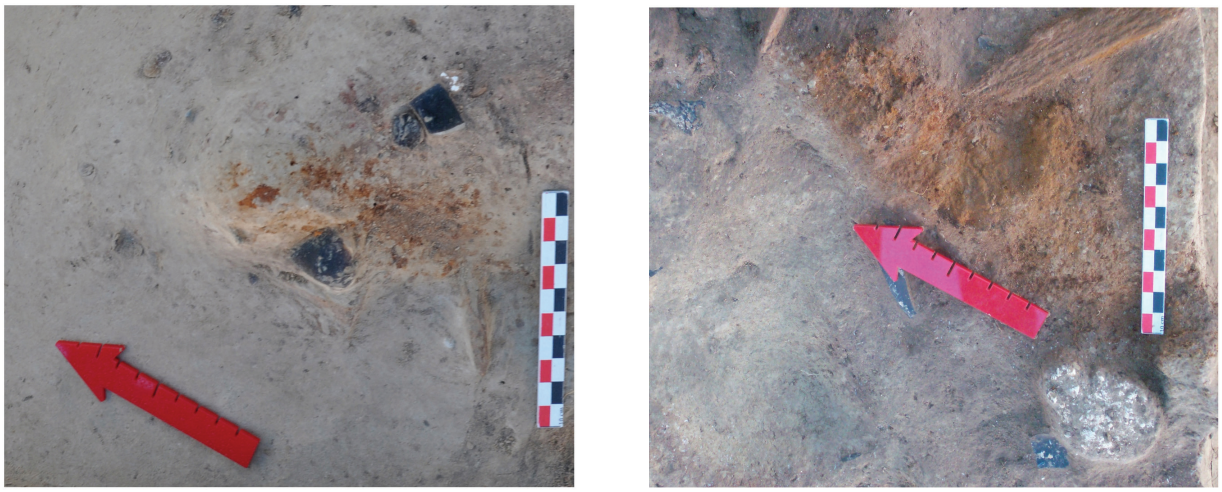

1 2

Fig. 2–29. Barmaky, archaeological horizons 2c, concentrations of ochre powder: 1 – square 9E; 2 – square 10E.

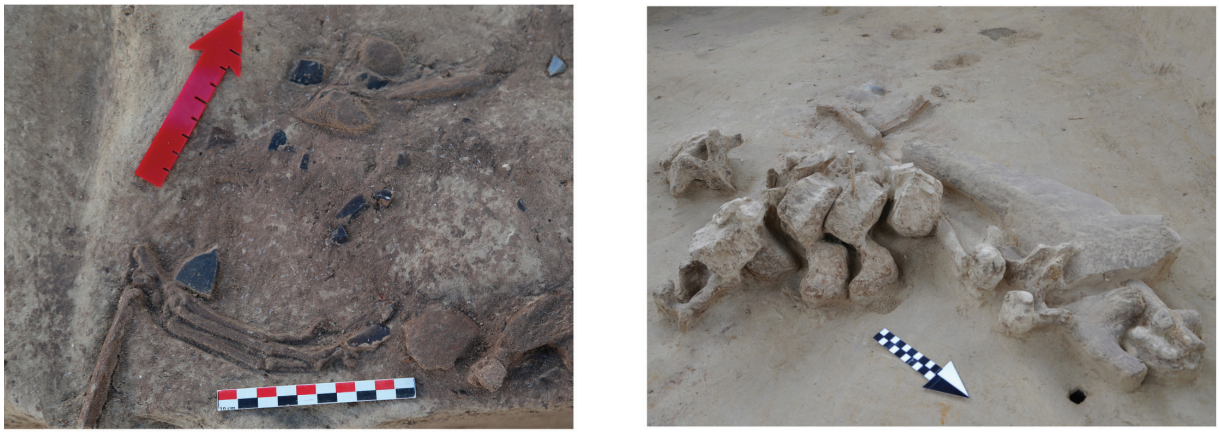

1 2

Fig. 2–30. Barmaky, bones in anatomical order: 1 – horizon 2c, square 10E, polar fox; 2 – horizon 2d, squares 4П, 4Р, 5П, 5Р, mammoth vertebrae.

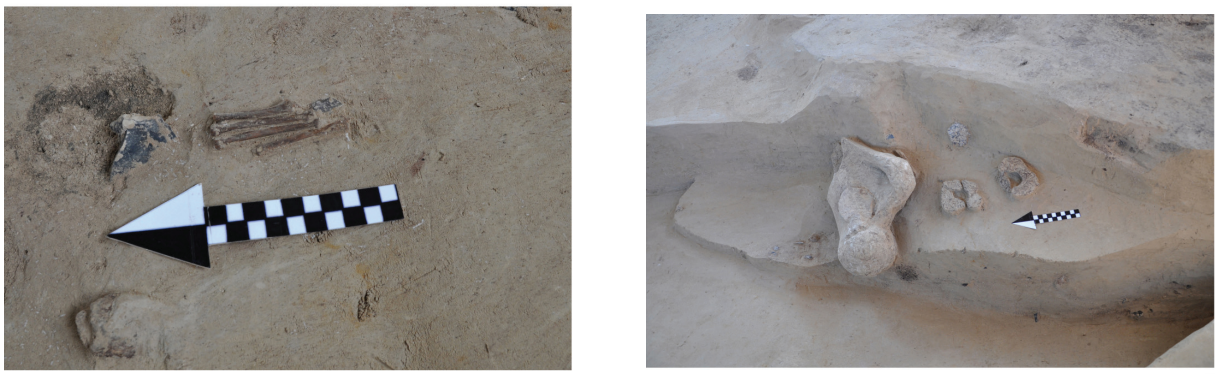

1 2

Fig. 2–31. Barmaky, archaeological horizon 2d, square 4Р: 1 – floor of a permafrost depression channel with polar fox bones in anatomical order; 2 – stepped wall of a permafrost depression channel, bones and artefacts in vertical and horizontal positions.

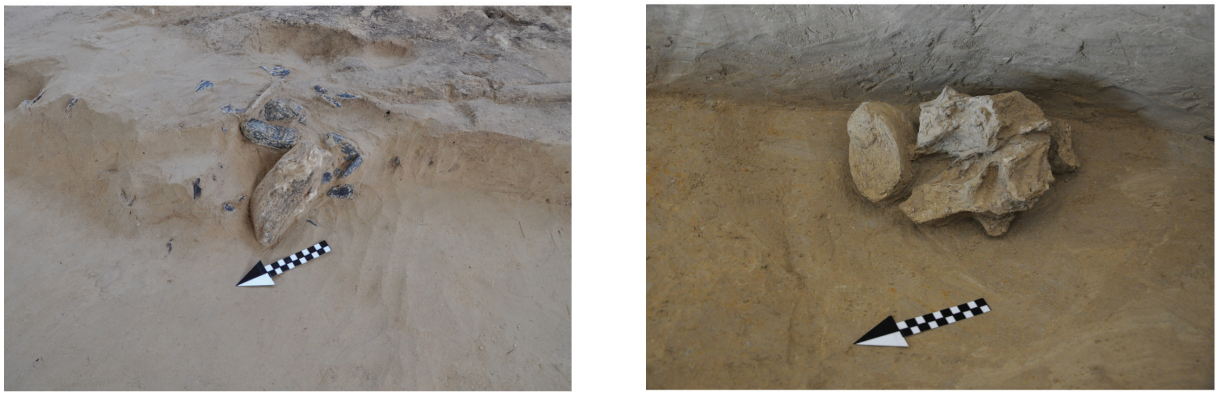

1 2

Fig. 2–32. Barmaky, archaeological horizon 2d. 1 – square 4Р, wall of a permafrost depression channel with bones and artefacts in the vertical position; 2 – square 6Т/6У, horizontal floor of a permafrost depression channel with a fragment of a mammoth skull.

considered a reliable argument for separating archaeological events and allow several interpretations.

Given that the occupation at Barmaky immediately post-dates the Last Glacial Maximum, it seems reasonable to assume that during the accumulation of archaeological level 2, at least two permafrost ice wedges were situated beneath the inhabited area at a depth of 0.2–1.2 m. During the subsequent climatic warming, the melting permafrost led to a vertical translocation of both sediments and archaeological material. Probably the net horizontal movement of both sediments and artefacts was not significant. After the permafrost degradation, the surface probably showed a shape close to the one proposed in Figure 2–33.

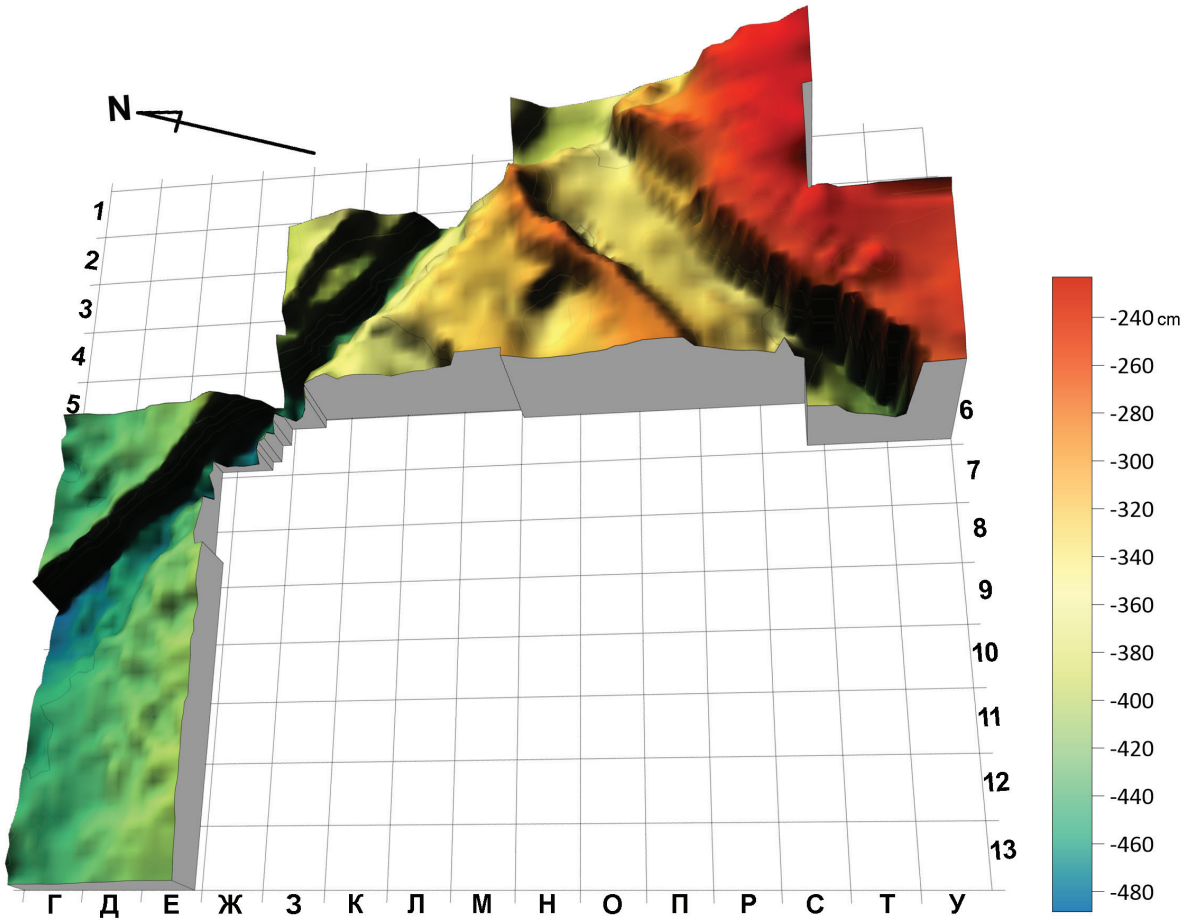


Fig. 2–33. Barmaky, archaeological horizons 2c and 2d, 3D reconstruction of the floor surface after permafrost degradation.

## STRUCTURES

Artificial structures at Barmaky are the chalk/marl crusts, two pits, and a dwelling structure.

### The chalk/marl crusts

Two thin crusts of chalk or marl deposits (horizon 2b), probably of anthropogenic origin, were documented during excavation. The material can be extracted as embedding material of a flint outcrop about 150–300 m from the site. The crusts have been applied directly above the cultural deposits of horizon 2c. The shape of the first crust from squares 4К, 4Л, 4М, 5Л, and 5М is amorphous. It covers an area of about 1.5 m2 and has a thickness of between 0.03 and 0.05 m. It consists of densely packed chalk/marl fragments of different sizes (Fig. 2–22). The maximum size of the fragments is 0.2×0.15×0.05 m. The relatively small artefact sample associated with the crust – archaeological horizon 2b – amounts to 276 pieces.

The second crust from squares 5У and 6У consists of a line of fragments with a total length of 0.5 m, a width of 0.2 m, and a thickness of 0.1 m (Fig. 2–23). It might be a part of a larger, not yet excavated structure. So far, no artefacts are associated with it.

A chalk/marl concentration is also known from the site of Samotoevka, where it was interpreted as a "floor" around a fireplace (Bessudnov, Bessudnov 2012).

### *Pit 1*

V. Piasetsky and V. Samoliuk (1990) already excavated and documented large parts of pit 1. It has an ovoid shape with a maximum diameter of 0.72 m, sloping walls, and a wavy floor with a maximum depth of 0.17 m (Fig. 2–34). Sediments of lithological layers 7 and 7a make up the filling of pit 1 (Fig. 2–21, *3*). The undisturbed stratigraphic sequence, including the archaeological horizon 2c (lithological layer 7a) at the bottom and walls of pit 1, might be evidence of a natural origin of this depression. The finds of archaeological horizon 2c in pit 1 amount to 3258 flint artefacts – mainly chips – and 31 faunal remains (Fig. 2–34, *1, 4*). Among the latter, two mandibles of young mammoths were identified. The densities of both lithic artefacts and bones in the neighbouring squares are ten times lower. The density of faunal remains in pit 1 also sets it apart from the wider surrounding areas, speaking against an accumulation by erosion. Considering the probable natural origin of pit 1, its faunal concentration might represent a cache in a natural depression.

### *Pit 2*

Like pit 1, pit 2 has also been partly excavated by V. Piasetsky. Unfortunately, however, he has not documented it as such. Pit 2 has an irregular to ovoid shape with a maximum length of 2.14 m and a maximum width of 1.71 m (Fig. 2–35, *1*). The walls are sloping and the floor is concave with a maximum depth of 0.35 m (Fig. 2–35, *2, 3*). Considering the post-depositional cryoturbation processes, it is difficult to be sure of its primary shape

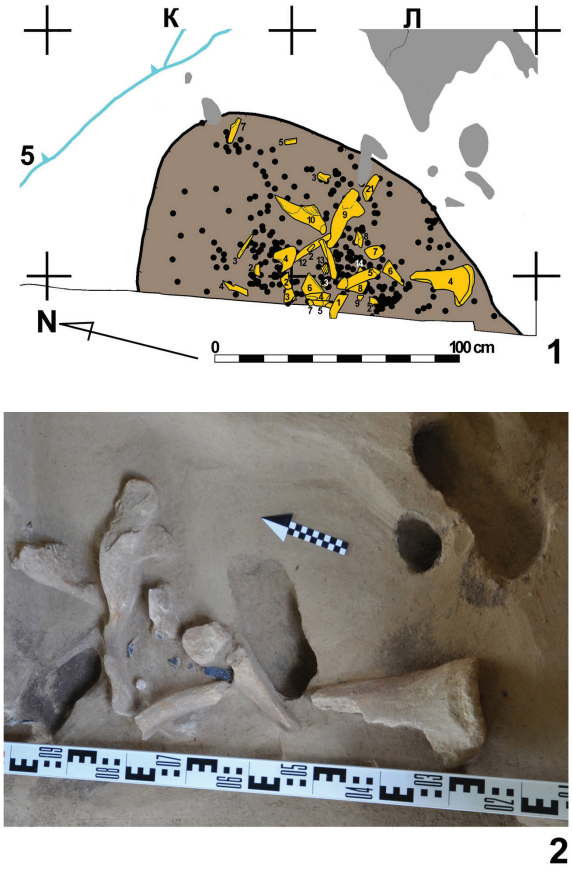


Fig. 2–34. Barmaky, pit 1: 1 – plan; 2 – bones and flints on the bottom of the pit.

and origin. The filling consists of sediments of lithological layer 6–7; the walls and bottom of pit 2 cut into lithological layer 8 (Fig. 2–14). The tiny lenses of brownish/greyish sediments and chalk/marl pieces in the filling suggest the presence of cultural deposits of horizons 2b and 2c, but exhibit neither vertical nor horizontal concentrations.

The archaeological material is represented by 5,289 pieces of flint artefacts, 1 fragment of amber, 6 perforated fossil shells, and 91 pieces of faunal remains, among others 20 mammoth ribs. These ribs are a distinctive feature (Fig. 2–36) since it is the only such concentration at the site. In addition, a skull fragment of a young mammoth has been recovered. The positions of artefacts and faunal pieces are mainly obliquely positioned and

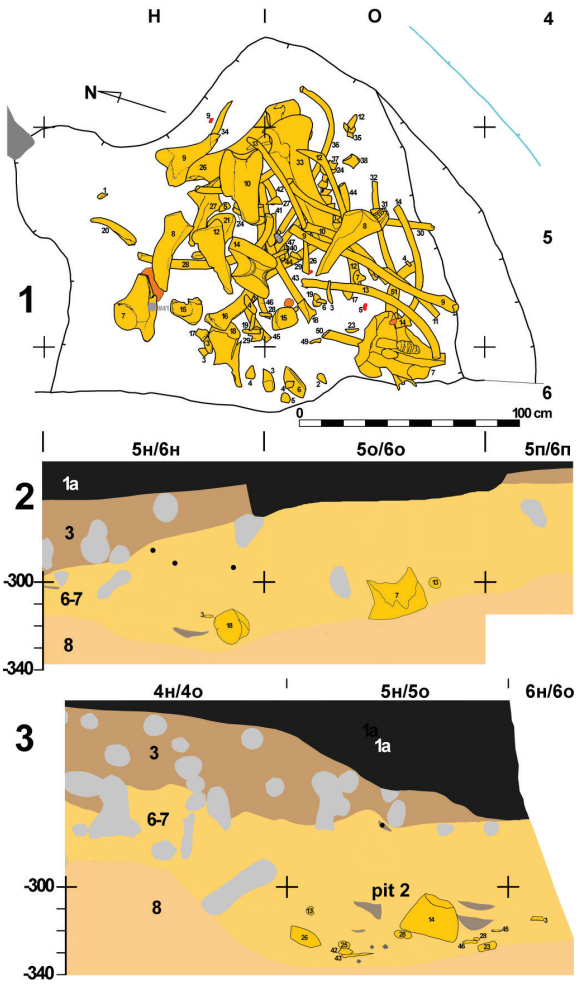


Fig. 2–35. Barmaky, pit 2: 1 – plan; 2 – section along square line 5/6; 3 – section along square line Н/О.

east–west oriented. Pit 2 was excavated by four artificial horizons. The fact that the long bones and ribs from the upper and lower horizons overlapped might be seen as evidence that the pit filling took place during a single episode. Sediments from the surrounding areas were used to cover the pit and form archaeological horizon 2a. The observed thickness of the cover is at least 0.3 m.

Directly above pit 2 on top of the mound-like cover made up by the deposits of archaeological horizon 2a, a scapula of a young mammoth was found, sq. 4О and 5О (Fig. 2–19, *1, 2*). It is the largest bone in the faunal assemblage of horizon 2a. The practice of marking a covered pit is also known from other Palaeolithic sites, such as Yeliseevichi, Kostenki 11, and Zaraiskaya (Polikarpovich 1968:70–71; Rogachev, Anikovich 1984: 196; Amirkhanov 2009: 23).

In contrast to the likely intentional deposition of large bones into and above pit 2, it seems probable that the flint artefacts, fossil shells, and the piece of unworked amber are rather the result of non-selective digging activity aimed to cover the pit with surrounding sediments, already containing these objects. The absence of the deposits of lithological layers 7 and 7a on the walls and bottom of pit 2 suggests its artificial origin.

## Dwelling structure

A complex of three settlement objects in the eastern part of the site, namely a fireplace (squares 4С, 4Т, 5С, 5Т), a patch of ashy sediments (squares 3Р, 3С, 4Р, 4С, 4Т, 5С, 5Т), and a line of seven big fragments of tube bones (squares 3С, 4Т, 5У) might be the remnants of a former dwelling structure (Fig. 2–37).

In the south-eastern part of the excavated area, there is a **cluster of intensively grey ashy/sooty sediments** with whitish carbonate concretions showing a clear eastern and partly northern border without gradual transitions, while the permafrost depression channel truncates its western and southern limits. The ashy cluster has a NE–SW extension and an irregular ovoid shape (Fig. 2–37). The preserved length is 2.86 m, the preserved width is 1.25 m, and the preserved thickness is 0.07 m. The grey ashy deposits contain 0.01–0.02 m thick yellowish solifluction lenses. The archaeologi-

1

2

Fig. 2-36. Barmaky, pit 2, bones and artefacts:
1 – square 5O; 2 – squares 4H, 4O, 5H, 5O.

cal finds from the ashy cluster consist of 1643 flint artefacts, 19 of which are burnt, and 21 bone fragments, 2 of which are burnt – although not intensively as indicated by their brown colour. In addition, 1 perforated fossil marine shell and 2 burnt chalk/marl fragments were found. The clear northern (sq. 3P) and eastern (3C, 4T, 5T) limits of the ash and artefact distribution might be evidence of some kind of former barrier or wall. On squares 5C and 5T, the part of the ashy cluster was translocated down by 0.1 m due to the permafrost depression. More than half of the finds were found in an oblique position, one-third lay horizontal, and about 10% vertical. There is no dominant orientation of both fauna and artefacts.

A **fireplace** is located in the southwestern part of the ashy cluster and probably is its source. It belongs to the simple type, i.e., not deepened and without additional constructions (Fig. 2-37; 2-38, *1*). It has an ovoid shape of 1.36 × 0.71 m extending in an NE-SW direction and a preserved thickness of 0.08 m. The black coloured sediments of the fireplace consist of an ashy/sooty component, which contrasts with both the ashy cluster and whitish silty-loess deposits of lithological layer 7. Solifluction lenses (max. thickness 0.02 m) of whitish, silty loess were found in the ashy/sooty deposits of the fireplace. 1374 flint artefacts (30 burnt), 18 fragments of bones (1 burnt), a concentration of burnt ochre powder (diameter ≈ 0.1 m, thickness ≈ 0.005 m), and one burnt chalk/marl fragment were found in the deposits of the fireplace.

The southern extremity of the fireplace was partly affected by permafrost depression and a small part was translocated 0.1 m down. Most of the finds from the fireplace exhibit oblique positions on different angles. At the same time, one-third of both bones and artefacts were found in a horizontal position, also characteristic of the burnt ochre powder concentration. A dominant orientation was not identified.

There is an alignment of **seven large fragments of tube bones** in squares 3C, 4T, and 5У, which show the same NE-SW orientation as the fireplace and the ashy cluster. Also, three of them are preserved in a vertical position, reaching about 5-7 cm below the level of other finds from this horizon (Fig. 2-37; 2-38, *2*). However, the relation of this bone line to both features remains unclear. The same is true for the small chalk/marl concentration with the same orientation in squares 5У and 6У. When considered together, the fireplace, the ashy cluster with its clear limits, and the alignment of seven large bone fragments might be the remnants of a light dwelling structure, such as a tent. However, since the feature's alignments run parallel with the permafrost depression, i.e., strung out in the north-south direction, taphonomic processes as agents in the formation of these features cannot be excluded.

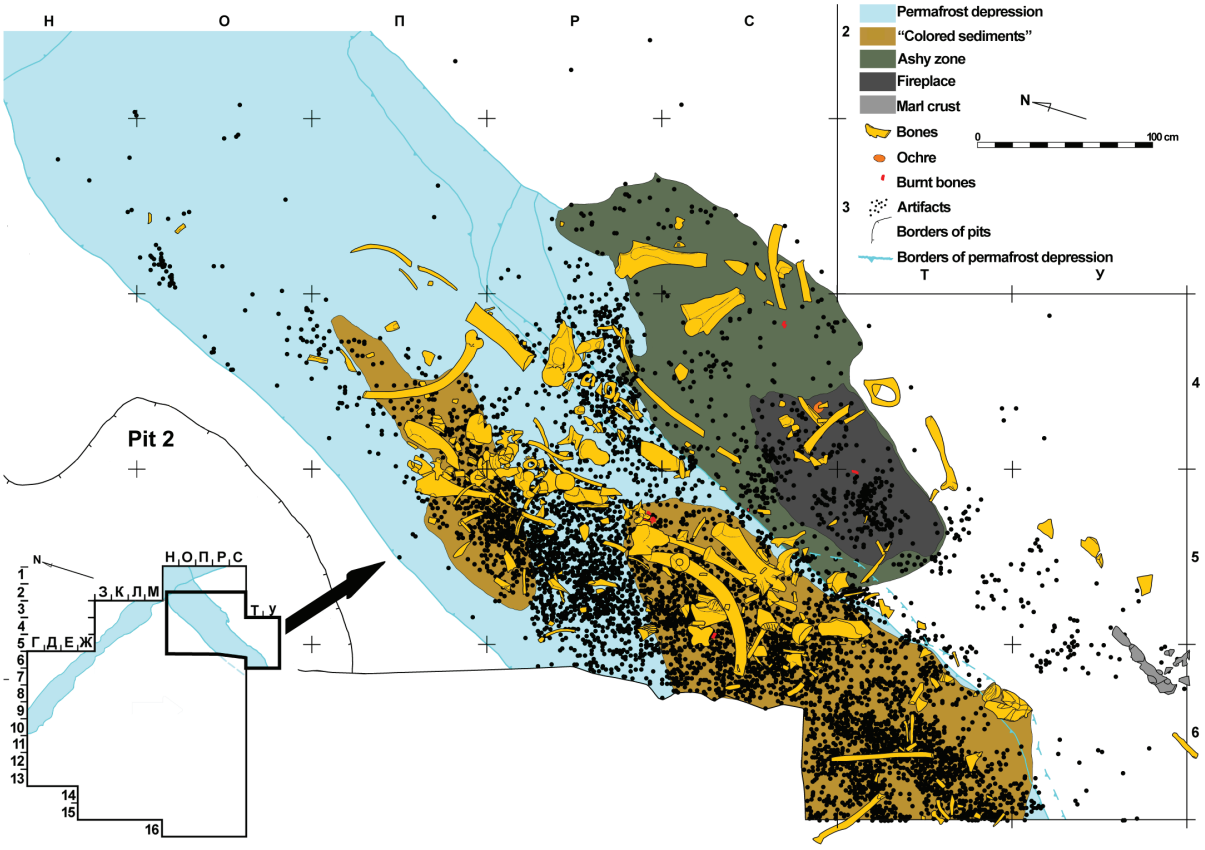


Fig. 2–37. Barmaky, archaeological horizons 2c and 2d: fireplace, ashy cluster, faunal material, artefacts, and permafrost depression channel.

1 2

Fig. 2–38. Barmaky, archaeological horizons 2c: 1 – section of the fireplace along square line 4С/5С; 2 – line of vertically positioned tube bone fragments.

## DISCUSSION AND CONCLUSION

Archaeological level 1 consists of redeposited material from level 2, mainly due to bioturbation. In the western part erosional processes also contributed to its formation.

The combined plan of Barmaky, level 2 is presented in Figure 2-39. Even taking into account the problematic methods of field investigations in 1982 and 1990, the complex character of the settlement structure is obvious. Unfortunately, defining the stratigraphical position of archaeological material excavated in the 1982 and 1990 field seasons is impossible. Nevertheless, the above-stated observations of the stratigraphy and site formation processes allow for a number of statements and assumptions.

Barmaky, level 2 occupations accumulated on top (square lines 1-5) and the upper slope (square lines 6-13) of the hill. The wavy boundaries and surfaces of the lithological layers and their discontinuous character seem to be the result of post-depositional cryoturbation processes, which also created the channels of the permafrost depression and solifluction lenses. During the accumulation of archaeological horizon 2c, pronounced traces of solifluction were observed. The solifluction process is likely caused by repeated seasonal melting and leads to the transportation of both sediments and archaeological material downslope.

The available stratigraphic sequence suggests the beginning of permafrost degradation during or shortly after the accumulation of lithological layer 4, that is sometime after the accumulation of the cultural deposits. Several depression channels signal this permafrost degradation, a feature observed at several Eastern European sites, such as Zaraisk, Yeliseevichi I, Timonovka I, and Yudinovo (Velichko et al. 1997: 51-66; Amirkhanov 2000: 88, 94; Sergin 2007: 14-15; Gribchenko & Kurenkova 2014: 107). In permafrost environments, a relative stability of the living floor during the accumulation of the cultural deposits is a necessary requirement for settlement activities (Sergin 2007; Grigorieva 2008: 53-54). At Barmaky, the living floor seems to have been generally stable during the accumulation of archaeological level 2 because of permafrost deposits about one meter below the surface. At the same time, the repeated solifluction processes suggest a seasonal instability of the occupation surface. Therefore, it seems that from the point of surface stability, the best period for settlement exploitation was after the time of the summer maximum temperatures. There are two kinds of seasonally distinctive faunal indicators: the remains infantile mammoth and the lower limbs of a polar fox in the anatomical connection (Chapter 6, this volume). The time of death of the mammoth is supposed to be February. Assuming that *Vulpes lagopus* was mainly hunted for fur, the best hunting time would have started at the end of September. Together, the available evidence and hints suggest that the occupation at Barmaky took place towards the winter and thus on a stable living floor. It is, however, impossible to determine whether the remains of archaeological horizon 2c accumulated as a result of a single prolonged stay or as a palimpsest of two or more events. The high density of artefacts in some squares and the relatively high degree of fragmentation of artefacts and fauna, bigger tool-to-core ratio in the western area can result from both a longer single stay or frequently repeated visits on the same living floor (Chapters 3, 6 and 9, this volume).

The absence of a stratigraphical connection between the eastern and western areas of lithological layers 7 and 7a does not allow to establish a general sequence of the site formation processes of archaeological level 2. Thus, the following separate sequences can be proposed.

The western area, archaeological level 2 accumulation sequence:

1. Accumulation of the materials of horizon 2c, including pit 1.
2. Accumulation of the horizon 2b – chalk/marl crust.
3. Accumulation of horizon 2a1 above pit 1 – i.e., the process of covering the pit by surrounding sediments, forming the cache in a natural depression.
4. Digging of pit 2 and filling with the sediments of lithological layer 6-7.
5. Accumulation of horizon 2a above pits 1 and 2 and partly above the chalk/marl crust – i.e., the covering of pits by surrounding sediments, which already contain the cultural deposits of horizon 2c.

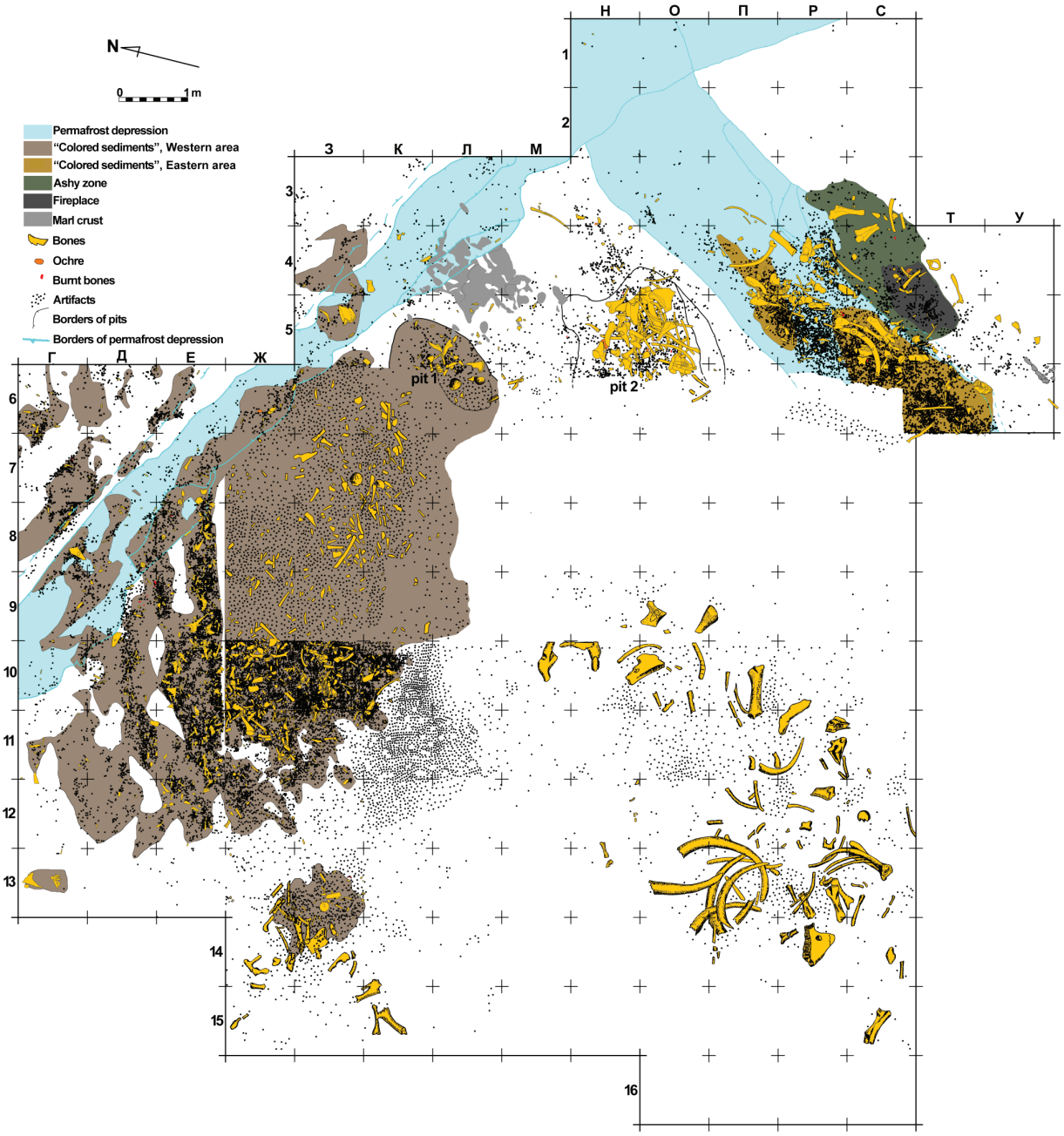


Fig. 2–39. Barmaky, archaeological level 2: combined plan of 1982–2020 field campaigns.

6. The accumulation of horizon 2d, as the degradation of permafrost deposits leads to the appearance of depression channels; the materials of horizons 2b and 2c are the two sources of horizon 2d formation.

Pit 2 appears to be the latest artificial object in the proposed sequence, which accumulates after the formation of 2b and 2c. The separate covering of pit 1 by horizon 2a1 deposits suggests that pit 1 was covered before the mound-like covering has been built above both pits using the sediments of horizon 2a.

At the same time, the absence of a stratigraphic connection between deposits and covering of pit 2 and the eastern area does not allow for temporal correlation.

The eastern area, archaeological level 2 accumulation sequence:

1. Accumulation of the materials of horizon 2c, including the ashy zone and hearth.
2. Accumulation of the horizon 2b – chalk/marl crust.
3. Accumulation of horizon 2d, as the degradation of permafrost deposits leads to the appearance of depression channels; the materials of horizons 2a and 2c are the two sources of horizon 2d formation.

The absence of direct stratigraphic contact of the deposits of horizon 2c in the western and eastern areas prevents a determination of their temporal correlation. In other words, the western and eastern areas might either represent two habitation zones of a single settlement or two temporally different events. Three assumptions for the temporal correlations of pit 2 and horizon 2c in the eastern and western areas might be proposed. First, pit 2 was constructed as a meat cache at the end of the western settlement. Second, pit 2 belongs to the economic activities of the eastern habitation area and accumulated after the western area had been abandoned. Third, if the western and eastern areas are contemporaneous, then there is no stratigraphic evidence to disentangle the palimpsest nature of horizon 2c occupation(s) in both areas.

Based on the presented stratigraphical observation the following subdivision of artefacts and fauna assemblages might be proposed.

1. Level 1 artefacts.
2. 2a complex, which include the materials from horizons 2a, 2a1, and 2ab.
3. Pit 2 complex.
4. Western area complex, which consists of the materials from horizons 2b, 2c, and 2d on square lines Г, Д, Е, Ж, З, К, and Л.
5. Eastern area complex, which consists of the materials from horizon 2c, including the ashy lens and fireplace, and horizon 2d on square lines Н, О, П, Р, С, Т, and У.
6. The archaeological material from sondages 3, 4 and 1990 field campaign.

# RADIOCARBON DATING OF BARMAKY AND THE WIDER CHRONOLOGICAL CONTEXT OF THE MID DNIEPER EPIGRAVETTIAN

# 3

ANDREAS MAIER

Before our work at Barmaky, a single conventional radiocarbon measurement on bone (KI-11087) was available for the site, with an age estimate of roughly 17.5 ka (Nuzhnyi 2008a). According to Nuzhnyi (2015: 210), this sample originates from a location with an uneven stratigraphic context. For better chronological control, we selected eight charcoal samples and five samples from fragmented mammalian tube bones with no further determination of the species from all areas of the excavation for AMS dating. Unfortunately, all attempts to date the charcoal samples and one attempt to date a thin long bone failed due to low $CO_2$ yield. Of the remaining four bone samples, three were dated at Oxford and one at Mannheim (Table 3-1). The samples dated at Oxford come from the Western Area and originate from those squares with the highest densities of bones and artefacts. The sample dated at Mannheim originates from the permafrost depression (Fig. 3-1). All AMS-dates returned consistent age estimates and can be combined to a weighted average (P =17,8 %, 15747±34) using CalPal-Beyond the Ghost, Version 2020.11 (Weninger and Jöris, 2008), which, using the IntCal20 curve (Reimer et al. 2020) as implemented in CalPal, results in a calendar date range of 19064 to 18944 calBP, i.e. roughly 19 ka calBP (Table 3-1).

Based on the technological and typological characteristics of the lithic and organic assemblage components (Chapters 8 and 9), Barmaky is taxonomically attributed to the East European Epigravettian. In Ukraine, the Epigravettian is further subdivided into several taxonomic sub-units, mainly based on the typological particularities of lithic projectile implements from 22 stratified assemblages in the periglacial zone of the mid-Dnieper basin (Chapter 11). For a chronological contextualisation of Barmaky, the most relevant of these sub-units are the Mizyn industry, to which Barmaky is attributed (Nuzhnyi 2008a, 2015; Chapter 11), the Mezhyrich industry, and the Yudinovo industry.

Chronologically, Early Epigravettian assemblages in Ukraine follow the latest manifestations of local Gravettian industries and are reported as early as 23–22 ka calBP in the river basins of Dniester and Prut, the Northern Black Sea steppe region, and the eastern part of Central Europe (Noiret 2009; Krotova 2013; Połtowicz-Bobak 2013). North of 50° latitude, however, comparable assemblages are not been reported before 19–18 ka calBP and thus show a hiatus of five to six thousand years during the Last Glacial Maximum (Chabai, Vasyliev 2021a).

The lithic assemblages of the Mizyn industry are characterised by straight-backed (and few lanceolate) micro-points with fine, abrupt, dorsal retouch on bladelets. In addition, micro-blades are common, which often show an obliquely retouched/truncated base. Narrow rectangles with one or two oblique truncations do occur, but are rather uncommon. The organic industry is marked by spindle-shaped and sometimes slotted points as well as batons percées. For the Mezhyrich industry, the distinctive lithic insets are narrow lanceolate points with fine dorsal and ventral abrupt and semi-abrupt retouch and numerous rectangles made on bladelets and micro-blades, sometimes by inverse and alternate retouch. Micro-burin technology is reported from the assemblages of Semenivka 1, 2 and 3, also attributed to the Mezhyrich industry. Just as for

| Site, horizon | Square | depth | Sample | Method | Lab.-Nr. | δ13C | C:N | C % | Collagen % | BP | Std | calBP | Std | P | wBP | wStd | wcalBP | wStd | References |
|---|---|---|---|---|---|---|---|---|---|---|---|---|---|---|---|---|---|---|---|
| Barmaky | | | bone | Conv | KI-11087 | | | | | 14300 | 220 | 17459 | 322 | | | | | | Nuznyi 2008a |
| Barmaky, 2c | 12E | -402 mm | bone | AMS | OxA-38249 | -18.57 | | | | 15610 | 80 | 18898 | 71 | * | | | | | Chabai et al. 2020b |
| Barmaky, 2c | 10E | -401 mm | bone | AMS | OxA-X-2804-40 | -21.34 | | | | 15720 | 80 | 18993 | 87 | * | | | | | Chabai et al. 2020b |
| Barmaky, 2d | 6Ж | -435 mm | bone | AMS | MAMS-49912 | | 3,2 | 40 | 5,2 | 15770 | 50 | 19026 | 70 | * | | | | | Chabai et al. 2022 |
| Barmaky, 2c | 12E | -417 mm | bone | AMS | OxA-38250 | -23.66 | | | | 15850 | 80 | 19137 | 123 | * | | | | | Chabai et al. 2020b |
| | | | | | | | | | | | | | | | 17,8 | 15747 | 34 | 19004 | 60 |

Table 3-1. Radiocarbon dates from Barmaky

P: dates combined in a weighted average (marked with *, a, or b) and probability in %. wBP/wStd/wCalBP: weighted averages, standard deviation and calibrated weighted averages. Calibrations using the IntCal20 curve (Reimer 2020), and weighted averages calculated with CalPal Beyond the Ghost, Version 2020.11 (Weninger and Jöris, 2008).

the Mizyn industry, the organic industry of the Mezhyrich industry is characterised by spindle-shaped and sometimes slotted points as well as batons percées. Typical for the Yudinovo industry are lanceolate points on flakes, blades, and bladelets with abrupt/semi-abrupt retouch as well as typical and atypical rectangles on blades and bladelets. For the organic industry, cylindrical points are typical.

The question thus arises whether the observed differences and similarities between these taxonomic sub-units are an expression of variability between contemporaneous groups or rather of a chronological succession?

For the three relevant industries, 129 radiocarbon dates from 13 sites (see Table 11-3) roughly suggest ages between 19 to 14 ka calBP (Chabai et al. 2020b). The exact chronological position and relation between the assemblages of the Mid Dnieper Epigravettian and their taxonomic units are, however, still debated. If all 129 available dates are considered indiscriminately, no chronological succession between the taxonomic nits and their respective assemblages is observable, and the age estimates for many assemblages cover several millennia (Table 11-3). However, many of the available dates are flawed, for instance, because their exact origin and thus stratigraphic position are unclear. Moreover, a large number of dates are made on mammoth remains, including teeth. Since mammoth remains often show a structural offset in comparison to other species towards an older age, such dates must be treated with caution. Larger accumulations of mammoth remains are a frequent feature at Epigravettian sites in Ukraine, and it is likely that many of these items were gathered in the landscape and are thus (much) older than the occupation in question. Furthermore, judging from the available radiocarbon dates, the highest number of dated Epigravettian occupations occur during a period between 18.5-17.0 ka cal BP. However, this impression might indeed be misleading and rather reflect oscillations of the mammoth population in the East European Plain, which peaked around the same time between 18 and 17.5 ka calBP (Nadachowski et al. 2018). Given the subsequent decrease of this species, it is highly likely that many mammoth remains that could be gathered in the landscape probably date to between 18 and 17.5 ka calBP. For the age

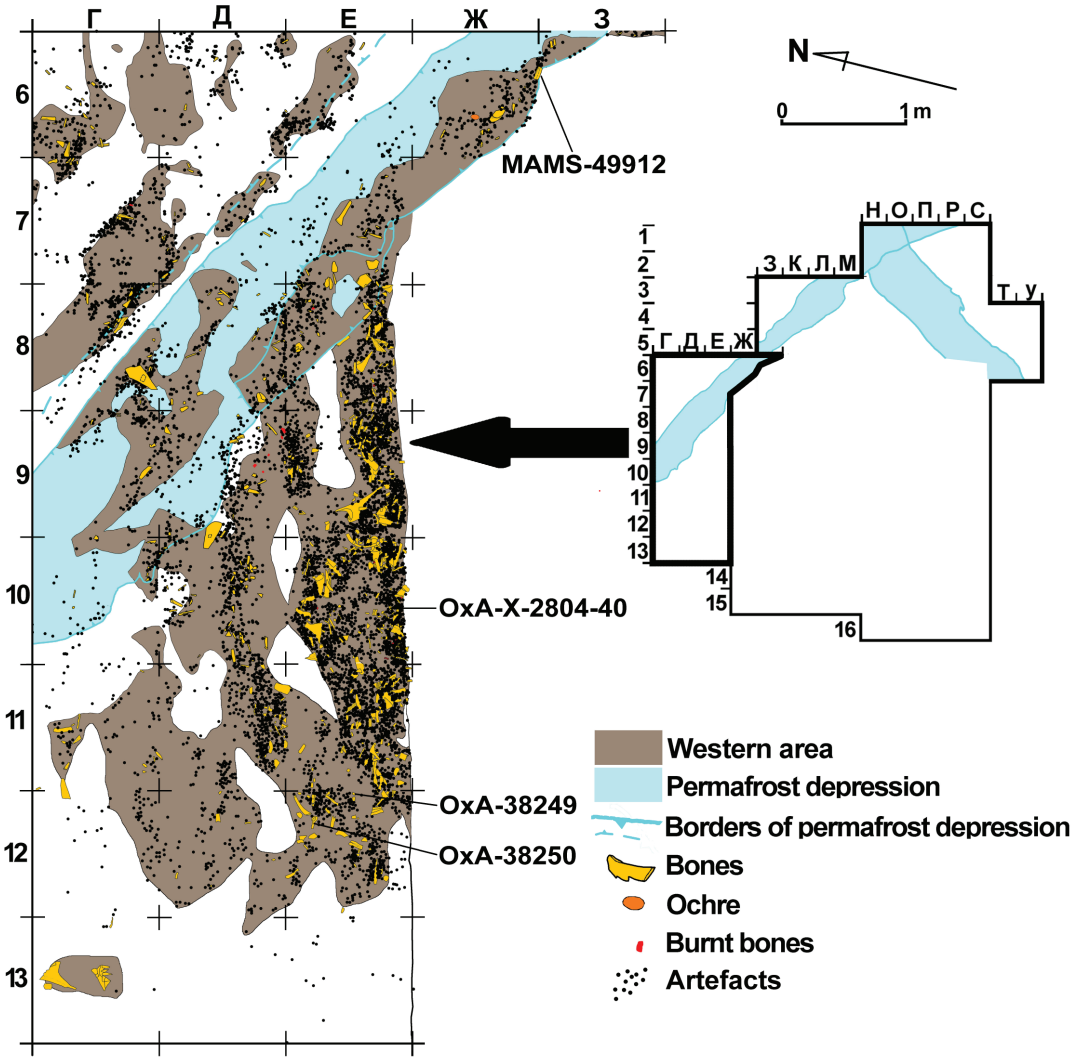


Fig. 3–1. Origin of the bone samples used for radiocarbon dating. For details see Table 3–1.

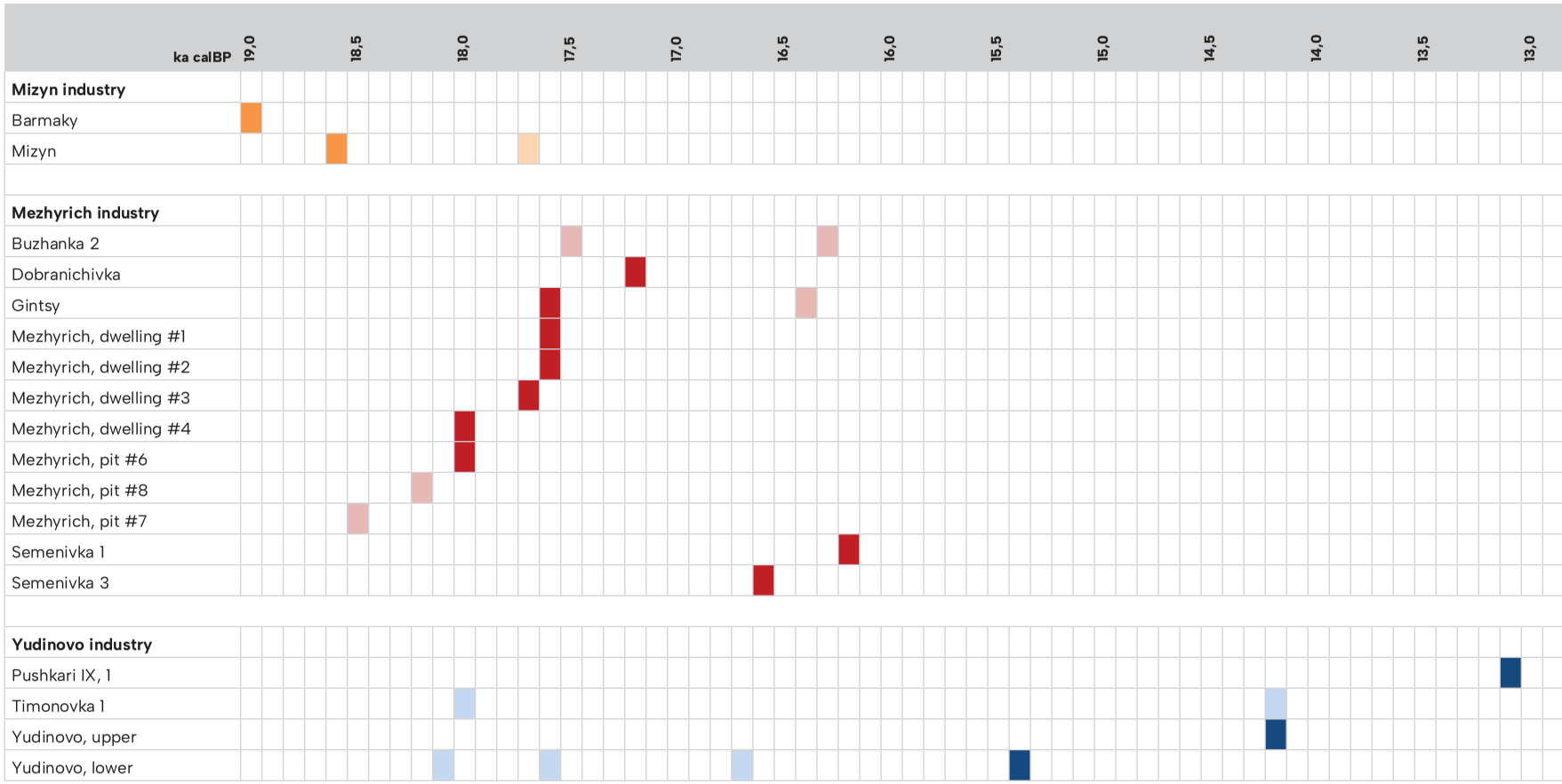


Fig. 3-2. Chronological position of dated assemblages from the Mizyn, Mezhyrich, and Yudinovo industries. Light colours: single dates and weighted averages including mammoth-only and conventional-only date clusters; dark colours: only weighted averages, no conventional-only date clusters, and only the youngest mammoth-only date clusters.

determination of occupations or dynamics of the human population, this signal is likely to be fallacious and should not be taken as a proxy.

If only repeatedly confirmed measurements in the form of weighted averages are accepted, a rather clear chronological succession emerges from the Mizyn industry over the Mezhyrich industry to the Yudinovo industry (Fig. 3-2). In light of these reflections, it seems likely that the Mizyn industry is currently the oldest manifestation of the Epigravettian in the Mid Dnieper region, roughly dated to between 19 and 18 ka calBP (Table 11-3). With the inclusion of Barmaky, level 2, the Mizyn industry also shows the largest extent of the discussed taxonomic units, spanning from the northwest to the northeast of Ukraine. Chronologically, it is followed by the Mezhyrich industry from around 18 to about 16 ka calBP and the Yudinovo industry between 16 and 13 ka calBP (see Chapter 11 for alternative hypotheses). Concerning the variability in lithic insets, this suggests a chronological development of straight-backed microliths into lanceolate microliths and a gain in importance of rectangular microliths in the Mezhyrich and Yudinovo industries.

# BARMAKY: MOLLUSCS (GASTROPODA)

# 4

STEFAN MENG

## SETTING

The archaeological site of Barmaky (50°37.700'N; 26°17.579'E) near Rivne is a part of the Volhynian loess plateau in the NW of Ukraine (see Chapters 1 and 2). The approximately 3 m thick loesses with very rich archaeological layers dated to the early post-LGM period (Nuzhnyi, 2015; see Chapter 3, this volume).

Molluscs (Gastropoda) were also included in the archaeological excavations. The interpretation of fossil terrestrial gastropod faunas is an important tool for palaeoecological reconstructions in the Quaternary. A prerequisite for this is an understanding of the distribution history and ecological requirements of the respective species or species communities. Molluscs can provide important parameters for climate and landscape history, as well as for the interpretation of archaeological sites (Ložek 1964; Mania 1973; Alexandrowicz 1987; Motuz 1987; Fűköh et al. 1995; Frank 2006; Alexandrowicz et al. 2014; Popiuk et al. 2021; Meng et al. 2021).

## RESULTS

Molluscs are rare in Barmaky. In 120 sediment samples, only 281 gastropod shells were found (Table 4-1). The present material comes from the eastern part of the excavation site from the archaeological levels 2a (squares 4M, 5M, 4H, 5H), 2c (squares 4C, 5C, 5T, 6T, 6У), 2d (squares 5E, 6E, 7E, 8E, 6Ж, 3O, 5O, 4P, 5P, 5C, 6C, 5T, 6T, 5У, 6У) and pit 2 (4H, 5H, 5O) (see Chapter 2).

Despite the small number of individuals, the gastropods (Table 4-1; Fig. 4-1) represent a typical regional cold period fauna of Central and Eastern Europe of a herb-rich tundra steppe.

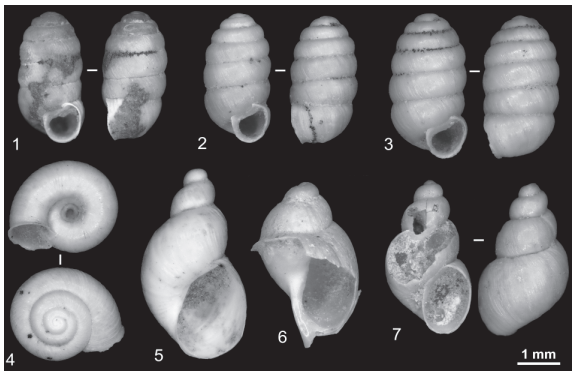


Fig. 4-1. Barmaky, Gastropods (levels/squares): 1 – *Pupilla muscorum* aff. (2c/ 5T), 2 – *Pupilla loessica* (2d/ 5P), 3 – *Pupilla alpicola* aff. (2d/ 5P), 4 – *Vallonia tenuilabris* (2a/ 5M), 5 – *Succinella oblonga* (2d/ 6T), 6 – *Radix* sp. (2pit/ 4H), 7 – *Galba truncatula* (2a/ 5M).

The dominant elements are *Pupilla loessica, Succinella oblonga, Vallonia tenuilabris* or *Trochulus hispidus*. Currently, *P. loessica* and *V. tenuilabris* can be found in large numbers in Central Asia, e.g., in the humid high mountain habitats of Altai and Tien Shan or, for example, in the permafrost regions of N Mongolia, e.g., around Lake Khövsgöl-Nuur (Meng 2009; Meng and Hoffmann 2009; Meng et al. 2021; Horsák et al. 2010; Haase et al. 2021). The relationship between cold-age *Pupilla* species and recent faunas is not yet fully understood. In a comprehensive study (e.g., Haase et al. 2021), recent *Pupilla* from Central Europe and Central Asia as well as fossil materials from Central Europe were compared with each other. It was found that the recent *P. pratensis* (Clessin) is genetically and the fossil *P. muscorum densegyrata* Ložek morphometrically identical to *P. alpicola*. *P. alpicola* of Barmaky is therefore also labelled with "aff.". This species prefers marshy meadows. Overall, the fauna does not describe extremely arid steppe habitats, but rather some-

| horizons | number of samples | squares | Terrestrial gastropods | | | | | | | Limnic gastropods | | | Total shells: |
|---|---|---|---|---|---|---|---|---|---|---|---|---|---|
| | | | *Succinella oblonga* (Drap.) | *Vallonia tenuilabris* (Al. Br.) | *Pupilla alpicola* aff. (Charp.) | *Pupilla loessica* (Ložek) | *Pupilla muscorum* aff. (L.) | *Pupilla* sp. | *Trochulus hispidus* (L.) | *Radix* sp. | *Galba truncatula* (O.F. M.) | *Planorbis planorbis* (L.) | |
| 2a | 3 | 4M | 1 | – | – | – | – | – | – | – | – | – | **1** |
| | 1 | 5M | 1 | 1 | 1 | – | – | – | – | – | 1 | – | **4** |
| | 1 | 4H | – | 1 | – | – | – | – | – | – | – | – | **1** |
| | 1 | 5H | – | – | – | 1 | 2 | – | – | – | – | – | **3** |
| 2c | 1 | 4C | 2 | – | – | – | – | – | – | – | – | – | **2** |
| | 1 | 5C | 1 | – | – | – | – | – | – | – | – | – | **1** |
| | 1 | 5T | 1 | – | – | – | – | – | – | – | – | – | **1** |
| | 1 | 6T | 1 | – | – | – | 1 | – | – | – | – | – | **2** |
| | 1 | 6У | – | – | – | – | – | – | 1 | – | – | – | **1** |
| 2d | 7 | 5E | 1 | – | – | – | – | – | 3 | – | – | 2 | **6** |
| | 2 | 6E | – | 1 | – | – | – | – | 1 | – | – | – | **2** |
| | 2 | 7E | – | – | – | – | – | – | 2 | – | – | – | **2** |
| | 6 | 8E | – | – | – | 3 | – | 1 | 2 | – | – | 1 | **7** |
| | 2 | 6Ж | 1 | – | – | – | – | – | – | – | – | 2 | **3** |
| | 1 | 3O | 2 | – | – | – | – | – | – | – | – | – | **2** |
| | 1 | 5O | – | 1 | – | – | – | – | – | – | – | – | **1** |
| | 3 | 4P | 1 | 1 | – | – | – | – | – | – | – | – | **2** |
| | 6 | 5P | 3 | 1 | 3 | – | – | 3 | – | – | – | – | **10** |
| | 13 | 5C | 6 | 3 | – | 5 | – | 1 | 2 | – | – | – | **17** |
| | 9 | 6C | 6 | – | 1 | 11 | – | 3 | 1 | – | – | – | **22** |
| | 11 | 5T | 17 | – | 3 | 23 | 1 | 1 | – | – | – | – | **45** |
| | 35 | 6T | 42 | 1 | 4 | 71 | – | 2 | 6 | – | – | – | **126** |
| | 1 | 5У | – | – | – | – | – | – | 1 | – | – | – | **1** |
| | 5 | 6У | 1 | – | 3 | 8 | – | – | 2 | – | – | – | **14** |
| pit 2 | 1 | 4H | – | – | – | – | – | – | – | 1 | – | – | **1** |
| | 3 | 5H | – | – | – | 1 | – | 2 | – | – | – | – | **3** |
| | 1 | 5O | – | – | – | – | – | – | 1 | – | – | – | **1** |
| **Total:** | **120** | **–** | **87** | **10** | **15** | **123** | **4** | **13** | **22** | **1** | **1** | **5** | **281** |

Table 4-1. Barmaky, Gastropods: total individuals, levels, squares, samples.

what more humid conditions, which can at least be confirmed by the rich vertebrate faunas (see Chapter 5).

Occasional freshwater gastropods were also found in Barmaky, such as *Radix* sp., *Galba truncatula* and *Planorbis planorbis* (Table 4-1; Fig. 4-1). These species are typical of temporary and standing waters (Glöer 2019). Due to the low density of individuals, however, the shells were likely relocated from the surrounding area, where moist areas with small bodies of water had developed.

As the investigated loess profile is crossed by numerous crotowinas, Holocene and subrecent gastropods, such as *Chondrula tridens* (O.F. M.), *Vallonia excentrica* (Sterki), *Oxychilius depressus* (Sterki) were relocated into the profile section. These species were therefore not considered in detail here.

In addition, small fragments of marine molluscs (Gastropoda, Bivalvia) from the Miocene, which is common in the neighbouring area, were found in the entire loess profile. This unusual phenomenon of relocated marine molluscs in loess is, however, widespread on the Volhynian loess plateau (Chapter 9, this volume).

# THE ANIMAL REMAINS OF BARMAKY, EXCAVATIONS 2018–2020 AND 1990

KERSTIN PASDA

5

## DOCUMENTING METHOD FOR MATERIALS FROM THE 2018–2020 EXCAVATIONS

First recording of the osteological material took place during the ongoing excavation in 2018 and 2019. The finds were carefully cleaned with tap water and air dried. All sediment was sieved, and the resulting identifiable material was recorded at the end of the campaigns.

In the 2018 campaign, each fragment was recorded according to the OssoBook coding system and computer programme (Kaltenthaler et al. 2018). From the 2019 campaign onwards, the data was recorded using ACCESS (Microsoft Office) and finally synchronised. The following parameters were recorded: Archaeological information: abbreviation, find location and year of excavation, find slip number, layer, square/quadrant, line-number, object-number, z-coordinates. Osteoarchaeological information: animal species, skeletal part, bone part, body side, sex, age estimate, age criteria, pathology, marks of slaughtering and dismemberment, marks of burning marks and combustion, weight, and dimensions. No osteological reference collection was available for the taxonomic determination and identification of the skeletal elements during the excavation campaigns from 2018–2029. Individual skeletal elements that could not be identified with certainty were taken to Germany after the recording to check the identification with a reference collection. Elements which had no morphological criteria for species identification wer-categorised into five size classes: mammoth, bison, reindeer, wolf, and hare. The material from 2020 was weighed using a precision scale. A suitcase scale was used for fragments weighing over 1200 g. In the 2019 and 2020 campaign, the largest length of the fragment, rounded up to 1 cm, was added to the 2018 recording criteria. Therefore, the fragment lengths of numerous elements in the western area were not recorded. Measurements were taken according to von den Driesch (1976) and extended with depth measurements according to Pasda (2009) with an electronic calliper to an accuracy of 0.01 mm. For teeth, the largest width and crown height was measured. The crown height was measured labially, for M1–M3 at the highest point, for Pd4 in the centre of the crown.

If a skeletal part was broken into several fragments, only one count was recorded and the state of fragmentation was noted in the database. The fragments were weighed during the 2018–2019 excavation using a simple kitchen scale. The material from the 2020 excavation campaign was exported to Germany in 2023 and was determined with the help of an osteological reference collection. In 2018 individual objects were photographed with a Nikon D5100 and from 2019 on with a Nikon D7500 and a microscope lens (Nikon DX AF-S Micro NIKKOR 40mm 1:2.8 G). In some cases, details were enlarged using a light microscope at the University of Hildesheim.

## DOCUMENTING METHOD FOR MATERIAL FROM THE 1990 EXCAVATION

The osteological material from the 1990 excavation was also recorded. This material was stored in the Rivne Regional Lore Museum. Numerous finds were exhibited in showcases in the exhibition rooms (Fig. 5–1), sometimes together with skeletal elements of other locations. Some of the showcases could be opened, but the objects could not be removed. Those finds clearly attributable to the Barmaky excavation were photographed, and an attempt was made to identify and attribute them based on the photos. The excavations square was noted on the object in many cases. In some cases, however, the labels could not be clearly assigned to an object. When the location of finds was not clearly recognisable, documentation did not take place.

In addition to the objects displayed in the exhibition, numerous larger bones in poorer condition were available in the museum's storage. The material was obviously selected, since only larger, clearly identifiable elements and complete skeletal elements were present. The documentation of this material took place in a fast-track procedure. The labels written on the objects were recorded in full, but it was not always possible to determine the body side. Given the lack of an appropriate scale, the weight was not recorded. The animal species, the skeletal part, the bone part, the rough age, the epiphyseal condition, pathological lesions, and traces of processing were noted, and, in a few cases, measurements and body side were taken. In some cases, the identification was later verified based on photographs.

Fig. 5–1. Barmaky, 1990 field campaign material in the Rivne Natural History Museum.

## Preservation and condition of the osteological material

Bone preservation of the excavations in 1990 and 2018–2020 was generally good. The surface of most specimens showed signs of dissolution due to root corrosion. Sometimes, the bones were perforated and permeated by roots. Some bones and teeth were in an advanced process of decay, only allowing for a classification at species size. Tusk fragments were often chipped off in layers (Fig. 5-2) and frequently only isolated lamellae were found. The substance of many elements was well preserved, making manipulations such as cutting (Fig. 5-3 – 5-6) or impacting (Fig. 5-7; 5-8; 5-9) and, in some cases, use wear on the surface of fragments easily identifiable (Fig. 5-10). No clear instances of carnivore gnawing were identifiable.

Fig. 5-2. Barmaky, *Mammuthus primigenius*: example of the decay of a tusk.

## Minimum Number of Individuals

To calculate the Minimum Number of Individuals (MNI), the most frequent skeletal element was analysed, considering the specific bone part, body side, and age.

## Spatial comparison

The differences in preservation and recording conditions between the osteological material from the 2018–2020 excavation on the one hand, and the selected material from the 1990 excavation on the other, had considerable influence on the analysis of the faunal elements, eventually limiting a joined evaluation of their spatial distribution and a comparison between both excavation campaigns. Additionally, sedimentological differences were observed between the western and the eastern areas of the 2018–2020 excavation (see Chapter 2). Therefore, these areas are considered individually in the following chapter. The evaluation was divided into the square lines Г, Д, Е, Ж, З, К, Л, representing the eastern area, and the squares Н, О, П, Р, С, Т, У, representing the western area. In addition, Pit 2, and horizon 2a were considered individually. As the material from the 1990 excavation cannot be assigned to one of these areas with certainty, this material is considered separately.

Fig. 5-3. Bartmaky, pit 2, *Mammuthus primigenius*, subadult/early Adultas: humerus right, prox. epiphyseal joint in fusion; with impact marks and cut marks (arrows).

Fig. 5–4. Bartmaky, pit 2, *Mammuthus primigenius*: cut marks on a rib.

Fig. 5–5. Barmaky, eastern area, *Mammuthus primigenius*, Infans: costa right; the magnification shows parallel cut marks on the rib corpus.

Fig. 5–6. Barmaky, pit 2, *Mammuthus primigenius*, Adultas: right costa; the corpus shows strong cut marks.

Fig. 5–7. Barmaky, western area, *Mammuthus primigenius*, Adultas: ilium exhibiting parallel indentations.

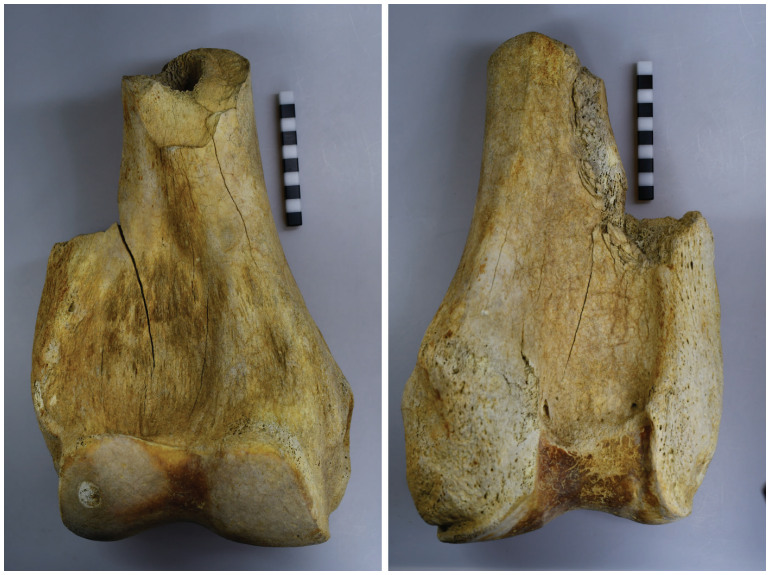

Fig. 5–8. Barmaky, pit 2, *Mammuthus primigenius*, Adultas: humerus left. Dynamic fractures, and impact marks in the distal diaphysis area.

Fig. 5–9. Barmaky, pit 2, *Mammuthus primigenius*, femur diaphysis, dist. unfused, Juvenis; diaphysis is broken up along the shaft in parallel strokes.

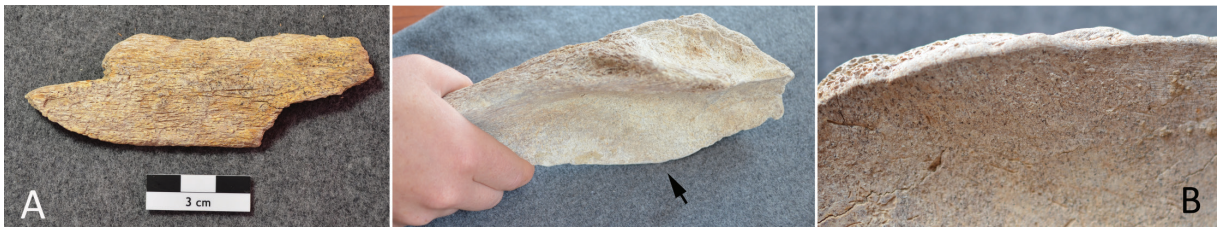


Fig. 5-10. Barmaky, the examples of bones with rounded edges: A – smaller bone fragment; B – mammoth bone.

## RESULTS

The material of the 2018-2020 excavation comprises 4797 fragments (number of identified specimens, NISP) with a weight of 96.7 kg (Table 5-1a). Eleven species were identified with certainty. The same species were represented in the 1990 material, except for saiga, hare and birds. A total of 218 objects could be identified according to species in the material from 1990. All in all, 5015 objects were documented. Remains of small rodents (n=65) could be a modern mixture and are therefore not discussed in detail. The same applies to a shark tooth, which probably originates from the Miocene sediments of the region. Additional sondages were also carried out during the campaigns, also yielding animal remains. However, as the connection with the material from the excavation campaigns is not certain, they are not included in the present analysis (Table 5-1b).

### Mammoth

With a total of 867 single finds (20% of the finds and 67% of the determinable material, 749 of the material from the 2018-2020 excavation) and a weight of 88.6 kg (93% of all weighed fragments) the mammoth is the dominant animal among the finds of Barmaky (Table 5-1a). One Scapula of an adult mammoth was found in a sondage during the 1990 campaign. In total an MNI of 8 mammoths could be calculated.

The age determination of mammoth usually follows age groups that were established on molars (for example Laws 1966). Since naming and numbering of the molars might differ (see overview in Table 5-2), this publication uses numbering from 1 to 6 following Laws (1966). Given the low number of dental remains, parts of the postcranial skeleton were also included in the age estimates following Haynes (2017), who compiled data on modern elephants. Since epiphyseal fusion gives ages prior to, during, or after the process of fusion, the finds were categorised according to the following age groups: 'Infans' (infantile), 'Juvenis' (juvenile), 'subadult/early Adultas' (subadult/early adult), and 'Adultas' (adult). In addition to the age criteria obtained from teeth and epiphyseal fusion of the postcranial bones (Table 5-3), the skeletal elements were also categorised according to their dimensions and bone surface structure (Table 5-4). However, it must be mentioned that both methods, the classification according to age by epiphyseal fusion, but above all the judgement of age based on personal estimation, are not very precise. In other mammals, the stage 'Infans' begins at birth and ends around the time when reaching sexual maturity. Sexual maturity occurs in many mammals with the fusion of the three pelvic parts in the acetabulum. According to Haynes (2017, fig. 1), the pelvic parts of female elephants' fuse at 6 years of age. Accordingly, the age of 0 to 5 years could be categorised as 'Infans'. After the onset of sexual maturity, mammals are generally not yet fully grown. There follows another long phase of skeletal maturity. It is only from the age of 18 that a period of epiphyseal fusion begins, which lasts until the age of 32 in female elephants according to Haynes (2017), and in male elephants, up to over 60 years. The period between 6 and 32 years is here referred to as 'Juvenis'. From the age of 33 in female animals, when all postcranial epiphyses have fused, elephants are likely to have reached the stage of 'Adultus'. In males, this seems to take considerably longer.

| | 2018–2020 | | | | | | | | | 1990 | | material total | |
|---|---|---|---|---|---|---|---|---|---|---|---|---|---|
| | west | | east* | | pit 2 | | horizon 2a | | MNI | | | NISP | MNI |
| **Spezies** | **NISP** | **g** | **NISP** | **g** | **NISP** | **g** | **NISP** | **g** | | **NISP** | **MNI** | | |
| **Mammalia indet. (size of)** | | | | | | | | | | | | | |
| hare | 4 | 1 | – | – | – | – | – | – | – | – | – | 4 | – |
| wolf | 24 | 3,61 | – | – | – | – | – | – | – | – | – | 24 | – |
| reindeer | 2456 | 2312,99 | 729 | 553,7 | 173 | 72,3 | 3 | 9,6 | – | – | – | 3429 | – |
| bison | 226 | 1422,96 | – | – | – | – | 8 | 125,6 | – | – | – | 226 | – |
| mammoth | 65 | 215,7 | – | – | – | – | 30 | 269,0 | – | – | – | 65 | – |
| **Ungulates** | | | | | | | | | | | | | |
| *Mammuthus primigenius* | 365 | 16150,4 | 236 | 15413,1 | 103 | 39900,4 | 45 | 17137,8 | 6 | 118 | 6 | 867 | 10 |
| *Bison* sp. | 33 | 1449,1 | 16 | 284,5 | – | – | 1 | 8,7 | 2 | 24 | 3 | 74 | 3 |
| *Equus* sp. | 1 | 32,6 | – | – | 1 | 31,1 | – | – | 1 | 2 | 1 | 4 | 1 |
| Equus/Bison | 2 | 65,1 | – | – | – | – | – | – | – | – | – | 2 | – |
| *Rangifer tarandus* | 36 | 417,4 | 7 | 370,3 | 1 | 54,4 | – | – | 4 | 22 | 1 | 66 | 4 |
| Bison/Rangifer | – | – | – | – | – | – | – | – | – | 4 | – | 4 | – |
| *Saiga tatarica* | 1 | 78 | – | – | – | – | – | – | 1 | – | – | 1 | 1 |
| **Carnivores** | | | | | | | | | | | | | |
| *Canis lupus* | – | – | – | – | – | – | – | – | – | 2 | 1 | 2 | 1 |
| *Vulpes lagopus* | 22 | 4,6 | 109 | 57,3 | 8 | 204,6 | 2 | 4,0 | 3 | 44 | 3 | 185 | 4 |
| *Ursus arctos* | – | – | 1 | 6,4 | – | – | – | – | 1 | 2 | 1 | 3 | 1 |
| **Rodents** | | | | | | | | | | | | | |
| *Lepus* sp. | – | – | 20 | 7,8 | – | – | – | – | 3 | – | – | 20 | 3 |
| Rodentia indet., small | – | – | 65 | 2,2 | – | – | – | – | – | – | – | 65 | – |
| **Aves/birds** | | | | | | | | | | | | | |
| *Larus argentatus* | – | – | 1 | 2,2 | – | – | – | – | 1 | – | – | 1 | 1 |
| *Phalacrocorax aristotelis* | – | – | 2 | 0,5 | – | – | – | – | 1 | – | – | 2 | 1 |
| **Pisces/fish** | | | | | | | | | | | | | |
| shark indet. | – | – | 1 | 0,1 | – | – | – | – | – | – | – | 1 | – |
| total det. | 460 | 18197,2 | 458 | 16144,4 | 113 | 40190,5 | 48 | 17554,7 | 23 | 218 | 16 | 1297 | 30 |
| total indet. | 2775 | 3956,26 | 729 | 553,7 | 173 | 72,3 | 41 | 9,6 | – | – | – | 3718 | – |
| **material total** | **3235** | **22153,46** | **1187** | **16698,1** | **286** | **40262,8** | **89** | **17564,3** | **23** | **218** | **16** | **5015** | **30** |

Table 5-1a. Barmaky, list of animal species; NISP: Number of Identified Specimen (n); MNI: Minimum Number of Individuals; g: weight in grams. *without horizon 2a and pit 2; pit 1 see Table 5-23.

**Individual 1:** one Adultas (ulna dist. fused).
According to Haynes (2017, fig. 1), the epiphysis at the ulna distalis in elephants fuses with 26–33 years in females, and with approx. 52–66 years in males. This corresponds to Laws' (1966) age group XVI–XIX/XX in females and XXVI/XXVII in males. Located skeleton elements of the Adultas age group see Fig. 5–11 – 5–13.

**Individual 2:** one subadult/early Adultas (humerus prox. in fusion).
The proximal humerus fuses at around 25–31 years of age in female elephants (Haynes 2017, fig. 1). This corresponds to Laws' (1966) age groups of XVI/XVII–XVIII. In males, the epiphysis does not fuse until 40–47 years of age, which corresponds to Laws' age groups of XXIIa–XXV. Located skeleton elements of the subadults/early Adultas age group see Fig. 5–14, and Fig. 5–15.

**Individual 3:** one Juvenis (radius proximal in fusion).
The proximal radius fuses at 24–26 years of age in female elephants (Haynes 2017, Fig. 1), however at > 60 years of age in males. This corresponds to Laws' (1966) age groups of XV–XVI for females and XXVII–XXX for males. Based on the bone dimensions, it is probably a smaller juvenile animal rather than an older bull. Located skeleton elements of the Juvenis age group see Fig. 5–16 – 5–18. A fragment of a smaller tusk (Fig. 5–19) also potentially belongs to this age group.

**Individuals 4–6:** three Infants (two left maxilla with M2 (Fig. 5–20; 5–21) and one isolated left maxilla M2 (Fig. 5–22).
The remains of one left maxilla M2 (Fig. 5–21), and one isolated left maxilla M2 (Fig. 5–22) show that at least two animals of identical age were present. Two sides of a mandibula with the same age as the two maxillae (Fig. 5–23) may belong to one of these individuals. Where the M1 was present, it was 100% worn, and in all M2 specimens, the foremost area of the dental crown was in use and showed 30–40% of wear. According to Laws (1966), these animals were between age group II and III, i.e. older than 6 months and younger than 12 months. According to a statement by P. Wojtal and G. Haynes, these animals were about 9 months old. Given the spatial distribution, these may be the remains of three individual calves. The lower jaw parts (Fig. 5–23) come from Pit 1, an upper jaw (Fig. 5–21) from Pit 2 and the isolated upper tooth (Fig. 5–22) from the channel. The available data suggests a minimum number of 2 individuals of this age.

A third and older infantile mammoth is represented by a maxilla fragment with M2 and M3 (Fig. 5–20). The M2 showed 100% wear, and the M3 50% wear. This corresponds to the age groups of Laws (1966) between IV and V, which is about 2.5 ± ½ years. Located skeleton elements of the Infans age group see Fig. 5–24 – Fig. 5–26.

The western area of the 2018–2020 excavation contains the remains of at least three animals, one early adult or adult (humerus dist. fused), and two infantiles (one left maxilla M2 and a jaw, age group II–III; maxilla with M2, age group IV–V). The eastern area contains the remains of at least five individuals, two adults (two left femur prox. fused), one juvenile (phalanx 2 in fusion), and two infantiles (one left maxilla M2 and one isolated left maxilla M2, age

| | 2018–2020 | | 1990 |
|---|---|---|---|
| **species** | **NISP** | **g** | **NISP** |
| *Mammuthus primigenius* | 6 | 365,75 | 1 |
| *Rangifer tarandus* | 1 | 123,04 | – |
| *Canis lupus* | 4 | 17,04 | – |
| indet. size of reindeer | 50 | 23,82 | – |
| indet. size of wolf | 24 | 3,61 | – |
| **total** | **67** | **533,26** | **1** |

Table 5–1b. Barmaky, animal species found in sondages.

| used in other publications | used in the present publication |
|---|---|
| dp2/pd2 | M1 |
| dp3/pd3 | M2 |
| dp4/pd4 | M3 |
| M1/m1 | M4 |
| M2/m2 | M5 |
| M3/m3 | M6 |

Table 5–2. Barmaky, *Mammuthus primigenius*: designation of the molars.

group II–III). In the material of the 1990 excavation, elements from all areas of the skeleton and at least four individuals were present. With remains of two adults (two tibia prox. fused), one early adult (humerus prox. and femur dist. in fusion), and one juvenile or infantile (two femora dist. unfused) animals, they show a different age distribution than those of the 2018–2020 material. When calculating the MNI for the entire collection, remains representing at least eight individuals are present: three adults (five femura dist. fused), one subadult/early adult (femur dist. and humerus prox. in fusion), one juvenile (phalanx 2, radius prox. in fusion.), and three infantiles (three left maxilla M2, two younger infantiles and one older infantile) animals. The measurements of *Mammuthus primigenius* remains are presented in Table 5-5.

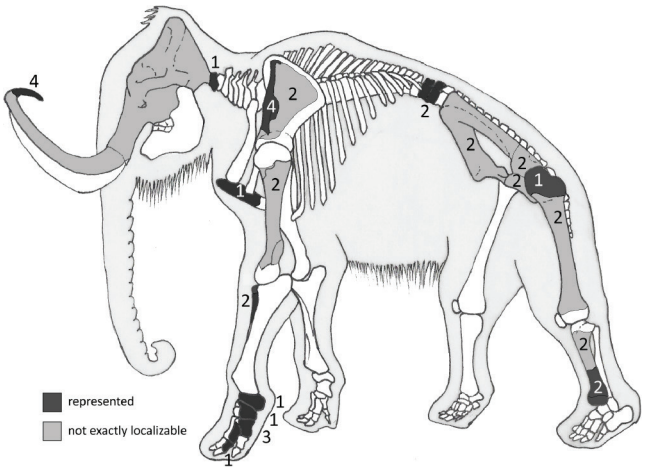


Fig. 5-11. Barmaky, *Mammuthus primigenius*, side undetermined: identified skeletal elements, epiphyses fused. Template redrawn according to Mol & van Essen (1987). Numbers represent the number of finds.

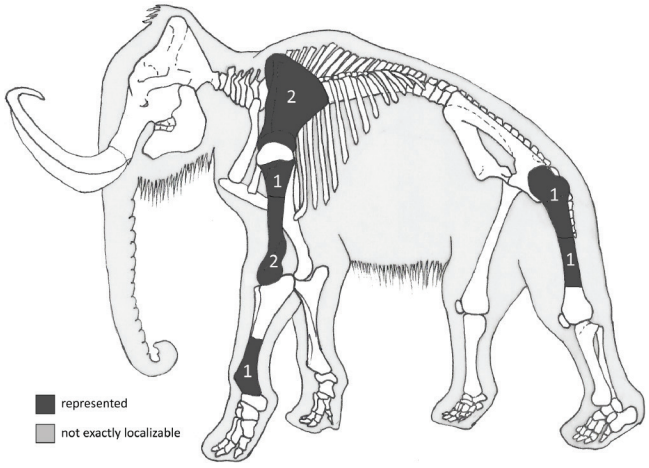


Fig. 5-13. Barmaky, *Mammuthus primigenius*, age group Adultas, left side: identified skeletal elements, epiphyses fused. Template redrawn according to Mol & van Essen (1987). Numbers represent the number of finds.

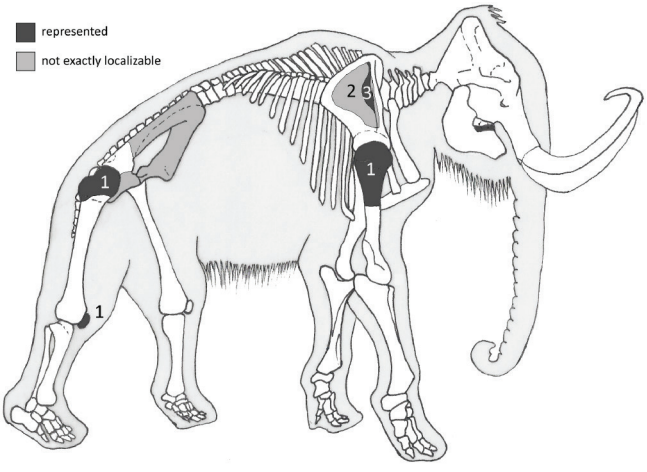


Fig. 5-12. Barmaky, *Mammuthus primigenius*, age group Adultas, right side: identified skeletal elements, epiphyses fused, humerus of subadult individual as the epiphyseal joint is "in fusion". Template redrawn according to Mol & van Essen (1987). Numbers represent the number of finds.

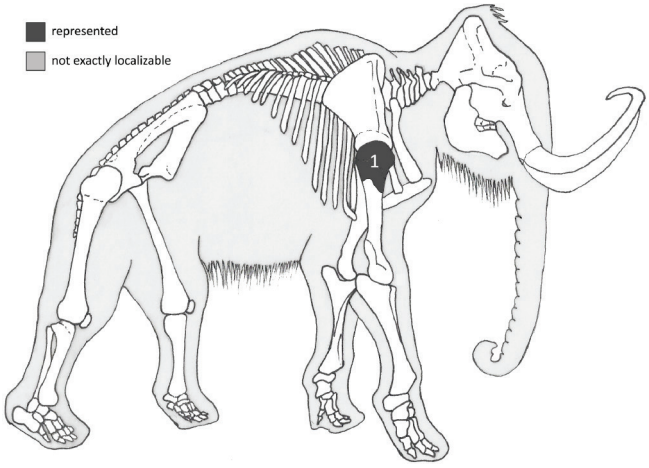


Fig. 5-14. Barmaky, *Mammuthus primigenius*, age group subadult/early Adultas, right side: identified skeletal elements, epiphyses in fusion. Template redrawn according to Mol & van Essen (1987). Numbers represent the number of finds.

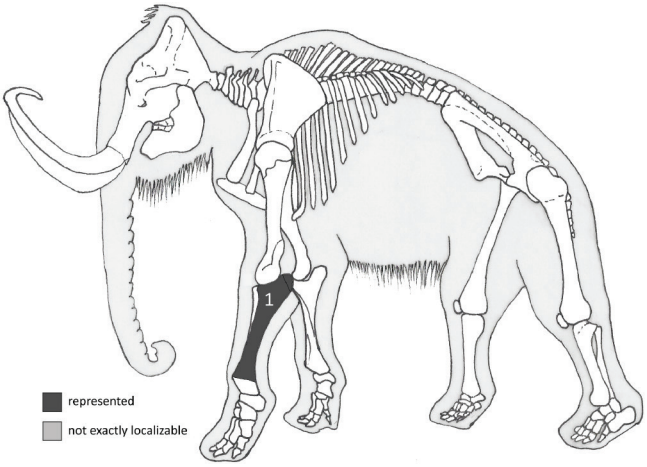


Fig. 5-15. Barmaky, *Mammuthus primigenius*, age group subadult/early Adult, left side: identified skeletal elements, epiphyses unfused. Template redrawn according to Mol & van Essen (1987). Numbers represent the number of finds.

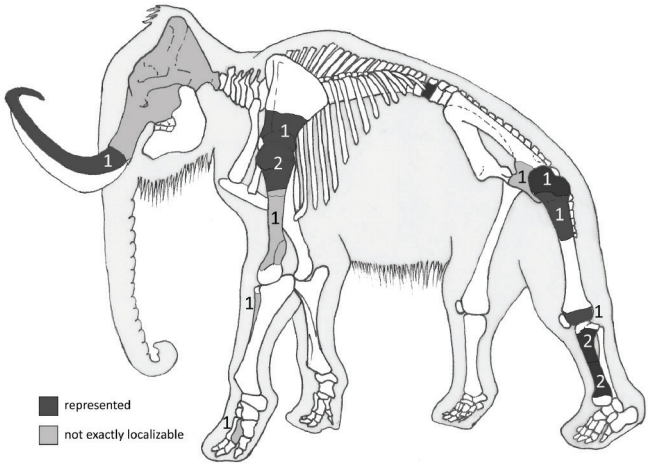


Fig. 5-16. Barmaky, *Mammuthus primigenius*, age group Juvenis, side undetermined: identified skeletal elements, epiphyses unfused. Template redrawn according to Mol & van Essen (1987). Numbers represent the number of finds.

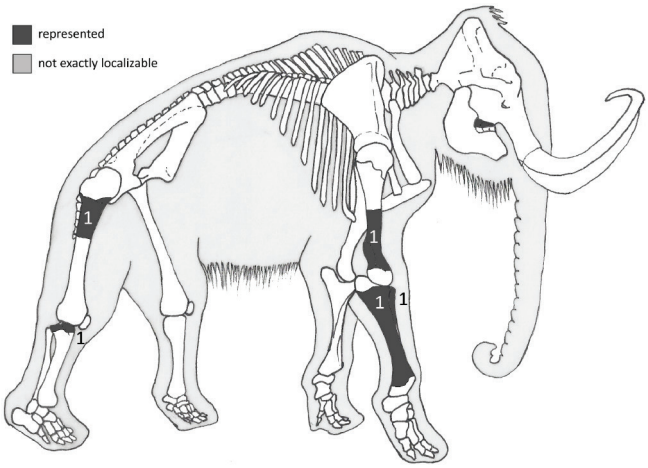


Fig. 5-17. Barmaky, *Mammuthus primigenius*, age group Juvenis, right side: identified skeletal elements of mammoth, epiphyses unfused. Template redrawn according to Mol & van Essen (1987). Numbers represent the number of finds.

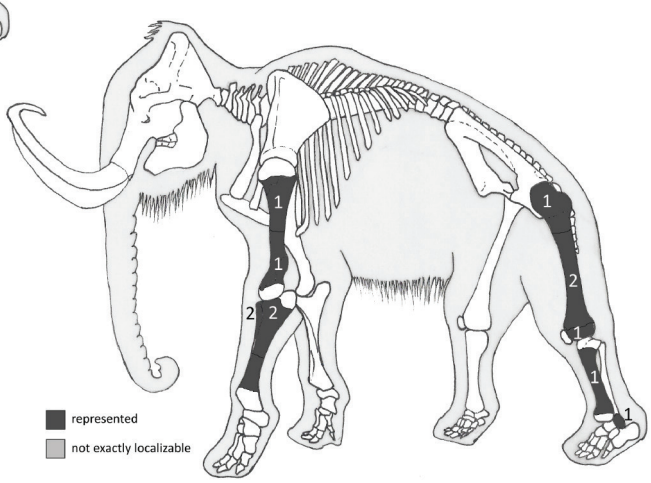


Fig. 5-18. Barmaky, *Mammuthus primigenius*, age group Juvenis, left side: identified skeletal elements, , epiphyses unfused. Template redrawn according to Mol & van Essen (1987). Numbers represent the number of finds.

Fig. 5–19. Barmaky, eastern area, *Mammuthus primigenius*, age group Juvenis: tusk.

Fig. 5–20. Barmaky, western area, *Mammuthus primigenius*, about 2.5 years old (range ½ ± year)/age group Infans: maxilla; M2 100% wear; M3 50% wear; age group between IV and V (Laws 1966).

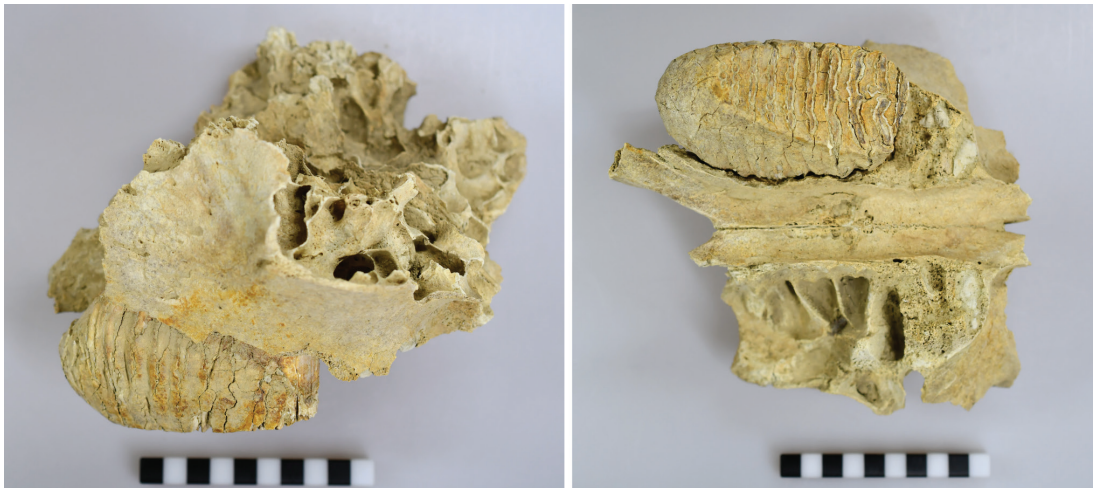

Fig. 5–21. Barmaky, pit 2, *Mammuthus primigenius*, about 9 months old/age group Infans: maxilla, with left M2; M2 30–40% wear; age group between II and III (Laws 1966).

Fig. 5–22. Barmaky, eastern area, *Mammuthus primigenius*, about 9 months old/age group Infans: left maxilla M2, 30–40% wear; age group II – III (Laws 1966).

Fig. 5–23. Barmaky, western area, pit 1, *Mammuthus primigenius*, about 9 months old/age group Infans: left mandibula, with M1 and M2; M1 100% wear; M2 30–40% wear; age group between II and III (Laws 1966).

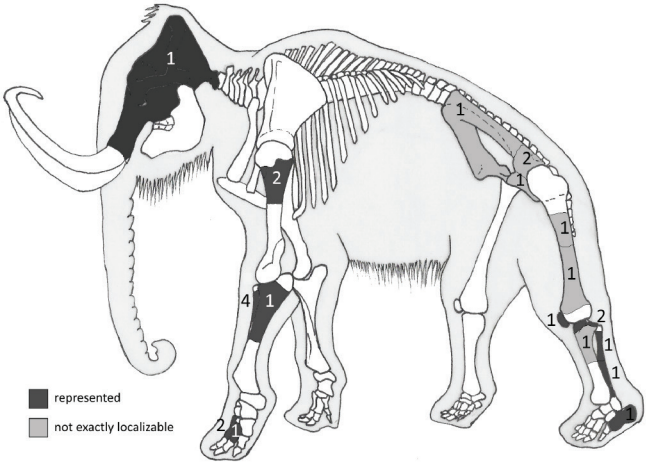


Fig. 5–24. Barmaky, *Mammuthus primigenius*, age group Infans, side undetermined: identified skeletal elements; epiphyses fused; Maxilla. Template redrawn according to Mol & van Essen (1987). Numbers represent the number of finds.

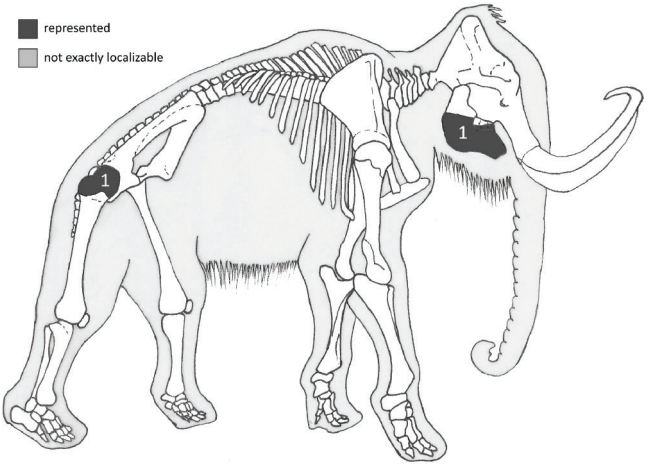


Fig. 5–25. Barmaky, *Mammuthus primigenius*, age group Infans, right side: identified skeletal elements, epiphyses fused. Template redrawn according to Mol & van Essen (1987). Numbers represent the number of finds.

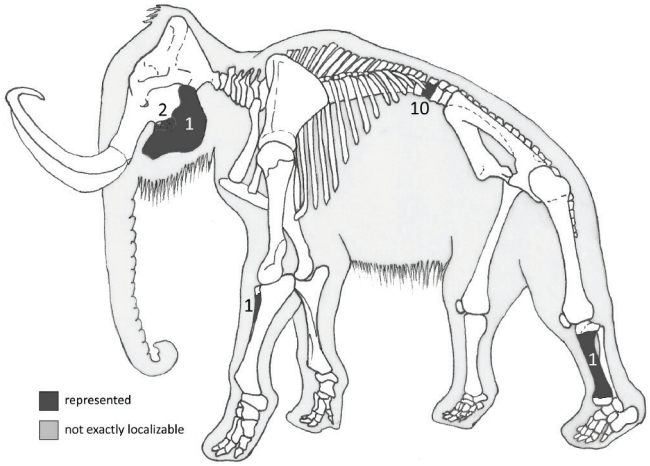


Fig. 5–26. Barmaky, *Mammuthus primigenius*, age group Infans, left side: identified skeletal elements, epiphyses fused – individuals 7–8. Template redrawn according to Mol & van Essen (1987). Numbers represent the number of finds.

| Females | | males | | | unfused | | | | | | | | | in fusion | | |
|---|---|---|---|---|---|---|---|---|---|---|---|---|---|---|---|---|
| Laws age groups | fusion in years | Laws age groups | fusion in years | skeletal element | west left side | west side? | east* right side | east* left side | east* side? | pit 2 right side | pit 2 left side | 1990 side? | **unfused total** | east side? | 1990 side? | **in fusion total** |
| | | | | scapula | – | – | – | – | – | – | – | – | **–** | – | – | **–** |
| VII–XII | approx.10–20,5 | IX–XV | ~10–20.5 | coxa acetabulum | – | – | – | – | – | – | – | 2 | **2** | – | – | **–** |
| XII | 18 | XV | 20,5 | humerus distal | 1 D, 1 E | – | – | – | – | 1 D | – | – | **3** | – | – | **–** |
| | | | | phal.2 | – | – | – | – | – | – | – | – | **–** | 1 | – | **1** |
| XV–XVI | 24–26 | XXVII–XXX | >60 | radius proximal | – | – | – | – | – | – | – | 2 D | **2** | – | 2 | **2** |
| | | | | phal.1 | – | – | – | – | – | – | – | – | **–** | – | – | **–** |
| | | | | metapodials | – | – | – | – | – | – | – | – | **–** | – | – | **–** |
| | | XV | 20,5 | tibia distal | – | – | – | – | – | – | – | – | **–** | – | – | **–** |
| XIII–XVIII | 20–31 | | | fibula distal | 1 E | – | – | – | – | – | – | – | **1** | – | – | **–** |
| | | | | calcaneus | – | – | – | – | – | – | – | – | **–** | – | – | **–** |
| XIII–XVIII | 20–31 | XV | 20,5 | ulna proximal | – | – | – | 1 D | – | – | – | – | **1** | – | – | **–** |
| XIII–XVIII | 20–31 | XIX–XX | 30–33 | femur distal | – | – | – | – | – | – | 3 D, 1 E | – | **4** | – | 1 | **1** |
| XVI/XVII–XVIII | 25–31 | XXIIa–XXV | 40–47 | humerus proximal | 1 D, 1 E | – | – | – | – | – | – | 1 D | **3** | – | 1 | **1** |
| XIII–XVIII | 20–31 | XXII/XXIIb | 37–42 | femur proximal | – | – | 1 D | – | – | 1 E | 1 E | 1 D, 1 E | **5** | – | – | **–** |
| XVII/XVIII–XIX | 29–32 | XVII/XVIII–XVIII/XIX | 28–29 | tibia proximal | – | 2 E | – | 2 D, 1 E | – | – | – | 1 D | **6** | – | – | **–** |
| XVI–XIX/XX | 26–33 | XXVI–XXVII | 52?–66? | radius distal | – | – | – | 1 D | – | – | – | 1 D | **2** | – | – | **–** |
| XVI–XIX/XX | 26–33 | XXVI–XXVII | 52?–66? | ulna distal | – | – | 1 D | 1 D | – | – | 1 D | – | **3** | – | – | **–** |

Table 5–3. Barmaky, *Mammuthus primigenius*, epiphysis fusion, by excavation area and body side; EA: eastern area; WA: western area; 2a: complex 2a and 1990: 1990 field campaign; "?": body side not determined; E: epiphysis; D: diaphysis. *without horizon 2a and pit 2

| Females | | males | | | fused | | | | | | | | | | | |
|---|---|---|---|---|---|---|---|---|---|---|---|---|---|---|---|---|
| Laws age groups | fusion in years | Laws age groups | fusion in years | skeletal element | west left side | east* right side | east* left side | east* side? | horizon 2a | pit 2 right side | pit 2a left side | pit 2 side? | 1990 right | 1990 left | 1990 side? | **fused total** |
| | | | | scapula | – | – | – | – | 1 | – | 1 | – | 1 | 1 | – | **4** |
| VII–XII | approx.10–20,5 | IX–XV | ~10–20.5 | coxa acetabulum | – | – | – | – | – | – | – | – | – | – | – | **–** |
| XII | 18 | XV | 20,5 | humerus distal | 1 | – | – | – | – | 1 | – | – | 1 | – | 1 | **4** |
| | | | | phal.2 | – | – | – | – | – | – | – | 1 | – | – | 2 | **3** |
| XV–XVI | 24–26 | XXVII–XXX | >60 | radius proximal | – | – | – | – | – | – | – | – | – | – | 2 | **2** |
| | | | | phal.1 | – | – | – | 1 | – | – | – | – | – | – | 2 | **3** |
| | | | | metapodials | – | – | – | – | – | – | – | – | – | – | 1 | **1** |
| | | XV | 20,5 | tibia distal | – | – | – | – | – | – | – | – | 1 | 1 | – | **2** |
| XIII–XVIII | 20–31 | | | fibula distal | – | – | – | – | – | – | – | – | – | – | – | **–** |
| | | | | calcaneus | – | – | – | – | – | – | – | – | – | – | 2 | **2** |
| XIII–XVIII | 20–31 | XV | 20,5 | ulna proximal | – | – | – | – | – | – | – | – | – | – | 4 | **4** |
| XIII–XVIII | 20–31 | XIX–XX | 30–33 | femur distal | – | – | – | – | – | – | – | – | 1 | 1 | 3 | **5** |
| XVI/XVII–XVIII | 25–31 | XXIIa–XXV | 40–47 | humerus proximal | – | – | – | – | – | 1 | – | – | 1 | 1 | 1 | **4** |
| XIII–XVIII | 20–31 | XXII/XXIIb | 37–42 | femur proximal | – | 1 | 2 | – | – | – | – | – | – | – | 1 | **4** |
| XVII/XVIII–XIX | 29–32 | XVII/XVIII–XVIII/XIX | 28–29 | tibia proximal | – | – | – | – | – | – | – | – | 1 | 1 | 2 | **4** |
| XVI–XIX/XX | 26–33 | XXVI–XXVII | 52?–66? | radius distal | – | – | – | – | – | – | – | – | – | – | – | **–** |
| XVI–XIX/XX | 26–33 | XXVI–XXVII | 52?–66? | ulna distal | – | – | 1 | – | – | – | – | – | – | – | – | **1** |

Table 5–3. continued.

| | 2018–2020, western area | | | | | | | | 2018–2020 eastern area | | | | | | | | | 2018–2020, horizon 2a | | |
|---|---|---|---|---|---|---|---|---|---|---|---|---|---|---|---|---|---|---|---|---|
| age group/ skel.element | Infans | Infans–Juvenis | Juvenis | Juvenils–early Adultas | early Adultas | early Adultas–Adultas | Adultas | without age criteria | Infans | Infans–Juvenis | Juvenis | Juvenils–early Adultas | not fully grown | early Adultas | early Adultas–Adultas | Adultas | without age criteria | Infans | Adultas | without age criteria |
| cranium | 1 | | | | | | | | 9 | 5 | 1 | | 6 | | | 10 | 8 | 1 | | |
| mandibula | 2 | | | | | | | | | | | | | | | | | | | |
| dens indet. | | | | | | 1 | | | | | | | | | | | | | | |
| maxilla M1 | | | | | | | | | 2 | | | | | | | | | | | |
| maxilla molar | | | | | | | | | | 1 | | | | | | | | | | |
| mandibula molar | | | | | | | | 1 | | | | | | | | | | | | |
| max./mand.molar | | | | | | | 4 | 9 | | | | | | | | | 4 | | | |
| tusk | | | | | | | 74 | 9 | | | 1 | | | | | 30 | | | 3 | |
| atlas | 1 | | | | | | | | | | | | | | | 16 | | | | |
| vertebra cervicalis | 1 | | | | | | | | 2 | | | | | | | | | | | |
| vertebra thoracalis | | | | | | | 2 | | 1 | | | | | | | | | | | |
| vertebra caudalis | | | | | 1 | | | | | | | | | 1 | | 2 | | | | |
| vertebra indet. | | | | | | | | | 8 | | 4 | 2 | 2 | | 1 | 1 | 1 | | | |
| sternum | | | | | | | | | | 1 | | | | | | 1 | | | | |
| costa | 1 | | 2 | | | | 20 | 10 | 2 | | | | 1 | 1 | | 34 | 3 | 2 | | |
| scapula | | | | | | | 6 | 2 | | | | | | | | 4 | | | 2 | |
| coxa | | | | | | | 9 | 7 | | | | | | | | 6 | | | 2 | |
| humerus | | | | | 4 | | 2 | | | | | | | | | | | | | |
| radius | | | 1 | | | | 1 | | 1 | | | | | | | | | | | |
| ulna | | | | | | | | | | | 1 | | | 2 | | | 1 | | | |
| mc III+IV | | | | | | | 1 | | | | | | | | | 1 | | | | |
| patella | | | | | | 1 | | | | | | | | | | | | | | |
| femur | | 2 | | 1 | | | 3 | 3 | | | 1 | | | | | 2 | 2 | | | |
| tibia | 1 | | 1 | 1 | | | 1 | | 1 | | 2 | | | | | | | | | |
| fibula | | | 1 | | | | | | | | | | | | | | | | | |
| phal.1 ant./post. | | | | | | | | | | | | | | | | 1 | | | | |
| phal.2 ant./post. | | | | | | | | | | 1 | | | | | | | | | | |
| sesamoid | 1 | | | | | | | | | | | | | | | | | | | |
| postcran. fragment | 2 | | | | | 1 | 41 | 138 | 13 | | | | 1 | | | 24 | 44 | 4 | 1 | 5 |
| **total** | **10** | **2** | **5** | **2** | **5** | **3** | **164** | **179** | **39** | **8** | **10** | **2** | **10** | **4** | **1** | **132** | **63** | **7** | **8** | **5** |

Table 5–4. Barmaky, *Mammuthus primigenius*, skeletal elements, by age and allocation to the areas; ant.: anterior; post.: posterior; mc: metacarpus; phal.1: phalanx 1/phalanx proximalis; phal.2: phalanx 2/phalanx medialis.

| | 2018–2020, pit 2 | | | | | 1990 | | | | | | 1990 sondage and not assignable finds | | | | | | total |
|---|---|---|---|---|---|---|---|---|---|---|---|---|---|---|---|---|---|---|
| age group/ skel.element | Infans | Juvenis | not fully grown | Adultas | without age criteria | Infans | Juvenis | Juvenils–early Adultas | early Adultas | Adultas | | Infans | Infans–Juvenis | Juvenis | Juvenils–early Adultas | early Adultas | Adultas | |
| cranium | 4 | | 2 | 9 | | | | | | | | | | | | | | **56** |
| mandibula | | | | | | | | | | | | | | | | | | **2** |
| dens indet. | | | | | | | | | | 2 | | | | | | | | **3** |
| maxilla M1 | | | | | | | | | | | | | | | | | | **2** |
| maxilla molar | | | | | | | | | | | | | | | | | | **1** |
| mandibula molar | | | | | | | | | | | | | | | | | | **1** |
| max./mand.molar | | | | | | | | | | 1 | | | | | | | | **18** |
| tusk | | | | 2 | | | | | | 6 | | | | | | | 2 | **127** |
| atlas | | | | | | | | | | | | | | | | | | **17** |
| vertebra cervicalis | | | | | | | | | | | | | | | | | | **3** |
| vertebra thoracalis | | | | | | | | | | | | | | | | | | **3** |
| vertebra caudalis | | | | | | | | | | | | | 1 | | | | | **5** |
| vertebra indet. | 1 | | | | | | | | | | | | | | | | | **20** |
| sternum | | | | | | | | | | | | | | | | | | **2** |
| costa | 2 | 1 | 1 | 23 | | 1 | | | 3 | 26 | 1 | | | | | 1 | 2 | **137** |
| scapula | | | | 8 | | | | | | 1 | | | | | 1 | | 1 | **25** |
| coxa | | | | | 1 | 2 | 1 | | | 3 | | 2 | | | | | | **33** |
| humerus | 1 | | | 3 | | 2 | 1 | | | 1 | | | | 2 | | | | **16** |
| radius | | | | | | 2 | | | | 1 | | 3 | | | | | | **9** |
| ulna | | | | | | 1 | | | | | | | | | | | | **5** |
| mc III+IV | | | | 1 | | | | | | | | | | | | | | **3** |
| patella | | | | | | 1 | | | | | | | | | | | | **2** |
| femur | 1 | 2 | 3 | 2 | | | | | 1 | 5 | | | | 2 | | | 2 | **32** |
| tibia | | | | 1 | | | | 1 | | 2 | | 1 | | | | | 1 | **13** |
| fibula | | | | | | 2 | | | | | | | | | | | | **3** |
| phal.1 ant./post. | | | | | | | | 1 | | | | | | | | | | **2** |
| phal.2 ant./post. | | | | 1 | | 1 | | | | 2 | | | | | | | | **5** |
| sesamoid | | | | | | | | | | | | | | | | | | **1** |
| postcran. fragment | | | | 9 | 21 | 1 | 1 | | 1 | 16 | 2 | | | | | | | **325** |
| **total** | **9** | **3** | **6** | **59** | **22** | **13** | **3** | **2** | **5** | **66** | **3** | **6** | **1** | **4** | **1** | **1** | **8** | **871** |

Table 5–4. continued.

| square, find # | ID | year | skeletal elements | | | | | | | | side |
|---|---|---|---|---|---|---|---|---|---|---|---|
| | | | | **LG** | **BG** | | | | | | |
| 5O, pit 2, #29 | 216 | 2020 | scapula | 125 | 75 | | | | | | left |
| | | | | **Bd** | **Dd** | **BT** | **SD** | **Bp** | | | |
| 5H, pit 2, #7 | 9 | 2019 | humerus | – | – | – | – | 173,7 | | | right |
| 43, pit 2, #10 | 25 | 2019 | humerus | 216,5 | 150 | 173,05 | 89,31 | – | | | left |
| 53, 2d, #10 | 263 | 2019 | humerus | 213,11 | 127,2 | 185,44 | – | – | | | left |
| | | | | **BPC** | **DPA** | **SDO** | **Loe** | | | | |
| 3P, 2a, ash, #1 | 313 | 2020 | ulna | 182,36 | 156,21 | 129,8 | – | | | | right |
| 5O, pit 2, #33 | 571 | 2020 | ulna | 176,94 | 170,79 | 119,18 | – | | | | left |
| 5C, 2d, #35 | 214 | 2020 | ulna | 177,91 | 147,91 | 109,01 | 502 | | | | left |
| | | | | **Bp** | **DC** | **SD** | **Bd** | | | | |
| 5H, pit 2, #21 | 12 | 2019 | femur | – | 143,82 | – | – | | | | left |
| 5H, pit 2, #18 | 519 | 2020 | femur | – | 138,56 | – | – | | | | left |
| 4P, 2d, #10 | 572 | 2020 | femur | 3050 | 134,85 | – | – | | | | left |
| 5H, pit 2, #26 | 575 | 2020 | femur | – | – | – | 210,05 | | | | left |
| 5H, pit 2, #26 | 607 | 2020 | femur | – | – | 120 | – | | | | left |
| | | | | **SD** | **GL** | | | | | | |
| 5C, 2d, #30 | 516 | 2020 | tibia | 50,6 | 247,5 | | | | | | left |
| | | | | **Bp** | **SD** | **Bd** | **Gpl** | **Dp** | **DD** | **Dd** | **GL** |

Table 5–5. Barmaky, *Mammuthus primigenius*, measurements (in mm); ant.: anterior; post.: posterior; phal.2: phalanx 2/ phalanx medialis.

**Abbreviations:**
**Scapula** – LG: length of the glenoid cavity; BG: breadth of the glenoid cavity.
**Humerus** – GLC: greatest length from caput; Bp: breadth of the proximal end; Dp: depth of the proximal end; SD: smallest breadth of the diaphysis; BT: breadth of the trochlea; Bd: breadth of the distal end; Dd: distal depth.
**Ulna** – SDO: smallest depth of the olecranon; DPA: depth across Processus anconaeus; BPC: greatest width of the proximal articular surface; GL: greatest length; Loe: Length of the olecranon.
**Femur** – Bp: greatest proximal width; DC: diameter of the Caput femoris; SD: smallest width of the diaphysis; Bd: greatest distal width.
**Tibia** – GL: greatest length; SD: smallest width of diaphysis; Bd: greatest distal width; Dd: distale Tiefe.
**Phalanx 1, 2** – Gpl: greatest peripheral length; GL: greatest length; Bp: greatest proximal width; SD: smallest width of the diaphysis; DD: smallest depth of the diaphysis; Bd: greatest distal width; Dp: depth proximal; Dd: depth distal.

## Bison

The bison was represented with 74 remains (Table 5-1a). The 33 remains in the western area of the 2018–2020 excavation originate exclusively from adult animals, as do 17 remains in the eastern area (Table 5-6) and come from all areas of the skeleton. At least two individuals can be identified based on four tibiae. In the spatial division of the 2018–2020 excavation areas, at least two bisons (three tibiae) are represented in the western, and at least one bison in the eastern area. A bison maxilla molar was recovered in horizon 2a and therefore represents one MNI. In the material from the 1990 excavation, 24 elements were identified as bison. Skeletal elements from all areas of the skeleton are present, however no cranium or mandibula, but one horn piece was found. The remains come from at least two adults (three patellae), and one juvenile or subadult (costa and tibia dist. unfused; Table 5-7). When looking at the entire material, the remains of at least three bisons are present, one juvenile/subadult, and two adults. The measurements of bison are presented in Table 5-8.

## Horse

Only four remains could be determined with certainty as horse (Table 5-1a). In the material from the 2018–2029 excavation, one tooth was recovered in the western area and one distal phalanx (anterior/posterior) in the eastern area, which came from at least one horse. Two single teeth come from the material of the 1990 excavation and represent the remains of at least one adult horse (Table 5-9). In total, the remains come from at least one adult horse. The measurements of horse are presented in Table 5-10.

## Reindeer

Reindeer could be identified by 67 remains, 66 in the excavation area (Table 5-1a), and one in a sondage (Table 5-1b). In the material of the 2018–2020 excavation, predominantly postcranial limb elements are represented, but no toes (Table 5-11). Given the large size of the remains, only males can be identified with an MNI of three: one adult (no epiphyseal areas present, age determination based on size and bone surface structure), one juvenile/subadult (tibia dist. unfused), one infantile (femur prox. unfused). In the western area, at least three adult reindeer are represented (six tibia diaphyses), along with one juvenile/subadult (one distal tibia unfused). The material from the 1990 excavation includes elements of all areas of the skeleton but no cranium or mandibula. Due to the different stages of epiphyseal fusion, at least three individuals are represented: one adult (ulna prox. fused), one juvenile (ulna and radius prox. unfused), and one infantile/juvenile (Mt III+IV unfused). In the eastern area, at least one male adult individual is represented. In total, at least four individuals are represented: one infant, one juvenile or subadult, and two adults. All bones showed traces of green bone breakage and impacts and therefore were probably smashed to be cooked to extract the fat (Fig. 5-27). The measurements of reindeer are presented in Table 5-12.

## Saiga

Saiga is represented by a single bone only. This bone was found in square 10E, find no. 4, western area. The proximal end with part of the diaphysis of a right femur had a prox. unfused epiphysis and so came from a juvenile or subadult animal. The femur measurements are presented in Table 5-13.

## Wolf

The wolf is represented by two finds in the material from the 1990 excavation (Table 5-1a). Another four finds came from sondages carried out during the 2018–2020 excavation campaigns (Tables 5-14; 5-15) with unclear connection to the excavation. Based on the remains, only one individual of a fully-grown wolf can be confirmed.

## Arctic fox

Arctic fox (or polar fox, *Vulpes lagopus or Alopex lagopus*) was represented by a total of 185 finds (Table 5-1a) from all areas of the skeleton (Table 5-16). All remains came from fully grown animals and most were complete

| skeletal element | 2018–2020, western area | | | | | | | | | | | 2018–2020, eastern area | | | | | | | | | | | horizon 2a |
|---|---|---|---|---|---|---|---|---|---|---|---|---|---|---|---|---|---|---|---|---|---|---|---|
| | 10Д | 5, 6Л | 5Г ? | 8Г | 6К | 2Е | 8Е | 9Е | 10Е | 11Е | 12Е | 2Р | 4Р | 4Т | 5Р | 5Т | 6Т | 4С | 4Р | 5С | 5Р | 6Т | 6П |
| processus cornualis (horn) | | | | | | | | | 1 | | | | | | | | | | | | | | |
| cranium | | | | | | | | | | | | | 1 | | 1 | | | | | | | 1 | |
| mandibula | | | | | | | | | | | | | | | | | | | | | | 1 (right) | |
| maxillamolar | | | | | | | | | | | | | | | | | | | | | | | 1 |
| mandibula M1 | | | | | | | | | | | | | | | | | | | | 1 (right) | | | |
| costa | | 1 | 1 | 1 | | | | 3 | 4 | 5 | 1 | | | 1 | 1 | 1 | 1 | 1 | | 1 | 2 | | |
| scapula | | | | | 1 | | | | 1 | | | | | | | | | | | | | | |
| humerus | | | | | | | | 1 (left) | | 1 (left) | | | | | | | | | | | | | |
| mc III+IV | | 1 | | | | | | 2 | | | | 1 | | | | | | | | | | | |
| femur | | | | | | | | 1 (left) | 1 (right) | | | | | | | | | | | | | | |
| tibia | | | | 1 | | | | | | 1 | 1 | | | | | | | | 1 (right) | | | | |
| phal.1, post. | 1 | | | | | | 1 | | | | | | | | | | | | | | | | |
| postcran. fragment | | | | | | 1 | 1 | | | | | | | | | | | | | | 1 | | |

Table 5–6. Barmaky, western and eastern areas by squares, *Bison* sp., skeletal elements, all adult/epiphyses fused; l: left; r: right; mc: metacarpus; phal.1: phalanx 1/phalanx proximalis; post.: posterior.

Fig. 5–27. Barmaky, 1990 field campaign (a) and pit 2 (b), *Rangifer tarandus*: a – humerus dist., radius prox., ulna prox.; b – left femur prox., male.

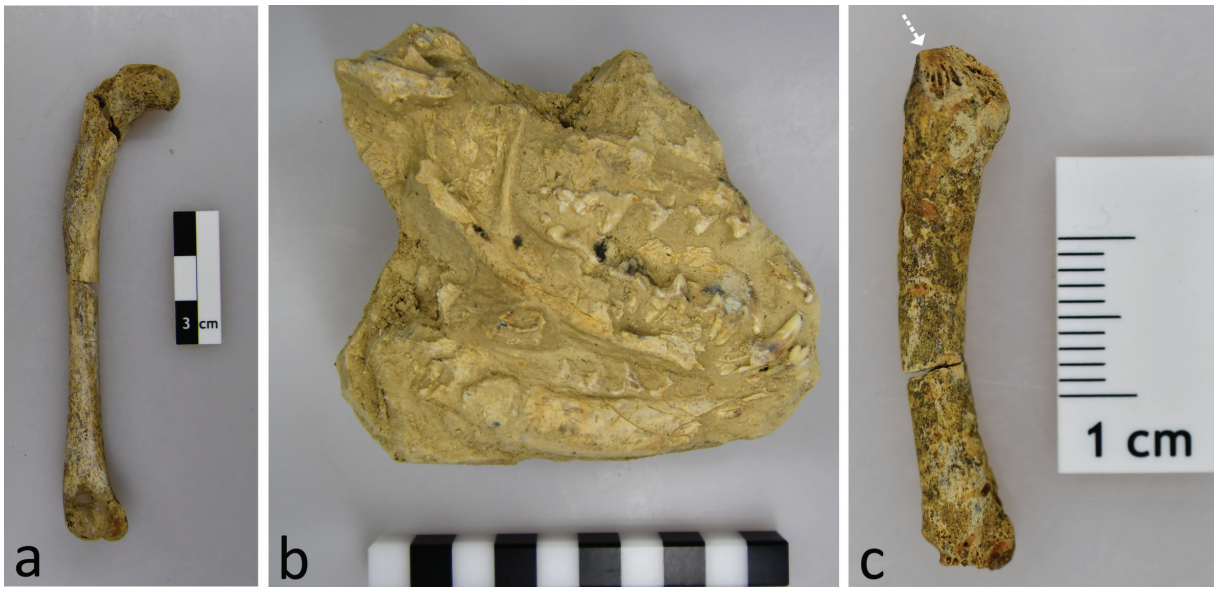


Fig. 5–28. Barmaky, pit 2 (a, b) and eastern area, pit 1 (c), *Vulpes lagopus*: a – right humerus; b – right and left Cranium and Mandibula; c – right MC IV, cut smoothly proximal to the joint end (arrow).

(example Fig. 5-28, a). The distribution of partial skeletons (predominantly paw bones in the bandage and complete head, Fig. 5-28, b) and multiple occurring elements suggest the presence of at least one fox in the western area and three foxes in the eastern area. If horizon 2a and Pit 2 are considered separately, there is at least one fox in horizon 2a and two foxes in Pit 2. Altogether, remains of at least three adult foxes are present in the excavation area from 2018-2020 (two complete right humeri, one right humerus proximalis). Fox bones from the 1990 excavation come from at least three adults (three right mandibulae, three left mandibulae). Due to the number of right mandibulae in the complete material, at least four adult individuals are represented. The measurements of arctic fox bones are presented in Table 5-17.

## Brown bear

Brown bear is present with three finds (Table 5-18). One right carpal (pyramidal/ulnar) of an adult bear was found in the 2018-2020 excavation. Two femora were present in the material from the 1990 excavation, one diaphysis and a right distal end with fused epiphysis, which are possibly of the same animal. The right femur – labelled with the species identification "bison" – shows remarkable arthritic destruction of the knee joint (Fig. 5-29). This indicates that the bear was relatively old and likely had some form of disability. All finds may come from a single individual.

## Hare

A total of 20 remains of hares were found (Table 5-1a), located exclusively in the eastern area of the excavation campaign of 2018-2020. Apart from four skull- and one radius fragment, the finds came from the paws (Table 5-19; measurements Table 5-20). The remains are from possibly three individuals, although the finds are in neighbouring quadrants (4P, 5C, 5P, 6T; eastern area), with two adults (fused epiphyses), and one juvenile animal (unfused epiphysis).

## Seagull

The distal end of a right humerus of an adult herring gull (or seagull, *Larus argentatus*) was found in square 6T, eastern area, find-no. 48 (Fig. 5-30).

## Shag

A shag (*Phalacrocorax aristotelis*) was represented by two bones from one individual found in square 6T, eastern area (find-no 113). One right radius diaphysis, right distal end and right diaphysis of an ulna are from an animal which was not fully grown.

Fig. 5-29. Barmaky, 1990 field campaign: *Ursus arctos*, femur distal. Pathological lesion at the margins of the distal articular surface: marginal exostosis (white arrow) and depression (black arrow) due to a localized inflammatory process.

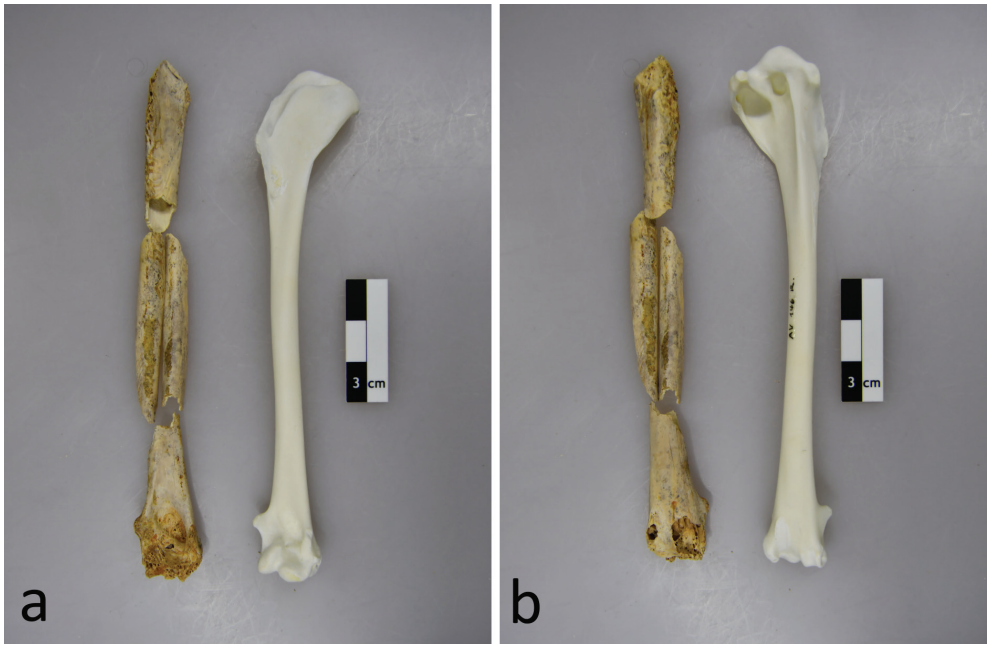


Fig. 5-30. *Larus argentatus*, humerus right adult: a – cranial view; b – caudal view; left – Barmaky, eastern area specimen, right – comparative skeleton of a seagull.

| skeletal elements | 9H | 7K | 6O | 6Ж | 6K | 63 | 7Ж | 7K | 8Ж | 9Ж | 93 | unclear |
|---|---|---|---|---|---|---|---|---|---|---|---|---|
| processus cornualis (horn) | | | | | | | | 1 | | | | |
| costa | | 1 - | 1 | 1 | 1 | 1 | | 3 | 2 | 1 | 1 | |
| humerus | | | | | | | | 1 | | | | |
| radius | | | | | | | | 1 | | | | 1 |
| ulna | | | | | | | | 1 | | | | |
| mc III+IV | | | | | | | | | | 1 | | |
| patella | | | | | 1 | | | 1 | | | | 1 |
| tibia | 1 dist. - | | | | | | | | | | | |
| tarsale | | | | | | | | 1 | | | | |
| phal.1 ant./post. | | | | | | | 1 | | | | | |

Table 5-7. Barmaky, 1990 field campaign by squares, *Bison* sp., skeletal elements; –: unfused; mc: metacarpus; phal.1: phalanx 1/phalanx proximalis; ant.: anterior; post.: posterior.

| square, find # | ID | year | skeletal elements | | | | | | | | side |
|---|---|---|---|---|---|---|---|---|---|---|---|
| | | | | LM1 | BM1 | ZhM1 | | | | | |
| 5C, 2d, #45 | 397 | 2020 | mandibula M1 | 31 | 15,03 | 42,92 | | | | | right |
| | | | | Bp | SD | Bd | Gpl | Dp | DD | Dd | GL | |
| 10Д, #13 | 157 | 2019 | phal.1, post. | 28,04 | 25,18 | 27,86 | 61,12 | 27,11 | 14,43 | 18,55 | 57,55 | – |
| 8E, #16 | 369 | 2019 | phal.1, post. | 26,15 | 21,79 | – | – | 27,2 | – | – | – | – |

Table 5–8. Barmaky, *Bison* sp.; measurements (in mm); post.: posterior; phal.1: phalanx 1/phalanx proximalis.

**Abbreviations:**
**Mandibula M1** – LM1: length of the M1 crown; BM1: breadth of the M1 crown; ZhM1: crown height labially at the centre of the crown.
**Phalanx 1, 2** – Gpl: greatest peripheral length; GL: greatest length; Bp: greatest proximal width; SD: smallest width of the diaphysis; DD: smallest depth of the diaphysis; Bd: greatest distal width; Dp: depth proximal; Dd: depth distal.

| skel. element | 2018–2020, western area sq. 43 | 2018–2020, pit 2 sq. 50 | 1990 sq. 83 |
|---|---|---|---|
| maxillamolar | – | – | 1 |
| mandibula M3 | – | – | 1 |
| mandibula P left | 1 | – | – |
| phal. 3 ant./post. | – | 1 | – |

Table 5–9. Barmaky, *Equus* sp., skeletal elements, all adult/epiphyses fused; phal.3: phalanx 3/phalanx distalis; ant.: anterior; post.: posterior.

| square, find # | ID | year | skeletal elements | | | | side |
|---|---|---|---|---|---|---|---|
| | | | | LP4 | BP4 | LhP4 | |
| level 1, sq.4E | 367 | 2018 | mandibula P4 | 29,28 | 16,51 | 39,01 | left |
| | | | | Ld | BF | | |
| 5O, pit 2, #24 | 238 | 2020 | phal.3, ant./post. | 52,28 | 49,96 | – | – |

Table 5–10. Barmaky, *Equus* sp., measurements (in mm); ant.: anterior; post.: posterior; phal.3: phalanx 3/phalanx distalis.

**Abbreviations:**
**Mandibula** – LP4 length of the P4 crown; BP4: breadth of the P4 crown; LhP4: crown height of the P4 labially at the centre of the crown.
**Phalanx 3** – BF: breadth of the Facies articularis, Ld: length of the dorsal surface.

| skel. element | 2018–2020, western area | 2018–2020, eastern area* | 2018–2020, pit 2 | sondage L–32 | 1990 |
|---|---|---|---|---|---|
| antler | 1 | 1 ma | | 1 ma | 1 |
| cranium | 3 | | | | |
| costa | 7 | 5 | | | 3 |
| vertebra thoracalis | | | | | 2 – |
| vertebra | | | | | 3 – |
| scapula | 2 | | | | |
| humerus | 1 | | | | 1 prox. +/–, 1 prox. E. – |
| ulna | | | | | 1 + |
| radius | 1 | | | | 1 + |
| mc III+IV | | | | | 1dist. D –, 1 dist. E – |
| femur | 3 D, 1 prox. E – | | 1 left prox. +, ma | | 1 dist. +/– |
| tibia | 6 D, 1 dist. D – | | | | 1 prox. – |
| fibula | 1 | | | | |
| centroquartale | | | | | 1 + |
| calcaneus | | 1 left +, ma | | | |
| astragalus | 1 | | | | |
| metapodium indet. | 1 | | | | |
| mt III+IV | 4 D, 1 D + | | | | 2 |
| sesamoideum | 1 | | | | |
| postcran. fragment | 2 | | | | |

Table 5–11. Barmaky, western area (WA), eastern area (EA), sondage 4 and 1990 field campaign (1990): *Rangifer tarandus*, skeletal elements divided according to area; ma: male; E: epiphysis, D: diaphysis; +: fused; –: unfused; +/–: in fusion; mc: metacarpus; mt: metatarsus. *without pit 2.

| square, find # | ID | year | skeletal elements | | | | | side | sex |
|---|---|---|---|---|---|---|---|---|---|
| | | | | **DC** | | | | | |
| 5O, pit 2, #19 | 513 | 2020 | femur | 42,2 | | | | left | male |
| | | | | **SD** | **Bd (unfused)** | **Dd (unfused)** | | | |
| 12E, #28 | 104 | 2018 | tibia | 36,9 | 49,34 | 36,97 | | left | – |
| | | | | **GLl** | **GLm** | **Dl** | **Bd** | | |
| 10E, #3 | 59 | 2018 | astragalus | 54,06 | 51,1 | 29,77 | 35,34 | right | – |
| | | | | **GL** | **GB** | | | | |
| 6T, 2d, #10 | 330 | 2020 | calcaneus | 106,03 | 51,34 | | | left | male |

Table 5–12. Barmaky, *Rangifer tarandus*: measurements (in mm).

**Abbreviations:**
**Femur** – Bp: greatest proximal width; DC: diameter of the Caput femoris; SD: smallest width of the diaphysis; Bd: greatest distal width.
**Tibia** – SD: smallest width of diaphysis; Bd: greatest distal width; Dd: distal depth.
**Astragalus** – GLl: lateral length; GLm: medial length; Dl: lateral depth; Bd: width of the caput.
**Calcaneus** – GL: greatest length; GB: greatest width.

| square, find # | ID | year | skeletal elements | | side |
|---|---|---|---|---|---|
| | | | | DC | |
| 10E, #48 | 105 | 2018 | femur | 42 | right |

Table 5-13. Barmaky, *Saiga tatarica*: measurements (in mm).

**Abbreviations:**
**Femur** – Bp: greatest proximal width; DC: diameter of the Caput femoris; SD: smallest width of the diaphysis; Bd: greatest distal width.

| skeletal elements | 1990, sq. 7K | 1990, sq. 73 | sondage 4 | sondage 4 |
|---|---|---|---|---|
| cranium | – | – | 1 | – |
| mandibula | – | – | 1 | – |
| dens indet. | – | – | 1 | – |
| costa | 1 | – | – | – |
| calcaneus | – | – | – | 1 (left) |
| vertebra cervicalis | – | 1 | – | – |

Table 5-14. Barmaky, *Canis lupus*, skeletal elements, all adult/epiphyses fused.

| square, find # | ID | year | skeletal elements | | side |
|---|---|---|---|---|---|
| | | | | GB | |
| sondage 4 | 274 | 2019 | calcaneus | 26,07 | left |

Table 5-15. Barmaky, *Canis lupus*: measurements (in mm).

**Abbreviations:**
**Calcaneus** – GB: greatest width.

## Proportion of animal species

Among the 2018–2019 faunal remains, mammoth makes up by far the largest part of the ungulates, both in terms of the numbers (Fig. 5-31, a) and weight (Fig. 5-31, b). Bison and reindeer were represented in about equal proportions (Fig. 5-31, a), while horse and saiga are only represented with a few finds. Since weight reflects the relevance for the human diet better than numbers, the latter is more significant. In this scenario, mammoth contributed the largest amount, while bison, reindeer, horse and saiga were apparently quite insignificant.

A comparison of the eastern and western areas of the 2018–2020 excavation shows differences in the proportions of animal species. Looking at the number of finds, carnivores are often represented in the eastern area (Fig. 5-32, c), among which arctic fox and wolf could be identified, with the former occurring in higher numbers. Reindeer and bison, on the other hand, are more common in the western area (Fig. 5-32, a). When comparing the weight of finds, bison and reindeer make up a larger proportion in the western area (Fig. 5-32, b).

From the 1990 excavation, 218 objects have been documented (Table 5-1a). Seven species corresponding to those from 2018–2020 could be identified. Saiga, birds and hare, however, are not represented. The proportions of the individual species (Fig. 5-33) also roughly correspond to the proportions of the 2018–2020 excavation. The observation that mammoth is less frequently represented in favour of the other species may result from the fact that only skeletal elements with clear morphological features were present in the museum. This may also be the reason for the absence of small species such as birds or hares.

The comparison of the MNI between the eastern and western areas (Fig. 5-34, a, b and Table 5-21) shows that the larger number of finds in the eastern area corresponds with the fact that more species are represented there. There is no major difference between the MNI proportions of the species represented between the 2018–2020 excavation and the 1990 archaeological material. In fact, the MNI in the eastern area of the 2018–2020 excavation and in the 1990 excavation is identical with 15 individuals each (Fig. 5-34, b, c), although the number of underlying observations is significantly different with 1715 in the 2018–2020 (Fig. 5-34, b), and at 218 in the 1990 (Fig. 5-34, c) material. To summarise, the species represented are the same in all areas except for minor deviations. This may indicate that there is no large temporal difference in the occupation of the areas.

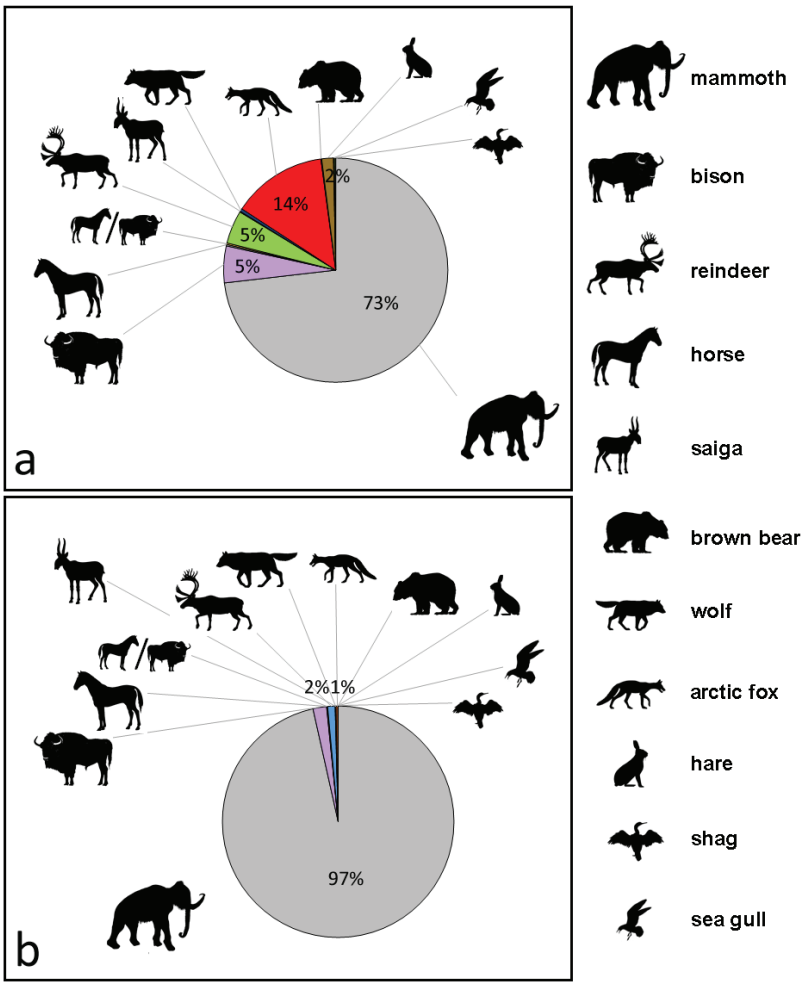


Fig. 5-31. Barmaky: faunal elements from the eastern and western areas, total amount; a – NISP of identifiable species; b – weight of identifiable skeletal elements.

## Anthropogenic traces

In addition to numerous impact scars and green fractures that suggest intentional smashing, several elements (such as those shown in Fig. 5-3, or Fig. 5-9) also displayed traces of cutting (Fig. 5-4 – Fig. 5-6). Cut marks were identified with certainty only at 24 finds from the 2018-2020 excavation campaign (Table 5-22). There is no clear difference in the number between the eastern and western areas. There is also no significant difference between the species. Although most cut marks have been identified in mammoth remains, the mammoth also represents by far the largest proportion of the total number of finds. No reliable interpretations can therefore be made based on the cut marks.

## Season

The youngest mammoth individuals can be used to determine the season. One right and one left mandibula fragment from Pit 1 (Fig. 5-26) probably originate from the same individual. One left maxilla found in square 6O in Pit 2 as part of an almost intact cranium (Fig. 5-24), and an isolated left maxilla M2 of the same age, found in square 5C in the eastern area (Fig. 5-25), originate from individuals which were about the same age.

It is reported that in principle, elephants can reproduce throughout the year, but a study on an elephant population in Myanmar showed that about 40% of births occur between December and March (Dierenfeld et al. 2020), corresponding to the cool, dry period. If the

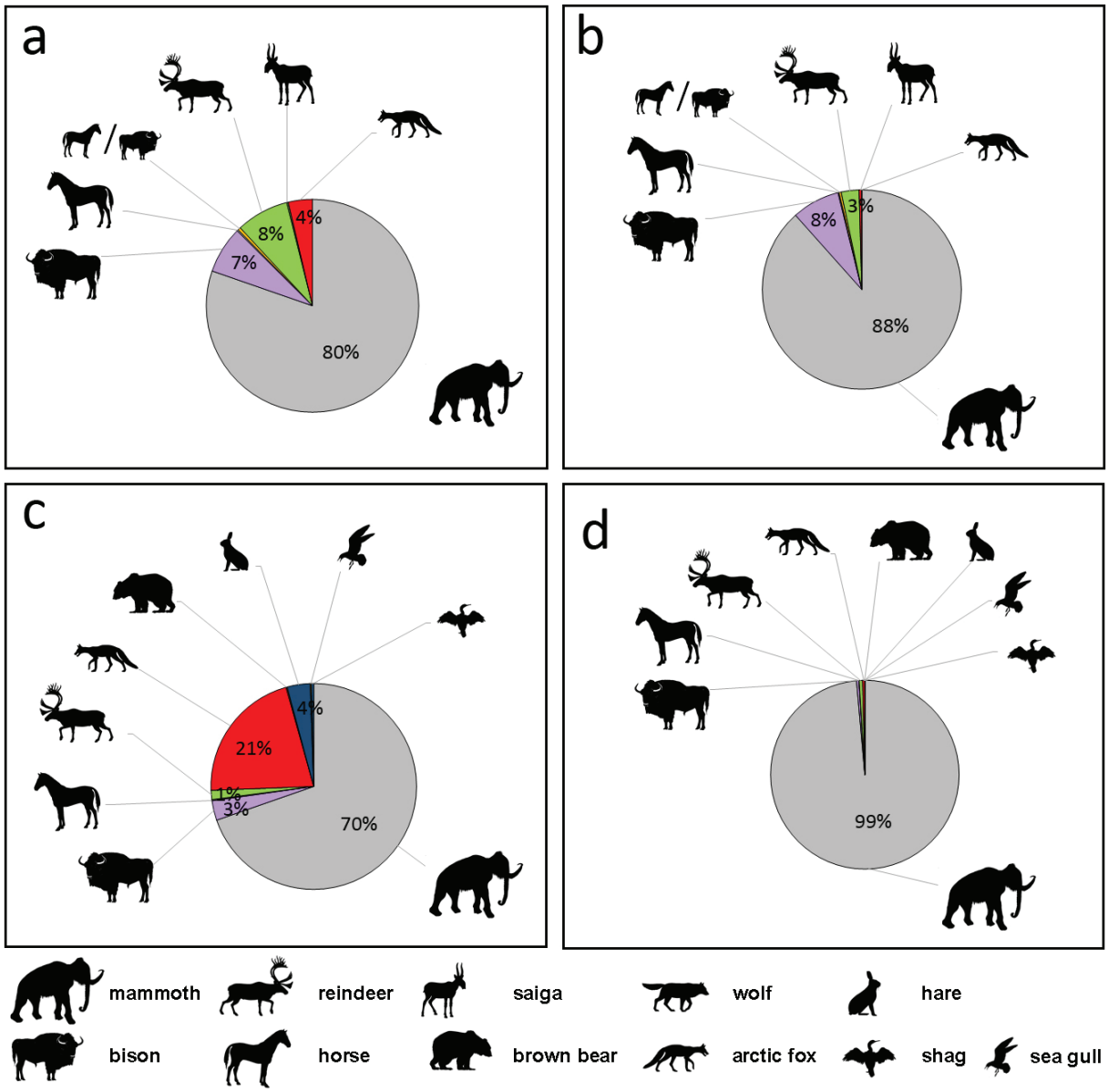


Fig. 5-32. Barmaky, faunal elements: a – western area, NISP 445 of identifiable species; b – western area, weight 48.5 kg of identifiable skeletal elements; c – eastern area, NISP 410 of identifiable species; d – eastern area, weight 73.2 kg of identifiable skeletal elements.

data can be applied to mammoths, then the birth of the Barmaky calf was also more likely to have taken place in the colder period. Under arctic conditions, this could have been between November and May. Rountrey et al. (2012, 188) assume that – with reference to elephants and other recent tundra ungulates – mammoths probably gave birth just before the start of the growing season, i.e. sometime in May.

In ungulates, teeth only erupt after birth. Elephants are fully lactating in the first few months of their lives and do not consume solid food. In elephants, the lactation period lasts anywhere from 2 to 8 years, and weaning is usually contingent. In the Mynamar population, the transition to solid food takes place between month 12 and 18, when protein and fat content increases and carbohydrate content decreases, while the final (late) lactation phase last from month

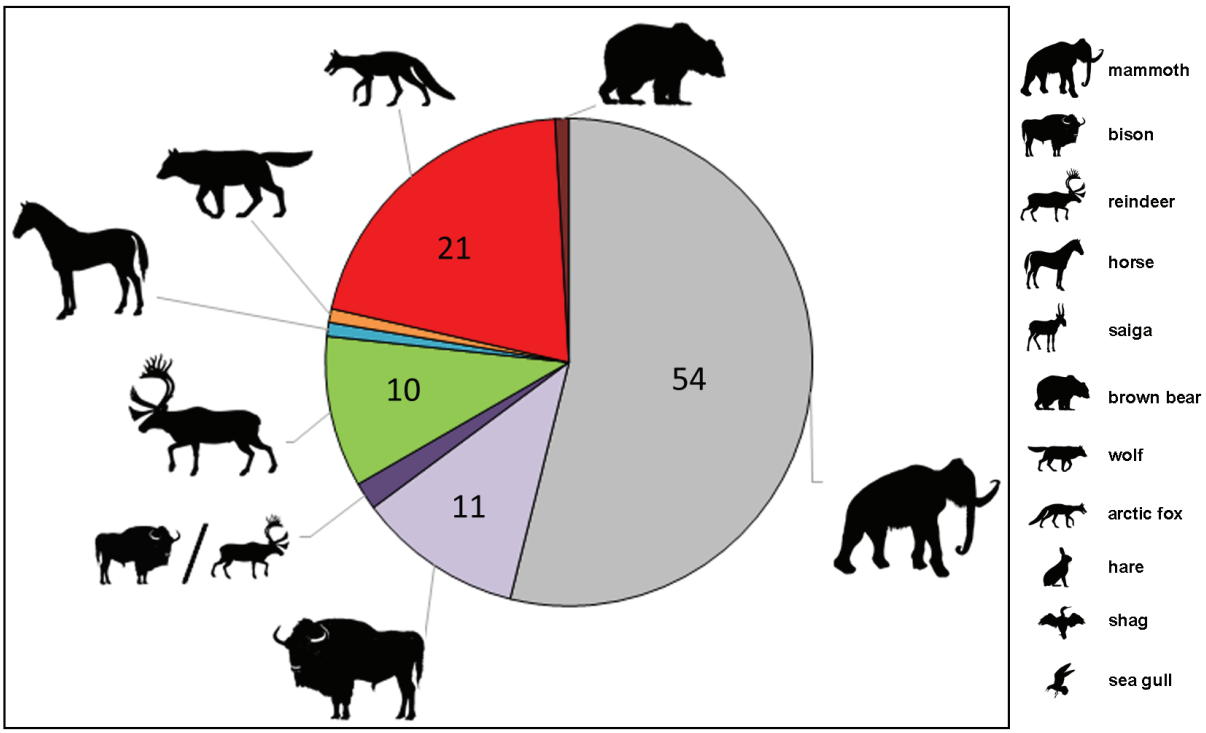


Fig. 5-33. Barmaky, 1990 field campaign: NISP. The numbers in the graph are percentages.

18 onwards, when the nutrient content stabilises but protein remains high (Dierenfeld et al. 2020). How long mammoths were nursed is unclear, but several months are likely before they were able to eat solid food. For the Barmaky mammoths, the development of the M1 should have been completed in summer. In one of the young individuals, the M1 shows already traces of use and the third deciduous molar was in the breakthrough with incipient wear at the foremost tip. Accordingly, the animal was no longer neonatal, but may have been a few months old. Since tooth wear had already taken place, the baby mammoth had eaten solid food at least over several weeks and was therefore several months old which is in line with G. Haynes' statement that the animal was about 9 months old. If one assumes that the birth took place around May, the time of death may have been around February. In the other young individual, the M2 was already chewed off over a larger area (100%) (Fig. 5-23) and the M3 was slightly worn at the foremost area (50%), while the rest of the tooth had not erupted completely. Within Laws' (1966) age group system, this individual falls between IV and V, which corresponds to about 2.5 years of age, give and take ½ year.

Elephant gestation lasts 22 months and fertile cows only become fertile at intervals of several years (Haynes 1991, 65; Kapustin et al. 1996; Whyte 2005). This was probably also the case with mammoths. If the two young individuals died at the same time, they are therefore unlikely to have had the same mother. Based on the teeth, it can be assumed that the juvenile animal may have died in the same season as the baby mammoths. Either the animals were killed at approximately the same time, or the settlement was visited several times in the same season but in different years.

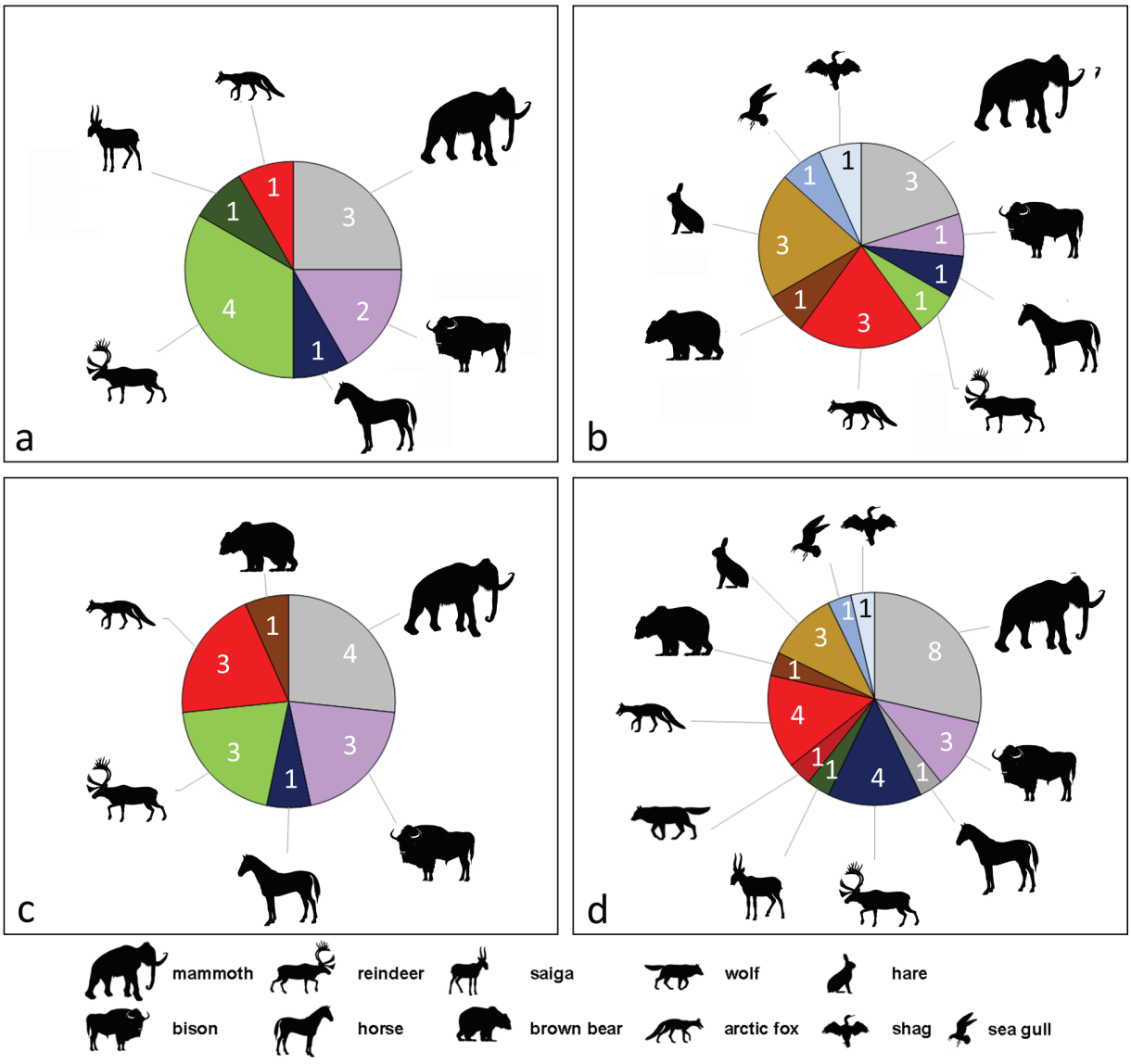


Fig. 5-34. Barmaky, MNI of animal species, by excavation areas: a – western area, NISP 1096/MNI 12; b – eastern area, NISP 1715/MNI 15; c – 1990 field campaign, NISP 218/MNI 15; d – total, NISP 3029/MNI 28. The numbers represent the MNI, data see Tables 5-1 and 5-21.

| skel. element | eastern area*, right side | eastern area*, left side | eastern area*, side? | horizon 2a, side? | pit 2, right side | pit 2, left side | pit 2, side? | western area, right side | 1990, right side | 1990, left side | 1990, side? | total |
|---|---|---|---|---|---|---|---|---|---|---|---|---|
| cranium fragm. | | | 4 | | | | | | | | 2 | **6** |
| cranium complete | | | | | | | 1 | | | | | **1** |
| maxilla | | | | | | | | | | | 4 | **4** |
| maxilla C | | | | | | | | | 1 | | | **1** |
| maxilla I2 | | | | | 2 | | | | | | | **2** |
| maxilla I3 | | | | | 1 | | | | | | | **1** |
| mandibula | 1 | 1 | | | | | | | 3 | 3 | | **8** |
| mandibula C | | | | | | | | | 2 | | | **2** |
| dens indet. | | | | | | | | | | | 4 | **4** |
| scapula | 1 | | | | | | | | | 1 | | **2** |
| humerus | 2 | 1 | 1 | | 1 | | | | 1 | 1 | 1 | **8** |
| radius | 1 | 2 | | | | | | | | | | **3** |
| ulna | 1 | 1 | | | | 1 | | | | | 2 | **5** |
| scaphoideum | | 1 | | | | | | | | | | **1** |
| metacarpus I | 1 | 2 | 2 | | | | | | | | | **5** |
| metacarpus II | 1 | 1 | | | | | | | | | | **2** |
| metacarpus III | 1 | 1 | 2 | | | | | | | | | **4** |
| metacarpus IV | 1 | 1 | 1 | | | | | | | | | **3** |
| metacarpus indet. | | | 3 | | | | | | | | | **3** |
| phalanx 1 ant. | | | 5 | | | | | | | | | **5** |
| phalanx 3 ant. | | | 2 | | | | | | | | | **2** |
| pelvis | | | | | | | | | | | 1 | **1** |
| femur | | | | | | | | | 1 | 1 | 3 | **5** |
| tibia | 2 | | | | | | | | 1 | 1 | 3 | **7** |
| astragalus | 1 | | | | | | | | | | | **1** |
| calcaneus | 1 | | | | | | | | | | 2 | **3** |
| tarsale | 5 | | | | | | | | | | | **5** |
| metatarsus II | 1 | 1 | | | | | | 2 | | | | **4** |
| metatarsus III | 2 | | | | | | | 2 | | | | **4** |
| metacarpus IV | | | | | | | | 2 | | | | **2** |
| metatarsus V | 1 | | 1 | | | | | | | | | **2** |
| metatarsus indet. | 6 | 1 | 6 | | | | | | | | | **13** |
| phalanx 1 post. | 6 | | 1 | | | | | 5 | | | | **12** |
| phalanx 2 post. | 2 | | 2 | | | | | 3 | | | | **7** |
| phalanx 3 post. | 5 | 1 | | | | | | 2 | | | | **8** |
| phalanx 1 ant./post. | | | 3 | | | | | | | | 1 | **4** |
| phalanx 2 ant./post. | | | | | | | | 2 | | | | **2** |
| phalanx 3 ant./post. | | | 1 | | | | | | | | | **1** |
| sesamoid | 4 | | 2 | | | | | 2 | | | | **8** |
| costa | | | | | | | | 2 | | | | **2** |
| atlas | | | 1 | | | | | | | | | **1** |
| vertebra cervicalis | | | | | | | | | | | 1 | **1** |
| vertebra thoracalis | | | | 1 | | | 1 | | | | 1 | **3** |
| vertebra caudalis | | | | | | | | | | | 2 | **2** |
| vertebra | | | 11 | | | | | | | | 1 | **12** |
| long bone fragment | | | 3 | | | | | | | | | **3** |

Table 5–16. Barmaky, *Vulpes lagopus*, skeletal elements divided according to body side and excavation area; all skeletal elements came from fully grown individuals; EA: eastern area; WA: western area; phal.1: phalanx 1/phalanx proximalis; phal.2: phalanx 2/phalanx medialis; phal.3: phalanx 3/phalanx distalis; ant.: anterior; post.: posterior. *without horizon 2a and pit 2.

| square, find # | ID | year | skeletal elements | | | | | | | side |
|---|---|---|---|---|---|---|---|---|---|---|
| | | | | GL | Bp | SD | Bd | | | |
| 10E, #38 | 173 | 2018 | radius | – | 9,06 | 6,87 | – | | | – |
| 10E, #96 | 317 | 2019 | radius | - | 8,84 | 6,30 | – | | | right |
| | | | | GLC | Dp | SD | Bd | Dd | BT | |
| 10E, #39 | 142 | 2018 | humerus | 91,97 | 18,23 | 6,02 | 15,15 | – | – | right |
| 6ǽ, #3 | 367 | 2020 | humerus | 97,64 | – | 6,15 | 16,46 | 12,12 | 12,12 | left |
| 5O, pit 2, #20 | 512 | 2020 | humerus | 98,58 | – | 6,44 | 15,06 | 11,81 | 9,49 | right |
| | | | | GL | SDO | DPA | BPC | | | |
| 10E, #38 | 172 | 2018 | ulna | – | 11,68 | – | 7,09 | | | left |
| 10E, #116 | 174 | 2018 | ulna | – | 11,60 | 10,24 | 7,27 | | | right |
| | | | | Bp | Dp | SD | Bd | Dd | GL | |
| 10E, #114 | 176 | 2018 | mc I | – | – | – | 5,58 | 4,83 | 14,58 | – |
| 9E, #9 | 316 | 2019 | mc I | 7,29 | – | 3,65 | 5,23 | – | 28,80 | right |
| 10E, #55 | 126 | 2018 | mc III | 41,34 | – | 5,33 | 6,87 | – | – | – |
| 5-6Л, #422 | 185 | 2019 | mc II | 3,99 | 5,86 | 3,62 | 5,89 | 4,87 | 37,39 | right |
| 5К, pit 1, #13 | 3 | 2019 | mc IV | 6,32 | 5,38 | 3,92 | 5,43 | 4,84 | 34,97 | right |
| 6Л, pit 1, #8 | 4 | 2019 | mc III | – | – | – | – | – | 41,51 | right |
| 5H, pit 1, #7 | 5 | 2019 | mc II | – | – | – | – | – | – | right |
| | | | | SD | Bd | Dd | | | | |
| 10E, #27 | 127 | 2018 | tibia | 7,25 | 13,18 | 8,42 | | | | right |
| 6Г, #13 | 215 | 2019 | tibia | 7,14 | – | – | | | | right |
| 11E, #10 | 414 | 2018 | tibia | 7,33 | – | – | | | | left |
| | | | | GLl | | | | | | |
| 10E, #27 | 128 | 2018 | astragalus | 15,78 | | | | | | left |
| | | | | GL | GB | | | | | |
| 10E, #27 | 135 | 2018 | calcaneus | 26,78 | 10,07 | | | | | right |
| | | | | Bp | Dp | SD | Bd | Dd | GL | |
| 10E, #27 | 137 | 2018 | mt II | – | – | 5,55 | – | 5,18 | 49,18 | |
| 9Г, #5 | 222 | 2019 | mt III | 4,60 | 7,47 | 3,65 | 4,61 | 4,97 | 47,01 | right |
| | | | | Gpl | Bp | SD | Bd | | | |
| 10E, #55 | 125 | 2018 | phal,1 post, | 14,34 | 5,58 | 3,31 | 4,47 | | | right |
| 10E, #27 | 130 | 2018 | phal,1 post, | 18,81 | 5,03 | 2,95 | 4,01 | | | right |

Table 5-17: Barmaky, *Vulpes lagopus*, measurements (in mm); post.: posterior; mc: metacarpus; mt: metatarsus; phal.1: phalanx 1/phalanx proximalis.

**Abbreviations:**
**Humerus** – GLC: greatest length from caput; Dp: depth of the proximal end; SD: smallest breadth of the diaphysis; BT: breadth of the trochlea; Bd: breadth of the distal end; Dd: distal depth.
**Radius** – Bp: greatest proximal width; SD: smallest width of the diaphysis.
**Ulna** – SDO: smallest depth of the olecranon; DPA: depth across Processus anconaeus; BPC: greatest width of the proximal articular surface; GL: greatest length.
**Tibia** – SD: smallest width of diaphysis; Bd: greatest distal width; Dd: greatest distal depth.
**Astragalus** – GLl: lateral length.
**Calcaneus** – GL: greatest length; GB: greatest width.
**Metacarpus/Metatarsus** – GL: greatest length; Bp: greatest proximal width; Dp: depth proximal; SD: smallest width of the diaphysis; Dd: distal depth; Bd: greatest distal width.
**Phalanx 1, 2** – Gpl: greatest peripheral length; Bp: greatest proximal width; SD: smallest width of the diaphysis; Bd: greatest distal width.

| Skeletal elements | EA, sq. 5C | 1990, sq. 7K | 1990, sq. 6Ж |
|---|---|---|---|
| carpale | 1 (dex) | – | – |
| femur | – | 1 | 1 |

Table 5-18. Barmaky, *Ursus arctos*, skeletal elements, all adult/epiphyses fused.

| Skeletal elements | 4P juv. | 4P ad. | 5C ad. | 5P ad. | 5P juv./subad. | 6T |
|---|---|---|---|---|---|---|
| cranium | – | – | – | – | – | 4 |
| radius | – | – | – | – | 1 | – |
| mc I | – | – | – | – | 1 | – |
| mc IV | – | – | – | – | 1 | – |
| mt II | – | 1 | – | – | – | – |
| mt III | – | 1 | – | – | – | – |
| mt IV | – | 1 | – | – | – | – |
| mt V | – | 1 | – | – | – | – |
| mt indet. | 1 | – | – | – | – | – |
| metapodium indet. | – | – | – | 1 | 1 | – |
| astragalus | – | – | – | 1 | – | – |
| calcaneus | – | – | – | 1 | – | – |
| phal.1 ant./post. | – | – | 1 | 1 | 1 | – |
| phal.1, post. | – | – | 1 | – | – | – |
| phal.2 ant./post. | – | – | 1 | 1 | 1 | – |

Table 5-19. Barmaky, *Lepus* sp., skeletal elements, eastern area, by squares; mc: metacarpus; mt: metatarsus; phal.1: phalanx 1/phalanx proximalis; phal.2: phalanx 2/phalanx medialis; ant.: anterior; post.: posterior.

| square, find # | ID | year | skeletal elements | | | side |
|---|---|---|---|---|---|---|
| | | | | GL | GB | |
| 5P, 2d, sieving | 196 | 2020 | calcaneus | 34,62 | 13,23 | left |

Table 5-20. Barmaky, *Lepus* sp., measurements (in mm).

**Abbreviations:**
**Calcaneus** – GL: greatest length; GB: greatest width.

| | 2018–2020, western area | | | | 2018–2020, eastern area* | | | | 2018–2020, pit 2 | | | |
|---|---|---|---|---|---|---|---|---|---|---|---|---|
| **spezies** | infantile | juvenile | juvenile/ subadult | adult | infantile | juvenile | juvenile/ subadult | adult | infantile | juvenile | juvenile/ subadult | adult |
| Mammuthus | 2 | | | 1 | 1 | | 2 | 2 | | 2 | | 1 |
| Bison | | | | 2 | | | | 1 | | | | |
| Equus | | | | 1 | | | | 1 | | | | 1 |
| Rangifer | | | 1 | 3 | | | | 1 | | | | 1 |
| Saiga | | | 1 | | | | | | | | | |
| Canis | | | | | | | | | | | | |
| Vulpes | | | | 1 | | | | 3 | | | | 2 |
| Ursus | | | | | | | | 1 | | | | |
| Lepus | | | | | | 1 | | 2 | | | | |
| Larus | | | | | | | | 1 | | | | |
| Phalacrocorax | | | | | | | 1 | | | | | |

Table 5–21. Barmaky, by areas and field campaigns: MNI of animal species. *without horizon 2a and pit 2.



| | 2018–2020, horizon 2a | | | | 1990 | | | | calculation for all areas | | | | |
|---|---|---|---|---|---|---|---|---|---|---|---|---|---|
| **spezies** | infantile | juvenile | juvenile/ subadult | adult | infantile | iInfantile/ juvenile | juvenile/ subadult | adult | infantile | juvenile | juvenile/ subadult | adult | **total all areas** |
| Mammuthus | | | | 1 | | 1 | | 3 | 3 | 2 | 2 | 3 | **8** |
| Bison | | | | 1 | | | 1 | 2 | | | 1 | 2 | **3** |
| Equus | | | | | | | | 1 | | | | 1 | **1** |
| Rangifer | | | | | 1 | | 1 | 1 | 1 | | 1 | 2 | **4** |
| Saiga | | | | | | | | | | | 1 | | **1** |
| Canis | | | | | | | | 1 | | | | 1 | **1** |
| Vulpes | | | | 1 | | | | 3 | | | | 4 | **4** |
| Ursus | | | | | | | | 1 | | | | 1 | **1** |
| Lepus | | | | | | | | | | 1 | | 2 | **3** |
| Larus | | | | | | | | | | | | 1 | **1** |
| Phalacrocorax | | | | | | | | | | | 1 | | **1** |

Table 5–21. continued.

| species | skeletal elements | eastern area | western area |
|---|---|---|---|
| Vulpes | mc IV | 1 | – |
| Bison | costa | – | 2 |
| Rangifer | calcaneus | 1 | 2 |
| | costa | 6 | 1 |
| | humerus | 1 | – |
| | radius | 1 | – |
| Mammuthus | ulna | 1 | – |
| | pelvis | – | 1 |
| | tibia | – | 1 |
| | femur | 1 | – |
| | fragment | – | 1 |
| indet. size of bison | fragment | – | 3 |
| indet. size of reindeer | fragment | 1 | – |
| | **Total:** | **13** | **11** |

Table 5-22. Barmaky: cut marks on skeletal elements of individual species; mc: metacarpus.

## SPATIAL DISTRIBUTION OF FAUNAL REMAINS IN THE EXCAVATION AREA FROM 2018–2020

### Comparison of the spatial distribution of the species

Looking at the distribution of the faunal elements, concentrations appear in several areas. Mammoth remains occur in the entire area (Fig. 5-35 – 5-42), but cluster in squares 5 К-П (Pit 1), 5Н, 5О (Pit 2), and in the permafrost depression channel from 3ПР, 4ПР, 5ПРСТ, 6Т (Fig. 5-43; 5-44). There is no clear difference in the distribution between the age groups of the mammoths. Bison and reindeer, in contrast, are scattered without visible concentration (Fig. 5-45 - 5-48). The horse remains were found in square 9E, hare in the channel in squares 4P and 5C, and saiga in 10E (Fig. 5-49). The remains of the carnivores are widely distributed but cluster in Pit 2, squares 5O, and in squares 9E, 10E, 11E (Fig. 5-50 - 5-54) and the bird remains are situated in the southern section of the channel. The skeletal elements in the channel appear to have been aligned or lay with their long sides parallel to the sides of the channel (Fig. 5-43), suggesting post-depositional movement. This levelling can neither be seen in Pit 1 and Pit 2, nor in the western excavation area.

### Comparison of the find weights between different areas

The total number of faunal elements in the western area is about three times larger than in the eastern area (without pit 2 and horizon 2a), while the total weight is only slightly higher, indicating a stronger fragmentation in the western area (Table 5-1a, Table 5-26; see also the comparison of the fragment lengths between the eastern and the western area in Fig. 5-55). While the average weight of a fragment in the eastern area is 14g, it is only 7g in the western area.

Pit 1, located in the western area, contained 69 finds (Table 5-23). The remains consist of mammoth, bison, and arctic fox, with an MNI of four animals: one adult bison (scapula blade, costa corpus, metacarpus III+IV diaphysis), three to four mammoth individuals including the calf: one adult (lamellae of a tusk and of a molar, four scapulae blades, several ribs, one pelvis), possibly of one subadult (humerus left, prox. unfused; vertebra caudalis, prox. unfused), one juvenile (fibula dist. Epi., unfused), and of one of the very young (infantile) specimens (tibia prox. diaphysis, unfused (not in the plan); mandibula left (Fig. 5-26) and right, M2 erupting, Laws (1966) age groups II to III), remains of three fox paws, including parts of two front and one rear paw, all with fused epiphyses.

Pit 2 contained 286 finds (Table 5-24), most of it from mammoth, but also one of horse and one of reindeer. Some cranial and postcranial elements of Arctic fox were also found. However, unlike in many other areas, there were no paw bones in anatomical order, but only one cranium with right and left mandibula (Fig. 5-28, b). Among the mammoths, the remains of at least four individuals were identified: one infantile (maxilla, Fig. 5-24, Laws' (1966) age group II-III; femur left dist. unfused), one juvenile (femur left, dist. unfused), one subadult (femur left prox. unfused), and one adult

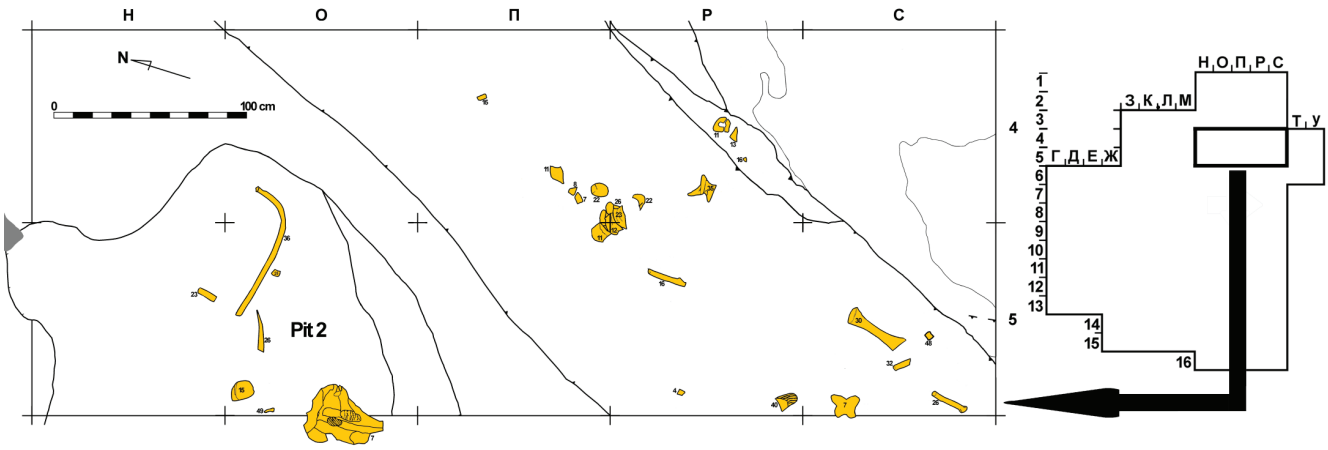


Fig. 5–35. Barmaky, eastern area, *Mammuthus primigenius*, age group Infans: the distribution of remains.

(scapula left, nearly complete, fused; humerus right prox. fused; ulna left dist. fused; costae fused) (see also Table 5–24). The mammoth maxilla had the same dental status as the two halves of the lower jaw from Pit 1, so it is possible that they are the remains of the same calf but could also come from a third infantile mammoth. This pit also contained numerous ribs from the right side, presumably from just one adult mammoth. Strong cut marks were visible on five of these ribs (e.g., Fig. 5–4; 5–6). What is striking in Pit 2 is that a particularly large number of remains of the scapula, humerus, femur and costae of various mammoths were found. These elements belong to those areas of the body where there is a particularly large amount of meat.

In Horizon 2a, 89 fragments with remains of three species and at least 4 individuals were identified: arctic fox, bison, and mammoth (Table 5–25). Apart from some unidentifiable skeletal remains of various mammals, there were remains of at least one adult arctic fox and one bison. The mammoth remains represent at least two individuals. Most of the skeletal elements belonged to adult animals, including an almost complete left scapula, several ribs, pelvic fragments, and some tusk remains (Table 5–4). In contrast, some ribs, skull fragments, and postcranial elements were from infantile animals.

| Skeletal elements | Bison | Mammuthus | Vulpes | indet. size of bison | indet. size of reindeer | Total: |
|---|---|---|---|---|---|---|
| cranium | – | – | – | 1 | 3 | **4** |
| mandibula | – | 2 | – | – | – | **2** |
| tusk | – | 2 | – | – | – | **2** |
| mandibulamolar | – | 1 | – | – | – | **1** |
| dens indet. | – | 1 | – | – | – | **1** |
| vertebra caudalis | – | 1 | – | – | – | **1** |
| costa | 1 | 8 | – | – | 1 | **10** |
| scapula | 1 | 4 | – | – | 1 | **6** |
| humerus | – | 1 | – | – | – | **1** |
| mc III+IV | 1 | – | – | – | – | **1** |
| mc I | – | – | 1 | – | – | **1** |
| mc II | – | – | 2 | – | – | **2** |
| mc III | – | – | 1 | – | – | **1** |
| mc IV | – | – | 1 | – | – | **1** |
| pelvis | – | 1 | – | – | – | **1** |
| tibia | – | 1 | – | – | – | **1** |
| fibula | – | 1 | – | – | – | **1** |
| phal.1, post. | – | – | 1 | – | – | **1** |
| postcran. fragment | – | 6 | – | 8 | 17 | **31** |
| **Total:** | **3** | **29** | **6** | **9** | **22** | **69** |

Table 5–23. Barmaky, pit 1: skeletal elements of animal species; mc: metacarpus; phal.1: phalanx 1/phalanx proximalis; post.: posterior.

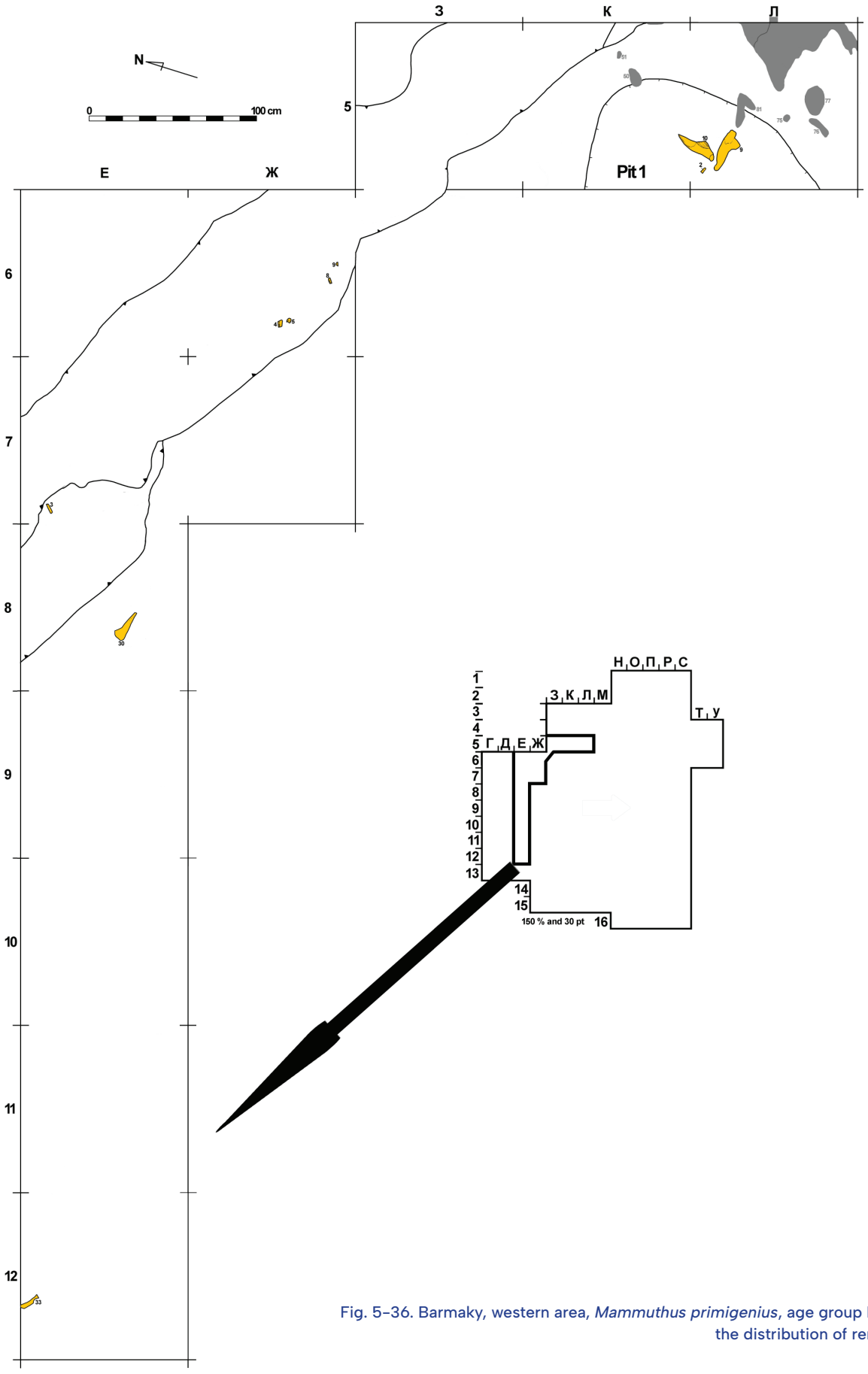


Fig. 5-36. Barmaky, western area, *Mammuthus primigenius*, age group Infans: the distribution of remains.

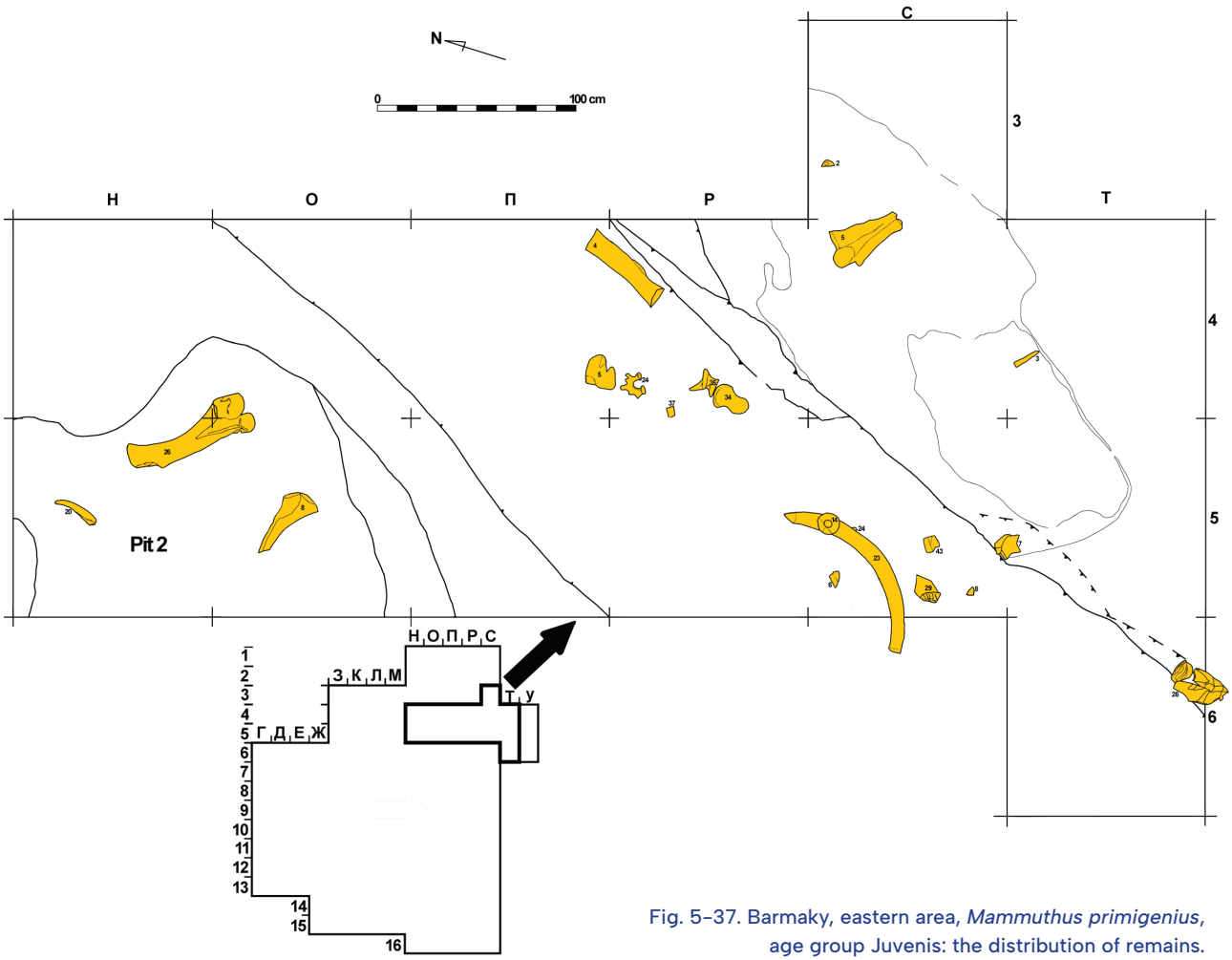


Fig. 5-37. Barmaky, eastern area, *Mammuthus primigenius*, age group Juvenis: the distribution of remains.

## Comparison of the fragment length of mammoth remains between the 2018–2020 excavation areas

A comparison of the fragment lengths of mammoth remains from the eastern and western excavation areas during the 2018–2020 period reveals, where recorded (see above), additional differences (Fig. 5-56). While most fragments in the western area have a length of 1–50 cm, the fragments in the eastern area have a range between 1–100 cm, therefore exhibiting a less marked degree of fragmentation. While varying soil conditions could account for the differing degrees of fragmentation in the remains, the consistently uniform fragmentation in the western area strongly suggests anthropogenic action.

When Pit 2 and horizon 2a in the eastern area are considered separately from the other material in the eastern area, a much more nuanced picture emerges (Fig. 5-56, a). In terms of absolute numbers, the results show little difference between the eastern and western areas. However, in Pit 2 and horizon 2a, the proportion of highly fragmented faunal remains is notably high, with larger fragments being rare. This trend becomes even more apparent when the fragment lengths are analysed in relation to their proportions within each feature (Fig. 5-56, b). Horizon 2a, in particular, is characterised by especially small fragments.

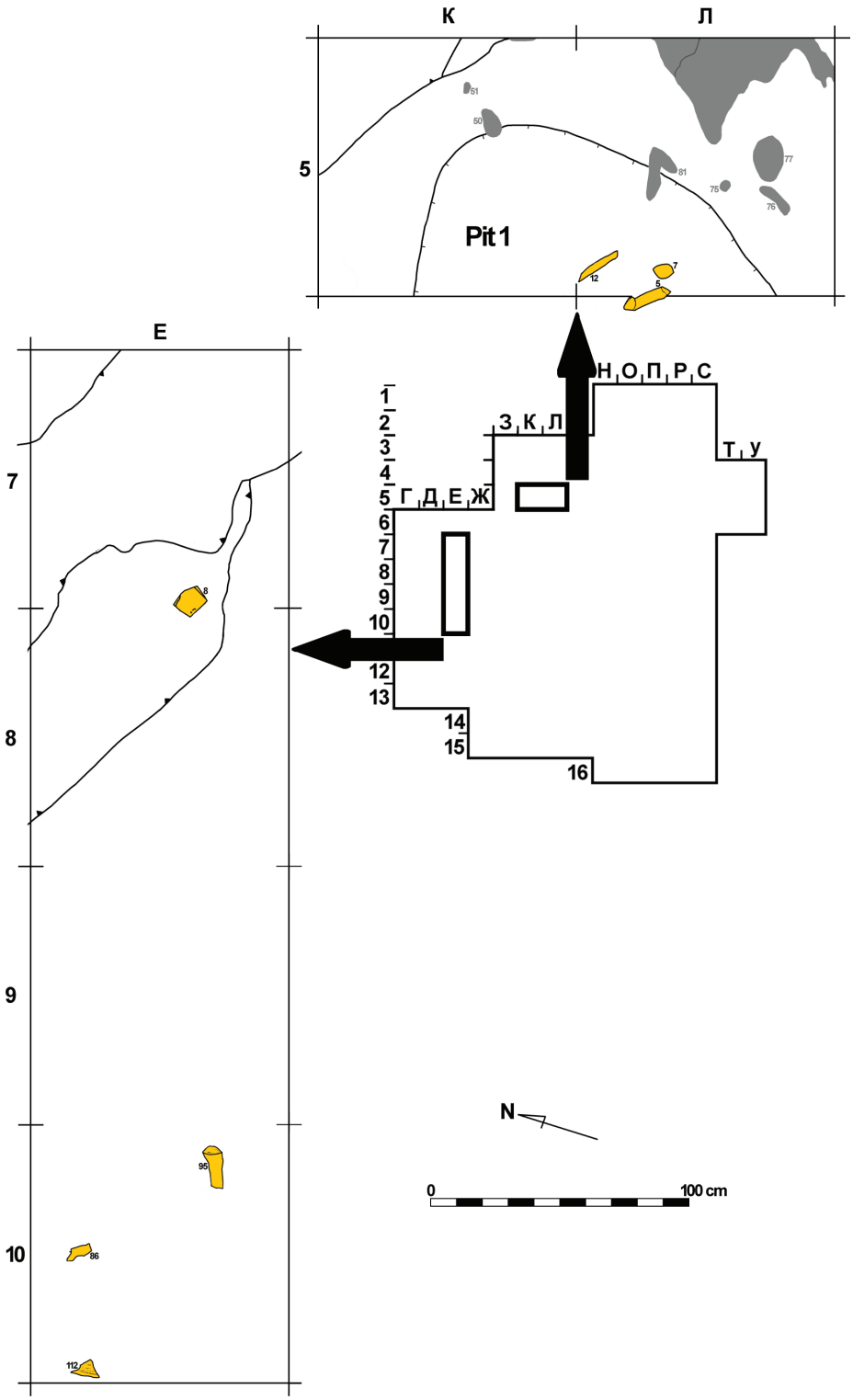


Fig. 5–38. Barmaky, western area, *Mammuthus primigenius*, age group Juvenis: the distribution of remains.

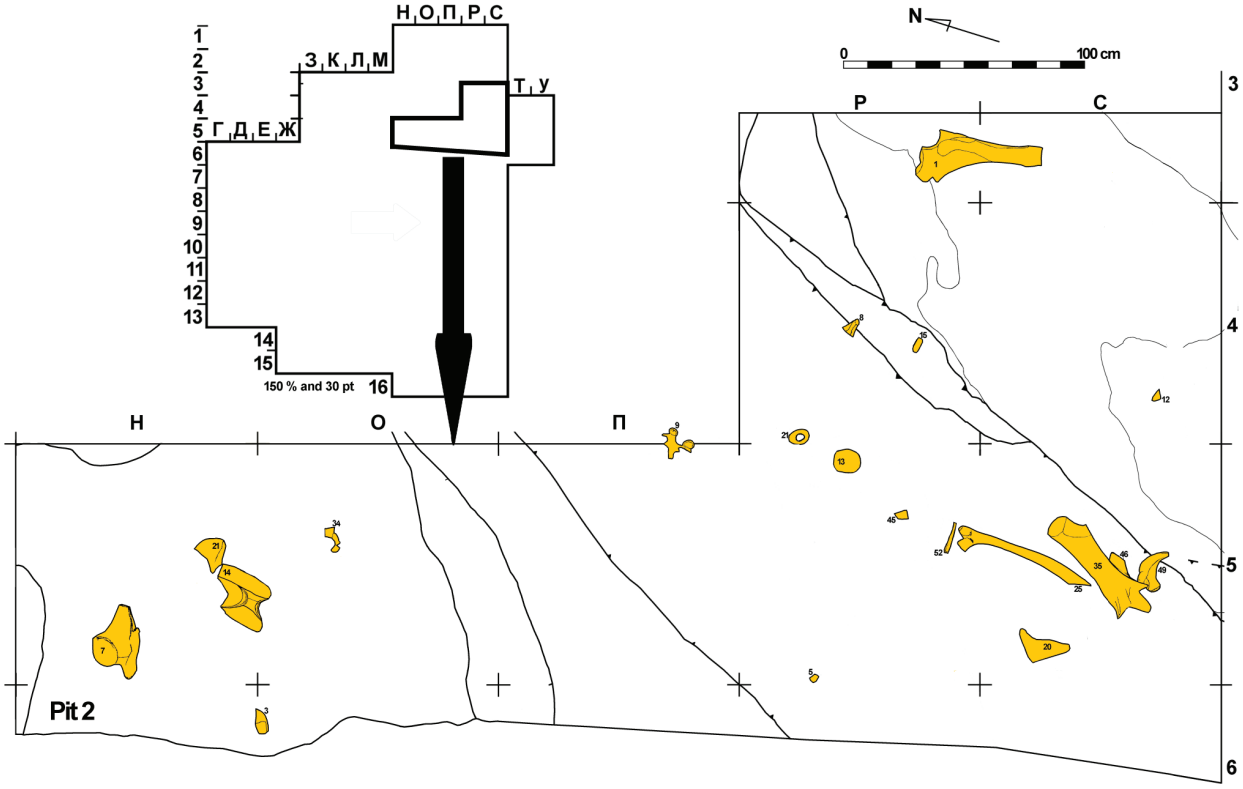


Fig. 5–39. Barmaky, eastern area, *Mammuthus primigenius*, age group subadult/early Adultas: the distribution of remains.

A potential explanation for the varying fragment sizes could be the different activities conducted within the settlement area. The area where mammoths were dismembered could have been in the eastern area, while skeletal elements were processed mainly in the western area. It is possible that specific skeletal elements were chosen during the butchering process and only those were smashed for cooking. After cooking, which may have taken place in the western area and in horizon 2a, the remains may have been dumped in Pit 2.

## Site function based on animal remains

Bones of ungulates (reindeer and bison) are strongly fractured. Many postcranial elements of mammoths also show traces of blows and breakup in fresh condition. However, several skeletal elements, especially those from the 1990 excavation and from the eastern area of the 2018–2020 excavations, were also quite large and not fractured. The average weight of ungulate bone fragments (determined species and undeterminable fragments in size classes) is 2 g while those of mammoth is 118 g. This might indicate that marrow and bone fat extraction was more important for the former. Whether mammoth bones were used for construction purposes and therefore left relatively large cannot be decided based on the recorded material. Due to the large size of the mammoths, it can be assumed that these animals were killed at this location and that the settlement site was built for the purpose of utilising the carcasses at the killing site. The presence of a minimum of eight individual mammoths from different age groups could indicate that a family with offspring from several years was killed. Based on the skeletal elements of bison and reindeer present, which came from all parts of the body, it can be assumed that these animals were introduced into the settlement site as complete carcasses. The same can be said for Arctic foxes. Due to the small number of remains from horse, saiga, hare, wolf, bear, statements as to the procurement strategy are not possible.

| skel. element | Vulpes | Equus | Mammuthus | Rangifer | indet. size of reindeer | total |
|---|---|---|---|---|---|---|
| cranium | 1 | – | 17 | – | 1 | **19** |
| maxilla I2 | 2 | – | – | – | – | **2** |
| maxilla I3 | 1 | – | – | – | – | **1** |
| tusk | – | – | 2 | – | – | **2** |
| costa | – | – | 28 | – | – | **28** |
| scapula | – | – | 8 | – | – | **8** |
| ulna | 1 | – | 1 | – | – | **2** |
| humerus | 1 | – | 4 | – | – | **5** |
| pelvis | – | – | 1 | – | – | **1** |
| femur | – | – | 9 | 1 | – | **10** |
| tibia | – | – | 1 | – | – | **1** |
| vertebra thoracalis | 2 (1 *) | – | – | – | – | **2** |
| vertebra | – | – | 1 | – | – | **1** |
| phal.2 ant./post. | – | – | 1 | – | – | **1** |
| phal.3 ant./post. | – | 1 | – | – | – | **1** |
| postcran. fragment | – | – | 30 | – | 172 | **202** |
| **total:** | **8** | **1** | **103** | **1** | **173** | **286** |

Table 5-24. Barmaky, pit 2, animal remains; phal.2: phalanx 2/phalanx medialis; phal.3: phalanx 3/phalanx distalis; post.: posterior. * also located in horizon 2a, Table 5-25. For a detailed age classification of the individual elements of mammoth see Table 5-5.

| skel. element | Vulpes | Bison | Mammuthus | size of mammoth | indet. size of bison | indet. size of reindeer | total |
|---|---|---|---|---|---|---|---|
| cranium | – | – | 2 | – | – | – | **2** |
| maxillamolar | – | 1 | – | – | – | – | **1** |
| tusk | – | – | 15 | – | – | – | **15** |
| vertebra thoracalis | 2 (1 *) | – | – | – | – | – | – |
| costa | – | – | – | – | – | – | – |
| scapula | – | – | – | – | – | – | – |
| pelvis | – | – | 4 | – | – | – | **4** |
| postcran. fragment | – | – | 18 | 30 | 8 | **3** | **59** |
| **total:** | **2** | **1** | **45** | **30** | **8** | **3** | **89** |

Table 5-25: Barmaky, skeletal elements of animal species found in horizon 2a. * also located in pit 2, Table 5-16. For a detailed age classification of the individual elements of mammoth, see Table 5-4.

| | fragment length in mm | | | | |
|---|---|---|---|---|---|
| excavation area | 1-10 | 11-500 | 500-1000 | > 1000 | total |
| west | 3 | 205 | 36 | 3 | **247** |
| pit 2 | 58 | 27 | 14 | 4 | **103** |
| horizon 2a | 43 | 2 | – | – | **45** |
| east (without hor. 2 a and pit 2) | – | 122 | 120 | – | **242** |

Table 5-26: Barmaky, fragment length in the various areas of the 2018-2020 excavation campaigns.

Fig. 5–40. Barmaky, western area, *Mammuthus primigenius*, age group subadult/early Adultas: the distribution of remains.

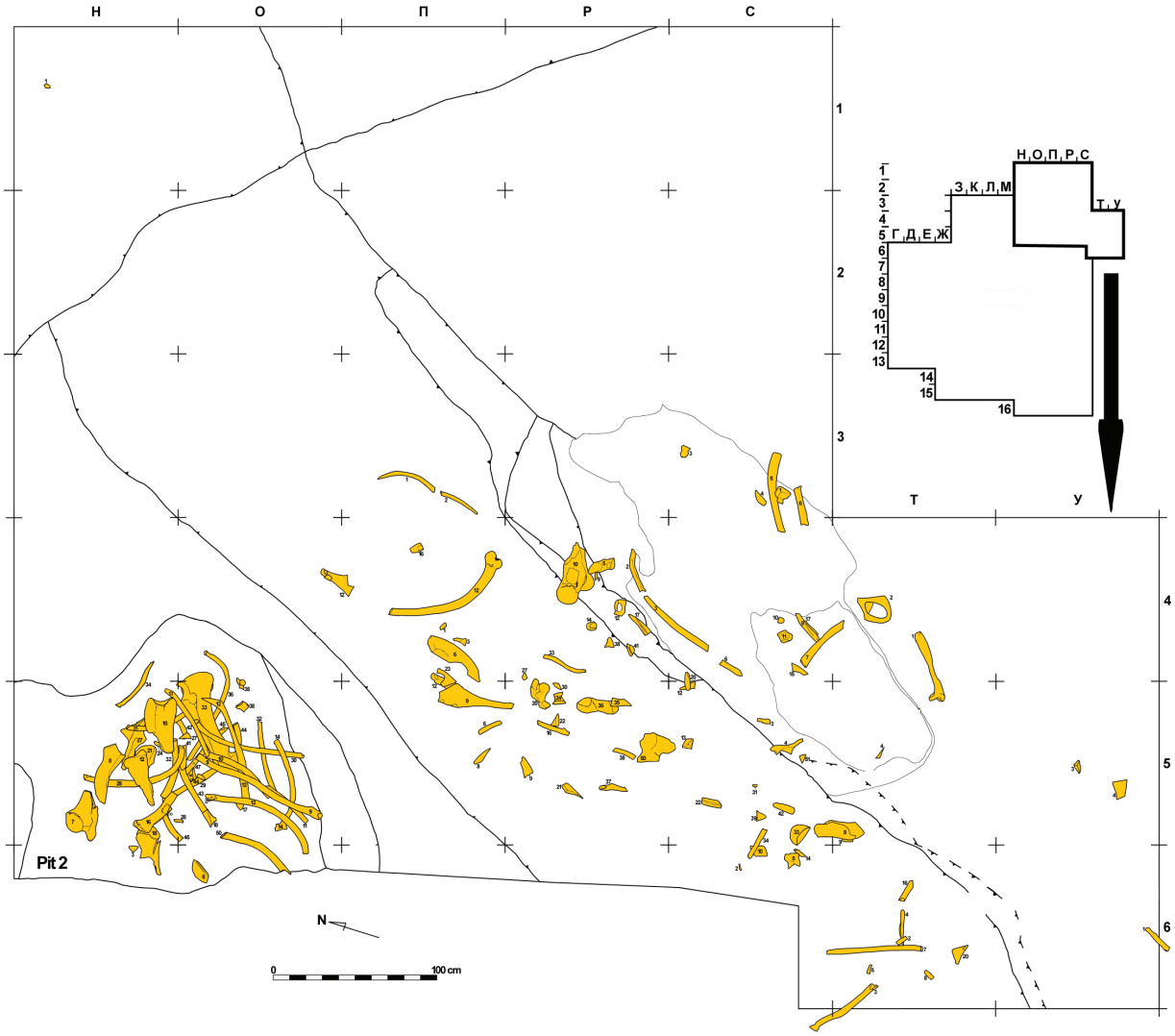


Fig. 5-41. Barmaky, eastern area, *Mammuthus primigenius*, age group Adultas: the distribution of remains.

Among the carnivores, three species could reliably be determined, arctic fox, wolf, and brown bear. All remains came from adult animals and most are located in the central area of the western part with an east-west scattering (Fig. 5-54). Wolf and brown bear were represented by only a few individual finds of possibly only one individual each (Tables 5-1a, 5-14, 5-18; Fig. 5-52). Of the wolf remains, only one came from the 1990 excavation. Other remains were found in sondages (Table 5-1b). Arctic fox was the most common carnivore with 179 finds of at least four individuals (Tables 5-1a, 5-16). Also, 76 items – all from lower limbs and paws – were found in anatomical connection (in Fig. 5-50; 5-51), and a straight cut around the metapodials (Fig. 5-28, c) suggests the separation of a paw. This may indicate the extraction of skins to which the feet were still attached. In contrast to the ungulates remains, those of arctic fox were predominantly complete and showed no systematic fracturing, speaking against their use as a source for nutrition, but rather suggesting that fur was of prime interest. The significance of carnivores as a source of fur for Palaeolithic hunter-gatherer has also been pointed out in other contexts (Wojtal et al. 2020).

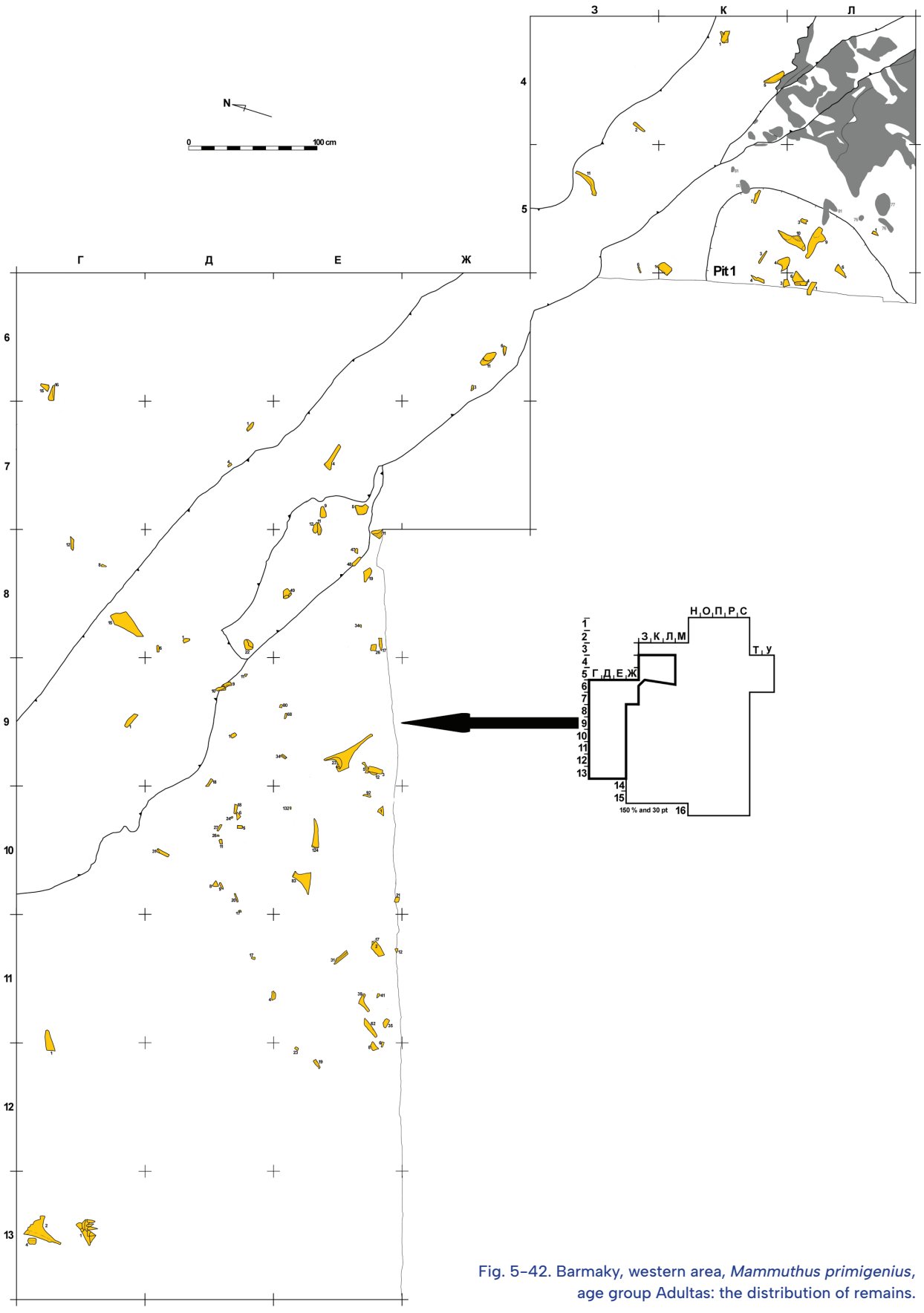


Fig. 5–42. Barmaky, western area, *Mammuthus primigenius*, age group Adultas: the distribution of remains.

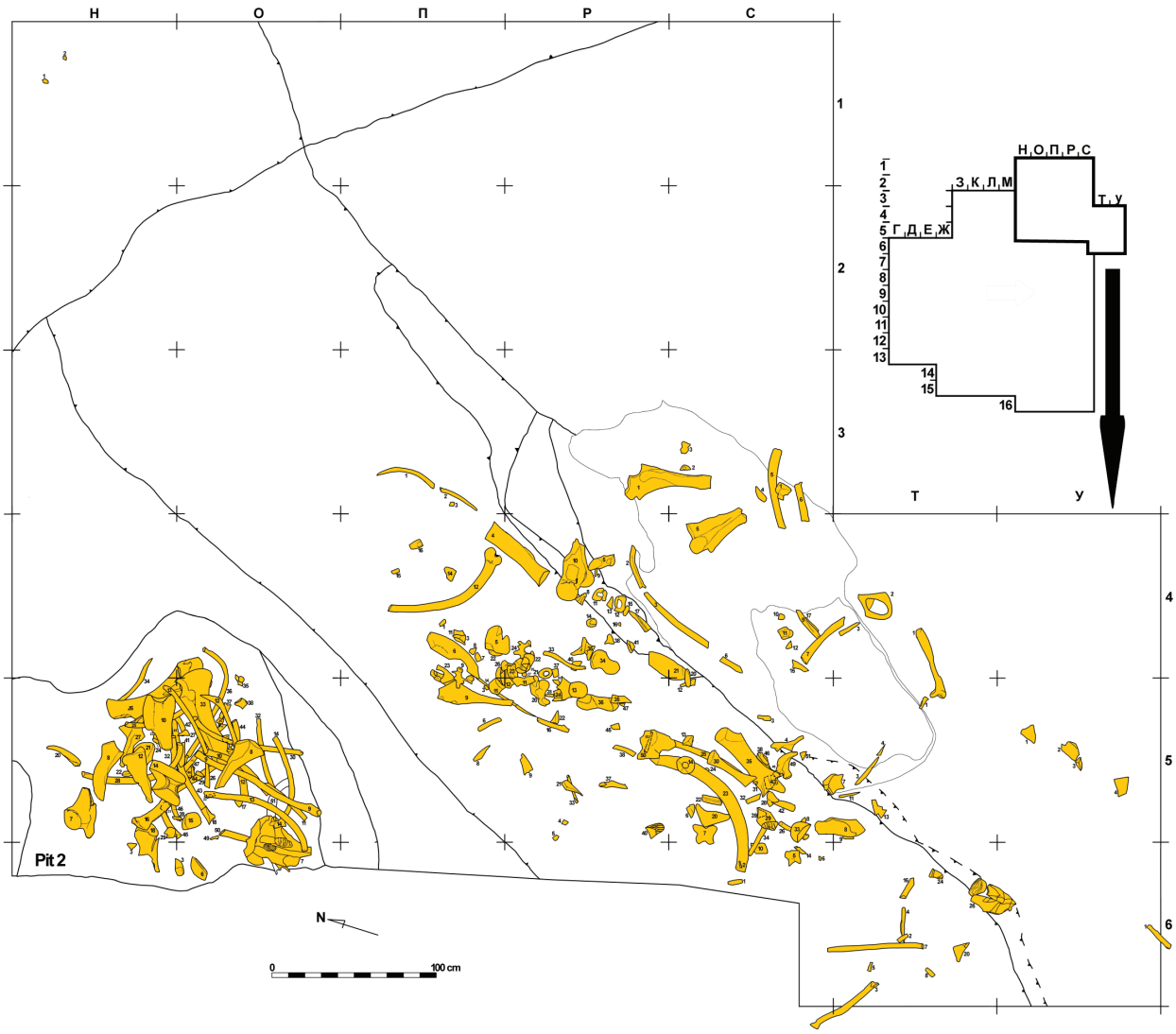


Fig. 5-43. Barmaky, eastern area, *Mammuthus primigenius*: the distribution of remains.

## Carnivore influence

As mentioned above, there is no case of unequivocal carnivore gnawing. Since decomposition of organic material in an arctic environment takes a long time (Pasda 2001, 2005: 5-7, 2009: 8), remaining organic material can attract carnivores even after years. Cervids are also known to eat skeletal substance in times of need, to compensate a lack of proteins and minerals, especially in the winter season (Herre 1986: 210; Kahlke 2001; Kierdorf 1993). The absence of gnawing marks and the fact that numerous skeletal elements were still in anatomical connection suggest that the site was covered by sediment relatively quickly and thus not accessible to carnivores and other bone eating animals.

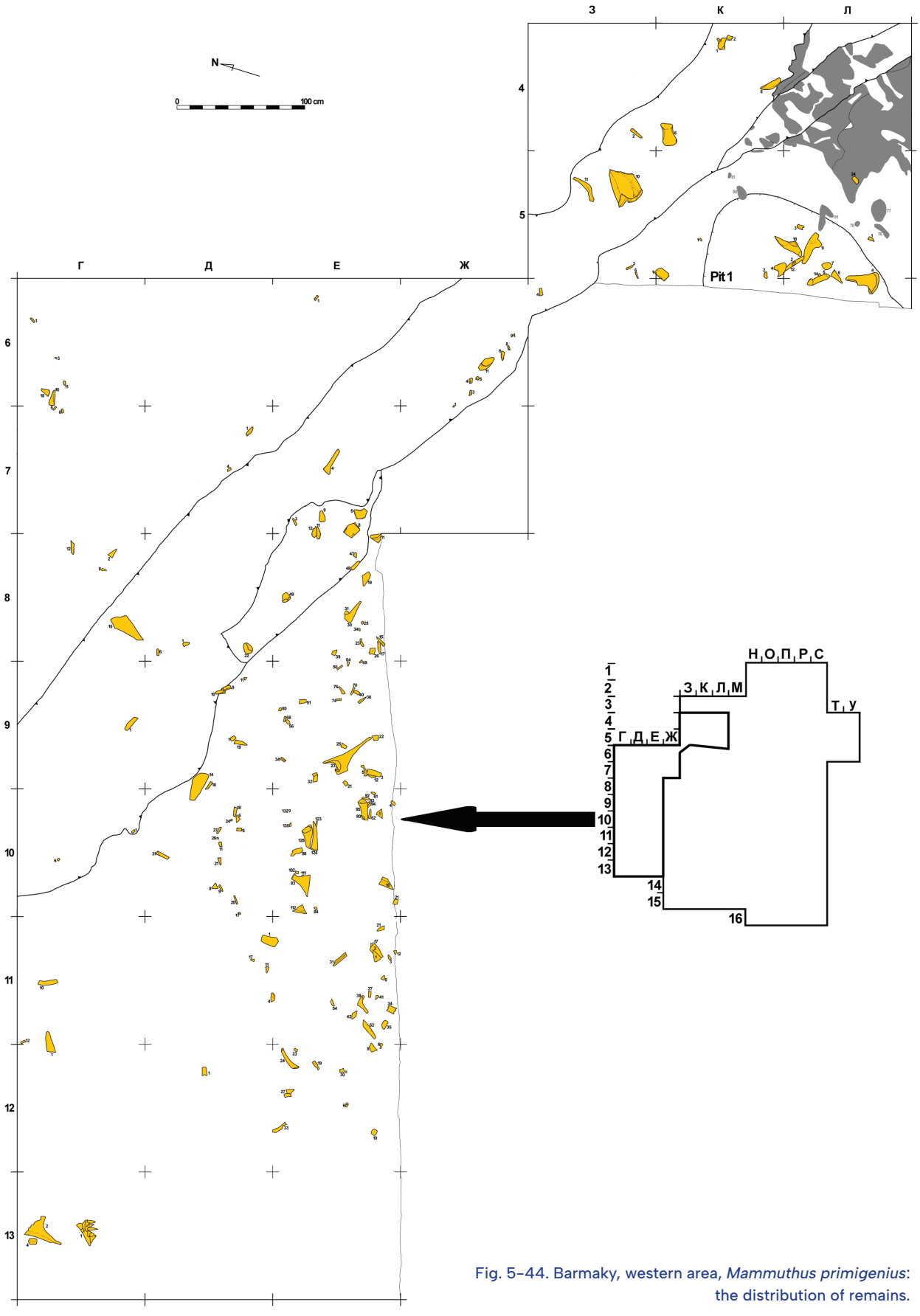


Fig. 5–44. Barmaky, western area, *Mammuthus primigenius*: the distribution of remains.

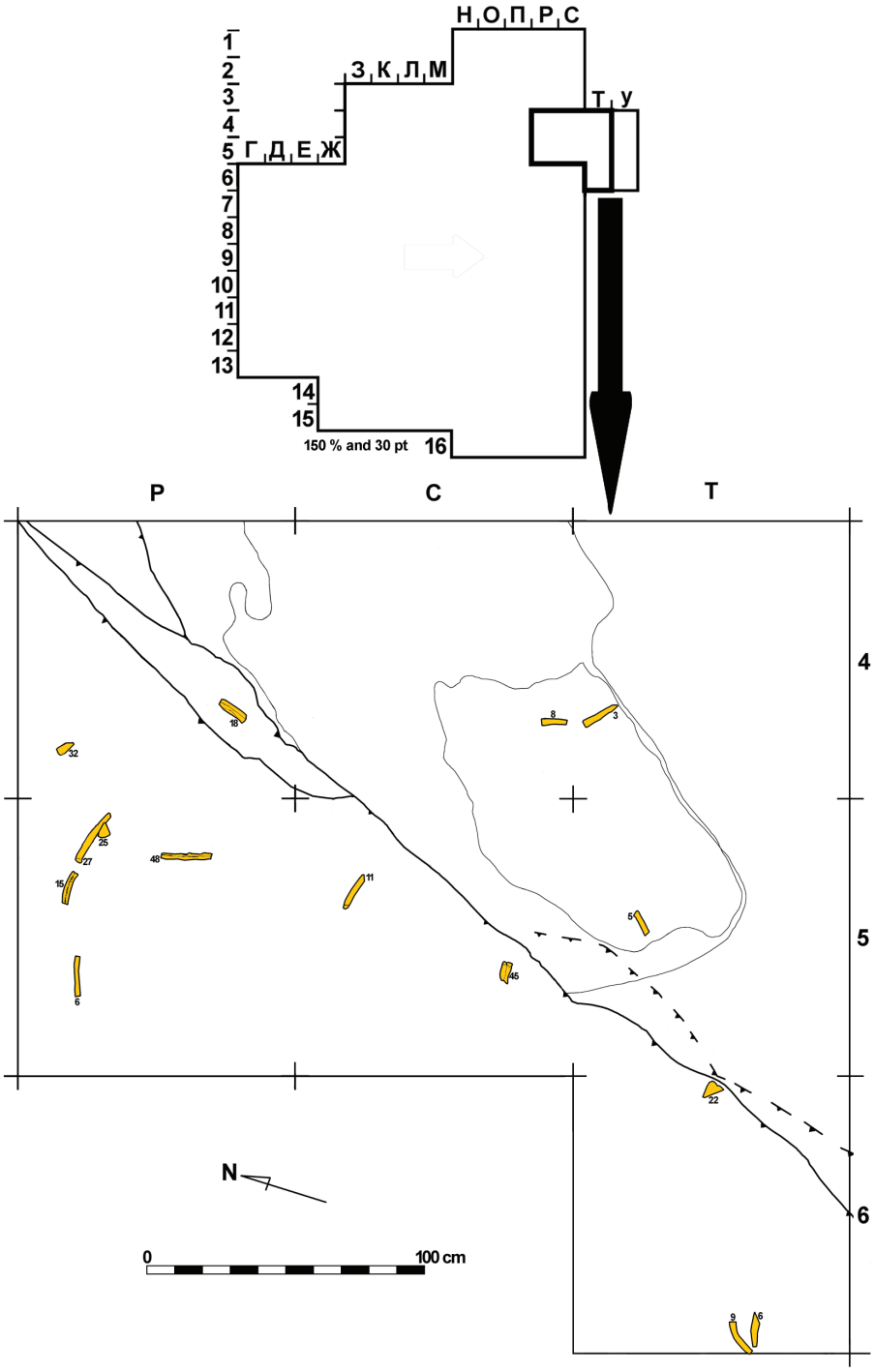


Fig. 5-45. Barmaky, eastern area, *Bison sp.*: the distribution of remains.

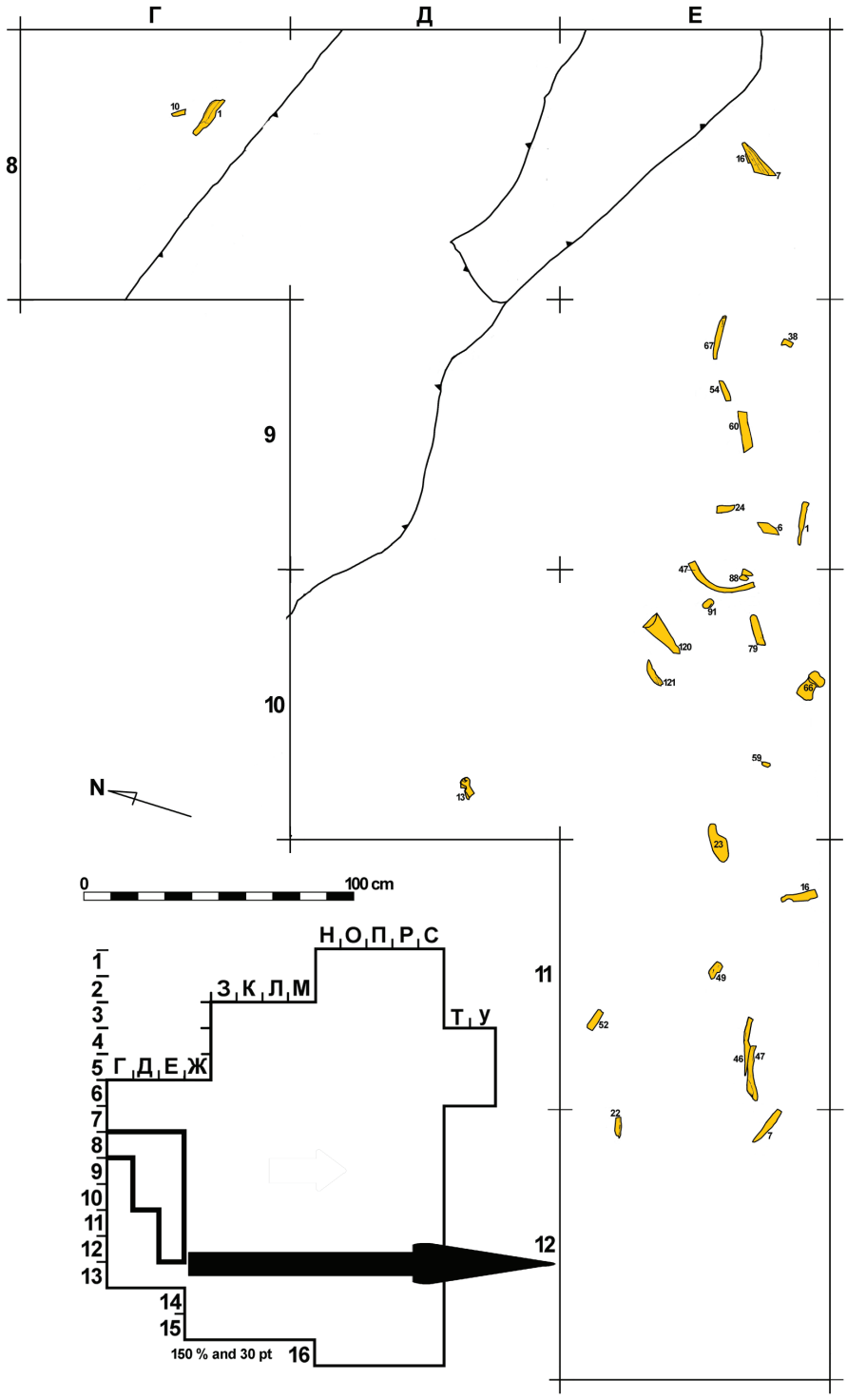


Fig. 5–46. Barmaky, western area, *Bison sp.*: the distribution of remains.

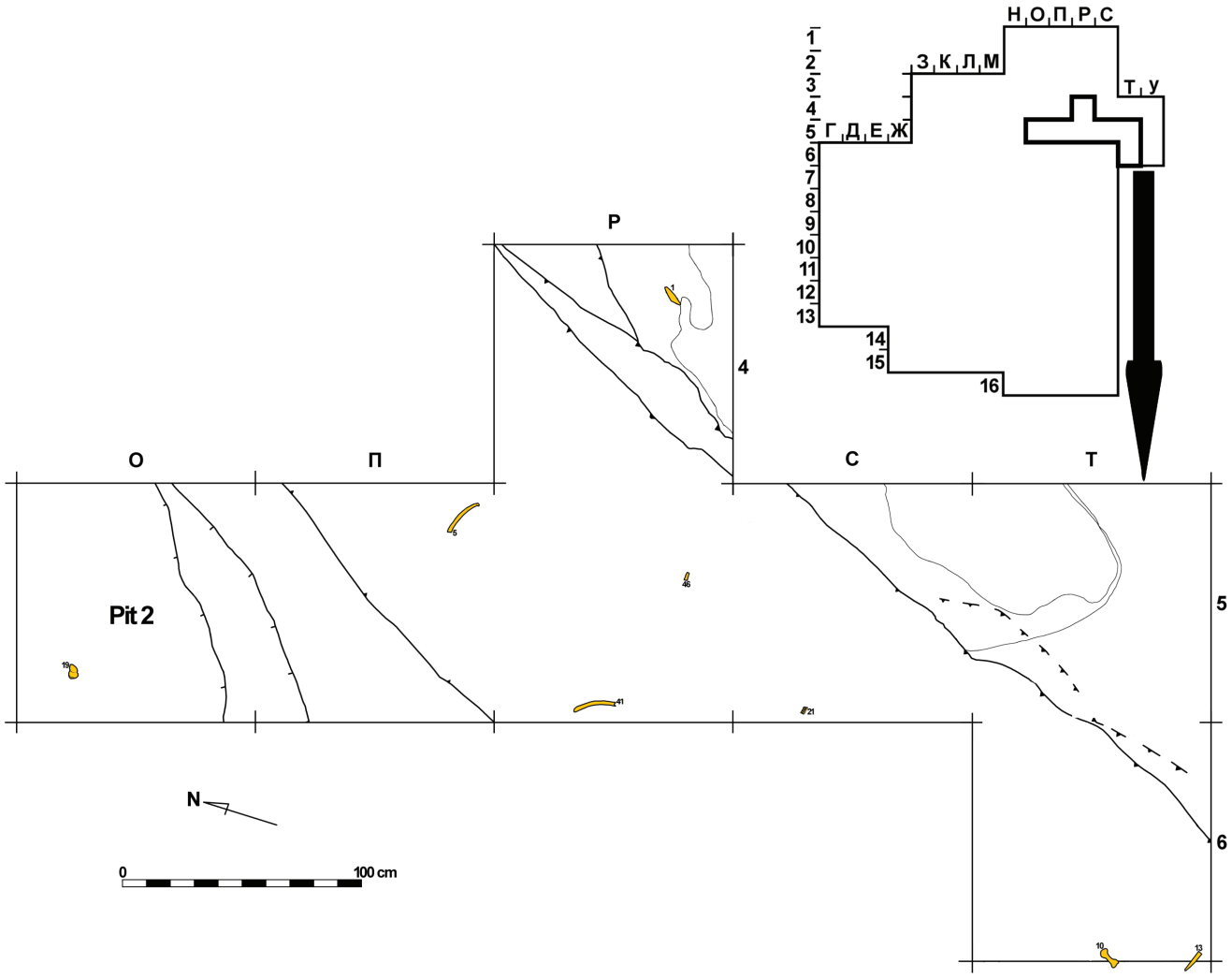


Fig. 5–47. Barmaky, eastern area, *Rangifer tarandus*: the distribution of remains.

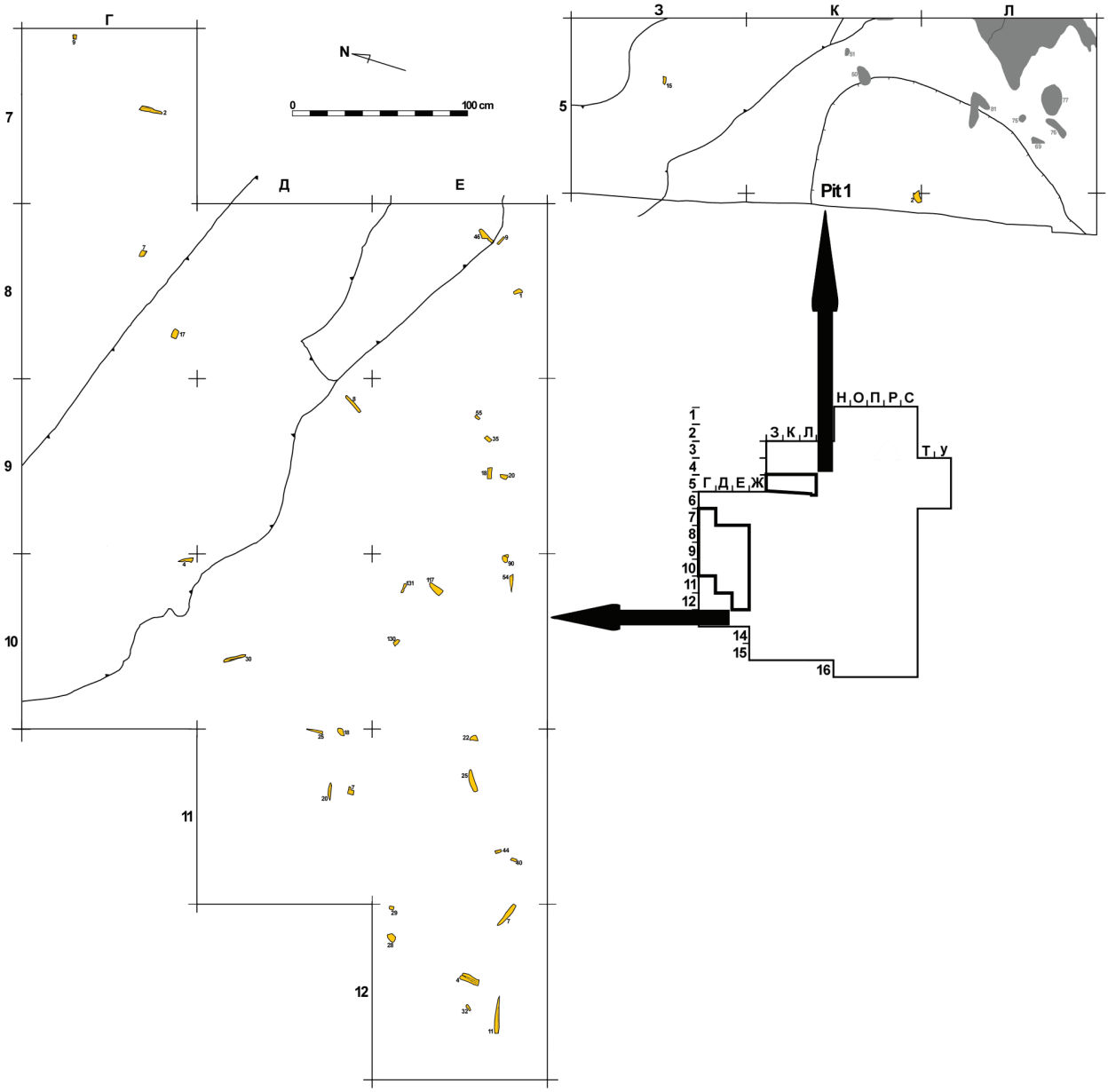


Fig. 5-48. Barmaky, western area, *Rangifer tarandus*: the distribution of remains.

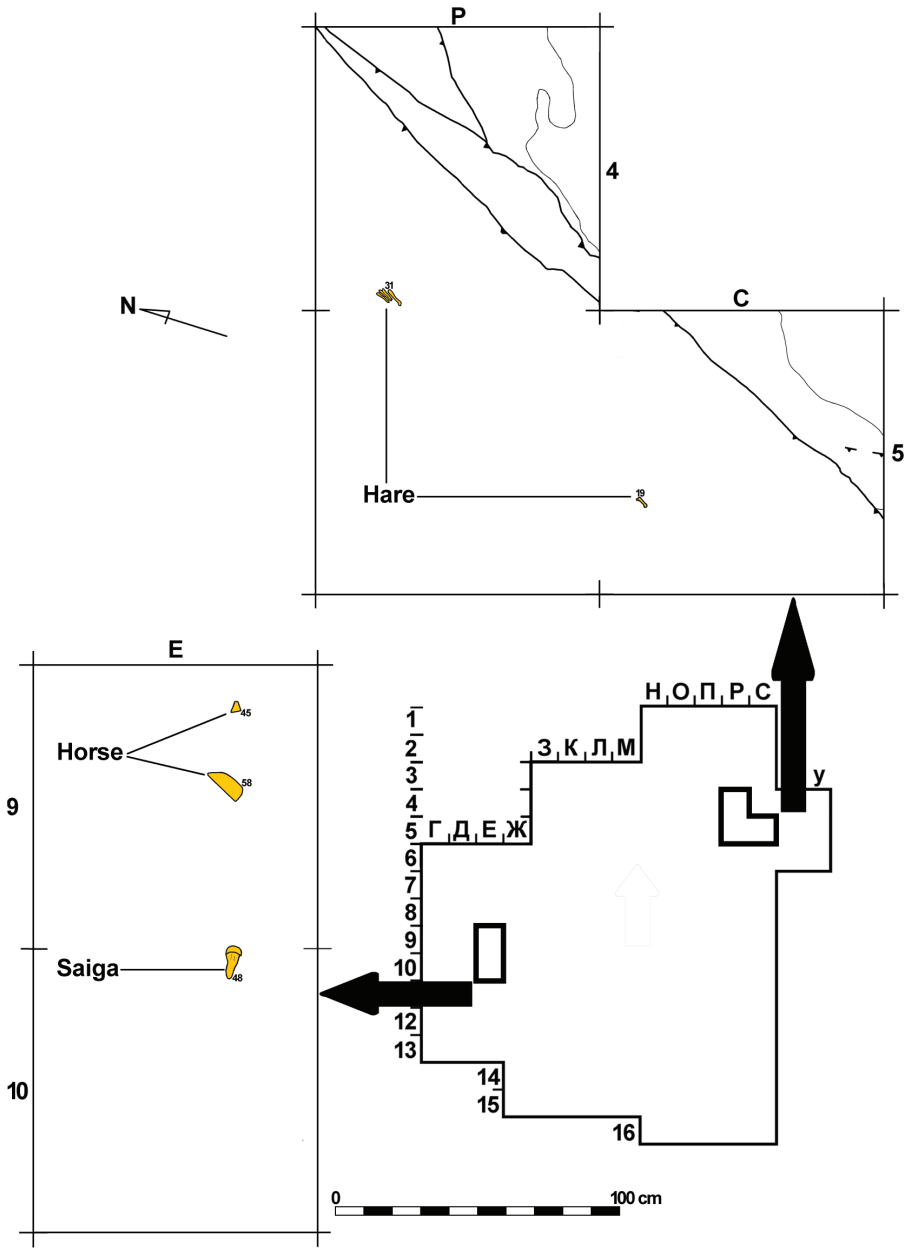


Fig. 5–49. Barmaky, horse, saiga, hare: the distribution of remains.

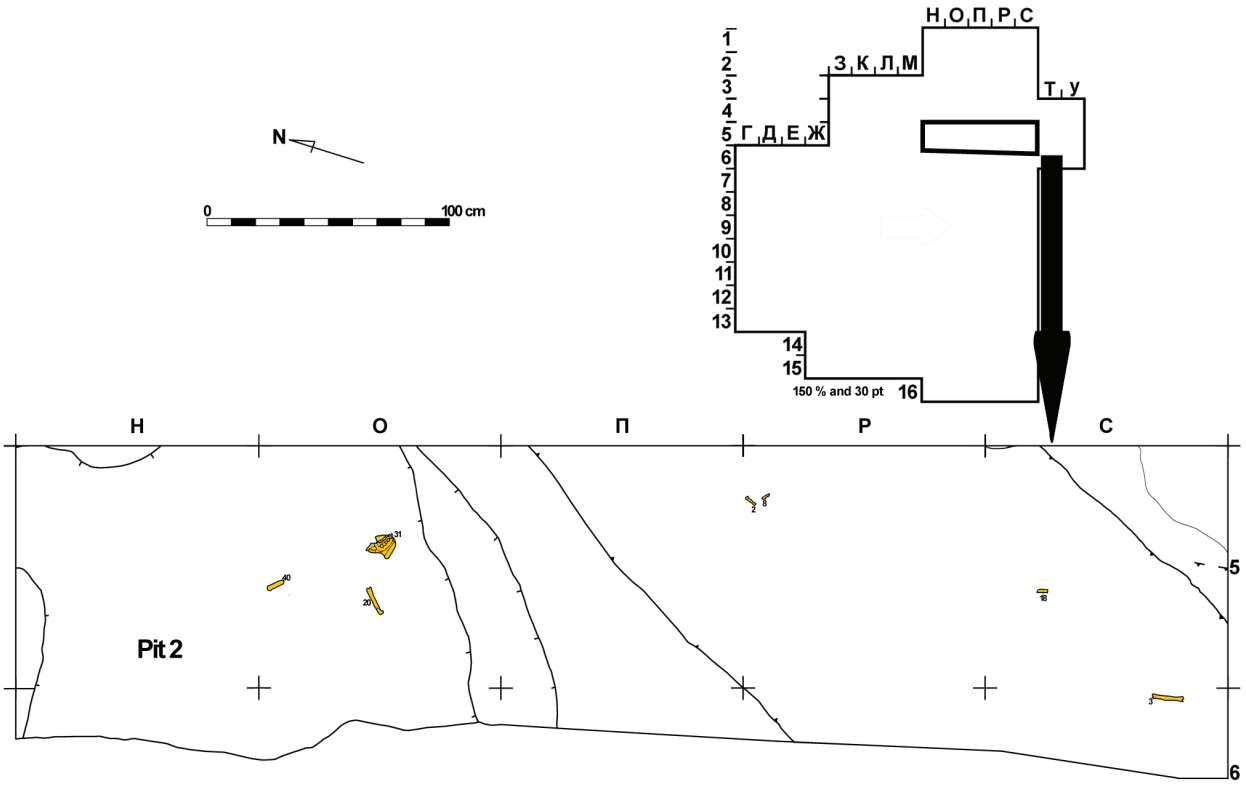


Fig. 5–50. Barmaky, eastern area, *Vulpes lagopus*: the distribution of remains.

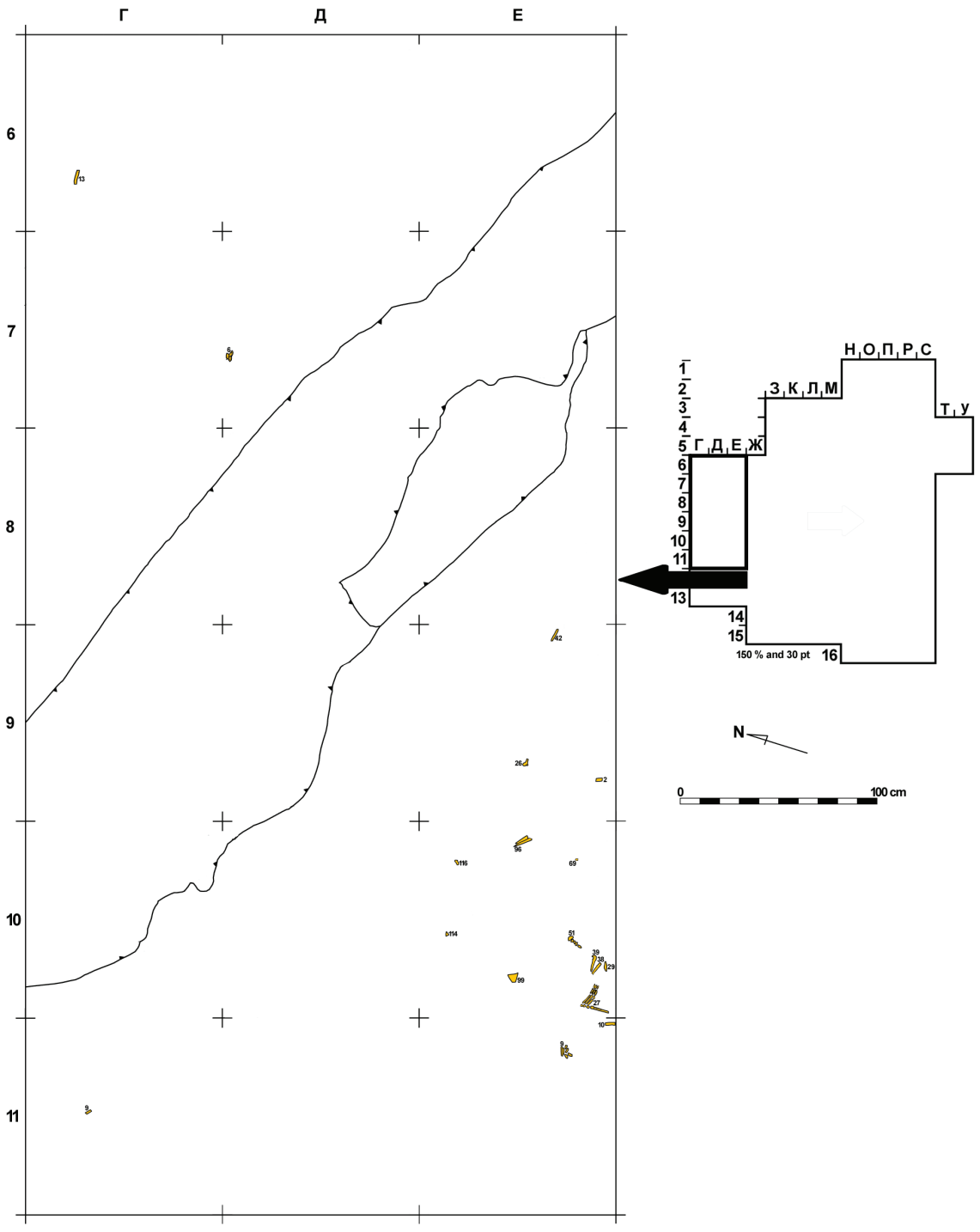


Fig. 5–51. Barmaky, western area, *Vulpes lagopus*: the distribution of remains.

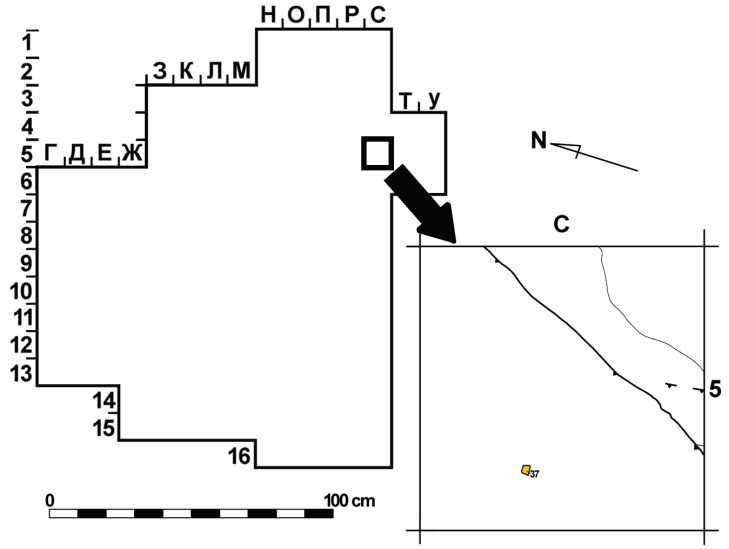


Fig. 5–52. Barmaky, eastern area, *Ursus*: the distribution of remains.

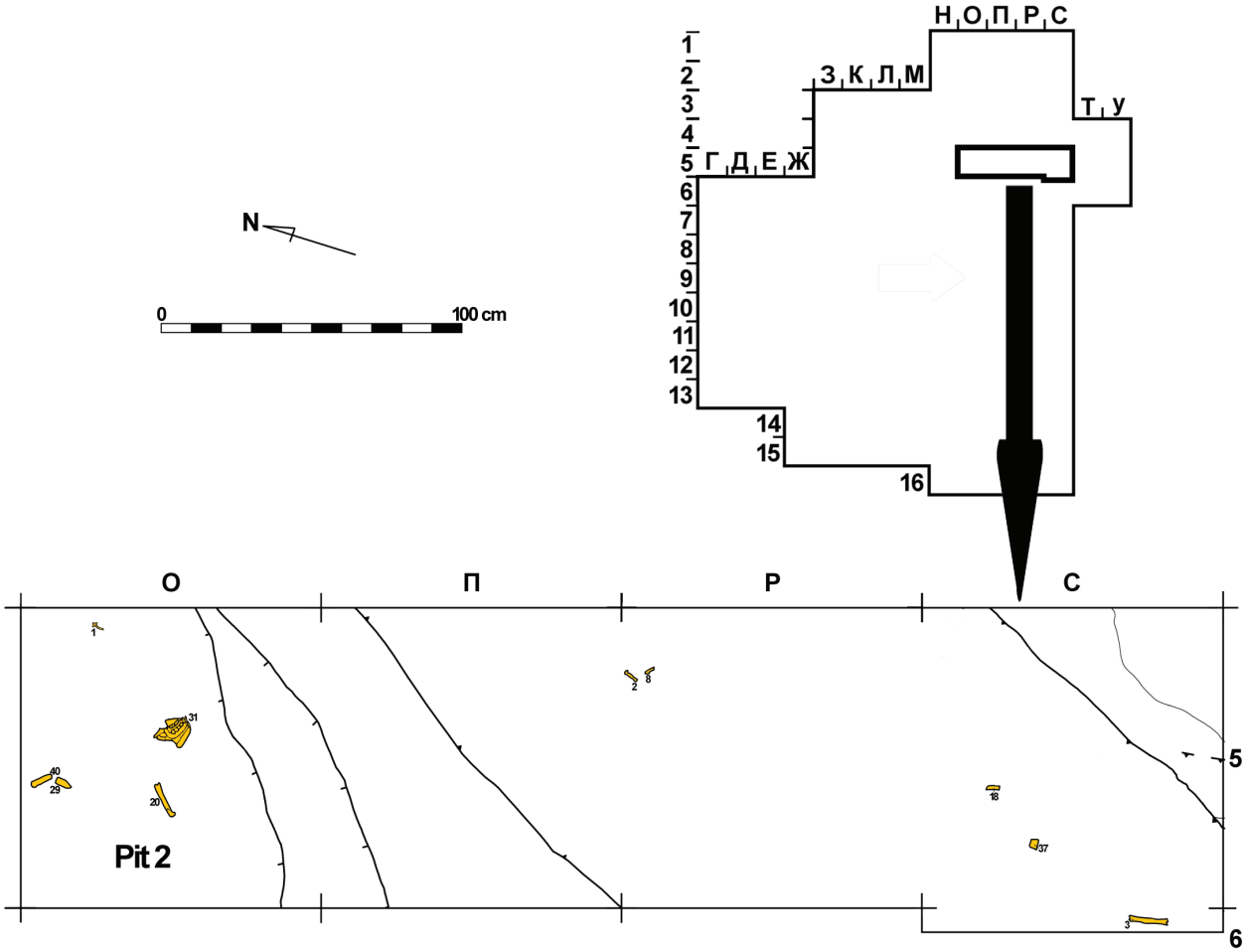


Fig. 5–53. Barmaky, eastern area, carnivors: the distribution of remains.

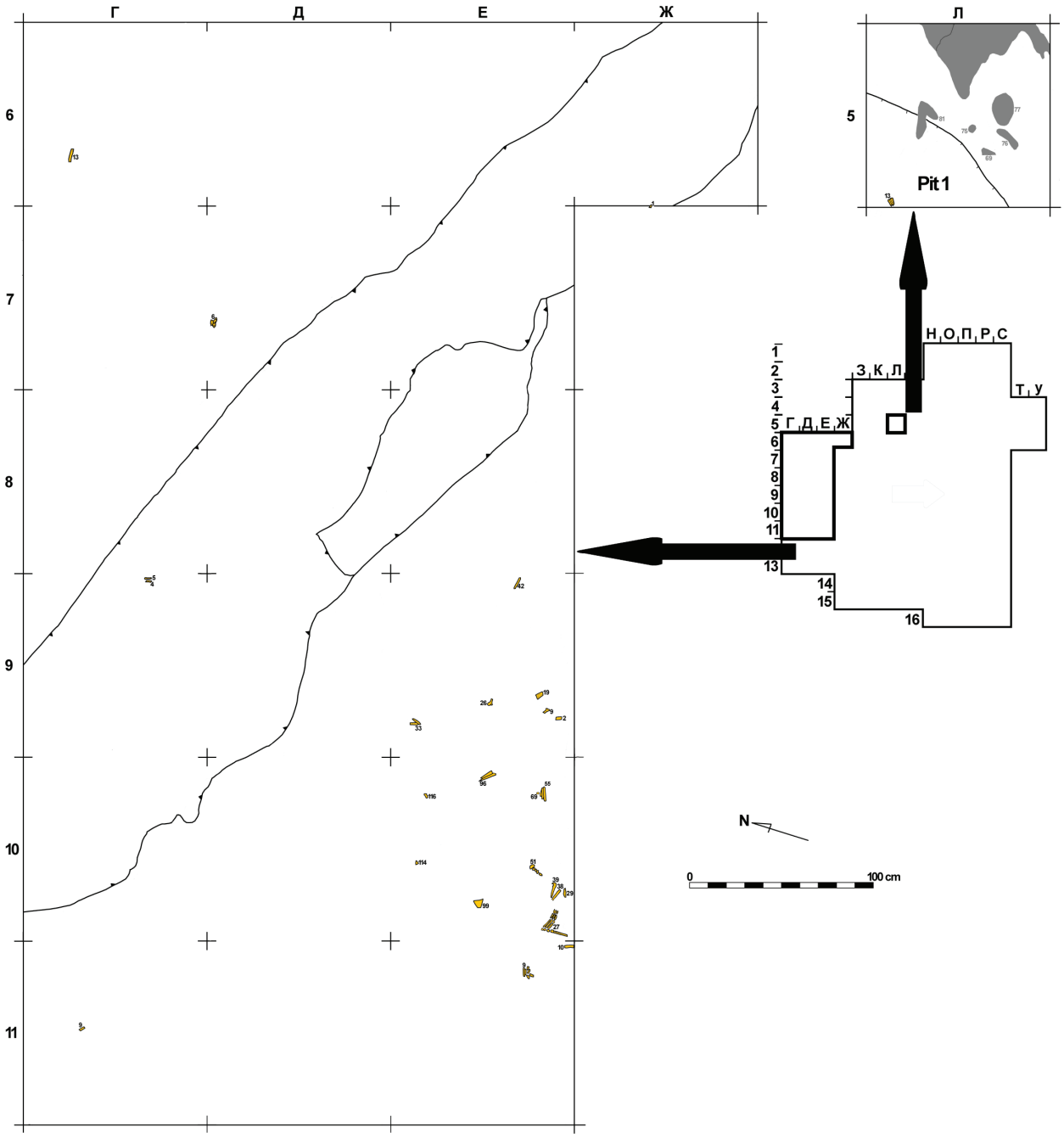


Fig. 5-54. Barmaky, western area, carnivors: the distribution of remains.

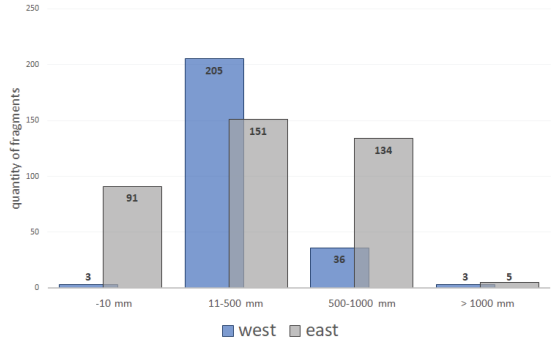


Fig. 5-55. Barmaky, western and eastern areas: comparison of mammoth fragment lengths.

## SUMMARY

In the osteological material of the excavation 2018-2020, 4797 fragments (NISP) with a weight of 97 kg could be documented. A total of 218 objects could be identified according to species in the material from 1990. In general, bone preservation of the excavations in 1990 and 2018-2020 was quite good. As the material was completely sieved during the excavation campaigns of 2018-2020, remains of small species could also be documented. The material from the 1990 excavation was obviously selected, as only larger skeletal elements of medium and large sized animals were present.

Eleven species were identified with certainty. With at least eight individuals (together with the material from the 1990 campaign), Mammoth is the dominant species and among the weighed material it makes up 93%. The eight mammoths could be differentiated into different age groups: three infantiles, one juvenile, one subadult, and three adults. It could have been a single group of animals of different ages that were killed at the same time. With mammoth, saiga, reindeer, and arctic fox, four animal species are represented that are typical representatives of a colder climate. Reindeer and arctic fox were represented by at least four, bison and hare by at least three and the other animals by at least one individual. The similar species composition in all areas of the site suggests that there is neither a large temporal difference in their use, nor a recognisable difference in subsistence practices.

The age and number of mammoth individuals are the same in the western and eastern areas of the 2018-2020 excavation, pointing towards a single settlement event with varying activities carried out at different locations. This impression is corroborated also by the different degree of fragmentation in the different areas. While dismemberment likely took place in the eastern area, selected elements were deliberately smashed, cooked, and finally deposited in the western area of the 2018-2020 excavation. The pattern of greater fragmentation can also be seen in horizon 2a and Pit 2, where the smaller fragments were possibly disposed immediately after cooking close to the place where consumption took place.

The material from the 1990 excavation is highly selective, making a clear interpretation difficult. However, as numerous complete skeletal elements were recovered, activites may have been similar to those conducted in the eastern area of the 2018-2020 excavation, i.e. dismembering of carcasses.

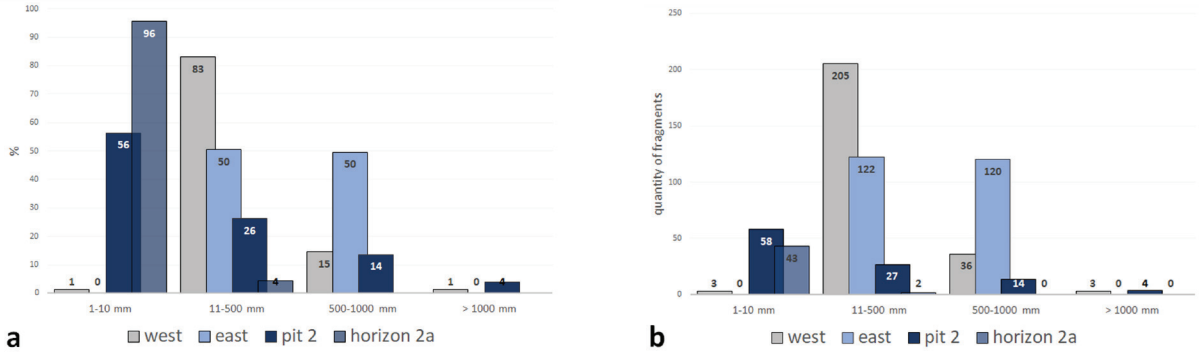


Fig. 5-56: Barmaky, comparison of mammoth fragment lengths between the different areas and findings of the 2018-2020 excavations. a: proportion of the numbers of finds in the individual areas (data indicated in the graphic), b: absolute numbers (data indicated in the graphic and in Table 5-26).

The season of occupation can be determined as winter based on the remains of the youngest mammoths and, given the amount of meat from eight individuals, may have lasted several weeks. Due to the size of the mammoths, especially the adult animals, and the presence of all parts of the body, it can be assumed that there was no long or even no transportation distance between the place where the animals were killed and the place where they were butchered. The other ungulates also presumably reached this place as complete animals. It can therefore also be assumed that their killing location was not too far from the site.

The presence of carnivores is probably related to the use of their fur, evidenced by several paw bones from foxes found in anatomical order, which could indicate that they remained on the skins.

## Acknowledgements

I am thankful to Dr. Stefan Ziegler, WWF Frankfurt, Germany, for providing information on elephant lactation. My heartfelt thanks go to Dr. Piotr Wojtal, Institute of Systematics and Evolution of Animals, Polish Academy of Sciences, Krakow, Poland, who helped me with literature, discussions on the time of mammoth's birth, and with determining the biological age of the young mammoths. I would like to thank Prof. Dr. Uwe Kierdorf, Prof. Dr. Horst Kierdorf, and Dr. Carsten Witzel, University of Hildesheim, Germany, whose department enabled me to take some detailed pictures with the optical microscope.

# STABLE ISOTOPE ANALYSES OF THE FAUNAL ASSEMBLAGE

LILIAN REISS, KERSTIN PASDA, CHRISTOPH MAYR, ANDREAS MAIER

6

The faunal assemblage documented at Barmaky is quite diverse (Chapter 5). For a better understanding of the food web, diet habits, and habitat situations of the animals at the site, we selected a spectrum of faunal material for stable isotope analyses from both herbivores and carnivores, i.e., woolly mammoth (*Mammuthus primigenius*), bison (*Bison* sp.), reindeer (*Rangifer tarandus*), horse (*Equus* sp.), hare (*Lepus* sp.), brown bear (*Ursus arctos*), arctic fox (*Vulpes lagopus*), and also aquatic birds, more precisely (European) shag (*Phalacrocorax aristotelis*) and (European) herring gull (*Larus argentatus*) (Reiss et al. 2025; Table 6-1). The reconstruction of food webs relies on the principle that isotopic fractionation varies between animals at different trophic levels. In addition, isotopic differences are also influenced by dietary isotopic variability at temporal and spatial scales, which is well reflected in bone collagen (DeNiro & Epstein 1978; Beijersbergen et al. 2021) as a regenerating tissue reflecting the average isotopic uptake of an individual over a period of up to ten years (Hedges et al. 2007; Drucker 2022).

## Methods

Stable isotope analysis of bone collagen has become an established tool for the reconstruction of palaeo-food webs and palaeoecological conditions (DeNiro & Epstein 1978, 1981; Bocherens et al. 2015). The following section briefly summarises the applied protocols for collagen extraction, quality control of extracted collagen, stable isotope analysis, and statistical analysis. In general, both the carbon ($\delta^{13}C$) and the nitrogen ($\delta^{15}N$) values in a terrestrial mammal depend on the isotopic signature of its food sources, which partly are controlled by various abiotic factors such as humidity and temperature.

The $\delta^{13}C$ values of bone collagen in herbivores allow inferences about light exposure of the consumed plants, $CO_2$ partial pressure and moisture (Peterson & Fry 1987; Bump et al. 2007; Kohn 2010). The relative $^{13}C$ enrichment between the bone collagen of a herbivorous mammal and plants is about 5‰ (e.g. Lee-Thorp et al. 1989; Ambrose & Norr 1993; Drucker 2022), while the carbon isotope carbon isotope fractionation between the consumer's collagen and the collagen of its prey lies between 0.8 and 1.3‰ (e.g. Bocherens & Drucker 2003; Fox-Dobbs et al. 2007; Krajcarz et al. 2016, 2018; Drucker 2022).

The $\delta^{15}N$ values can depend on nutritional as well as physiological factors (Peterson & Fry 1987; Vanderklift & Ponsard 2003). For instance, prolonged fasting (Hobson et al. 1993) or lactation (Bocherens et al. 1994; Fizet et al. 1995) can significantly affect the $\delta^{15}N$ values, while the consumption of mother's milk can lead to an increase in the $^{15}N$ content in body tissues of young animals (Fogel 1989; Bocherens et al. 1994; Jenkins et al. 2001). Even more important for food webs studies, the $^{15}N$ enrichment ranges between 3 and 5‰ per trophic level (e.g. DeNiro & Epstein 1981; Schoeninger & DeNiro 1984; Minagawa & Wada 1984; Bocherens & Drucker 2003; Fox-Dobbs et al. 2007; Krajcarz et al. 2018; Drucker 2022).

| Sample ID | Species | C (%) | N (%) | C/N atomar | Yield (wt. %) | n |
|---|---|---|---|---|---|---|
| N 114 * | *Bison* sp. | 44.2 | 10.8 | 4.8 | 2.3 | 2 |
| ID 411 * | *Bison* sp. | 22.4 | 7.7 | 3.4 | 0.6 | 3 |
| N 115 | *Bison* sp. | 36.2 | 13.3 | 3.2 | 0.6 | 3 |
| ID 582 * | *Bison* sp. | 28.6 | 10.2 | 3.3 | 0.8 | 3 |
| ID 238 * | *Equus* sp. | 12.1 | 4 | 3.5 | 0.7 | 3 |
| ID 530 | *Larus argentatus* | 35.6 | 13.1 | 3.2 | 2.1 | 3 |
| ID 196 * | *Lepus* sp. | 16.8 | 5.8 | 3.4 | 0.9 | 3 |
| ID 181 | *Lepus* sp. | 32.9 | 11.6 | 3.3 | 5.6 | 3 |
| N 177 | *Lepus* sp. | 36.6 | 13.5 | 3.2 | 2.2 | 3 |
| ID 361 | *Lepus* sp. | 34.4 | 12.7 | 3.2 | 3.9 | 3 |
| ID 11 * | *Mammuthus primigenius* | 15.6 | 5.2 | 3.5 | 1.2 | 3 |
| N 113 * | *Mammuthus primigenius* | 25 | 8.9 | 3.3 | 4.4 | 3 |
| N 11 * | *Mammuthus primigenius* | 21.5 | 7.3 | 3.4 | 1.6 | 3 |
| N 119 * | *Mammuthus primigenius* | 76.9 | 2.7 | 33.2 | 2.8 | 3 |
| N 121 | *Mammuthus primigenius* | 43.2 | 16.2 | 3.1 | 3.9 | 3 |
| N 20 | *Mammuthus primigenius* | 33.4 | 11.2 | 3.5 | n.d. | 1 |
| N 10 | *Mammuthus primigenius* | 40.9 | 14.8 | 3.2 | 2.8 | 3 |
| N 13 | *Mammuthus primigenius* | 40.9 | 14.2 | 3.4 | 5.1 | 1 |
| N 14 | *Mammuthus primigenius* | 41.6 | 14.9 | 3.3 | 3.8 | 2 |
| N 16 | *Mammuthus primigenius* | 32.9 | 11.8 | 3.3 | 4.5 | 3 |
| N 21 | *Mammuthus primigenius* | 38 | 13.8 | 3.2 | 7.4 | 3 |
| ID 8 | *Mammuthus primigenius* | 37.1 | 13.4 | 3.2 | 3.1 | 3 |
| ID 10 | *Mammuthus primigenius* | 39.5 | 14.4 | 3.2 | 2.8 | 3 |
| ID 214 | *Mammuthus primigenius* | 38.2 | 13.8 | 3.2 | 1.6 | 3 |
| ID 357 | *Phalacrocorax aristotelis* | 31.8 | 11.2 | 3.3 | 1.1 | 1 |
| ID 222 * | *Rangifer tarandus* | 8.6 | 3 | 3.4 | 1.1 | 3 |
| ID 416 * | *Rangifer tarandus* | 27 | 9.2 | 3.4 | 0.5 | 2 |
| ID 513 | *Rangifer tarandus* | 39.4 | 14.6 | 3.1 | 4.6 | 3 |
| ID 330 | *Rangifer tarandus* | 41 | 15.3 | 3.1 | 9 | 3 |
| N 64 | *Ursus arctos* | 39.2 | 14.6 | 3.1 | 2.7 | 3 |
| ID 3 * | *Vulpes lagopus* | 62.7 | 22.1 | 3.3 | 5.5 | 2 |
| N 22 | *Vulpes lagopus* | 38.6 | 13.7 | 3.3 | n.d. | 2 |
| N 112 | *Vulpes lagopus* | 40.1 | 13.9 | 3.4 | n.d. | 1 |
| ID 273 | *Vulpes lagopus* | 36.2 | 13.1 | 3.2 | 2.6 | 3 |
| ID 187-191 | *Vulpes lagopus* | 38.9 | 14 | 3.2 | 3.8 | 3 |
| ID 367 | *Vulpes lagopus* | 41.7 | 15.5 | 3.1 | 5.6 | 3 |
| ID 512 | *Vulpes lagopus* | 36.7 | 13.6 | 3.1 | 2 | 3 |

Table 6-1. Barmaky. List of chemical results of the analysed material. Given are the carbon and nitrogen composition, the C/N ratio, the weight percentage (wt.%) of the collagen yield and the number of analyses per specimen (n). Samples marked with an asterisk indicate values outside the range of well-preserved collagen and are thus not discussed any further due to their anomalous chemical composition; n.d. means 'not determined' (Table from Reiss et al. 2025).

## Collagen extraction protocol and quality check

Collagen extraction was performed using a slightly modified protocol based on Bocherens et al. (1991). Bone fragments weighing approximately 0.25 to 1.0 g were carefully cut from each specimen using a rotary tool (Proxxon-Micromot, Germany) equipped with a circular diamond blade. The samples were cleaned with sandpaper, soaked in deionized water for 30 minutes, briefly cleaned in an ultrasonic bath (10 seconds), and dried overnight at 40 °C. Subsequently, the dried samples were ground into a fine powder using a mortar and pestle.

From each powdered sample (grain size: 0.3–0.7 mm), 0.25 to 1.0 g was weighed into centrifuge tubes, soaked in 1 M HCl, and agitated on a rotator for 20 minutes to remove carbonate components. The samples were then washed repeatedly with distilled water and centrifuged (Heraeus Multifuge 3L-R, Thermo Electron Corporation, USA) at 3000 rpm for five minutes per wash until a neutral pH was achieved. To eliminate humic acids, the samples were treated with 0.125 M NaOH and left under a fume hood for 20 hours. Afterwards, the samples were washed again with distilled water and centrifuged until neutral pH was restored.

In the final stage, the pellets were immersed in 0.01 M HCl (pH 2) and incubated in a water bath (Julabo, SW23, Germany) at 95 °C for 10 to 17 hours to solubilize the gelatin. The resulting solution was filtered through MF-Millipore membrane filters (5.0 µm) using a vacuum filtration apparatus, washed with deionized water, frozen, and lyophilized.

To mitigate the potential bias in isotope values caused by impurities or diagenetic alterations in prehistoric bone collagen, preservation quality was assessed using criteria such as atomic C/N ratios, elemental contents, and collagen yields. Pure, well-preserved collagen is characterized by atomic C/N ratios ranging between 2.9 and 3.6. Consequently, samples with C/N ratios exceeding 3.6 were excluded from analysis (DeNiro 1985; Ambrose 1990; van Klinken 1999; Grupe et al. 2003; Coltrain et al. 2004; Bösl et al. 2006).

The minimum acceptable yield of extracted collagen varies between 0.5 and 2 wt.%, depending on the study (DeNiro & Weiner 1988; Ambrose 1990; van Klinken 1999; Ambrose & Norr 1993; Dobberstein et al. 2009). For elemental contents, well-preserved collagen should contain 11–16 wt.% nitrogen and approximately 35±9 wt.% carbon (van Klinken 1999) (Table 6-1).

## Stable isotope analysis

Based on the amount of extracted collagen, samples were analysed in duplicates or triplicates whenever feasible at the stable isotope laboratory of the Institute of Geography, Friedrich-Alexander-Universität Erlangen-Nürnberg. For analysis, 240–260 µg of collagen was encapsulated in tin capsules and combusted in an elemental analyser (Flash 2000, Thermo Scientific, USA). The evolved gases ($CO_2$ and $N_2$) were transferred via a CONFLO-IV interface (Thermo Scientific, USA) to an isotope ratio mass spectrometer (Delta V Advantage, Thermo Scientific, USA) for isotopic analysis.

Isotope results are expressed as delta (δ) values in per mil (‰) using the equation:

$$\delta = R_{Sample} / R_{Standard} - 1 \quad (1)$$

where R is the mass ratio of the heavier to the lighter isotope ($^{13}C/^{12}C$ or $^{15}N/^{14}N$) of the sample and the international standards Vienna Pee Dee Belemnite (VPDB) for carbon and atmospheric nitrogen (AIR) for nitrogen (Coplen 2011).

The weight percentages of carbon (wt.%) and nitrogen (wt.%) were determined by comparing the peak areas of the sample gases to the sample weights. Calibration for elemental content was performed using the standards atropine and cyclohexanone 2,4-dinitrophenylhydrazone, with a measurement error of <5%. The elemental contents and atomic C/N ratios derived from these measurements were used to assess the chemical purity and preservation of the collagen.

## Statistical analysis

Statistical calculations were carried out with R studio (version R-4.2.2). Shapiro-Wilk tests were used to check for normal distribution of data (Dytham 2011). For all analyses performed, a significance level of 0.05 was chosen. The determination of isotopic niche widths of the different analysed animal taxa was performed using the Stable Isotope Bayesian Ellipses in R (SIBER) package (Jackson et al. 2011). This method is based on the calculation of bivariate ellipses and substitutes the previously common use of convex hulls, which were dependent on the sample size (Laymann et al. 2007; Jackson et al. 2011). The estimates of ellipses using a Bayesian approach provide a robust comparison between data sets with different sample sizes and therefore allow a direct comparison of isotopic niches in different communities (Jackson et al. 2011). We determined the convex hulls, i.e. the total area (TA) and the standard ellipse area (SEA, in ‰²) and the standard ellipse area corrected by sample size (SEAc) of the taxa represented by n ≥ 3. Our calculation of the SEAc using a Bayesian probability estimation includes 40% of all potential specimens that would fit into the respective niches.

## Results

Based on the quality criterion considered, a total of 12 samples were either outside of the range of acceptable and sufficient collagen preservation or other chemical characteristics, such as nitrogen or carbon contents (wt.%) were either too high or too low (Table 6-1). Therefore, they neither underwent further analysis nor are they included in the data evaluation and discussion.

The remaining samples have a normal data distribution according to Shapiro Wilk test ($\delta^{13}C$: W = 0.93696, p = 0.1259; $\delta^{15}N$: W = 0.9542, p = 0.3111).

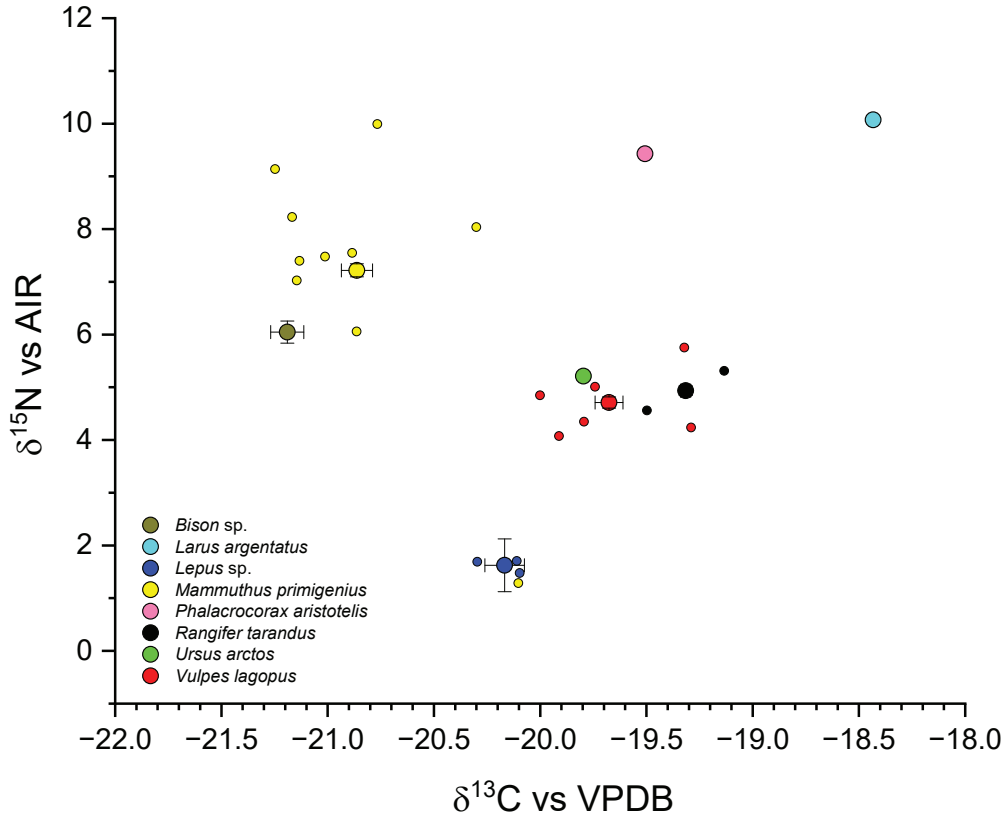


Fig. 6-1. Nitrogen vs. carbon stable isotope values of bone collagen from the Upper Palaeolithic site Barmaky. Mean values are represented as big circles and whiskers represent the respective standard deviations. Small symbols indicate individual (multiple) measurements for taxa with n > 1 (Fig. from Reiss et al. 2025).

The isotope-inferred food web of Barmaky reveals a niche partitioning that reflects differences in habitat and/or dietary behaviour (Stewart et al. 2003; Bocherens et al. 2015; Schwartz-Narbonne et al. 2015, 2019).

Mammoth and bison exhibit the lowest $\delta^{13}C$ mean values, ranging from −20.9±0.1‰ to −21.2±0.1‰, respectively, while the measured sample of the European herring gull has the highest $\delta^{13}C$ value of −18.4‰ (Fig. 6-1). Among the mammals, reindeer shows the highest $\delta^{13}C$ mean value of −19.3±0.3‰ followed by arctic fox (−19.7±0.1‰), brown bear (−19.8±0.03‰) and hare (−20.2±0.1‰).

Both single specimens of aquatic birds, i.e., European herring gull and European shag, exhibit the highest $\delta^{15}N$ values of 10.1‰ and 9.4‰, respectively. Mammoth (7.2±0.1‰) and bison (6.0±0.2‰) have also high $\delta^{15}N$ mean values. Among the herbivores, hare exhibits the lowest $\delta^{15}N$ mean value of 1.6±0.5‰. However, a single mammoth bone specimen exhibits an equally low $\delta^{15}N$ value (1.3‰). Interestingly, arctic fox (4.7±0.1‰) as reindeer (4.9±0.5‰) and brown bear (5.2±0.2‰) (Fig. 6-1).

SIBER analyses revealed the highest total area for mammoth (4.34‰²) followed by arctic fox (0.77‰²) and hare (0.02‰²) (Fig. 6-2). However, as hare is only represented with three data points, its SEA should be considered with caution. The SEA of mammoth is 2.17‰² and the SEAc 2.44‰². Arctic fox exhibits a SEA of 0.56‰² and a SEAc of 0.70‰², whereas hare shows the smallest ellipses with a SEA of 0.03‰² and, corrected for sample size, a SEAc of 0.07‰².

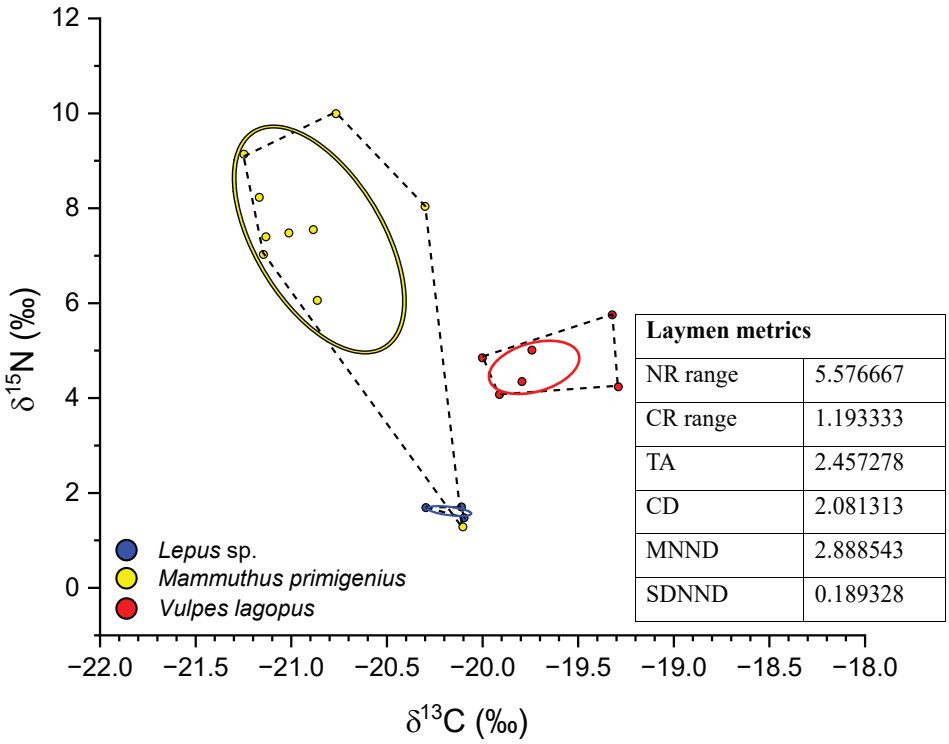


Fig. 6-2. Standard ellipse areas (SEAc) (solid ellipses) and convex hulls (dashed lines) of woolly mammoth, hare, and arctic fox. Abbreviations of Laymen metrics are as follows: NR = $\delta^{15}N$ range; CR = $\delta^{13}C$ range; CD = mean distance to centroid; MNND = mean nearest neighbour distance; SDNND = standard deviation of the nearest neighbour distance (Fig. from Reiss et al. 2025).

## DISCUSSION AND CONCLUSION

### Food web and reconstruction of diet and habitat

In general, the carbon isotope composition of plants is influenced by a variety of factors, such as humidity, $CO_2$ partial pressure, light intensity, and temperature (Tieszen 1991; Bonafini et al. 2013). Whereas decreased $\delta^{13}C$ plant values result from reduced light, higher atmospheric $CO_2$ partial pressure, and increased water availability, increased $\delta^{13}C$ plant values are the result of decreased temperatures, drier conditions, and a lower atmospheric $CO_2$ partial pressure (Pataki et al. 2003; Kohn 2010; Drucker 2022).

### Mammoth and bison

Mammoths exhibit the lowest $\delta^{13}C$ values in the faunal assemblage of Barmaky. Shrubs, forbs and graminoids (grasses and sedges) exhibited the lowest $\delta^{13}C$ values in modern arctic realms (Fizet et al. 1995) and in combination with freshwater plants (Kirillova et al. 2016) have frequently been discussed as the main diet of mammoth in previous studies (e.g. Vereshchagin & Baryshnikov 1982; Olivier 1982; Tütken et al. 2007; Kosintsev et al. 2012; Metcalfe et al. 2013; Drucker 2022; Malikov et al. 2023; Reiss et al. 2025). Based on tooth wear analyses, Eurasian mammoths show plasticity in diet between grazing and browsing (Rivals et al. 2010, 2012, 2015). They can be described as grass-dominated mixed feeders, whose wide dietary range indicates the adaptability of their feeding behaviour to the available vegetative resources (Rivals et al. 2012; Fig. 6-2). Consequently, the mammoths documented at Barmaky were probably living in the more humid parts of the environment, such as riparian habitats and often consumed grasses and sedges (Guthrie 2001; Wooller et al. 2007; Drucker et al. 2008; Kirillova et al. 2016; Drucker 2022).

The $\delta^{15}N$ values of mammoths, in contrast, are the highest in the entire assemblage, even higher than those of the arctic fox (see below). High $\delta^{15}N$ values in mammoths, often comparable to those of carnivores, are a common phenomenon throughout Eurasia (Bocherens et al. 1994, 1997, 2001, 2011, 2015; Iacumin et al. 2000, 2010; Fox-Dobbs et al. 2008; Drucker et al. 2003, 2015, 2018; Szpak et al. 2010; Reiss et al. 2023). This anomalously high $\delta^{15}N$ signature of the mammoths is still subject of scientific debate and has not been conclusively clarified. However, it has been demonstrated that physiological characteristics can largely be ruled out (Schwartz-Narbonne et al. 2015; Naito et al. 2016). Rather, high $\delta^{15}N$ values may result from dietary habits and the occupation of a certain ecological niche (McKendrigk et al. 1980; Bocherens 2003; Schwartz-Narbonne et al. 2019; Drucker 2022; Malikov et al. 2023). Coprophagy in mammoths could be another reason of high $\delta^{15}N$ values (van Geel et al. 2011; Metcalfe et al. 2013). The high variability in $\delta^{15}N$ values and large niche breath of mammoth, as indicated by their SEAc (Fig. 6-2), however, could also be the consequence of individual mobile behaviour in geographically and climatically different regions. Variability in mammoth mobility pattern between high and low $\delta^{15}N$ groups, which could be translated as highly mobile versus sedentary individuals, has not yet been documented, but is very likely.

A single data point of bison suggests a co-occupation of the mammoth niche and/or a highly mobile behaviour as well.

### Reindeer

Reindeer have the highest $\delta^{13}C$ values among the herbivorous taxa, indicating feeding in an edaphically drier habitat with less vegetation and the consumption of large amounts of lichen (Bocherens et al. 2015; Finstad & Kielland 2011; Drucker et al. 2011). Just as mammoth, reindeer are considered to be migratory animals and thus their isotopic values may just as well reflect isotopic signatures from geographically distinct environments (Wooller et al. 2021).

### Hare

Hare exhibits an intermediate position between mammoth and reindeer, and most probably reflects local site conditions as hares are non-migratory/sedentary animals (Fig. 6-3), feeding mostly on herbs.

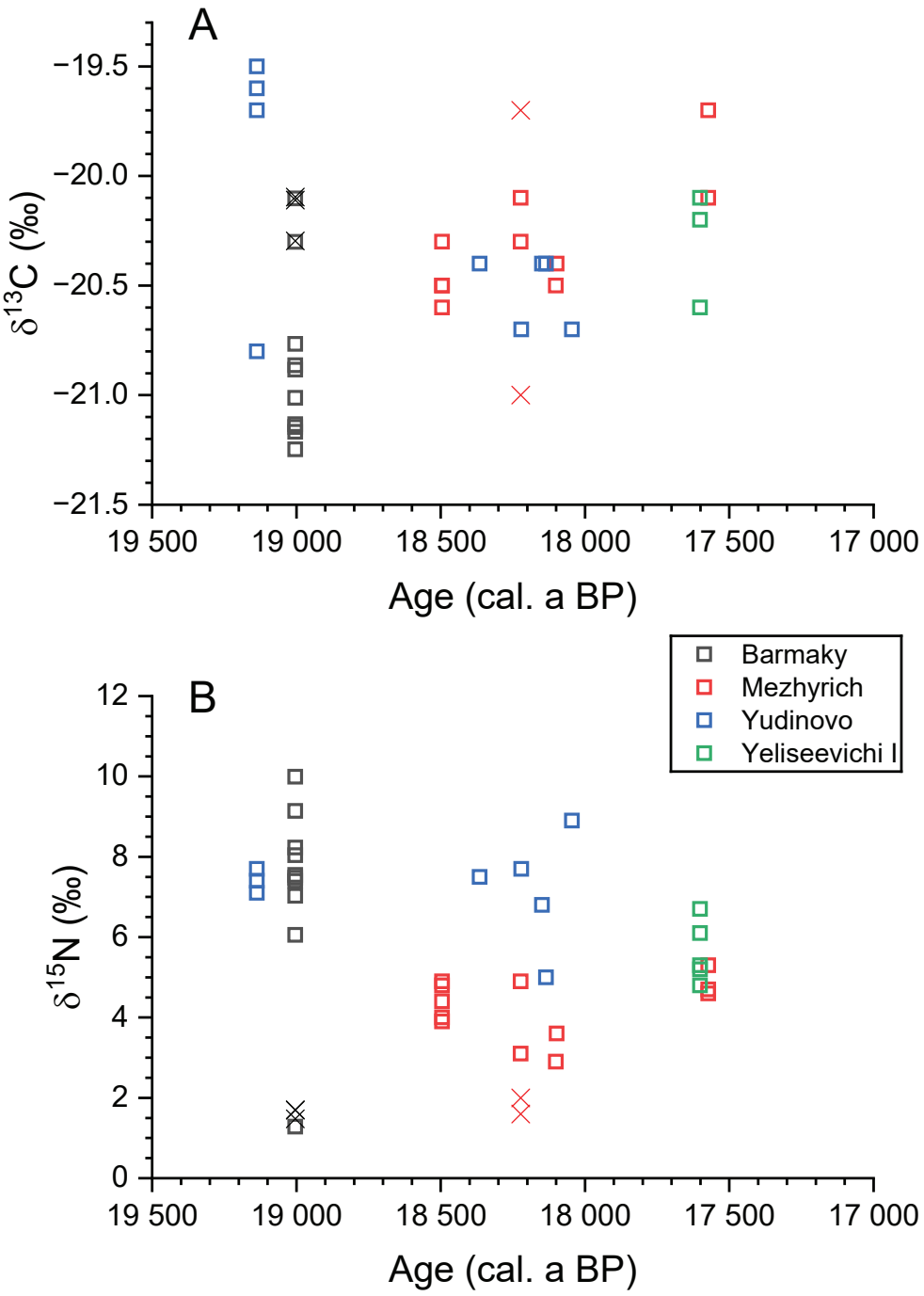


Fig. 6–3. Mammoth (open boxes) and hare (crosses) collagen isotope data from different Epigravettian sites in the East European Plain versus age. A. $\delta^{13}C$ of bone collagen. B. $\delta^{15}N$ of bone collagen. Isotope values from Barmaky (this study) are compared to Yudinovo (Drucker et al. 2018; Iacumin et al. 2000), Mezhyrich (Iacumin et al. 2000; Drucker et al. 2014), and Yeliseevichi (Iacumin et al. 2000) (Fig. from Reiss et al. 2025).

## Arctic fox and brown bear

Arctic fox exhibits relatively low $\delta^{15}N$ values (4.7±0.1‰) and is on the same isotopic level as reindeer and brown bear, the latter, at least during late Pleniglacial conditions, considered an omnivorous species (Matheus 1995; Hofreiter et al. 2004; Drucker et al. 2018). Interestingly, arctic fox and brown bear do not show niche partitioning but rather share an isotopic niche. However, brown bear is only represented by a single data point and therefore should be considered with caution. As foxes are often described as generalist feeders, their decreased $\delta^{15}N$ values may be the result of a diet based on micromammals with low $\delta^{15}N$ values close to the isotopic baseline, carrion, or even partly an omnivorous diet (Baumann et al. 2020; Baumann 2023). In fact, the application of a linear dietary model results in local hares probably making up a large proportion of the diet of arctic foxes as their collagen is enriched by about 3‰ in $^{15}N$ and by about 1‰ in $^{13}C$ (Reiss et al. 2025).

## Birds

The high $\delta^{15}N$ values of the bird specimens most probably result from their limnic and/or marine feeding habits (Schoeninger & DeNiro 1984) and therefore could also indicate migratory behaviour. At the same time, they also exhibit the highest $\delta^{13}C$ values.

## Palaeoenvironmental conditions around Barmaky

Before the Last Glacial Maximum, a steppe and tundra-like ecosystem, also referred to as the "mammoth steppe" (Guthrie 2001), was prevalent in the East European Plain. This ecosystem was characterised by a highly diversified niche partitioning, particularly between different herbivorous taxa, and most notably a specific mammoth niche with particularly high values of nitrogen (Iacumin et al. 2000, 2006, 2010; Drucker et al. 2003, 2018; Stevens and Hedges 2004; Stevens et al. 2008; Bocherens et al. 2015; Krajcarz et al. 2016; Fox-Dobbs et al. 2008; Drucker & Fontana 2024). It has been shown that significant environmental changes that affected the base of terrestrial food webs could have had an impact on isotopic niche partitioning (Stevens et al. 2008; Schwartz-Narbonne et al. 2015; Drucker et al. 2018; Reiss et al. 2023) and local environmental conditions played an important role in $\delta^{15}N$ signatures of Central European mammoths (Iacumin et al. 2000; Drucker et al. 2018). Environmental changes during and after the LGM may have led to spatio-temporal differences at a regional-centennial scale of the isotopic baseline. As a consequence, the mammoth steppe ecosystem seems to have become depleted in some regions and during some periods, apparently leading to a regional collapse of former independent herbivorous niches into a single niche and the loss of a specific mammoth niche. Evidence of such environmental depletion are reported for instance from Kammern-Grubgraben in Lower Austria and Mezhyrich in Central Ukraine, where mammoth remains with exceptionally low $\delta^{15}N$ values were found, while those from Yeliseevichi (Russia) had intermediate $\delta^{15}N$ values (Iacumin et al. 2000; Drucker et al. 2018; Reiss et al. 2023).

At Mezhyrich, mammoths also exhibited unusually low $\delta^{15}N$ values, which corresponded to those of the associated hares (Iacumin et al. 2000; Drucker et al. 2014). At Barmaky, however, the mammoth $\delta^{15}N$ values and those of hares differ significantly from each other with one exception (Fig. 6-3B). That leads us to suggest an alternative explanation to the mammoth niche hypothesis, according to which the mammoths from Mezhyrich were killed closer to their main habitat, while the mammoths from Barmaky may have spent most of their lives in a different location from where they died, reflecting their highly mobile behaviour. This could mean that the $\delta^{15}N$ baseline value, which is determined by the $\delta^{15}N$ signature of the soil, was higher in the main habitat of the Barmaky mammoths than at their death place. On a longer timescale, climate model results suggest that the sites had different climatic conditions (Reiss et al. 2025). For example, the Mezhyrich site was always located outside the area with continuous permafrost, while the largely contemporaneous Yudinovo site (Drucker et al. 2018; Iacumin et al. 2000), located almost 400 km further northeast, was always located within the area with continuous permafrost (Reiss et al. 2025). Such climatic differences should be reflected in the $\delta^{15}N$

values, but the lack of more complete food webs in the region makes it difficult to currently draw precise conclusions.

Interestingly, the mammoths from Barmaky exhibit very low $\delta^{13}C$ values, which differ significantly from those of the other Epigravettian sites in the region (Fig. 6-3). This could reflect a more diverse landscape with a vegetation cover that included scattered stand of trees (Tieszen 1991; Pataki et al. 2003; Kohn 2010; Bonafini et al. 2013) and/or could be the result of a regional precipitation gradient with slightly wetter conditions closer to the Carpathian Arc.The food web reconstructed for the faunal assemblage documented at Barmaky shows a characteristic structure with differences in the trophic ecology between herbivores, carnivores and water-bound birds. A $\delta^{13}C$ clustering between the herbivorous species hare and mammoth on the one hand and reindeer on the other indicates a niche partitioning between both herbivorous groups associated with differences in diet and habitats along a moisture gradient.

Shifts in temperature and aridity between 19 and 17 ka may have altered the ecological situation in the East European plain, with the region of Volhynia shifting in and out of permafrost conditions and concomitant vegetational responses, influencing supply and quality of the available food for herbivores (Reiss et al. 2025). The diverse herbivorous niches documented at Barmaky, including a well-marked mammoth niche, might signal relatively favourable conditions in the region at the time of the occupation of the site around 19 ka, probably coinciding with a shift of the permafrost line north of the Volhynian region.

# 7

# LITHIC RAW MATERIALS

MICHAEL BRANDL

The lithic artefacts discovered at Barmaky are exclusively made from high-quality Turonian flint. This material is prevalent throughout the Volhynian Uplands, occurring in nodular or flat forms that appear macroscopically similar. The nearest flint outcrop lies just 300 meters south of the site, within chalk and marl deposits on an eroded hillside. To date, there is no evidence of imported, non-local flint in the Barmaky assemblage. Ongoing analyses aim to determine the provenance of the raw material used at Barmaky. This report presents the initial findings from background sampling of lithic outcrops at the site and outcrops in the surrounding region.

To explore the potential for differentiating specific varieties of locally available high-quality Upper Cretaceous (Cenomanian and predominantly Turonian) flint within the study area, geological samples were collected from various locations near Rivne and Barmaky. The most suitable reference samples thus far originate from a quarry at Ostriv, located approximately 30 km southwest of Barmaky, where three distinct flint layers were analysed using the Multi-Layered Chert Sourcing Approach (MLA: Brandl 2016; Brandl et al. 2018). Using Ostriv as a baseline, samples from Rivne 1 and Barmaky (spots 326–329) were examined, including both residual and transported materials. Stereomicroscopic analysis revealed a broader range of microfacies in the Rivne and Barmaky samples compared to those from Ostriv's primary sequence (Fig. 7-1).

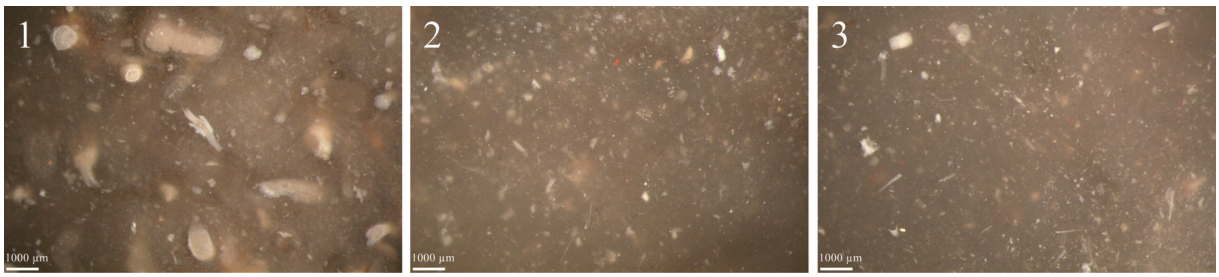


Fig. 7-1. Microfacies of the three examined layers at Ostriv. 1 – layer 1; 2 – layer 2; 3 – layer 3.
Layer 1 displays larger bioclastic remains (sponge remains, bryozoa and echinoderms), while layers 2 and 3 are dominated by demosponge microscleres. Layer 3 is also rich in echinoderm remains (predominantly trochites from crinoids).

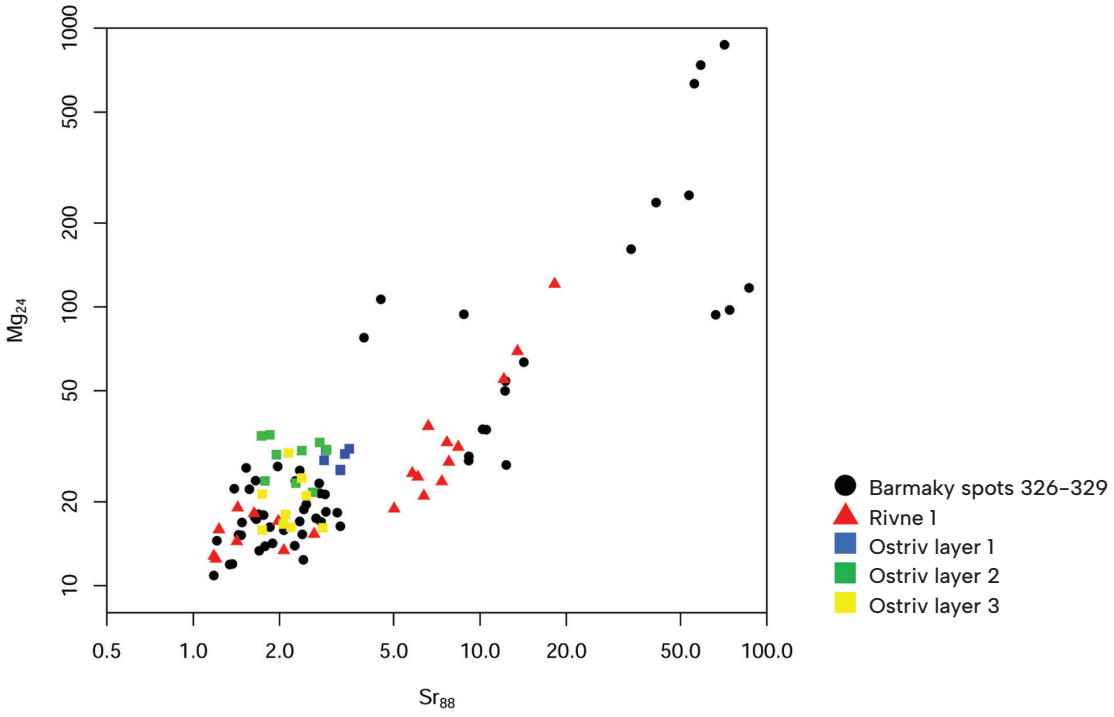


Fig. 7-2. Strontium (Sr) versus magnesium (Mg) concentration plot indicating the chemofacies of the tested geological samples. Graph: Michael Brandl.

In addition to microfacies analysis, geochemical testing using Laser Ablation–Inductively Coupled Plasma–Mass Spectrometry (LA-ICP-MS) was conducted on representative samples from all three sites at the NAWI Geocenter, University of Graz, Austria. A comprehensive report is forthcoming, but preliminary geochemical findings suggest the Ostriv sequence can be defined by a narrow chemofacies characterised by elements such as strontium (Sr) and magnesium (Mg) (Fig. 7-2). Strontium, in particular, appears to be a significant marker, likely tied to bioproductivity in specific depositional settings. The analysis may also distinguish individual layers within the primary outcrop; however, the current sample size is insufficient for definitive conclusions.

When test samples from Rivne and Barmaky were incorporated into the geochemical analysis, some aligned with the narrow chemofacies identified for Ostriv's primary sequence, while others corresponded to the broader chemofacies of the Upper Cretaceous depositional environment in the Volhynian region (Fig. 7-2). These preliminary results highlight the potential for targeted future studies but underscore the need for systematic geoarchaeological surveys and a more extensive microfacial and geochemical database. Such efforts will enable the integration of archaeological materials into provenance analyses, offering valuable insights for research across the Volhynian region.

# 8

# BARMAKY: LITHIC ARTEFACTS

V. CHABAI & D. DUDNYK

## INTRODUCTION

The total number of lithic artefacts excavated during the 2018–2020 field campaigns is 153,348 pieces. They were excavated from level 1 and, containing most of the finds, level 2 (Table 8-1).

This chapter presents the technologically significant attributes of core-like pieces, tools, and *débitage*, adopted from previous studies of Palaeolithic stone assemblages from the Crimea, Portuguese Estremadura, Levant, Central Europe, Romanian Banat, Central Asia, and Altai (Chabai, Demidenko 1998; Almeida 2000; Monigal 2002; Demidenko 2012; Sitlivy et al. 2012; Kolobova 2014; Maier 2015; Derevianko et al. 2018). Each artefact is characterised via several attributes, such as preservation conditions, shapes, the axis of detachment, lateral and distal profiles, cross-sections, dorsal scar patterns, cortex cover and placements, striking platform characteristics, and the blank and striking platform dimensions.

Tool typology follows the common approaches (Sonneville-Bordes, Perrot 1954–1956; Movius et al. 1968; Gladilin 1976; Marks 1976; Demars, Laurent 1992; Demidenko 2012).

The typology of core-like pieces is based on V. Gladilin's classification, allowing for a precise description of core variety (Galdilin 1976). Differentiating between burin spalls and micro-blades is often plagued with uncertainties (Demidenko, Chabai 2012: 269). The present study follows J. Tixier (1974), supplemented by the following attributes: lateral or bilateral steep mid-point cross-sections; oblique, not abraded, untrimmed, finely faceted or plain striking platforms.

| | level 1 | level 2 | Σ | % | esse, % |
|---|---|---|---|---|---|
| **pre-cores** | – | 43 | **43** | 0,03 | 0,27 |
| **cores** | – | 131 | **131** | 0,09 | 0,81 |
| **tools** | 16 | 811 | **827** | 0,54 | 5,10 |
| **flakes** | 85 | 7717 | **7802** | 5,09 | 48,16 |
| **blades** | 45 | 2698 | **2743** | 1,79 | 16,93 |
| **bladelets** | 39 | 2488 | **2527** | 1,65 | 15,60 |
| **micro-blades** | 11 | 1359 | **1370** | 0,89 | 8,46 |
| **burin spalls** | 15 | 668 | **683** | 0,45 | 4,22 |
| **truncation spalls** | 1 | 73 | **74** | 0,05 | 0,46 |
| **chips** | 478 | 132553 | **133031** | 86,75 | – |
| **unidentifiable *débitage*** | 44 | 4002 | **4046** | 2,64 | – |
| **chunks** | – | 71 | **71** | 0,05 | – |
| **TOTAL:** | **734** | **152614** | **153348** | 100,00 | 100,00 |

Table 8-1. Barmaky, by levels: artefact totals

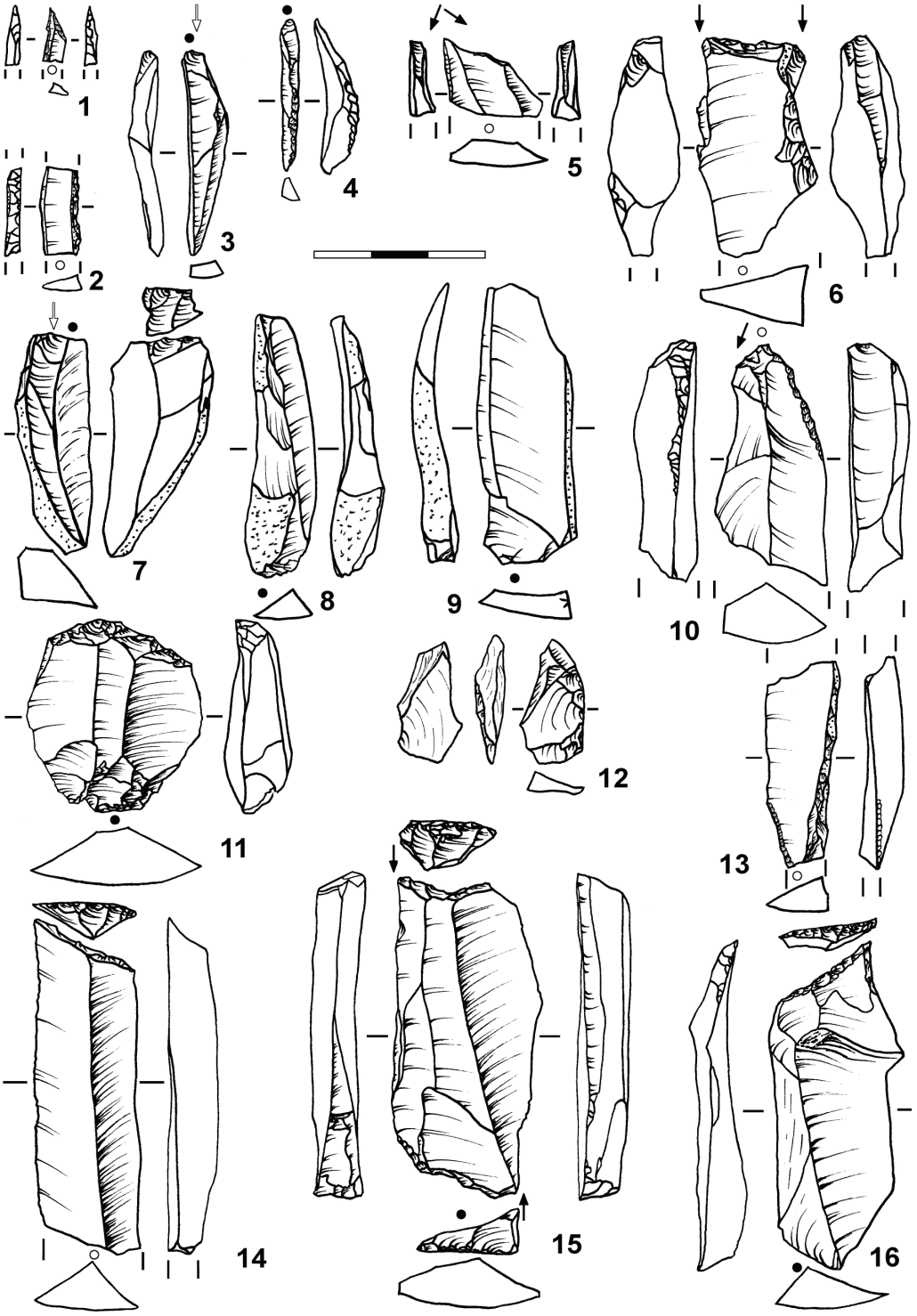

Fig. 8-1. Barmaky, level 1, horizons 1 (11), 1.1 (2, 3, 9), 1.2 (5–7, 10, 12, 13, 15, 16), 1.3 (1, 4, 8, 14): 1 – microlithic point on micro-blade, straightly dorsally backed; 2 – unidentifiable microlithic on micro-blade, wavy dorsally backed; 3, 7 – burin spalls multiple; 4 – burin spall, primary, retouched; 5 – dihedral-asymmetrical burin on blade; 6 – burin on straightly proximally dorsally truncated crested / *débordante* blade; 8 – secondary crested bladelet, unidirectional; 9 – *débordante* blade, cortical; 10 – burin on obliquely-convexly proximally dorsally truncated secondary crested blade; 11 – end-scraper on flake, simple-convex, distal, dorsal; 12 – truncation spall, secondary; 13 – retouched piece lateral, dorsal, on secondary crested blade; 14 – truncated piece on blade, oblique, distal, dorsal; 15 – opposite-alternative burin on the bi-terminally obliquely-concavely dorsally truncated blade; 16 – borer-perforator on blade, distal.

The ENTRER 4 program (McPherron, Dibble 2002: 127–148) and Mitutoyo digital calliper were used to analyse the proposed attributes; measurements were taken with up to 0.01 mm accuracy.

## ARCHAEOLOGICAL LEVEL 1

The artefacts of Level 1 originate from two clusters: western and eastern. The western cluster represents the aggregation of three levels. In total, their number (n = 734) is too *small* for reliable statistical analyses (Table 8–2). Core-like pieces and chunks are absent. Flakes dominate the *débitage* assemblage and the sum of bladelets and micro-blades prevails over the number of blades. Some tools, tool trimming elements, chips, and unidentifiable *débitage* are present.

*Débordantes* and crested pieces were identified in flakes and lamellar blanks (Table 8–3; Fig. 8–1, *8, 9, 10*). The sum of secondary and multiple burin spalls prevails over primary ones (Fig. 8–1, *3, 4, 7*). A single truncation spall was also found (Fig. 8–1, *12*).

While broken pieces dominate the lamellar assemblages, complete specimens prevail over broken flakes (Table 8–4). Flake assemblages are dominated by trapezoidal off-axis pieces (Table 8–5). The insufficient number of lamellar pieces does not allow for reliable statements about the shape and axis of the lamellar assemblages. Pieces with straight lateral profiles and feathering distal extremities are characteristic of all *débitage* classes (Tables 8–6, 8–7). In addition, curved mid-point profiles are an important feature of the lamellar assemblages, whereas triangular and trapezoidal mid-point cross-sections are most characteristic for all classes of *débitage* (Table 8–8). Relatively numerous are lateral steep cross-sections, which correspond with débordante and crested pieces. Non-cortical pieces with unidirectional scar patterns are the most numerous among flake and lamellar assemblages (Table 8–9, *10*). Among the cortical *débitage*, pieces with lateral cortex are most common. Plain, untrimmed striking platforms without abrasion traces and lipping are most characteristic for all *débitage* classes (Tables 8–11, 8–12, 8–13, 8–14). In addition, right-angle striking platforms with pronounced bulbs dominate the *débitage* assemblage (Tables 8–15, 8–16).

Nine tools were made on blades, two on micro-blades, two on flakes, and three pieces are classified as unidentifiable fragments of *débitage*. The most numerous tool classes are burins and retouched pieces on blades; the other tool classes are only represented by single pieces (Table 8–17). The only end-scraper belongs to the simple-convex distal type, made

| | Western area | | | | | | | |
|---|---|---|---|---|---|---|---|---|
| | **1** | **1.1** | **1.2** | **1.3** | **Eastern area** | **Σ** | **%** | **esse, %** |
| **tools** | 1 | 1 | 11 | 3 | – | **16** | 2,18 | 7,55 |
| **flakes** | 12 | 10 | 40 | 12 | 11 | **85** | 11,58 | 40,09 |
| **blades** | 3 | 12 | 19 | 7 | 4 | **45** | 6,13 | 21,23 |
| **bladelets** | 5 | 6 | 17 | 6 | 5 | **39** | 5,31 | 18,40 |
| **micro-blades** | 1 | – | 2 | 8 | – | **11** | 1,50 | 5,19 |
| **burin spalls** | – | 1 | 8 | 6 | – | **15** | 2,04 | 7,08 |
| **truncation spalls** | – | – | 1 | – | – | **1** | 0,14 | 0,47 |
| **chips** | 8 | 8 | 20 | 434 | 8 | **478** | 65,12 | – |
| **unidentifiable *débitage*** | 5 | 3 | 13 | 12 | 11 | **44** | 5,99 | – |
| **TOTAL:** | **35** | **41** | **131** | **488** | **39** | **734** | 100,00 | 100,00 |

Table 8–2. Barmaky, level 1, by horizons: artefact totals

| | Western area | | | | | |
|---|---|---|---|---|---|---|
| | 1 | 1.1 | 1.2 | 1.3 | Eastern area | Σ |
| **FLAKES** | | | | | | |
| regular | 10 | 7 | 31 | 10 | 7 | **65** |
| lateral *débordantes* | – | 2 | 3 | 1 | – | **6** |
| cortical *débordantes* | – | – | – | 1 | – | **1** |
| crested | 1 | – | 1 | – | 3 | **5** |
| *Kantenabschläge* | – | 1 | 1 | – | – | **2** |
| core tablet | – | – | 3 | – | – | **3** |
| primary | 2 | – | 2 | – | 1 | **5** |
| **BLADES** | | | | | | |
| regular | 3 | 11 | 16 | 7 | 2 | **39** |
| lateral *débordantes* | – | – | 1 | – | 1 | **2** |
| cortical *débordantes* | – | 1 | 4 | – | – | **5** |
| natural *débordantes* | – | – | 1 | – | – | **1** |
| crested | – | – | 5 | 1 | – | **6** |
| primary | – | – | – | – | 1 | **1** |
| **BLADELETS** | | | | | | |
| regular | 2 | 4 | 15 | 4 | 5 | **30** |
| lateral *débordantes* | 1 | 1 | – | – | – | **2** |
| cortical *débordantes* | – | – | 1 | – | – | **1** |
| natural *débordantes* | – | – | 1 | 1 | – | **2** |
| crested | 2 | 1 | – | 1 | – | **4** |
| **MICRO-BLADES** | | | | | | |
| regular | 1 | 1 | 2 | 9 | – | **13** |
| **BURIN SPALLS** | | | | | | |
| primary | – | – | 1 | 1 | – | **2** |
| primary, retouched | – | – | 1 | 2 | – | **3** |
| secondary | – | – | 2 | 2 | – | **4** |
| secondary, retouched | – | – | 1 | 1 | – | **2** |
| multiple | – | 1 | 2 | – | – | **3** |
| multiple, retouched | – | – | 1 | – | – | **1** |
| **TRUNCATION SPALLS** | | | | | | |
| secondary | – | – | 1 | – | – | **1** |
| **UNIDENTIFIABLE *DÉBITAGE*** | | | | | | |
| unidentifiable *débitage* | 5 | 3 | 15 | 13 | 11 | **47** |

Table 8-3. Barmaky, level 1, by horizons: *débitage* structure (including tools)

by continuous scalar obverse abrupt retouch: 33.15×29.68×10.49 mm (Fig. 8-1, *11*). The burins on truncated blades were made on straight, 38,27×19,62×11,73 mm, and oblique-convex, 42,64×19,84×9,55 mm, truncations (Fig. 8-1, *6, 10*). One burin uses the opposite alternative and is made on bi-terminal oblique concave truncations: 56.94×24.77×8.13 mm (Fig. 8-1, *15*). There also is a distal fragment of a dihedral asymmetrical burin on a blade (Fig. 8-1, *5*). One blade (Fig. 8-1, *14*) and a piece of unidentifiable *débitage* show oblique distal dorsal truncations. A single borer-perforator on a blade was made by distal, partial scalar, obverse abrupt retouch: 57.53×23.64×5.15 mm (Fig. 8-1, *16*). A distal fragment of a straight-backed microgravette point (Fig. 8-1, *1*) and a medial fragment of a wavy-backed unidentifiable microlithic tool (Fig. 8-1, *2*) represent the backed pieces on micro-blades. The lateral (Fig. 8-1, *13*), bi-lateral, and proximal sides of retouched pieces demonstrate the partial scalar/micro-scalar/marginal obverse/inverse flat/semi-abrupt retouching.

Despite the poor statistical reliability, the flint assemblage of Level 1 contains several characteristic features of the Epigravettian techno-complex, such as the prevalence of the sum of bladelets and micro-blades over blades, the dominance of unidirectional dorsal scar patterns, the dominance of burins on truncated blades over dihedral burins, and the presence of backed micro-blades.

| | | Western area | | | | | |
|---|---|---|---|---|---|---|---|
| | | **1** | **1.1** | **1.2** | **1.3** | **Eastern area** | **Σ** |
| **flakes** | complete | 8 | 7 | 23 | 5 | 10 | **53** |
| | distal | – | 2 | 8 | 5 | – | **15** |
| | lateral | 2 | – | 1 | 1 | – | **4** |
| | medial | 1 | – | 3 | – | – | **4** |
| | proximal | 2 | 1 | 6 | 1 | 1 | **11** |
| **blades** | complete | – | 3 | 9 | 3 | 1 | **16** |
| | distal | 2 | 2 | 4 | 4 | 2 | **14** |
| | medial | 1 | 4 | 7 | – | – | **12** |
| | proximal | – | 3 | 7 | 1 | 1 | **12** |
| **bladelets** | complete | 1 | 1 | 3 | 3 | 2 | **10** |
| | distal | 2 | – | 3 | 1 | 3 | **9** |
| | medial | 1 | 3 | 6 | – | – | **10** |
| | proximal | 1 | 2 | 5 | 2 | – | **10** |
| **micro-blades** | complete | 1 | – | – | 1 | – | **2** |
| | distal | – | – | 1 | 1 | – | **2** |
| | medial | – | 1 | 1 | 4 | – | **6** |
| | proximal | – | – | – | 3 | – | **3** |

Table 8-4. Barmaky, level 1, by horizons: *débitage* conditions (including tools)

| | | | flakes | blades | bladelets | micro-blades | Σ |
|---|---|---|---|---|---|---|---|
| horizon 1 | rectangular | on-axis | 1 | 1 | – | – | **2** |
| | | off-axis | – | – | 2 | – | **2** |
| | trapezoidal | on-axis | 1 | – | – | – | **1** |
| | | off-axis | 3 | – | – | – | **3** |
| | ovoid | on-axis | 1 | – | – | – | **1** |
| | | off-axis | – | – | – | 1 | **1** |
| | expanding | on-axis | 1 | 1 | – | – | **2** |
| | | off-axis | – | – | 1 | – | **1** |
| | irregular | off-axis | 2 | – | 1 | – | **3** |
| | unidentifiable | | 4 | 1 | 1 | – | **6** |
| horizon 1.1 | rectangular | on-axis | 2 | 2 | – | – | **4** |
| | trapezoidal | on-axis | 1 | – | – | – | **1** |
| | | off-axis | 4 | 2 | 1 | – | **7** |
| | triangular | on-axis | 1 | 1 | – | – | **2** |
| | expanding | on-axis | – | 1 | 2 | – | **3** |
| | unidentifiable | | 2 | 6 | 3 | 1 | **12** |
| horizon 1.2 | rectangular | on-axis | 3 | 4 | 2 | 1 | **10** |
| | | off-axis | 4 | 1 | – | – | **5** |
| | trapezoidal | on-axis | 1 | – | – | – | **1** |
| | | off-axis | 14 | 2 | 3 | – | **19** |
| | triangular | on-axis | 1 | – | 1 | – | **2** |
| | | off-axis | 1 | – | – | – | **1** |
| | leaf-shaped | on-axis | – | 1 | – | – | **1** |
| | ovoid | off-axis | 2 | | – | – | **2** |
| | crescent | off-axis | 2 | 2 | – | – | **4** |
| | expanding | on-axis | – | 1 | – | – | **1** |
| | | off-axis | – | 1 | – | – | **1** |
| | irregular | off-axis | 3 | 1 | – | – | **4** |
| | unidentifiable | | 10 | 14 | 11 | 1 | **36** |
| horizon 1.3 | rectangular | on-axis | 1 | – | 2 | – | **3** |
| | | off-axis | 2 | – | – | – | **2** |
| | trapezoidal | off-axis | 5 | 2 | – | – | **7** |
| | triangular | on-axis | – | – | – | 1 | **1** |
| | | off-axis | 1 | 1 | – | – | **2** |
| | crescent | off-axis | – | 2 | 2 | 1 | **5** |
| | expanding | on-axis | 1 | – | – | – | **1** |
| | irregular | off-axis | – | 1 | – | – | **1** |
| | unidentifiable | off-axis | – | – | 1 | – | **1** |
| | unidentifiable | | 2 | 2 | 1 | 7 | **12** |
| eastern area | rectangular | on-axis | – | – | 2 | – | **2** |
| | trapezoidal | off-axis | 6 | – | 1 | – | **7** |
| | triangular | off-axis | 1 | – | – | – | **1** |
| | ovoid | on-axis | – | 1 | – | – | **1** |
| | | off-axis | 2 | | – | – | **2** |
| | crescent | off-axis | – | 1 | 2 | – | **3** |
| | irregular | off-axis | 1 | 1 | – | – | **2** |
| | unidentifiable | | 1 | 1 | – | – | **2** |

Table 8-5. Barmaky, level 1, by horizons: *débitage* shapes & axis (including tools)

| | | flakes | blades | bladelets | micro-blades | Σ |
|---|---|---|---|---|---|---|
| horizon 1 | straight | 7 | – | 4 | – | **11** |
| | incurvate medial | 3 | – | – | 1 | **4** |
| | incurvate distal | 3 | 1 | – | – | **4** |
| | twisted | – | 2 | 1 | – | **3** |
| horizon 1.1 | straight | 3 | 2 | 2 | 1 | **8** |
| | convex | 1 | – | – | – | **1** |
| | incurvate proximal | – | 1 | – | – | **1** |
| | incurvate medial | 4 | 7 | 2 | – | **13** |
| | incurvate distal | 2 | – | – | – | **2** |
| | twisted | – | 2 | 2 | – | **4** |
| horizon 1.2 | straight | 16 | 11 | 8 | 2 | **37** |
| | convex | 4 | – | – | – | **4** |
| | incurvate proximal | 1 | – | 1 | – | **2** |
| | incurvate medial | 7 | 7 | 4 | – | **18** |
| | incurvate distal | 9 | 2 | 2 | – | **13** |
| | twisted | 3 | 7 | 2 | – | **12** |
| | unidentifiable | 1 | – | – | – | **1** |
| horizon 1.3 | straight | 6 | 2 | 1 | 6 | **15** |
| | convex | 2 | – | – | 1 | **3** |
| | incurvate medial | – | 5 | 2 | 2 | **9** |
| | incurvate distal | 3 | 1 | 1 | – | **5** |
| | twisted | 1 | – | 1 | – | **2** |
| | unidentifiable | – | – | 1 | – | **1** |
| eastern area | straight | 4 | 2 | 3 | – | **9** |
| | convex | – | – | 1 | – | **1** |
| | incurvate medial | 1 | 2 | – | – | **3** |
| | incurvate distal | 3 | – | – | – | **3** |
| | twisted | 2 | – | 1 | – | **3** |
| | unidentifiable | 1 | – | – | – | **1** |

Table 8–6. Barmaky, western area, level 1, by horizons: *débitage* lateral profiles (including tools)

| | | flakes | blades | bladelets | micro-blades | Σ |
|---|---|---|---|---|---|---|
| horizon 1 | feathering | 7 | 2 | 2 | 1 | **12** |
| | hinged | 2 | – | 1 | – | **3** |
| | missing | 2 | 1 | 2 | – | **5** |
| | modified | 1 | – | – | – | **1** |
| | unidentifiable | 1 | – | – | – | **1** |
| horizon 1.1 | feathering | 7 | 4 | – | – | **11** |
| | blunt | 1 | – | – | – | **1** |
| | hinged | 1 | 1 | 1 | | **3** |
| | missing | 1 | 7 | 5 | 1 | **14** |
| horizon 1.2 | feathering | 22 | 4 | 4 | – | **30** |
| | blunt | 2 | 4 | 1 | – | **7** |
| | hinged | 8 | 2 | 1 | 1 | **12** |
| | missing | 9 | 14 | 11 | 1 | **35** |
| | modified | – | 3 | – | – | **3** |
| horizon 1.3 | feathering | 7 | 2 | 2 | 1 | **12** |
| | blunt | – | 1 | 1 | – | **2** |
| | hinged | 4 | 2 | 1 | – | **7** |
| | overpassed | – | 1 | – | – | **1** |
| | missing | 1 | 1 | 2 | 7 | **11** |
| | modified | – | 1 | – | 1 | **2** |
| eastern area | feathering | 9 | 3 | – | 4 | **16** |
| | hinged | 1 | – | – | 1 | **2** |
| | missing | 1 | 1 | – | – | **2** |

Table 8–7. Barmaky, western area, level 1 by horizons: *débitage* distal profiles (including tools)

| | | flakes | blades | bladelets | micro-blades | Σ |
|---|---|---|---|---|---|---|
| horizon 1 | triangular | 2 | 3 | 2 | – | **7** |
| | trapezoidal | 5 | – | 1 | 1 | **7** |
| | multiple | 2 | – | 1 | – | **3** |
| | lateral steep | – | – | 1 | – | **1** |
| | convex | 1 | – | – | – | **1** |
| | flat | 1 | – | – | – | **1** |
| | unidentifiable | 2 | – | – | – | **2** |
| horizon 1.1 | triangular | 2 | 4 | 4 | – | **10** |
| | trapezoidal | 2 | 5 | 1 | – | **8** |
| | multiple | 3 | 2 | – | – | **5** |
| | lateral steep | 3 | 1 | 1 | 1 | **6** |
| horizon 1.2 | triangular | 15 | 5 | 11 | 1 | **32** |
| | trapezoidal | 15 | 7 | 2 | 1 | **25** |
| | multiple | 3 | 5 | 2 | – | **10** |
| | lateral steep | 4 | 9 | 2 | – | **15** |
| | convex | 2 | – | – | – | **2** |
| | irregular | 1 | – | – | – | **1** |
| | unidentifiable | 1 | 1 | – | – | **2** |
| horizon 1.3 | triangular | 6 | 2 | 2 | 4 | **14** |
| | trapezoidal | 3 | 4 | 3 | 4 | **14** |
| | multiple | – | 1 | – | 1 | **2** |
| | lateral steep | 2 | 1 | 1 | – | **4** |
| | unidentifiable | 1 | – | – | – | **1** |
| eastern area | triangular | 2 | 2 | 5 | – | **9** |
| | trapezoidal | 5 | – | – | – | **5** |
| | lateral steep | 3 | 1 | – | – | **4** |
| | convex | – | 1 | – | – | **1** |
| | flat | 1 | – | – | – | **1** |

Table 8-8. Barmaky, level 1, by horizons: *débitage* cross-sections (including tools)

| | | flakes | blades | bladelets | micro-blades | Σ |
|---|---|---|---|---|---|---|
| horizon 1 | cortex | 2 | – | – | – | **2** |
| | lateral | 2 | 1 | – | – | **3** |
| | unidirectional | 6 | 2 | 2 | 1 | **11** |
| | bidirectional | 1 | – | 1 | – | **2** |
| | crested "one side" | – | – | 1 | – | **1** |
| | crested+unidirectional | – | – | 1 | – | **1** |
| | crested secondary, unidirectional | 1 | – | – | – | **1** |
| | semi-crossed | 1 | – | – | – | **1** |
| horizon 1.1 | lateral | 1 | 1 | – | – | **2** |
| | unidirectional | 6 | 10 | 5 | 1 | **22** |
| | bidirectional | 1 | 1 | – | – | **2** |
| | crested+unidirectional | – | – | 1 | – | **1** |
| | orthogonal | 2 | – | – | – | **2** |
| horizon 1.2 | cortex | 3 | – | – | – | **3** |
| | lateral | 4 | 1 | – | – | **5** |
| | bi-lateral | 1 | – | – | – | **1** |
| | unidirectional | 22 | 17 | 17 | 2 | **58** |
| | bidirectional | 3 | 3 | – | – | **6** |
| | crested "double sides" | 1 | – | – | – | **1** |
| | crested+unidirectional | – | 2 | – | – | **2** |
| | crested secondary, unidirectional | – | 2 | – | – | **2** |
| | crested secondary, bidirectional | – | 1 | – | – | **1** |
| | orthogonal | 6 | 1 | – | – | **7** |
| | unidentifiable | 1 | – | – | – | **1** |
| horizon 1.3 | lateral | 2 | – | – | – | **2** |
| | unidirectional | 8 | 5 | 4 | 9 | **26** |
| | bidirectional | – | 2 | 1 | – | **3** |
| | crested "double sides" | – | 1 | – | – | **1** |
| | crested secondary, unidirectional | – | – | 1 | – | **1** |
| | orthogonal | 2 | – | – | – | **2** |
| eastern area | cortex | 1 | 2 | – | – | **3** |
| | lateral | 1 | – | – | – | **1** |
| | unidirectional | 6 | 2 | 5 | – | **13** |
| | crested "double sides" | 2 | – | – | – | **2** |
| | crested+unidirectional | 1 | – | – | – | **1** |

Table 8-9. Barmaky, level 1, by horizons: *débitage* dorsal scars (including tools)

| | | | flakes | blades | bladelets | micro-blades | Σ |
|---|---|---|---|---|---|---|---|
| horizon 1 | none | 0% | 7 | 2 | 2 | 1 | **12** |
| | primary | >75% | 2 | – | – | – | **2** |
| | proximal | 1–25% | – | – | 1 | – | **1** |
| | | 26–50% | – | – | 1 | – | **1** |
| | lateral | 1–25% | 3 | – | – | – | **3** |
| | | 26–50% | – | – | 1 | – | **1** |
| | distal | 1–25% | 1 | 1 | – | – | **2** |
| horizon 1.1 | none | 0% | 3 | 9 | 3 | – | **15** |
| | lateral | 1–25% | 2 | 2 | 1 | 1 | **6** |
| | | 26–50% | 1 | – | 1 | – | **2** |
| | | 51–75% | – | 1 | – | – | **1** |
| | distal-lateral | 26–50% | 1 | – | 1 | – | **2** |
| | | 51–75% | 3 | – | | – | **3** |
| horizon 1.2 | none | 0% | 26 | 13 | 11 | 2 | **52** |
| | primary | >75% | 3 | – | – | – | **3** |
| | proximal | 26–50% | 1 | – | – | – | **1** |
| | central | 1–25% | – | – | 1 | – | **1** |
| | lateral | 1–25% | 3 | 5 | 1 | – | **9** |
| | | 26–50% | 1 | 4 | 2 | – | **7** |
| | | 51–75% | 2 | 1 | 1 | – | **4** |
| | bi-lateral | 1–25% | 1 | – | – | – | **1** |
| | | 26–50% | – | 1 | – | – | **1** |
| | | 51–75% | 1 | – | – | – | **1** |
| | distal | 26–50% | – | 1 | – | – | **1** |
| | | 51–75% | 1 | – | – | – | **1** |
| | distal-lateral | 1–25% | 1 | 1 | – | – | **2** |
| | | 26–50% | – | 1 | – | – | **1** |
| | | 51–75% | 1 | – | 1 | – | **2** |
| horizon 1.3 | none | 0% | 8 | 4 | 2 | 9 | **23** |
| | primary | >75% | 1 | – | – | – | **1** |
| | proximal | 51–75% | – | 1 | – | – | **1** |
| | lateral | 1–25% | 1 | – | 2 | – | **3** |
| | | 26–50% | – | 3 | 2 | – | **5** |
| | distal | 1–25% | 1 | – | – | – | **1** |
| | distal-lateral | 51–75% | 1 | – | – | – | **1** |
| eastern area | none | 0% | 3 | 2 | 3 | – | **8** |
| | primary | >75% | 1 | 2 | – | – | **3** |
| | proximal | 1–25% | 1 | – | – | – | **1** |
| | lateral | 1–25% | 1 | – | – | – | **1** |
| | | 26–50% | 1 | – | – | – | **1** |
| | | 51–75% | – | – | 1 | – | **1** |
| | distal | 26–50% | 2 | – | – | – | **2** |
| | | 51–75% | 1 | – | – | – | **1** |
| | distal-lateral | 1–25% | – | – | 1 | – | **1** |
| | | 26–50% | 1 | – | – | – | **1** |

Table 8–10. Barmaky, western area, level 1, by horizons: *débitage* primary surfaces placement & percentages (including tools)

| | | flakes | blades | bladelets | micro-blades | Σ |
|---|---|---|---|---|---|---|
| horizon 1 | plain | 7 | – | 2 | – | **9** |
| | linear | 1 | – | – | – | **1** |
| | dihedral | 1 | – | – | – | **1** |
| | faceted | 1 | – | – | – | **1** |
| | crushed | 1 | – | – | 1 | **2** |
| | missing | 2 | 3 | 3 | – | **8** |
| horizon 1.1 | plain | 5 | 4 | 1 | – | **10** |
| | dihedral | 1 | 1 | – | – | **2** |
| | polyhedral | – | 1 | – | – | **1** |
| | faceted | 1 | – | – | – | **1** |
| | crushed | 1 | – | 2 | – | **3** |
| | missing | 2 | 6 | 3 | 1 | **12** |
| horizon 1.2 | cortex | 1 | – | – | – | **1** |
| | plain | 13 | 6 | 2 | – | **21** |
| | linear | – | 2 | 2 | – | **4** |
| | dihedral | 6 | 1 | 1 | – | **8** |
| | polyhedral | 2 | – | – | – | **2** |
| | faceted | 1 | 1 | – | – | **2** |
| | crushed | 5 | 3 | 3 | – | **11** |
| | modified | 1 | 3 | – | – | **4** |
| | missing | 12 | 11 | 9 | 2 | **34** |
| horizon 1.3 | plain | 4 | 2 | 2 | 2 | **10** |
| | linear | – | – | 2 | – | **2** |
| | pointed | – | 1 | – | – | **1** |
| | dihedral | 1 | 1 | 1 | – | **3** |
| | crushed | 2 | – | – | 2 | **4** |
| | missing | 5 | 4 | 1 | 5 | **15** |
| eastern area | cortex | 1 | – | – | – | **1** |
| | plain | 6 | 2 | 1 | – | **9** |
| | linear | – | – | 1 | – | **1** |
| | polyhedral | 1 | – | – | – | **1** |
| | crushed | 3 | – | – | – | **3** |
| | | – | 2 | 3 | – | **5** |

Table 8–11. Barmaky, level 1, by horizons: *débitage* striking platform types (including tools)

| | | flakes | blades | bladelets | micro-blades | Σ |
|---|---|---|---|---|---|---|
| horizon 1 | trimmed | 3 | – | – | – | **3** |
| | untrimmed | 8 | – | 2 | 1 | **11** |
| | missing | 2 | 3 | 3 | – | **8** |
| | unidentifiable | – | – | – | – | **–** |
| horizon 1.1 | trimmed | – | 2 | – | – | **2** |
| | untrimmed | 7 | 4 | 2 | – | **13** |
| | missing | 2 | 6 | 3 | 1 | **12** |
| | unidentifiable | 1 | – | 1 | – | **2** |
| horizon 1.2 | trimmed | 4 | 7 | 4 | – | **15** |
| | untrimmed | 24 | 6 | 3 | – | **33** |
| | missing | 12 | 11 | 9 | 2 | **34** |
| | unidentifiable | 1 | 3 | 1 | – | **5** |
| horizon 1.3 | trimmed | – | 2 | 3 | 1 | **6** |
| | untrimmed | 6 | 2 | 2 | 3 | **13** |
| | missing | 5 | 4 | 1 | 5 | **15** |
| | unidentifiable | 1 | – | – | – | **1** |
| eastern area | trimmed | – | 1 | 2 | – | **3** |
| | untrimmed | 10 | 1 | – | – | **11** |
| | missing | – | 2 | 3 | – | **5** |
| | unidentifiable | 1 | – | – | – | **1** |

Table 8–12. Barmaky, level 1, by horizons: *débitage* overhang trimming (including tools)

| | | flakes | blades | bladelets | micro-blades | Σ |
|---|---|---|---|---|---|---|
| horizon 1 | abrased | – | – | – | – | **–** |
| | unabrased | 11 | – | 2 | 1 | **14** |
| | missing | 2 | 3 | 3 | – | **8** |
| | unidentifiable | – | – | – | – | **–** |
| horizon 1.1 | abrased | – | – | – | – | **–** |
| | unabrased | 7 | 6 | 2 | – | **15** |
| | missing | 2 | 6 | 3 | 1 | **12** |
| | unidentifiable | 1 | – | 1 | – | **2** |
| horizon 1.2 | abrased | – | – | – | – | **–** |
| | unabrased | 27 | 13 | 8 | – | **48** |
| | missing | 12 | 11 | 9 | 2 | **34** |
| | unidentifiable | 2 | 3 | – | – | **5** |
| horizon 1.3 | abrased | – | – | – | – | **–** |
| | unabrased | 6 | 4 | 5 | 4 | **19** |
| | missing | 5 | 4 | 1 | 5 | **15** |
| | unidentifiable | 1 | – | – | – | **1** |
| eastern area | abrased | – | – | – | – | **–** |
| | unabrased | 10 | 2 | 2 | – | **14** |
| | missing | – | 2 | 3 | – | **5** |
| | unidentifiable | 1 | – | – | – | **1** |

Table 8–13. Barmaky, level 1, by horizons: *débitage* butt abrasion (including tools)

## ARCHAEOLOGICAL LEVEL 2

According to the stratigraphic observations, the following complexes represent the archaeological material of level 2:

1. Complex 2a, which include the materials from horizons 2a, 2a1, and 2ab;
2. The artefact complex from pit 2.
3. The western area (WA) complex, which consists of the materials from horizons 2b, 2c, and horizon 2d on square lines Г, Д, Е, Ж, З, К, and Л;
4. The eastern area (EA) complex, which consists of the materials from horizon 2c, including the ashy lens and fireplace, and horizon 2d on square lines Н, О, П, Р, С, Т, and У.

The total number of artefacts from archaeological level 2 amounts to 152,614 pieces (Table 8–18). The most numerous collections of artefacts originate from the WA, horizon 2c – 93,548 items, and the EA, horizon 2d – 46,783 items.

## COMPLEX 2A: ARCHAEOLOGICAL LEVEL 2, HORIZONS 2A, 2A1 & 2AB

Eighteen squares contain 6,994 artefacts of complex 2a (Table 8–19). The majority belongs to horizon 2a (n = 6637) and originates from three squares 4Н, 5Н, and 5О, which directly overlie pit 2, while a few finds were discovered in squares as 2Н, 2Р, and 3М. The total number of artefacts from horizon 2a1 is 229, found mainly in square 6Л (n = 156), while single pieces come from squares 5К, 5Л, and 6К. All mentioned squares correlate directly with the position of pit 1.

Except for 123 chips and 4 pieces of unidentifiable *débitage*, one medial fragment of lateral *débordante* bladelet originated from horizon 2ab. These artefacts were found during the cleaning of the chalk/marl crust in the squares 4Л and 5Л. For a quantitative techno-typological analysis, the number of artefacts is too small.

| | | flakes | blades | bladelets | micro-blades | Σ |
|---|---|---|---|---|---|---|
| horizon 1 | lipped | 1 | – | – | – | **1** |
| | semi-lipped | 3 | – | – | – | **3** |
| | unlipped | 7 | – | 2 | 1 | **10** |
| | missing | 2 | 3 | 3 | – | **8** |
| horizon 1.1 | semi-lipped | – | 2 | 1 | – | **3** |
| | unlipped | 7 | 4 | 1 | – | **12** |
| | missing | 2 | 6 | 3 | 1 | **12** |
| | unidentifiable | 1 | – | 1 | – | **2** |
| horizon 1.2 | lipped | 2 | – | – | – | **2** |
| | semi-lipped | 1 | 1 | – | – | **2** |
| | unlipped | 20 | 9 | 6 | – | **35** |
| | missing | 12 | 11 | 9 | 2 | **34** |
| | unidentifiable | 6 | 6 | 2 | – | **14** |
| horizon 1.3 | lipped | – | 1 | – | – | **1** |
| | semi-lipped | – | – | 1 | – | **1** |
| | unlipped | 6 | 3 | 3 | 4 | **16** |
| | missing | 5 | 4 | 1 | 5 | **15** |
| | unidentifiable | 1 | – | 1 | – | **2** |
| eastern area | lipped | – | – | – | – | **–** |
| | semi-lipped | 1 | 1 | – | – | **2** |
| | unlipped | 7 | 1 | 2 | – | **10** |
| | missing | – | 2 | 3 | – | **5** |
| | unidentifiable | 3 | – | – | – | **3** |

Table 8-14. Barmaky, 1 level, by horizons: *débitage* butts lipping (including tools)

| | | flakes | blades | bladelets | micro-blades | Σ |
|---|---|---|---|---|---|---|
| horizon 1 | absent | – | – | – | – | **–** |
| | defused | 1 | – | – | – | **1** |
| | pronounced | 10 | – | 2 | 1 | **13** |
| | missing | 2 | 3 | 3 | – | **8** |
| horizon 1.1 | absent | – | – | – | – | **–** |
| | defused | 1 | 2 | – | – | **3** |
| | pronounced | 6 | 4 | 2 | – | **12** |
| | missing | 2 | 6 | 3 | 1 | **12** |
| | unidentifiable | 1 | – | 1 | – | **2** |
| horizon 1.2 | absent | – | – | – | – | **–** |
| | defused | 9 | 3 | 3 | – | **15** |
| | pronounced | 14 | 7 | 3 | – | **24** |
| | missing | 12 | 11 | 9 | 2 | **34** |
| | unidentifiable | 6 | 6 | 2 | – | **14** |
| horizon 1.3 | absent | – | – | – | – | **–** |
| | defused | 2 | 2 | 2 | – | **6** |
| | pronounced | 4 | 2 | 2 | 4 | **12** |
| | missing | 5 | 4 | 1 | 5 | **15** |
| | unidentifiable | 1 | – | 1 | – | **2** |
| eastern area | absent | – | – | – | – | **–** |
| | defused | 2 | 1 | 1 | – | **4** |
| | pronounced | 6 | 1 | 1 | – | **8** |
| | missing | – | 2 | 3 | – | **5** |
| | unidentifiable | 3 | – | – | – | **3** |

Table 8-15. Barmaky, level 1, by horizons: *débitage* bulbs (including tools)

Despite the marked difference in the number of artefacts from horizons 2a and 2a1, **the typological structures** are very similar (Table 8-19). The main characteristic is the low number or even absence of core-like pieces compared to the number of tools. In general, the cores-to-tools ratio is 1 to 12 in the 2a complex. The sum of bladelets and micro-blades prevails over the number of blades.

## Unmodified raw material

Seven of 13 **chunks** show maximum measurements >50 mm. Thus, these pieces might be evaluated as raw material reserves. Two of them are natural flakes, one is a rounded nodule, and the rest are unidentifiable; the average dimensions are 78.29×53.69×25.36 mm.

## Pre-cores & cores

**Four core-like pieces** originate from horizon 2a (Table 8-20). A relatively large and broken single bladelet pre-core (>58.23×14.29×>28.23 mm) is of the narrow flaking surface type with the prepared crested ridge. A bi-directional sub-cylindrical core for blades, probably on a natural flake (70.48×46.41×27.21 mm), exhibits two main opposed striking platforms and traces of lateral crested ridge preparation. In addition, there are two unidirectional narrow flaking surface cores for blades/bladelets on natural flakes. The larger specimen (82.51×26.92×65.71 mm) shows the preparation of a crested ridge on the back and distal parts (Fig. 8-2). The smaller core (62.96×24.86×42.28 mm) has a prepared but unused opposite striking platform and a crested ridge on the back (Fig. 8-3).

| | | flakes | blades | bladelets | micro-blades | Σ |
|---|---|---|---|---|---|---|
| horizon 1 | right | 6 | – | 2 | – | **8** |
| | acute | 4 | – | – | – | **4** |
| | missing | 2 | 3 | 3 | – | **8** |
| | unidentifiable | 1 | – | – | 1 | **2** |
| horizon 1.1 | right | 5 | 3 | 1 | – | **9** |
| | acute | 2 | 3 | 1 | – | **6** |
| | missing | 2 | 6 | 3 | 1 | **12** |
| | unidentifiable | 1 | – | 1 | – | **2** |
| horizon 1.2 | right | 14 | 8 | 4 | – | **26** |
| | acute | 9 | 2 | 1 | – | **12** |
| | missing | 12 | 11 | 9 | 2 | **34** |
| | unidentifiable | 6 | 6 | 3 | – | **15** |
| horizon 1.3 | right | 4 | 2 | 3 | 3 | **12** |
| | acute | 1 | 2 | 2 | – | **5** |
| | missing | 5 | 4 | 1 | 5 | **15** |
| | unidentifiable | 2 | – | – | 1 | **3** |
| eastern area | right | 3 | 1 | 2 | – | **6** |
| | acute | 4 | 1 | – | – | **5** |
| | obtuse | 1 | – | – | – | **1** |
| | missing | – | 2 | 3 | – | **5** |
| | unidentifiable | 3 | – | – | – | **3** |

Table 8-16. Barmaky, level 1, by horizons: *débitage* striking platform angels (including tools)

## *Débitage*

The nearly equal proportions of flakes and the sum of lamellar pieces characterise the ***débitage* structure**. Technological pieces make up 20–33 % of each blank class: flakes, blades, bladelets, and micro-blades (Table 8-21). The different types of *débordante* blanks are most numerous – 10–16 % (Fig. 8-4, *4, 6, 7, 10, 12, 17*). Crested pieces are important among the blades – 13.38 % (Fig. 8-4, *5, 11, 15, 16*). Primary blanks make up 3.5 % of all flakes and lamellar pieces. The specific *Kantenabschläge* amounts to 3.56 % of the flake assemblage (Fig. 8-4, *9, 13*). The tool trimming *débitage* is represented by burin and truncation spalls (Fig. 8-4, *1-3, 8, 14)*. Altogether, these spalls compose less than 2 % of the total number of blanks. Such percentages and the variety of technological blanks and tool trimming *débitage* suggest intensive on-site core reduction and tool production processes.

The degree of **fragmentation** of lamellar pieces – either by flaking accidents or by trampling – is higher than for flakes (Table 8-22), maybe as a result of the reduced thickness of lamellar items. About 45 % of flakes have trapezoidal **shapes** (Table 8-23). Rectangular shapes are more characteristic of blades and bladelets (≈33 %), while micro-blades show a preference for crescent shapes (≈33 %). Two-thirds of the flakes were detached off-axis (Table 8-23). The lamellar *débitage*, in contrast, is more symmetrical: 42–54 % were detached on-axis. In sum, trapezoidal **off-axis** flakes amount to about 40 % of the flake assemblage. Rectangular on-axis items are more common for blade (≈27 %) and bladelet (≈32 %) assemblages, while crescent off-axis forms are more characteristic (≈35 %) of micro-blades (Table 8-23).

Straight **lateral profiles** dominate the *débitage* assemblages of both "regular" and "technical" blanks (Table 8-24) with about one-third of the flakes and blades and 45–46 % of the bladelets and micro-blades.

Feathering **distal terminations** dominate all blank classes (Table 8-25). Hinged distal ends make up about 30 % of flake and lamellar assemblages, while blunt and overshot forms are distributed over the blank classes in approximately equal proportions.

Triangular and trapezoidal **cross-sections** dominate the blank assemblages (Table 8-26). Multiple cross-sections are not numerous. The relatively high values of lateral steep cross-sections reflect the amounts of *débordante* and crested pieces among the lamellar *débitage*.

The unidirectional **dorsal scars** dominate among all classes of *débitage* (Table 8-27), also in combination with crested forms. Such "combined" unidirectional scars amount to 54.45 % of flakes, 72.54 % of blades, 82.95 % of bladelets, and 82.71 % of micro-blades. Different variants of crested dorsal scar patterns show ratios of 4.58 % for flakes, 13.38 % for blades, 7.75 % for bladelets, and 7.70 % for micro-blades. These findings suggest that the main aim of the *débitage* process was the production of unidirectional lamellar blanks using crested ridge preparation of the flaking surface.

Cortex and/or natural planes are the **primary dorsal surfaces** and make up about 8 % of the assemblage (Table 8-28). Partly cortical surfaces prevail among flakes and blades, while

| | 1 | 1.1 | 1.2 | 1.3 | Σ |
|---|---|---|---|---|---|
| **END-SCRAPERS ON FLAKES** | | | | | |
| simple-convex, distal, dorsal | 1 | – | – | – | **1** |
| **BURINS ON TRUNCATED BLADES** | | | | | |
| on straight proximal dorsal truncation | – | – | 1 | – | **1** |
| on oblique-convex proximal dorsal truncation | – | – | 1 | – | **1** |
| opposite-alternative, on bi-terminal oblique-concave dorsal truncations | – | – | 1 | – | **1** |
| **BURINS DIHEDRAL ON BLADES** | | | | | |
| asymmetrical, distal | – | – | 1 | – | **1** |
| **TRUNCATED PIECES ON BLADES** | | | | | |
| oblique, distal, dorsal | – | – | – | 1 | **1** |
| **TRUNCATED PIECES ON UNIDENTIFIABLE *DEBITAGE*** | | | | | |
| oblique, distal, dorsal | – | – | – | 1 | **1** |
| **BORER-PERFORATORS ON BLADES** | | | | | |
| distal, dorsal | – | – | 1 | – | **1** |
| **BACKED POINTS ON MICRO-BLADES** | | | | | |
| straightly dorsally backed | – | – | – | 1 | **1** |
| **BACKED UNIDENTIFIABLE PIECES ON MICRO-BLADES** | | | | | |
| wavy dorsally backed | – | 1 | – | – | **1** |
| **RETOUCHED PIECES ON BLADES** | | | | | |
| lateral, dorsal | – | – | 2 | – | **2** |
| bilateral, ventral | – | – | 1 | – | **1** |
| **RETOUCHED PIECES ON FLAKES** | | | | | |
| proximal, ventral | – | – | 1 | – | **1** |
| **UNIDENTIFIABLE TOOLS ON UNIDENTIFIABLE *DEBITAGE*** | | | | | |
| distal, dorsal | – | – | 1 | – | **1** |
| lateral-distal, dorsal | – | – | 1 | – | **1** |
| **TOTAL:** | **1** | **1** | **11** | **3** | **16** |

Table 8-17. Barmaky, level 1, by horizons: tools

| | 2a | pit 2 | EA | WA | Σ | % | esse, % |
|---|---|---|---|---|---|---|---|
| **pre-cores** | 1 | 5 | 12 | 25 | **43** | 0,03 | 0,27 |
| **cores** | 3 | 6 | 59 | 63 | **131** | 0,09 | 0,82 |
| **tools** | 48 | 14 | 90 | 659 | **811** | 0,53 | 5,07 |
| **flakes** | 403 | 278 | 3264 | 3772 | **7717** | 5,06 | 48,27 |
| **blades** | 131 | 99 | 1053 | 1415 | **2698** | 1,77 | 16,88 |
| **bladelets** | 126 | 83 | 1058 | 1221 | **2488** | 1,63 | 15,56 |
| **micro-blades** | 76 | 42 | 552 | 689 | **1359** | 0,89 | 8,50 |
| **burin spalls** | 19 | 8 | 71 | 570 | **668** | 0,44 | 4,18 |
| **truncation spalls** | 1 | – | 14 | 58 | **73** | 0,05 | 0,46 |
| **chips** | 5870 | 4591 | 39117 | 82975 | **132553** | 86,86 | – |
| **unidentifiable *débitage*** | 303 | 159 | 1480 | 2060 | **4002** | 2,62 | – |
| **chunks** | 13 | 4 | 13 | 41 | **71** | 0,05 | – |
| **TOTAL:** | **6994** | **5289** | **46783** | **93548** | **152614** | **100,00** | **100,00** |

Table 8-18. Barmaky, level 2, by complexes: artefact totals

| | complex 2a | | | | | complex pit 2 | |
|---|---|---|---|---|---|---|---|
| | **2a** | **2a1** | **2ab** | Σ | esse,% | # | esse,% |
| **pre-cores** | 1 | – | – | **1** | 0,12 | **5** | 0,93 |
| **cores** | 3 | – | – | **3** | 0,37 | **6** | 1,12 |
| **tools** | 46 | 2 | – | **48** | 5,94 | **14** | 2,62 |
| **flakes** | 386 | 17 | – | **403** | 49,88 | **278** | 51,96 |
| **blades** | 122 | 9 | – | **131** | 16,21 | **99** | 18,50 |
| **bladelets** | 121 | 4 | 1 | **126** | 15,59 | **83** | 15,51 |
| **micro-blades** | 73 | 3 | – | **76** | 9,41 | **42** | 7,85 |
| **burin spalls** | 18 | 1 | – | **19** | 2,35 | **8** | 1,50 |
| **truncation spalls** | 1 | – | – | **1** | 0,12 | **–** | – |
| **chips** | 5563 | 184 | 123 | **5870** | – | **4591** | – |
| **unidentifiable *débitage*** | 290 | 9 | 4 | **303** | – | **159** | – |
| **chunks** | 13 | – | – | **13** | – | **4** | – |
| **TOTAL:** | **6637** | **229** | **128** | **6994** | 100,00 | **5289** | 100,00 |

Table 8-19. Barmaky, complexes pit 2 & 2a, by horizons: artefact totals

| | 2a | pit 2 |
|---|---|---|
| **BLADE PRE-CORES** | | |
| unidirectional, sub-cylindrical | – | 1 |
| **BLADE / BLADELET PRE-CORES** | | |
| unidirectional, narrow flaking surface | – | 1 |
| bidirectional, narrow flaking surface | – | 1 |
| unidentifiable, narrow flaking surface | – | 1 |
| **BLADELET PRE-CORES** | | |
| narrow flaking surface, unidentifiable | 1 | – |
| **UNIDENTIFIABLE PRE-CORES** | | |
| unidentifiable | – | 1 |
| **BLADE CORES** | | |
| bidirectional, sub-cylindrical | 1 | 1 |
| bidirectional-adjacent, sub-cylindrical | – | 1 |
| bidirectional, narrow flaking surface | – | 1 |
| **BLADE / BLADELET CORES** | | |
| bidirectional, narrow flaking surface | – | 1 |
| **BLADELET CORES** | | |
| unidirectional, narrow flaking surface | 2 | – |
| bidirectional, sub-cylindrical | – | 1 |
| bidirectional-alternate, cylindrical | – | 1 |
| **TOTAL:** | **4** | **11** |

Table 8-20. Barmaky, pit 2 and horizon 2a: core-like pieces

non-cortical surfaces dominate among the bladelet and micro-blade assemblages. Lateral positions of the primary surfaces dominate among all of the blanks. The relatively high amount of lamellar *débitage* with lateral primary surfaces might be evidence of intensive narrow flaking surface core exploitation. The relatively high percentages of blanks with distal primary surfaces of lamellar *débitage* reflect the insufficient role of bidirectional flaking.

About half of all **striking platforms** are plain (Table 8-29). Linear platforms become more important among lamellar *débitage*, while the percentages of dihedral platforms are more or less equally represented for all blank classes. Also noteworthy is the large number of crushed striking platforms among all classes of *débitage*.

The methods of overhang trimming and butt abrasion were rarely used for flakes (Tables 8-30; 8-31). Abraded platforms are also absent in lamellar assemblages, while the majority of lamellar butts demonstrate pronounced traces of overhang trimming. Right-angled, unlipped platforms with pronounced bulbs dominate the blank assemblages (Table 8-32; 8-33; 8-34).

## Tool trimming pieces

The number of primary (Fig. 8-4, *1*) **burin spalls** is equal to the sum of secondary and multiple burin spalls (Table 8-21; Fig. 8-4, *2, 3, 8*). Eight of 19 burin spalls exhibit traces of dorsal retouch. Five pieces are complete. Thirteen pieces have different laterally curved or twisted profiles. The sum of blunt, overpassed, and hinged terminations exceeds feathering distal ends. Nearly all burin spalls show a lateral steep cross-section. The sum of dihedral, polyhedral, and faceted platforms is higher than the sum of plain and pointed butts. The overhangs of burin spalls are untrimmed and not abraded, but mainly lipped/semi-lipped with diffuse and/or absent bulbs. Among the complete platforms, those with an acute angle prevail.

The only **truncation spall** originates from horizon 2a1 (Fig. 8-4, *14*). It belongs to the rejuvenation type: a dorsal single blow intentionally removes the distal part of the burin on the truncated piece.

## *Débitage* dimensions

The thicknesses of the *débitage* platforms are about three times smaller than the widths (Table 8-35). This points to the importance of overhang trimming during the preparation of striking platforms. The careful platform preparation of lamellar products is also reflected in the blank-to-platform widths ratios. The widths of the lamellar products are more than twice as wide as the width of their platforms. The moderate values of width and length are characteristic of blades. The length-to-width ratios of blades, bladelets, and micro-blades are 2.67, 2.76, and 3.25, respectively. On average, blades are thicker than flakes. In sum, the lamellar products are relatively thick, rather narrow, and not very elongated.

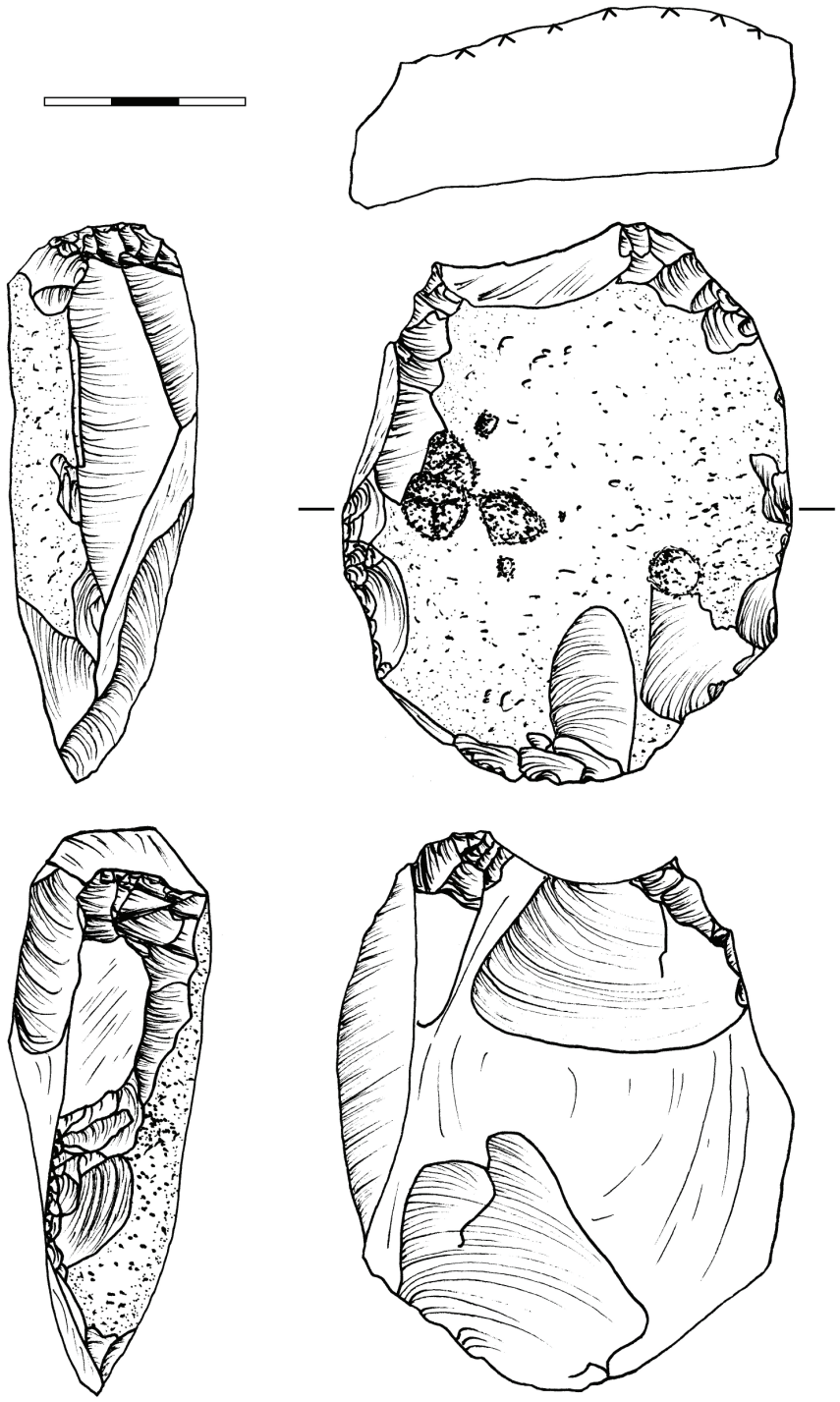

Fig. 8–2. Barmaky, complex 2a, horizon 2a: core for blades/bladelets, unidirectional, narrow flaking surface.

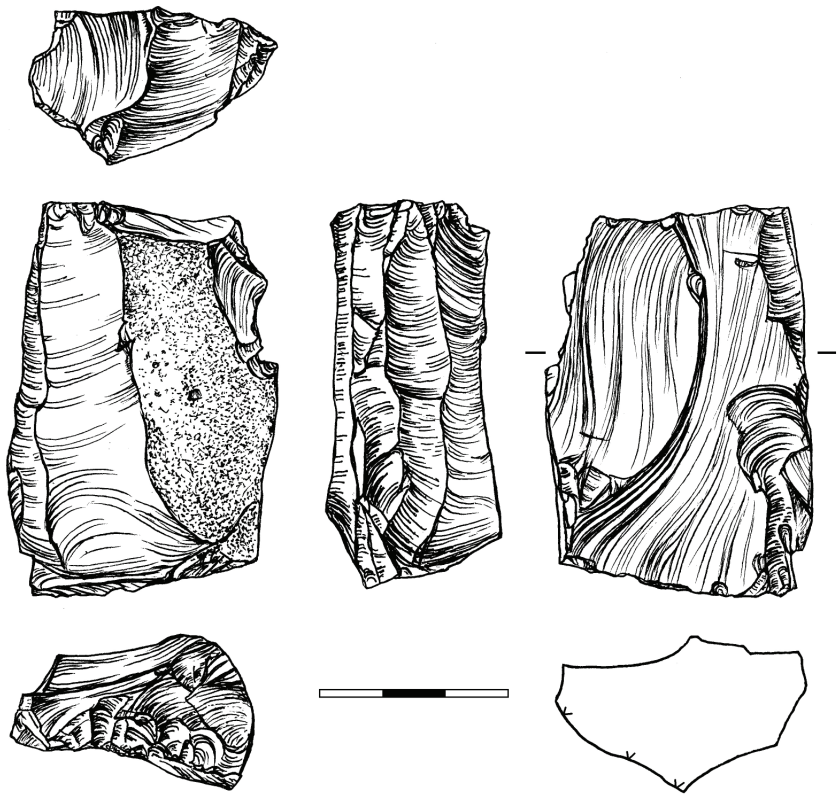

Fig. 8-3. Barmaky, complex 2a, horizon 2a: core for blade/bladelets, unidirectional, narrow flaking surface.

## Tools

The tool assemblage is not very diverse and retouched pieces, burins, and microliths play a significant role (Table 8-36). All but eleven tools were made on lamellar *débitage*: 21 on blades, 8 on bladelets and 8 on micro-blades. Non-lamellar blanks comprise 7 flakes and 4 unidentifiable blanks.

Nine **burins** were produced on blades, one on flake, and one on an unidentifiable piece of *débitage*. Four of the nine blades are crested. One burin on the blade belongs to the angle type, eight burins were made on truncations, and one is unidentifiable. The following combinations of truncations and burin working edges were identified: single working edge are found on straight proximal, oblique-convex distal, concave proximal, oblique-concave distal truncations (Fig. 8-5, *4*). Two working edges are observed in combination with a bi-lateral burin on straight distal truncation and opposite-alternate working edges on bi-terminal oblique truncations (Fig. 8-5, *7, 9*). Furthermore, a burin on a flake with distal straight truncation and a burin on an unidentifiable blank with proximal oblique truncation were found. In general, truncations were made by obverse, continuous, scalar, and abrupt retouch. Burins on truncations are dominant; the ratio of burins spall negatives and burins is 2.36:1; the ratio of burin spalls and burins is 1.72:1. The average dimension of burins on blade is 61.53×22.27×7.80 mm.

Blades also serve as blanks for **truncated pieces** (Table 8-36). All but one are broken. Both distal (2 pieces) and proximal (2 pieces) truncations were identified (Fig. 8-5, *5, 6, 8*). Obverse, continuous, scalar, and abrupt retouching were used to produce nearly all of the truncated blades, showing three oblique and one straight truncation. The average dimensions of complete truncated blades are 90.31×19.85×8.71 mm (Fig. 8-5, *6*). Truncated pieces are thus considerably longer than burins.

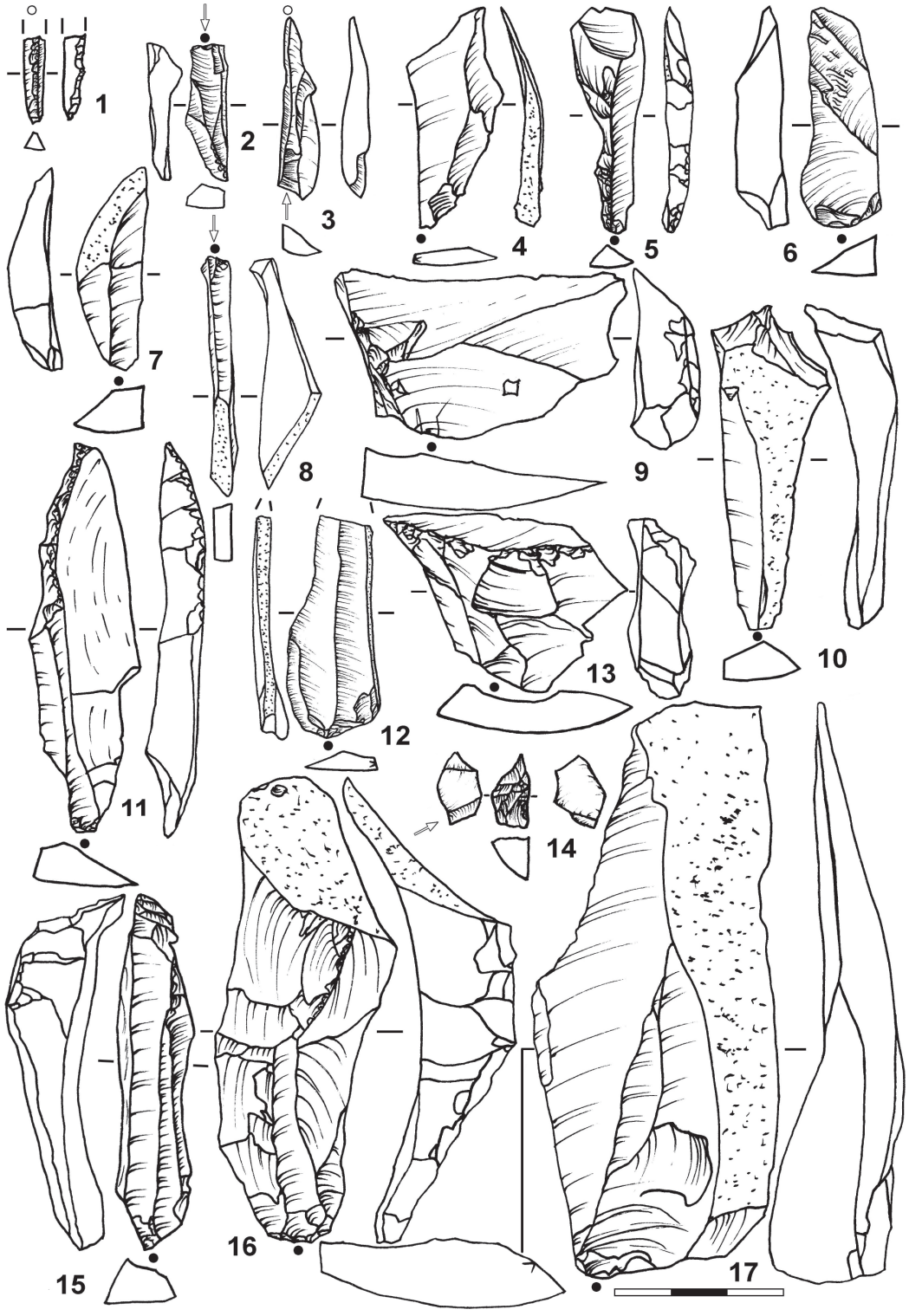


Fig. 8–4. Barmaky, complex 2a, horizons 2a (1–13, 15–17) and 2a1 (14): 1 – burin spall, primary, retouched; 2 – burin spall, secondary; 3 – burin spall, multiple, bidirectional; 4, 12 – cortical *débordante* blades; 5 – crested blade, bidirectional; 6, 10 – lateral *débordante* blades; 7 – natural *débordante* bladelet; 8 – burin spall, multiple; 9, 13 – *Kantenabschläge*; 11, 16 – one-side crested blades, unidirectional; 14 – truncation spall, rejuvenating; 15 – secondary crested blade, unidirectional; 17 – natural *débordante* blade.

| | 2a | | 2a1 | | pit 2 | |
|---|---|---|---|---|---|---|
| | # | % | # | % | # | % |
| **FLAKES** | | | | | | |
| regular | **291** | 74,05 | **11** | 64,71 | **199** | 70,32 |
| lateral *débordantes* | **25** | 6,36 | **1** | 5,88 | **22** | 7,77 |
| cortical *débordantes* | **7** | 1,78 | **–** | – | **5** | 1,77 |
| natural *débordantes* | **7** | 1,78 | **–** | – | **5** | 1,77 |
| crested | **16** | 4,07 | **1** | 5,88 | **10** | 3,53 |
| core tablet | **1** | 0,25 | **–** | – | **2** | 0,71 |
| *Kantenabschläge* | **14** | 3,56 | **1** | 5,88 | **7** | 2,47 |
| primary | **31** | 7,89 | **3** | 17,65 | **30** | 10,60 |
| natural | **1** | 0,25 | **–** | – | **3** | 1,06 |
| **TOTAL**: | **393** | 100,00 | **17** | 100,00 | **283** | 100,00 |
| **BLADES** | | | | | | |
| regular | **96** | 67,61 | **6** | 60,00 | **67** | 62,62 |
| lateral *débordantes* | **11** | 7,75 | **1** | 10,00 | **6** | 5,61 |
| cortical *débordantes* | **5** | 3,52 | **2** | 20,00 | **3** | 2,80 |
| natural *débordantes* | **7** | 4,93 | **–** | – | **4** | 3,74 |
| crested | **19** | 13,38 | **1** | 10,00 | **21** | 19,63 |
| core tablet | **–** | – | **–** | – | **2** | 1,87 |
| primary | **4** | 2,82 | **–** | – | **4** | 3,74 |
| **TOTAL:** | **142** | 100,00 | **10** | 100,00 | **107** | 100,00 |
| **BLADELETS** | | | | | | |
| regular | **103** | 79,84 | **3** | 75,00 | **62** | 74,70 |
| lateral *débordantes* | **7** | 5,43 | **–** | – | **5** | 6,02 |
| cortical *débordantes* | **2** | 1,55 | **–** | – | **5** | 6,02 |
| natural *débordantes* | **6** | 4,65 | **–** | – | **3** | 3,61 |
| crested | **10** | 7,75 | **1** | 25,00 | **8** | 9,64 |
| primary | **1** | 0,78 | **–** | – | **–** | – |
| **TOTAL:** | **129** | 100,00 | **4** | 100,00 | **83** | 100,00 |
| **MICRO-BLADES** | | | | | | |
| regular | **66** | 81,48 | **1** | 33,33 | **34** | 80,95 |
| lateral *débordantes* | **8** | 9,88 | **1** | 33,33 | **4** | 9,52 |
| cortical *débordantes* | **1** | 1,23 | **–** | – | **2** | 4,76 |
| natural *débordantes* | **3** | 3,70 | **–** | – | **–** | – |
| crested | **3** | 3,70 | **1** | 33,33 | **2** | 4,76 |
| **TOTAL:** | **81** | 100,00 | **3** | 100,00 | **42** | 100,00 |

Table 8-21. Barmaky, pit 2 & complex 2a, by horizons: *débitage* structure (including tools)

| | 2a | | 2a1 | | pit 2 | |
|---|---|---|---|---|---|---|
| | # | % | # | % | # | % |
| **BURIN SPALLS** | | | | | | |
| primary | **3** | 16,67 | **–** | – | **3** | 37,50 |
| primary, retouched | **5** | 27,78 | **1** | 100,00 | **1** | 12,50 |
| secondary | **5** | 27,78 | **–** | – | **3** | 37,50 |
| secondary, retouched | **2** | 11,11 | **–** | – | **–** | – |
| multiple | **2** | 11,11 | **–** | – | **1** | 12,50 |
| multiple, bidirectional | **1** | 5,56 | **–** | – | **–** | – |
| **TOTAL:** | **18** | 100,00 | **1** | 100,00 | **8** | 100,00 |
| **TRUNCATION SPALLS** | | | | | | |
| rejuvenating | **1** | 100,00 | **–** | – | **–** | – |
| **TOTAL:** | **1** | 100,00 | **–** | – | **–** | – |
| unidentifiable *débitage* | 293 | – | 10 | – | 160 | – |

Table 8–21. continued.

| | | flakes | | blades | | bladelets | | micro-blades | |
|---|---|---|---|---|---|---|---|---|---|
| | | # | % | # | % | # | % | # | % |
| HORIZON 2a | complete | **221** | 56,23 | **47** | 33,10 | **34** | 26,36 | **19** | 23,46 |
| | distal | **46** | 11,70 | **43** | 30,28 | **35** | 27,13 | **26** | 32,10 |
| | lateral | **44** | 11,20 | **–** | – | **–** | – | **–** | – |
| | medial | **17** | 4,33 | **17** | 11,97 | **23** | 17,83 | **23** | 28,40 |
| | proximal | **65** | 16,54 | **35** | 24,65 | **37** | 28,68 | **13** | 16,05 |
| | unidentifiable | **–** | – | **–** | – | **–** | – | **–** | – |
| | **TOTAL:** | **393** | 100,00 | **142** | 100,00 | **129** | 100,00 | **81** | 100,00 |
| HORIZON 2a1 | complete | **8** | 47,06 | **3** | 30,00 | **–** | – | **–** | – |
| | distal | **5** | 29,41 | **3** | 30,00 | **3** | 75,00 | **2** | 66,66 |
| | lateral | **1** | 5,88 | **–** | – | **–** | – | **–** | – |
| | medial | **–** | – | **–** | – | **–** | – | **1** | 33,33 |
| | proximal | **3** | 17,65 | **4** | 40,00 | **1** | 25,00 | **–** | – |
| | unidentifiable | **–** | – | **–** | – | **–** | – | **–** | – |
| | **TOTAL:** | **17** | 100,00 | **10** | 100,00 | **4** | 100,00 | **3** | 100,00 |
| PIT 2 | complete | **149** | 52,65 | **52** | 48,60 | **27** | 32,53 | **8** | 19,05 |
| | distal | **54** | 19,08 | **27** | 25,23 | **20** | 24,10 | **15** | 35,71 |
| | lateral | **25** | 8,83 | **–** | – | **–** | – | **–** | – |
| | medial | **12** | 4,24 | **12** | 11,21 | **12** | 14,46 | **15** | 35,71 |
| | proximal | **43** | 15,19 | **16** | 14,95 | **24** | 28,92 | **4** | 9,52 |
| | **TOTAL:** | **283** | 100,00 | **107** | 100,00 | **83** | 100,00 | **42** | 100,00 |

Table 8–22. Barmaky, complex 2a, by horizons: *débitage* conditions (including tools)

| | | | flakes | | blades | | bladelets | | micro-blades | |
|---|---|---|---|---|---|---|---|---|---|---|
| | | | # | % | # | % | # | % | # | % |
| HORIZON 2a | rectangular | on-axis | **49** | 18,35 | **26** | 27,66 | **25** | 32,47 | **9** | 18,37 |
| | | off-axis | **16** | 5,99 | **5** | 5,32 | **1** | 1,30 | **2** | 4,08 |
| | trapezoidal | on-axis | **13** | 4,87 | **2** | 2,13 | **–** | – | **1** | 2,04 |
| | | off-axis | **106** | 39,70 | **15** | 15,96 | **7** | 9,09 | **6** | 12,24 |
| | | unidentifiable | **1** | 0,37 | **–** | – | **–** | – | **–** | – |
| | triangular | on-axis | **3** | 1,12 | **–** | – | **6** | 7,79 | **3** | 6,12 |
| | | off-axis | **2** | 0,75 | **–** | – | **4** | 5,19 | **–** | – |
| | leaf-shaped | on-axis | **5** | 1,87 | **7** | 7,45 | **8** | 10,39 | **6** | 12,24 |
| | | off-axis | **–** | – | **2** | 2,13 | **1** | 1,30 | **–** | – |
| | ovoid | on-axis | **9** | 3,37 | **1** | 1,06 | **–** | – | **–** | – |
| | | off-axis | **9** | 3,37 | **1** | 1,06 | **–** | – | **–** | – |
| | | unidentifiable | **1** | 0,37 | **–** | – | **–** | – | **–** | – |
| | crescent | off-axis | **4** | 1,50 | **18** | 19,15 | **15** | 19,48 | **17** | 34,69 |
| | expanding | on-axis | **11** | 4,12 | **6** | 6,38 | **2** | 2,60 | **1** | 2,04 |
| | | off-axis | **7** | 2,62 | **1** | 1,06 | **2** | 2,60 | **1** | 2,04 |
| | irregular | off-axis | **31** | 11,61 | **10** | 10,64 | **5** | 6,49 | **3** | 6,12 |
| | | unidentifiable | **–** | – | **–** | – | **1** | 1,30 | **–** | – |
| | | **TOTAL:** | **267** | 100,00 | **94** | 100,00 | **77** | 100,00 | **49** | 100,00 |
| | unidentifiable | off-axis | 4 | – | – | – | 1 | – | 1 | – |
| | | unidentifiable | 122 | – | 48 | – | 51 | – | 31 | – |
| HORIZON 2a1 | rectangular | on-axis | **4** | 30,77 | **1** | 14,29 | **–** | – | **–** | – |
| | trapezoidal | on-axis | **1** | 7,69 | **–** | – | **–** | – | **–** | – |
| | | off-axis | **7** | 53,85 | **–** | – | **–** | – | **–** | – |
| | triangular | on-axis | **–** | – | **–** | – | **1** | 33,33 | **1** | 50,00 |
| | | off-axis | **–** | – | **2** | 28,57 | **–** | – | **–** | – |
| | leaf-shaped | on-axis | **–** | – | **1** | 14,29 | **–** | – | **–** | – |
| | crescent | off-axis | **–** | – | **2** | 28,57 | **1** | 33,33 | **1** | 50,00 |
| | irregular | off-axis | **1** | 7,69 | **1** | 14,29 | **1** | 33,33 | **–** | – |
| | | **TOTAL:** | **13** | 100,00 | **7** | 100,00 | **3** | 100,00 | **2** | 100,00 |
| | unidentifiable | | 4 | – | 3 | – | 1 | – | 1 | – |

Table 8-23. Barmaky, pit 2 & complex 2a, by horizons: *débitage* shapes & axis (including tools)

The only **denticulate piece** was made on a flake (16.75×16.97×6.91 mm) by obverse, continuous, scalar, semi-abrupt retouching of the distal and lateral edges. The medial part of a blade, in contrast, served as blank for a laterally **notched piece**; the retouch is partial, obverse, sub-parallel, and abrupt. Obverse, continuous micro-scalar flat obverse retouching forms the tip of a **lateral point** on a bladelet; the proximal part is broken (>35.67×11.31×4.57 mm).

Three **microliths** were made on bladelets (Table 8-36) and eight on micro-blades. Eight microliths belong to the type of dorsally straight-backed points with obliquely truncated/retouched bases – i.e. microgravette points (Fig. 8-5, *2, 3*). Two microliths are too fragmented to be precisely identified (Fig. 8-5, *1*) and one medial fragment of a bladelet with wavy backing was classified as an unfinished broken microlith. Five microlithic points exhibit

| | | | flakes | | blades | | bladelets | | micro-blades | |
|---|---|---|---|---|---|---|---|---|---|---|
| | | | # | % | # | % | # | % | # | % |
| PIT 2 | rectangular | on-axis | **29** | 15,18 | **16** | 20,25 | **10** | 19,23 | **2** | 8,33 |
| | | off-axis | **13** | 6,81 | **8** | 10,13 | **3** | 5,77 | **2** | 8,33 |
| | trapezoidal | on-axis | **11** | 5,76 | **3** | 3,80 | **5** | 9,62 | **–** | – |
| | | off-axis | **77** | 40,31 | **13** | 16,46 | **8** | 15,38 | **3** | 12,50 |
| | | unidentifiable | **2** | 1,05 | **–** | – | **–** | – | **–** | – |
| | triangular | on-axis | **4** | 2,09 | **4** | 5,06 | **2** | 3,85 | **4** | 16,67 |
| | | off-axis | **7** | 3,66 | **1** | 1,27 | **3** | 5,77 | **1** | 4,17 |
| | | unidentifiable | **–** | – | **–** | – | **–** | – | **1** | 4,17 |
| | leaf-shaped | on-axis | **1** | 0,52 | **7** | 8,86 | **4** | 7,69 | **3** | 12,50 |
| | | off-axis | **2** | 1,05 | **2** | 2,53 | **1** | 1,92 | **–** | – |
| | ovoid | on-axis | **8** | 4,19 | **1** | 1,27 | **–** | – | **–** | – |
| | | off-axis | **6** | 3,14 | **1** | 1,27 | **–** | – | **–** | – |
| | | unidentifiable | **1** | 0,52 | **–** | – | **–** | – | **–** | – |
| | crescent | on-axis | **–** | – | **1** | 1,27 | **–** | – | **–** | – |
| | | off-axis | **6** | 3,14 | **9** | 11,39 | **9** | 17,31 | **4** | 16,67 |
| | expanding | on-axis | **5** | 2,62 | **1** | 1,27 | **1** | 1,92 | **–** | – |
| | | off-axis | **3** | 1,57 | **–** | – | **–** | – | **–** | – |
| | irregular | on-axis | **–** | – | **1** | 1,27 | **2** | 3,85 | **–** | – |
| | | off-axis | **14** | 7,33 | **10** | 12,66 | **4** | 7,69 | **4** | 16,67 |
| | | unidentifiable | **2** | 1,05 | **1** | 1,27 | **–** | – | **–** | – |
| | | **TOTAL:** | **191** | 100,00 | **79** | 100,00 | **52** | 100,00 | **24** | 100,00 |
| | unidentifiable | on-axis | – | – | 5 | – | 4 | – | 5 | – |
| | | off-axis | 2 | – | 4 | – | 2 | – | 1 | – |
| | | unidentifiable | 90 | – | 19 | – | 25 | – | 12 | – |

Table 8-23. continued.

a broken tip. The microliths were produced by obverse, scalar/micro-scalar/sub-parallel, continuous, abrupt retouch. The average dimensions of microliths on the bladelets and micro-blades are 35.02×7.65×2.51 and 21.85×5.80×2.05 mm, respectively.

Blades (7), bladelets (4), and flakes (5) served as blanks for **retouched pieces** (Table 8-36). One blank was too fragmented for identification. The most common retouch combination is obverse-lateral, partial, micro-scalar, and semi-abrupt. The average dimensions of retouched blades, bladelets, and flakes are >45,54×21.19×7.89, 28.33×10.45×3.25, and 44,57×34.21×6.44 mm, accordingly.

Two *débitage* fragments with obverse, continuous, marginal/obverse, and flat/semi-abrupt retouch are classified as **unidentifiable tools**.

## Flaking instruments

Seven small fragments of **sandstone** pieces without clear traces of flaking originate from horizon 2a and might be fragments of hammer stones.

| | | flakes | | blades | | bladelets | | micro-blades | |
|---|---|---|---|---|---|---|---|---|---|
| | | # | % | # | % | # | % | # | % |
| HORIZON 2a | straight | **113** | 31,92 | **44** | 33,08 | **57** | 46,34 | **36** | 45,00 |
| | convex | **30** | 8,47 | **4** | 3,01 | **2** | 1,63 | **3** | 3,75 |
| | incurvate proximal | **16** | 4,52 | **4** | 3,01 | **4** | 3,25 | **8** | 10,00 |
| | incurvate medial | **78** | 22,03 | **30** | 22,56 | **27** | 21,95 | **10** | 12,50 |
| | incurvate distal | **83** | 23,45 | **18** | 13,53 | **11** | 8,94 | **7** | 8,75 |
| | twisted | **34** | 9,60 | **33** | 24,81 | **22** | 17,89 | **16** | 20,00 |
| | **TOTAL:** | **354** | 100,00 | **133** | 100,00 | **123** | 100,00 | **80** | 100,00 |
| | unidentifiable | 39 | – | 9 | – | 6 | – | 1 | – |
| HORIZON 2a1 | straight | **5** | 31,25 | **1** | 10,00 | **3** | 75,00 | **2** | 66,66 |
| | convex | **4** | 25,00 | **–** | – | **–** | – | **–** | – |
| | incurvate proximal | **2** | 12,50 | **1** | 10,00 | **–** | – | **–** | – |
| | incurvate medial | **2** | 12,50 | **3** | 30,00 | **–** | – | **–** | – |
| | incurvate distal | **3** | 18,75 | **3** | 30,00 | **1** | 25,00 | **1** | 33,33 |
| | twisted | **–** | – | **2** | 20,00 | **–** | – | **–** | – |
| | **TOTAL:** | **16** | 100,00 | **10** | 100,00 | **4** | 100,00 | **3** | 100,00 |
| | unidentifiable | 1 | – | – | – | – | – | – | – |
| PIT 2 | straight | **101** | 39,00 | **33** | 33,67 | **33** | 47,14 | **21** | 61,76 |
| | convex | **34** | 13,13 | **2** | 2,04 | **–** | – | **–** | – |
| | incurvate proximal | **4** | 1,54 | **5** | 5,10 | **6** | 8,57 | **–** | – |
| | incurvate medial | **44** | 16,99 | **24** | 24,49 | **9** | 12,86 | **2** | 5,88 |
| | incurvate distal | **54** | 20,85 | **15** | 15,31 | **11** | 15,71 | **3** | 8,82 |
| | twisted | **22** | 8,49 | **19** | 19,39 | **11** | 15,71 | **8** | 23,53 |
| | **TOTAL:** | **259** | 100,00 | **98** | 100,00 | **70** | 100,00 | **34** | 100,00 |
| | unidentifiable | 24 | – | 9 | – | 13 | – | 8 | – |

Table 8-24. Barmaky, pit 2 & complex 2a, by horizons: *débitage* lateral profiles (including tools)

## PIT 2 COMPLEX: ARCHAEOLOGICAL LEVEL 2

From the about two m² large pit 2 originate 5,289 flint artefacts (mostly chips) and 10 sandstone pieces (Table 8-19). The tool-to-core ratio is 1.27 to 1 and the sum of bladelets and micro-blades prevails over the number of blades.

### Unmodified raw material

One flint plaquette and one rounded nodule were identified among 4 flint chunks. The plaquette (68.99×43.49×17.46 mm) and one unidentifiably shaped piece (82.83×55.81×20.03 mm) may be a possible reserve of raw material.

### Core-like pieces

Five pre-cores and six cores were found in pit 2 (Table 8-20). Unidirectional and bidirectional pre-cores for blades and blades/bladelets are identified. Sub-cylindrical piece on a rounded nodule and pieces with a narrow flaking surface on plaquettes were recognised (Fig. 8-6, *1*). Two pieces show prepared striking platforms, two have crested ridges on the flaking surfaces, and one piece has a hinge fracture on the unprepared flaking surface. The pre-cores' average dimension is 79.91×39.75×51.83 mm.

The lamellar core assemblage is characterised by bidirectional pieces (Table 8-20; Fig. 8-6, *2, 3*; 8-7, *1, 2*). The sum of sub-cylindrical and cylindrical pieces prevails over the number of narrow flaking surface cores. One

| | | flakes | | blades | | bladelets | | micro-blades | |
|---|---|---|---|---|---|---|---|---|---|
| | | # | % | # | % | # | % | # | % |
| HORIZON 2a | feathering | **175** | 58,14 | **43** | 51,81 | **45** | 65,22 | **28** | 63,64 |
| | blunt | **30** | 9,97 | **7** | 8,43 | **3** | 4,35 | **3** | 6,82 |
| | hinged | **84** | 27,91 | **25** | 30,12 | **20** | 28,99 | **12** | 27,27 |
| | overpassed | **12** | 3,99 | **8** | 9,64 | **1** | 1,45 | **1** | 2,27 |
| | **TOTAL:** | **301** | 100,00 | **83** | 100,00 | **69** | 100,00 | **44** | 100,00 |
| | missing | 90 | – | 52 | – | 60 | – | 36 | – |
| | modified | 1 | – | 7 | – | – | – | 1 | – |
| | unidentifiable | 1 | – | – | – | – | – | – | – |
| HORIZON 2a1 | feathering | **6** | 46,15 | **2** | 33,33 | **1** | 33,33 | **2** | 100,00 |
| | blunt | **1** | 7,69 | **2** | 33,33 | **1** | 33,33 | **–** | – |
| | hinged | **6** | 46,15 | **1** | 16,67 | **1** | 33,33 | **–** | – |
| | overpassed | **–** | – | **1** | 16,67 | **–** | – | **–** | – |
| | **TOTAL:** | **13** | 100,00 | **6** | 100,00 | **3** | 100,00 | **2** | 100,00 |
| | missing | 4 | – | 4 | – | 1 | – | 1 | – |
| PIT 2 | feathering | **134** | 62,04 | **45** | 60,81 | **38** | 80,85 | **16** | 69,57 |
| | blunt | **18** | 8,33 | **11** | 14,86 | **1** | 2,13 | **2** | 8,70 |
| | hinged | **59** | 27,31 | **16** | 21,62 | **6** | 12,77 | **3** | 13,04 |
| | overpassed | **5** | 2,31 | **2** | 2,70 | **2** | 4,26 | **2** | 8,70 |
| | **TOTAL:** | **216** | 100,00 | **74** | 100,00 | **47** | 100,00 | **23** | 100,00 |
| | missing | 64 | – | 28 | – | 34 | – | 18 | – |
| | modified | 2 | – | 5 | – | – | – | – | – |
| | unidentifiable | 1 | – | – | – | 2 | – | 1 | – |

Table 8-25. Barmaky, pit 2 & complex 2a, by horizons: *débitage* distal profiles (including tools)

rounded nodule and one plaquette show natural shapes suited for core production. The original shapes of four more cores are unidentifiable. The sub-cylindrical bidirectional blade and bladelet cores are very exhausted and the latter has a secondary crested lateral ridge and a pronounced opposite supplementary platform (Fig. 8-7, *2*). Despite the predominance of sub-cylindrical and cylindrical cores, the average dimension is close to those of narrow flaking surface cores: 62.57×38.79×40.10 mm.

## *Débitage*

The *débitage* structure is characterised by high percentages of technical blanks: crested (Fig. 8-8, *5, 6, 9, 10, 13, 16*), *débordante* (Fig. 8-8, *1, 2, 7, 8, 11, 12, 14, 15*), *Kantenabschläge*, core-tablets, and primary pieces (Table 8-21). The latter are more frequent among flakes, while crested pieces are common for blades.

The low amount of **complete** lamellar pieces (20-50%) is a characteristic feature of the *débitage* assemblage from pit 2 (Table 8-22).

Different **shapes and axis** attributes characterise the flake and lamellar assemblages (Table 8-23). Trapezoidal off-axis pieces dominate the flake assemblage. Along with the latter, rectangular on-axis blanks characterise the blade assemblage, while rectangular on-axis and crescent off-axis pieces are characteristic of bladelets. Triangular on-axis and crescent off-axis pieces are common for micro-blades.

Straight **lateral profiles** dominate the *débitage* assemblages (Table 8-24), but differently curved blanks also play a significant role. Feathering **distal extremities** are the dominant type of distal ends (Table 8-25), but hinges make up more than 20 % of flakes and blades and more than 12 % of bladelets and micro-blades. Triangular and trapezoidal

| | | flakes | | blades | | bladelets | | micro-blades | |
|---|---|---|---|---|---|---|---|---|---|
| | | # | % | # | % | # | % | # | % |
| HORIZON 2a | triangular | **141** | 38,95 | **38** | 26,76 | **54** | 41,86 | **45** | 55,56 |
| | trapezoidal | **108** | 29,83 | **55** | 38,73 | **47** | 36,43 | **19** | 23,46 |
| | multiple | **24** | 6,63 | **16** | 11,27 | **9** | 6,98 | **3** | 3,70 |
| | lateral steep | **50** | 13,81 | **31** | 21,83 | **17** | 13,18 | **13** | 16,05 |
| | convex | **24** | 6,63 | **2** | 1,41 | **2** | 1,55 | **–** | – |
| | flat | **12** | 3,31 | **–** | – | **–** | – | **1** | 1,23 |
| | irregular | **3** | 0,83 | **–** | – | **–** | – | **–** | – |
| | **TOTAL:** | **362** | 100,00 | **142** | 100,00 | **129** | 100,00 | **81** | 100,00 |
| | unidentifiable | 31 | – | – | – | – | – | – | – |
| HORIZON 2a1 | triangular | **6** | 37,50 | **4** | 40,00 | **2** | 50,00 | **–** | – |
| | trapezoidal | **3** | 18,75 | **3** | 30,00 | **2** | 50,00 | **1** | 33,33 |
| | multiple | **1** | 6,25 | **–** | – | **–** | – | **–** | – |
| | lateral steep | **3** | 18,75 | **3** | 30,00 | **–** | – | **2** | 66,66 |
| | convex | **3** | 18,75 | **–** | – | **–** | – | **–** | – |
| | **TOTAL:** | **16** | 100,00 | **10** | 100,00 | **4** | 100,00 | **3** | 100,00 |
| | unidentifiable | 1 | – | – | – | – | – | – | – |
| PIT 2 | triangular | **87** | 33,21 | **31** | 28,97 | **42** | 50,60 | **28** | 66,67 |
| | trapezoidal | **73** | 27,86 | **31** | 28,97 | **19** | 22,89 | **6** | 14,29 |
| | multiple | **21** | 8,02 | **13** | 12,15 | **4** | 4,82 | **–** | – |
| | lateral steep | **42** | 16,03 | **30** | 28,04 | **18** | 21,69 | **8** | 19,05 |
| | convex | **20** | 7,63 | **2** | 1,87 | **–** | – | **–** | – |
| | flat | **16** | 6,11 | **–** | – | **–** | – | **–** | – |
| | irregular | **3** | 1,15 | **–** | – | **–** | – | **–** | – |
| | **TOTAL:** | **262** | 100,00 | **107** | 100,00 | **83** | 100,00 | **42** | 100,00 |
| | unidentifiable | 21 | – | – | – | – | – | – | – |

Table 8-26. Barmaky, pit 2 & complex 2a, by horizons: *débitage* cross-sections (including tools)

**cross-sections** dominate (Table 8-26), while lateral steep cross-sections amount to 16-28 % of all *débitage* classes and reflect the importance of *débordante* pieces.

Unidirectional **dorsal scar patterns** are most common among all classes of *débitage* (Table 8-27), whereas the sum of different bidirectional scars hardly exceeds 15 %. Primary blanks represent about 10 % of flakes but are virtually absent in lamellar pieces. Crested pieces have higher shares in blade assemblage (up to 20 %) than in flake, bladelet, and micro-blade collections. The combination of crested and unidirectional scars reflects the repeated shaping of the cores' flaking surfaces.

The percentage of completely cortical flakes contrasts with the percentages of primary lamellar pieces (Table 8-28). Lateral locations of cortical areas are common for lamellar *débitage*. Among others, this observation underlines the importance of narrow flaking surface knapping, while the relative representation of pieces with distal cortex suggests the prevalence of unipolar flaking.

Plain **platforms** are nearly equally represented among all classes of *débitage* (Table 8-29). Linear platforms are more important for lamellar assemblages. **Overhang trimming** is common for lamellar blanks, while the overhangs on flakes are mainly untrimmed (Table 8-30).

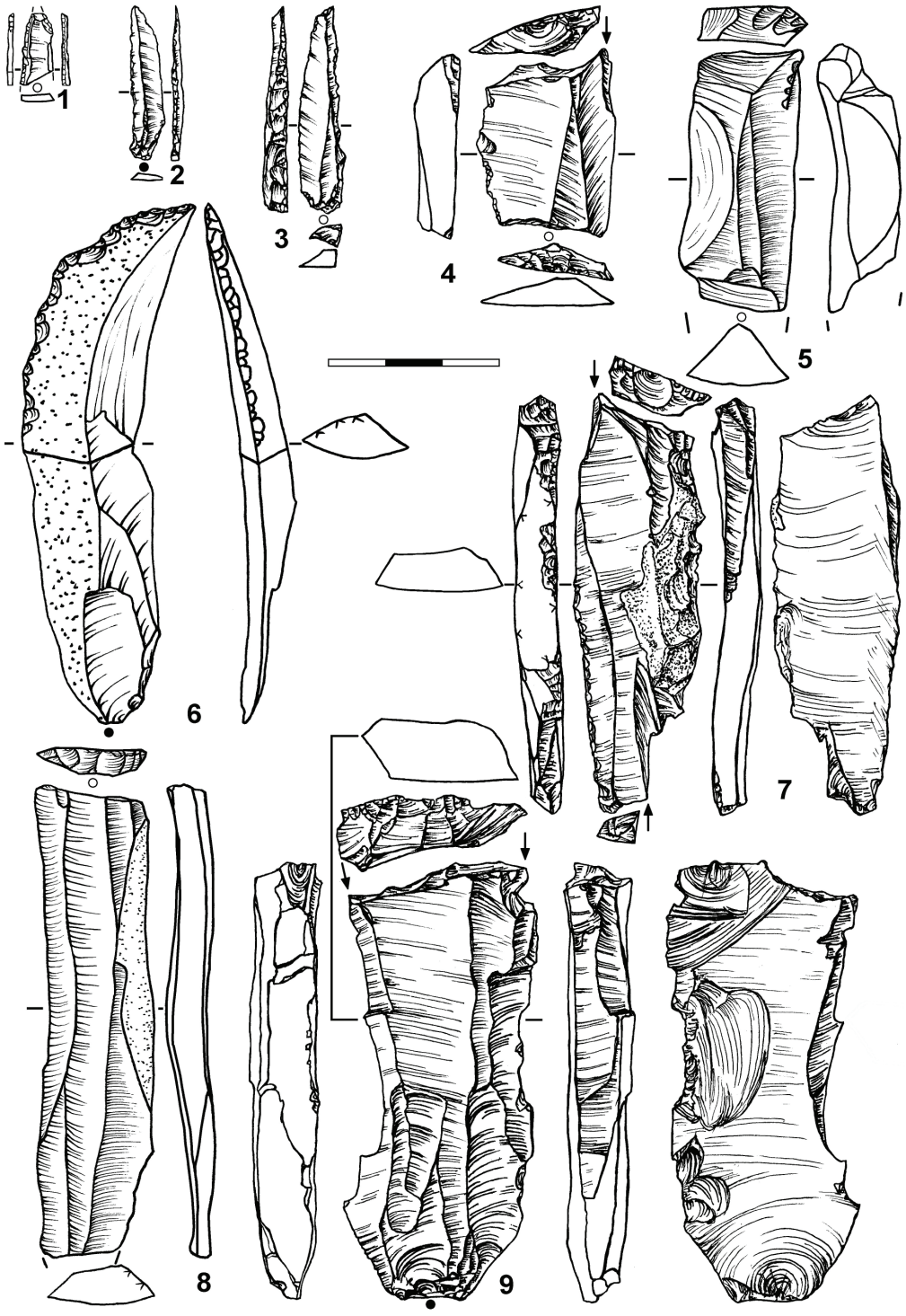


Fig. 8–5. Barmaky, complex 2a, horizon 2a: 1 – the microlithic point on micro-blade, straightly dorsally backed, laterally dorsally retouched; 2 – the microlithic point on micro-blade, straightly dorsally backed, dorsally retouched base; 3 – the microlithic point on bladelet, straightly dorsally backed, obliquely dorsally truncated base; 4 – burin on oblique-concave distal dorsal truncation, on a bi-terminally truncated blade; 5 – truncated piece on blade, straight, distal, dorsal; 6 – truncated piece on blade, oblique-convex, distal-lateral, dorsal; 7 – opposite-alternative burin on bi-terminally, obliquely dorsally truncated blade; 8 – truncated blade, oblique, proximal, dorsal; 9 – bi-lateral burin on straightly distally dorsally truncated and on the laterally ventrally thinned blade.

| | | flakes | | blades | | bladelets | | micro-blades | |
|---|---|---|---|---|---|---|---|---|---|
| | | # | % | # | % | # | % | # | % |
| HORIZON 2a | cortex | **32** | 8,14 | **4** | 2,82 | **1** | 0,78 | **–** | – |
| | lateral | **32** | 8,14 | **1** | 0,70 | **3** | 2,33 | **4** | 4,94 |
| | bi-lateral | **3** | 0,76 | **–** | – | **–** | – | **–** | – |
| | unidirectional | **202** | 51,40 | **90** | 63,38 | **102** | 79,07 | **65** | 80,25 |
| | bidirectional | **13** | 3,31 | **10** | 7,04 | **9** | 6,98 | **5** | 6,17 |
| | crested "one side" | **1** | 0,25 | **2** | 1,41 | **1** | 0,78 | **1** | 1,23 |
| | crested "double sides" | **2** | 0,51 | **–** | – | **1** | 0,78 | **–** | – |
| | crested+unidirectional | **9** | 2,29 | **7** | 4,93 | **3** | 2,33 | **1** | 1,23 |
| | crested+bidirectional | **3** | 0,76 | **3** | 2,11 | **1** | 0,78 | | |
| | crested secondary, unidirectional | **3** | 0,76 | **6** | 4,23 | **2** | 1,55 | **1** | 1,23 |
| | crested secondary, bidirectional | **–** | – | **1** | 0,70 | **2** | 1,55 | **–** | – |
| | orthogonal | **80** | 20,36 | **14** | 9,86 | **3** | 2,33 | **1** | 1,23 |
| | semi-crossed | **10** | 2,54 | **3** | 2,11 | **–** | – | **1** | 1,23 |
| | crossed | **1** | 0,25 | **–** | – | **–** | – | **–** | – |
| | opposite directional | **2** | 0,51 | **1** | 0,70 | **1** | 0,78 | **2** | 2,47 |
| | **TOTAL:** | **393** | 100,00 | **142** | 100,00 | **129** | 100,00 | **81** | 100,00 |
| HORIZON 2a1 | cortex | **3** | 17,65 | **–** | – | **–** | – | **–** | – |
| | lateral | **–** | – | **1** | 10,00 | **–** | – | **–** | – |
| | unidirectional | **7** | 41,18 | **7** | 70,00 | **3** | 75,00 | **1** | 33,33 |
| | bidirectional | **–** | – | **1** | 10,00 | **1** | 25,00 | **1** | 33,33 |
| | crested+unidirectional | **1** | 5,88 | **–** | – | **–** | – | **1** | 33,33 |
| | crested+bidirectional | **–** | – | **1** | 10,00 | **–** | – | **–** | – |
| | orthogonal | **5** | 29,41 | **–** | – | **–** | – | **–** | – |
| | semi-crossed | **1** | 5,88 | **–** | – | **–** | – | **–** | – |
| | **TOTAL:** | **17** | 100,00 | **10** | 100,00 | **4** | 100,00 | **3** | 100,00 |
| PIT 2 | cortex | **31** | 11,11 | **5** | 4,72 | **–** | – | **–** | – |
| | lateral | **29** | 10,39 | **3** | 2,83 | **–** | – | **–** | – |
| | bi-lateral | **1** | 0,36 | **–** | – | **–** | – | **–** | – |
| | unidirectional | **142** | 50,90 | **55** | 51,89 | **59** | 71,08 | **35** | 83,33 |
| | bidirectional | **12** | 4,30 | **14** | 13,21 | **6** | 7,23 | **2** | 4,76 |
| | bidirectional-crossed | **–** | – | **2** | 1,89 | **1** | 1,20 | **–** | – |
| | crested "one side" | **1** | 0,36 | **5** | 4,72 | **2** | 2,41 | **–** | – |
| | crested "double sides" | **2** | 0,72 | **–** | – | **–** | – | **–** | – |
| | crested+unidirectional | **6** | 2,15 | **10** | 9,43 | **4** | 4,82 | **1** | 2,38 |
| | crested+bidirectional | **–** | – | **1** | 0,94 | **2** | 2,41 | **–** | – |
| | crested secondary, unidirectional | **1** | 0,36 | **6** | 5,66 | **1** | 1,20 | **1** | 2,38 |
| | crested secondary, bidirectional | **1** | 0,36 | **–** | – | **–** | – | **–** | – |
| | orthogonal | **39** | 13,98 | **3** | 2,83 | **7** | 8,43 | **2** | 4,76 |
| | semi-crossed | **11** | 3,94 | **1** | 0,94 | **–** | – | **–** | – |
| | opposite directional | **3** | 1,08 | **1** | 0,94 | **1** | 1,20 | **1** | 2,38 |
| | **TOTAL:** | **279** | 100,00 | **106** | 100,00 | **83** | 100,00 | **42** | 100,00 |
| | unidentifiable | 4 | – | 1 | – | – | – | – | – |

Table 8-27. Barmaky, pit 2 & complex 2a, by horizons: *débitage* dorsal scar patterns (including tools)

| | | | flakes | | blades | | bladelets | | micro-blades | |
|---|---|---|---|---|---|---|---|---|---|---|
| | | | # | % | # | % | # | % | # | % |
| HORIZON 2a | none | 0% | **182** | 46,31 | **53** | 37,32 | **71** | 55,04 | **57** | 70,37 |
| | primary | >75% | **31** | 7,89 | **3** | 2,11 | **1** | 0,78 | | |
| | proximal | 1–25% | **24** | 6,11 | **1** | 0,70 | **1** | 0,78 | **1** | 1,23 |
| | | 26–50% | **1** | 0,25 | **–** | – | **–** | – | **–** | – |
| | central | 1–25% | **2** | 0,51 | **–** | – | **1** | 0,78 | **–** | – |
| | | 51–75% | **–** | – | **–** | – | **2** | 1,55 | **–** | – |
| | lateral | 1–25% | **44** | 11,20 | **28** | 19,72 | **13** | 10,08 | **6** | 7,41 |
| | | 26–50% | **21** | 5,34 | **26** | 18,31 | **24** | 18,60 | **9** | 11,11 |
| | | 51–75% | **6** | 1,53 | **7** | 4,93 | **9** | 6,98 | **3** | 3,70 |
| | bi-lateral | 1–25% | **1** | 0,25 | **–** | – | **–** | – | **–** | – |
| | | 26–50% | **1** | 0,25 | **1** | 0,70 | **–** | – | **1** | 1,23 |
| | | 51–75% | **1** | 0,25 | **1** | 0,70 | **–** | – | **–** | – |
| | distal | 1–25% | **34** | 8,65 | **5** | 3,52 | **2** | 1,55 | **1** | 1,23 |
| | | 26–50% | **10** | 2,54 | **4** | 2,82 | **1** | 0,78 | **–** | – |
| | | 51–75% | **5** | 1,27 | **–** | – | **–** | – | **–** | – |
| | distal-lateral | 1–25% | **10** | 2,54 | **7** | 4,93 | **1** | 0,78 | **1** | 1,23 |
| | | 26–50% | **8** | 2,04 | **1** | 0,70 | **1** | 0,78 | **1** | 1,23 |
| | | 51–75% | **8** | 2,04 | **5** | 3,52 | **2** | 1,55 | **1** | 1,23 |
| | distal-proximal | 1–25% | **3** | 0,76 | **–** | – | **–** | – | **–** | – |
| | | 26–50% | **1** | 0,25 | **–** | – | **–** | – | **–** | – |
| | | **TOTAL:** | **393** | 100,00 | **142** | 100,00 | **129** | 100,00 | **81** | 100,00 |
| HORIZON 2a1 | none | 0% | **6** | 35,29 | **6** | 60,00 | **3** | 75,00 | **3** | 100,00 |
| | primary | >75% | **3** | 17,65 | **–** | – | **–** | – | **–** | – |
| | proximal | 1–25% | **1** | 5,88 | **–** | – | **–** | – | **–** | – |
| | lateral | 1–25% | **–** | – | **2** | 20,00 | **–** | – | **–** | – |
| | | 26–50% | **4** | 23,53 | **1** | 10,00 | **–** | – | **–** | – |
| | | 51–75% | **–** | – | **1** | 10,00 | **–** | – | **–** | – |
| | distal | 1–25% | **1** | 5,88 | **–** | – | **–** | – | **–** | – |
| | | 26–50% | **1** | 5,88 | **–** | – | **–** | – | **–** | – |
| | distal-lateral | 1–25% | **1** | 5,88 | **–** | – | **1** | 25,00 | **–** | – |
| | | **TOTAL:** | **17** | 100,00 | **10** | 100,00 | **4** | 100,00 | **3** | 100,00 |

Table 8–28. Barmaky, pit 2 & complex 2a, by horizons: *débitage* primary surfaces placement & percentages (including tools)

| | | | flakes | | blades | | bladelets | | micro-blades | |
|---|---|---|---|---|---|---|---|---|---|---|
| | | | # | % | # | % | # | % | # | % |
| PIT 2 | none | 0% | **132** | 46,64 | **52** | 48,60 | **46** | 55,42 | **33** | 78,57 |
| | primary | >75% | **31** | 10,95 | **4** | 3,74 | **–** | – | **–** | – |
| | proximal | 1–25% | **10** | 3,53 | **2** | 1,87 | **1** | 1,20 | **–** | – |
| | | 26–50% | **5** | 1,77 | **–** | – | **–** | – | **–** | – |
| | central | 1–25% | **–** | – | **1** | 0,93 | **1** | 1,20 | **–** | – |
| | | 26–50% | **3** | 1,06 | **–** | – | **–** | – | **–** | – |
| | | 51–75% | **1** | 0,35 | **–** | – | **–** | – | **–** | – |
| | lateral | 1–25% | **27** | 9,54 | **17** | 15,89 | **11** | 13,25 | **3** | 7,14 |
| | | 26–50% | **12** | 4,24 | **7** | 6,54 | **12** | 14,46 | **3** | 7,14 |
| | | 51–75% | **12** | 4,24 | **6** | 5,61 | **6** | 7,23 | **3** | 7,14 |
| | bi-lateral | 1–25% | **1** | 0,35 | **1** | 0,93 | **–** | – | **–** | – |
| | | 26–50% | **3** | 1,06 | **–** | – | **–** | – | **–** | – |
| | | 51–75% | **1** | 0,35 | **2** | 1,87 | **–** | – | **–** | – |
| | distal | 1–25% | **15** | 5,30 | **–** | – | **2** | 2,41 | **–** | – |
| | | 26–50% | **5** | 1,77 | **1** | 0,93 | **–** | – | **–** | – |
| | | 51–75% | **2** | 0,71 | **–** | – | **–** | – | **–** | – |
| | distal-lateral | 1–25% | **4** | 1,41 | **4** | 3,74 | **2** | 2,41 | **–** | – |
| | | 26–50% | **8** | 2,83 | **4** | 3,74 | **1** | 1,20 | **–** | – |
| | | 51–75% | **8** | 2,83 | **6** | 5,61 | **1** | 1,20 | **–** | – |
| | distal-proximal | 1–25% | **1** | 0,35 | **–** | – | **–** | – | **–** | – |
| | | 26–50% | **1** | 0,35 | **–** | – | **–** | – | **–** | – |
| | | 51–75% | **1** | 0,35 | **–** | – | **–** | – | **–** | – |
| | | **TOTAL:** | **283** | 100,00 | **107** | 100,00 | **83** | 100,00 | **42** | 100,00 |

Table 8-28. continued.

At the same time, **butt abrasion** and **lipped** platforms are virtually absent (Tables 8-31; 8-32). Pronounced **bulbs** in combination with **right-angle platforms** are characteristic for all blank types (Tables 8-33; 8-34).

## Tool trimming pieces

Primary and secondary/multiple **burin spalls** are equally represented (Table 8-21; Fig. 8-8, *3, 4*). Only one burin spall was preliminarily retouched before detachment. They occur as distal and proximal fragments as well as complete pieces. Crescent off-axis shapes, twisted lateral profiles, hinged distal ends, lateral steep cross-sections, untrimmed, unlipped, non-abraded, acute platforms, and pronounced/diffuse bulbs are characteristic.

## *Débitage* dimensions

Despite the limited number of artefacts, the main metrical characteristics of pit 2 and other complexes are fairly similar (Table 8-35).

## Tools

Only 14 tools originate from pit 2 (Table 8-36), eight on blades, five on flakes, and one on an unidentifiable blank.

**Burins** are made on rather regular blades and comprise one distally symmetrical dihedral burin (Fig. 8-9, *3*), as well as one burin on oblique distal (Fig. 8-9, *1*), oblique proximal (Fig. 8-9, *7*), and oblique-convex distal (Fig. 8-9, *5*) truncation, respectively. The truncations were made by continuous, scalar/sub-parallel obverse semi-abrupt/abrupt retouch. The burin on oblique-convex truncation is a reutilized piece: opposite of the burin spall

a former burin negative, is partly removed by truncation. A total of 10 burin spall negatives is observed on four burin edges, six of them on the dihedral burin. The average dimensions of burins are 60.32×21.19×6.53 mm.

**Truncated pieces** comprise a distally obliquely truncated blade, a bi-terminally truncated blade, and a distally straightly truncated flake (Table 8-36). Regular blades (67.00×20.58×4.47 and 81.95×20.44×5.77 mm) and a *débordante* flake (26.04×17.17×2.44 mm) serve as blanks. Continuous/partial scalar/sub-parallel obverse abrupt retouch was applied for the truncation. The bi-terminally truncated blade is a former burin on proximal truncation; the newly made proximal truncation partly removed the burin spall negative on the lateral side (Fig. 8-9, *6*).

The **retouched pieces** were made on one "regular" blade (>40.51×22.94×5.57 mm), two "regular" flakes, and two *débordante* flakes (Table 8-36; Fig. 8-9, *2, 4*). The blade was modified by lateral partial scalar obverse abrupt retouch and the flakes by distal/proximal partial scalar obverse/inverse semi-abrupt/abrupt retouch. The average dimensions of the latter are >24.42×26.47×5.99 mm.

There are two **unidentifiable tools**: a medial fragment of a blade and a lateral fragment of an unknown blank (Table 8-36). A continuous sub-parallel obverse semi-abrupt retouch modified the lateral side of the blade and a partial micro-scalar obverse abrupt retouch modified the lateral edge of the unknown blank.

### Flaking instruments

There are 4 small chunks and 1 flake from sandstone pebbles. These are probably fragments of hammer-stones.

## EASTERN AREA COMPLEX: ARCHAEOLOGICAL LEVEL 2, HORIZONS 2C & 2D

The artefacts from the eastern area originate from 17 square meters, which is characterised by five features: a hearth, an ashy zone, coloured sediments of horizon 2c, material from a permafrost depression (horizon 2d), and a chalk/ marl crust (horizon 2b), the latter without artefacts (Chapter 2, Fig. 2-22, this volume). Stratigraphically, the hearth and ashy zone belong to horizon 2c. Horizon 2d appears to contain relocated material of horizon 2c. Thus, the horizons 2c and 2d in the eastern area might be the remnants of temporary close economic episodes. The squares 4P (3332 items), 5P (12419 items), 5C (7113 items), 6C (5511 items), and 6T (8891 items) of horizon 2d have the highest artefact densities.

The main characteristic feature of the **artefact assemblages** is the relatively large amount of pre-cores and cores (Table 8-37). The tool-to-core-like pieces ratio is 1.26 to 1, showing an intensive core reduction in the area. At the same time, the presence of tool trimming pieces, such as burin and truncation spalls (Table 8-37), suggests on-site tool production. The sum of bladelets and micro-blades prevails over the number of blades. The high percentage of chips (83.61 %) indicates a low rate of post-depositional transportation.

### Unmodified raw material

The maximum dimensions of nine **chunks** exceed 50 mm. These pieces probably served as raw material reserves, four of them exhibit the negatives of testing blows. Four natural flakes and their fragments, one rounded nodule, five plaquettes, and three unidentifiable pieces represent the chunk collection. The mean values of maximum measurements are 77.88×49.11×25.61 mm. Predominantly, plate-like shapes of middle-size raw materials were transported to the site area.

### Pre-cores & cores

Both **pre-cores** and cores mainly originate from horizon 2d (Table 8-38). Unidirectional pre-cores prevail over bidirectional ones and specimens for blade/bladelet and bladelet production dominate the assemblage. All identifiable pre-cores belong to the narrow flaking surface type (Fig. 8-10; 8-11; 8-12, *1*). Flakes (2 pieces), natural flakes (3 pieces), and flint plaquettes (5 pieces) were used as blanks for the production of narrow flaking surface pre-cores. In seven cases, the initial flaking starts from the preparation of crested ridges. A single pre-core on flake with a unidirectional narrow flaking surface shows a wedge-like preparation of the distal part (Fig. 8-12, *1*). The length varies

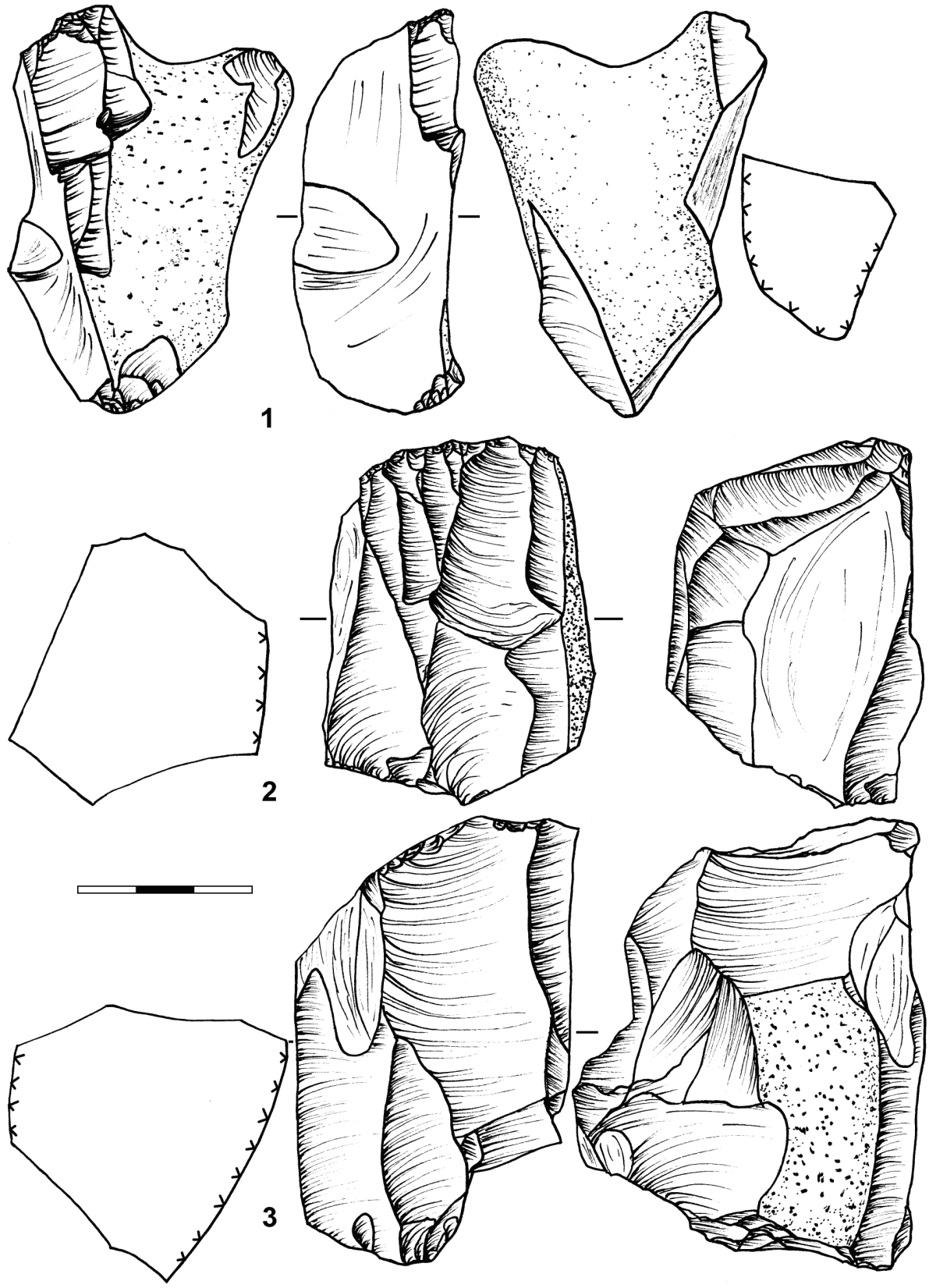


Fig. Fig. 8–6. Barmaky, pit 2 complex: 1 – pre-core, bidirectional, narrow flaking surface; 2 – core for blades /bladelets, bidirectional, narrow flaking surface; 3 – core for blades, bidirectional, narrow flaking surface.

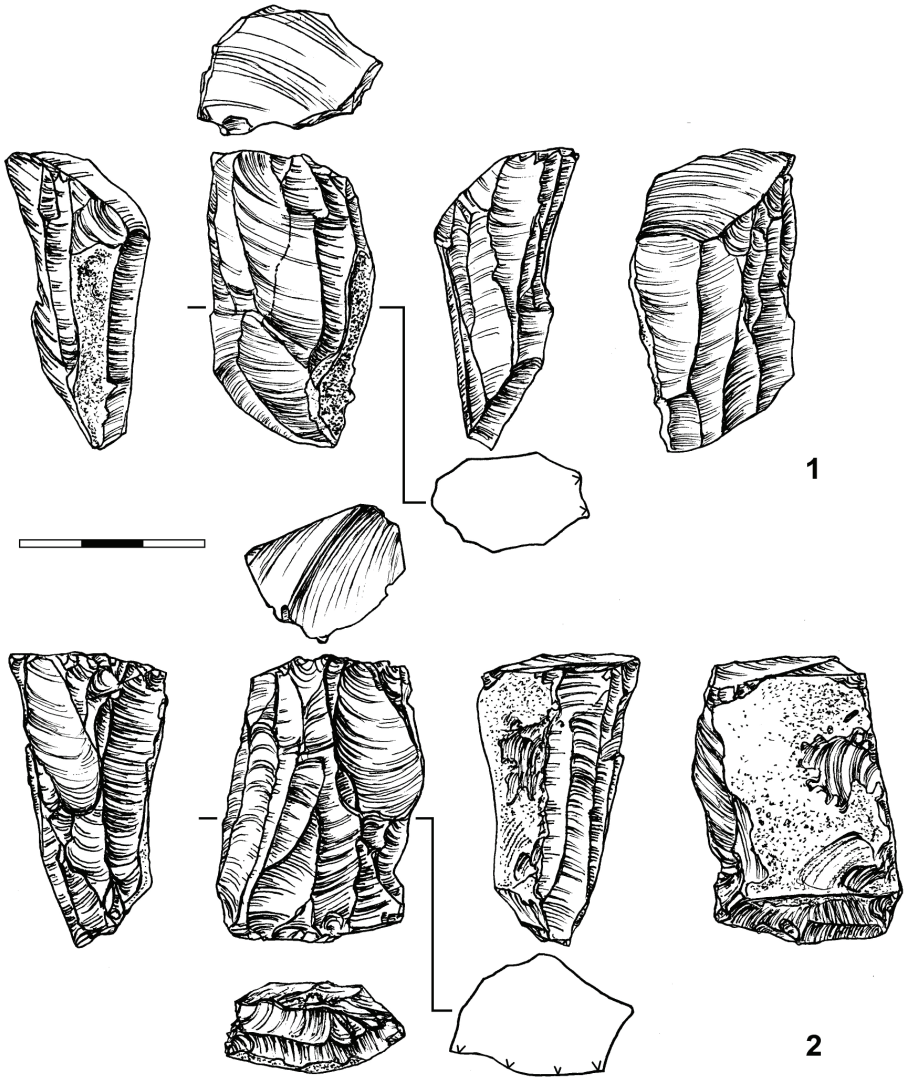


Fig. 8–7. Barmaky, pit 2 complex: 1 – core for bladelets, bidirectional-alternate, cylindrical; 2 – core for bladelets, bidirectional, sub-cylindrical.

from 95.72 to 45.39 mm (mean 64.63 mm), the width from 65.38 to 18.02 mm (mean 31.65 mm), and the thickness from 70.27 to 34.58 mm (mean 58.91 mm). The fact that the values for thickness exceed those of width underlines the significance of narrow flaking surfaces.

**Cores** for blades (18 items), blades/bladelets (18 items), and bladelets (17 items) occur in equal numbers (Table 8–38). In addition, there are two cores for flakes and five unidentifiable core fragments. The cores for flakes are both sub-cylindrical: bidirectional-alternate (41.52×68.10×59.72 mm) and multidirectional (60.29×65.06×47.52 mm). The latter was made on a natural flake; the blank for the former is unidentifiable.

Bidirectional **cores for blades** (11 pieces) prevail over unidirectional (7 pieces) ones (Table 8–38; Fig. 8–12, *2, 3*; 8–13; 8–14, *2*). Among the former, specimens with sub-cylindrical/cylindrical shapes and narrow flaking surfaces show about equal numbers. The same is true for unidirectional blade cores. Three bidirectional blade cores show adjacent flaking surfaces and three exhibit two opposite main striking platforms, while the rest show supplementary opposite platforms (Fig. 8–12, *3*; 8–14, *2*).

Two rounded nodules, three natural flakes, three flint plaquettes, and 12 unidentifiable pieces serve as raw volume for the blade cores (Fig. 8–13). As can be expected, the metric parameters of sub-cylindrical/cylindrical blade

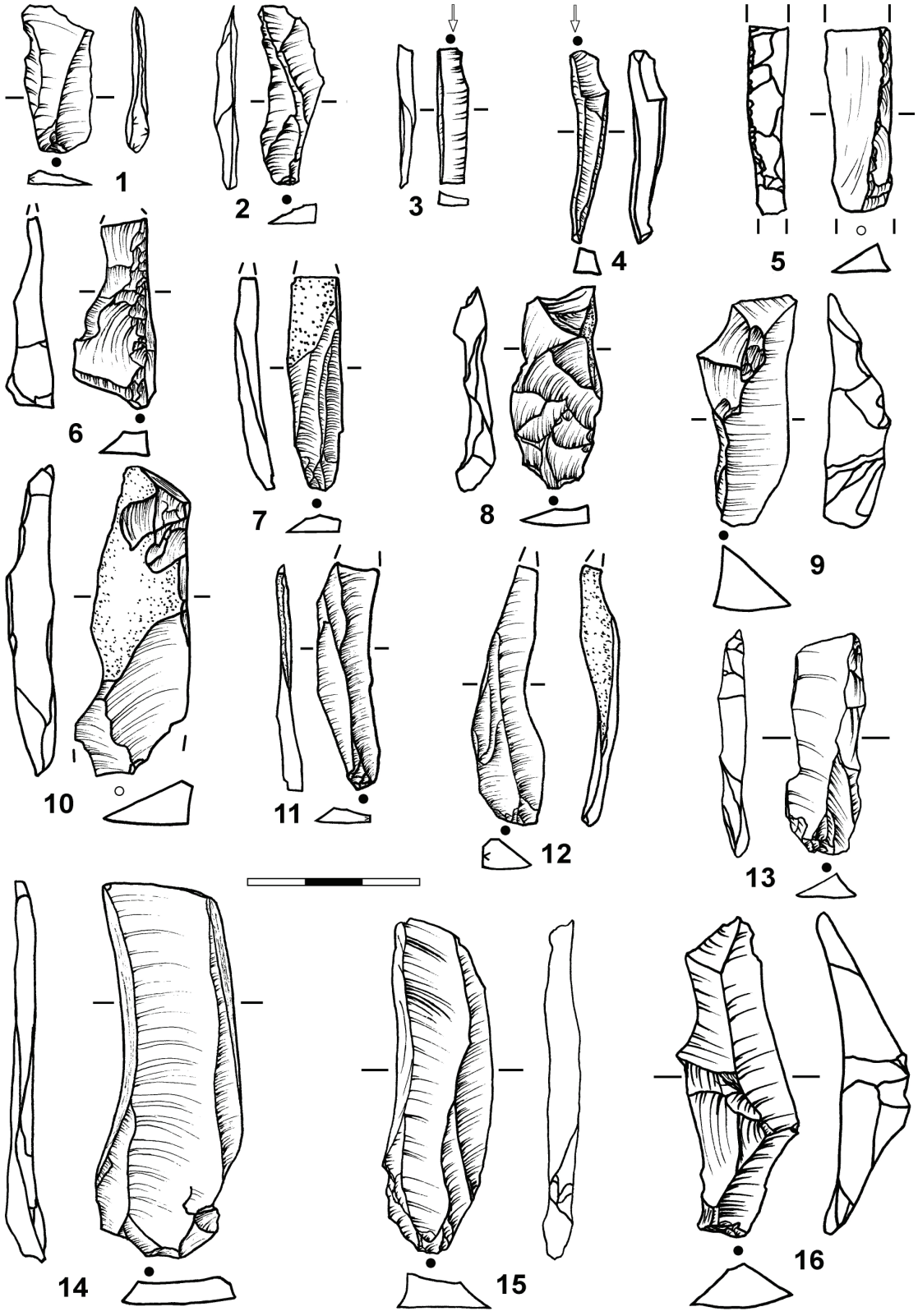


Fig. 8-8. Barmaky, pit 2 complex: 1, 11, 12 – cortical *débordante* bladelets; 2 – natural *débordante* bladelets; 3 – burin spall, secondary; 4 – burin spall, multiple; 5 – one-side crested bladelet; 6, 9 – one-side crested blades; 7 – natural *débordante* bladelets; 8 – lateral *débordante* blades; 10 – crested blade, unidirectional, on lateral *débordante* piece; 13 – secondary crested blade, unidirectional; 14, 15 – natural *débordante* blades; 16 – one-side crested blade, bidirectional.

| | | | flakes | | blades | | bladelets | | micro-blades | |
|---|---|---|---|---|---|---|---|---|---|---|
| | | | # | % | # | % | # | % | # | % |
| HORIZON 2a | cortex | | **22** | 8,98 | **1** | 1,89 | **1** | 2,17 | **–** | – |
| | plain | | **126** | 51,43 | **27** | 50,94 | **18** | 39,13 | **8** | 50,00 |
| | linear | | **28** | 11,43 | **13** | 24,53 | **17** | 36,96 | **5** | 31,25 |
| | pointed | | **2** | 0,82 | **–** | – | **2** | 4,35 | **–** | – |
| | dihedral | | **29** | 11,84 | **6** | 11,32 | **6** | 13,04 | **3** | 18,75 |
| | polyhedral | | **16** | 6,53 | **1** | 1,89 | **1** | 2,17 | **–** | – |
| | faceted | | **22** | 8,98 | **5** | 9,43 | **1** | 2,17 | **–** | – |
| | | **TOTAL:** | **245** | 100,00 | **53** | 100,00 | **46** | 100,00 | **16** | 100,00 |
| | crushed | | 52 | – | 24 | – | 21 | – | 13 | – |
| | modified | | – | – | 6 | – | 2 | – | 4 | – |
| | unidentifiable | | 4 | – | – | – | – | – | – | – |
| | missing | | 92 | – | 59 | – | 60 | – | 48 | – |
| HORIZON 2a1 | cortex | | **1** | 9,09 | **–** | – | **–** | – | **–** | – |
| | plain | | **5** | 45,45 | **3** | 42,86 | **1** | 100,00 | **–** | – |
| | linear | | **–** | – | **2** | 28,57 | **–** | – | **–** | – |
| | dihedral | | **2** | 18,18 | **1** | 14,29 | **–** | – | **–** | – |
| | faceted | | **3** | 27,27 | **1** | 14,29 | **–** | – | **–** | – |
| | | **TOTAL:** | **11** | 100,00 | **7** | 100,00 | **1** | 100,00 | **–** | – |
| | crushed | | 1 | – | – | – | – | – | – | – |
| | missing | | 5 | – | 3 | – | 3 | – | 3 | – |
| PIT 2 | cortex | | **20** | 12,27 | **–** | – | **1** | 2,94 | **–** | – |
| | plain | | **87** | 53,37 | **20** | 42,55 | **21** | 61,76 | **5** | 55,56 |
| | linear | | **13** | 7,98 | **15** | 31,91 | **8** | 23,53 | **4** | 44,44 |
| | pointed | | **–** | – | **2** | 4,26 | **2** | 5,88 | **–** | – |
| | dihedral | | **13** | 7,98 | **7** | 14,89 | **1** | 2,94 | **–** | – |
| | polyhedral | | **14** | 8,59 | **–** | – | **–** | – | **–** | – |
| | faceted | | **16** | 9,82 | **3** | 6,38 | **1** | 2,94 | **–** | – |
| | | **TOTAL:** | **163** | 100,00 | **47** | 100,00 | **34** | 100,00 | **9** | 100,00 |
| | crushed | | 40 | – | 19 | – | 16 | – | 3 | – |
| | modified | | 1 | – | 2 | – | – | – | – | – |
| | unidentifiable | | 3 | – | – | – | 1 | – | – | – |
| | missing | | 76 | – | 39 | – | 32 | – | 30 | – |

Table 8–29. Barmaky, pit 2 & complex 2a, by horizons: *débitage* striking platform types (including tools)

| | | | flakes | | blades | | bladelets | | micro-blades | |
|---|---|---|---|---|---|---|---|---|---|---|
| | | | # | % | # | % | # | % | # | % |
| HORIZON 2a | trimmed | | **52** | 17,39 | **32** | 45,07 | **38** | 57,58 | **12** | 42,86 |
| | untrimmed | | **247** | 82,61 | **39** | 54,93 | **28** | 42,42 | **16** | 57,14 |
| | | **TOTAL:** | **299** | 100,00 | **71** | 100,00 | **66** | 100,00 | **28** | 100,00 |
| | missing | | 92 | – | 59 | – | 60 | – | 48 | – |
| | unidentifiable | | 2 | – | 12 | – | 3 | – | 5 | – |
| HORIZON 2a1 | trimmed | | **1** | 8,33 | **1** | 14,29 | **1** | 100,00 | **–** | – |
| | untrimmed | | **11** | 91,67 | **6** | 85,71 | **–** | – | **–** | – |
| | | **TOTAL:** | **12** | 100,00 | **7** | 100,00 | **1** | 100,00 | **–** | – |
| | missing | | 5 | – | 3 | – | 3 | – | 3 | – |
| PIT 2 | trimmed | | **12** | 5,91 | **37** | 59,68 | **30** | 62,50 | **6** | 54,55 |
| | untrimmed | | **191** | 94,09 | **25** | 40,32 | **18** | 37,50 | **5** | 45,45 |
| | | **TOTAL:** | **203** | 100,00 | **62** | 100,00 | **48** | 100,00 | **11** | 100,00 |
| | missing | | 76 | – | 41 | – | 32 | – | 30 | – |
| | unidentifiable | | 4 | – | 4 | – | 3 | – | 1 | – |

Table 8–30. Barmaky, pit 2 & complex 2a, by horizons: *débitage* overhang trimming (including tools)

| | | | flakes | | blades | | bladelets | | micro-blades | |
|---|---|---|---|---|---|---|---|---|---|---|
| | | | # | % | # | % | # | % | # | % |
| HORIZON 2a | abrased | | **–** | – | **–** | – | **–** | – | **–** | – |
| | unabrased | | **299** | 100,00 | **71** | 100,00 | **65** | 100,00 | **28** | 100,00 |
| | | **TOTAL:** | **299** | 100,00 | **71** | 100,00 | **65** | 100,00 | **28** | 100,00 |
| | missing | | 92 | – | 59 | – | 60 | – | 48 | – |
| | unidentifiable | | 2 | – | 12 | – | 4 | – | 5 | – |
| HORIZON 2a1 | abrased | | **–** | – | **–** | – | **–** | – | **–** | – |
| | unabrased | | **12** | 100,00 | **7** | 100,00 | **1** | 100,00 | **–** | – |
| | | **TOTAL:** | **12** | 100,00 | **7** | 100,00 | **1** | 100,00 | **–** | – |
| | missing | | 5 | – | 3 | – | 3 | – | 3 | – |
| | unidentifiable | | **–** | – | **–** | – | **–** | – | **–** | – |
| PIT 2 | abrased | | **3** | 1,48 | **–** | – | **–** | – | **–** | – |
| | unabrased | | **200** | 98,52 | **61** | 100,00 | **47** | 100,00 | **11** | 100,00 |
| | | **TOTAL:** | **203** | 100,00 | **61** | 100,00 | **47** | 100,00 | **11** | 100,00 |
| | missing | | 76 | – | 41 | – | 32 | – | 30 | – |
| | unidentifiable | | 4 | – | 5 | – | 4 | – | 1 | – |

Table 8–31. Barmaky, pit 2 & complex 2a, by horizons: *débitage* butt abrasion (including tools)

| | | | flakes | | blades | | bladelets | | micro-blades | |
|---|---|---|---|---|---|---|---|---|---|---|
| | | | # | % | # | % | # | % | # | % |
| HORIZON 2a | lipped | | **12** | 4,46 | **1** | 1,59 | **1** | 1,85 | **2** | 10,00 |
| | semi-lipped | | **16** | 5,95 | **6** | 9,52 | **–** | – | **2** | 10,00 |
| | unlipped | | **241** | 89,59 | **56** | 88,89 | **53** | 98,15 | **16** | 80,00 |
| | | **TOTAL:** | **269** | 100,00 | **63** | 100,00 | **54** | 100,00 | **20** | 100,00 |
| | missing | | 92 | – | 59 | – | 60 | – | 48 | – |
| | unidentifiable | | 32 | – | 20 | – | 15 | – | 13 | – |
| HORIZON 2a1 | lipped | | **–** | – | **–** | – | **–** | – | **–** | – |
| | semi-lipped | | **2** | – | **2** | – | **–** | – | **–** | – |
| | unlipped | | **–** | – | **–** | – | **1** | – | **–** | – |
| | | **TOTAL:** | **2** | – | **2** | – | **1** | – | **–** | – |
| | missing | | 5 | – | 3 | – | 3 | – | 3 | – |
| | unidentifiable | | 10 | – | 5 | – | – | – | – | – |
| PIT 2 | lipped | | **11** | 5,73 | **2** | 3,70 | **1** | 2,27 | **1** | 9,09 |
| | semi-lipped | | **16** | 8,33 | **4** | 7,41 | **3** | 6,82 | **1** | 9,09 |
| | unlipped | | **165** | 85,94 | **48** | 88,89 | **40** | 90,91 | **9** | 81,82 |
| | | **TOTAL:** | **192** | 100,00 | **54** | 100,00 | **44** | 100,00 | **11** | 100,00 |
| | missing | | 76 | – | 39 | – | 32 | – | 30 | – |
| | unidentifiable | | 15 | – | 14 | – | 7 | – | 1 | – |

Table 8–32. Barmaky, pit 2 & complex 2a, by horizons: *débitage* butts lipping (including tools)

| | | | flakes | | blades | | bladelets | | micro-blades | |
|---|---|---|---|---|---|---|---|---|---|---|
| | | | # | % | # | % | # | % | # | % |
| HORIZON 2a | absent | | **6** | 2,23 | **–** | – | **1** | 1,85 | **1** | 5,00 |
| | defused | | **45** | 16,73 | **9** | 14,06 | **3** | 5,56 | **4** | 20,00 |
| | pronounced | | **218** | 81,04 | **55** | 85,94 | **50** | 92,59 | **15** | 75,00 |
| | | **TOTAL:** | **269** | 100,00 | **64** | 100,00 | **54** | 100,00 | **20** | 100,00 |
| | missing | | 92 | – | 59 | – | 60 | – | 48 | – |
| | unidentifiable | | 32 | – | 19 | – | 15 | – | 13 | – |
| HORIZON 2a1 | absent | | **–** | – | **–** | – | **–** | – | **–** | – |
| | defused | | **4** | – | **2** | – | **–** | – | **–** | – |
| | pronounced | | **4** | – | **4** | – | **1** | – | **–** | – |
| | | **TOTAL:** | **8** | – | **6** | – | **1** | – | **–** | – |
| | missing | | 5 | – | 3 | – | 3 | – | 3 | – |
| | unidentifiable | | 4 | – | 1 | – | – | – | – | – |
| PIT 2 | absent | | **9** | 4,69 | **1** | 1,85 | **–** | – | **–** | – |
| | defused | | **36** | 18,75 | **9** | 16,67 | **12** | 27,27 | **3** | 27,27 |
| | pronounced | | **147** | 76,56 | **44** | 81,48 | **32** | 72,73 | **8** | 72,73 |
| | | **TOTAL:** | **192** | 100,00 | **54** | 100,00 | **44** | 100,00 | **11** | 100,00 |
| | missing | | 76 | – | 39 | – | 32 | – | 30 | – |
| | unidentifiable | | 15 | – | 14 | – | 7 | – | 1 | – |

Table 8–33. Barmaky, pit 2 & complex 2a, by horizons: *débitage* bulbs (including tools)

| | | | flakes | | blades | | bladelets | | micro-blades | |
|---|---|---|---|---|---|---|---|---|---|---|
| | | | # | % | # | % | # | % | # | % |
| HORIZON 2a | right | | **177** | 71,37 | **42** | 79,25 | **44** | 93,62 | **11** | 68,75 |
| | acute | | **70** | 28,23 | **11** | 20,75 | **3** | 6,38 | **5** | 31,25 |
| | obtuse | | **1** | 0,40 | **–** | – | **–** | – | **–** | – |
| | | **TOTAL:** | **248** | 100,00 | **53** | 100,00 | **47** | 100,00 | **16** | 100,00 |
| | missing | | 92 | – | 59 | – | 60 | – | 48 | – |
| | unidentifiable | | 53 | – | 30 | – | 22 | – | 17 | – |
| HORIZON 2a1 | right | | **5** | 45,45 | **5** | 71,43 | **1** | 100,00 | **–** | – |
| | acute | | **6** | 54,55 | **2** | 28,57 | **–** | – | **–** | – |
| | obtuse | | **–** | – | **–** | – | **–** | – | **–** | – |
| | | **TOTAL:** | **11** | 100,00 | **7** | 100,00 | **1** | 100,00 | **–** | – |
| | missing | | 5 | – | 3 | – | 3 | – | 3 | – |
| | unidentifiable | | 1 | – | – | – | – | – | – | – |
| PIT 2 | right | | **119** | 72,12 | **41** | 87,23 | **31** | 91,18 | **6** | 66,67 |
| | acute | | **46** | 27,88 | **6** | 12,77 | **3** | 8,82 | **3** | 33,33 |
| | | **TOTAL:** | **165** | 100,00 | **47** | 100,00 | **34** | 100,00 | **9** | 100,00 |
| | missing | | 76 | – | 39 | – | 32 | – | 30 | – |
| | unidentifiable | | 42 | – | 21 | – | 17 | – | 3 | – |

Table 8–34. Barmaky, pit 2 & complex 2a, by horizons: *débitage* striking platform angels (including tools)

| | | flakes | blades | bladelets | micro-blades |
|---|---|---|---|---|---|
| complex 2a | platform, W | **10,12** (1,36–44.61) | **8,18** (1,75–35,89) | **4,42** (1,09–8,36) | **3,01** (1,53–5,47) |
| | platform, Th | **2,92** (0,16–21,55) | **2,73** (0,49–14,27) | **1,50** (0,31–7,19) | **1,21** (0,55–2,95) |
| | blank, L | **24,27** (1,46–73,91) | **50,72** (26,78–100,57) | **25,59** (16,11–42,66) | **18,18** (15,16–26,74) |
| | blank, W | **22,41** (8,39–66,80) | **19,03** (12,06–43,49) | **9,26** (7,00–11,98) | **5,60** (2,91–6,96) |
| | blank, Th | **4,15** (0,57–21,06) | **5,80** (1,37–22,09) | **2,60** (0,93–6,58) | **1,91** (0,68–4,87) |
| complex PIT 2 | platform, W | **11,32** (2,20–90,62) | **7,16** (1,93–27,13) | **4,04** (0,55–7,32) | **3,53** (1,49–5,90) |
| | platform, Th | **3,69** (0,39–30,63) | **2,44** (0,52–13,16) | **1,56** (0,56–6,54) | **1,30** (0,37–2,65) |
| | blank, L | **25,85** (7,58–72,61) | **48,82** (30,15–118,68) | **27,35** (16,25–61,90) | **17,67** (15,25–22,80) |
| | blank, W | **23,12** (8,51–102,11) | **18,34** (12,00–47,86) | **9,21** (7,07–11,92) | **5,92** (4,39–6,99) |
| | blank, Th | **4,49** (0,83–27,20) | **5,12** (1,28–20,05) | **2,52** (0,87–7,51) | **1,53** (0,74–2,92) |
| complex EA | platform, W | **6,66** (0,95–60,97) | **7,43** (0,38–22,37) | **4,46** (0,64–11,97) | **2,74** (0,37–5,64) |
| | platform, Th | **3,17** (0,18–26,94) | **2,69** (0,43–13,13) | **1,57** (0,22–8,25) | **1,02** (0,22–3,75) |
| | blank, L | **25,39** (1,43–100,21) | **46,07** (25,02–112,20) | **27,22** (14,75–83,06) | **19,54** (14,56–52–48) |
| | blank, W | **21,75** (7,59–110,08) | **17,00** (12,00–43,60) | **9,22** (7,00–11,98) | **5,57** (2,19–6,99) |
| | blank, Th | **4,09** (0,61–43,71) | **4,76** (0,99–27,61) | **2,58** (0,61–15,76) | **1,73** (0,62–6,68) |
| complex WA | platform, W | **10,55** (0,54–75,02) | **8,00** (1,25–40,68) | **4,71** (0,93–11,67) | **3,16** (0,82–7,52) |
| | platform, Th | **3,24** (0,23–36,65) | **2,86** (0,16–20,45) | **1,66** (0,04–7,87) | **1,23** (0,17–5,22) |
| | blank, L | **24,35** (3,00–93,51) | **50,94** (25,40–106,54) | **26,35** (15,46–58,40) | **19,78** (14,96–53,21) |
| | blank, W | **22,08** (7,61–91,70) | **18,02** (12,00–41,71) | **9,31** (7,00–11,99) | **5,42** (2,54–6,99) |
| | blank, Th | **4,37** (0,64–37,60) | **5,86** (1,00–29,33) | **2,97** (0,80–13,18) | **1,99** (0,57–6,82) |

Table 8–35. Barmaky, level 2, by complexes: *débitage* average dimensions and the ranges (in brackets), in mm (including tools)

| | 2a | 2a1 | pit 2 |
|---|---|---|---|
| **BURINS ON TRUNCATED BLADES** | | | |
| on straight proximal dorsal truncation | 1 | – | – |
| on oblique distal dorsal truncation | – | – | 1 |
| on oblique proximal dorsal truncation | – | – | 1 |
| on oblique-convex distal dorsal truncation | 2 | – | 1 |
| on oblique-concave distal dorsal truncation | 1 | – | – |
| on concave proximal ventral truncation | 1 | – | – |
| bi-lateral, on straight distal dorsal truncation | 1 | – | – |
| opposite-alternative, on bi-terminal oblique dorsal truncations | 1 | – | – |
| **BURINS ON BLADES, DIHEDRAL** | | | |
| symmetrical, distal | – | – | 1 |
| **BURINS ON TRUNCATED FLAKES** | | | |
| on straight distal dorsal truncation | 1 | – | – |
| **BURINS ON TRUNCATED UNIDENTIFIABLE *DEBITAGE*** | | | |
| on oblique proximal dorsal truncation | – | 1 | – |
| **BURINS ON BLADES, ANGLE** | | | |
| distal | 1 | – | – |
| **BURINS ON BLADES, UNIDENTIFIABLE** | | | |
| distal; on laterally dorsally retouched blade | 1 | – | – |
| **TRUNCATED PIECES ON BLADES** | | | |
| straight, distal, dorsal | 1 | – | – |
| oblique, distal, dorsal | – | – | 1 |
| oblique, proximal, dorsal, | 2 | – | – |
| oblique-convex, distal-lateral, dorsal | 1 | – | – |
| bi-terminal, oblique, dorsal | – | – | 1 |
| **TRUNCATED PIECES ON FLAKES** | | | |
| straight, distal, dorsal | – | – | 1 |
| **DENTICULATED PIECES ON FLAKES** | | | |
| distal-lateral, dorsal | 1 | – | – |
| **NOTCHED PIECES ON BLADES** | | | |
| lateral, dorsal | 1 | – | – |
| lateral, dorsal | 1 | – | – |
| **BACKED POINTS ON BLADELETS** | | | |
| straightly dorsally backed, obliquely dorsally truncated base | 2 | – | – |
| **BACKED POINTS ON MICRO-BLADES** | | | |
| distally backed / truncated, dorsal | 1 | – | – |
| straightly dorsally backed, dorsally retouched base | 1 | – | – |
| straightly dorsally backed, obliquely dorsally truncated base (broken tip) | 4 | – | – |
| **UNFINISHED BACKED PIECES ON BLADELETS** | | | |
| unfinished, wavy dorsaly backed | 1 | – | – |

Table 8-36. Barmaky, pit 2 & complex 2a, by horizons: tools

| | 2a | 2a1 | pit 2 |
|---|---|---|---|
| **UNIDENTIFIABLE BACKED PIECES ON MICRO-BLADES** | | | |
| unidentifiable, straightly dorsaly backed | 2 | – | – |
| **RETOUCHED PIECES ON BLADES** | | | |
| distal / lateral, dorsal | – | 1 | – |
| lateral, dorsal | 3 | – | 1 |
| lateral, ventral | 2 | – | – |
| bi-lateral, alternate | 1 | – | – |
| **RETOUCHED PIECES ON BLADELETS** | | | |
| lateral, dorsal | 4 | – | – |
| **RETOUCHED PIECES ON FLAKES** | | | |
| distal, dorsal | 1 | – | 2 |
| distal, ventral | – | – | 1 |
| lateral, dorsal | 4 | – | – |
| proximal, dorsal | – | – | 1 |
| **RETOUCHED PIECES ON UNIDENTIFIABLE *DEBITAGE*** | | | |
| lateral, dorsal | 1 | – | – |
| **UNIDENTIFIABLE TOOLS ON BLADES** | | | |
| lateral, dorsal | – | – | 1 |
| **UNIDENTIFIABLE TOOLS ON UNIDENTIFIABLE *DEBITAGE*** | | | |
| lateral, dorsal | 1 | – | 1 |
| bi-lateral, dorsal | 1 | – | – |
| **TOTAL:** | 46 | 2 | 14 |

Table 8-36. continued.

cores and those with narrow flaking surfaces are quite different. The mean measurements of the former are 66.30×43.84×32.63 mm. and for the latter 73.25×34.15×47.69 mm. It cannot be excluded that some cylindrical cores are indeed exhausted cores with a narrow flaking surface. The best example of such transformation is the unidirectional narrow flaking surface core (55.87×46,32×47.99 mm) with hinge fracture on the flaking surface which probably led to its discard (Fig. 8-12, *2*). Along with hinge fractures, longitudinal breakages are the main reasons for discard. An undoubtedly exhausted blade core is the only example of a broken flattened unidirectional specimen. The average dimensions of the sub-cylindrical blade cores are 65.89×43.14×31.97 mm; the average dimensions of narrow flaking surface blade cores are 69.76×34.15×48.06 mm.

The **blade/bladelet cores** are subdivided into four main groups: unidirectional – 9 pieces, perpendicular – 2 pieces, bidirectional – 6 pieces, and multidirectional – 1 item (Table 8-38; Fig. 8-14, *1*; 8-15; 8-16, *1, 2, 3*). Narrow flaking surfaces prevail among the unidirectional cores, two of which have an additional flaking surface on the opposite side (Fig. 8-14, *1*). This type is reminiscent of the bilateral burins on truncation. The difference between unidirectional cores of pyramidal and sub-cylindrical shape consists in the exploitation of a 360° striking platform for the former. Two unidirectional blade/bladelet cores show a combination of a narrow and a flattened/sub-cylindrical flaking surface, perpendicular-adjacent at about 90° (Fig. 8-15, *2*). The same kind of flattened flaking surface is characteristic of the bidirectional blade/bladelet core with a narrow flaking surface (Fig. 8-16, *3*).

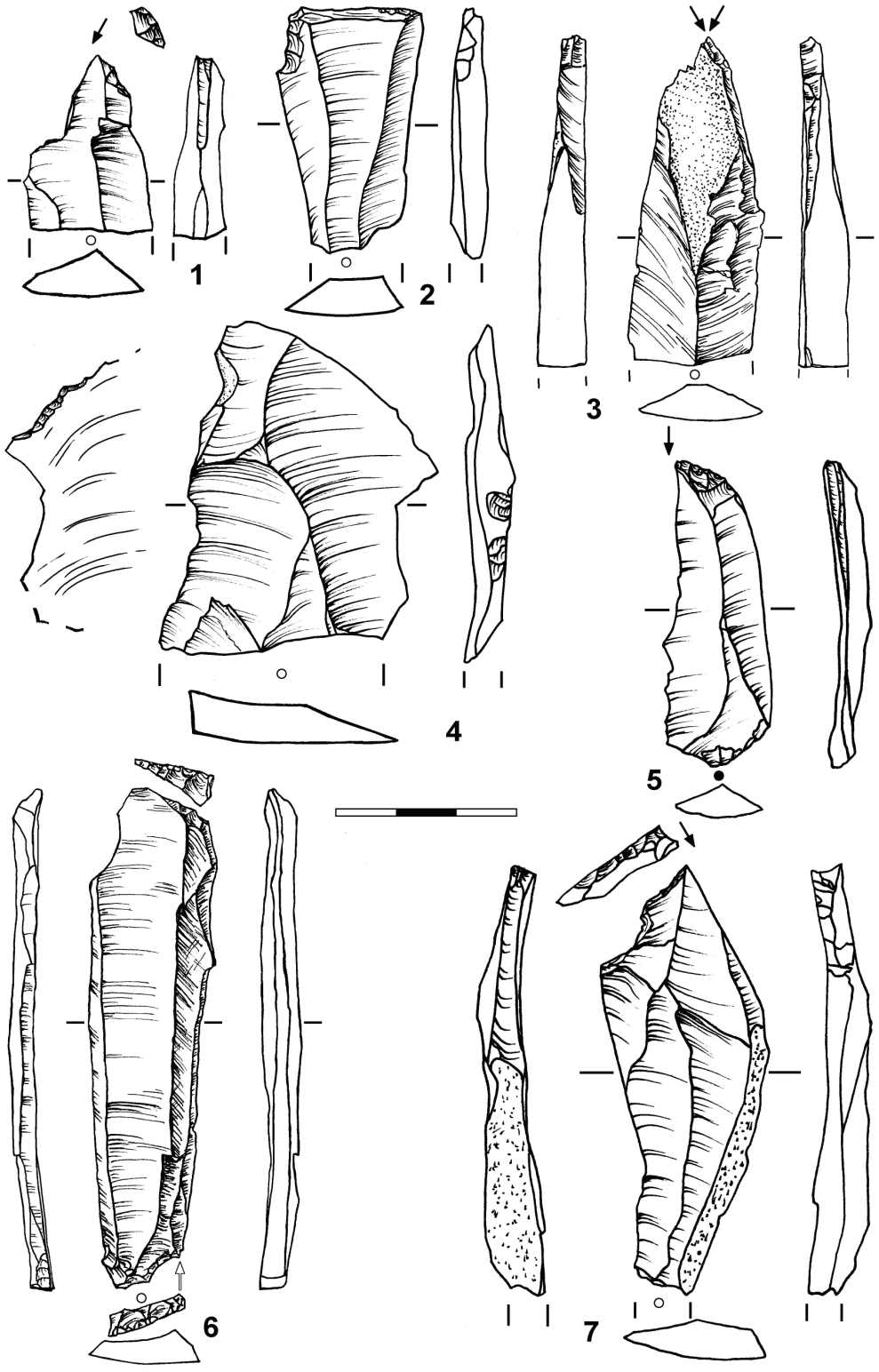


Fig. 8-9. Barmaky, pit 2 complex: 1 – burin on obliquely distally dorsally truncated blade; 2 – retouched piece on blade, lateral, dorsal; 3 – dihedral-symmetrical burin on blade, distal; 4 – retouched piece on flake, distal, ventral; 5 – burin on oblique-convexly distally dorsally truncated blade; 6 – truncated piece on blade, bi-terminal, oblique, dorsal; 7 – burin on obliquely proximally dorsally truncated blade. The bi-terminally truncated blade (6) is the former burin on proximal truncation.

The bidirectional blade/bladelet cores with sub-cylindrical shape and a narrow flaking surface (Table 8-38; Fig. 8-15, *1*; 8-16, *1, 2*), show a clear difference between the main and the supplementary striking platforms. Only one specimen is equipped with two main striking platforms opposite of each other (Fig. 8-15, *1*).

A single exhausted blade/bladelet core with multi-directional narrow flaking surface (43.31×29.86×39.43 mm) is also present.

Plate-like core blanks dominate in the blade/bladelet cores assemblage: one flake, one flint plaquette, and seven natural flakes (Fig. 8-14, *1*; 8-15, *1, 2*). In addition, a single rounded nodule and seven pieces of unidentifiable shapes were used. The average dimensions of sub-cylindrical/pyramidal blade/bladelet cores and those with narrow flaking surfaces are 44.97×40.63×37.28 mm and 60.37×29.91×63.38 mm, respectively. The fact that cores with narrow flaking surfaces are longer and thicker suggests that some blade/bladelet cores with narrow flaking surfaces were reduced to sub-cylindrical ones. The preparation of a back and distal crested ridge is common for all types of blade/bladelet cores. The main reason for discarding is longitudinal fragmentation.

**Bladelet cores** are represented by 10 unidirectional, 4 bidirectional, 1 perpendicular, and 1 multidirectional specimens (Table 8-38; Fig. 8-17; 8-18; 8-19; 8-20). The unidirectional cores are further subdivided into sub-cylindrical – 1 (Fig. 8-19, *1*), pyramidal – 1 (Fig. 8-19, *3*), narrow flaking surface – 8 (Fig. 8-17; 8-18, *1, 2*), and unidentifiable due to their fragmentation – 1. The measurements of sub-cylindrical (39.94×29.87×20.21 mm) and pyramidal (52.59×25.78×25.75 mm) cores might again indicate that these pieces are exhausted versions of those with a narrow flaking surface. One pyramidal core exhibits an unused supplementary striking platform opposite of the used one (Fig. 8-19, *3*). Among the bladelet cores with narrow flaking surfaces, two pieces show a wedge-like distal part (Fig. 8-18, *2*). One item demonstrates a special method of narrowing the flaking surface by lateral flattened removals, and one piece has both flattened lateral removals and a wedge-like distal part. The back and distal crested ridges are common for bladelet cores with a narrow flaking surface, as is the preparation of secondary crested ridges on the flaking surfaces.

All but one bidirectional bladelet cores have a narrow flaking surface (Table 8-38; Fig. 8-19, *2*; 8-20, *3*). The other was classified as intermediate between sub-cylindrical and sub-pyramidal (Fig. 8-19, *2*). Two of five bidirectional cores with narrow flaking surfaces exhibit clear supplementary striking platforms opposite of one another. One exhausted core has a multidirectional narrow flaking

| | 2c | | 2c, ash | | 2c, hearth | | 2d | | | | |
|---|---|---|---|---|---|---|---|---|---|---|---|
| | # | esse, % | # | esse, % | # | esse, % | # | esse, % | Σ | % | esse, % |
| **pre-cores** | 1 | 0,39 | – | – | 1 | 0,35 | 10 | 0,19 | **12** | 0,03 | 0,19 |
| **cores** | 5 | 1,95 | 1 | 0,33 | 2 | 0,70 | 51 | 0,96 | **59** | 0,13 | 0,96 |
| **tools** | 3 | 1,17 | 2 | 0,66 | 6 | 2,10 | 79 | 1,48 | **90** | 0,19 | 1,46 |
| **flakes** | 131 | 50,97 | 169 | 55,59 | 134 | 46,85 | 2830 | 53,15 | **3264** | 6,98 | 52,88 |
| **blades** | 54 | 21,01 | 42 | 13,82 | 67 | 23,43 | 890 | 16,71 | **1053** | 2,25 | 17,06 |
| **bladelets** | 36 | 14,01 | 52 | 17,11 | 54 | 18,88 | 916 | 17,20 | **1058** | 2,26 | 17,14 |
| **micro-blades** | 23 | 8,95 | 30 | 9,87 | 19 | 6,64 | 480 | 9,01 | **552** | 1,18 | 8,94 |
| **burin spalls** | 4 | 1,56 | 6 | 1,97 | 3 | 1,05 | 58 | 1,09 | **71** | 0,15 | 1,15 |
| **truncation spalls** | – | – | 2 | 0,66 | – | – | 12 | 0,23 | **14** | 0,03 | 0,23 |
| **chips** | 980 | – | 1262 | – | 1043 | – | 35832 | – | **39117** | 83,61 | – |
| **unidentifiable *débitage*** | 62 | – | 76 | – | 44 | – | 1298 | – | **1480** | 3,16 | – |
| **chunks** | 1 | – | 1 | – | 1 | – | 10 | – | **13** | 0,03 | – |
| **TOTAL:** | **1300** | 100,00 | **1643** | 100,00 | **1374** | 100,00 | **42466** | 100,02 | **46783** | 100,00 | 100,00 |

Table 8-37. Barmaky, eastern area complex, by horizons and structures: artefact totals

surface (38.92×23.71×36.64 mm), and another one shows narrow and sub-cylindrical flaking surfaces, perpendicular-adjacent at about 90° (36.56×18.87×35.76 mm)(Fig. 8-20, *1, 2*). The bidirectional bladelet cores with sub-cylindrical/pyramidal shape show mean measurements of 46.99×26.97×24.42 mm, while those with a narrow flaking surface measure on average 61.83×21.15×41.32 mm. Again, the sub-cylindrical/pyramidal shapes may be simply reduced versions of cores with a narrow flaking surface. Four bladelet cores were made on flakes (Fig. 8-20, *1*): one on a flint plaquette, five on natural flakes (Fig. 8-17; 8-18; *1, 2*; 8-20, *2*). For 7 pieces, the initial blanks are unidentifiable. The reasons for discard are the decrease in sizes and hinge fractures on the flaking surfaces.

Five more cores are fragments of unidentifiable typology. Three of them probably belong to the unidirectional cores.

One of the most pronounced features of the core assemblage from the eastern area is the clear increase of specimens with a narrow flaking surface from blade through blade/bladelet to bladelet cores (Table 8-38). Compared to the sizes of the pieces interpreted as raw material reserve (77.88×49.11×25.61 mm), the reduction of most uni- and bidirectional cores with a narrow flaking surface (65.29×27.29×52.35 mm) was not very intensive. As can be expected, multidirectional and perpendicular cores are most reduced (39.59×24.14×37.27 mm), while sub-cylindrical and pyramidal cores (57.67×38.27×33.29 mm) occupy an intermediate position.

## *Débitage*

The main characteristic of the ***débitage*** consists in the high amount of bladelets and micro-blades, which in sum prevail over blades (Table 8-37). Also characteristic is the high amount of technological pieces: *débordante* (Fig. 8-21, *1, 3-8*, *10-21*; 8-22, *10, 14*), crested pieces (Fig. 8-22, *1, 3-5, 7, 9, 13*; 8-23, *1, 5, 6,* 8-12; 8-24, *3*), crested pieces on *débordantes* (Fig. 8-21, *2, 9*; 8-22, *2, 6, 8, 11, 12*; 8-23, 2-4, *7*; 8-24, *10*), *Kantenabschläge* (Fig. 8-24, *4, 15*) primary flakes, and core-tablets among the *débitage* classes (Table 8-39). Here, different types of *débordante* blanks play the main role: 9.23 % of flakes, 16.25 % of blades, 16.67 % of bladelets, and 12.86 % of micro-blades. The percentages of crested lamellar pieces underline their significant role in the shaping of the cores' flaking surfaces (Table 8-39).

Complete flakes are more frequent than **complete** blades, bladelets, and micro-blades (Table 8-40), probably as a result of a combination of several factors, such as blank parameters, trampling, and hard-hammer percussion.

Most numerous are trapezoidal **off-axis** flakes. The lamellar assemblage is dominated by rectangular on-axis pieces (Table 8-41). In addition, crescent off-axis and triangular on-axis pieces are important among micro-blades. Such differences between flake and lamellar assemblages underline their different technological role: flakes are mainly the result of core shaping and repair, while lamellar banks are the desired products of core reduction.

Straight **lateral profiles** dominate in all blank assemblages (Table 8-42), particularly among bladelets and micro-blades. Within curved blanks, those curved in mid-part are the most numerous. In addition, twisted lateral profiles are abundant in blade, bladelet, and micro-blade assemblages.

Feathering ends are the most common type of **distal terminations** (Table 8-43), while blunt and overshot forms are not numerous. Hinges make up about 20 %, maybe because of predominantly unipolar flaking.

Triangular **cross-sections** are the most numerous among all classes of blanks (Table 8-44). Trapezoidal cross-sections are important among blade and bladelet assemblages. The high number of lateral-steep cross-sections reflects the amount of *débordante* pieces.

More than half of the **dorsal scars** of flakes and blades are unidirectional (Table 8-45), while bladelet and micro-blade assemblages show up to 80 % unidirectional dorsal scars. The shares of different types of bidirectional scars, including the combination of crested, crossed, and opposite patterns, are 4.82 % for flakes, 15.40 % for blades, 10.18 % for bladelets, and 5.91 % for micro-blades, highlighting the leading role of the unipolar core reduction strategy. The shares of crested blanks (flakes – 5.67 %, blades – 15.39 %, bladelets – 9.52 %, micro-blades – 7.55 %) as well as about 10 % cortical flakes indicate on-site core reduction (Table 8-45).

| | 2c | 2c, ash | 2c, hearth | 2d | Σ | % |
|---|---|---|---|---|---|---|
| **FLAKE / BLADE PRE-CORES** | | | | | | |
| unidirectional, unidentifiable | – | – | – | 1 | **1** | 1,41 |
| **BLADE PRE-CORES** | | | | | | |
| unidirectional, narrow flaking surface | – | – | – | 1 | **1** | 1,41 |
| unidirectional, unidentifiable | – | – | – | 1 | **1** | 1,41 |
| **BLADE / BLADELET PRE-CORES** | | | | | | |
| bidirectional, narrow flaking surface | – | – | – | 1 | **1** | 1,41 |
| unidentifiable, narrow flaking surface | – | – | – | 3 | **3** | 4,23 |
| **BLADELET PRE-CORES** | | | | | | |
| unidirectional, narrow flaking surface | 1 | – | – | 1 | **2** | 2,82 |
| unidirectional, narrow flaking surface, wedge-shaped | – | – | 1 | – | **1** | 1,41 |
| bidirectional, narrow flaking surface | – | – | – | 1 | **1** | 1,41 |
| **UNIDENTIFIABLE PRE-CORES** | | | | | | |
| unidentifiable, narrow flaking surface | – | – | – | 1 | **1** | 1,41 |
| **FLAKE CORES** | | | | | | |
| bidirectional-alternate, sub-cylindrical | – | – | – | 1 | **1** | 1,41 |
| multidirectional, sub-cylindrical | – | – | – | 1 | **1** | 1,41 |
| **BLADE CORES** | | | | | | |
| unidirectional, sub-cylindrical | – | – | – | 3 | **3** | 4,23 |
| unidirectional, narrow flaking surface | – | – | – | 2 | **2** | 2,82 |
| unidirectional, flattened | – | – | – | 1 | **1** | 1,41 |
| unidirectional, unidentifiable | – | – | – | 1 | **1** | 1,41 |
| bidirectional, sub-cylindrical | 2 | – | – | 2 | **4** | 5,63 |
| bidirectional, cylindrical | – | – | – | 1 | **1** | 1,41 |
| bidirectional-adjacent, sub-cylindrical | – | – | – | 1 | **1** | 1,41 |
| bidirectional, narrow flaking surface | 1 | – | – | 2 | **3** | 4,23 |
| bidirectional-adjacent, narrow flaking surfaces | – | – | – | 1 | **1** | 1,41 |
| bidirectional-adjacent, unidentifiable | 1 | – | – | – | **1** | 1,41 |
| **BLADE / BLADELET CORES** | | | | | | |
| unidirectional, sub-cylindrical | – | – | – | 1 | **1** | 1,41 |
| unidirectional, pyramidal | – | – | – | 1 | **1** | 1,41 |
| unidirectional, narrow flaking surface | – | – | 1 | 2 | **3** | 4,23 |
| unidirectional-alternate, narrow flaking surface | – | – | – | 1 | **1** | 1,41 |
| unidirectional-alternate, narrow flaking surface, syb-pyramidal | – | – | – | 1 | **1** | 1,41 |
| unidirectional, unidentifiable | – | – | – | 2 | **2** | 2,82 |
| bidirectional, sub-cylindrical | – | – | – | 2 | **2** | 2,82 |
| bidirectional-adjacent, sub-cylindrical | – | – | – | 2 | **2** | 2,82 |
| bidirectional, narrow flaking surface | – | – | – | 1 | **1** | 1,41 |
| bidirectional, laterally narrowed flaking surface | – | – | 1 | – | **1** | 1,41 |

Table 8-38. Barmaky, eastern area complex, by horizons and structures: pre-cores and cores

| | 2c | 2c, ash | 2c, hearth | 2d | Σ | % |
|---|---|---|---|---|---|---|
| **BLADELET CORES** | | | | | | |
| unidirectional, sub-cylidrical | – | – | – | 1 | **1** | 1,41 |
| unidirectional, pyramidal | – | – | – | 1 | **1** | 1,41 |
| unidirectional, narrow flaking surface | 1 | – | – | 3 | **4** | 5,63 |
| unidirectional, narrow flaking surface, wedge-shaped | – | – | – | 1 | **1** | 1,41 |
| unidirectional, laterally narrowed flaking surface | – | – | – | 1 | **1** | 1,41 |
| unidirectional, laterally narrowed flaking surface, wedge-shaped | – | – | – | 1 | **1** | 1,41 |
| unidirectional, unidentifiable | – | – | – | 1 | **1** | 1,41 |
| bidirectional, sub-cylindrical / sub-pyramidal | – | – | – | 1 | **1** | 1,41 |
| bidirectional, narrow flaking surface | – | – | – | 1 | **1** | 1,41 |
| bidirectional-alternate, narrow flaking surface | – | – | – | 1 | **1** | 1,41 |
| bidirectional-bilateral, narrow flaking surface | – | – | – | 1 | **1** | 1,41 |
| perpendicular-adjacent, narrow flaking surface / sub-cylindrical | – | – | – | 1 | **1** | 1,41 |
| multi-directional, narrow flaking surface | – | 1 | – | – | **1** | 1,41 |
| **UNIDENTIFIABLE CORES** | | | | | | |
| unidentifiable | – | – | – | 5 | **5** | 7,04 |
| **TOTAL:** | **6** | **1** | **3** | **61** | **71** | 100,00 |

Table 8-38. continued.

Most flakes and blades are still carrying **cortex** (Table 8-46), mostly with lateral location, and more than 8 % of flakes are completely cortex-covered. Bladelets and micro-blades, however, are less cortical (Table 8-46). Cortex in lateral position is found on about half of the blades and nearly one-third of the bladelets and micro-blades, partly underlining the importance of cores with narrow flaking surfaces on flat raw volumes and cortical débordantes including crested pieces among the lamellar assemblages (Fig. 8-21, *7, 10, 12, 13, 17, 18, 21*; 8-22, *8, 10, 12*; 8-23, *2, 3, 4*). In general, the amount of cortical pieces reflects an intensive on-site core reduction.

Plain **striking platform remnants** dominate the flake and blade assemblages (Table 8-47), while linear platforms are more frequent among bladelets and micro-blades. The latter reflects the width-to-thickness dimensions of bladelets and blades rather than a specific method of platform preparation. There is a comparatively high number of flakes with cortical platforms, correlating with the above-stated conclusion about intensive on-site core reduction. At least 20 % of blanks have crushed platforms, which might be evidence of the use of hard-hammers.

**Overhang trimming** appears to be the main method for a modification of the angle between the striking platform and flaking surface (Table 8-48), more frequently applied to lamellar assemblage. **Butt abrasion**, in contrast, is not important (Table 8-49). The dominance of **unlipped platforms** and **pronounced butts** in all classes of blanks reflects the application of hard hammer percussion (Tables 8-50; 8-51). In addition, **right-angle platforms** dominate among all blanks (Table 8-52).

## Tool trimming pieces

Truncation and **burin spalls** represent the tool trimming elements. Secondary (Fig. 8-24, *5*) burin spalls prevail over primary (Fig. 8-24, *1, 2, 6, 9*) ones (Table 8-39) and multiple (Fig. 8-24, *7, 8*) forms are not numerous. However, the sum of multiple and secondary burin spalls indicates a relatively intensive burin reduction. Burin spalls occur complete (25.35 %), and as distal (33.80 %), medial (19.72 %), and proximal (21.13 %) fragments. More than half are rectangular (55.10 %) in shape, but crescent (16.33 %) and triangular (12.24 %) forms are also important. About half of the burin spalls were removed off-axis (52.00 %). Lateral profiles are straight

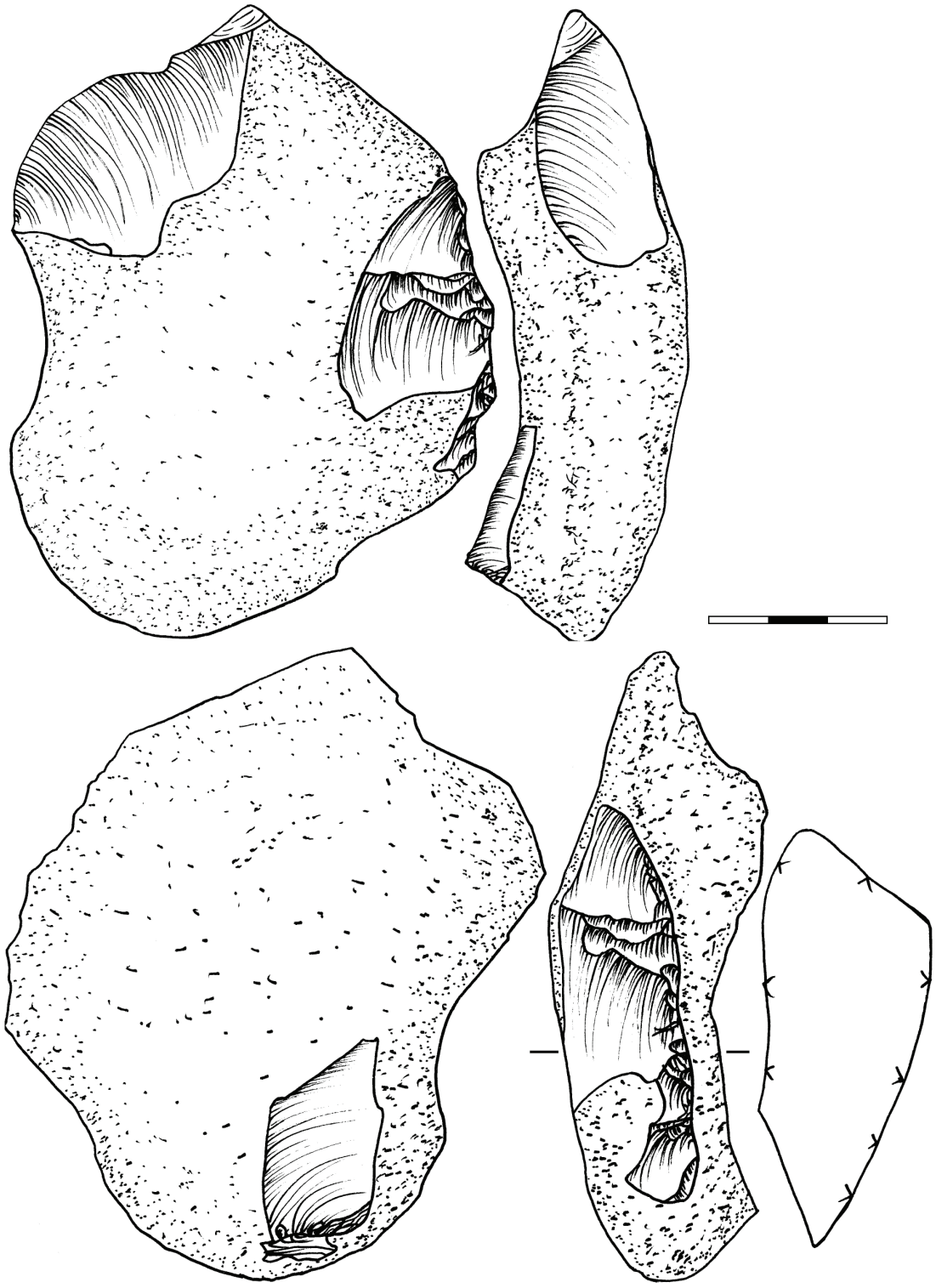

Fig. 8–10. Barmaky, eastern area complex, horizon 2d: pre-core for blades/bladelets, narrow flaking surface.

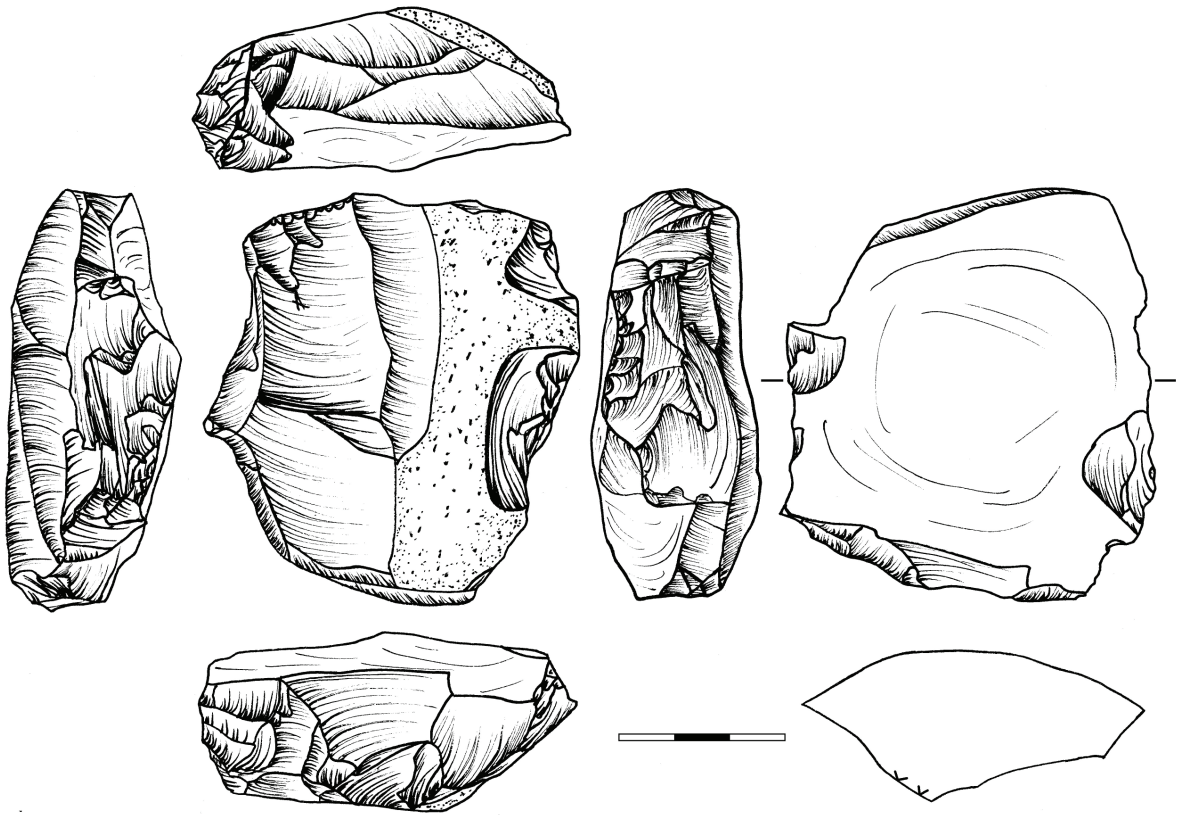

Fig. 8-11. Barmaky, eastern area complex, horizon 2d: pre-core for blades/bladelets, narrow flaking surface.

(38.24 %) and twisted (26.47 %), with usually hinged distal (56.10 %) terminations and lateral steep cross-sections (67.61 %). The platforms are often faceted (50 %), untrimmed (87.09 %), not abraded (100 %), and unlipped (70.37 %), with pronounced and diffuse bulbs (50 on 50 %). The platform angles are both right (72 %) and acute (18 %).

Initial (Fig. 8-24, *11, 12, 14*) truncation spalls prevail over rejuvenating and secondary (Fig. 8-24, *13, 16*) ones (Table 8-39).

## *Débitage* dimensions

In general, the main metric parameters of the *débitage* from horizon 2a and EA complexes do not differ (Table 8-35), except for the average width of the striking platform remnants of flakes. The reason for this difference is unclear.

## Tools

Four classes dominate the tool assemblage: burins, truncated pieces, microliths, and retouched pieces (Table 8-53). Flakes serve as blanks for 20, blades for 38, bladelets for 8, micro-blades for 10, and unidentifiable forms for 2 tools.

An **end-scraper** (Fig. 8-25, *4*) is of the simple-convex type on the distal part of a broken blade (>37.76×21.44×7.84 mm). Continuous sub-parallel obverse abrupt retouching formed its working edge.

Most of the **burins** originate from the permafrost depression – horizon 2d. One piece was found in horizon 2c and one burin originates from horizon 2c, the ashy zone. Twenty blades and three flakes served as blanks for burin production.

Thirteen of 23 burins are made **on truncated blades and truncated flakes** (Table 8-54; Fig. 8-25, *1-3, 5, 7-10*). Those on truncated blades

| | 2c | | 2c, ash | | 2c, hearth | | 2d | |
|---|---|---|---|---|---|---|---|---|
| | # | % | # | % | # | % | # | % |
| **FLAKES** | | | | | | | | |
| regular | **95** | 71,97 | **109** | 63,74 | **76** | 56,30 | **2106** | 73,89 |
| lateral *débordantes* | **10** | 7,58 | **15** | 8,77 | **13** | 9,63 | **129** | 4,53 |
| cortical *débordantes* | **3** | 2,27 | **6** | 3,51 | **12** | 8,89 | **71** | 2,49 |
| natural *débordantes* | **3** | 2,27 | **3** | 1,75 | **3** | 2,22 | **63** | 2,21 |
| crested | **6** | 4,55 | **7** | 4,09 | **14** | 10,37 | **145** | 5,09 |
| core tablet | **–** | – | **1** | 0,58 | **4** | 2,96 | **8** | 0,28 |
| *Kantenabschläge* | **5** | 3,79 | **8** | 4,68 | **1** | 0,74 | **79** | 2,77 |
| primary | **8** | 6,06 | **14** | 8,19 | **7** | 5,19 | **218** | 7,65 |
| natural | **2** | 1,52 | **8** | 4,68 | **5** | 3,70 | **31** | 1,09 |
| **TOTAL:** | **132** | 100,00 | **171** | 100,00 | **135** | 100,00 | **2850** | 100,00 |
| **BLADES** | | | | | | | | |
| regular | **29** | 51,79 | **22** | 52,38 | **39** | 54,17 | **602** | 64,80 |
| lateral *débordantes* | **3** | 5,36 | **2** | 4,76 | **3** | 4,17 | **59** | 6,35 |
| cortical *débordantes* | **9** | 16,07 | **6** | 14,29 | **6** | 8,33 | **47** | 5,06 |
| natural *débordantes* | **5** | 8,93 | **2** | | **7** | 9,72 | **45** | 4,84 |
| crested | **6** | 10,71 | **9** | 21,43 | **11** | 15,28 | **143** | 15,39 |
| core tablet | **–** | – | **1** | 2,38 | **–** | – | **4** | 0,43 |
| primary | **4** | 7,14 | **–** | – | **6** | 8,33 | **29** | 3,12 |
| **TOTAL:** | **56** | 100,00 | **42** | 100,00 | **72** | 100,00 | **929** | 100,00 |
| **BLADELETS** | | | | | | | | |
| regular | **26** | 72,22 | **39** | 75,00 | **33** | 61,11 | **670** | 72,51 |
| lateral *débordantes* | **1** | 2,78 | **–** | – | **2** | 3,70 | **59** | 6,39 |
| cortical *débordantes* | **–** | – | **2** | 3,85 | **3** | 5,56 | **40** | 4,33 |
| natural *débordantes* | **5** | 13,89 | **4** | 7,69 | **5** | 9,26 | **55** | 5,95 |
| crested | **4** | 11,11 | **5** | 9,62 | **10** | 18,52 | **87** | 9,42 |
| primary | **–** | – | **2** | 3,85 | **1** | 1,85 | **13** | 1,41 |
| **TOTAL:** | **36** | 100,00 | **52** | 100,00 | **54** | 100,00 | **924** | 100,00 |
| **MICRO-BLADES** | | | | | | | | |
| regular | **17** | 73,91 | **22** | 73,33 | **14** | 73,68 | **385** | 78,57 |
| lateral *débordantes* | **1** | 4,35 | **2** | 6,67 | **2** | 10,53 | **27** | 5,51 |
| cortical *débordantes* | **–** | – | **1** | 3,33 | **–** | – | **18** | 3,67 |
| natural *débordantes* | **2** | 8,70 | **3** | 10,00 | **1** | 5,26 | **18** | 3,67 |
| crested | **3** | 13,04 | **2** | 6,67 | **2** | 10,53 | **39** | 7,96 |
| primary | **–** | – | **–** | – | **–** | – | **3** | 0,61 |
| **TOTAL:** | **23** | 100,00 | **30** | 100,00 | **19** | 100,00 | **490** | 100,00 |
| **BURIN SPALLS** | | | | | | | | |
| primary | **1** | 25,00 | **3** | 50,00 | **1** | 33,33 | **13** | 22,41 |
| primary, retouched | **–** | – | **–** | – | **–** | – | **12** | 20,69 |
| secondary | **3** | 75,00 | **3** | 50,00 | **2** | 66,67 | **20** | 34,48 |
| secondary, retouched | **–** | – | **–** | – | **–** | – | **6** | 10,34 |
| multiple | **–** | – | **–** | – | **–** | – | **6** | 10,34 |
| multiple, bidirectional | **–** | – | **–** | – | **–** | – | **1** | 1,72 |
| **TOTAL:** | 4 | 100,00 | 6 | 100,00 | 3 | 100,00 | 58 | 100,00 |

Table 8–39. Barmaky, eastern area complex, by horizons and structures: *débitage* structure (including tools)

| | 2c | | 2c, ash | | 2c, hearth | | 2d | |
|---|---|---|---|---|---|---|---|---|
| | # | % | # | % | # | % | # | % |
| **TRUNCATION SPALLS** | | | | | | | | |
| initial | **–** | – | **1** | 50,00 | **–** | – | **7** | 58,33 |
| rejuvenating | **–** | – | **1** | 50,00 | **–** | – | **4** | 33,33 |
| secondary | **–** | – | **–** | – | **–** | – | **1** | 8,33 |
| **TOTAL:** | **–** | – | **2** | 100,00 | **–** | – | **12** | 100,00 |
| unidentifiable *débitage* | **62** | – | **76** | – | **44** | – | **1300** | – |

Table 8-39. continued.

include one primary blade and two crested pieces. Single-edge burins on oblique and oblique-convex truncations prevail (Fig. 8-25, *2, 3, 5, 7, 8*). Straight and concave truncations are rare (Fig. 8-25, *1, 9*), as are burins with two distal or opposite (Fig. 8-25, *10*) edges (Table 8-54). In seven cases, laterally scalar/irregular, partial/discontinuous, and semi-abrupt/flat retouched pieces were used: dorsal – 5 (Fig. 8-25, *2, 5, 8, 10*), ventral – 1 (Fig. 8-24, *3*), and alternate – 1. The average dimensions are 70.45×20.24×7.73 mm. The only complete burin on a truncated flake measures 79.14×41.75×14.78 mm (Fig. 8-25, *8*).

**Angle burins** are not numerous: four are made on blades (two on dorsally lateral and ventrally retouched pieces) including one *débordante* piece, and one on a lateral inversely retouched flake (Table 8-54; Fig. 8-25, *6*). Scalar, obverse/inverse and flat/semi-abrupt retouch combinations shaped the lateral edges of two angle burins on blades and one on flake. The average dimensions of angle burins on blades are >36.35×19.08×4.36 mm, while the one on flake measures 26.42×44.96×43.71 mm.

Three blades served as blanks for distally asymmetrical **dihedral** burins (Table 8-54, Fig. 8-26, *3*). Their lateral edges were shaped by partial, scalar, obverse, flat, and continuous, scalar stepped, alternating, and semi-abrupt retouch. All dihedral burins occur as distal fragments of blades with average dimensions of >41.27×25.75×7.98 mm.

Two **transversal burins** were produced on the distal and proximal ends of crested blades with average dimensions of 56.14×25.59×8.00 mm (Table 8-54). The proximal specimen was made on a partial lateral truncation (Fig. 8-26, *6*).

The 23 burins exhibit 26 burin edges formed by 46 burin spalls negatives. The ratio of burins spall negatives and burins is 2 to 1; the ratio of burin spalls and burins is 3.08 to 1.

All but one of the **truncated pieces** are made on blades, including one crested and one *débordante* piece (Table 8-55). Six blades show an oblique truncation: distal – 4 (Fig. 8-26, *4, 7*) and proximal – 2 (Fig. 8-26, *1, 9*). Straight truncations were observed three times on distal (Fig. 8-26, *2*) and two times on proximal parts of the blades. Two blades show oblique-convex truncations on their distal and proximal part (Fig. 8-26, *5*), respectively. Oblique-concave and bi-terminal oblique/concave truncated blades (Fig. 8-26, *10*) are not numerous (Table 8-55). One flake with lateral retouch and distal oblique truncation was identified (61.99×31.65×8.33 mm). One oblique distal truncation was made on a lateral alternatingly retouched blade, and a lateral obverse retouched blade and flake were also truncated. The combinations of continuous, scalar/sub-parallel, obverse, and abrupt retouches are mainly used for truncations. The average dimension of truncated pieces on blades is 58.76×20.65×4.76 mm.

There are three **denticulate pieces**: one on the distal part of a blade and two on flakes (Table 8-53; Fig. 8-26, *8*; 8-27, *13*). The denticulated edge on the blade was made by lateral continuous scalar obverse abrupt retouch. The distal part of the flake was modified by continuous scalar obverse flat retouches (Fig. 8-27, *13*). Another denticulate was done on the already dorsally retouched distal end of a flake by lateral continuous scalar stepped obverse abrupt retouch (Fig. 8-26, *8*). The denticulates made on flakes are relatively large: 60.23×44.07×18.25 and 61.48×54.92×12.81 mm.

| | | | flakes | | blades | | bladelets | | micro-blades | |
|---|---|---|---|---|---|---|---|---|---|---|
| | | | # | % | # | % | # | % | # | % |
| HORIZON 2c | complete | | **82** | 62,12 | **28** | 50,00 | **17** | 47,22 | **5** | 21,74 |
| | distal | | **20** | 15,15 | **15** | 26,79 | **7** | 19,44 | **10** | 43,48 |
| | lateral | | **9** | 6,82 | **1** | 1,79 | **1** | 2,78 | **–** | – |
| | medial | | **3** | 2,27 | **7** | 12,50 | **3** | 8,33 | **6** | 26,09 |
| | proximal | | **17** | 12,88 | **5** | 8,93 | **8** | 22,22 | **2** | 8,70 |
| | unidentifiable | | **1** | 0,76 | **–** | – | **–** | – | **–** | – |
| | | **TOTAL:** | **132** | 100,00 | **56** | 100,00 | **36** | 100,00 | **23** | 100,00 |
| HORIZON 2c, ash | complete | | **107** | 62,57 | **15** | 35,71 | **13** | 25,00 | **12** | 40,00 |
| | distal | | **24** | 14,04 | **11** | 26,19 | **17** | 32,69 | **9** | 30,00 |
| | lateral | | **8** | 4,68 | **–** | – | **2** | 3,85 | **–** | – |
| | medial | | **6** | 3,51 | **5** | 11,90 | **13** | 25,00 | **6** | 20,00 |
| | proximal | | **23** | 13,45 | **11** | 26,19 | **7** | 13,46 | **3** | 10,00 |
| | unidentifiable | | **3** | 1,75 | **–** | – | **–** | – | **–** | – |
| | | **TOTAL:** | **171** | 100,00 | **42** | 100,00 | **52** | 100,00 | **30** | 100,00 |
| HORIZON 2c, hearth | complete | | **80** | 59,26 | **23** | 31,94 | **17** | 31,48 | **8** | 42,11 |
| | distal | | **22** | 16,30 | **21** | 29,17 | **13** | 24,07 | **3** | 15,79 |
| | lateral | | **12** | 8,89 | **–** | – | **1** | 1,85 | **–** | – |
| | medial | | **1** | 0,74 | **5** | 6,94 | **8** | 14,81 | **3** | 15,79 |
| | proximal | | **19** | 14,07 | **23** | 31,94 | **15** | 27,78 | **5** | 26,32 |
| | unidentifiable | | **1** | 0,74 | **–** | – | **–** | – | **–** | – |
| | | **TOTAL:** | **135** | 100,00 | **72** | 100,00 | **54** | 100,00 | **19** | 100,00 |
| HORIZON 2d | complete | | **1747** | 61,30 | **393** | 42,30 | **331** | 35,82 | **159** | 32,45 |
| | distal | | **416** | 14,60 | **237** | 25,51 | **265** | 28,68 | **177** | 36,12 |
| | lateral | | **191** | 6,70 | **3** | 0,32 | **2** | 0,22 | **–** | – |
| | medial | | **83** | 2,91 | **91** | 9,80 | **160** | 17,32 | **88** | 17,96 |
| | proximal | | **405** | 14,21 | **205** | 22,07 | **166** | 17,97 | **66** | 13,47 |
| | unidentifiable | | **8** | 0,28 | **–** | – | **–** | – | **–** | – |
| | | **TOTAL:** | **2850** | 100,00 | **929** | 100,00 | **924** | 100,00 | **490** | 100,00 |

Table 8–40. Barmaky, eastern area complex, by horizons and structures: *débitage* conditions (including tools)

A single **borer-perforator** belongs to the distal type (Table 8–53). The tip of the bladelet (>29.24×9.21×5.84 mm) was shaped by partial sub-parallel inverse flat retouch.

There are four distal fragments of lateral **points**: one on a blade, two on a crested blade, and one on a *débordante* bladelet (Table 8–53; Fig. 8–27, *9*). All of them were made by partial scalar obverse semi-abrupt retouches. The average dimensions of the points on blades are >47.25×16.50×7.40. The point on the bladelet measures >50.64×9.03×6.25 mm.

The lateral and distal sides of a **raclette** on a flake (46.69×33.45×6.76 mm) were shaped by continuous sub-parallel obverse abrupt retouch (Fig. 8–27, *11*).

The **combined tool** of a bi-lateral burin on the distal concave dorsal truncation and a proximal simple-convex end-scraper modified by continuous, sub-parallel obverse abrupt retouch (Fig. 8–27, *12*) was made on a bi-lateral dorsally retouched crested blade (64.74×27.27×10.11 mm).

| | | | flakes | | blades | | bladelets | | micro-blades | |
|---|---|---|---|---|---|---|---|---|---|---|
| | | | # | % | # | % | # | % | # | % |
| HORIZON 2c | rectangular | on-axis | **1** | 1,01 | **7** | 14,00 | **4** | 15,38 | **3** | 16,67 |
| | | off-axis | **10** | 10,10 | **–** | – | **1** | 3,85 | **1** | 5,56 |
| | trapezoidal | on-axis | **11** | 11,11 | **6** | 12,00 | **2** | 7,69 | **2** | 11,11 |
| | | off-axis | **18** | 18,18 | **1** | 2,00 | **–** | – | **1** | 5,56 |
| | triangular | on-axis | **1** | 1,01 | **3** | 6,00 | **3** | 11,54 | **4** | 22,22 |
| | | off-axis | **3** | 3,03 | **2** | 4,00 | **1** | 3,85 | **–** | – |
| | leaf-shaped | on-axis | **–** | – | **3** | 6,00 | **1** | 3,85 | **–** | – |
| | | off-axis | **2** | 2,02 | **–** | – | **1** | 3,85 | **–** | – |
| | ovoid | on-axis | **11** | 11,11 | **2** | 4,00 | **–** | – | **–** | – |
| | | off-axis | **6** | 6,06 | **–** | – | **–** | – | **–** | – |
| | crescent | on-axis | **–** | – | **1** | 2,00 | **1** | 3,85 | **–** | – |
| | | off-axis | **3** | 3,03 | **1** | 2,00 | **2** | 7,69 | **–** | – |
| | expanding | on-axis | **3** | 3,03 | **6** | 12,00 | **–** | – | **–** | – |
| | | off-axis | **7** | 7,07 | **2** | 4,00 | **–** | – | **–** | – |
| | | unidentifiable | **–** | – | **1** | 2,00 | **–** | – | **–** | – |
| | irregular | off-axis | **22** | 22,22 | **15** | 30,00 | **10** | 38,46 | **7** | 38,89 |
| | | unidentifiable | **1** | 1,01 | **–** | – | **–** | – | **–** | – |
| | | **TOTAL:** | **99** | 100,00 | **50** | 100,00 | **26** | 100,00 | **18** | 100,00 |
| | unidentifiable | on-axis | – | – | 2 | – | – | – | – | – |
| | | off-axis | 2 | – | – | – | – | – | – | – |
| | | unidentifiable | 31 | – | 4 | – | 10 | – | 5 | – |
| HORIZON 2c, ash | rectangular | on-axis | **6** | 4,41 | **5** | 13,51 | **10** | 24,39 | **3** | 12,00 |
| | | off-axis | **4** | 2,94 | **1** | 2,70 | **1** | 2,44 | **2** | 8,00 |
| | | unidentifiable | **3** | 2,21 | **1** | 2,70 | **6** | 14,63 | **–** | – |
| | trapezoidal | on-axis | **22** | 16,18 | **6** | 16,22 | **5** | 12,20 | **1** | 4,00 |
| | | off-axis | **35** | 25,74 | **1** | 2,70 | **–** | – | **–** | – |
| | | unidentifiable | **4** | 2,94 | **–** | – | **–** | – | **–** | – |
| | triangular | on-axis | **5** | 3,68 | **2** | 5,41 | **5** | 12,20 | **7** | 28,00 |
| | | off-axis | **4** | 2,94 | **–** | – | **1** | 2,44 | **–** | – |
| | leaf-shaped | on-axis | **2** | 1,47 | **3** | 8,11 | **–** | – | **2** | 8,00 |
| | | off-axis | **1** | 0,74 | **1** | 2,70 | **1** | 2,44 | **–** | – |
| | | unidentifiable | **–** | – | **–** | – | **1** | 2,44 | **–** | – |
| | ovoid | on-axis | **4** | 2,94 | **–** | – | **–** | – | **–** | – |
| | | off-axis | **7** | 5,15 | **–** | – | **–** | – | **–** | – |
| | crescent | on-axis | **1** | 0,74 | **–** | – | **–** | – | **–** | – |
| | | off-axis | **7** | 5,15 | **1** | 2,70 | **2** | 4,88 | **3** | 12,00 |
| | expanding | on-axis | **4** | 2,94 | **1** | 2,70 | **1** | 2,44 | **–** | – |
| | | off-axis | **6** | 4,41 | **2** | 5,41 | **–** | – | **–** | – |
| | | unidentifiable | **–** | – | **2** | 5,41 | **–** | – | **–** | – |
| | irregular | off-axis | **18** | 13,24 | **11** | 29,73 | **8** | 19,51 | **7** | 28,00 |
| | | unidentifiable | **3** | 2,21 | **–** | – | **–** | – | **–** | – |
| | | **TOTAL:** | **136** | 100,00 | **37** | 100,00 | **41** | 100,00 | **25** | 100,00 |
| | unidentifiable | off-axis | 2 | – | 1 | – | – | – | 1 | – |
| | | unidentifiable | 33 | – | 4 | – | 11 | – | 4 | – |

Table 8-41. Barmaky, eastern area complex, by horizons and structures: *débitage* shapes & axis (including tools)

| | | | flakes | | blades | | bladelets | | micro-blades | |
|---|---|---|---|---|---|---|---|---|---|---|
| | | | # | % | # | % | # | % | # | % |
| HORIZON 2c, hearth | rectangular | on-axis | **4** | 3,74 | **7** | 12,28 | **5** | 16,13 | **3** | 27,27 |
| | | off-axis | **5** | 4,67 | **3** | 5,26 | **–** | – | **–** | – |
| | | unidentifiable | **–** | – | **3** | 5,26 | **–** | – | **–** | – |
| | trapezoidal | on-axis | **19** | 17,76 | **6** | 10,53 | **–** | – | **–** | – |
| | | off-axis | **26** | 24,30 | **2** | 3,51 | **1** | 3,23 | **–** | – |
| | | unidentifiable | **1** | 0,93 | **–** | – | **–** | – | **–** | – |
| | triangular | on-axis | **3** | 2,80 | **6** | 10,53 | **7** | 22,58 | **3** | 27,27 |
| | | off-axis | **2** | 1,87 | **–** | – | **–** | – | **2** | 18,18 |
| | leaf-shaped | on-axis | **1** | 0,93 | **3** | 5,26 | **4** | 12,90 | **–** | – |
| | | off-axis | **1** | 0,93 | **1** | 1,75 | **1** | 3,23 | **–** | – |
| | ovoid | on-axis | **3** | 2,80 | **–** | – | **–** | – | **–** | – |
| | | off-axis | **4** | 3,74 | **–** | – | **–** | – | **–** | – |
| | crescent | on-axis | **–** | – | **–** | – | **–** | – | **1** | 9,09 |
| | | off-axis | **2** | 1,87 | **3** | 5,26 | **1** | 3,23 | **1** | 9,09 |
| | | unidentifiable | **1** | 0,93 | **–** | – | **–** | – | **–** | – |
| | expanding | on-axis | **2** | 1,87 | **3** | 5,26 | **2** | 6,45 | **–** | – |
| | | off-axis | **4** | 3,74 | **6** | 10,53 | **1** | 3,23 | **–** | – |
| | irregular | off-axis | **29** | 27,10 | **13** | 22,81 | **9** | 29,03 | **1** | 9,09 |
| | | unidentifiable | **–** | – | **1** | 1,75 | **–** | – | **–** | – |
| | | **TOTAL:** | **107** | 100,00 | **57** | 100,00 | **31** | 100,00 | **11** | 100,00 |
| | unidentifiable | off-axis | 2 | – | – | – | 1 | – | – | – |
| | | unidentifiable | 26 | – | 15 | – | 22 | – | 8 | – |

Table 8-41. continued 1

Five bladelets and nine micro-blades, including two *débordante*, served as blanks for the production of three types of **microliths** (Table 8-56): dorsally straight-backed points (Fig. 8-27, *1-5, 8*), unfinished (Fig. 8-27, *7*), and unidentifiable microliths (Fig. 8-27, *6, 10*). All microliths are only preserved in fragments: 2 distal, 3 medial, and 9 proximal. Both distal fragments belong to the straight-backed points on micro-blades. The identification of the proximal fragments as points comes with an uncertainty, but seems warranted by the presence of obliquely retouched/truncated bases. As D. Nuzhnyi demonstrated for Barmaky and Mizyn, complete pieces with obliquely retouched/truncated bases belong to straight-backed points on bladelets/micro-blades (Nuzhnyi 2015: 166-167) and non-pointed, complete microliths with an obliquely retouched/truncated base are unknown. Pointed straight-backed microliths with unmodified bases, however, are known. So, an obliquely retouched/truncated base, present in six out of the nine proximal fragments, can be seen as indicative of a pointed tip (Fig. 8-27, *3-5, 8*). One straight-backed bladelet (Fig. 8-27, *6*) and one straight-backed micro-blade with an unworked base cannot be assigned to a type. The same applies to the medial parts of two bladelets and one micro-blade with straight backing (Fig. 8-27, *6, 10*). A broken bladelet with partial backing and an unworked base belongs to the unfinished microliths (Fig. 8-27, *7*). The main combination of retouch kinds is continuous, scalar, obverse, and abrupt and was used for the backing of 10 microliths. The combination of partial scalar obverse abrupt retouches was applied twice. Two more pieces were modified by continuous, scalar, obverse semi-abrupt, and continuous, scalar, bifacial abrupt retouches. The average dimensions of microliths on bladelets and micro-blades are >25.14×7.94×2.60 and >17.28×5.45×2.39 mm, respectively.

| | | | flakes | | blades | | bladelets | | micro-blades | |
|---|---|---|---|---|---|---|---|---|---|---|
| | | | # | % | # | % | # | % | # | % |
| HORIZON 2d | rectangular | on-axis | **215** | 10,28 | **150** | 21,25 | **186** | 28,01 | **89** | 24,12 |
| | | off-axis | **150** | 7,17 | **34** | 4,82 | **29** | 4,37 | **19** | 5,15 |
| | | unidentifiable | **1** | 0,05 | **4** | 0,57 | **3** | 0,45 | **–** | – |
| | trapezoidal | on-axis | **143** | 6,84 | **61** | 8,64 | **37** | 5,57 | **21** | 5,69 |
| | | off-axis | **550** | 26,29 | **55** | 7,79 | **40** | 6,02 | **31** | 8,40 |
| | | unidentifiable | **7** | 0,33 | **3** | 0,42 | **4** | 0,60 | **3** | 0,81 |
| | triangular | on-axis | **27** | 1,29 | **44** | 6,23 | **65** | 9,79 | **52** | 14,09 |
| | | off-axis | **54** | 2,58 | **19** | 2,69 | **22** | 3,31 | **13** | 3,52 |
| | | unidentifiable | **–** | – | **2** | 0,28 | **4** | 0,60 | **5** | 1,36 |
| | leaf-shaped | on-axis | **56** | 2,68 | **43** | 6,09 | **52** | 7,83 | **22** | 5,96 |
| | | off-axis | **70** | 3,35 | **20** | 2,83 | **16** | 2,41 | **4** | 1,08 |
| | | unidentifiable | **1** | 0,05 | **6** | 0,85 | **1** | 0,15 | **–** | – |
| | ovoid | on-axis | **86** | 4,11 | **12** | 1,70 | **3** | 0,45 | **1** | 0,27 |
| | | off-axis | **104** | 4,97 | **4** | 0,57 | **1** | 0,15 | **–** | – |
| | | unidentifiable | **12** | 0,57 | **–** | – | **–** | – | **1** | 0,27 |
| | crescent | on-axis | **10** | 0,48 | **4** | 0,57 | **10** | 1,51 | **4** | 1,08 |
| | | off-axis | **96** | 4,59 | **33** | 4,67 | **49** | 7,38 | **57** | 15,45 |
| | | unidentifiable | **1** | 0,05 | **1** | 0,14 | **–** | – | **–** | – |
| | expanding | on-axis | **81** | 3,87 | **28** | 3,97 | **12** | 1,81 | **4** | 1,08 |
| | | off-axis | **52** | 2,49 | **23** | 3,26 | **12** | 1,81 | **5** | 1,36 |
| | | unidentifiable | **2** | 0,10 | **6** | 0,85 | **4** | 0,60 | **–** | – |
| | irregular | off-axis | **371** | 17,73 | **152** | 21,53 | **113** | 17,02 | **38** | 10,30 |
| | | unidentifiable | **3** | 0,14 | **2** | 0,28 | **1** | 0,15 | **–** | – |
| | | **TOTAL:** | **2092** | 100,00 | **706** | 100,00 | **664** | 100,00 | **369** | 100,00 |
| | unidentifiable | off-axis | 64 | – | 15 | – | 21 | – | 4 | – |
| | | unidentifiable | 694 | – | 208 | – | 239 | – | 117 | – |

Table 8-41. continued 2.

**Retouched pieces** were made on 4 natural flakes, 4 *débordante* flakes, 1 primary flake, 8 flakes (Fig. 8-28, *3, 4*), 3 blades (Fig. 8-28, *2*), 2 crested blades, 1 bladelet (Fig. 8-28, *1*), and 1 micro-blade (Table 8-57). The location of the retouch is lateral dorsal (9 pieces) followed by distal dorsal (7 pieces). The partial scalar obverse flat (6 items) and semi-abrupt (7 items) retouch is most common. The average dimensions of retouched pieces on blades and flakes are 42.10×17.73×5.55 and 49.11×35.79×9.98 mm, respectively.

Two tiny lateral fragments of unknown *débitage* modified by continuous scalar obverse flat and abrupt retouching are classified as **unidentifiable tools** (Table 8-53).

## Flaking instruments

A hammer stone (64.17×36.05×26.60 mm) on a flint pebble with clear traces of use on its distal side originates from horizon 2c. Three more flint pebbles (53.91×55.61×39.52; 35.7×29.58×15.31; 17.94×11.12×9.11 mm) without traces of usage were found in horizon 2d. Twenty-nine small pieces of sandstone probably come from crushed hammer-stones. Three chips and eight flakes with recognisable dorsal and ventral surfaces were identified among the sandstone fragments.

| | | flakes | | blades | | bladelets | | micro-blades | |
|---|---|---|---|---|---|---|---|---|---|
| | | # | % | # | % | # | % | # | % |
| HORIZON 2c | straight | **47** | 39,50 | **27** | 50,94 | **18** | 52,94 | **15** | 68,18 |
| | convex | **12** | 10,08 | **1** | 1,89 | **–** | – | **1** | 4,55 |
| | incurvate proximal | **5** | 4,20 | **–** | – | **1** | 2,94 | **–** | – |
| | incurvate medial | **17** | 14,29 | **15** | 28,30 | **6** | 17,65 | **–** | – |
| | incurvate distal | **23** | 19,33 | **5** | 9,43 | **4** | 11,76 | **2** | 9,09 |
| | twisted | **15** | 12,61 | **5** | 9,43 | **5** | 14,71 | **4** | 18,18 |
| | **TOTAL:** | **119** | 100,00 | **53** | 100,00 | **34** | 100,00 | **22** | 100,00 |
| | unidentifiable | **13** | – | **3** | – | **2** | – | **1** | – |
| HORIZON 2c, ash | straight | **81** | 50,63 | **20** | 51,28 | **34** | 70,83 | **19** | 65,52 |
| | convex | **16** | 10,00 | **–** | – | **–** | – | **–** | – |
| | incurvate proximal | **4** | 2,50 | **–** | – | **–** | – | **1** | 3,45 |
| | incurvate medial | **25** | 15,63 | **9** | 23,08 | **6** | 12,50 | **7** | 24,14 |
| | incurvate distal | **21** | 13,13 | **4** | 10,26 | **1** | 2,08 | **1** | 3,45 |
| | twisted | **13** | 8,13 | **6** | 15,38 | **7** | 14,58 | **1** | 3,45 |
| | **TOTAL:** | **160** | 100,00 | **39** | 100,00 | **48** | 100,00 | **29** | 100,00 |
| | unidentifiable | **11** | – | **3** | – | **4** | – | **1** | – |
| HORIZON 2c, hearth | straight | **66** | 51,56 | **38** | 54,29 | **31** | 59,62 | **16** | 84,21 |
| | convex | **6** | 4,69 | **2** | 2,86 | **2** | 3,85 | **–** | – |
| | incurvate proximal | **2** | 1,56 | **2** | 2,86 | **–** | – | **–** | – |
| | incurvate medial | **32** | 25,00 | **17** | 24,29 | **12** | 23,08 | **1** | 5,26 |
| | incurvate distal | **15** | 11,72 | **3** | 4,29 | **1** | 1,92 | **1** | 5,26 |
| | twisted | **7** | 5,47 | **8** | 11,43 | **6** | 11,54 | **1** | 5,26 |
| | **TOTAL:** | **128** | 100,00 | **70** | 100,00 | **52** | 100,00 | **19** | 100,00 |
| | unidentifiable | **7** | – | **2** | – | **2** | – | **–** | – |
| HORIZON 2d | straight | **1228** | 46,08 | **407** | 47,44 | **490** | 58,33 | **260** | 56,03 |
| | convex | **258** | 9,68 | **8** | 0,93 | **8** | 0,95 | **2** | 0,43 |
| | incurvate proximal | **60** | 2,25 | **16** | 1,86 | **14** | 1,67 | **8** | 1,72 |
| | incurvate medial | **430** | 16,14 | **237** | 27,62 | **156** | 18,57 | **77** | 16,59 |
| | incurvate distal | **433** | 16,25 | **79** | 9,21 | **53** | 6,31 | **32** | 6,90 |
| | twisted | **256** | 9,61 | **111** | 12,94 | **119** | 14,17 | **85** | 18,32 |
| | **TOTAL:** | **2665** | 100,00 | **858** | 100,00 | **840** | 100,00 | **464** | 100,00 |
| | unidentifiable | **185** | – | **71** | – | **84** | – | **26** | – |

Table 8–42. Barmaky, eastern area complex, by horizons and structures: *débitage* lateral profiles (including tools)

| | | | flakes | | blades | | bladelets | | micro-blades | |
|---|---|---|---|---|---|---|---|---|---|---|
| | | | # | % | # | % | # | % | # | % |
| HORIZON 2c | feathering | | **63** | 58,33 | **21** | 48,84 | **15** | 60,00 | **10** | 66,67 |
| | blunt | | **19** | 17,59 | **6** | 13,95 | **4** | 16,00 | **1** | 6,67 |
| | hinged | | **25** | 23,15 | **14** | 32,56 | **6** | 24,00 | **3** | 20,00 |
| | overpassed | | **1** | 0,93 | **2** | 4,65 | **–** | – | **1** | 6,67 |
| | | **TOTAL:** | **108** | 100,00 | **43** | 100,00 | **25** | 100,00 | **15** | 100,00 |
| | missing | | 22 | – | 12 | – | 11 | – | 8 | – |
| | modified | | – | – | 1 | – | – | – | – | – |
| | unidentifiable | | 2 | – | – | – | – | – | – | – |
| HORIZON 2c, ash | feathering | | **77** | 56,62 | **8** | 32,00 | **19** | 61,29 | **17** | 80,95 |
| | blunt | | **21** | 15,44 | **8** | 32,00 | **–** | – | **–** | – |
| | hinged | | **38** | 27,94 | **8** | 32,00 | **11** | 35,48 | **4** | 19,05 |
| | overpassed | | **–** | – | **1** | 4,00 | **1** | 3,23 | **–** | – |
| | | **TOTAL:** | **136** | 100,00 | **25** | 100,00 | **31** | 100,00 | **21** | 100,00 |
| | missing | | 30 | – | 16 | – | 21 | – | 9 | – |
| | modified | | – | – | 1 | – | – | – | – | – |
| | unidentifiable | | 5 | – | – | – | – | – | – | – |
| HORIZON 2c, hearth | feathering | | **69** | 61,61 | **24** | 58,54 | **19** | 61,29 | **9** | 81,82 |
| | blunt | | **21** | 18,75 | **3** | 7,32 | **2** | 6,45 | **–** | – |
| | hinged | | **22** | 19,64 | **13** | 31,71 | **10** | 32,26 | **2** | 18,18 |
| | overpassed | | **–** | – | **1** | 2,44 | **–** | – | **–** | – |
| | | **TOTAL:** | **112** | 100,00 | **41** | 100,00 | **31** | 100,00 | **11** | 100,00 |
| | missing | | 22 | – | 28 | – | 23 | – | 8 | – |
| | modified | | – | – | 3 | – | – | – | – | – |
| | unidentifiable | | 1 | – | – | – | – | – | – | – |
| HORIZON 2d | feathering | | **1465** | 64,31 | **374** | 62,02 | **395** | 66,61 | **250** | 74,63 |
| | blunt | | **227** | 9,96 | **93** | 15,42 | **70** | 11,80 | **24** | 7,16 |
| | hinged | | **542** | 23,79 | **104** | 17,25 | **125** | 21,08 | **59** | 17,61 |
| | overpassed | | **44** | 1,93 | **32** | 5,31 | **3** | 0,51 | **2** | 0,60 |
| | | **TOTAL:** | **2278** | 100,00 | **603** | 100,00 | **593** | 100,00 | **335** | 100,00 |
| | missing | | 539 | – | 295 | – | 324 | – | 154 | – |
| | modified | | 10 | – | 28 | – | 2 | – | 1 | – |
| | unidentifiable | | 23 | – | 3 | – | 5 | – | – | – |

Table 8–43. Barmaky, eastern area complex, by horizons and structures: *débitage* distal profiles (including tools)

| | | | flakes | | blades | | bladelets | | micro-blades | |
|---|---|---|---|---|---|---|---|---|---|---|
| | | | # | % | # | % | # | % | # | % |
| HORIZON 2c | triangular | | **46** | 35,94 | **15** | 26,79 | **12** | 34,29 | **16** | 69,57 |
| | trapezoidal | | **40** | 31,25 | **13** | 23,21 | **11** | 31,43 | **2** | 8,70 |
| | multiple | | **6** | 4,69 | **4** | 7,14 | **3** | 8,57 | **–** | – |
| | lateral steep | | **21** | 16,41 | **22** | 39,29 | **9** | 25,71 | **5** | 21,74 |
| | convex | | **6** | 4,69 | **2** | 3,57 | **–** | – | **–** | – |
| | flat | | **9** | 7,03 | **–** | – | **–** | – | **–** | – |
| | | **TOTAL:** | **128** | 100,00 | **56** | 100,00 | **35** | 100,00 | **23** | 100,00 |
| | unidentifiable | | 4 | – | – | – | 1 | – | – | – |
| HORIZON 2c, ash | triangular | | **62** | 38,04 | **11** | 26,19 | **23** | 45,10 | **17** | 56,67 |
| | trapezoidal | | **45** | 27,61 | **12** | 28,57 | **17** | 33,33 | **6** | 20,00 |
| | multiple | | **7** | 4,29 | **4** | 9,52 | **–** | – | **–** | – |
| | lateral steep | | **32** | 19,63 | **15** | 35,71 | **9** | 17,65 | **7** | 23,33 |
| | convex | | **10** | 6,13 | **–** | – | **1** | 1,96 | **–** | – |
| | flat | | **7** | 4,29 | **–** | – | **1** | 1,96 | **–** | – |
| | | **TOTAL:** | **163** | 100,00 | **42** | 100,00 | **51** | 100,00 | **30** | 100,00 |
| | unidentifiable | | 8 | – | – | – | 1 | – | – | – |
| HORIZON 2c, hearth | triangular | | **38** | 29,69 | **15** | 20,83 | **16** | 29,63 | **10** | 52,63 |
| | trapezoidal | | **35** | 27,34 | **23** | 31,94 | **19** | 35,19 | **4** | 21,05 |
| | multiple | | **4** | 3,13 | **6** | 8,33 | **3** | 5,56 | **–** | – |
| | lateral steep | | **43** | 33,59 | **25** | 34,72 | **16** | 29,63 | **5** | 26,32 |
| | convex | | **4** | 3,13 | **3** | 4,17 | **–** | – | **–** | – |
| | flat | | **4** | 3,13 | **–** | – | **–** | – | **–** | – |
| | | **TOTAL:** | **128** | 100,00 | **72** | 100,00 | **54** | 100,00 | **19** | 100,00 |
| | unidentifiable | | 7 | – | – | – | – | – | – | – |
| HORIZON 2d | triangular | | **953** | 35,39 | **284** | 30,60 | **414** | 44,95 | **275** | 56,24 |
| | trapezoidal | | **775** | 28,78 | **318** | 34,27 | **252** | 27,36 | **119** | 24,34 |
| | multiple | | **265** | 9,84 | **87** | 9,38 | **41** | 4,45 | **8** | 1,64 |
| | lateral steep | | **384** | 14,26 | **214** | 23,06 | **207** | 22,48 | **87** | 17,79 |
| | convex | | **153** | 5,68 | **23** | 2,48 | **6** | 0,65 | **–** | – |
| | flat | | **144** | 5,35 | **1** | 0,11 | **1** | 0,11 | **–** | – |
| | irregular | | **19** | 0,71 | **1** | 0,11 | **–** | – | **–** | – |
| | | **TOTAL:** | **2693** | 100,00 | **928** | 100,00 | **921** | 100,00 | **489** | 100,00 |
| | unidentifiable | | 157 | – | 1 | – | 3 | – | 1 | – |

Table 8–44. Barmaky, eastern area complex, by horizons and structures: *débitage* cross-sections (including tools)

| | | flakes | | blades | | bladelets | | micro-blades | |
|---|---|---|---|---|---|---|---|---|---|
| | | # | % | # | % | # | % | # | % |
| HORIZON 2c | cortex | **8** | 6,20 | **2** | 3,57 | **–** | – | **–** | – |
| | lateral | **10** | 7,75 | **–** | – | **–** | – | **–** | – |
| | bi-lateral | **1** | 0,78 | **–** | – | **–** | – | **–** | – |
| | unidirectional | **75** | 58,14 | **36** | 64,29 | **30** | 83,33 | **19** | 82,61 |
| | bidirectional | **4** | 3,10 | **8** | 14,29 | **–** | – | **–** | – |
| | crested "one side" | **3** | 2,33 | **2** | 3,57 | **1** | 2,78 | **2** | 8,70 |
| | crested+unidirectional | **2** | 1,55 | **2** | 3,57 | **2** | 5,56 | **1** | 4,35 |
| | crested+bidirectional | **1** | 0,78 | | 0,00 | **1** | 2,78 | **–** | – |
| | crested secondary, unidirectional | **2** | 1,55 | **1** | 1,79 | **1** | 2,78 | **–** | – |
| | crested secondary, bidirectional | **–** | – | **1** | 1,79 | **–** | – | **–** | – |
| | orthogonal | **22** | 17,05 | **3** | 5,36 | **–** | – | **–** | – |
| | semi-crossed | **–** | – | **1** | 1,79 | **1** | 2,78 | **1** | 4,35 |
| | opposite directional | **1** | 0,78 | **–** | – | **–** | – | **–** | – |
| | **TOTAL:** | **129** | 100,00 | **56** | 100,00 | **36** | 100,00 | **23** | 100,00 |
| | unidentifiable | 3 | – | – | – | – | – | – | – |
| HORIZON 2c, ash | cortex | **20** | 11,76 | **–** | – | **2** | 3,85 | **–** | – |
| | lateral | **17** | 10,00 | **–** | – | **1** | 1,92 | **–** | – |
| | unidirectional | **100** | 58,82 | **27** | 64,29 | **41** | 78,85 | **28** | 93,33 |
| | bidirectional | **2** | 1,18 | **4** | 9,52 | **1** | 1,92 | | 0,00 |
| | crested "one side" | **3** | 1,76 | **5** | 11,90 | **3** | 5,77 | **1** | 3,33 |
| | crested "double sides" | **1** | 0,59 | **–** | – | **–** | – | **–** | – |
| | crested+unidirectional | **3** | 1,76 | **4** | 9,52 | **–** | – | **1** | 3,33 |
| | crested secondary, unidirectional | **1** | 0,59 | **1** | 2,38 | **2** | 3,85 | **–** | – |
| | crested secondary, bidirectional | **–** | – | **–** | – | **1** | 1,92 | **–** | – |
| | orthogonal | **17** | 10,00 | **–** | – | **–** | – | **–** | – |
| | semi-crossed | **4** | 2,35 | **–** | – | **1** | 1,92 | **–** | – |
| | opposite directional | **2** | 1,18 | **1** | 2,38 | **–** | – | **–** | – |
| | **TOTAL:** | **170** | 100,00 | **42** | 100,00 | **52** | 100,00 | **30** | 100,00 |
| | unidentifiable | 1 | – | – | – | – | – | – | – |

Table 8-45. Barmaky, eastern area complex, by horizons and structures: *débitage* dorsal scars (including tools)

| | | flakes | | blades | | bladelets | | micro-blades | |
|---|---|---|---|---|---|---|---|---|---|
| | | # | % | # | % | # | % | # | % |
| HORIZON 2c, hearth | cortex | **10** | 7,46 | **4** | 5,56 | **1** | 1,85 | **–** | – |
| | lateral | **5** | 3,73 | **1** | 1,39 | **1** | 1,85 | **2** | 10,53 |
| | bi-lateral | **1** | 0,75 | **–** | – | **–** | – | **–** | – |
| | unidirectional | **82** | 61,19 | **44** | 61,11 | **36** | 66,67 | **14** | 73,68 |
| | bidirectional | **7** | 5,22 | **8** | 11,11 | **6** | 11,11 | **1** | 5,26 |
| | crested "one side" | **8** | 5,97 | **5** | 6,94 | **2** | 3,70 | **–** | – |
| | crested "double sides" | **1** | 0,75 | **–** | – | **–** | – | **–** | – |
| | crested alternating | **–** | – | **–** | – | **–** | – | **1** | 5,26 |
| | crested+unidirectional | **3** | 2,24 | **3** | 4,17 | **4** | 7,41 | **1** | 5,26 |
| | crested+bidirectional | **–** | – | **2** | 2,78 | **–** | – | **–** | – |
| | crested secondary, unidirectional | **2** | 1,49 | **3** | 4,17 | **4** | 7,41 | **–** | – |
| | crested secondary, bidirectional | **1** | 0,75 | **–** | – | **–** | – | **–** | – |
| | orthogonal | **8** | 5,97 | **–** | – | **–** | – | **–** | – |
| | semi-crossed | **6** | 4,48 | **1** | 1,39 | **–** | – | **–** | – |
| | opposite directional | **–** | – | **1** | 1,39 | **–** | – | **–** | – |
| | **TOTAL:** | **134** | 100,00 | **72** | 100,00 | **54** | 100,00 | **19** | 100,00 |
| | unidentifiable | 1 | – | – | – | – | – | – | – |
| HORIZON 2d | cortex | **240** | 8,50 | **29** | 3,12 | **13** | 1,41 | **3** | 0,61 |
| | lateral | **208** | 7,37 | **11** | 1,18 | **7** | 0,76 | **2** | 0,41 |
| | bi-lateral | **30** | 1,06 | **–** | – | **–** | – | **1** | 0,20 |
| | unidirectional | **1503** | 53,22 | **541** | 58,23 | **677** | 73,27 | **402** | 82,04 |
| | bidirectional | **103** | 3,65 | **112** | 12,06 | **81** | 8,77 | **26** | 5,31 |
| | bidirectional-crossed | **1** | 0,04 | **6** | 0,65 | **4** | 0,43 | **–** | – |
| | crested "one side" | **39** | 1,38 | **21** | 2,26 | **21** | 2,27 | **17** | 3,47 |
| | crested "double sides" | **11** | 0,39 | **2** | 0,22 | **3** | 0,32 | **–** | – |
| | crested alternating | **4** | 0,14 | **8** | 0,86 | **3** | 0,32 | **–** | – |
| | crested+unidirectional | **58** | 2,05 | **61** | 6,57 | **32** | 3,46 | **7** | 1,43 |
| | crested+bidirectional | **6** | 0,21 | **12** | 1,29 | **7** | 0,76 | **1** | 0,20 |
| | crested secondary, unidirectional | **38** | 1,35 | **31** | 3,34 | **21** | 2,27 | **11** | 2,24 |
| | crested secondary, bidirectional | **4** | 0,14 | **8** | 0,86 | **1** | 0,11 | **1** | 0,20 |
| | orthogonal | **512** | 18,13 | **77** | 8,29 | **52** | 5,63 | **17** | 3,47 |
| | semi-crossed | **44** | 1,56 | **5** | 0,54 | **1** | 0,11 | **1** | 0,20 |
| | crossed | **1** | 0,04 | **–** | – | **–** | – | **–** | – |
| | opposite directional | **22** | 0,78 | **5** | 0,54 | **1** | 0,11 | **1** | 0,20 |
| | **TOTAL:** | **2824** | 100,00 | **929** | 100,00 | **924** | 100,00 | **490** | 100,00 |
| | unidentifiable | 26 | – | – | – | – | – | – | – |

Table 8-45. continued.

| | | | flakes | | blades | | bladelets | | micro-blades | |
|---|---|---|---|---|---|---|---|---|---|---|
| | | | # | % | # | % | # | % | # | % |
| HORIZON 2c | none | 0% | **52** | 39,39 | **12** | 21,43 | **19** | 52,78 | **14** | 60,87 |
| | primary | >75% | **8** | 6,06 | **2** | 3,57 | **–** | – | **–** | – |
| | proximal | 1–25% | **4** | 3,03 | **–** | – | **–** | – | **–** | – |
| | | 26–50% | **–** | – | **1** | 1,79 | **–** | – | **–** | – |
| | central | 1–25% | **1** | 0,76 | **1** | 1,79 | **3** | 8,33 | **–** | – |
| | lateral | 1–25% | **23** | 17,42 | **17** | 30,36 | **7** | 19,44 | **3** | 13,04 |
| | | 26–50% | **4** | 3,03 | **10** | 17,86 | **4** | 11,11 | **4** | 17,39 |
| | | 51–75% | **2** | 1,52 | **1** | 1,79 | **–** | – | **–** | – |
| | bi-lateral | 1–25% | **3** | 2,27 | **1** | 1,79 | **–** | – | **–** | – |
| | | 51–75% | **–** | – | **1** | 1,79 | **–** | – | **–** | – |
| | distal | 1–25% | **16** | 12,12 | **3** | 5,36 | **1** | 2,78 | **1** | 4,35 |
| | | 26–50% | **7** | 5,30 | **–** | – | **–** | – | **–** | – |
| | | 51–75% | **2** | 1,52 | **1** | 1,79 | **–** | – | **–** | – |
| | distal-lateral | 1–25% | **2** | 1,52 | **1** | 1,79 | **1** | 2,78 | **–** | – |
| | | 26–50% | **3** | 2,27 | **3** | 5,36 | **1** | 2,78 | **–** | – |
| | | 51–75% | **1** | 0,76 | **–** | – | **–** | – | **1** | 4,35 |
| | distal-proximal | 1–25% | 3 | 2,27 | – | – | – | – | – | – |
| | | 51–75% | **1** | 0,76 | **2** | 3,57 | **–** | – | **–** | – |
| | | **TOTAL:** | **132** | 100,00 | **56** | 100,00 | **36** | 100,00 | **23** | 100,00 |
| HORIZON 2c, ash | none | 0% | **53** | 30,99 | **10** | 23,81 | **26** | 50,00 | **19** | 63,33 |
| | primary | >75% | **20** | 11,70 | **–** | – | **2** | 3,85 | **–** | – |
| | proximal | 1–25% | **13** | 7,60 | **–** | – | **1** | 1,92 | **–** | – |
| | | 26–50% | **–** | – | **–** | – | **1** | 1,92 | **–** | – |
| | central | 26–50% | **2** | 1,17 | **–** | – | **–** | – | **–** | – |
| | | 51–75% | **1** | 0,58 | **1** | 2,38 | **–** | – | **–** | – |
| | lateral | 1–25% | **24** | 14,04 | **14** | 33,33 | **10** | 19,23 | **10** | 33,33 |
| | | 26–50% | **12** | 7,02 | **3** | 7,14 | **6** | 11,54 | **–** | – |
| | | 51–75% | **5** | 2,92 | **4** | 9,52 | **2** | 3,85 | **–** | – |
| | bi-lateral | 1–25% | **3** | 1,75 | **–** | – | **1** | 1,92 | **–** | – |
| | | 26–50% | **1** | 0,58 | **2** | 4,76 | **–** | – | **–** | – |
| | | 51–75% | **1** | 0,58 | **–** | – | **–** | – | **–** | – |
| | distal | 1–25% | **12** | 7,02 | **4** | 9,52 | **2** | 3,85 | **1** | 3,33 |
| | | 26–50% | **4** | 2,34 | **–** | – | **–** | – | **–** | – |
| | | 51–75% | **1** | 0,58 | **–** | – | **–** | – | **–** | – |
| | distal-lateral | 1–25% | **3** | 1,75 | **1** | 2,38 | **–** | – | **–** | – |
| | | 26–50% | **10** | 5,85 | **2** | 4,76 | **–** | – | **–** | – |
| | | 51–75% | **1** | 0,58 | **–** | – | **1** | 1,92 | **–** | – |
| | distal-proximal | 1–25% | **4** | 2,34 | **1** | 2,38 | **–** | – | **–** | – |
| | | 26–50% | **1** | 0,58 | **–** | – | **–** | – | **–** | – |
| | | **TOTAL:** | **171** | 100,00 | **42** | 100,00 | **52** | 100,00 | **30** | 100,00 |

Table 8–46. Barmaky, eastern area complex, by horizons and structures: *débitage* primary surfaces placement & percentages (including tools)

| | | | flakes | | blades | | bladelets | | micro-blades | |
|---|---|---|---|---|---|---|---|---|---|---|
| | | | # | % | # | % | # | % | # | % |
| HORIZON 2c, hearth | none | 0% | **50** | 37,04 | **18** | 25,00 | **28** | 51,85 | **10** | 52,63 |
| | primary | >75% | **11** | 8,15 | **6** | 8,33 | **1** | 1,85 | **–** | – |
| | proximal | 1–25% | **3** | 2,22 | **–** | – | **1** | 1,85 | **–** | – |
| | | 26–50% | **2** | 1,48 | **–** | – | **–** | – | **–** | – |
| | | 51–75% | **1** | 0,74 | **–** | – | **–** | – | **–** | – |
| | central | 1–25% | **–** | – | **1** | 1,39 | **–** | – | **–** | – |
| | | 51–75% | **1** | 0,74 | **–** | – | **–** | – | **–** | – |
| | lateral | 1–25% | **25** | 18,52 | **17** | 23,61 | **14** | 25,93 | **2** | 10,53 |
| | | 26–50% | **8** | 5,93 | **13** | 18,06 | **5** | 9,26 | **6** | 31,58 |
| | | 51–75% | **3** | 2,22 | **4** | 5,56 | **1** | 1,85 | **–** | – |
| | bi-lateral | 1–25% | **3** | 2,22 | **–** | – | **–** | – | **–** | – |
| | | 26–50% | **–** | – | **1** | 1,39 | **1** | 1,85 | **1** | 5,26 |
| | | 51–75% | **1** | 0,74 | **1** | 1,39 | **–** | – | **–** | – |
| | distal | 1–25% | **12** | 8,89 | **2** | 2,78 | **2** | 3,70 | **–** | – |
| | | 26–50% | **7** | 5,19 | **1** | 1,39 | **–** | – | **–** | – |
| | | 51–75% | **1** | 0,74 | **–** | – | **–** | – | **–** | – |
| | distal-lateral | 1–25% | **–** | – | **4** | 5,56 | **–** | – | **–** | – |
| | | 26–50% | **7** | 5,19 | **2** | 2,78 | **1** | 1,85 | **–** | – |
| | | 51–75% | **–** | – | **2** | 2,78 | **–** | – | **–** | – |
| | | **TOTAL:** | **135** | 100,00 | **72** | 100,00 | **54** | 100,00 | **19** | 100,00 |
| HORIZON 2d | none | 0% | **1225** | 42,98 | **325** | 34,98 | **512** | 55,41 | **323** | 65,92 |
| | primary | >75% | **239** | 8,39 | **25** | 2,69 | **11** | 1,19 | **2** | 0,41 |
| | proximal | 1–25% | **104** | 3,65 | **9** | 0,97 | **6** | 0,65 | **3** | 0,61 |
| | | 26–50% | **7** | 0,25 | **3** | 0,32 | **3** | 0,32 | **–** | – |
| | | 51–75% | **1** | 0,04 | **2** | 0,22 | **1** | 0,11 | **–** | – |
| | central | 1–25% | **5** | 0,18 | **4** | 0,43 | **–** | – | **1** | 0,20 |
| | | 26–50% | **10** | 0,35 | **4** | 0,43 | **1** | 0,11 | **–** | – |
| | | 51–75% | **11** | 0,39 | **2** | 0,22 | **1** | 0,11 | **2** | 0,41 |
| | lateral | 1–25% | **422** | 14,81 | **222** | 23,90 | **158** | 17,10 | **49** | 10,00 |
| | | 26–50% | **136** | 4,77 | **117** | 12,59 | **132** | 14,29 | **61** | 12,45 |
| | | 51–75% | **60** | 2,11 | **52** | 5,60 | **30** | 3,25 | **24** | 4,90 |
| | bi-lateral | 1–25% | **17** | 0,60 | **5** | 0,54 | **–** | – | **–** | – |
| | | 26–50% | **17** | 0,60 | **9** | 0,97 | **1** | 0,11 | **–** | – |
| | | 51–75% | **15** | 0,53 | **8** | 0,86 | **1** | 0,11 | **–** | – |
| | distal | 1–25% | **197** | 6,91 | **45** | 4,84 | **26** | 2,81 | **7** | 1,43 |
| | | 26–50% | **72** | 2,53 | **6** | 0,65 | **6** | 0,65 | **1** | 0,20 |
| | | 51–75% | **20** | 0,70 | **1** | 0,11 | **1** | 0,11 | **1** | 0,20 |
| | distal-lateral | 1–25% | **82** | 2,88 | **27** | 2,91 | **17** | 1,84 | **9** | 1,84 |
| | | 26–50% | **77** | 2,70 | **32** | 3,44 | **9** | 0,97 | **6** | 1,22 |
| | | 51–75% | **80** | 2,81 | **29** | 3,12 | **8** | 0,87 | **1** | 0,20 |
| | distal-proximal | 1–25% | **34** | 1,19 | **2** | 0,22 | **–** | – | **–** | – |
| | | 26–50% | **18** | 0,63 | **–** | – | **–** | – | **–** | – |
| | | 51–75% | **1** | 0,04 | **–** | – | **–** | – | **–** | – |
| | | **TOTAL:** | **2850** | 100,00 | **929** | 100,00 | **924** | 100,00 | **490** | 100,00 |

Table 8–46. continued.

| | | flakes | | blades | | bladelets | | micro-blades | |
|---|---|---|---|---|---|---|---|---|---|
| | | # | % | # | % | # | % | # | % |
| HORIZON 2c | cortex | **13** | 17,11 | ***1*** | 4,00 | **1** | 6,67 | **–** | – |
| | plain | **37** | 48,68 | ***15*** | 60,00 | **5** | 33,33 | **–** | – |
| | linear | **11** | 14,47 | ***5*** | 20,00 | **7** | 46,67 | **3** | 100,00 |
| | pointed | **1** | 1,32 | ***2*** | 8,00 | **–** | – | **–** | – |
| | dihedral | **5** | 6,58 | ***1*** | 4,00 | **1** | 6,67 | **–** | – |
| | polyhedral | **3** | 3,95 | ***1*** | 4,00 | **1** | 6,67 | **–** | – |
| | faceted | **6** | 7,89 | **–** | – | **–** | – | **–** | – |
| | **TOTAL:** | **76** | 100,00 | ***25*** | 100,00 | **15** | 100,00 | **3** | 100,00 |
| | crushed | 25 | – | 7 | – | 10 | – | 4 | – |
| | modified | | – | 1 | – | – | – | – | – |
| | unidentifiable | 4 | – | – | – | – | – | – | – |
| | missing | 27 | – | 23 | – | 11 | – | 16 | – |
| HORIZON 2c, ash | cortex | **21** | 21,43 | **–** | – | **–** | – | **–** | – |
| | plain | **48** | 48,98 | ***12*** | 50,00 | **5** | 41,67 | **2** | 20,00 |
| | linear | **14** | 14,29 | ***8*** | 33,33 | **4** | 33,33 | **6** | 60,00 |
| | pointed | **2** | 2,04 | ***1*** | 4,17 | **2** | 16,67 | **2** | 20,00 |
| | dihedral | **9** | 9,18 | ***1*** | 4,17 | **–** | – | **–** | – |
| | polyhedral | **–** | – | ***2*** | 8,33 | **1** | 8,33 | **–** | – |
| | faceted | **4** | 4,08 | **–** | – | **–** | – | **–** | – |
| | **TOTAL:** | **98** | 100,00 | ***24*** | 100,00 | **12** | 100,00 | **10** | 100,00 |
| | crushed | 32 | – | 2 | – | 9 | – | 5 | – |
| | unidentifiable | 7 | – | – | – | – | – | – | – |
| | missing | 34 | – | 16 | – | 31 | – | 15 | – |
| HORIZON 2c, hearth | cortex | **6** | 7,89 | **–** | – | **–** | – | **–** | – |
| | plain | **37** | 48,68 | ***16*** | 55,17 | **3** | 15,79 | **–** | – |
| | linear | **16** | 21,05 | ***4*** | 13,79 | **11** | 57,89 | **4** | 57,14 |
| | pointed | **1** | 1,32 | ***1*** | 3,45 | **2** | 10,53 | **–** | – |
| | dihedral | **9** | 11,84 | ***6*** | 20,69 | **1** | 5,26 | **3** | 42,86 |
| | polyhedral | **1** | 1,32 | ***2*** | 6,90 | **1** | 5,26 | **–** | – |
| | faceted | **6** | 7,89 | **–** | – | **1** | 5,26 | **–** | – |
| | **TOTAL:** | **76** | 100,00 | ***29*** | 100,00 | **19** | 100,00 | **7** | 100,00 |
| | crushed | 28 | – | 15 | – | 13 | – | 6 | – |
| | modified | – | – | 1 | – | – | – | – | – |
| | unidentifiable | 4 | – | | – | – | – | – | – |
| | missing | 27 | – | 27 | – | 22 | – | 6 | – |

Table 8–47. Barmaky, eastern area complex, by horizons and structures: *débitage* striking platform types (including tools)

| | | flakes | | blades | | bladelets | | micro-blades | |
|---|---|---|---|---|---|---|---|---|---|
| | | # | % | # | % | # | % | # | % |
| HORIZON 2d | cortex | **177** | 10,03 | ***8*** | 1,88 | **11** | 3,48 | **2** | 1,64 |
| | plain | **853** | 48,36 | ***185*** | 43,43 | **107** | 33,86 | **30** | 24,59 |
| | linear | **269** | 15,25 | ***119*** | 27,93 | **138** | 43,67 | **71** | 58,20 |
| | pointed | **17** | 0,96 | ***8*** | 1,88 | **23** | 7,28 | **15** | 12,30 |
| | dihedral | **208** | 11,79 | ***59*** | 13,85 | **28** | 8,86 | **3** | 2,46 |
| | polyhedral | **111** | 6,29 | ***25*** | 5,87 | **3** | 0,95 | **–** | – |
| | faceted | **128** | 7,26 | ***22*** | 5,16 | **6** | 1,90 | **1** | 0,82 |
| | en eperon | **1** | 0,06 | **–** | – | **–** | – | **–** | – |
| | **TOTAL:** | **1764** | 100,00 | ***426*** | 100,00 | **316** | 100,00 | **122** | 100,00 |
| | crushed | 463 | – | 162 | – | 182 | – | 100 | – |
| | modified | 1 | – | 11 | – | 2 | – | 3 | – |
| | unidentifiable | 35 | – | – | – | – | – | 1 | – |
| | missing | 587 | – | 330 | – | 424 | – | 264 | – |

Table 8–47. continued.

| | | flakes | | blades | | bladelets | | micro-blades | |
|---|---|---|---|---|---|---|---|---|---|
| | | # | % | # | % | # | % | # | % |
| HORIZON 2c | trimmed | **14** | 15,73 | ***8*** | 29,63 | **3** | 17,65 | **–** | – |
| | untrimmed | **75** | 84,27 | ***19*** | 70,37 | **14** | 82,35 | **4** | 100,00 |
| | **TOTAL:** | **89** | 100,00 | ***27*** | 100,00 | **17** | 100,00 | **4** | 100,00 |
| | missing | 27 | – | 23 | – | 11 | – | 16 | – |
| | unidentifiable | 16 | – | 6 | – | 8 | – | 3 | – |
| HORIZON 2c, ash | trimmed | **9** | 8,91 | ***11*** | 42,31 | **3** | 21,43 | **2** | 18,18 |
| | untrimmed | **92** | 91,09 | ***15*** | 57,69 | **11** | 78,57 | **9** | 81,82 |
| | **TOTAL:** | **101** | 100,00 | ***26*** | 100,00 | **14** | 100,00 | **11** | 100,00 |
| | missing | 34 | – | 16 | – | 31 | – | 15 | – |
| | unidentifiable | 36 | – | – | – | 7 | – | 4 | – |
| HORIZON 2c, hearth | trimmed | **7** | 8,24 | **9** | 26,47 | **7** | 30,43 | **–** | – |
| | untrimmed | **78** | 91,76 | **25** | 73,53 | **16** | 69,57 | **7** | 100,00 |
| | **TOTAL:** | **85** | 100,00 | **34** | 100,00 | **23** | 100,00 | **7** | 100,00 |
| | missing | 27 | – | 27 | – | 22 | – | 6 | – |
| | unidentifiable | 23 | – | 11 | – | 9 | – | 6 | – |
| HORIZON 2d | trimmed | **238** | 11,52 | **233** | 44,13 | **215** | 47,46 | **95** | 50,80 |
| | untrimmed | **1828** | 88,48 | **295** | 55,87 | **238** | 52,54 | **92** | 49,20 |
| | **TOTAL:** | **2066** | 100,00 | **528** | 100,00 | **453** | 100,00 | **187** | 100,00 |
| | missing | 499 | – | 337 | – | 427 | – | 267 | – |
| | unidentifiable | 285 | – | 64 | – | 44 | – | 36 | – |

Table 8–48. Barmaky, eastern area complex, by horizons and structures: *débitage* overhang trimming (including tools)

| | | flakes | | blades | | bladelets | | micro-blades | |
|---|---|---|---|---|---|---|---|---|---|
| | | # | % | # | % | # | % | # | % |
| HORIZON 2c | abrased | **3** | 3,49 | **–** | – | **1** | 6,25 | **1** | 33,33 |
| | unabrased | **83** | 96,51 | ***26*** | 100,00 | **15** | 93,75 | **2** | 66,67 |
| | **TOTAL:** | **86** | 100,00 | ***26*** | 100,00 | **16** | 100,00 | **3** | 100,00 |
| | missing | 27 | – | 23 | – | 11 | – | 16 | – |
| | unidentifiable | 19 | – | 7 | – | 9 | – | 4 | – |
| HORIZON 2c, ash | abrased | **3** | 3,00 | ***5*** | 20,00 | **2** | 15,38 | **–** | – |
| | unabrased | **97** | 97,00 | ***20*** | 80,00 | **11** | 84,62 | **11** | 100,00 |
| | **TOTAL:** | **100** | 100,00 | ***25*** | 100,00 | **13** | 100,00 | **11** | 100,00 |
| | missing | 34 | – | 16 | – | 31 | – | 15 | – |
| | unidentifiable | 37 | – | 1 | – | 8 | – | 4 | – |
| HORIZON 2c, hearth | abrased | **2** | 2,50 | **2** | 6,25 | **1** | 5,00 | **–** | – |
| | unabrased | **78** | 97,50 | **30** | 93,75 | **19** | 95,00 | **7** | 100,00 |
| | **TOTAL:** | **80** | 100,00 | **32** | 100,00 | **20** | 100,00 | **7** | 100,00 |
| | missing | 27 | – | 27 | – | 22 | – | 6 | – |
| | unidentifiable | 28 | – | 13 | – | 12 | – | 6 | – |
| HORIZON 2d | abrased | **32** | 1,57 | **24** | 4,64 | **22** | 4,94 | **9** | 4,89 |
| | unabrased | **2009** | 98,43 | **493** | 95,36 | **423** | 95,06 | **175** | 95,11 |
| | **TOTAL:** | **2041** | 100,00 | **517** | 100,00 | **445** | 100,00 | **184** | 100,00 |
| | missing | 499 | – | 337 | – | 427 | – | 267 | – |
| | unidentifiable | 310 | – | 75 | – | 52 | – | 39 | – |

Table 8-49. Barmaky, eastern area complex, by horizons and structures: *débitage* butt abrasion (including tools)

## ARCHAEOLOGICAL LEVEL 2, WESTERN AREA COMPLEX, HORIZONS 2B, 2C, AND 2D

The 93,548 flint artefacts from the western area were found on 35 square meters. In addition, 1 flint hammer-stone, 1 unmodified flint pebble, and 651 sandstone pieces originate from the same area. The squares 11E, 10E, and 9E have the highest density of artefacts: up to 14,000 pieces. Stratigraphically, horizons 2b, 2c, and 2d of the western area might be a palimpsest of temporarily close economic episodes.

Chips represent over 80 % of artefacts (Table 8-58). The sum of bladelets and micro-blades exceeds the number of blades. The tool-to-core ratio is 7.5 to 1, indicating intensive tool production and rejuvenation, corroborated by the abundant burin and truncation spalls. The unmodified pieces of raw material and the relatively high number of core-like pieces also suggest on-site core reduction (Table 8-58).

### Unmodified raw material

Three flint plaquettes, 9 natural flakes, 12 nodules, and 17 pieces of unknown shape compose the chunk collection (Table 8-58). Seventeen chunks exhibit reasonable sizes for raw material reserve: >50 mm. The reserve is composed of one plaquette, 5 natural flakes, 10 rounded nodules, and 1 unidentifiable piece. One rounded nodule is a relatively brittle piece of raw material, diminishing its potential as a reserve. The nodules and flat pieces measure on average 69.66×57.21×30.89 and 67.47×49.10×21.95 mm, respectively.

| | | flakes | | blades | | bladelets | | micro-blades | |
|---|---|---|---|---|---|---|---|---|---|
| | | # | % | # | % | # | % | # | % |
| HORIZON 2c | lipped | **1** | 1,28 | ***2*** | 6,90 | **–** | – | **–** | – |
| | semi-lipped | **6** | 7,69 | ***6*** | 20,69 | **2** | 12,50 | **–** | – |
| | unlipped | **71** | 91,03 | ***21*** | 72,41 | **14** | 87,50 | **3** | 100,00 |
| | **TOTAL:** | **78** | 100,00 | ***29*** | 100,00 | **100,00** | 100,00 | **3** | 100,00 |
| | missing | 27 | – | 23 | – | 11 | – | 16 | – |
| | unidentifiable | 27 | – | 4 | – | 9 | – | 4 | – |
| HORIZON 2c, ash | lipped | **11** | 11,00 | **–** | – | **–** | – | **–** | – |
| | semi-lipped | **12** | 12,00 | ***2*** | 8,00 | **2** | 16,67 | **1** | 8,33 |
| | unlipped | **77** | 77,00 | ***23*** | 92,00 | **10** | 83,33 | **11** | 91,67 |
| | **TOTAL:** | **100** | 100,00 | ***25*** | 100,00 | **12** | 100,00 | **12** | 100,00 |
| | missing | 34 | – | 16 | – | 31 | – | 15 | – |
| | unidentifiable | 37 | – | 1 | – | 9 | – | 3 | – |
| HORIZON 2c, hearth | lipped | **2** | 2,47 | **–** | – | **–** | – | **–** | – |
| | semi-lipped | **9** | 11,11 | **7** | 21,21 | **3** | 13,04 | **1** | 12,50 |
| | unlipped | **70** | 86,42 | **26** | 78,79 | **20** | 86,96 | **7** | 87,50 |
| | **TOTAL:** | **81** | 100,00 | **33** | 100,00 | **23** | 100,00 | **8** | 100,00 |
| | missing | 27 | – | 27 | – | 22 | – | 6 | – |
| | unidentifiable | 27 | – | 12 | – | 9 | – | 5 | – |
| HORIZON 2d | lipped | **42** | 2,23 | **4** | 0,81 | **6** | 1,46 | **1** | 0,61 |
| | semi-lipped | **177** | 9,41 | **48** | 9,70 | **22** | 5,37 | **6** | 3,68 |
| | unlipped | **1661** | 88,35 | **443** | 89,49 | **382** | 93,17 | **156** | 95,71 |
| | **TOTAL:** | **1880** | 100,00 | **495** | 100,00 | **410** | 100,00 | **163** | 100,00 |
| | missing | 499 | – | 331 | – | 425 | – | 265 | – |
| | unidentifiable | 471 | – | 103 | – | 89 | – | 62 | – |

Table 8-50. Barmaky, eastern area complex, by horizons and structures: *débitage* butts lipping (including tools)

## Core-like pieces

**Pre-cores** (n = 25) represent about one-third of the core-like pieces (Table 8-59; Fig. 8-29, 8-30, 8-31). Only specimens for blades and bladelets were identified and all but five exhibit unidirectional negatives on the flaking surface (Fig. 8-29; 8-31, *2*). One piece is unidentifiable because of fragmentation and 4 pre-cores are bidirectional (Fig. 8-30; 8-31, *1*).

There are 18 specimens with narrow flaking surfaces and 2 sub-cylindrical pieces. Twelve show prepared crested ridges on the flaking surface and/or distal/back sides. The only bi-directional pre-core for blades/bladelets with narrow flaking surface exhibits two main striking platforms (Fig. 8-30), while the other three show distinct main and supplementary striking platforms.

The importance of pre-cores with a narrow flaking surface correlates with the chosen raw material (15 natural flakes; 3 plaquettes; 4 rounded nodules; and 3 unidentifiable shapes) and is also reflected in the dimension of flat raw material volumes (69.86×26.79×61.01 mm). The latter shows the following ranges: length 46.14-108.04 mm; width 14.40-48.94 mm; thickness 23.98-106.90 mm.

The **core** assemblage consists of the pieces for flakes – 4.76 %, blades – 44.44 %, blades/bladelets – 28.57 %, bladelets – 17.46 %, micro-blades – 1.59 %, and unidentifiable – 3.17 % items (Table 8-59).

The **cores for blades** show a rather equal ratio of unidirectional (13) and bidirectional (15) pieces (Fig. 8-32, 8-33, 8-34; 8-35, *3*). The most common (n = 10) are unidi-

| | | flakes | | blades | | bladelets | | micro-blades | |
|---|---|---|---|---|---|---|---|---|---|
| | | # | % | # | % | # | % | # | % |
| HORIZON 2c | absent | **1** | 1,30 | ***3*** | 10,00 | **–** | – | **–** | – |
| | defused | **11** | 14,29 | ***12*** | 40,00 | **9** | 45,00 | **–** | – |
| | pronounced | **65** | 84,42 | ***15*** | 50,00 | **11** | 55,00 | **3** | 100,00 |
| | **TOTAL:** | **77** | 100,00 | ***30*** | 100,00 | **20** | 100,00 | **3** | 100,00 |
| | missing | 27 | – | 23 | – | 11 | – | 16 | – |
| | unidentifiable | 28 | – | 3 | – | 5 | – | 4 | – |
| HORIZON 2c, ash | absent | **5** | 4,95 | **–** | – | **–** | – | **–** | – |
| | defused | **20** | 19,80 | ***11*** | 42,31 | **6** | 46,15 | **7** | 50,00 |
| | pronounced | **76** | 75,25 | ***15*** | 57,69 | **7** | 53,85 | **7** | 50,00 |
| | **TOTAL:** | **101** | 100,00 | ***26*** | 100,00 | **13** | 100,00 | **14** | 100,00 |
| | missing | 34 | – | 16 | – | 31 | – | 15 | – |
| | unidentifiable | 36 | – | – | – | 8 | – | 1 | – |
| HORIZON 2c, hearth | absent | **–** | – | **–** | – | **1** | 3,70 | **–** | – |
| | defused | **32** | 37,65 | **14** | 38,89 | **7** | 25,93 | **2** | 25,00 |
| | pronounced | **53** | 62,35 | **22** | 61,11 | **19** | 70,37 | **6** | 75,00 |
| | **TOTAL:** | **85** | 100,00 | **36** | 100,00 | **27** | 100,00 | **8** | 100,00 |
| | missing | 27 | – | 27 | – | 22 | – | 6 | – |
| | unidentifiable | 23 | – | 9 | – | 5 | – | 5 | – |
| HORIZON 2d | absent | **37** | 1,97 | **7** | 1,40 | **11** | 2,66 | **2** | 1,20 |
| | defused | **345** | 18,38 | **83** | 16,57 | **60** | 14,53 | **34** | 20,36 |
| | pronounced | **1495** | 79,65 | **411** | 82,04 | **342** | 82,81 | **131** | 78,44 |
| | **TOTAL:** | **1877** | 100,00 | **501** | 100,00 | **413** | 100,00 | **167** | 100,00 |
| | missing | 499 | – | 331 | – | 425 | – | 265 | – |
| | unidentifiable | 474 | – | 97 | – | 86 | – | 58 | – |

Table 8-51. Barmaky, eastern area complex, by horizons and structures: *débitage* bulbs (including tools)

rectional cores with a narrow flaking surface (Table 8-59) with a ratio of seven unidirectional and three bidirectional specimens (Fig. 8-33). The opposite striking platforms on bidirectional cores play a supplementary role, show very sharp angles to the flaking surfaces (Fig. 8-32, *1, 4*), and are sometimes made on a distal crested ridge, which gives a wedge-like shape to the flaking surface (Fig. 8-33). Back and distal crested ridges are characteristic of both unidirectional and bidirectional cores for blades.

Sub-cylindrical bidirectional blade cores prevail over unidirectional ones (Table 8-59). Most bidirectional flaking surfaces are adjacent and alternate (Fig. 8-34, *1, 2*). Two main opposed striking platforms are only occasionally observed (Fig. 8-34, *2*) as are cores with alternating negatives in opposite directions on one flaking surface. The main purpose of opposite striking platforms is thus to repair the flaking surfaces. Back and distal crested ridges are common (Fig. 8-35, *3*). The main reasons for core discard are hinge fractures on the flaking surface, smashing of the striking platforms, and fragmentation. Complete but exhausted cores show a significantly reduced thickness of down to 20 mm. Close to the dimensions of exhausted cores are those of bidirectional-adjacent sub-cylindrical / sub-pyramidal ones: 59.35×34.58×23.08 mm.

The blade cores were made on a flake (1), natural flakes (6) flint plaquettes (2), rounded nodules (2) and unidentifiable raw volumes (17).

| | | flakes | | blades | | bladelets | | micro-blades | |
|---|---|---|---|---|---|---|---|---|---|
| | | # | % | # | % | # | % | # | % |
| HORIZON 2c | right | **41** | 52,56 | ***14*** | 56,00 | **11** | 73,33 | **2** | 66,67 |
| | acute | **36** | 46,15 | ***11*** | 44,00 | **4** | 26,67 | **1** | 33,33 |
| | obtuse | **1** | 1,28 | **–** | – | **–** | – | **–** | – |
| | **TOTAL:** | **78** | 100,00 | ***25*** | 100,00 | **15** | 100,00 | **3** | 100,00 |
| | missing | 27 | – | 23 | – | 11 | – | 16 | – |
| | unidentifiable | 27 | – | 8 | – | 10 | – | 4 | – |
| HORIZON 2c, ash | right | **80** | 81,63 | ***14*** | 56,00 | **10** | 83,33 | **7** | 70,00 |
| | acute | **18** | 18,37 | ***11*** | 44,00 | **2** | 16,67 | **3** | 30,00 |
| | obtuse | **–** | – | **–** | – | **–** | – | **–** | – |
| | **TOTAL:** | **98** | 100,00 | ***25*** | 100,00 | **12** | 100,00 | **10** | 100,00 |
| | missing | 34 | – | 16 | – | 31 | – | 15 | – |
| | unidentifiable | 39 | – | 1 | – | 9 | – | 5 | – |
| HORIZON 2c, hearth | right | **70** | 90,91 | **19** | 63,33 | **20** | 100,00 | **6** | 85,71 |
| | acute | **6** | 7,79 | **10** | 33,33 | **–** | – | **1** | 14,29 |
| | obtuse | **1** | 1,30 | **1** | 3,33 | **–** | – | **–** | – |
| | **TOTAL:** | **77** | 100,00 | **30** | 100,00 | **20** | 100,00 | **7** | 100,00 |
| | missing | 27 | – | 27 | – | 22 | – | 6 | – |
| | unidentifiable | 31 | – | 15 | – | 12 | – | 6 | – |
| HORIZON 2d | right | **1354** | 75,26 | **351** | 80,32 | **276** | 85,45 | **111** | 89,52 |
| | acute | **426** | 23,68 | **82** | 18,76 | **46** | 14,24 | **13** | 10,48 |
| | obtuse | **19** | 1,06 | **4** | 0,92 | **1** | 0,31 | **–** | – |
| | **TOTAL:** | **1799** | 100,00 | **437** | 100,00 | **323** | 100,00 | **124** | 100,00 |
| | missing | 499 | – | 331 | – | 425 | – | 265 | – |
| | unidentifiable | 552 | – | 161 | – | 176 | – | 101 | – |

Table 8-52. Barmaky, eastern area complex, by horizons and structures: *débitage* striking platform angels (including tools)

Predictably, the mean dimensions of cores with narrow flaking surfaces and sub-cylindrical cores are quite different: 65.12×34.53×50.75 and 60.71×36.99×29.26 mm, respectively.

**Cores for blades/bladelets** can be subdivided into unidirectional (10 items), bidirectional (7 items), and unsystematic (1 item) specimens (Table 8-59; Fig. 8-35, *1, 2*). Cores with a narrow flaking surface (8 items) and sub-cylindrical cores (8 items) occur in both unidirectional and bidirectional types. For one bidirectional core with the narrow flaking surface, the narrowing of the flaking surface is achieved by lateral removals detached from the same striking platform that is used for *debitage*. Nearly all of the blade/bladelet cores show a prepared crested ridge on the distal ends and/or backsides. In a few cases, the crested ridge on the back was used for an additional alternate flaking surface. The unsystematically reduced core has reached a maximal stage of exhaustion: the flaking surfaces serve as striking platforms, resulting in a multiplatform multidirectional cubic core. The usual reasons for discard are transversal and longitudinal breakage, hinge fractures on flaking surfaces, and smashed striking platforms.

Two flakes, 6 natural flakes, one rounded nodule, and one flint plaquette serve as the blanks for blade/bladelet core production; the rest of the cores were produced on unidentifiable blanks. The cores with a narrow flaking surface and sub-cylindrical blade/bladelet cores demonstrate the following average dimensions: 48.92×21.09×36.55 mm and 54.24×32.59×27.03 mm, respectively.

| | 2c | 2c, ash | 2c, hearth | 2d | Σ | % | esse, % |
|---|---|---|---|---|---|---|---|
| **end-scrapers** | – | – | – | 1 | **1** | 1,11 | 1,56 |
| **burins** | 1 | 1 | – | 21 | **23** | 25,56 | 35,94 |
| **truncated pieces** | 1 | – | 3 | 12 | **16** | 17,78 | 25,00 |
| **denticulates** | – | – | 1 | 2 | **3** | 3,33 | 4,69 |
| **borers** | – | – | – | 1 | **1** | 1,11 | 1,56 |
| **points** | – | – | – | 4 | **4** | 4,44 | 6,25 |
| **raclette** | – | – | – | 1 | **1** | 1,11 | 1,56 |
| **composite tools** | – | – | – | 1 | **1** | 1,11 | 1,56 |
| **microliths** | – | – | – | 14 | **14** | 15,56 | 21,88 |
| **retouched pieces** | 1 | 1 | 2 | 20 | **24** | 26,67 | – |
| **unidentifiable** | – | – | – | 2 | **2** | 2,22 | – |
| **TOTAL:** | **3** | **2** | **6** | **79** | **90** | 100,00 | 100,00 |

Table 8-53. Barmaky, eastern area, by horizons and structures: tools

| | 2c | 2c, ash | 2d | Σ |
|---|---|---|---|---|
| **BURINS ON TRUNCATED BLADES** | | | | |
| on straight distal dorsal truncation | – | – | 1 | **1** |
| on oblique distal dorsal truncation | 1 | – | 4 | **5** |
| on oblique proximal dorsal truncation | – | – | 1 | **1** |
| on oblique-convex distal dorsal truncation | – | – | 2 | **2** |
| opposite, on oblique biterminal dorsal truncations | – | – | 2 | **2** |
| **BURINS ON TRUNCATED FLAKES** | | | | |
| on oblique-convex distal dorsal truncation | – | – | 1 | **1** |
| bi-lateral, on concave distal dorsal truncation | – | – | 1 | **1** |
| **BURINS ON BLADES, ANGLE** | | | | |
| distal | – | – | 4 | **4** |
| **BURINS ON FLAKES, ANGLE** | | | | |
| proximal | – | 1 | – | **1** |
| **BURINS ON BLADES, DIHEDRAL** | | | | |
| asymmetrical, distal | – | – | 3 | **3** |
| **BURINS ON BLADES, TRANSVERSAL** | | | | |
| distal | – | – | 1 | **1** |
| proximal | – | – | 1 | **1** |
| **TOTAL:** | **1** | **1** | **21** | **23** |

Table 8-54. Barmaky, eastern area, by horizons and structures: burins

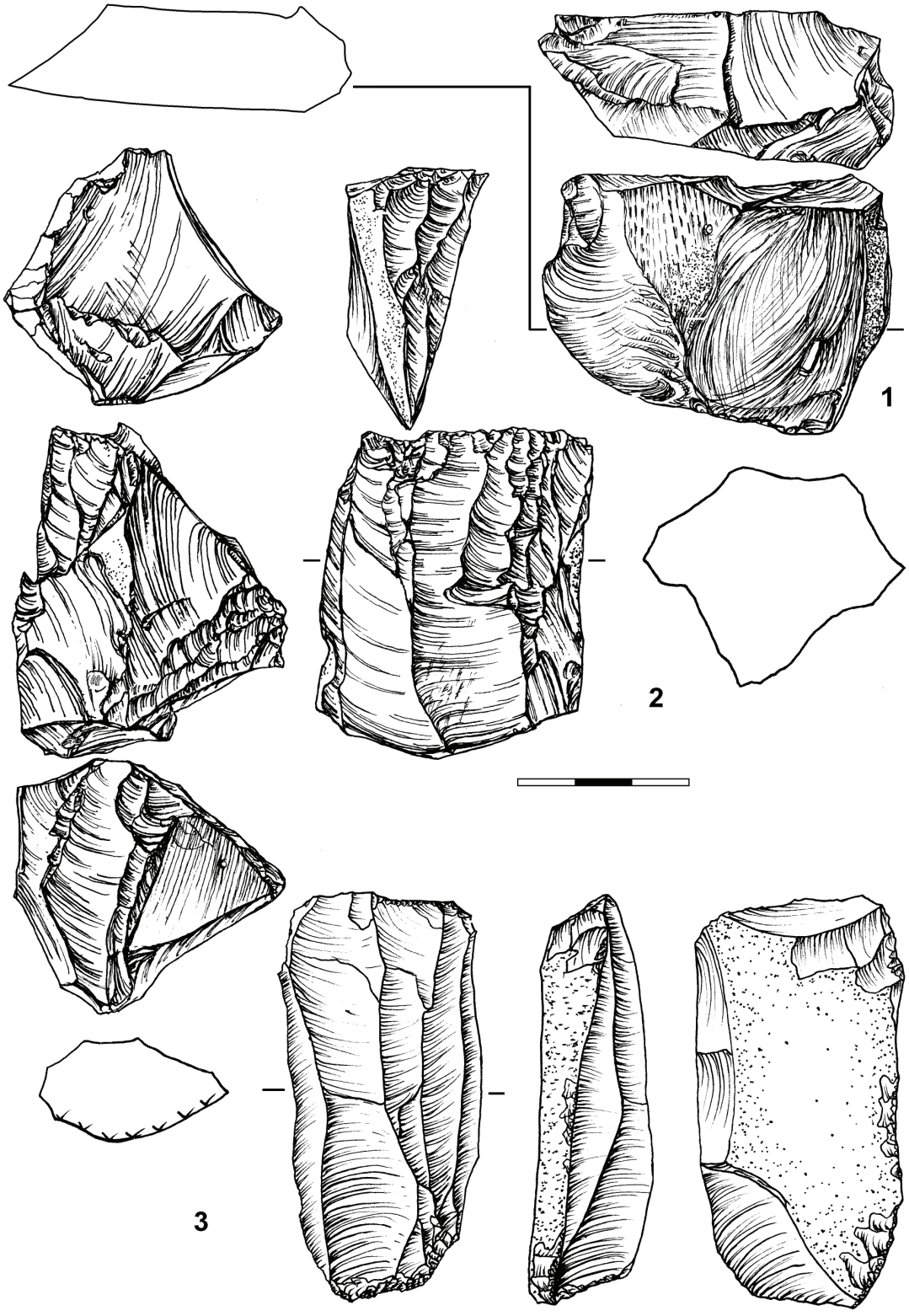


Fig. 8–12. Barmaky, eastern area complex, hearth (1), horizon 2d (2, 3): 1 – pre-core for bladelets, unidirectional, narrow flaking surface, wedge-shaped; 2 – core for blades, unidirectional, narrow flaking surface; 3 – core for blades, bidirectional, sub-cylindrical.

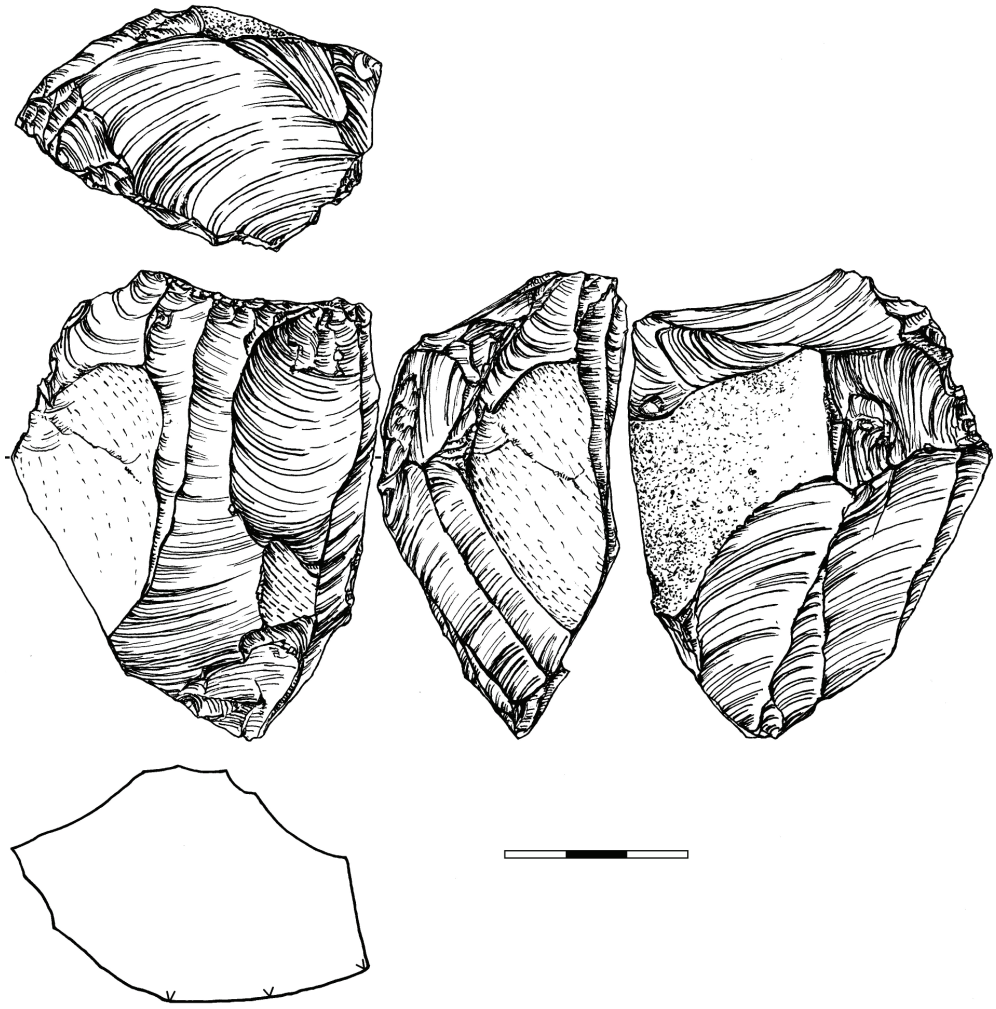

Fig. 8-13. Barmaky, eastern area complex, horizon 2d: core for blades, unidirectional, sub-cylindrical.

Narrow flaking surface types dominate the bladelet core assemblage (Table 8-59). The only bidirectional core with sub-cylindrical shape has a clear supplementary striking platform (Fig. 8-36, *2*), while the only bidirectional core with a narrow flaking surface exhibits two opposed main striking platforms. Crested ridges on the distal back sides are common. The distal trimming of one of the unidirectional cores with a narrow flaking surface led to a wedge-like working surface (Fig. 8-36, *1*).

Five flakes, two natural flakes, one rounded nodule, and three unidentifiable pieces of raw material serve as the blanks for bladelet cores. The single sub-cylindrical core measures 59.15×31.79×25.09 mm, while the average dimensions of bladelet cores with a narrow flaking surface are 51.09×20.04×33.84 mm.

A single **micro-blade core** was made on a natural *débordante* flake, belongs to the carinated type, and measures 24.53×14.21×44.29 mm (Table 8-59). The lateral natural surface of the flake serves as the striking platform for lamellar removals.

Two more cores are **unidentifiable** and represented by fragments of their striking platforms (Table 8-59).

## *Débitage*

The *débitage* assemblage is characterised by the dominant role of flakes (Tables 8-58; 8-60). The sum of bladelets and micro-blades exceeds the number of blades (Table 8-60). The technological *débitage* comprises about a

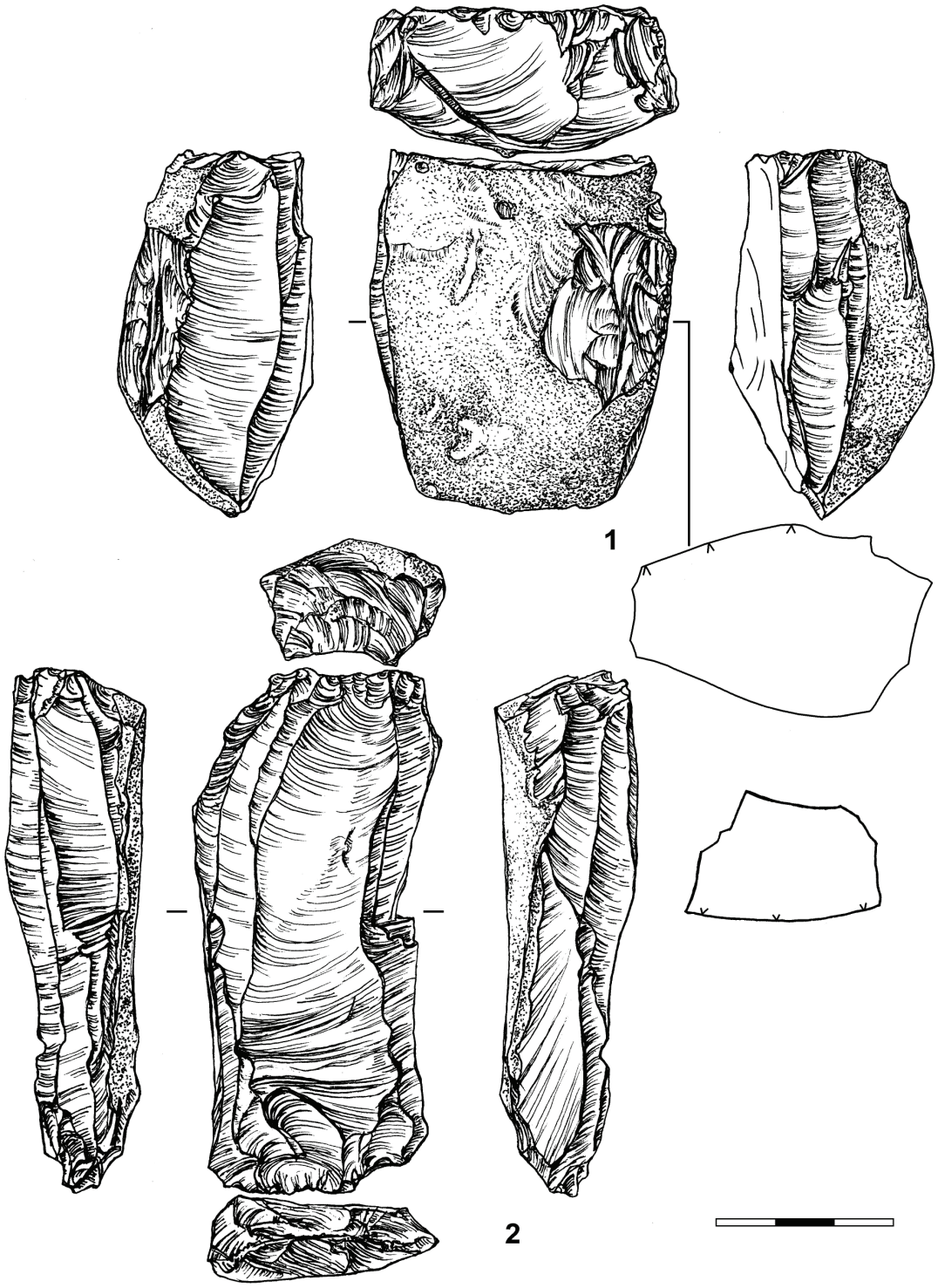


Fig. 8–14. Barmaky, eastern area complex, horizons 2d (1) & 2c (2): 1 – core for blades/bladelets, unidirectional–alternative, narrow flaking surface; 2 – core for blades, bidirectional, sub–cylindrical.

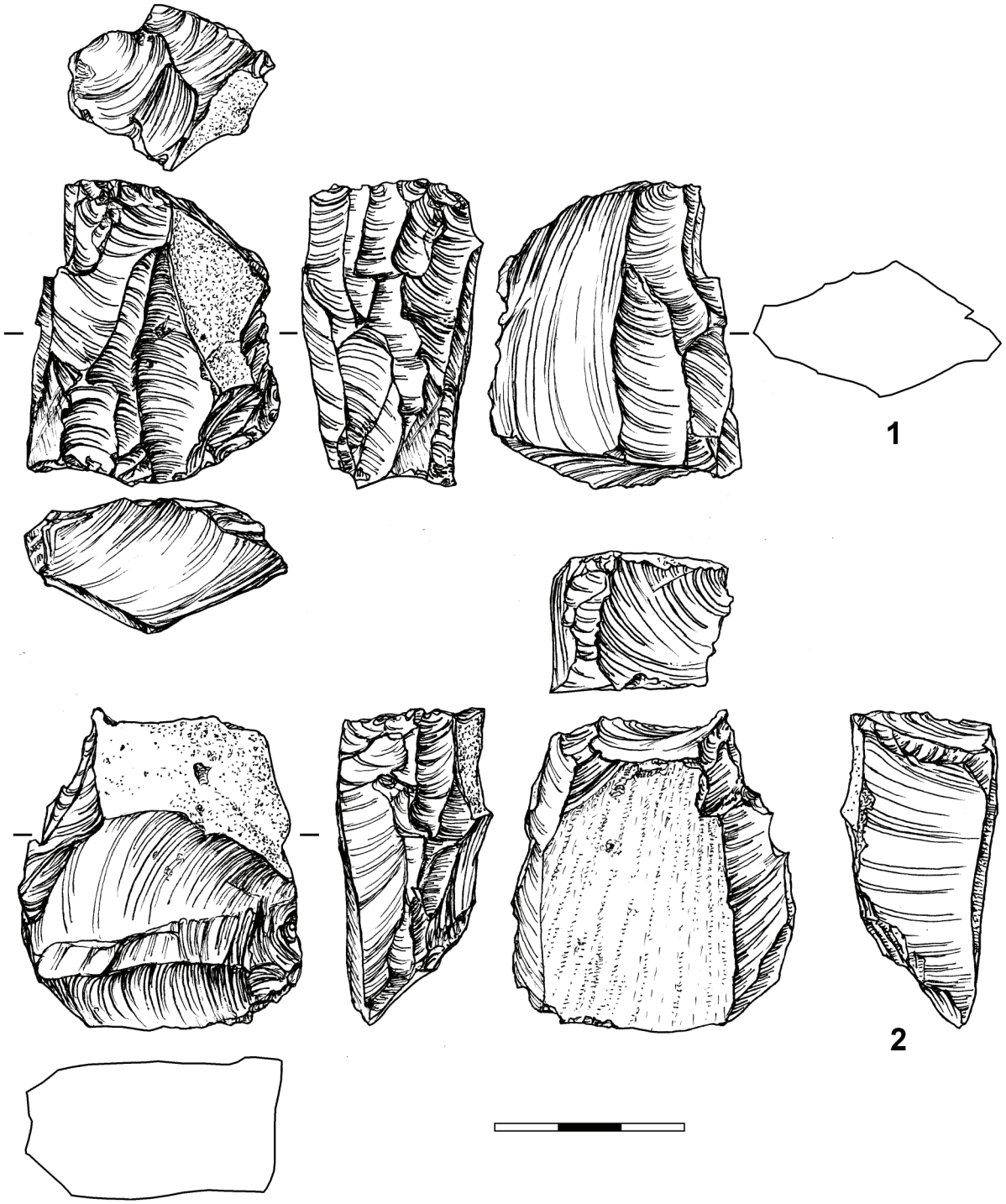


Fig. 8–15. Barmaky, eastern area complex, horizon 2d: 1 – core for blades/bladelets, bidirectional, narrow flaking surface; 2 – core perpendicular–adjacent, narrow / sub–cylindrical flaking surfaces.

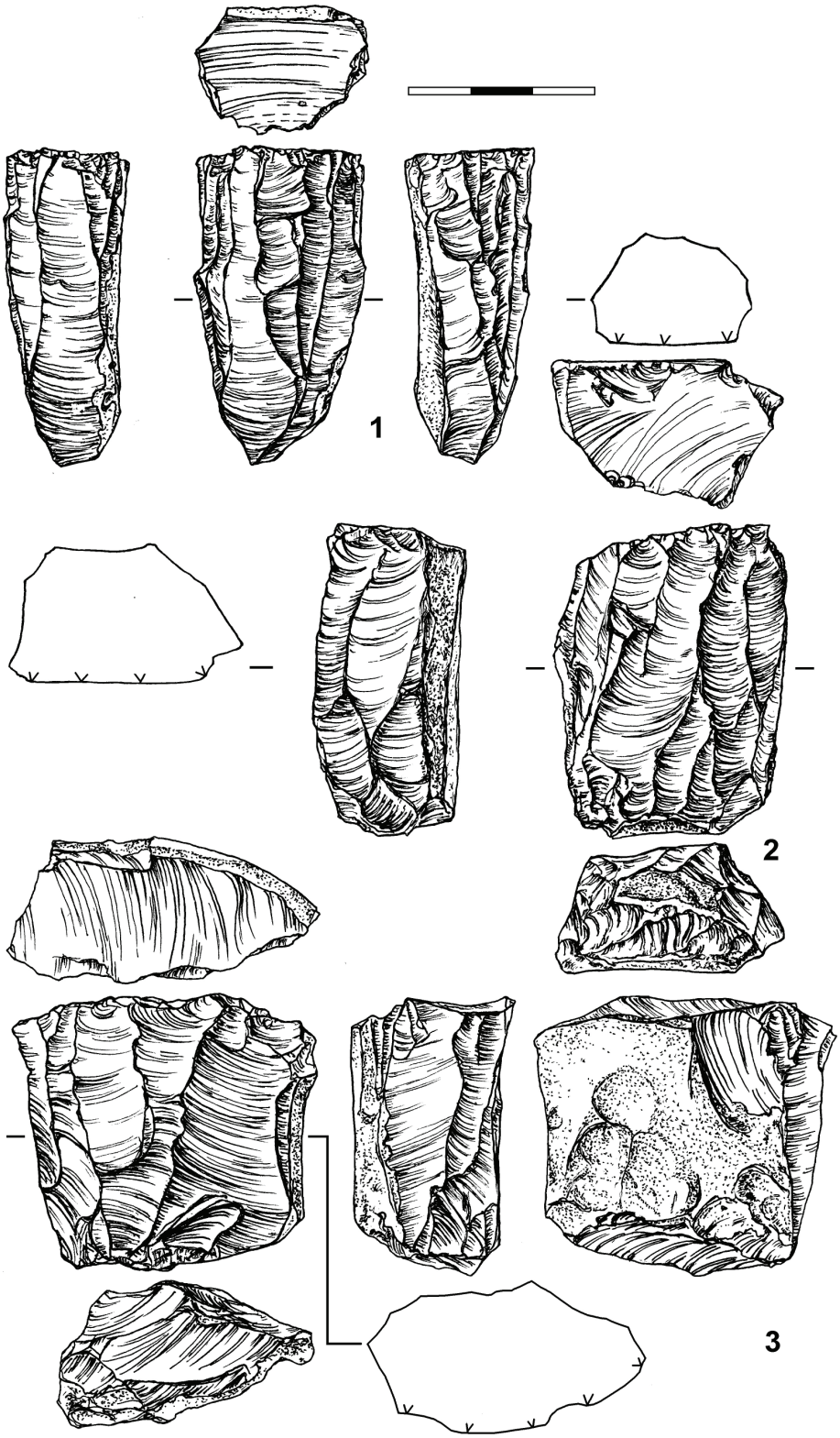


Fig. 8-16. Barmaky, eastern area complex, horizon 2d (1, 2,) & hearth (3): 1, 2 – cores for blades/bladelets, bidirectional-adjacent, sub-cylindrical; 3 – core for blades/bladelets, bidirectional, narrow flaking surfaces / laterally narrowed flaking surface.

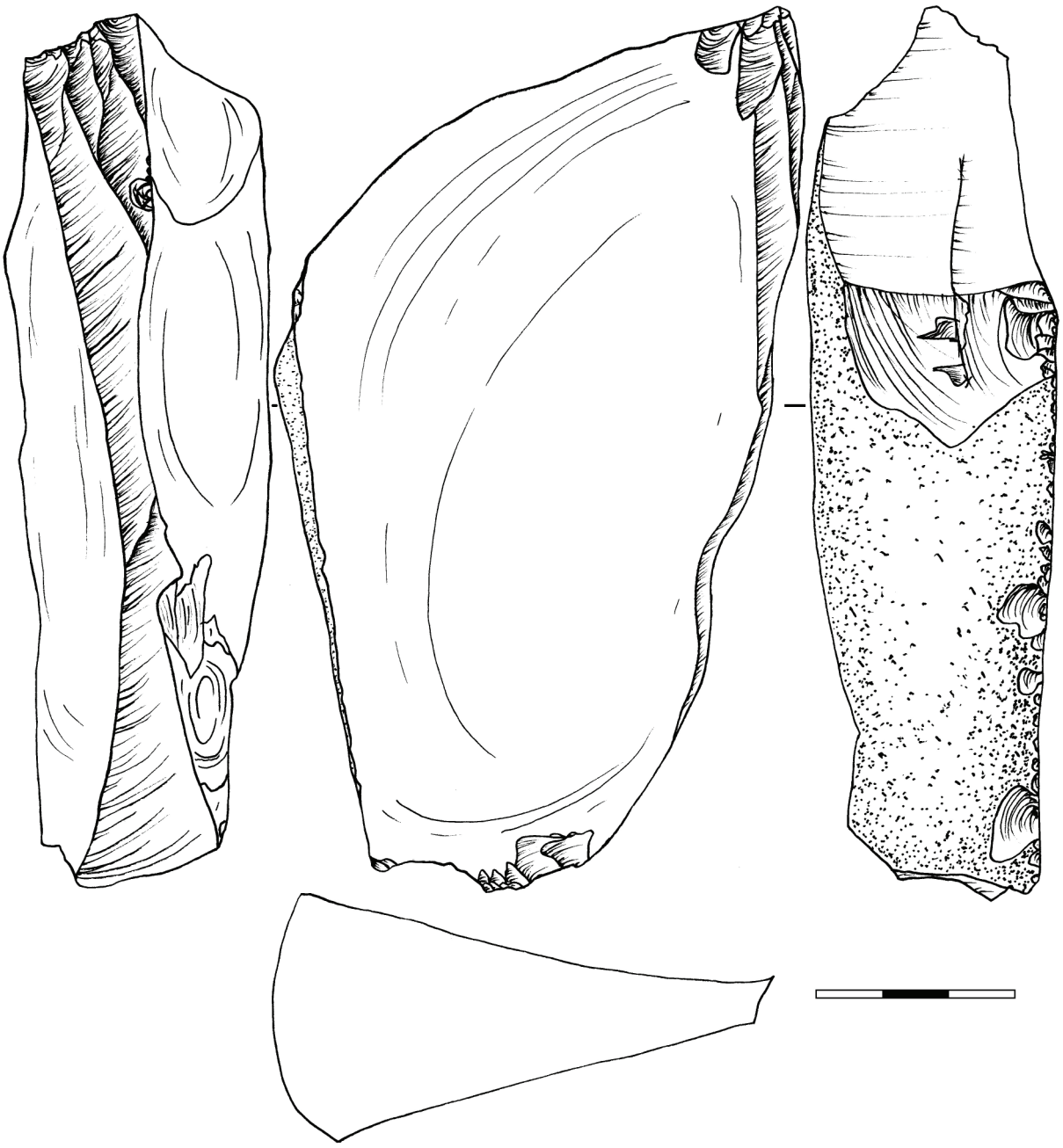

Fig. 8–17. Barmaky, eastern area complex, horizon 2c: core for bladelets, unidirectional, narrow flaking surface.

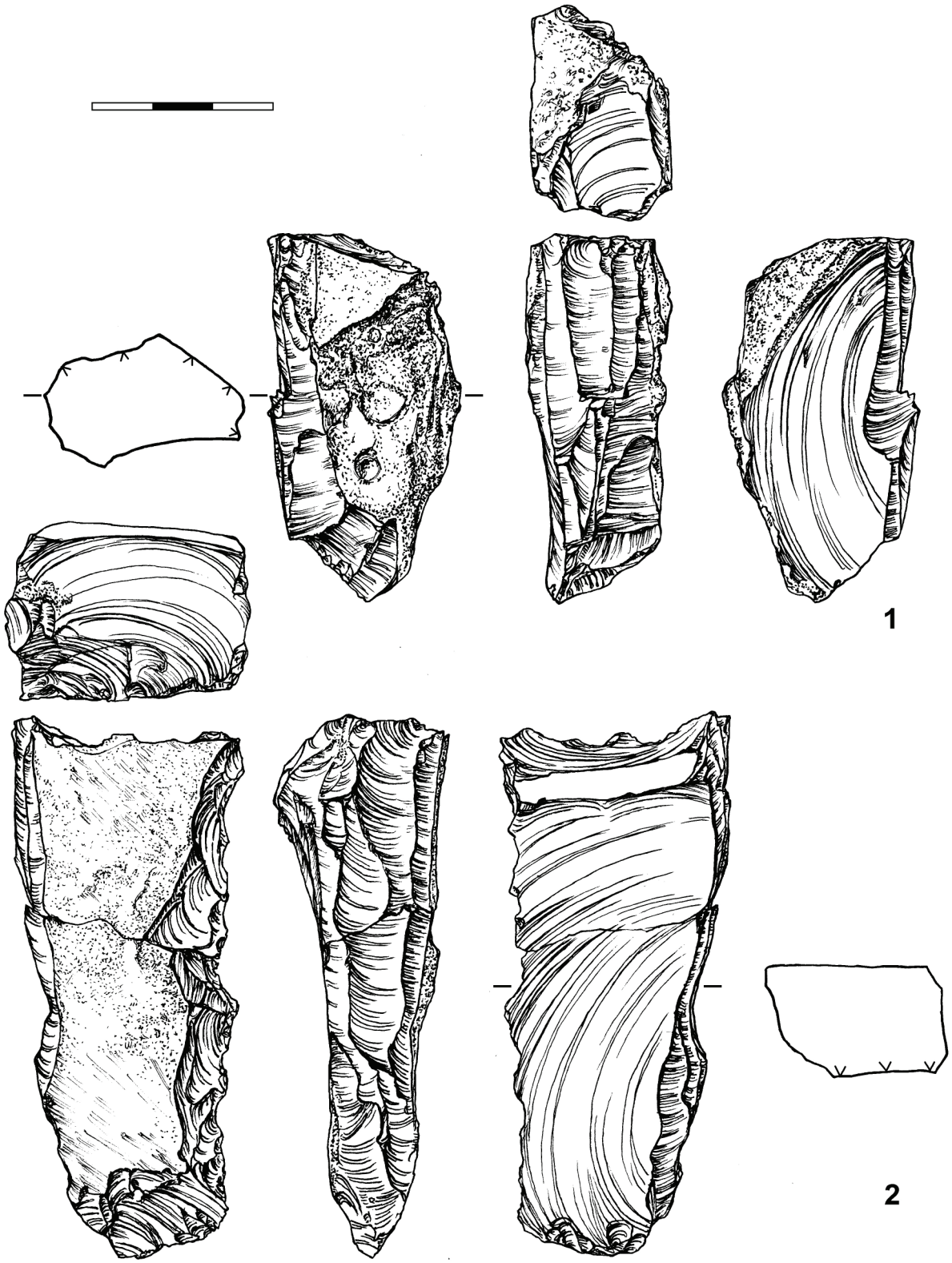


Fig. 8–18. Barmaky, eastern area complex, horizon 2d: 1 –core for bladelets, unidirectional, narrow flaking surface; 2 – core for bladelets, unidirectional, narrow flaking surface, wedge-shaped.

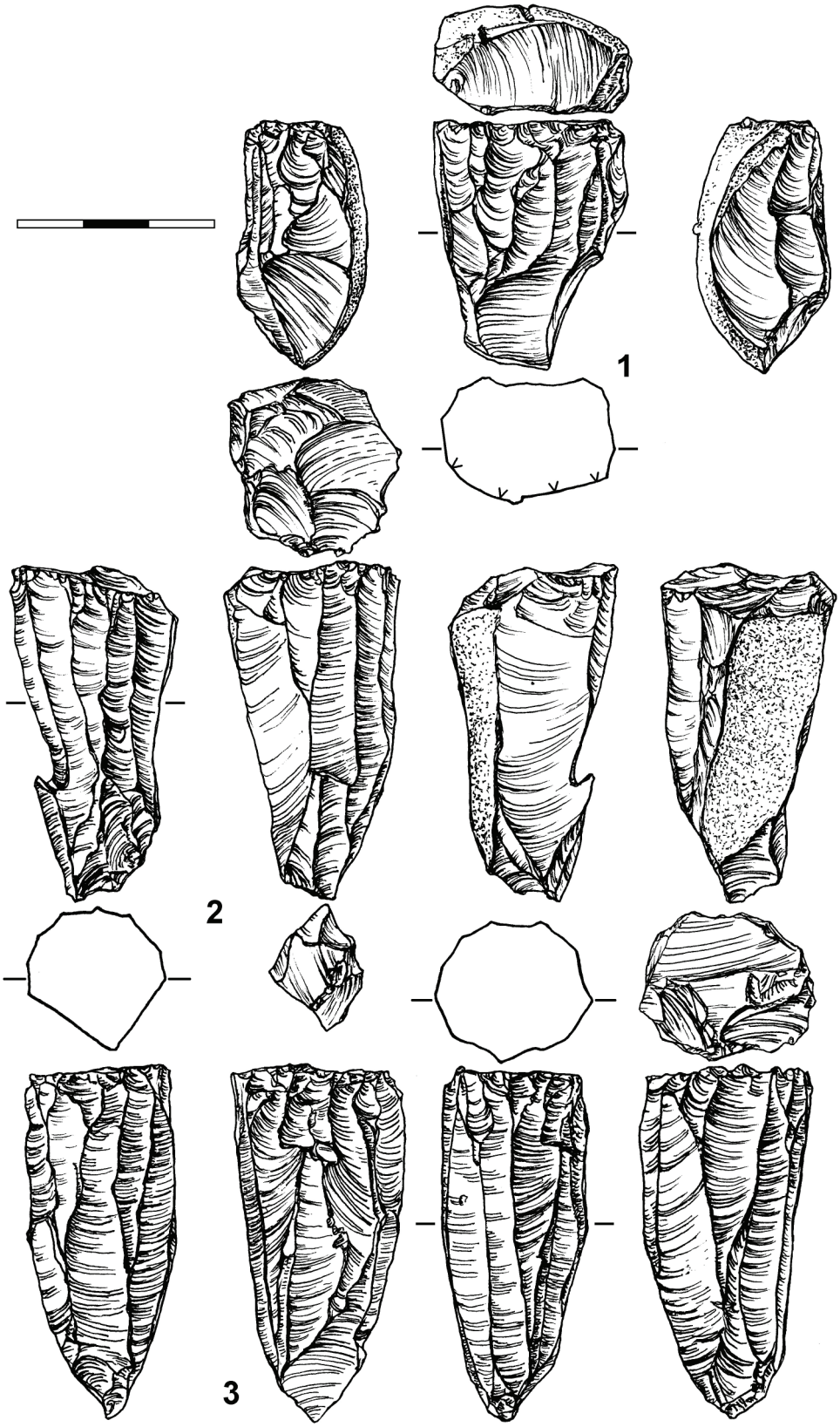


Fig. 8–19. Barmaky, eastern area complex, horizon 2d, cores for bladelets: 1 – unidirectional, sub-cylindrical; 2 – bidirectional, sub-cylindrical/sub-pyramidal; 3 – unidirectional, pyramidal.

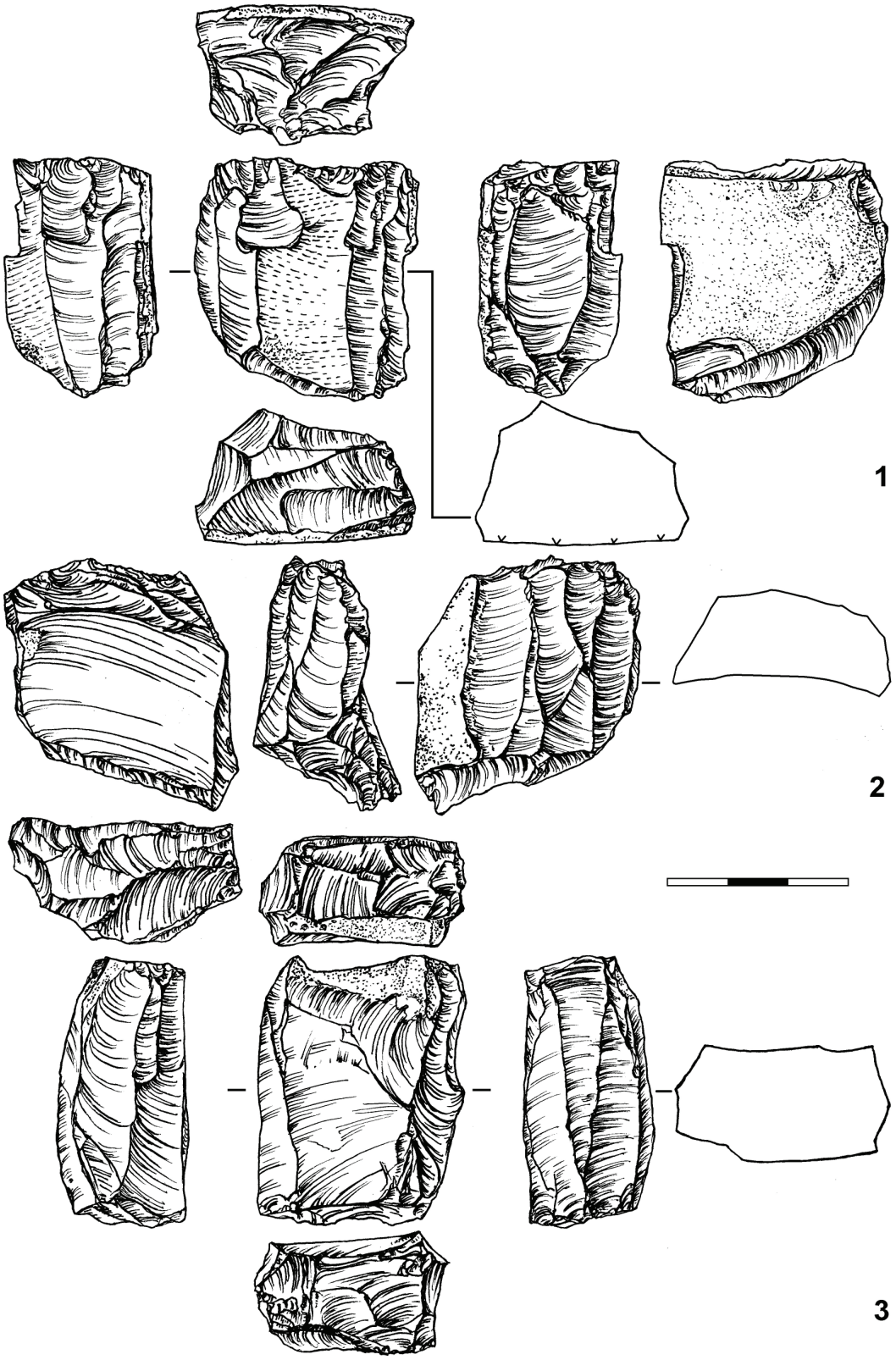


Fig. 8–20. Barmaky, eastern area complex, ash (1) & horizon 2d (2, 3), cores for bladelets: 1 – multi-directional, narrow flaking surface; 2 – perpendicular-adjacent, narrow flaking surface/sub-cylindrical; 3 – bidirectional-alternate, narrow flaking surface.

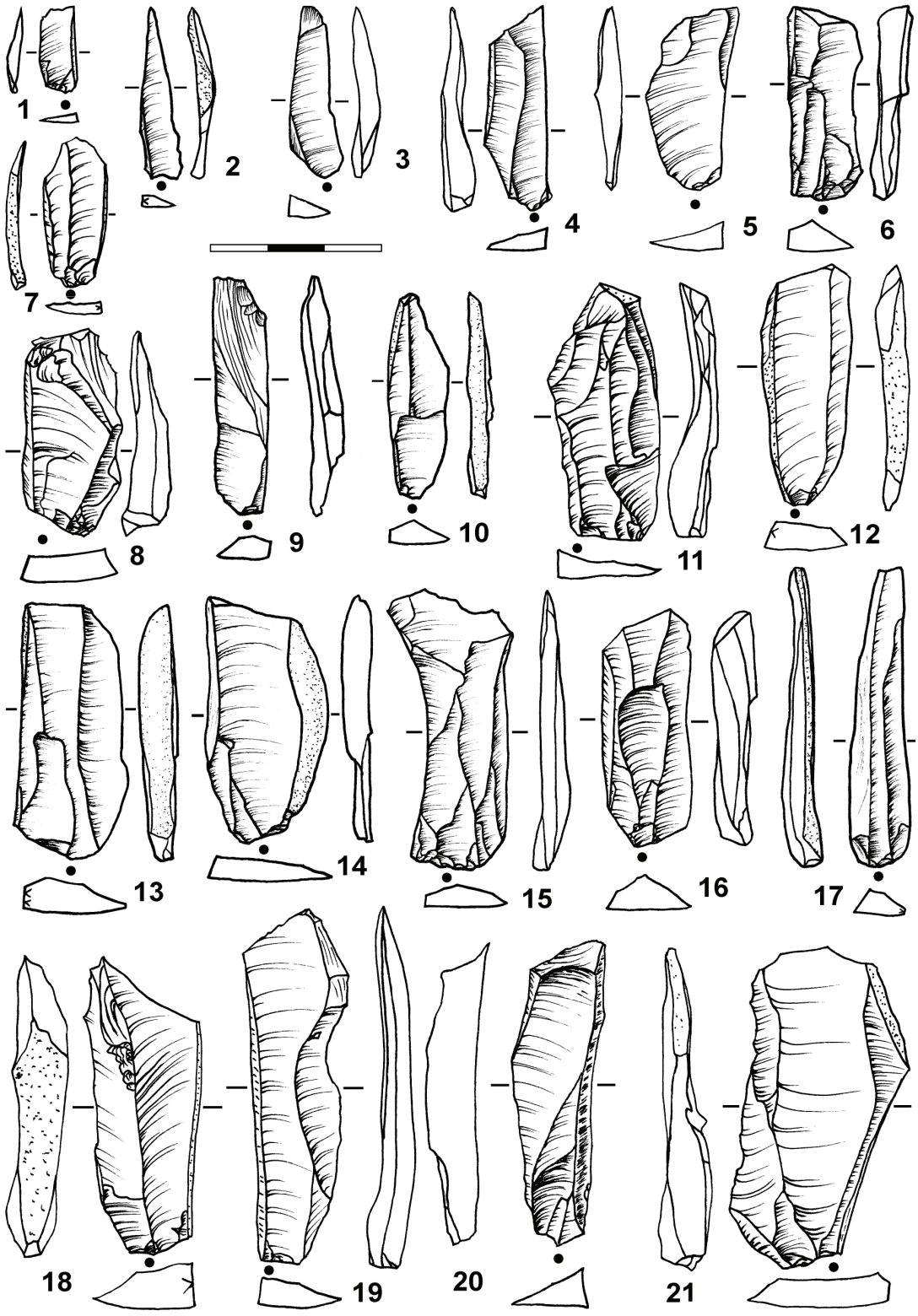


Fig. 8–21. Barmaky, eastern area complex, ash (1, 8), horizons 2d (2–4, 6, 9, 10, 13–17, 20), 2c (5, 12) & hearth (7, 11, 18, 19, 21): 1 – natural *débordante* micro-blade; 2 – secondary crested micro-blade, unidirectional on cortical *débordante*; 3, 4 – natural *débordante* bladelets; 5, 8, 11, 15, 19 – natural *débordante* blades; 6, 14, 16, 20 – lateral *débordante* blades; 7, 10, 17 – cortical *débordante* bladelets; 9 – crested bladelet, unidirectional on lateral *débordante*; 12, 13, 18, 21 – cortical *débordante* blades.

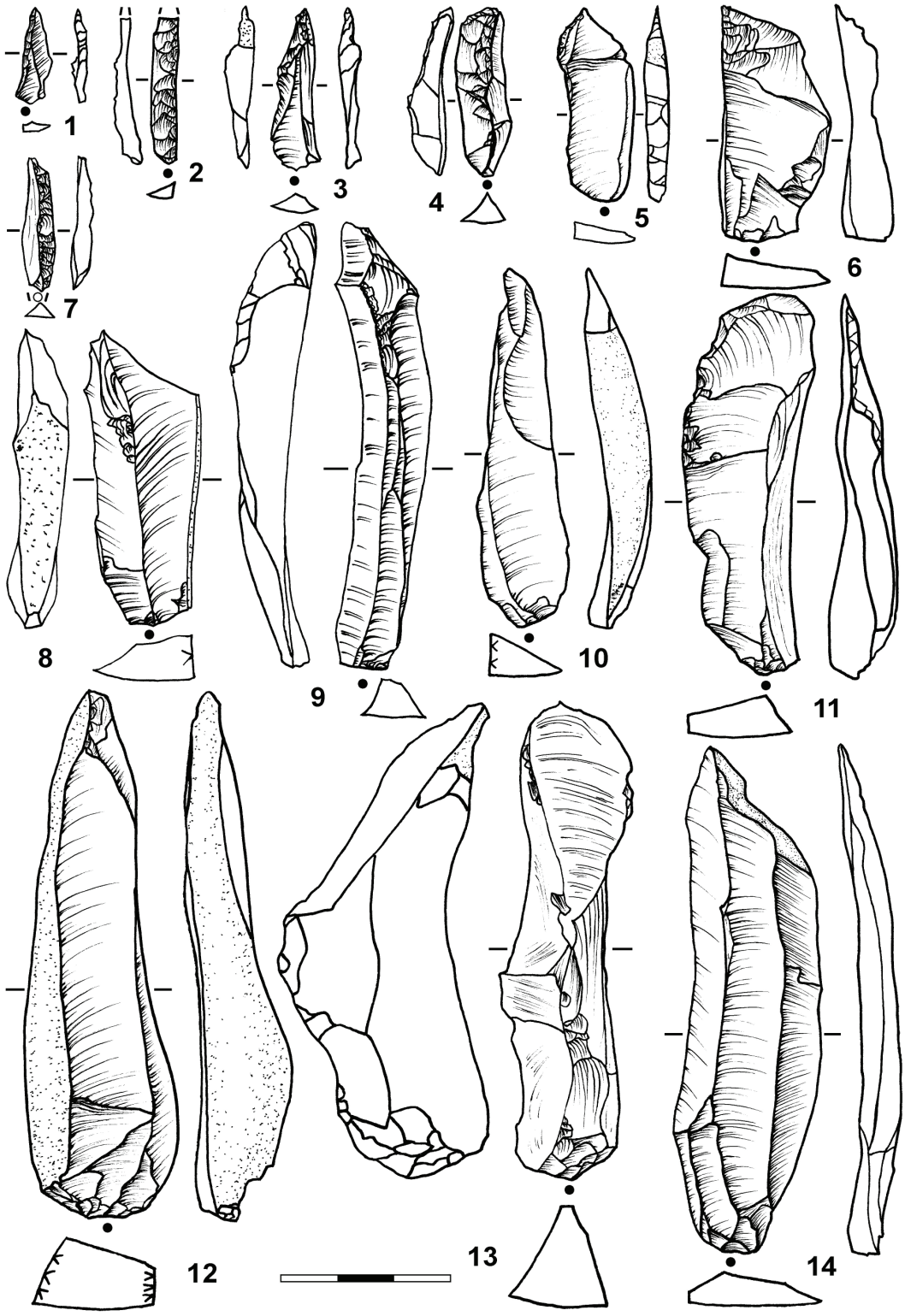


Fig. 8-22. Barmaky, eastern area complex, hearth (1, 3, 8), 2d (2, 4-7, 10-13), 2c, ash (9) and horizon 2c (14): 1 – one-side crested micro-blade, unidirectional; 2 – one-side crested micro-blade on natural *débordante*; 3 – one-side crested bladelet, unidirectional; 4 – crested bladelet; 5 – secondary crested bladelet, unidirectional; 6, 11 – one-side crested, unidirectional blade on natural *débordante*; 7 – one-side crested micro-blades; 8, 12 – one-side crested, unidirectional blade on cortical *débordante*; 9 – one-side crested blade, unidirectional; 10 – cortical *débordante* blade, bidirectional; 13 – crested blade; 14 – natural *débordante* blade, unidirectional.

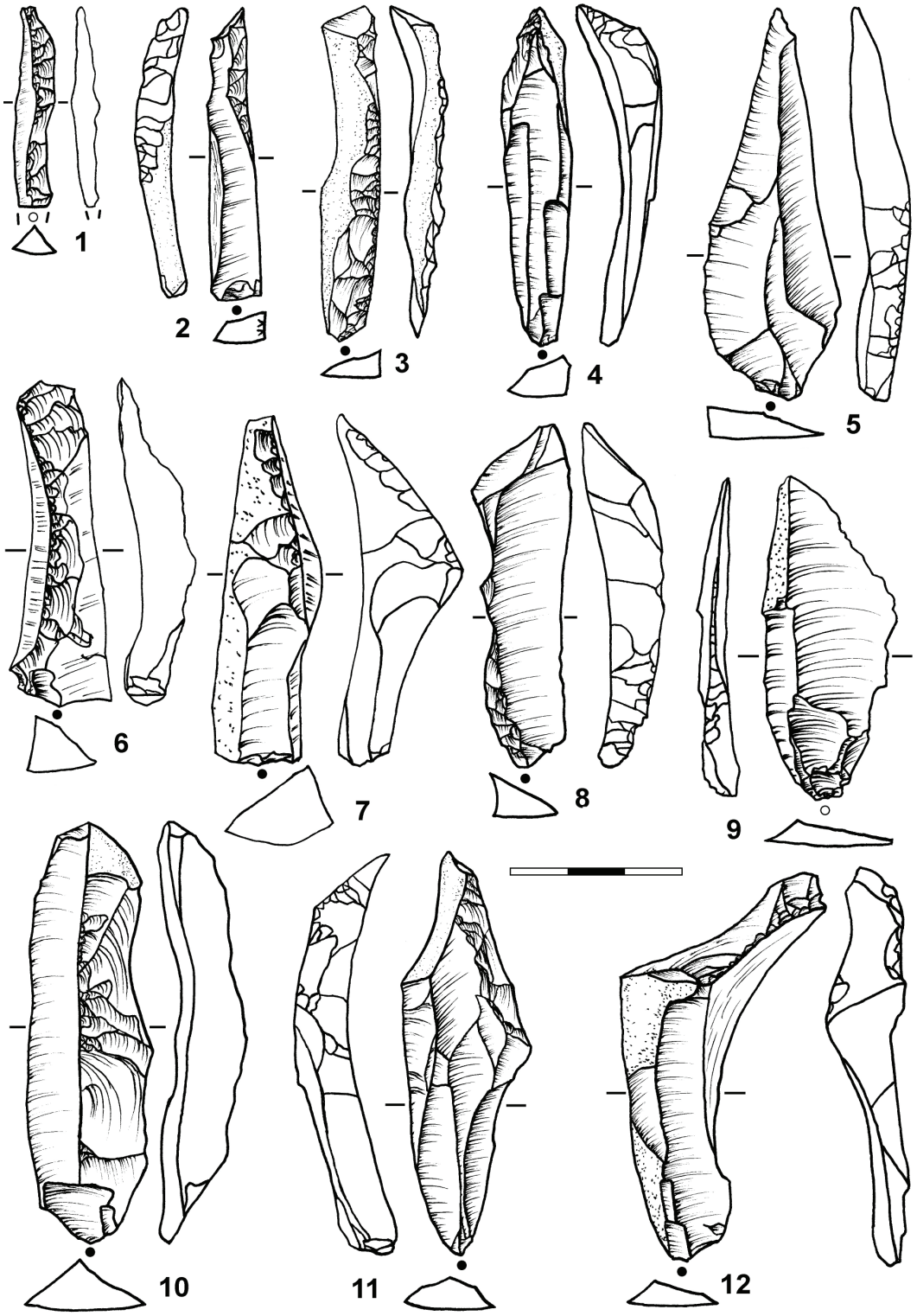


Fig. 8-23. Barmaky, eastern area complex, horizon 2d (1-5, 8, 10-12), ash (6-7) & hearth (9): 1 – one-side crested micro-blade; 2 – one-side crested, unidirectional bladelet on cortical *débordante*; 3 – one-side crested bladelet on cortical *débordante*; 4 – one-side crested, unidirectional bladelet on cortical *débordante*; 5, 8 – one-side crested blades, bidirectional; 6, 9, 10, 11, 12 – one-side crested blade, unidirectional; 7 – one-side unidirectional, crested blade on lateral *débordante* blade.

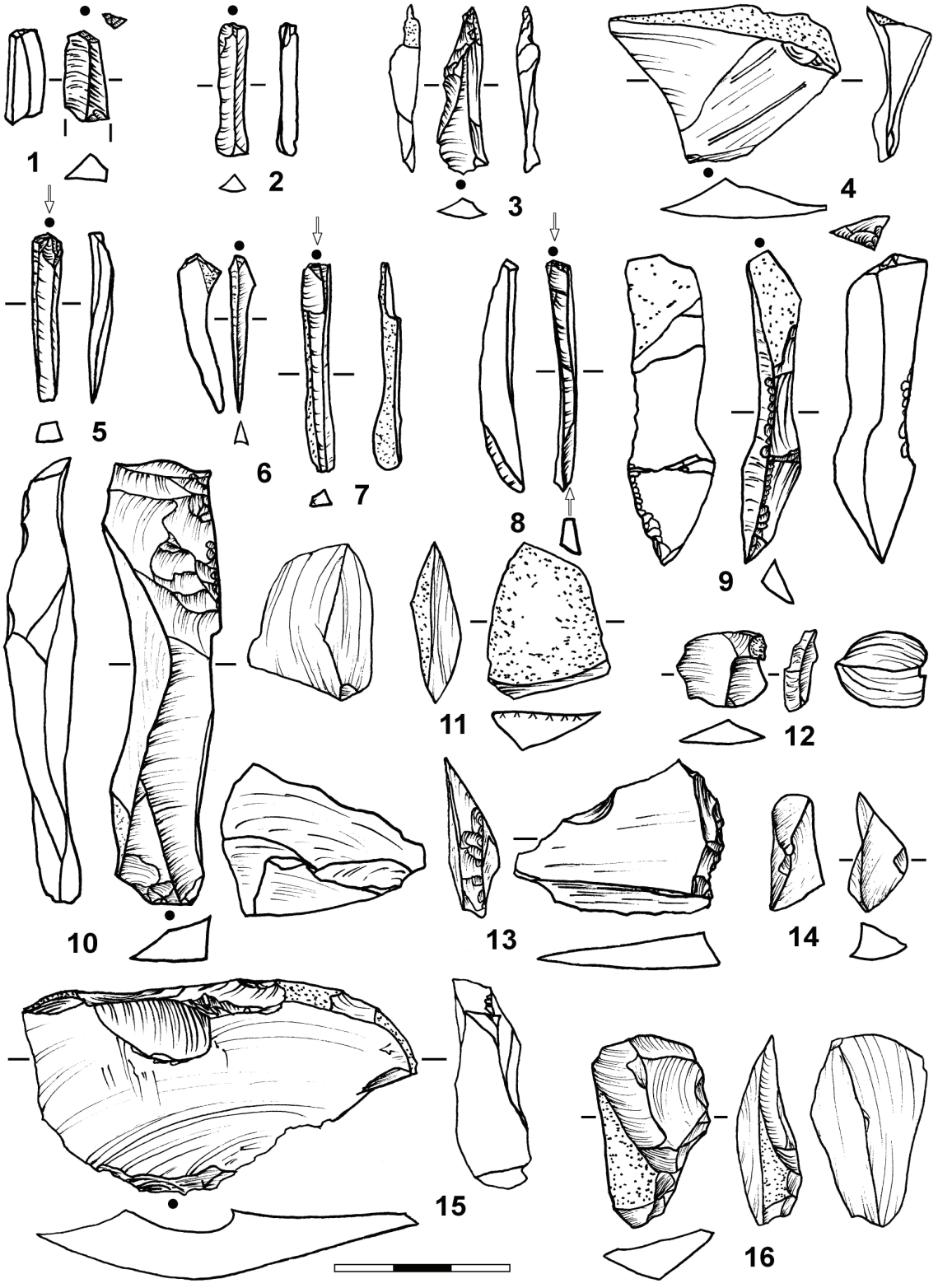


Fig. 8–24. Barmaky, eastern area complex, hearth (3, 4), horizons 2c (1) & 2d (2, 5–16): 1, 2, 6 – burin spalls, primary; 3 – secondary crested bladelet, unidirectional; 4, 15 – *Kantenabschläge*; 5 – burin spall, secondary; 7 – burin spall, multiple; 8 – burin spall, multiple, bidirectional; 9 – burin spall, primary, retouched; 10 – one-side crested, unidirectional blade on / *débordante* blade, unidirectional; 11, 12, 14 – truncation spalls, initial; 13, 16 – truncation spalls, secondary.

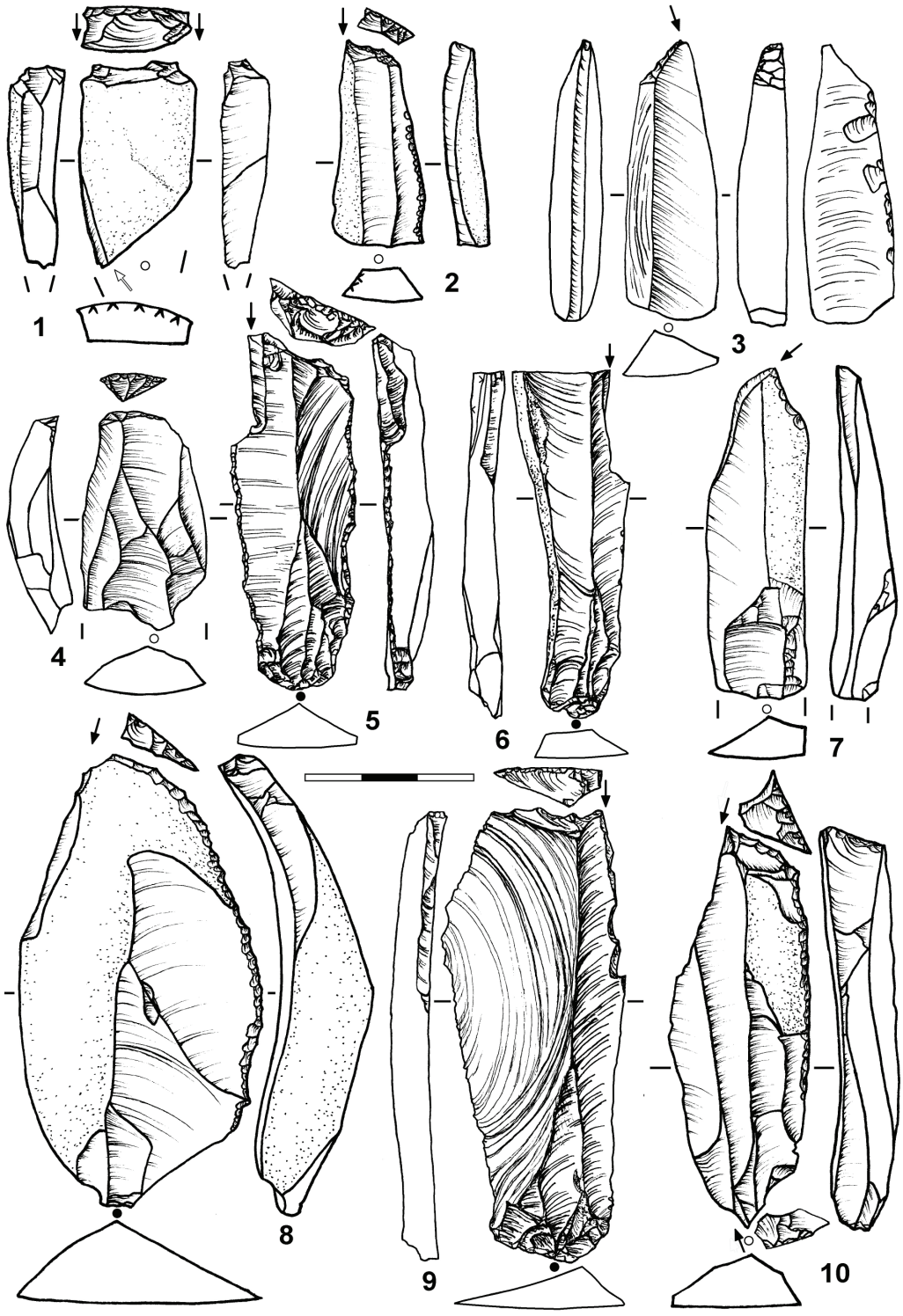


Fig. 8–25. Barmaky, eastern area complex, horizons 2d (1, 2, 4–10) & 2c (3): 1 – bi-lateral burin on concavely distally dorsally truncated flake; 2 – burin on obliquely-convexly distally dorsally truncated and laterally dorsally retouched blade; 3 – burin on obliquely distally dorsally truncated and laterally ventrally retouched blade; 4 – end-scraper on blade simple-convex, distal, dorsal; 5 – burin on obliquely distally dorsally truncated and bilaterally dorsally retouched blade; 6 – angle burin on blade; 7 – burin on obliquely distally dorsally truncated blade; 8 – burin on obliquely-convexly distally dorsally truncated and laterally dorsally retouched flake; 9 – burin on straightly distally dorsally truncated blade; 10 – opposite burin on obliquely bi-terminally dorsally truncated and laterally dorsally retouched blade.

quarter of the flakes, over a third of the blades, about 30 % of the bladelets, and over 20 % of the micro-blades. The primary and natural pieces compose about 10 % of the flakes and about 1 % of the lamellar *débitage*. The *débordantes* (Fig. 8-37; 8-38, *1, 3-9, 11, 12*; 8-39, *7, 10, 11, 13, 15*) and crested (Fig. 8-38, *2, 10*; 8-39, *1-5, 8, 9, 14, 16*; 8-40, *1, 2-8*) pieces are more common in lamellar assemblages than among flakes (Table 8-60). The combination of *débordante* and crested pieces was identified very frequently in the lamellar assemblage (Fig. 8-38, *2, 10*; 8-39, *6, 12, 16*; 8-40, *2*). The *Kantenabschläge* (Fig. 8-41, *12, 14, 15*) and primary pieces constitute about 5 % and nearly 10 % of the flake assemblage, respectively.

Half of the flakes are broken, while **fragmented** lamellar *débitage* is 4-5 times more frequent than complete blades, bladelets, and micro-blades (Table 8-61). Distal, medial, and proximal parts of lamellar products occur in about equal percentages (Table 8-61). Along with the application of hard hammer percussion, this pattern might reflect a significant influence of trampling.

About one-third of the flakes have trapezoidal **shapes**, which were removed off-axis (Table 8-62). Rectangular, on-axis blades/bladelets/micro-blades (20-23 %) dominate the lamellar assemblage, followed by trapezoidal off-axis (10-17 %), crescent off-axis (12-19 %), and irregular off-axis (11-15 %) shapes. Irregular off-axis blanks are equally characteristic for flake, blade, bladelet, and micro-blade assemblages. In general, off-axis blanks dominate the *débitage* assemblage. While trapezoidal shapes are more common for flakes, rectangular shapes are more characteristic for lamellar blanks (Table 8-62).

Straight **lateral profiles** dominate all blanks (Table 8-63), but are more frequent in bladelets and micro-blades than in flake assemblages. At the same time, the sum of differently curved *débitage* exceeds the number of straight profiles among all blanks except micro-blades (Table 8-63).

Feathering **distal extremities** make up more than half of all blank classes (Table 8-64). Being a usual knapping problem of unidirectional flaking, hinges can be observed in roughly equal shares in flake and lamellar assemblages.

The dominance of trapezoidal **cross-sections** in blades mainly reflects both the width and pronounced convexity of the flaking surfaces (Table 8-65). The narrow flaking surface of bladelet and micro-blade cores, in contrast, leads to the prevalence of triangular cross-sections in bladelets and micro-blades. Lateral steep cross-sections reflect the importance of *débordante* blanks (Table 8-65).

The dominance of unidirectional **scars** is the most characteristic feature of the blank assemblages: 50-85 % (Table 8-66). The sum of all types of bidirectional dorsal scar patterns rarely exceeds 20 % of blades and 10 % of both bladelets and micro-blades. Cortical dorsal

| | 2c | 2c, hearth | 2d | Σ |
|---|---|---|---|---|
| **TRUNCATED PIECES ON BLADES** | | | | |
| straight, distal, dorsal | – | 1 | 2 | **3** |
| straight, proximal, dorsal | 1 | – | 1 | **2** |
| oblique, distal, dorsal | – | – | 3 | **3** |
| oblique, distal, alternating | – | – | 1 | **1** |
| oblique, proximal, dorsal | – | – | 2 | **2** |
| oblique-convex, distal, dorsal | – | 1 | – | **1** |
| oblique-convex, proximal, dorsal | – | 1 | – | **1** |
| oblique-concave, proxinal, dorsal | – | – | 1 | **1** |
| bi-terminal, oblique (distal) / concave (base), dorsal | – | – | 1 | **1** |
| **TRUNCATED PIECES ON FLAKES** | | | | |
| oblique, distal, dorsal | – | – | 1 | **1** |
| **TOTAL:** | **1** | **3** | **12** | **16** |

Table 8-55. Barmaky, eastern area, by horizons and structures: truncated pieces

| | Σ |
|---|---|
| **BACKED POINTS ON BLADELETS** | |
| straightly dorsally backed, obliquely dorsally truncated base (broken tip) | 1 |
| **BACKED POINTS ON MICRO-BLADES** | |
| straightly dorsally backed (broken base) | 2 |
| straightly dorsally backed; obliquely dorsally truncated base (broken tip) | 1 |
| straightly dorsally backed, obliquely bifacialy truncated base (broken tip) | 1 |
| straightly dorsally backed, obliquely dorsally truncated/broken base (broken tip) | 2 |
| straightly dorsally backed, convex dorsally truncated base (broken tip) | 1 |
| **UNFINISHED BACKED PIECES ON BLADELETS** | |
| partially backed, dorsal | 1 |
| **UNIDENTIFIABLE BACKED PIECES ON BLADELETS** | |
| straightly dorsally backed | 2 |
| wavy dorsally backed | 1 |
| **UNIDENTIFIABLE BACKED PIECES ON MICRO-BLADES** | |
| straightly bifacially backed | 1 |
| concave dorsally backed | 1 |
| **TOTAL:** | **14** |

Table 8-56. Barmaky, eastern area, horizon 2d: microliths

| | 2c | 2c, ash | 2c, hearth | 2d | Σ |
|---|---|---|---|---|---|
| **RETOUCHED PIECES ON BLADE** | | | | | |
| distal, dorsal | – | – | 2 | – | **2** |
| distal, alternating | – | – | – | 1 | **1** |
| lateral, ventral | – | – | – | 1 | **1** |
| bi-lateral, alternate | – | – | – | 1 | **1** |
| **RETOUCHED PIECES ON BLADELET** | | | | | |
| bi-lateral, dorsal | – | – | – | 1 | **1** |
| **RETOUCHED PIECES ON MICRO-BLADE** | | | | | |
| lateral, dorsal | – | – | – | 1 | **1** |
| **RETOUCHED PIECES ON FLAKE** | | | | | |
| distal, dorsal | – | – | – | 5 | **5** |
| lateral, dorsal | 1 | – | – | 6 | **7** |
| lateral, ventral | – | – | – | 1 | **1** |
| lateral, bifacial | – | – | – | 1 | **1** |
| bi-lateral, dorsal | – | – | – | 1 | **1** |
| **RETOUCHED PIECES ON NATURAL FLAKE** | | | | | |
| lateral, dorsal | – | 1 | – | – | **1** |
| bi-lateral, alternate | – | – | – | 1 | **1** |
| **TOTAL:** | **1** | **1** | **2** | **20** | **24** |

Table 8-57. Barmaky, eastern area, by horizons and structures: retouched pieces

| | 2b | | 2c, pit 1 | | 2c | | 2d | | | | |
|---|---|---|---|---|---|---|---|---|---|---|---|
| | # | esse,% | # | esse,% | # | esse,% | # | esse,% | Σ | % | esse,% |
| **pre-cores** | – | – | – | – | 19 | 0,31 | 6 | 0,30 | 25 | 0,03 | 0,30 |
| **cores** | 1 | 2,27 | 4 | 1,40 | 45 | 0,73 | 13 | 0,66 | **63** | 0,07 | 0,74 |
| **tools** | 5 | 11,36 | 21 | 7,34 | 483 | 7,84 | 150 | 7,58 | **659** | 0,70 | 7,78 |
| **flakes** | 22 | 50,00 | 147 | 51,40 | 2649 | 42,98 | 954 | 48,21 | **3772** | 4,03 | 44,52 |
| **blades** | 6 | 13,64 | 41 | 14,34 | 1031 | 16,73 | 337 | 17,03 | **1415** | 1,51 | 16,70 |
| **bladelets** | 6 | 13,64 | 40 | 13,99 | 871 | 14,13 | 304 | 15,36 | **1221** | 1,31 | 14,41 |
| **micro-blades** | 3 | 6,82 | 20 | 6,99 | 538 | 8,73 | 128 | 6,47 | **689** | 0,74 | 8,13 |
| **burin spalls** | 1 | 2,27 | 13 | 4,55 | 473 | 7,67 | 83 | 4,19 | **570** | 0,61 | 6,73 |
| **truncation spalls** | – | – | – | – | 54 | 0,88 | 4 | 0,20 | **58** | 0,06 | 0,68 |
| **chips** | 217 | – | 2885 | – | 60612 | – | 19261 | – | **82975** | 88,70 | – |
| **unidentifiable *débitage*** | 15 | – | 87 | – | 1259 | – | 699 | – | **2060** | 2,20 | – |
| **chunks** | – | – | – | – | 34 | – | 7 | – | **41** | 0,04 | – |
| **TOTAL:** | **276** | 100,00 | **3258** | 100,00 | **68068** | 100,00 | **21946** | 100,00 | **93548** | 100,00 | 100,00 |

Table 8-58. Barmaky, western area complex, by horizons and structures: artefact totals

surfaces are more characteristic for flakes: up to 10 %. Crested pieces are common for blades: about 15 %. Along with primary pieces, the orthogonal dorsal scar pattern of flakes (about 20 %) reflects the role of flakes in the core shaping procedure.

Most flakes and blades exhibit cortex cover (Table 8-67). Primary pieces make up about 10 % of the flakes. Non-cortical pieces dominate the bladelet and micro-blade assemblages. Pieces with lateral cortex are most common among the partly cortical blanks. Lamellar pieces with lateral cortex amount to 20-40 %, underlining the importance of flat raw volumes for blade and bladelet cores with a narrow flaking surface.

Plain **striking platform remnants** make up about half of all identifiable butts of all blank classes (Table 8-68). The share of linear platforms rises with the decrease of the platform thickness as can be seen in their gradual increase from blade over bladelet to micro-blade assemblages (Table 8-68). Another specific feature of platform typology consists of the high amount (up to 20 %) of crushed butts. The method of **overhang trimming** was applied to about 40-50 % of platforms, but is more common for lamellar *débitage* (Table 8-69). Butt **abrasion** was not applied (Table 8-70). Unlipped **right-angle platforms** with pronounced bulbs dominate the blank assemblage (Tables 8-71; 8-72; 8-73). Together, the mentioned butt characteristics reflect the application of hard hammer percussion.

## Tool trimming pieces

Tool trimming pieces (Fig. 8-41, *1-11, 13*; 8-42) are more frequent in the western than in the eastern area (Tables 8-39; 8-58). About 60 % of the burin spalls belong to the secondary and multiple types (Table 8-60; Fig. 8-42, *1-16, 18, 20-22*) and about 45 % were retouched before detachment (Fig. 8-42, *4, 5, 7, 10, 12, 14, 15, 17-22*). Complete burin spalls and their distal and proximal fragments are represented by about the same numbers. One-third exhibits rectangular shapes, but irregular (≈16 %), triangular (≈14 %), and crescent (≈14 %) shapes are also common. Twisted (≈26 %), curved in mid part (≈20 %), and straight (≈26 %) lateral profiles are characteristic of burin spalls. Hinges make up more than half of the identifiable ends and lateral steep pieces represent about 80-90 % of the cross-sections. The striking platform attributes show a dominant role of faceted (>33 %) and plain (≈30 %) types. Others are untrimmed – about 100 %; not abraded – about 100 %; unlipped – >80 %; diffuse bulbs – >50 %; acute angle – >50 %.

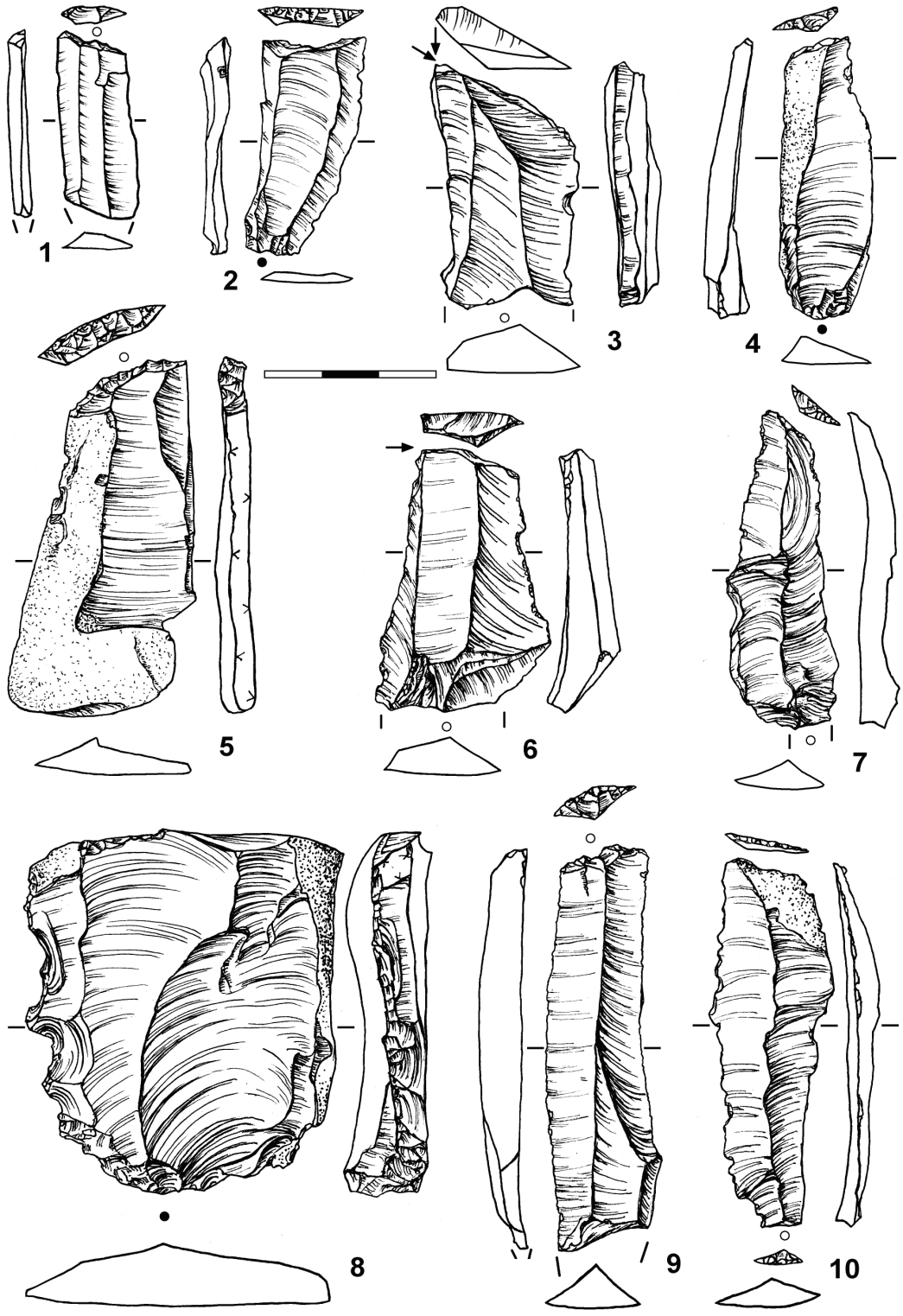


Fig. 8-26. Barmaky, eastern area complex, horizons 2d (1, 3, 4, 6, 7, 9, 10) & hearth (2, 5, 8): 1, 9 – truncated blades, oblique, proximal, dorsal; 2 – truncated blade, straight, distal, dorsal; 3 – dihedral-asymmetrical burin, distal, on laterally dorsally retouched blade; 4 – truncated blade, oblique, distal, alternating; 5 – truncated blade, oblique-convex, proximal, dorsal; 6 – transversal burin of "Suponevo type", proximal, on laterally partially dorsally truncated blade; 7 – truncated blade, oblique, distal, dorsal; 8 – denticulate piece on distally/laterally dorsally retouched flake; 10 – truncated blade, bi-terminal, distal oblique/proximal concave, dorsal.

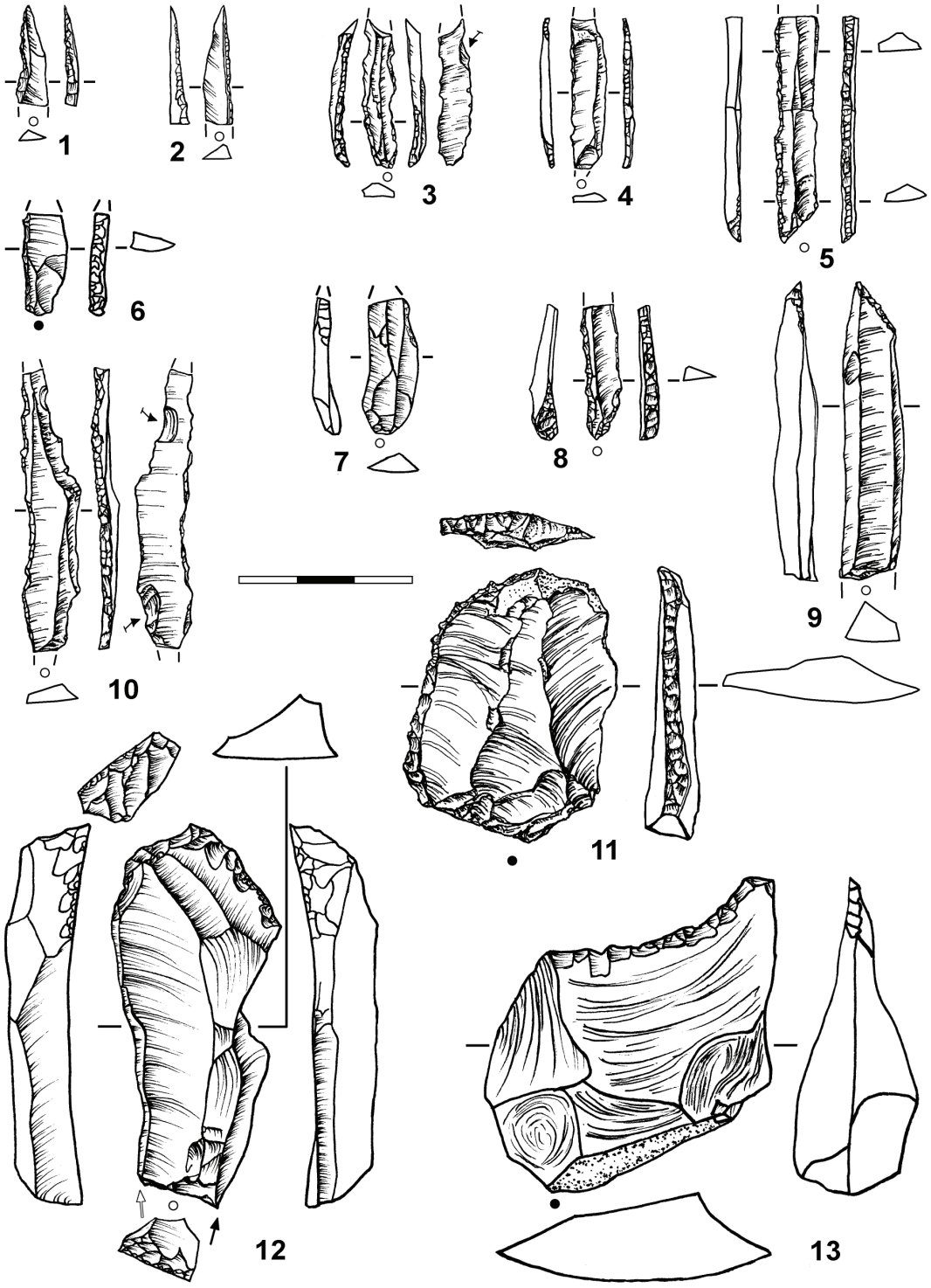


Fig. 8–27. Barmaky, eastern area complex, horizon 2d: 1, 2 – microlithic points on micro-blades, straightly dorsally backed (broken base); 3 – microlithic point on micro-blade, straightly dorsally backed, convex dorsally truncated base (broken tip); 4, 8 – microlithic points on micro-blades, straightly dorsally backed, obliquely dorsally truncated base (broken tip); 5 – microlithic point on bladelet, straightly dorsally backed, obliquely dorsally truncated base (broken tip); 6 – microlith unidentifiable on bladelet, straightly dorsally backed; 7 – unfinished microlith on bladelet, partially dorsally backed; 9 – point on bladelet, distally oblique, dorsal; 10 – microlith unidentifiable on bladelet, wavy dorsally backed; 11 – raclette on flake lateral-distal, dorsal; 12 – end-scraper – burin, the combination of simple-convex, distal, dorsal end-scraper & bi-lateral burin on proximally dorsally concavely truncated blade; 13 – denticulate piece on flake, distal, dorsal.

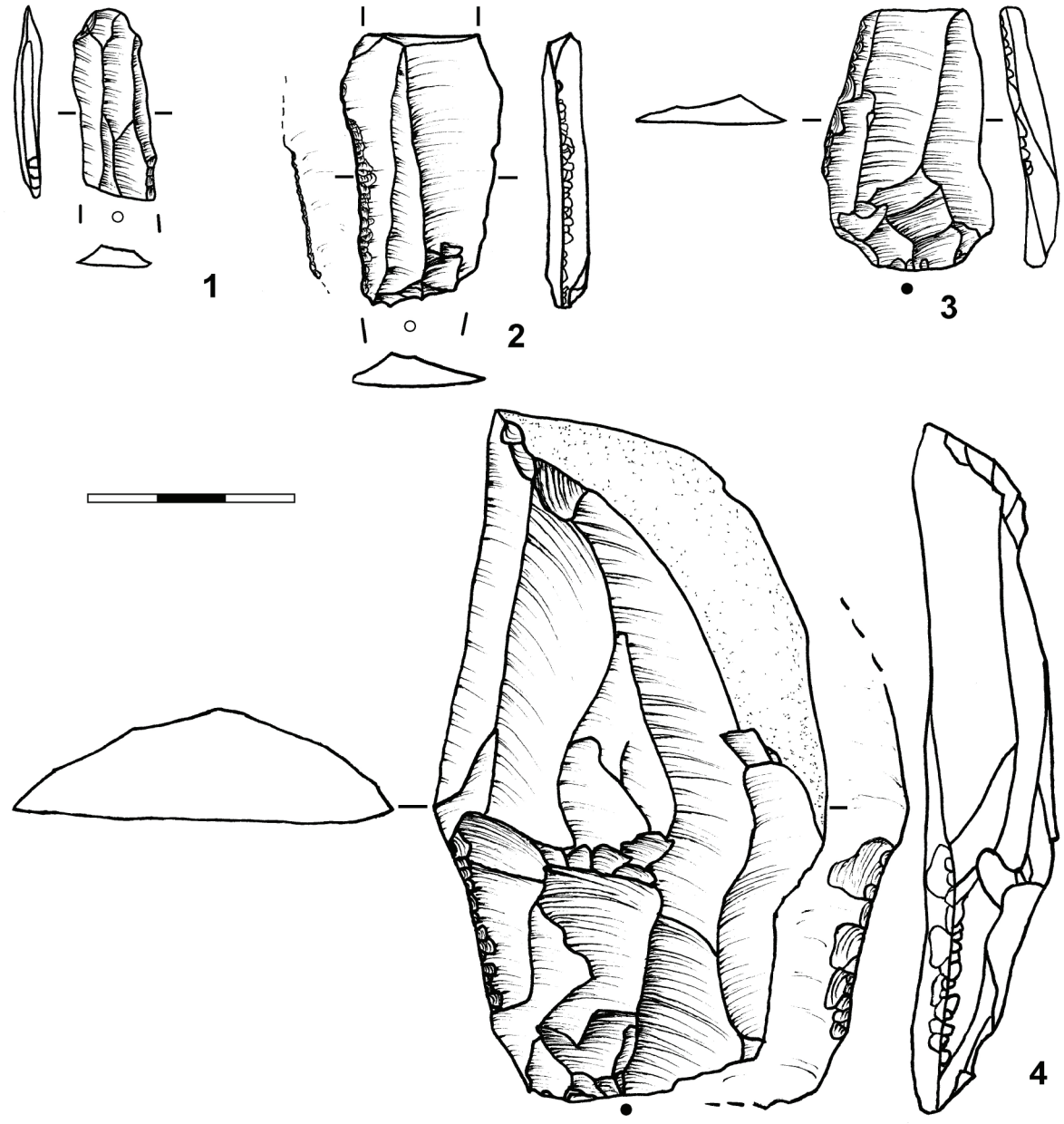


Fig. 8-28. Barmaky, eastern area complex, horizon 2d: 1 – retouched bladelet, bi-lateral, dorsal; 2 – retouched blade, bi-lateral, alternate; 3 – retouched flake, lateral, dorsal; 4 – retouched flake, lateral, bifacial.

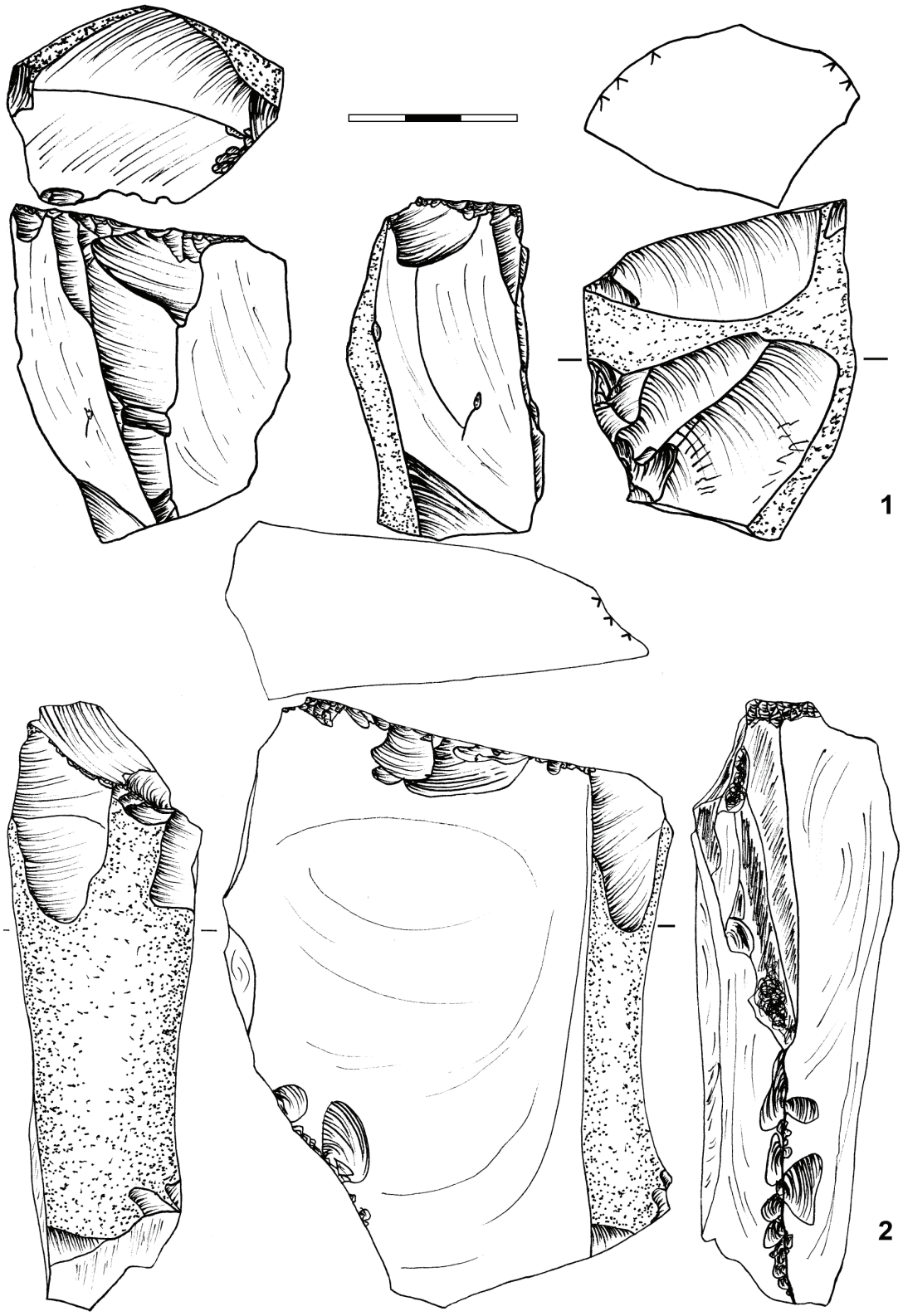


Fig. 8-29. Barmaky, western area complex, horizons 2d (1) & 2c (2): 1 – pre-core for blades, unidirectional, sub-cylindrical; 2 – pre-core for blades/bladelets, unidirectional, narrow flaking surface.

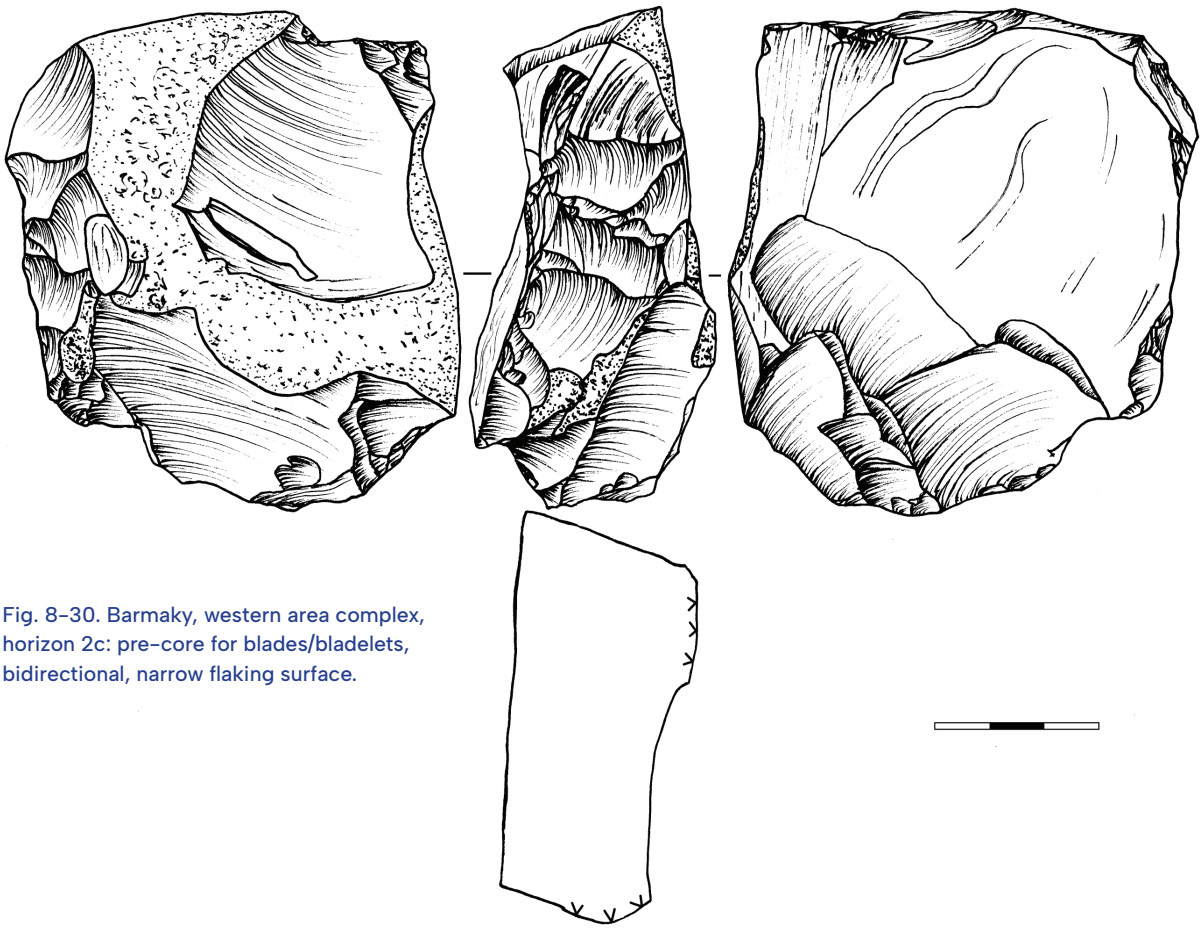

Fig. 8-30. Barmaky, western area complex, horizon 2c: pre-core for blades/bladelets, bidirectional, narrow flaking surface.

The sum of secondary (37.93 %) and rejuvenating (24.14 %) **truncation spalls** exceeds the initial (37.93 %) ones (Table 8-60; (Fig. 8-41, *1-5, 7, 8, 11, 13*), pointing towards relatively intensive on-site burin rejuvenation.

## *Débitage* dimensions

The differences between the *débitage* dimensions of the WA and other complexes are negligible (Table 8-35).

## Tools

Lamellar pieces serve as the main blank for tool production: blades 56.36 %, bladelets 9.97 %, micro-blades 14.43 %. Flakes serves as blanks for 19.07 % of the tools, and a single burin spall (0.17 %) was modified into a borer-perforator. More than 20 % of the tools were made on lamellar *débordantes* and crested pieces. In addition, 9 of 29 natural flakes were used for tool production. The most numerous tool classes are burins, retouched pieces, microliths, and truncated pieces (Table 8-74).

The **end-scrapers** are all simple-convex, 13 are made on blades (Fig. 8-43, *1, 2, 4, 5, 7*) 3 on flakes (Fig. 8-43, *3, 6*), and one on an unidentifiable fragment of *débitage*. Among the blades, 1 crested, 1 lateral *débordante*, and 1 primary item were identified. Two pieces also show a lateral dorsal retouch (Fig. 8-43, *5*), three pieces are bi-laterally dorsally retouched (Fig. 8-43, *7*), one item demonstrates the proximal concave dorsal truncation (Fig. 8-43, *4*), and one more piece is obliquely-concavely proximally dorsally truncated (Fig. 8-43, *1*). The most common combination of retouch for the working edges of end-scrapers is continuous sub-parallel obverse abrupt/semi-abrupt. The combinations of partial/discontinuous, marginal/scalar, obverse, and flat/

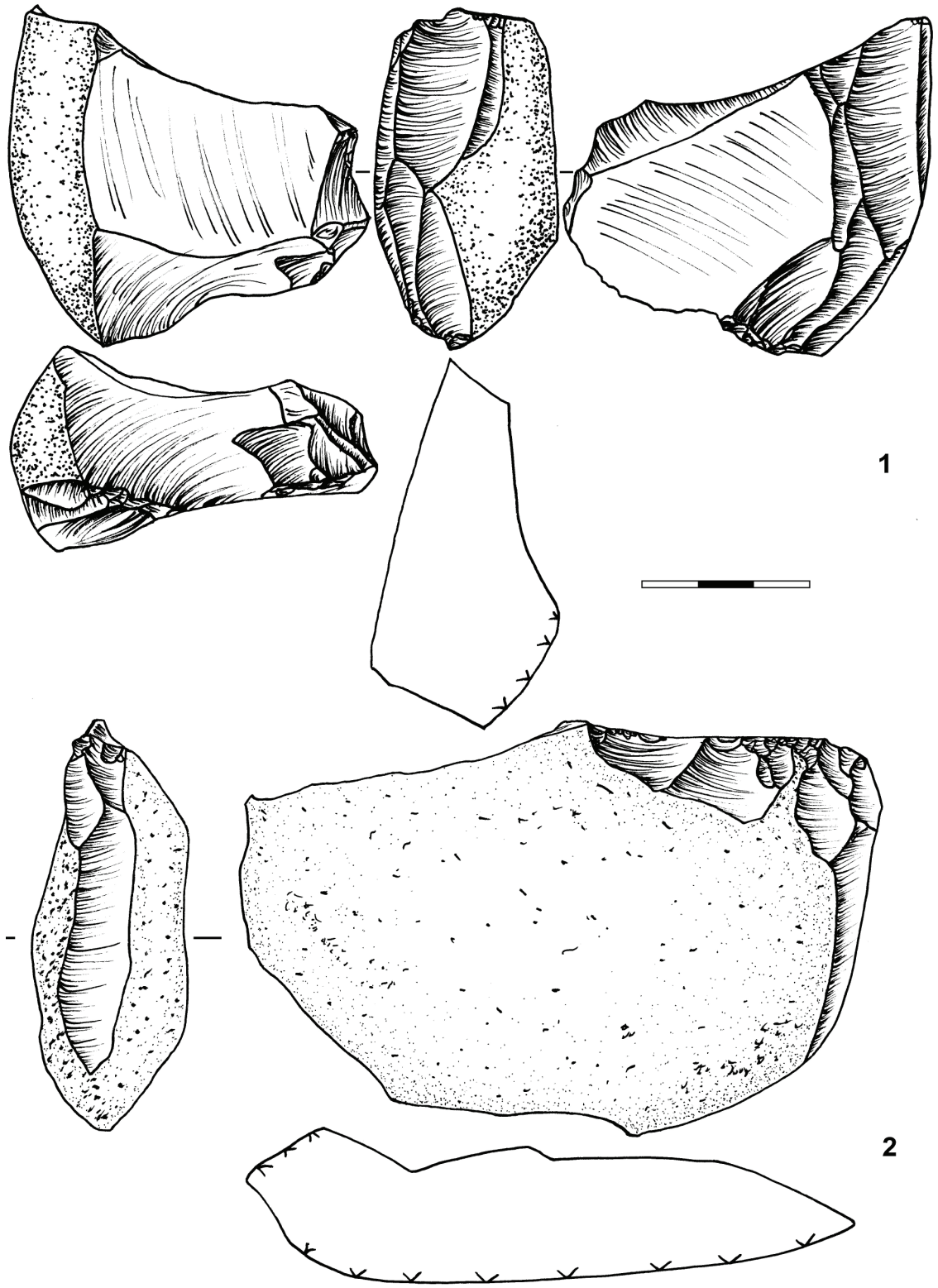


Fig. 8-31. Barmaky, western area complex, horizon 2c: 1 – pre-core for blades/bladelets, bidirectional, narrow flaking surface; 2 – pre-core for bladelets, unidirectional, narrow flaking surface.

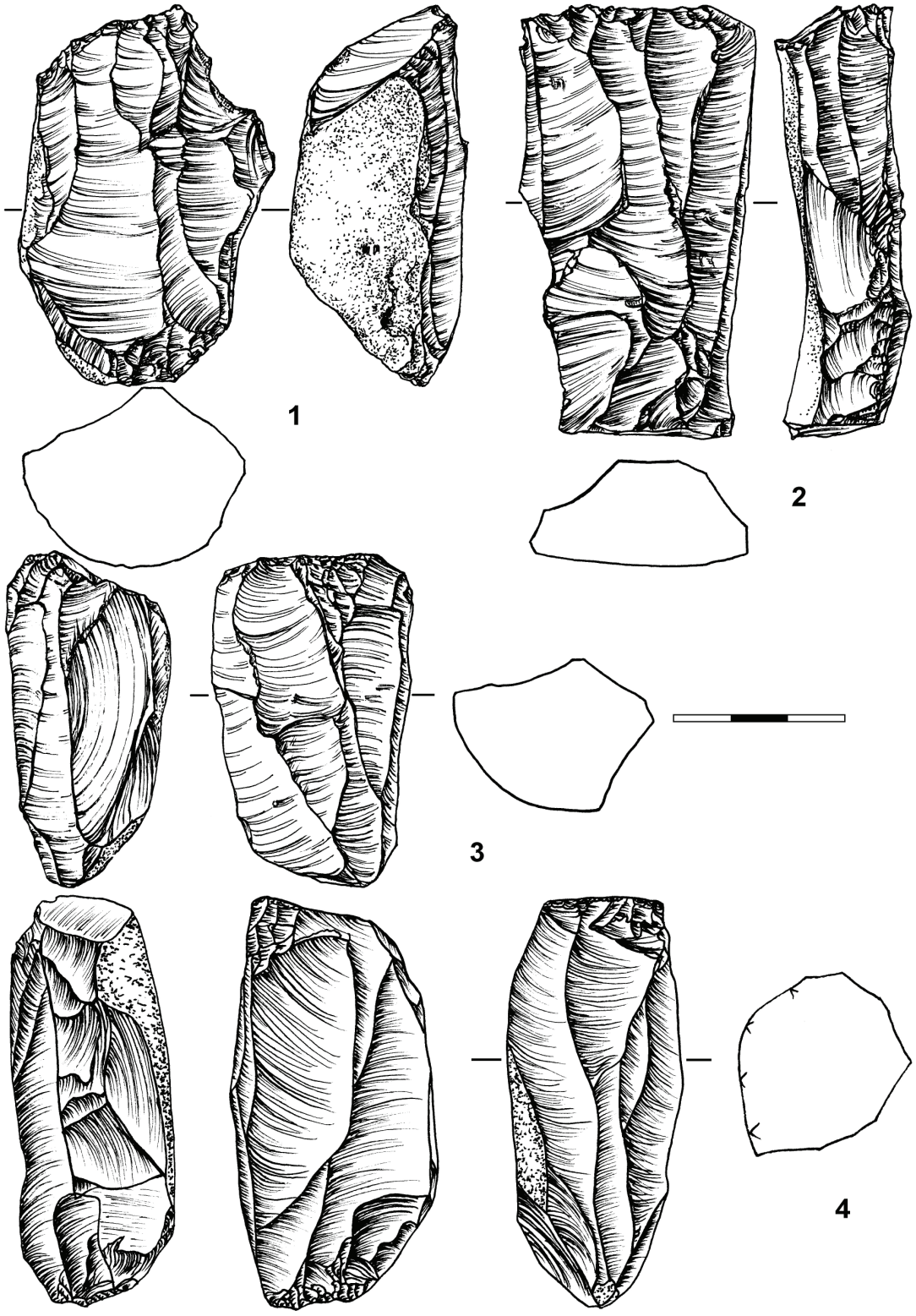


Fig. 8-32. Barmaky, western area complex, horizons 2c (1, 2, 4) & 2d (3), cores for blades: 1, 2, 4 – bidirectional, sub-cylindrical; 3 – unidirectional, sub-cylindrical.

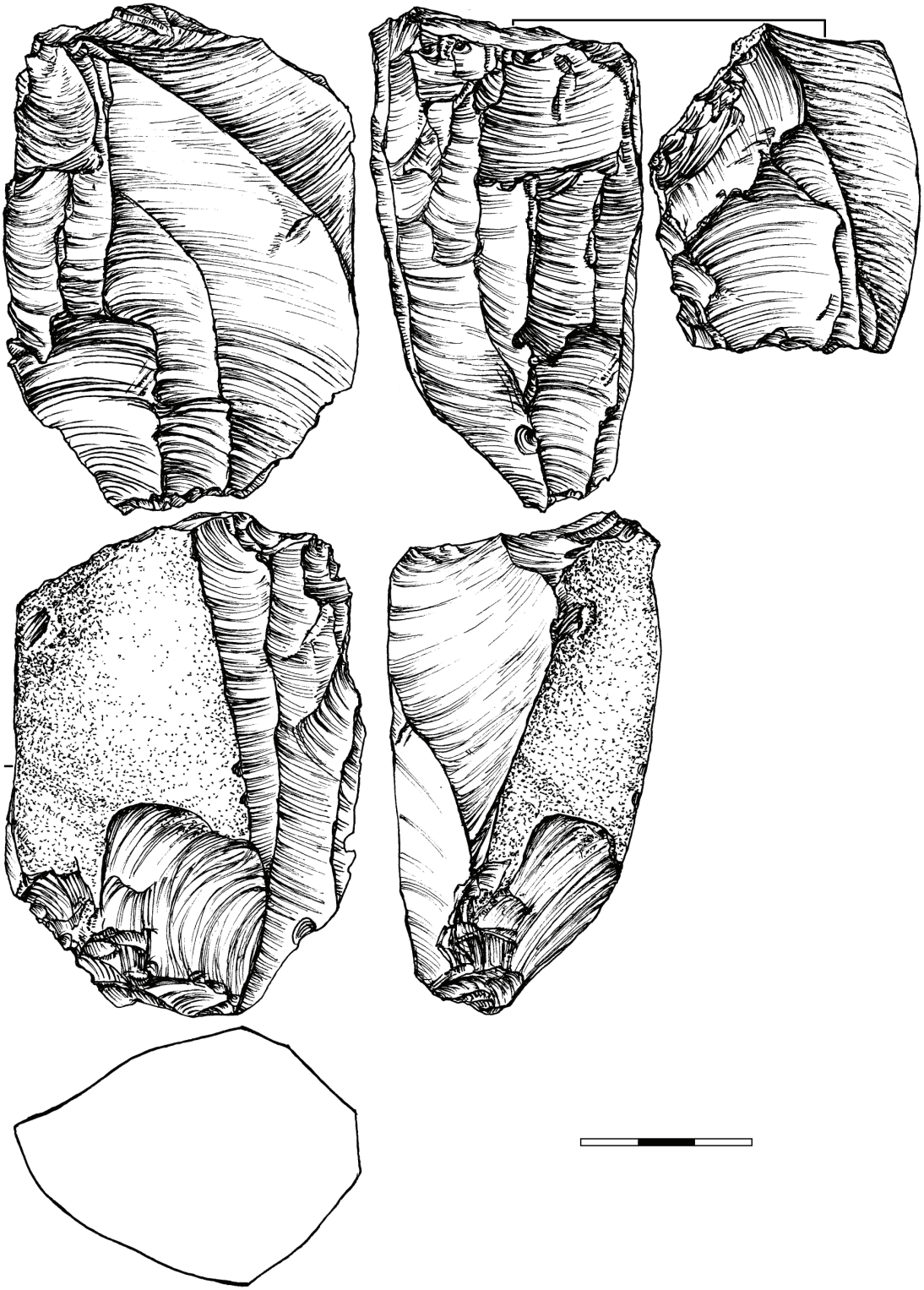

Fig. 8–33. Barmaky, western area complex, horizon 2c: core for blades, bidirectional, narrow flaking surface, wedge-shaped.

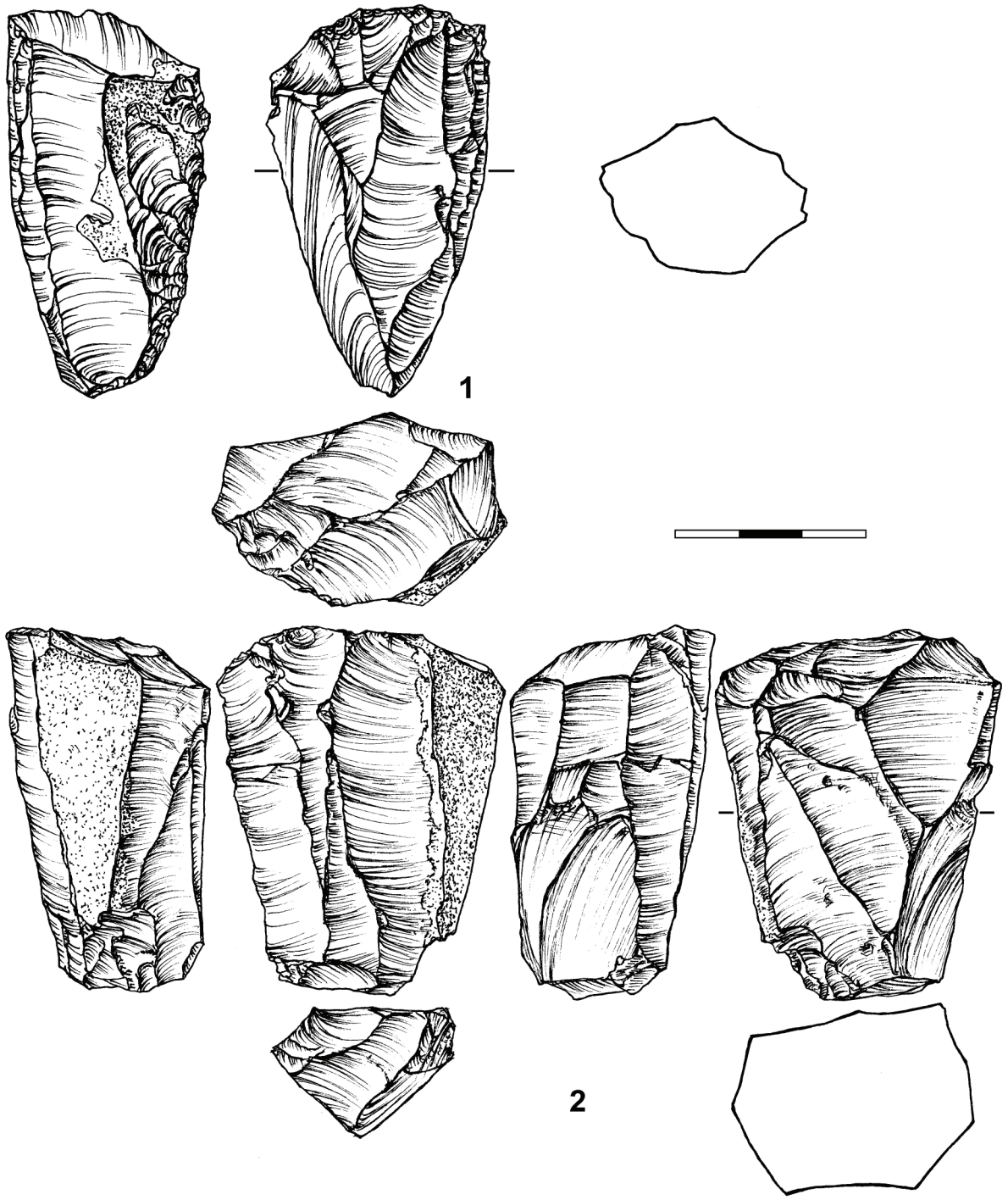


Fig. 8-34. Barmaky, western area complex, horizons 2d (1) & 2c (2), cores for blades: 1 – bidirectional-adjacent, sub-cylindrical/sub-pyramidal; 2 – bidirectional-alternate, sub-cylindrical.

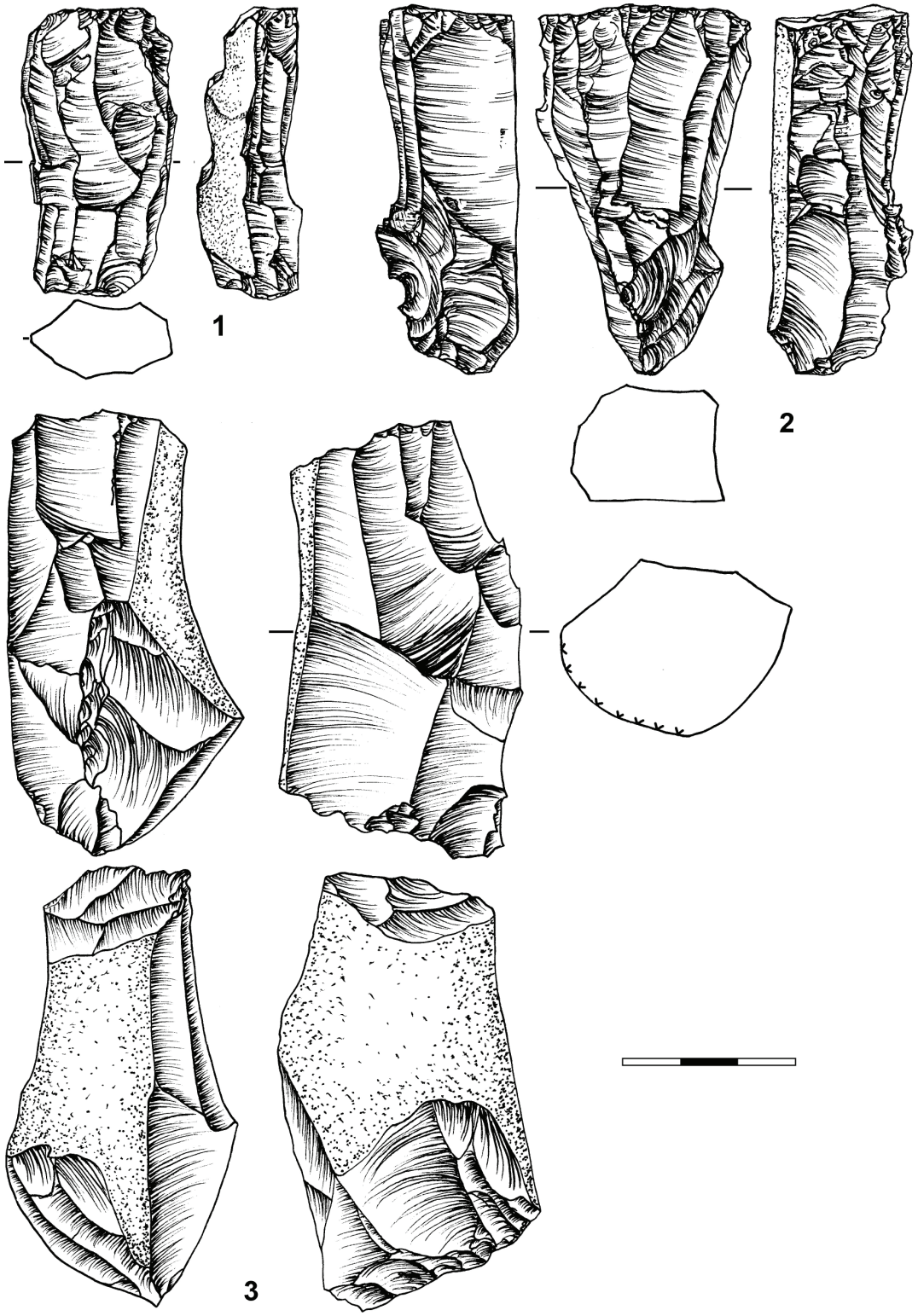


Fig. 8–35. Barmaky, western area complex, horizons 2d (1), 2c (2) & pit 1 (3): 1 – core for blades/bladelets, bidirectional, sub-cylindrical; 2 – core for blades/bladelets, bidirectional, sub-cylindrical/sub-pyramidal; 3 – core for blades, bidirectional, sub-cylindrical.

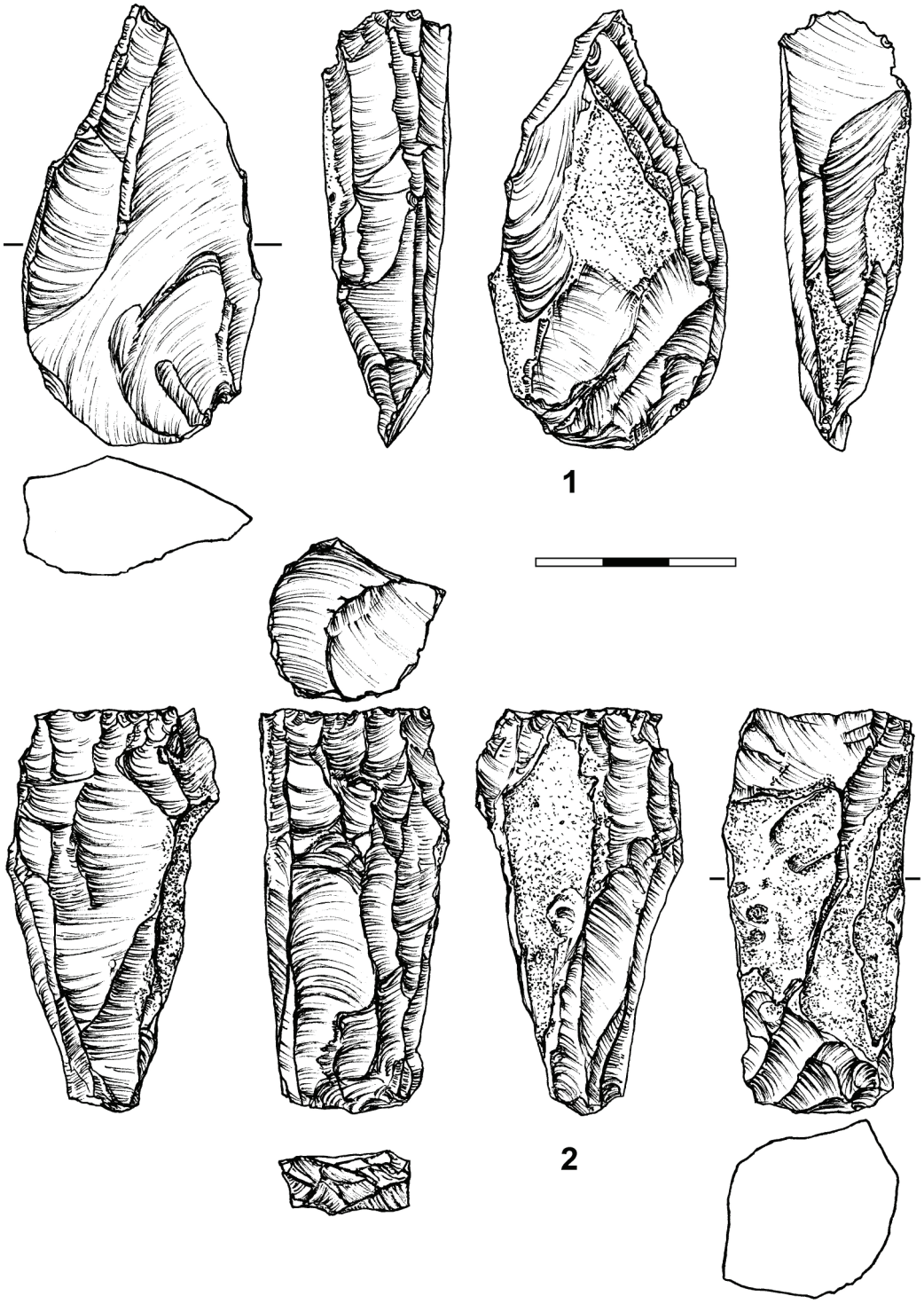


Fig. 8-36. Barmaky, western area complex, horizon 2c, cores for bladelets: 1 – unidirectional, narrow flaking surface, wedge-shaped; 2 – bidirectional, sub-cylindrical.

| | 2b | 2c, pit 1 | 2c | 2d | Σ | % |
|---|---|---|---|---|---|---|
| **BLADE PRE-CORES** | | | | | | |
| unidirectional, sub-cylindrical | – | – | – | 1 | **1** | 1,14 |
| unidirectional, narrow flaking surface | – | – | 1 | – | **1** | 1,14 |
| **BLADE / BLADELET PRE-CORES** | | | | | | |
| unidirectional, sub-cylindrical | – | – | – | 1 | **1** | 1,14 |
| unidirectional, narrow flaking surface | – | – | 7 | 2 | **9** | 10,23 |
| bidirectional, narrow flaking surface | – | – | 4 | – | **4** | 4,55 |
| **BLADELET PRE-CORES** | | | | | | |
| unidirectional, narrow flaking surface, wedge-shaped | – | – | – | 1 | **1** | 1,14 |
| unidirectional, narrow flaking surface | – | – | 3 | – | **3** | 3,41 |
| **UNIDENTIFIABLE PRE-CORES** | | | | | | |
| unidirectional, unidentifiable | – | – | 3 | 1 | **4** | 4,55 |
| unidentifiable | – | – | 1 | – | **1** | 1,14 |
| **FLAKE CORES** | | | | | | |
| bidirectional, sub-cylindrical | – | – | 1 | – | **1** | 1,14 |
| bidirectiomal-adjacent, sub-cylindrical | – | – | 1 | – | **1** | 1,14 |
| bidirectional-transversal, unidentifiable | – | – | – | 1 | **1** | 1,14 |
| **BLADE CORES** | | | | | | |
| unidirectional, sub-cylindrical | 1 | – | 1 | 2 | **4** | 4,55 |
| unidirectional, narrow flaking surface | – | 1 | 5 | – | **6** | 6,82 |
| unidirectional-alternate, narrow flaking surface | – | – | 1 | – | **1** | 1,14 |
| unidirectional, unidentifiable | – | – | 1 | 1 | **2** | 2,27 |
| bidirectional, sub-cylindrical | – | 1 | 3 | – | **4** | 4,55 |
| bidirectional-adjacent, syb-cylindrical | – | – | 1 | – | **1** | 1,14 |
| bidirectional-adjacent, sub-cylindrical / sub-pyramidal | – | – | – | 1 | **1** | 1,14 |
| bidirectional-alternate, sub-cylindrical | – | – | 3 | 1 | **4** | 4,55 |
| bidirectional, narrow flaking surface, wedge-shaped | – | – | 1 | – | **1** | 1,14 |
| bidirectional, narrow flaking surface | – | – | – | 1 | **1** | 1,14 |
| bidirectional-bilateral, narrow flaking surface | – | – | 1 | – | **1** | 1,14 |
| bidirectional, unidentifiable | – | 1 | – | 1 | **2** | 2,27 |
| **BLADE / BLADELET CORES** | | | | | | |
| unidirectional, syb-cylindrical | – | – | 2 | 1 | **3** | 3,41 |
| unidirectional, narrow flaking surface | – | – | 5 | – | **5** | 5,68 |
| unidirectional-alternate, narrow flaking surface | – | – | 1 | – | **1** | 1,14 |
| unidirectional, unidentifiable | – | – | 1 | – | **1** | 1,14 |
| bidirectional, syb-cylindrical | – | – | 1 | 2 | **3** | 3,41 |
| bidirectional, sub-cylindrical / sub-pyramidal | – | – | 1 | – | **1** | 1,14 |
| bidirectional-alternate, sub-cylindrical | – | – | 1 | – | **1** | 1,14 |
| bidirectional, laterally narrowed flaking surface | – | – | 1 | – | **1** | 1,14 |
| bidirectional-bilateral, narrow flaking surface | – | – | – | 1 | **1** | 1,14 |
| unsystematic, cubic | – | – | 1 | – | **1** | 1,14 |

Table 8-59. Barmaky, western area complex, by horizons and structures: core-like pieces

| | 2b | 2c, pit 1 | 2c | 2d | Σ | % |
|---|---|---|---|---|---|---|
| **BLADELET CORES** | | | | | | |
| unidirectional, narrow flaking surface, wedge-shaped | – | – | 1 | – | **1** | 1,14 |
| unidirectional, narrow flaking surface | – | – | 2 | – | **2** | 2,27 |
| bidirectional, sub-cylindrical | – | – | 1 | – | **1** | 1,14 |
| bidirectional, narrow flaking surface | – | – | 3 | 1 | **4** | 4,55 |
| multi-directional, narrow flaking surface | – | – | 3 | – | **3** | 3,41 |
| **MICRO-BLADE CORES** | | | | | | |
| unidirectional, narrow flaking surface, carinated | – | – | 1 | – | **1** | 1,14 |
| **UNIDENTIFIABLE CORES** | | | | | | |
| unidentifiable | – | 1 | 1 | – | **2** | 2,27 |
| **TOTAL:** | **1** | **4** | **64** | **19** | **88** | 100,00 |

Table 8-59. continued.

semi-abrupt retouch were applied to the lateral edges. Continuous scalar obverse abrupt retouch produced the proximal truncations. The average dimensions of end-scrapers on the blade and flake are 56.21×24.84×7.17 and 58.10×32.13×9.54 mm, respectively.

**Burins** on truncations (129 items) are the dominant type of this tool (Table 8-75), followed by angle (31), dihedral (35), transversal (2), combined (12), and unidentifiable (5) pieces. The vast majority of burins were made on blades (173 items), including crested (28), *débordantes* (32), and primary (4) pieces. Twenty flakes served as blanks for burins, including solitary crested, natural, primary, and four *débordante* pieces. In addition, 3 bladelets and 18 fragments of unidentifiable *débitage* were modified into burins.

Seventy "regular" blades, 17 crested, 18 *débordantes*, and 2 primary pieces represent the blanks for **burins on truncated blades** (Fig. 8-43*, 8, 9*; 8-44, 8-45, 8-46, 8-47; 8-48, *1, 3, 5, 6, 7*).

The most common type of truncation is oblique – 46 items (Fig. 8-43, *8, 9*; 8-44, *1-8*; 8-45, *1-6*), followed by oblique-convex (17) and oblique-concave (10) truncations (Fig. 8-44, *9*; 8-45, *7-9*; 8-46, *1, 4, 5-8*). In addition, straight and concave truncations were identified (Fig. 8-46, *2, 3*; 8-47, *1*). Burins on opposite, bi-terminal truncations show different combinations of truncations (Fig. 8-47, *2-6*; 8-48, *1, 3, 5-7*). In general, the simple one-edge forms dominate (83.18 %) the assemblage (Table 8-75).

Distal truncations made by scalar obverse abrupt retouch (45 pieces) compose about half of the identifiable modifications (Fig. 8-43, *8, 9*; 8-44, *1*, 8-45, *1, 2*; 8-46, *1, 3, 4*; 8-47, *1*). In addition, the same kind of retouch was found on 18 proximal parts of blades. A single blow oriented towards the dorsal surface truncated three blades; 14 blades show distal truncations made by sub-parallel obverse abrupt retouch. Other combinations of retouch are not numerous.

The 232 negatives of burin spalls and 128 burin edges are observed on 107 burins on truncated blades, indicating tool reutilisation/rejuvenation.

Twenty-one burins on truncated blades show clear traces of tool rejuvenation. The method of burin rejuvenation consists of the reorientation of the distal/proximal obliquely truncated part of the blade by rejuvenating truncation, which made the sharp angle between the newly truncated part and the lateral side opposite to the former burin edge. The byproducts of such rejuvenating truncation are the rejuvenating truncation spalls (Fig. 8-41, *2, 4, 8, 13*). Thus, the newly made burin negative on the lateral side is related to the sharp angle of distal/proximal truncation, while the former burin negative connects to the acute angle of present truncation (Fig. 8-47, *6*; 8-48, *7*). The reorientation of the truncation allows for removing another burin spall from the opposite lateral side of the blade (Fig. 8-44, *8, 9*; 8-46, *3, 7*; 8-47, *6*; 8-48, *3, 7*).

| | 2b | | 2c, pit 1 | | 2c | | 2d | |
|---|---|---|---|---|---|---|---|---|
| | # | % | # | % | # | % | # | % |
| **FLAKES** | | | | | | | | |
| regular | **17** | 73,91 | **110** | 74,83 | **1899** | 69,46 | **718** | 73,34 |
| lateral *débordantes* | **2** | 8,70 | **4** | 2,72 | **172** | 6,29 | **42** | 4,29 |
| cortical *débordantes* | **–** | – | **1** | 0,68 | **73** | 2,67 | **20** | 2,04 |
| natural *débordantes* | **–** | – | **1** | 0,68 | **40** | 1,46 | **12** | 1,23 |
| crested | **2** | 8,70 | **3** | 2,04 | **162** | 5,93 | **41** | 4,19 |
| core tablet | **1** | 4,35 | **1** | 0,68 | **24** | 0,88 | **12** | 1,23 |
| *Kantenabschläge* | **–** | – | **16** | 10,88 | **111** | 4,06 | **42** | 4,29 |
| primary | **1** | 4,35 | **10** | 6,80 | **228** | 8,34 | **89** | 9,09 |
| natural | **–** | | **1** | 0,68 | **25** | 0,91 | **3** | 0,31 |
| **TOTAL:** | **23** | 100,00 | **147** | 100,00 | **2734** | 100,00 | **979** | 100,00 |
| **BLADES** | | | | | | | | |
| regular | **8** | 88,89 | **23** | 45,10 | **810** | 63,53 | **265** | 64,95 |
| lateral *débordantes* | **–** | – | **4** | 7,84 | **109** | 8,55 | **29** | 7,11 |
| cortical *débordantes* | **–** | – | **8** | 15,69 | **79** | 6,20 | **20** | 4,90 |
| natural *débordantes* | **–** | – | **2** | 3,92 | **50** | 3,92 | **20** | 4,90 |
| crested | **–** | – | **12** | 23,53 | **201** | 15,76 | **64** | 15,69 |
| core tablet | **–** | – | **1** | 1,96 | **4** | 0,31 | **1** | 0,25 |
| primary | **1** | 11,11 | **1** | 1,96 | **22** | 1,73 | **9** | 2,21 |
| **TOTAL:** | **9** | 100,00 | **51** | 100,00 | **1275** | 100,00 | **408** | 100,00 |
| **BLADELETS** | | | | | | | | |
| regular | **4** | 57,14 | **33** | 78,57 | **642** | 70,39 | **223** | 70,13 |
| lateral *débordantes* | **2** | 28,57 | **1** | 2,38 | **83** | 9,10 | **23** | 7,23 |
| cortical *débordantes* | **–** | – | **3** | 7,14 | **48** | 5,26 | **15** | 4,72 |
| natural *débordantes* | **–** | – | **2** | 4,76 | **32** | 3,51 | **22** | 6,92 |
| crested | **1** | 14,29 | **3** | 7,14 | **94** | 10,31 | **32** | 10,06 |
| core tablet | **–** | – | **–** | – | **1** | 0,11 | **–** | – |
| primary | **–** | – | **–** | – | **12** | 1,32 | **3** | 0,94 |
| **TOTAL:** | **7** | 100,00 | **42** | 100,00 | **912** | 100,00 | **318** | 100,00 |
| **MICRO-BLADES** | | | | | | | | |
| regular | **2** | 66,67 | **20** | 83,33 | **446** | 74,21 | **112** | 77,24 |
| lateral *débordantes* | **1** | 33,33 | **1** | 4,17 | **87** | 14,48 | **21** | 14,48 |
| cortical *débordantes* | **–** | – | **1** | 4,17 | **17** | 2,83 | **–** | – |
| natural *débordantes* | **–** | – | **–** | – | **17** | 2,83 | **2** | 1,38 |
| crested | **–** | – | **2** | 8,33 | **33** | 5,49 | **10** | 6,90 |
| primary | **–** | – | **–** | – | **1** | 0,17 | **–** | – |
| **TOTAL:** | **3** | 100,00 | **24** | 100,00 | **601** | 100,00 | **145** | 100,00 |

Table 8-60. Barmaky, western area complex, by horizons and structures: *débitage* structure (including tools)

| | 2b | | 2c, pit 1 | | 2c | | 2d | |
|---|---|---|---|---|---|---|---|---|
| | # | % | # | % | # | % | # | % |
| **BURIN SPALLS** | | | | | | | | |
| primary | – | – | **6** | 46,15 | **78** | 16,49 | **11** | 13,25 |
| primary, retouched | – | – | – | – | **114** | 24,10 | **22** | 26,51 |
| secondary | **1** | 100,00 | **4** | 30,77 | **127** | 26,85 | **25** | 30,12 |
| secondary, retouched | – | – | **1** | 7,69 | **40** | 8,46 | **9** | 10,84 |
| multiple | – | – | **1** | 7,69 | **88** | 18,60 | **10** | 12,05 |
| multiple, retouched | – | – | **1** | 7,69 | **11** | 2,33 | **5** | 6,02 |
| multiple, bidirectional | – | – | – | – | **9** | 1,90 | – | – |
| multiple, bidirectional, retouched | – | – | – | – | **6** | 1,27 | **1** | 1,20 |
| **TOTAL:** | **1** | 100,00 | **13** | 100,00 | **473** | 100,00 | **83** | 100,00 |
| **TRUNCATION SPALLS** | | | | | | | | |
| initial | – | – | – | – | **20** | 37,04 | **2** | 50,00 |
| rejuvenating | – | – | – | – | **13** | 24,07 | **1** | 25,00 |
| secondary | – | – | – | – | **21** | 38,89 | **1** | 25,00 |
| **TOTAL:** | – | – | – | – | **54** | 100,00 | **4** | 100,00 |
| unidentifiable *débitage* | **15** | – | **92** | – | **1308** | – | **722** | – |

Table 8–60. continued.

Four more burins relate to the rejuvenation process. Two of them show obverse partial semi-abrupt retouch on the burin spall negative, probably as preparation for the removal of another spall. A burin on proximal truncation was made on a bi-terminally truncated blade; the distal truncation might be viewed as reserve for a burin spall in the opposite direction. The fourth burin shows an oblique proximal dorsal truncation, made after the burin spall detachment.

The burins on truncated blades were made on 37 retouched (Fig. 8-43, *8, 9*; 8-44, *1, 6*; 8-45, *3, 5*; 8-46, 1-3, *6, 8*; 8-47, *2*; 8-48, *6*), one notched (Fig. 8-48, *1*), and two inversely thinned pieces (Fig. 8-47, *6*; 8-48, *5*). Most parts of the blades were shaped by partial/discontinuous, scalar/marginal, obverse, and flat/semi-abrupt retouch. The average dimensions are 59.63×21.22×7.90 mm.

There are eight **burins on truncated flakes**, subdivided into seven types (Table 8-75). Five specimens have a single and three a double-working edge. One *débordante*, one primary, and six regular flakes served as the blanks. Straight, oblique-convex, concave, and oblique-concave distal/proximal truncations made by continuous, scalar, obverse, and abrupt retouch serve as striking platforms (Fig. 8-48, *2, 4, 8*). Eight burins exhibit 11 working edges shaped by 20 burin spalls negatives. Burins on oblique-concave distal dorsal truncation and on bi-lateral concave distal dorsal truncation show clear traces of rejuvenation, namely the reorientation of the distal truncation angles to the lateral sides. Four laterally retouched flakes serve as blanks for burin production (Fig. 8-48, *4, 8*). The combinations of retouch are continuous/discontinuous, marginal/scalar, obverse/alternating, and flat. The average dimensions are 51.26×34.19×10.44 mm.

Distal and proximal fragments of 14 tools represent **burins on truncated unidentifiable *débitage*** (Table 8-75; Fig. 8-49, *2, 4*). The straight and oblique truncated pieces prevail. Ten distal and four proximal parts of blanks were used for truncations. Two pieces were modified by obverse and inverse single-blow truncations. The continuous, scalar, obverse, abrupt retouch is the main method of truncation for eight pieces. Five burins were made on retouched pieces. The combinations of retouch are variable: continuous/discontinuous/partial, marginal/scalar/sub-parallel, and abrupt/semi-abrupt/flat. The only common attribute is the

| | | flakes | | blades | | bladelets | | micro-blades | |
|---|---|---|---|---|---|---|---|---|---|
| | | # | % | # | % | # | % | # | % |
| HORIZON 2b | complete | **14** | 60,87 | **3** | 33,33 | **–** | – | **1** | 33,33 |
| | distal | **5** | 21,74 | **2** | 22,22 | **3** | 42,86 | **–** | – |
| | lateral | **2** | 8,70 | **–** | – | **–** | – | **–** | – |
| | medial | **–** | – | **1** | 11,11 | **2** | 28,57 | **1** | 33,33 |
| | proximal | **2** | 8,70 | **3** | 33,33 | **2** | 28,57 | **1** | 33,33 |
| | **TOTAL:** | **23** | 100,00 | **9** | 100,00 | **7** | 100,00 | **3** | 100,00 |
| HORIZON 2c, pit 1 | complete | **90** | 61,22 | **24** | 47,06 | **15** | 35,71 | **5** | 20,83 |
| | distal | **21** | 14,29 | **15** | 29,41 | **6** | 14,29 | **9** | 37,50 |
| | lateral | **10** | 6,80 | **–** | – | **–** | – | **–** | – |
| | medial | **3** | 2,04 | **1** | 1,96 | **7** | 16,67 | **8** | 33,33 |
| | proximal | **23** | 15,65 | **11** | 21,57 | **14** | 33,33 | **2** | 8,33 |
| | **TOTAL:** | **147** | 100,00 | **51** | 100,00 | **42** | 100,00 | **24** | 100,00 |
| HORIZON 2c | complete | **1497** | 54,75 | **449** | 35,22 | **238** | 26,10 | **125** | 20,80 |
| | distal | **403** | 14,74 | **317** | 24,86 | **242** | 26,54 | **161** | 26,79 |
| | lateral | **277** | 10,13 | **1** | 0,08 | **–** | – | **1** | 0,17 |
| | medial | **126** | 4,61 | **218** | 17,10 | **205** | 22,48 | **179** | 29,78 |
| | proximal | **424** | 15,51 | **289** | 22,67 | **227** | 24,89 | **135** | 22,46 |
| | unidentifiable | **7** | 0,26 | **1** | 0,08 | **–** | – | **–** | – |
| | **TOTAL:** | **2734** | 100,00 | **1275** | 100,00 | **912** | 100,00 | **601** | 100,00 |
| HORIZON 2d | complete | **467** | 47,70 | **100** | 24,51 | **63** | 19,81 | **24** | 16,55 |
| | distal | **146** | 14,91 | **96** | 23,53 | **77** | 24,21 | **35** | 24,14 |
| | lateral | **137** | 13,99 | **–** | – | **–** | – | **1** | 0,69 |
| | medial | **61** | 6,23 | **101** | 24,75 | **93** | 29,25 | **63** | 43,45 |
| | proximal | **167** | 17,06 | **110** | 26,96 | **85** | 26,73 | **22** | 15,17 |
| | unidentifiable | **1** | 0,10 | **1** | 0,25 | **–** | – | **–** | – |
| | **TOTAL:** | **979** | 100,00 | **408** | 100,00 | **318** | 100,00 | **145** | 100,00 |

Table 8-61. Barmaky, western area complex, by horizons and structures: *débitage* conditions (including tools)

place of retouch: obverse. Twenty-one negatives of burin spalls form 14 working edges. The average width and thickness dimensions are 16.46 and 6.94, mm accordingly.

The **angle burins on blades** are subdivided into four groups: distal – 7 (Fig. 8-49, *1, 3, 6, 8*); proximal – 12 (Fig. 8-49, *9*); opposite – 1; and opposite-alternative – 1 (Table 8-75). Eight regular, 4 crested, 7 *débordante*, and 2 primary blades served as blanks. Eight burins were made on retouched blades (Fig. 8-49, *1, 8, 9*). The combinations of retouch are very variable: continuous/discontinuous/partial, marginal/scalar, obverse/alternating/ alternate, abrupt/semi-abrupt/flat. Twenty-one burin edges exhibit 30 burin spall negatives. The mean length, width, and thickness dimensions are >48.89, 23.83, and 8.61 mm. One of the burins was rejuvenated by oblique proximal dorsal truncations (Fig. 8-49, *9*).

Two fragments of distal **angle burins on bladelets** (>26.63×10.01×3.69 and >22.85×11.40×4.54 mm) were identified. Three negatives of burin spalls form two burin edges.

The **angle burins on flakes** consist of four distal and four proximal specimens (Table 8-75; Fig. 8-49, *5*; 8-50, *4-6*). Four regular flakes, 3 *débordantes*, and one natural flake served as the blanks. Two angle burins were made on laterally and laterally-distally retouched flakes (Fig. 8-49, *5*). These tools were shaped by partial/continuous, scalar, obverse, and semi-abrupt retouch. Eight burin edges were made by 11 burin spalls. The average dimensions are >46.54×33.37×9.74 mm.

The **dihedral burins on blades** are represented by symmetrical – 13 pieces (Fig. 8-49, *7*; 8-50, *1-3*, *7*; 8-51, *5*), asymmetrical – 13 pieces (Fig. 8-51, *1, 2, 4*; 8-52, *5, 6*), and bi-terminal symmetrical and asymmetrical pieces

| | | | flakes | | blades | | bladelets | | micro-blades | |
|---|---|---|---|---|---|---|---|---|---|---|
| | | | # | % | # | % | # | % | # | % |
| HORIZON 2b | rectangular | on-axis | **4** | 21,05 | **3** | 50,00 | **–** | – | **–** | – |
| | | off-axis | **2** | 10,53 | **1** | 16,67 | **–** | – | **–** | – |
| | trapezoidal | on-axis | **2** | 10,53 | **–** | – | **–** | – | **–** | – |
| | | off-axis | **4** | 21,05 | **–** | – | **1** | 33,33 | **–** | – |
| | triangular | on-axis | **2** | 10,53 | **–** | – | **–** | – | **–** | – |
| | | off-axis | **1** | 5,26 | **–** | – | **–** | – | **–** | – |
| | | unidentifiable | **–** | – | **1** | 16,67 | **–** | – | **–** | – |
| | crescent | off-axis | **1** | 5,26 | **–** | – | **1** | 33,33 | **1** | 100,00 |
| | irregular | off-axis | **3** | 15,79 | **1** | 16,67 | **1** | 33,33 | **–** | – |
| | | **TOTAL:** | **19** | 100,00 | **6** | 100,00 | **3** | 100,00 | **1** | 100,00 |
| | unidentifiable | | 4 | – | 3 | – | 4 | – | 2 | – |
| HORIZON 2c, pit 1 | rectangular | on-axis | **11** | 9,91 | **10** | 26,32 | **–** | – | **1** | 6,67 |
| | | off-axis | **8** | 7,21 | **6** | 15,79 | **3** | 13,64 | **3** | 20,00 |
| | trapezoidal | on-axis | **7** | 6,31 | **–** | – | **–** | – | **–** | – |
| | | off-axis | **41** | 36,94 | **9** | 23,68 | **4** | 18,18 | **4** | 26,67 |
| | | unidentifiable | **1** | 0,90 | **–** | – | **–** | – | **–** | – |
| | triangular | on-axis | **–** | – | **1** | 2,63 | **–** | – | **2** | 13,33 |
| | | off-axis | **10** | 9,01 | **1** | 2,63 | **3** | 13,64 | **1** | 6,67 |
| | leaf-shaped | on-axis | **2** | 1,80 | **–** | – | **1** | 4,55 | **1** | 6,67 |
| | | off-axis | **1** | 0,90 | **4** | 10,53 | **–** | – | **1** | 6,67 |
| | ovoid | on-axis | **2** | 1,80 | **–** | – | **1** | 4,55 | **–** | – |
| | | off-axis | **5** | 4,50 | **–** | – | **–** | – | **–** | – |
| | crescent | off-axis | **3** | 2,70 | **3** | 7,89 | **4** | 18,18 | **2** | 13,33 |
| | expanding | on-axis | **–** | – | **–** | – | **1** | 4,55 | **–** | – |
| | irregular | off-axis | **20** | 18,02 | **4** | 10,53 | **5** | 22,73 | **–** | – |
| | | **TOTAL:** | **111** | 100,00 | **38** | 100,00 | **22** | 100,00 | **15** | 100,00 |
| | unidentifiable | | 36 | – | 13 | – | 20 | – | 9 | – |

Table 8-62. Barmaky, western area complex, by horizons and structures: *débitage* shapes & axis (including tools)

– 3 pieces (Fig. 8-52, *1, 2, 4*) (Table 8-75). Twenty regular, 7 crested, and 2 *débordantes* pieces served as blanks. Nine burins show the following combinations of lateral retouch: continuous/partial, marginal/scalar/micro-scalar/sub-parallel, obverse/inverse, and flat/semi-abrupt/abrupt. There are no dominant retouch combinations for the lateral modification of dihedral burins. Twice, the proximal parts of dihedral burins were modified by dorsal and ventral truncations (Fig. 8-51, *5*; 8-52, *6*). A total of 92 burin spall negatives formed 32 burin edges. The average dimensions are 63.36×23.19×8.38 mm.

There are two more **dihedral burins on flakes**, one distal symmetrical (9.05×18.89×3.94 mm) and one distal asymmetrical (56.37×36.56×6.91 mm) piece (Fig. 8-51, *3, 6*; Table 8-75). Both were shaped by lateral dorsal and ventral retouch. Eight negatives of burin spalls form two burin edges.

The **dihedral burins on unidentifiable *débitage*** belong to the symmetrical (1 item) and asymmetrical (3 items) type (Table 8-75). One of the asymmetrical dihedral burins was made on the laterally continuously dorsally modified piece by micro-scalar abrupt retouch. This piece exhibits traces of oblique truncation on the distal end, which was removed by burin spalls. Thus, the former burin on oblique truncation was modified into the dihedral asymmetrical type. Thirteen negatives of burin spalls formed four burin edges. The average dimensions are >20.40×14.95×6.57 mm.

| | | | flakes | | blades | | bladelets | | micro-blades | |
|---|---|---|---|---|---|---|---|---|---|---|
| | | | # | % | # | % | # | % | # | % |
| HORIZON 2c | rectangular | on-axis | **220** | 11,82 | **157** | 20,79 | **120** | 23,39 | **70** | 23,26 |
| | | off-axis | **143** | 7,68 | **48** | 6,36 | **25** | 4,87 | **13** | 4,32 |
| | | unidentifiable | **3** | 0,16 | **2** | 0,26 | **–** | – | **1** | 0,33 |
| | trapezoidal | on-axis | **90** | 4,83 | **15** | 1,99 | **12** | 2,34 | **5** | 1,66 |
| | | off-axis | **629** | 33,78 | **127** | 16,82 | **75** | 14,62 | **33** | 10,96 |
| | | unidentifiable | **6** | 0,32 | **2** | 0,26 | **–** | – | **1** | 0,33 |
| | triangular | on-axis | **25** | 1,34 | **21** | 2,78 | **30** | 5,85 | **27** | 8,97 |
| | | off-axis | **54** | 2,90 | **27** | 3,58 | **36** | 7,02 | **16** | 5,32 |
| | | unidentifiable | **–** | – | **1** | 0,13 | **1** | 0,19 | **2** | 0,66 |
| | leaf-shaped | on-axis | **35** | 1,88 | **51** | 6,75 | **25** | 4,87 | **18** | 5,98 |
| | | off-axis | **31** | 1,66 | **38** | 5,03 | **14** | 2,73 | **9** | 2,99 |
| | | unidentifiable | **1** | 0,05 | **–** | – | **–** | – | **–** | – |
| | ovoid | on-axis | **93** | 4,99 | **9** | 1,19 | **3** | 0,58 | **–** | – |
| | | off-axis | **80** | 4,30 | **7** | 0,93 | **2** | 0,39 | **–** | – |
| | | unidentifiable | **2** | 0,11 | **–** | – | **–** | – | **–** | – |
| | crescent | on-axis | **3** | 0,16 | **1** | 0,13 | **2** | 0,39 | **4** | 1,33 |
| | | off-axis | **81** | 4,35 | **92** | 12,19 | **72** | 14,04 | **59** | 19,60 |
| | | unidentifiable | **2** | 0,11 | **–** | – | **–** | – | **–** | – |
| | expanding | on-axis | **52** | 2,79 | **23** | 3,05 | **9** | 1,75 | **3** | 1,00 |
| | | off-axis | **65** | 3,49 | **19** | 2,52 | **6** | 1,17 | **4** | 1,33 |
| | | unidentifiable | **–** | – | **4** | 0,53 | **1** | 0,19 | **–** | – |
| | irregular | on-axis | **–** | – | **–** | – | **2** | 0,39 | **–** | – |
| | | off-axis | **243** | 13,05 | **111** | 14,70 | **78** | 15,20 | **36** | 11,96 |
| | | unidentifiable | **4** | 0,21 | **–** | – | **–** | – | **–** | – |
| | | **TOTAL:** | **1862** | 100,00 | **755** | 100,00 | **513** | 100,00 | **301** | 100,00 |
| | unidentifiable | on-axis | 5 | – | 19 | – | 13 | – | 6 | – |
| | | off-axis | 53 | – | 31 | – | 23 | – | 11 | – |
| | | unidentifiable | 814 | – | 470 | – | 363 | – | 283 | – |

Table 8-62. continued 1

A regular flake (43.24×43.76×11.42 mm) and a *débordante* blade (>40.76×32.51×13.94 mm) served as blanks for distal **transversal burins** (Table 8-75; Fig. 8-52, *3*) with four and two negatives of burin spalls, respectively.

**Combined burins on blades** (Table 8-75) comprise burins on truncations and dihedral burins – 6 items (Fig. 8-52, *7*; 8-53, *3, 4, 6, 7*; 8-54, *6*), burins on truncations and angle burins – 4 items (Fig. 8-53, *1, 2, 5*), angle and dihedral burin – 1 item, and dihedral and transversal burin – 1 item (Fig. 8-54, *9*). Seven regular, one crested, and four *débordantes* served as blanks. The combined burin on oblique-convex distal dorsal truncation / dihedral-asymmetrical, proximal shows bilateral partial scalar/parallel obverse retouch (Fig. 8-53, *4*). Obverse and inverse abrupt one-blow distal truncation was applied for modifications of two distal extremities. Eight truncations were done by continuous, marginal/scalar/sub-parallel, obverse, and abrupt/semi-abrupt retouch. Twelve combined burins exhibit 22 working edges shaped by 61 burin spalls negatives. The average dimensions are 67.08×24.01×11.04 mm.

Four blades and one flake fragment are classified as **unidentifiable burins** (Table 8-75). The burin edges were made on the distal (3 items), proximal (1 item), and lateral (1 item) sides of the blanks. One distal burin was produced on the distal part of a blade, shaped by bi-lateral continuous scalar obverse flat retouch. A bilateral, partial scalar obverse flat

| | | | flakes | | blades | | bladelets | | micro-blades | |
|---|---|---|---|---|---|---|---|---|---|---|
| | | | # | % | # | % | # | % | # | % |
| HORIZON 2d | rectangular | on-axis | **90** | 15,28 | **48** | 25,00 | **29** | 19,59 | **12** | 20,69 |
| | | off-axis | **42** | 7,13 | **28** | 14,58 | **8** | 5,41 | **2** | 3,45 |
| | | unidentifiable | **1** | 0,17 | **–** | – | **–** | – | **1** | 1,72 |
| | trapezoidal | on-axis | **35** | 5,94 | **1** | 0,52 | **–** | – | **1** | 1,72 |
| | | off-axis | **241** | 40,92 | **34** | 17,71 | **22** | 14,86 | **8** | 13,79 |
| | | unidentifiable | **–** | – | **1** | 0,52 | **–** | – | **–** | – |
| | triangular | on-axis | **3** | 0,51 | **9** | 4,69 | **13** | 8,78 | **9** | 15,52 |
| | | off-axis | **22** | 3,74 | **13** | 6,77 | **11** | 7,43 | **2** | 3,45 |
| | | unidentifiable | **–** | – | **1** | 0,52 | **–** | – | **–** | – |
| | leaf-shaped | on-axis | **13** | 2,21 | **10** | 5,21 | **10** | 6,76 | **3** | 5,17 |
| | | off-axis | **11** | 1,87 | **2** | 1,04 | **4** | 2,70 | **–** | – |
| | ovoid | on-axis | **17** | 2,89 | **2** | 1,04 | **1** | 0,68 | **–** | – |
| | | off-axis | **14** | 2,38 | **–** | – | **–** | – | **–** | – |
| | crescent | off-axis | **12** | 2,04 | **25** | 13,02 | **32** | 21,62 | **17** | 29,31 |
| | expanding | on-axis | **16** | 2,72 | **4** | 2,08 | **2** | 1,35 | **–** | – |
| | | off-axis | **3** | 0,51 | **–** | – | **1** | 0,68 | **1** | 1,72 |
| | irregular | off-axis | **68** | 11,54 | **14** | 7,29 | **14** | 9,46 | **2** | 3,45 |
| | | unidentifiable | **1** | 0,17 | **–** | – | **1** | 0,68 | **–** | – |
| | | **TOTAL:** | **589** | 100,00 | **192** | 100,00 | **148** | 100,00 | **58** | 100,00 |
| | unidentifiable | on-axis | – | – | 1 | – | 2 | – | – | – |
| | | off-axis | 2 | – | 6 | – | 5 | – | – | – |
| | | unidentifiable | 388 | – | 209 | – | 163 | – | 87 | – |

Table 8-62. continued 2.

retouch modified the unidentifiable burin on the flake fragment (>47.04×33.05×5.33 mm). Probably five working edges were done by six burin spalls. The average dimensions are >39.40×18.64×5.22 mm.

Overall, 214 burins exhibit 256 burin edges created by 507 burin spall negatives. The burin spall negatives–to–burin ratio is 2.37 to 1; the burin spalls–to–burin ratio is 2.66 to 1.

**Truncated pieces on blades** constitute about 60 % of all truncated pieces (Table 8-76; Fig. 8-54, *1-5, 7, 8*; 8-55, *3, 4, 6, 7, 8, 10-12*), made on 42 regular, 7 crested, and 8 *débordante* pieces. Straight (7 items), oblique (27 items), oblique-convex (10 items), oblique-concave (4 items), convex (3 items), concave (2 items), bi-terminal oblique (2 items), bi-terminal oblique/convex (1 item), and bi-terminal oblique/wavy truncations are observed. Thirty-one distal (Fig. 8-54, *1, 3, 4, 7, 8*; 8-55, *3, 4, 7, 11*), 22 proximal (Fig. 8-54, *2, 5*; 8-55, *6, 8*), and 4 bi-terminal (Fig. 8-55, *10, 12*) parts of blades were truncated. The most common variants of retouch used for truncations are continuous scalar obverse abrupt (27 pieces) and continuous sub-parallel obverse abrupt (11 pieces). Two distal parts of blades were truncated by single-blow obverse abrupt retouch. Eleven truncated blades were done on laterally (9 items) and bi-laterally (2 items) dorsally retouched pieces (Fig. 8-54, *8*; 8-55, *11*). The obverse lateral retouch is the only common attribute, among a vast variety of combinations: continuous/discontinuous/partial, marginal/scalar/sub-parallel, and flat/semi-abrupt/abrupt. The average dimensions are 52.70×18.90×6.23 mm.

**Truncated pieces on bladelets** are not numerous and are represented by straight (3 items), oblique (5 items), oblique-convex (2 items), and oblique-concave (3 items) truncations (Table 8-76; Fig. 8-55, *1, 2*). Ten regular, two crested, and one *débordante* bladelets served as the blanks for truncated

| | | flakes | | blades | | bladelets | | micro-blades | |
|---|---|---|---|---|---|---|---|---|---|
| | | # | % | # | % | # | % | # | % |
| HORIZON 2b | straight | **5** | 22,73 | **4** | 44,44 | **1** | 16,67 | **–** | – |
| | convex | **3** | 13,64 | **–** | – | **1** | 16,67 | **1** | 50,00 |
| | incurvate proximal | **2** | 9,09 | **1** | 11,11 | **–** | – | **1** | 50,00 |
| | incurvate medial | **5** | 22,73 | **–** | – | **1** | 16,67 | **–** | – |
| | incurvate distal | **3** | 13,64 | **1** | 11,11 | **2** | 33,33 | **–** | – |
| | twisted | **4** | 18,18 | **3** | 33,33 | **1** | 16,67 | **–** | – |
| | **TOTAL:** | **22** | 100,00 | **9** | 100,00 | **6** | 100,00 | **2** | 100,00 |
| | unidentifiable | 1 | – | – | – | 1 | – | 1 | – |
| HORIZON 2c, pit 1 | straight | **51** | 37,23 | **15** | 29,41 | **13** | 31,71 | **10** | 43,48 |
| | convex | **15** | 10,95 | **3** | 5,88 | **1** | 2,44 | **2** | 8,70 |
| | incurvate proximal | **6** | 4,38 | **3** | 5,88 | **3** | 7,32 | **–** | – |
| | incurvate medial | **22** | 16,06 | **11** | 21,57 | **5** | 12,20 | **1** | 4,35 |
| | incurvate distal | **35** | 25,55 | **11** | 21,57 | **2** | 4,88 | **3** | 13,04 |
| | twisted | **8** | 5,84 | **8** | 15,69 | **17** | 41,46 | **7** | |
| | **TOTAL:** | **137** | 100,00 | **51** | 100,00 | **41** | 100,00 | **23** | 69,57 |
| | unidentifiable | 10 | – | – | – | 1 | – | 1 | – |
| HORIZON 2c | straight | **976** | 39,77 | **440** | 39,53 | **341** | 44,81 | **250** | 50,40 |
| | convex | **294** | 11,98 | **25** | 2,25 | **18** | 2,37 | **17** | 3,43 |
| | incurvate proximal | **75** | 3,06 | **52** | 4,67 | **32** | 4,20 | **13** | 2,62 |
| | incurvate medial | **389** | 15,85 | **241** | 21,65 | **115** | 15,11 | **54** | 10,89 |
| | incurvate distal | **463** | 18,87 | **147** | 13,21 | **73** | 9,59 | **39** | 7,86 |
| | twisted | **257** | 10,47 | **208** | 18,69 | **182** | 23,92 | **123** | 24,80 |
| | **TOTAL:** | **2454** | 100,00 | **1113** | 100,00 | **761** | 100,00 | **496** | 100,00 |
| | unidentifiable | 280 | – | 162 | – | 151 | – | 105 | – |
| HORIZON 2d | straight | **360** | 40,77 | **145** | 38,16 | **126** | 41,86 | **75** | 55,97 |
| | convex | **84** | 9,51 | **5** | 1,32 | **7** | 2,33 | **2** | 1,49 |
| | incurvate proximal | **27** | 3,06 | **16** | 4,21 | **14** | 4,65 | **5** | 3,73 |
| | incurvate medial | **141** | 15,97 | **87** | 22,89 | **55** | 18,27 | **13** | 9,70 |
| | incurvate distal | **179** | 20,27 | **48** | 12,63 | **25** | 8,31 | **8** | 5,97 |
| | twisted | **92** | 10,42 | **79** | 20,79 | **74** | 24,58 | **31** | 23,13 |
| | **TOTAL:** | **883** | 100,00 | **380** | 100,00 | **301** | 100,00 | **134** | 100,00 |
| | unidentifiable | 96 | – | 28 | – | 17 | – | 11 | – |

Table 8-63. Barmaky, western area complex, by horizons and structures: *débitage* lateral profiles (including tools)

pieces. All except one exhibit distal dorsal truncations. The exception, an obliquely proximally ventrally truncated bladelet, is the only complete piece (30.59×11.37×4.58 mm). The continuous scalar obverse semi-abrupt/abrupt retouch (8 pieces) is the most characteristic type of truncation. A single bladelet with a straight distal dorsal truncation shows an additional modification of the lateral edge, a dorsal notch. The average dimensions are 30.59×9.85×3.59 mm.

There is a single **truncated piece on a *débordante* micro-blade** (Table 8-76), measuring 32.49×6.94×2.92 mm. The distal oblique truncation was done by the continuous micro-scalar inverse abrupt retouch. Most likely, the truncated pieces on bladelets and micro-blades are unfinished microlithic insets for distant weapons. At least, the obliquely truncated base is the common component of microgravette straight-backed points in Barmaky assemblage.

| | | flakes | | blades | | bladelets | | micro-blades | |
|---|---|---|---|---|---|---|---|---|---|
| | | # | % | # | % | # | % | # | % |
| HORIZON 2b | feathering | **8** | 40,00 | **2** | 66,67 | **1** | 50,00 | **–** | – |
| | blunt | **3** | 15,00 | **1** | 33,33 | **–** | – | **–** | – |
| | hinged | **9** | 45,00 | **–** | – | **1** | 50,00 | **1** | 100,00 |
| | **TOTAL:** | **20** | 100,00 | **3** | 100,00 | **2** | 100,00 | **1** | 100,00 |
| | missing | 2 | – | 4 | – | 4 | – | 2 | – |
| | modified | – | – | 2 | – | 1 | – | – | – |
| | unidentifiable | 1 | – | – | – | – | – | – | – |
| HORIZON 2c, pit 1 | feathering | **71** | 60,17 | **15** | 45,45 | **16** | 76,19 | **10** | 76,92 |
| | blunt | **12** | 10,17 | **5** | 15,15 | **2** | 9,52 | **2** | 15,38 |
| | hinged | **34** | 28,81 | **11** | 33,33 | **3** | 14,29 | **1** | 7,69 |
| | overpassed | **1** | 0,85 | **2** | 6,06 | **–** | – | **–** | – |
| | **TOTAL:** | **118** | 100,00 | **33** | 100,00 | **21** | 100,00 | **13** | 100,00 |
| | missing | 29 | – | 12 | – | 21 | – | 10 | – |
| | modified | – | – | 6 | – | – | – | 1 | – |
| HORIZON 2c | feathering | **1186** | 58,02 | **333** | 52,86 | **284** | 60,43 | **182** | 65,00 |
| | blunt | **228** | 11,15 | **87** | 13,81 | **44** | 9,36 | **14** | 5,00 |
| | hinged | **601** | 29,40 | **158** | 25,08 | **136** | 28,94 | **83** | 29,64 |
| | overpassed | **29** | 1,42 | **52** | 8,25 | **6** | 1,28 | **1** | 0,36 |
| | **TOTAL:** | **2044** | 100,00 | **630** | 100,00 | **470** | 100,00 | **280** | 100,00 |
| | missing | 632 | – | 491 | – | 427 | – | 314 | – |
| | modified | 36 | – | 151 | – | 11 | – | 6 | – |
| | unidentifiable | 22 | – | 3 | – | 4 | – | 1 | – |
| HORIZON 2d | feathering | **395** | 57,25 | **79** | 49,07 | **90** | 66,18 | **42** | 71,19 |
| | blunt | **75** | 10,87 | **23** | 14,29 | **11** | 8,09 | **–** | – |
| | hinged | **206** | 29,86 | **36** | 22,36 | **32** | 23,53 | **14** | 23,73 |
| | overpassed | **14** | 2,03 | **23** | 14,29 | **3** | 2,21 | **3** | 5,08 |
| | **TOTAL:** | **690** | 100,00 | **161** | 100,00 | **136** | 100,00 | **59** | 100,00 |
| | missing | 282 | – | 206 | – | 177 | – | 83 | – |
| | modified | 4 | – | 38 | – | 4 | – | 1 | – |
| | unidentifiable | 3 | – | 3 | – | 1 | – | 2 | – |

Table 8-64. Barmaky, western area, by horizons and structures: *débitage* distal profiles (including tools)

Straight (3 items), oblique (5 items), oblique-convex (2 items), oblique concave (1 item) convex (1 item), and bi-terminal straight (2 items) truncations make up the **truncated pieces on flakes** (Table 8-76; Fig. 8-55, *5, 9*). Nine regular, one crested, one *débordante*, one *Kantenabschlag*, and 2 primary flakes served as blanks for truncated pieces on flakes. The following combinations of retouch for truncations were observed: single-blow truncations – 3 pieces; continuous scalar inverse/obverse semi-abrupt/abrupt – 8 pieces; continuous sub-parallel obverse semi-abrupt/abrupt – 2 pieces; partial sub-parallel inverse flat – 1 piece. Two pieces show a lateral partial scalar obverse semi-abrupt retouch. The average dimensions are 44.45×30.57×9.42 mm.

There are two **truncated pieces on natural flakes**: straightly and concavely truncated (Table 8-76). Both truncations were made by continuous scalar inverse abrupt retouches. The dimensions of these pieces are 51.50×62.89×17.86 and 63.92×47.02×24.99 mm. These truncated pieces on natural flakes are technologically and typologically very close to the narrow flaking surface pre-cores; the truncated parts might serve as striking platforms.

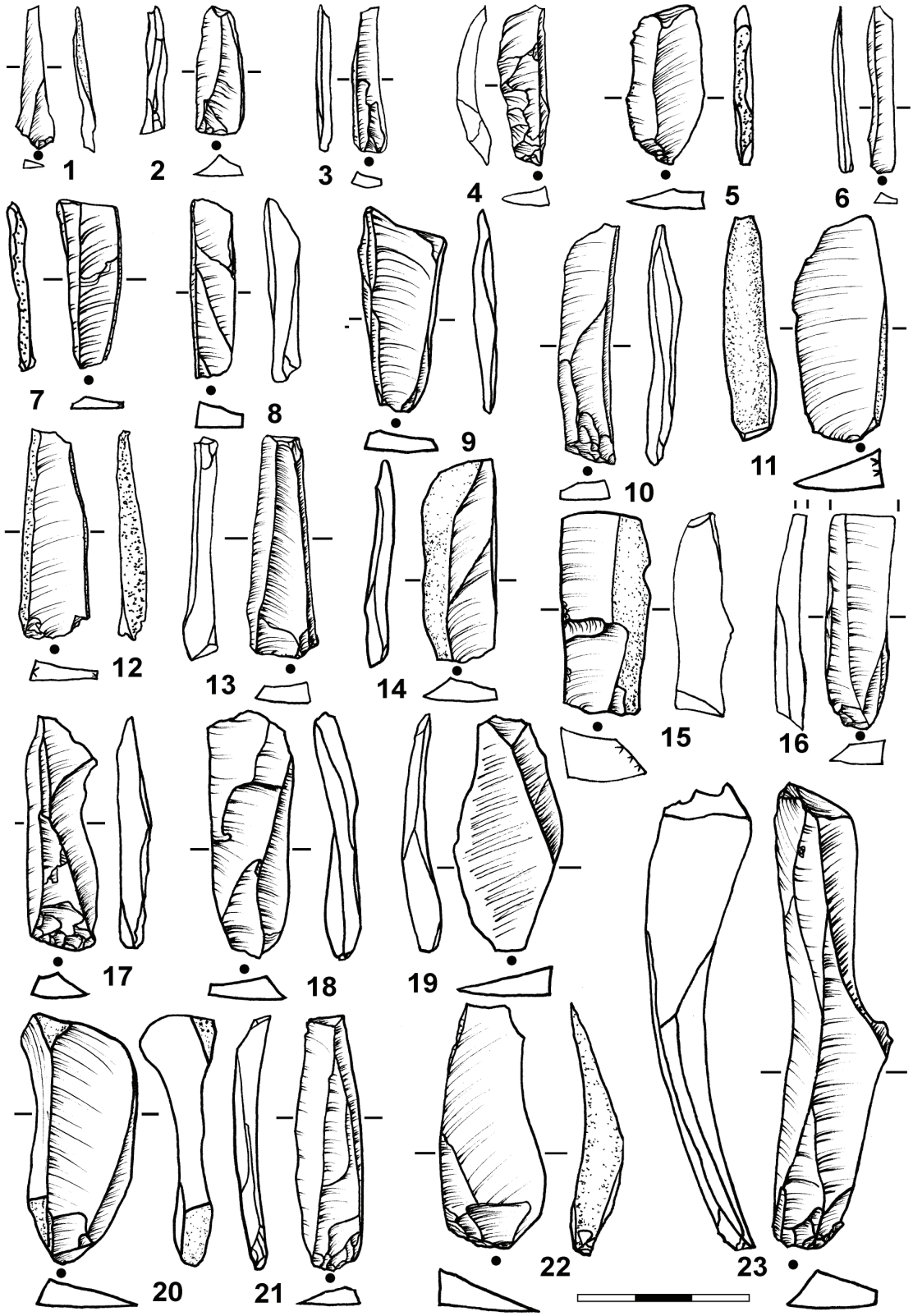


Fig. 8–37. Barmaky, western area complex, horizons 2c (1–7, 9–14, 17–23) & pit 1 (8, 15, 16): 1 – cortical *débordante* micro-blade; 2, 4, 8, 10, 21 – lateral *débordante* bladelets; 3, 6 – lateral *débordante* micro-blades; 5, 11, 22 – cortical *débordante* blades; 7, 12 – cortical *débordante* bladelets; 9, 14, 15, 17–20 – lateral *débordante* blades; 13, 16 – natural *débordante* bladelets; 23 – natural *débordante* blade.

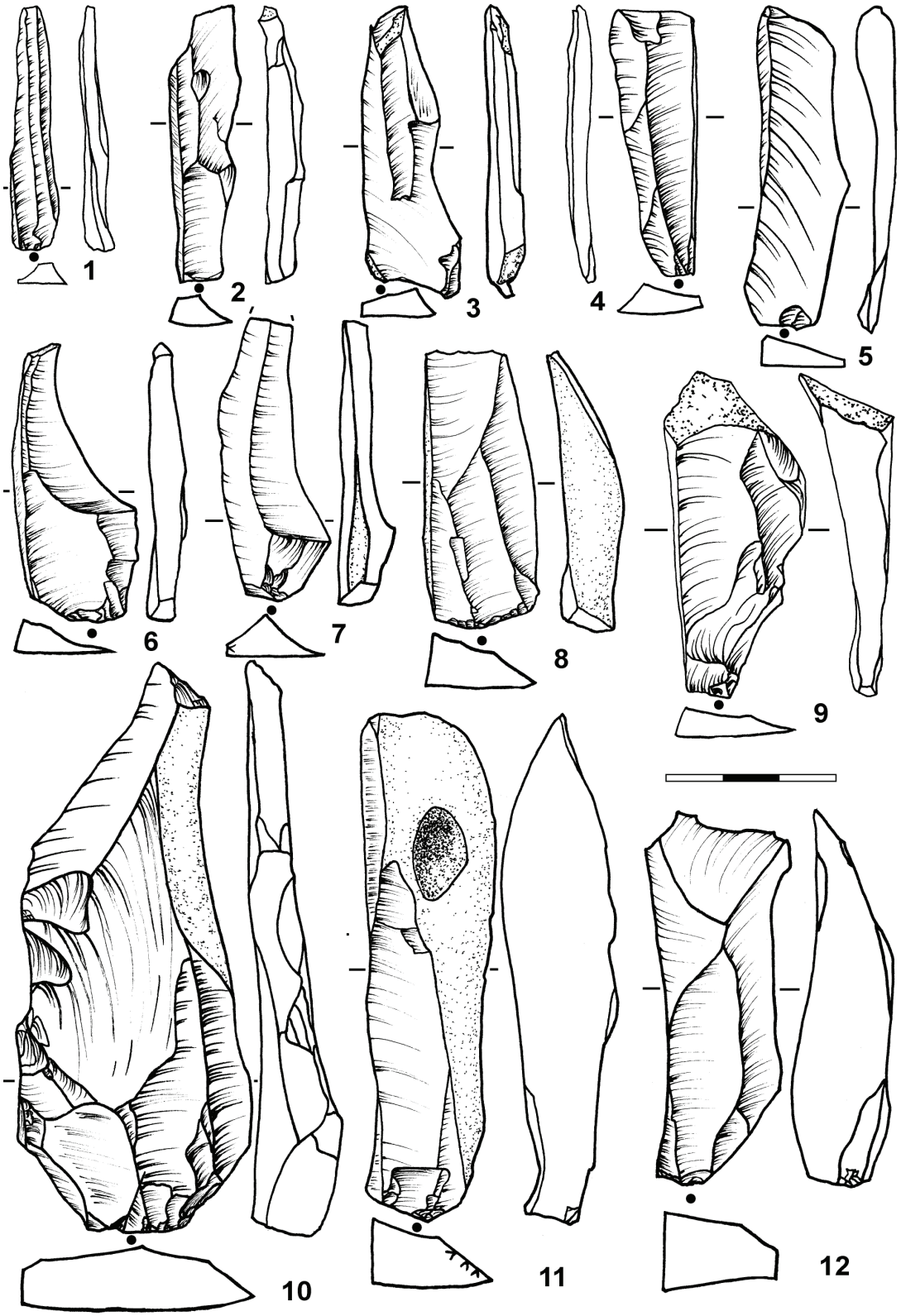


Fig. 8–38. Barmaky, western area complex, pit 1 (1, 5) & 2c horizon (2–4, 6–8, 10–12), 2d (9): 1 – lateral *débordante* bladelet; 2 – secondary crested bladelet, unidirectional on lateral *débordante*; 3 – lateral *débordante* blade; 4–6, 9, 11, 12 – natural *débordante* blades; 7, 8 – cortical *débordante* blades; 10 – one-side crested blade, unidirectional, on lateral *débordante*.

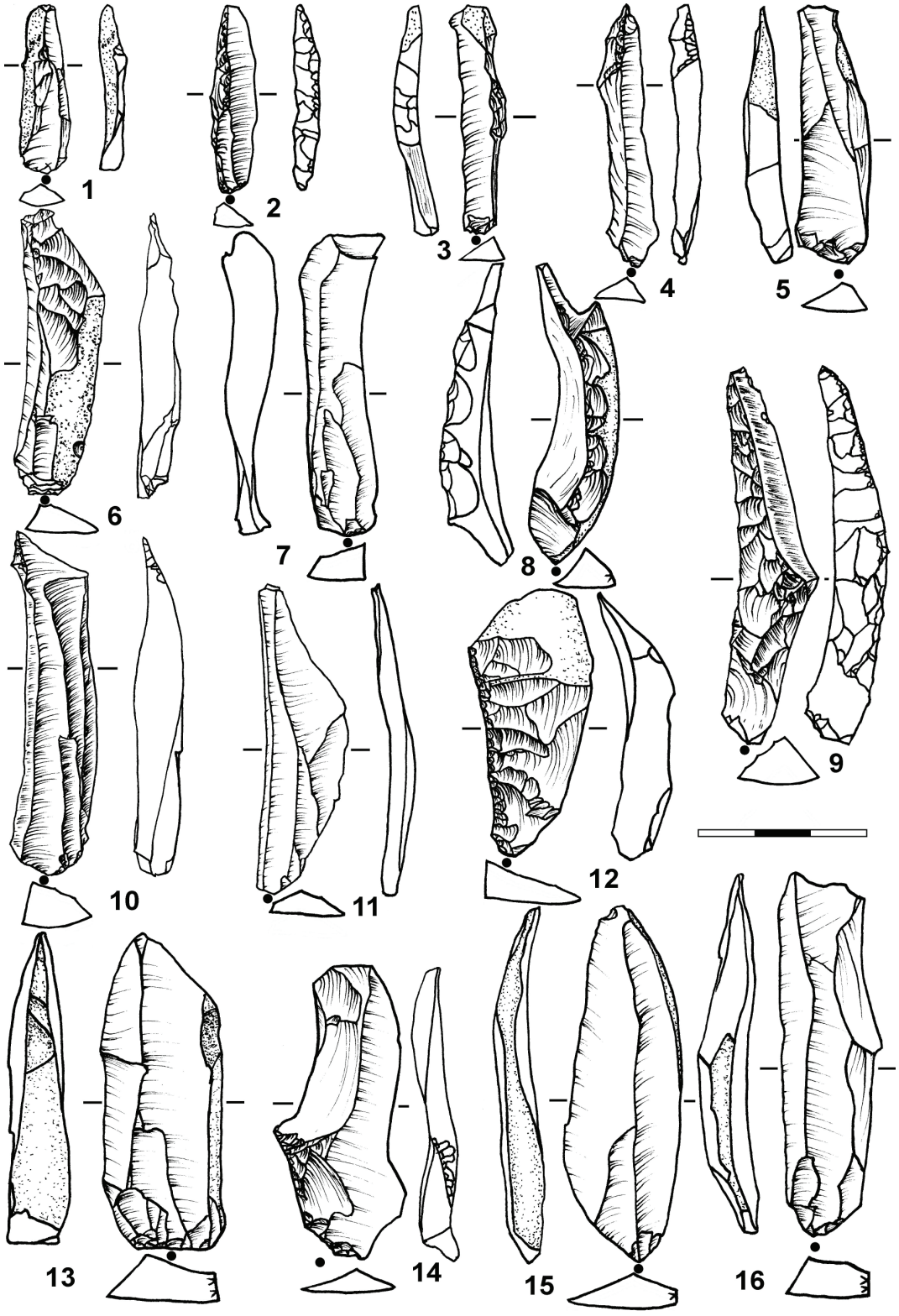


Fig. 8-39. Barmaky, western area complex, horizons 2d (1, 4, 7, 10) & 2c (2, 3, 5, 6, 8, 9, 11-16): 1 – one-side crested bladelet, bidirectional; 2-4 – one-side crested bladelets, bidirectional; 5 – secondary crested blade, bidirectional; 6, 12 – one-side crested bladelets on lateral *débordante*; 7 – lateral *débordante* blade; 8 – one-side crested blade; 9 – crested blade; 10, 13 – natural *débordante* blades; 11 – lateral *débordante* blade; 14 – one-side crested blade, unidirectional; 15 – cortical *débordante* blade; 16 – secondary crested blade, bidirectional, on cortical *débordante*.

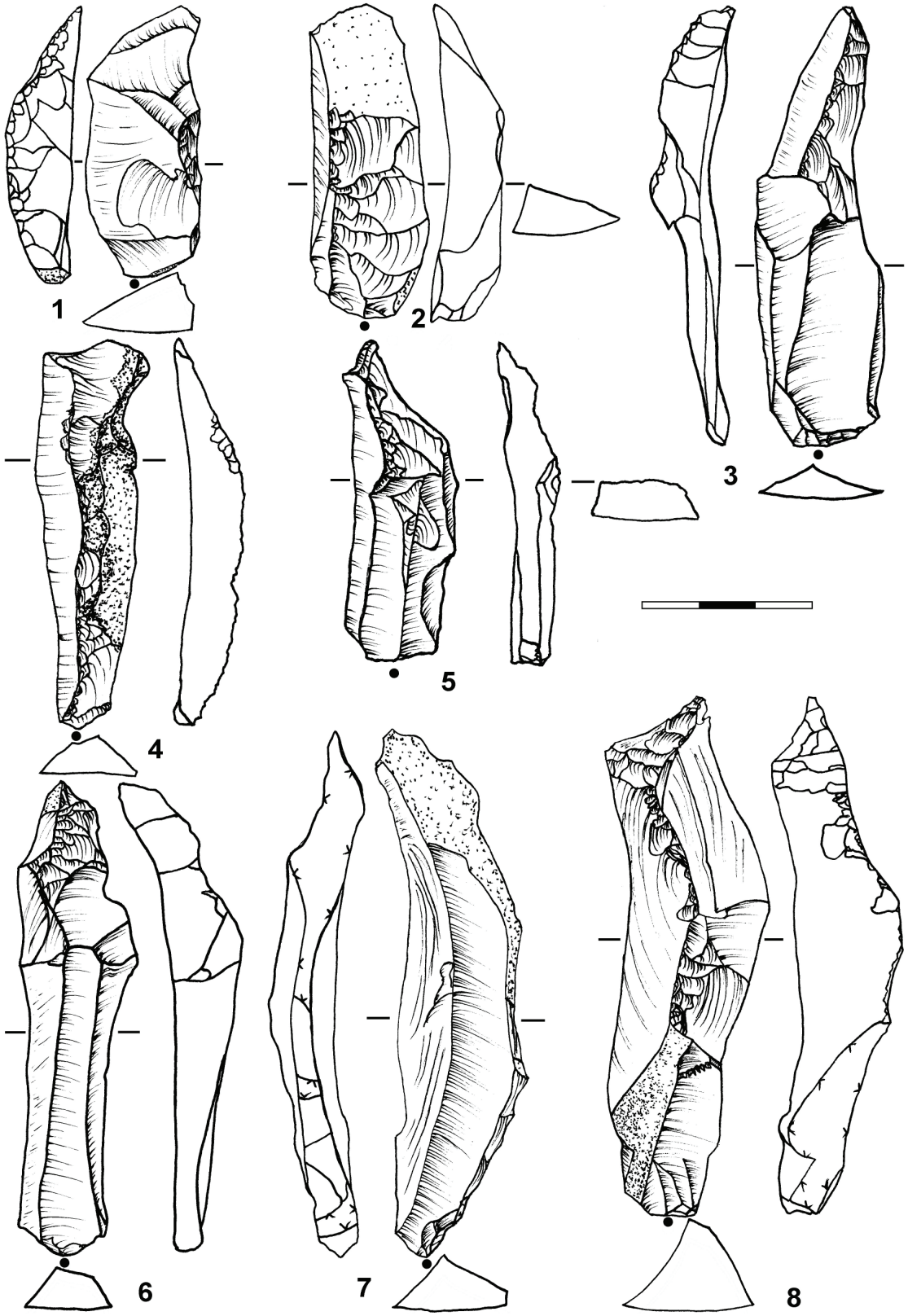


Fig. 8–40. Barmaky, western area complex, pit 1 (1, 8), horizons 2d (2, 4, 5) & 2c (3, 6, 7): 1 – crested blade; 2 – one-side crested blade on lateral *débordante*; 3, 4 – one-side crested blades, bidirectional; 5 – one-side crested blade, unidirectional; 6 – crested blade, unidirectional; 7 – secondary crested blade, unidirectional; 8 – alternatingly crested blade.

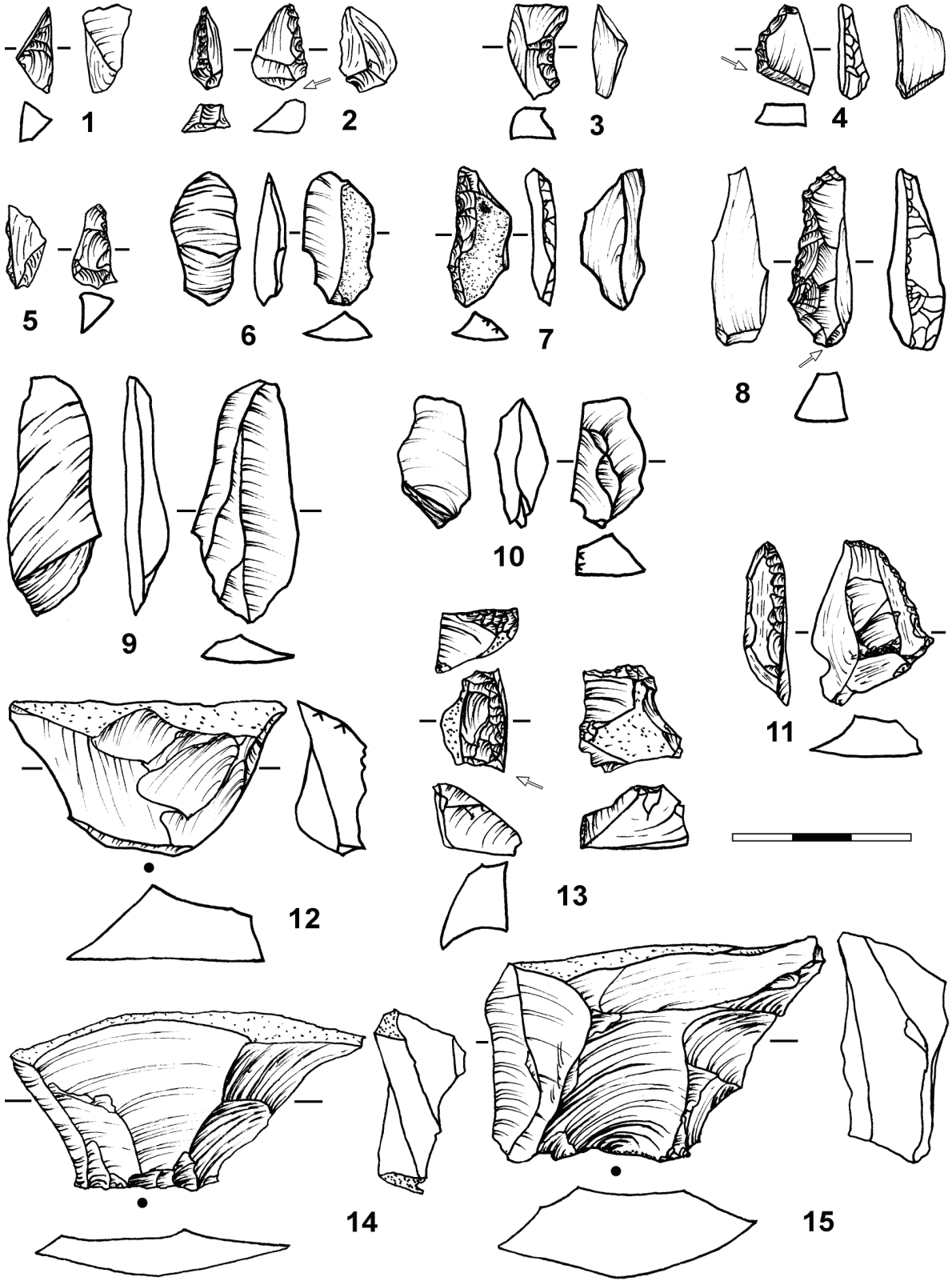


Fig. 8–41. Barmaky, western area complex, horizon 2c (1–11, 13, 15) & pit 1 (12, 14): 1, 3, 5, 7, 11 – secondary truncation spalls; 2, 4, 8, 13 – rejuvenating truncation spalls; 6, 9, 10 – initial truncation spalls; 12, 14, 15 – *Kantenabschläge.*

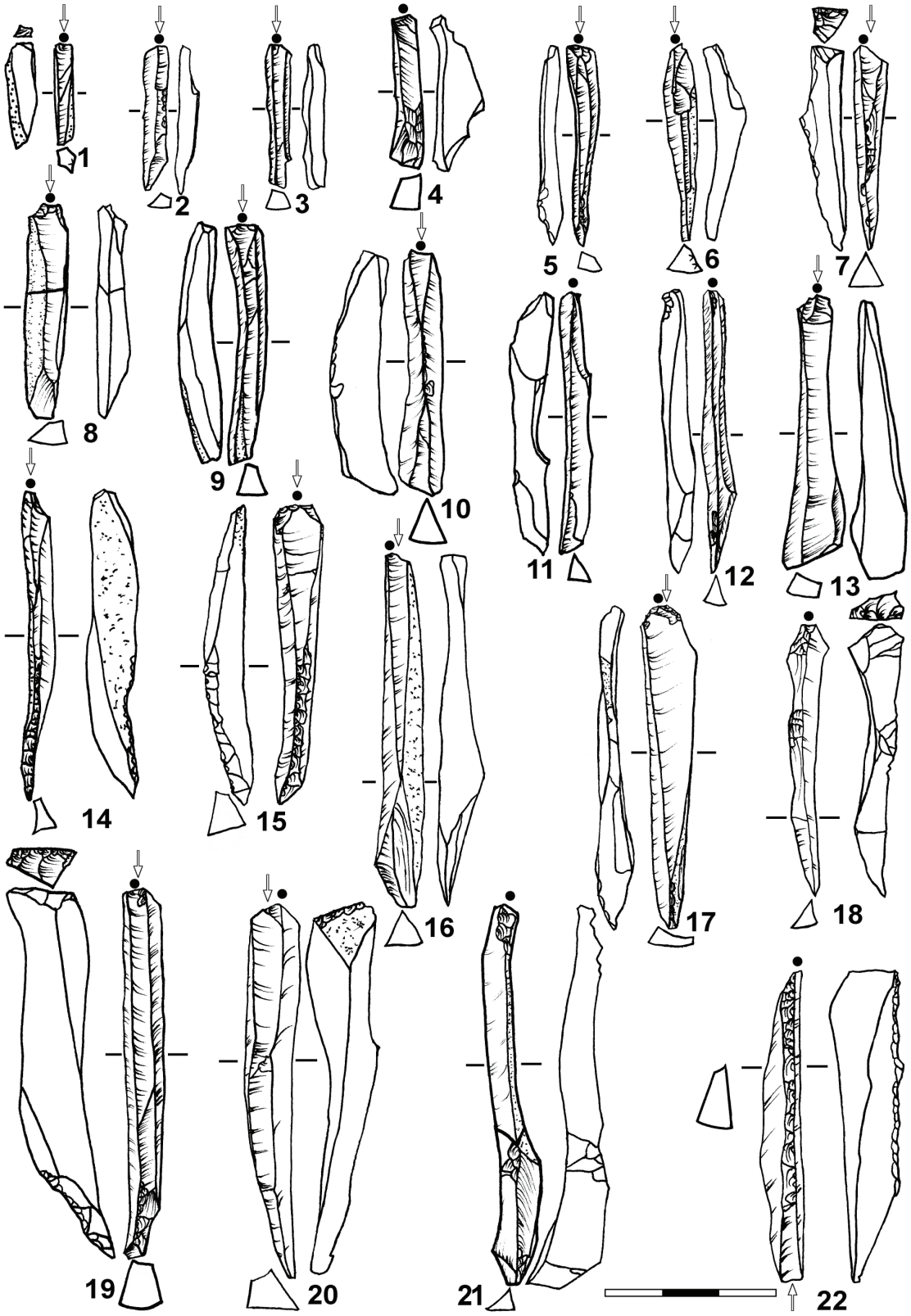


Fig. 8–42. Barmaky, western area complex, horizons 2d (1, 15) & 2c (2–14, 16–22), burin spalls: 1, 6, 9 – multiple; 2, 16 – multiple, bidirectional; 3, 8, 13 – secondary; 4, 12, 18, 21 – primary, retouched; 5, 10, 22 – multiple, bidirectional, retouched; 7, 14, 15, 20 – multiple, retouched; 11 – primary; 17, 19 – secondary, retouched.

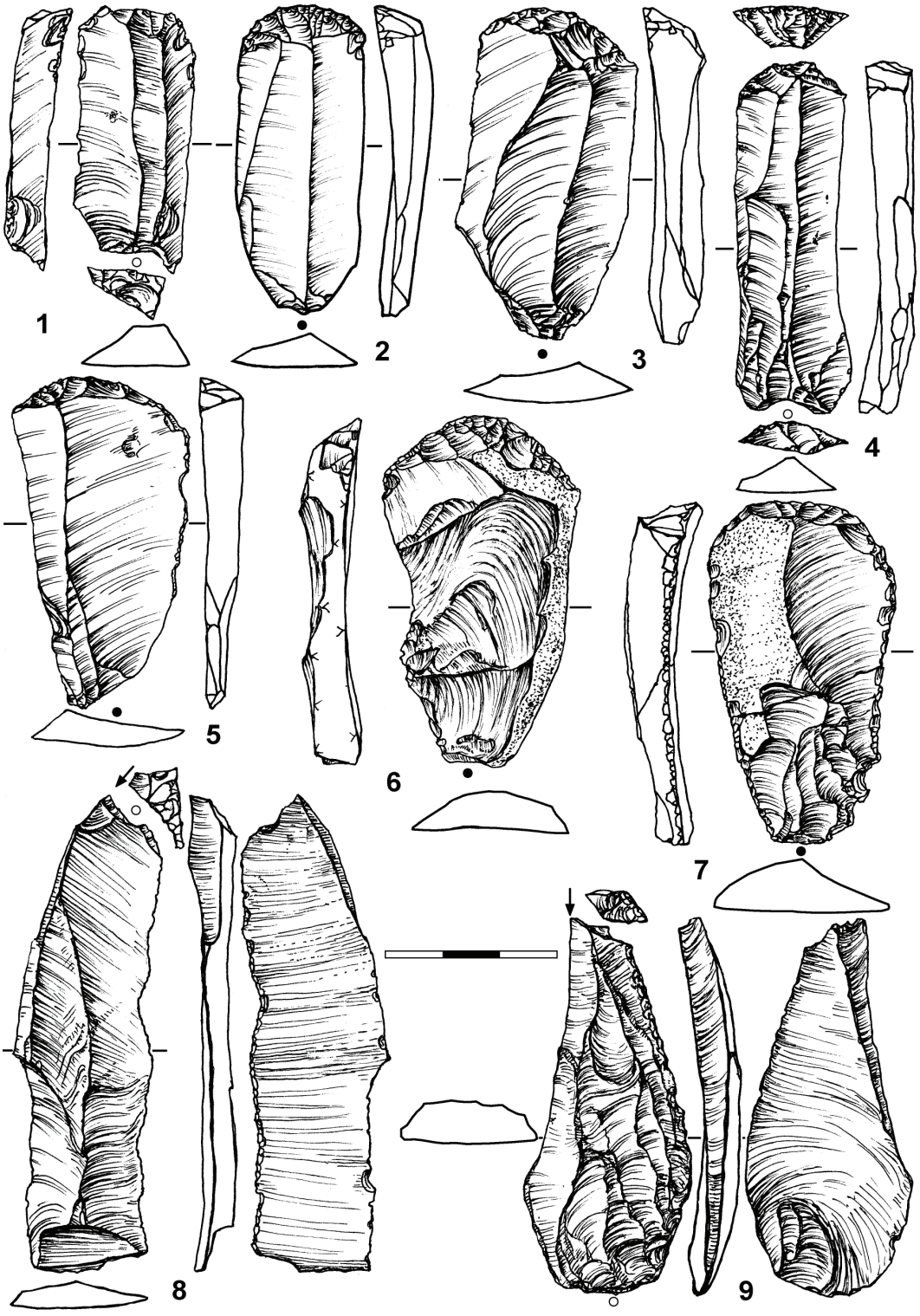


Fig. 8–43. Barmaky, western area complex, horizons 2c (1, 2, 5–9) & 2d (3, 4): 1 – end-scraper on blade, simple-convex, distal, on the obliquely-concavely proximally dorsally truncated piece; 2 – end-scraper on blade, simple-convex, distal; 3, 6 – end-scrapers on flakes, simple-convex, distal; 4 – end-scraper on blade, simple-convex, distal, on concavely proximally dorsally truncated piece; 5 – end-scraper on blade, simple-convex, distal, dorsal; on laterally dorsally retouched piece; 7 – end-scraper on blade, simple-convex, distal, dorsal; on bi-laterally dorsally retouched piece; 8 – burin on obliquely distally dorsally truncated and laterally ventrally retouched blade; 9 – burin on obliquely distally dorsally truncated and laterally dorsally retouched blade.

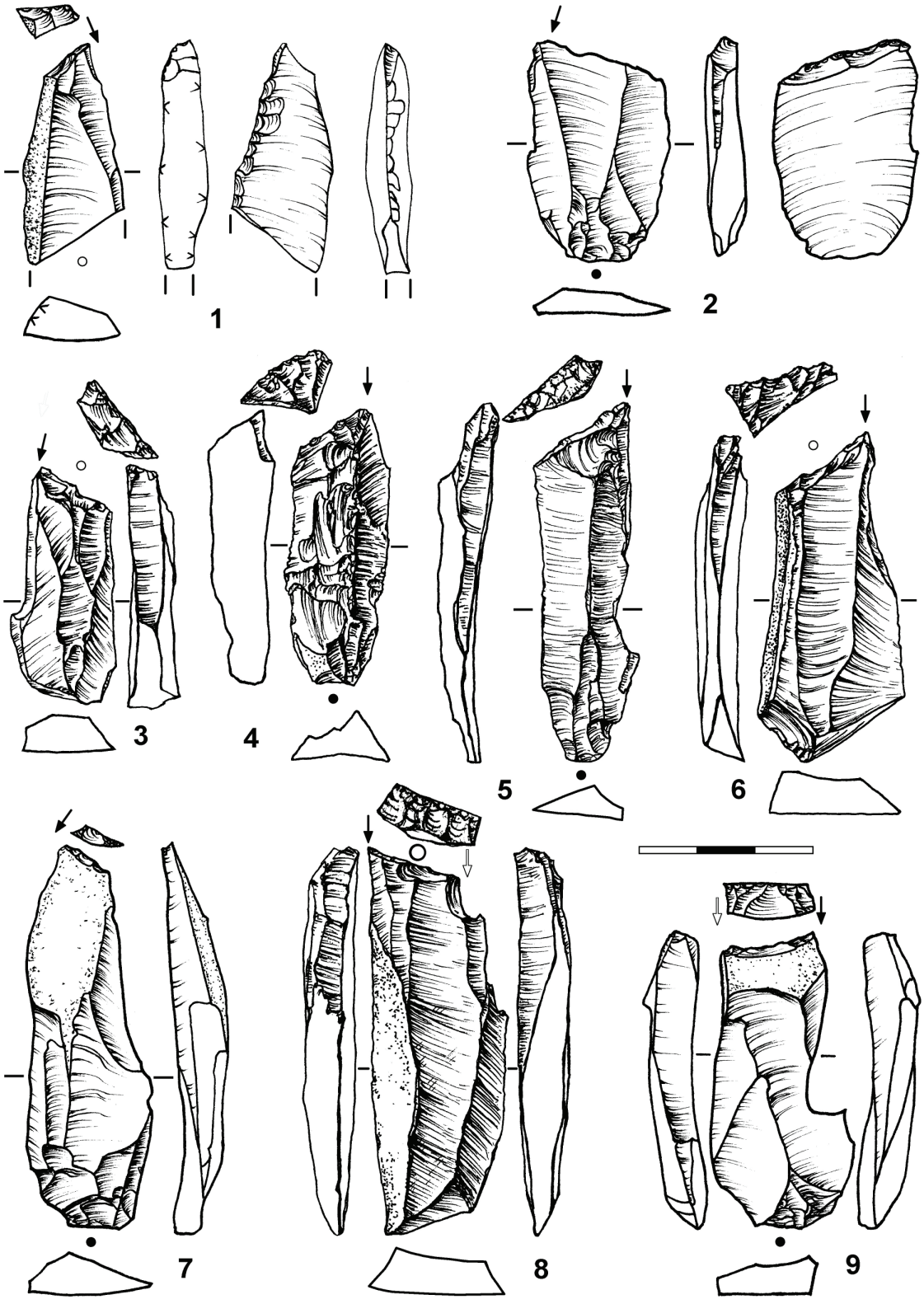


Fig. 8-44. Barmaky, western area complex, pit 1 (1, 4) & horizon 2c (2, 3, 5-9), burins on truncated blades: 1 – on oblique distal, dorsal truncation, on laterally ventrally retouched piece; 2 – on oblique distal, ventral truncation; 3 – on oblique proximal, dorsal truncation; 4, 5, 7 – on oblique distal, dorsal truncation; 6 – on oblique proximal, dorsal truncation, on laterally dorsally retouched piece; 8 – on oblique proximal, dorsal truncation; 9 – on oblique-concave distal, dorsal truncation. Burins 8 and 9 were rejuvenated by truncations.

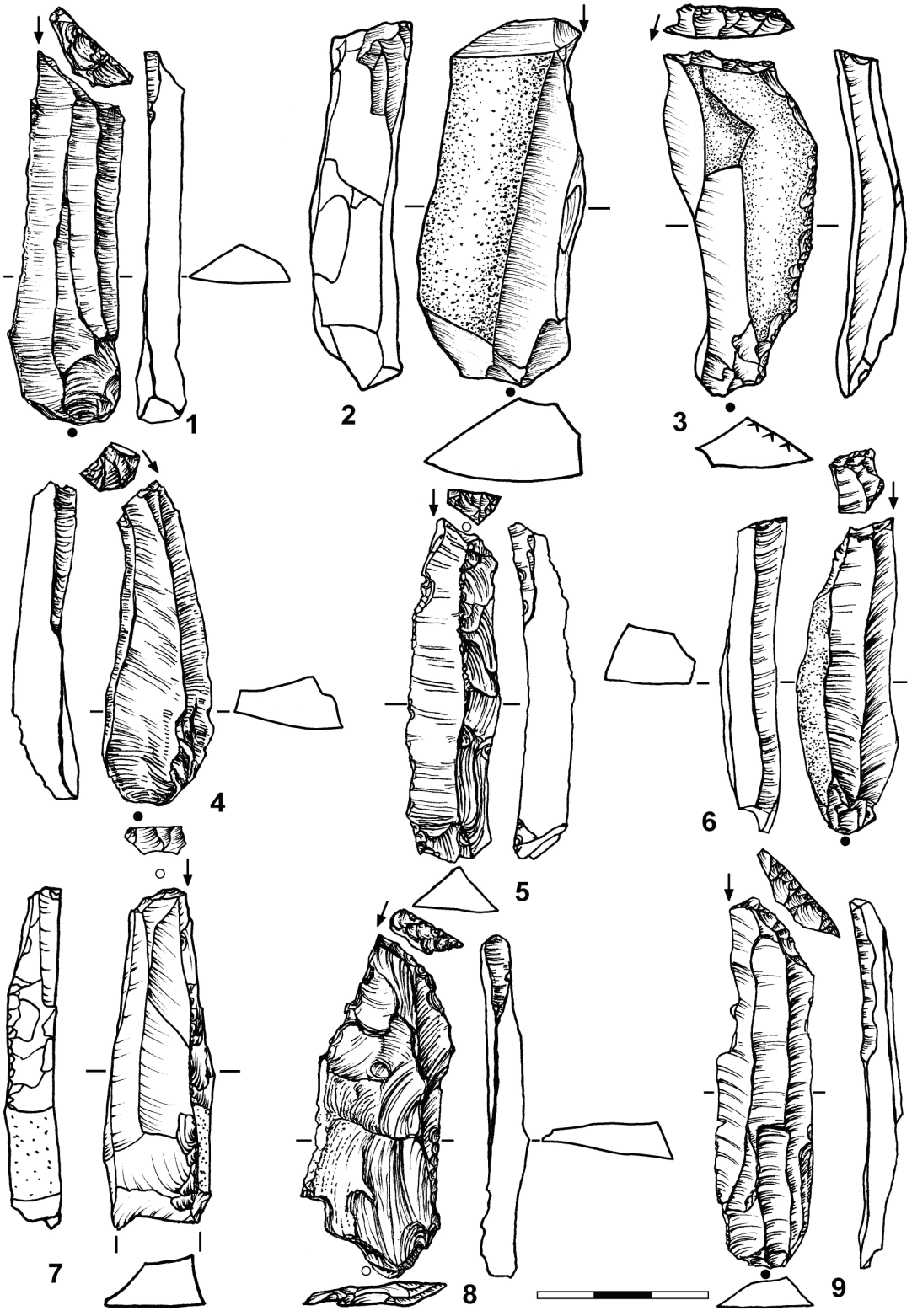


Fig. 8-45. Barmaky, western area complex, horizons 2c (1-6, 8, 9) & pit 1 (7), burins on truncated blades: 1, 2, 4, 6 – on oblique, distal, dorsal truncation; 3 – on oblique, distal, dorsal truncation, on laterally dorsally retouched piece; 5 – on oblique, proximal, dorsal truncation, on laterally/distally alternatingly retouched piece; 7 – on oblique-convex, proximal, dorsal truncation; 8 – on oblique-convex, distal, dorsal truncation, on bi-terminal oblique-convex / oblique-wavy truncated piece; 9 – on oblique-convex, distal, dorsal truncation.

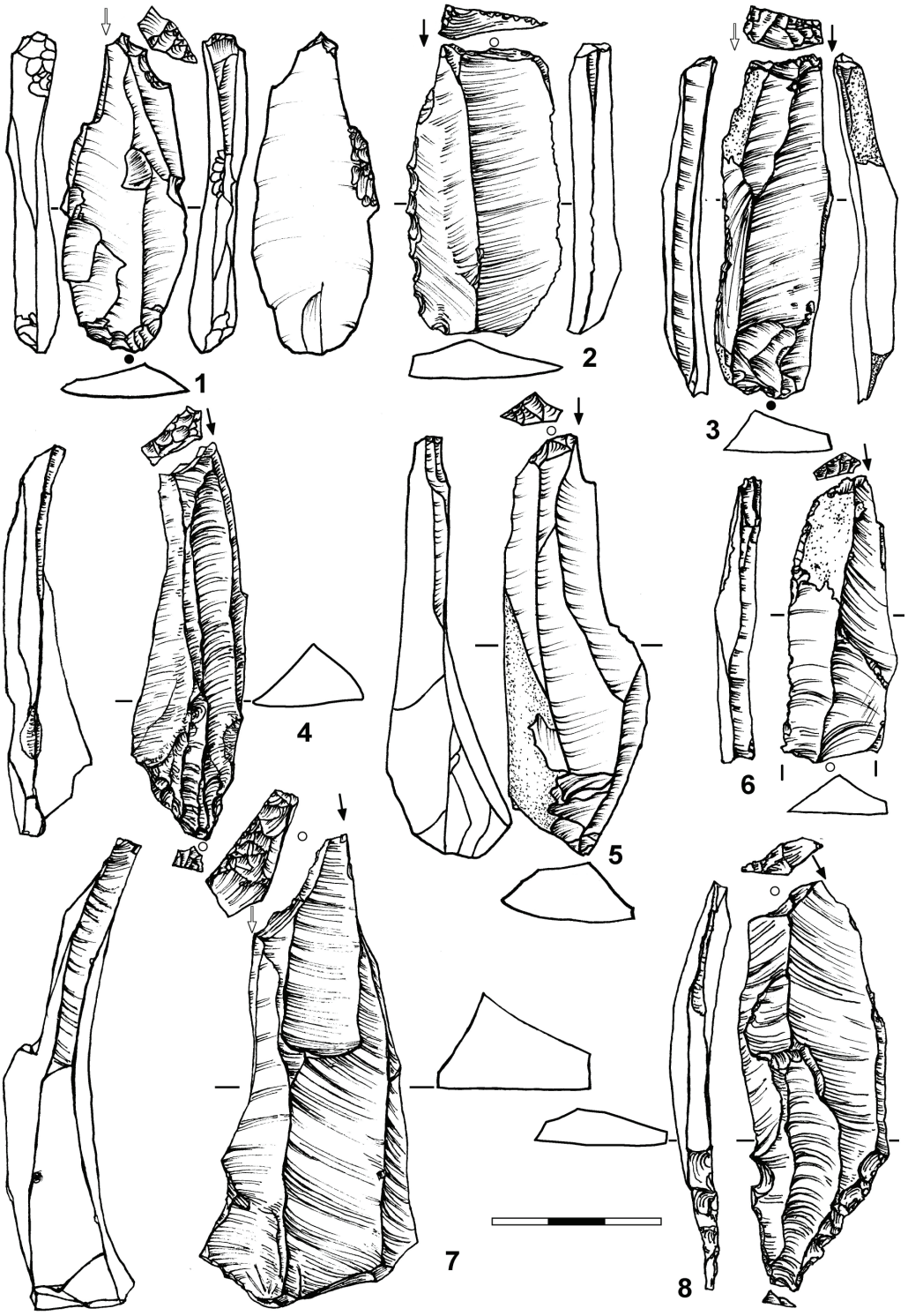


Fig. 8-46. Barmaky, western area complex, horizons 2c (1, 2, 4, 5, 8) & 2d (3, 6, 7), burins on truncated blades: 1 – on oblique-convex, distal, dorsal truncation, on laterally ventrally retouched piece; 2 – on concave, proximal, dorsal truncation, on laterally dorsally retouched piece; 3 – on concave, distal, dorsal truncation, on laterally dorsally retouched piece; 4 – on bi-terminal oblique-concave / oblique dorsal truncated piece; 5 – on oblique-convex, proximal, dorsal truncation; 6 – on oblique-convex, distal, dorsal truncation, on laterally dorsally retouched piece; 7 – on oblique-concave, proximal, dorsal truncation; 8 – on bi-terminal oblique distal & oblique-concave proximal, dorsal truncations, on bi-laterally dorsally retouched piece. Burins 1, 3, and 7 were rejuvenated by truncations.

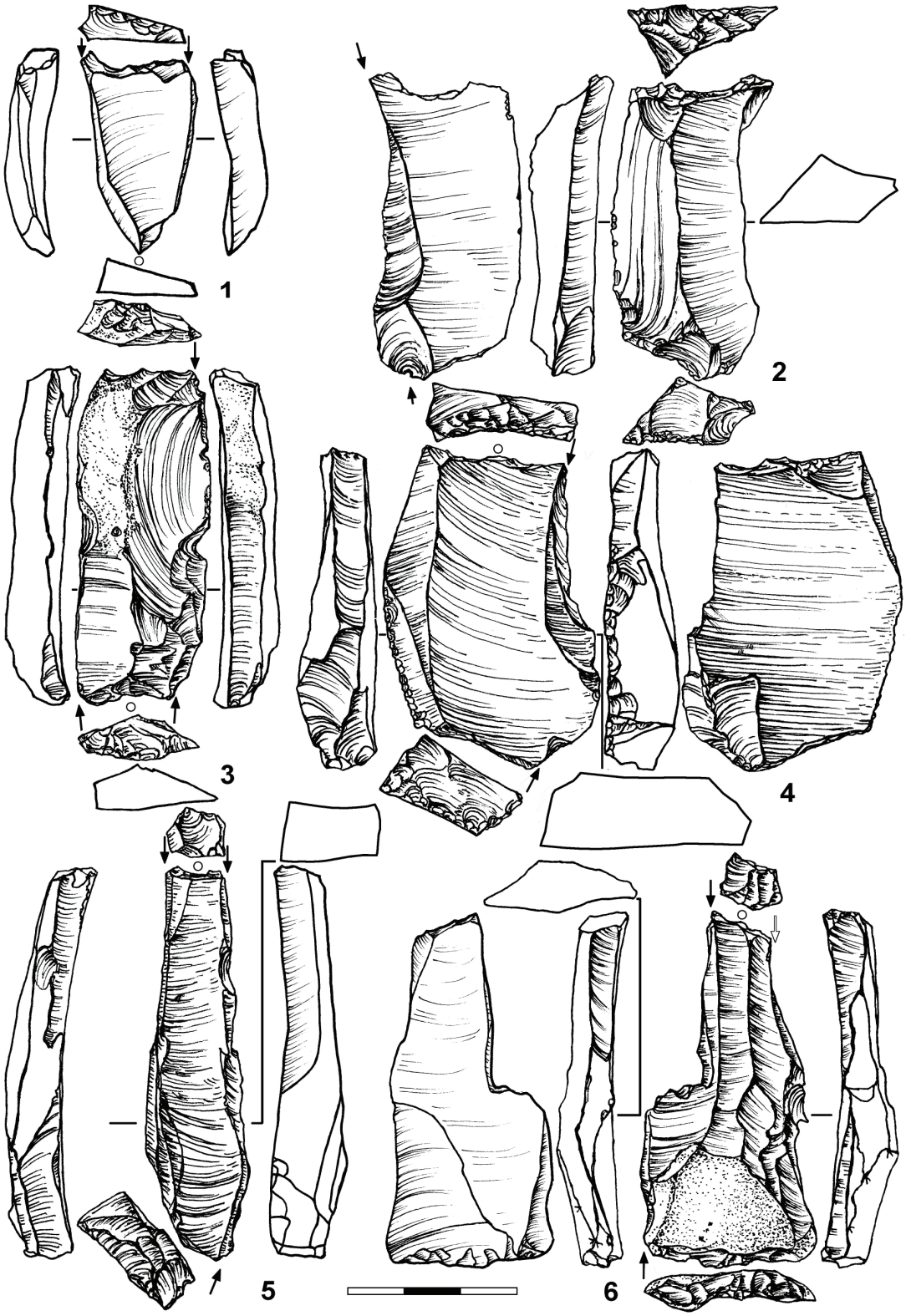


Fig. 8-47. Barmaky, western area complex, horizon 2c, burins on truncated blades: 1 – bi-lateral, on concave, distal, dorsal truncation; 2 – opposite, on oblique-concave bi-terminal, dorsal truncations; on laterally dorsally retouched piece; 3 – opposite and bi-lateral – 3-edges, on straight bi-terminal dorsal truncations; 4 – opposite, on bi-terminal straight & oblique dorsal truncations; 5 – opposite and bi-lateral – 3-edges, on bi-terminal concave and oblique-convex, dorsal truncations; 6 – opposite, on-bi-terminal oblique and straight, dorsal truncations. Burin 6 was rejuvenated by truncations.

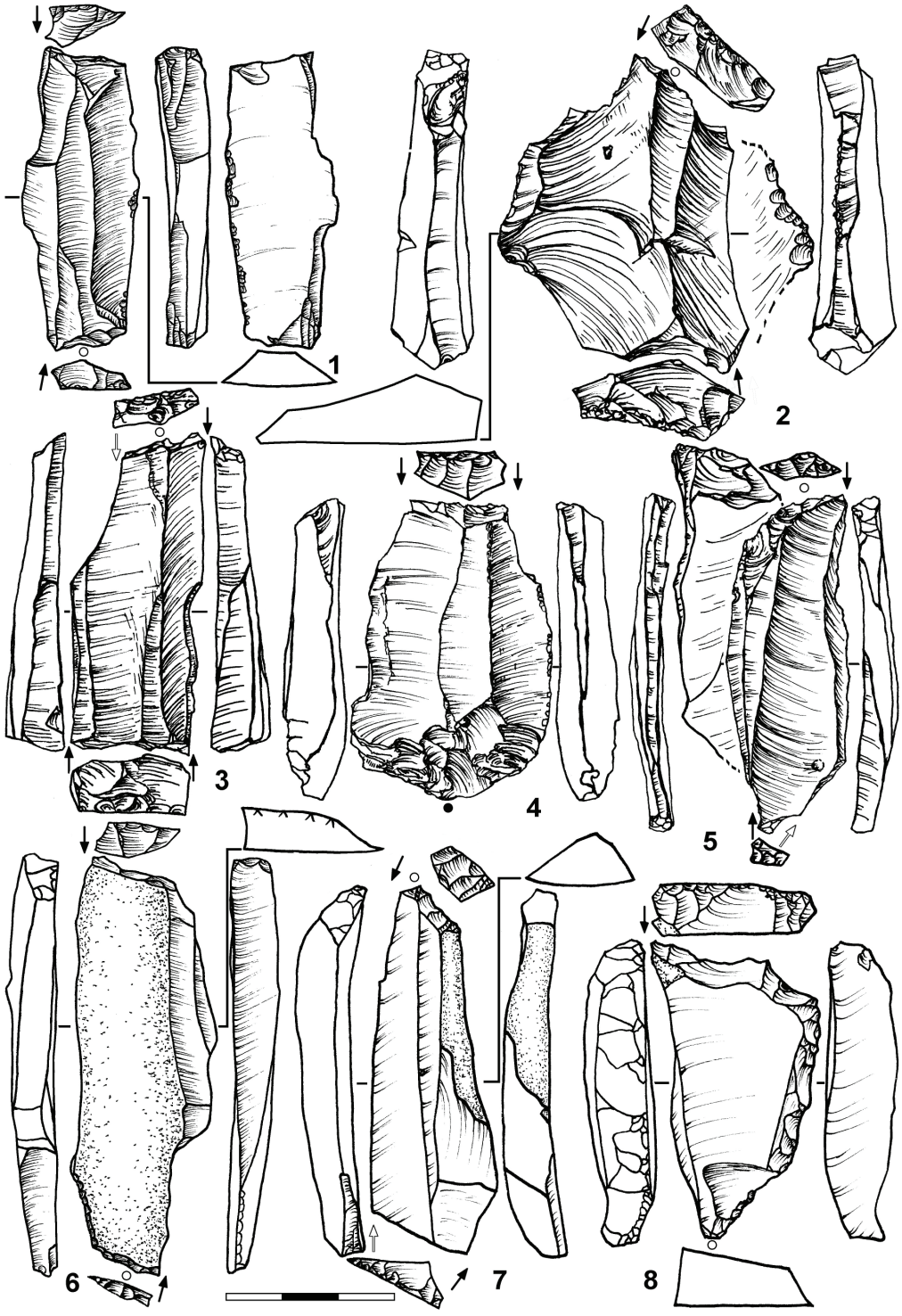


Fig. 8–48. Barmaky, western area complex, horizon 2c, burins: 1 – opposite, on bi-terminally, dorsally, obliquely truncated, and laterally, ventrally retouched blade; 2 – opposite-alternative, on bi-terminally obliquely-concavely, dorsally truncated, and on laterally, ventrally retouched flake; 3 – opposite and bi-lateral – 3 edges, on bi-terminally, concavely / obliquely dorsally truncated blade; 4 – bi-lateral, on straight, distal, dorsal truncation, on laterally, dorsally retouched flake; 5 – opposite-alternative, on bi-terminally, obliquely, dorsally truncated, and on proximally ventrally thinned blade; 6 – opposite-alternative, on bi-terminally, obliquely, dorsally truncated, and on laterally dorsally retouched blade; 7 – opposite-alternative, on bi-terminally obliquely dorsally truncated blade; 8 – on straight, distal, dorsal truncation, on laterally dorsally retouched flake. Burins 3, 5 and 7 were rejuvenated by truncations.

| | | flakes | | blades | | bladelets | | micro-blades | |
|---|---|---|---|---|---|---|---|---|---|
| | | # | % | # | % | # | % | # | % |
| HORIZON 2b | triangular | **7** | 33,33 | **4** | 44,44 | **3** | 42,86 | **1** | 33,33 |
| | trapezoidal | **8** | 38,10 | **4** | 44,44 | **1** | 14,29 | **1** | 33,33 |
| | multiple | **2** | 9,52 | **–** | – | **–** | – | **–** | – |
| | lateral steep | **3** | 14,29 | **–** | – | **3** | 42,86 | **1** | 33,33 |
| | convex | **–** | – | **1** | 11,11 | **–** | – | **–** | – |
| | flat | **1** | 4,76 | **–** | – | **–** | – | **–** | – |
| | **TOTAL:** | **21** | 100,00 | **9** | 100,00 | **7** | 100,00 | **3** | 100,00 |
| | unidentifiable | 2 | – | – | – | – | – | – | – |
| HORIZON 2c, PIT 1 | triangular | **55** | 39,86 | **15** | 29,41 | **19** | 45,24 | **13** | 54,17 |
| | trapezoidal | **45** | 32,61 | **14** | 27,45 | **12** | 28,57 | **6** | 25,00 |
| | multiple | **11** | 7,97 | **3** | 5,88 | **3** | 7,14 | **1** | 4,17 |
| | lateral steep | **12** | 8,70 | **18** | 35,29 | **8** | 19,05 | **4** | 16,67 |
| | convex | **5** | 3,62 | **1** | 1,96 | **–** | – | **–** | – |
| | flat | **6** | 4,35 | **–** | – | **–** | – | **–** | – |
| | irregular | **4** | 2,90 | **–** | – | **–** | – | **–** | – |
| | **TOTAL:** | **138** | 100,00 | **51** | 100,00 | **42** | 100,00 | **24** | 100,00 |
| | unidentifiable | 9 | – | – | – | – | – | – | – |
| HORIZON 2c | triangular | **883** | 35,11 | **344** | 27,15 | **373** | 40,94 | **322** | 53,67 |
| | trapezoidal | **682** | 27,12 | **454** | 35,83 | **284** | 31,17 | **130** | 21,67 |
| | multiple | **208** | 8,27 | **132** | 10,42 | **29** | 3,18 | **6** | 1,00 |
| | lateral steep | **426** | 16,94 | **317** | 25,02 | **216** | 23,71 | **141** | 23,50 |
| | convex | **155** | 6,16 | **18** | 1,42 | **7** | 0,77 | **–** | – |
| | flat | **127** | 5,05 | **–** | – | **1** | 0,11 | **1** | 0,17 |
| | irregular | **34** | 1,35 | **2** | 0,16 | **1** | 0,11 | **–** | – |
| | **TOTAL:** | **2515** | 100,00 | **1267** | 100,00 | **911** | 100,00 | **600** | 100,00 |
| | unidentifiable | 219 | – | 8 | – | 1 | – | 1 | – |
| HORIZON 2d | triangular | **315** | 36,71 | **110** | 27,03 | **145** | 45,60 | **73** | 50,69 |
| | trapezoidal | **253** | 29,49 | **160** | 39,31 | **80** | 25,16 | **40** | 27,78 |
| | multiple | **66** | 7,69 | **42** | 10,32 | **11** | 3,46 | **2** | 1,39 |
| | lateral steep | **111** | 12,94 | **89** | 21,87 | **79** | 24,84 | **29** | 20,14 |
| | convex | **63** | 7,34 | **6** | 1,47 | **3** | 0,94 | **–** | – |
| | flat | **31** | 3,61 | **–** | – | **–** | – | **–** | – |
| | irregular | **19** | 2,21 | **–** | – | **–** | – | **–** | – |
| | **TOTAL:** | **858** | 100,00 | **407** | 100,00 | **318** | 100,00 | **144** | 100,00 |
| | unidentifiable | 121 | – | 1 | – | – | – | 1 | – |

Table 8-65. Barmaky, western area complex, by horizons and structures: *débitage* cross-sections (including tools)

| | | flakes | | blades | | bladelets | | micro-blades | |
|---|---|---|---|---|---|---|---|---|---|
| | | # | % | # | % | # | % | # | % |
| HORIZON 2b | cortex | 1 | 4,35 | 1 | 11,11 | – | – | – | – |
| | lateral | 3 | 13,04 | – | – | – | – | – | – |
| | bi-lateral | – | – | – | – | 1 | 14,29 | – | – |
| | unidirectional | 11 | 47,83 | 5 | 55,56 | 5 | 71,43 | 3 | 100,00 |
| | bidirectional | – | | 3 | 33,33 | – | – | – | – |
| | crested alternating | 1 | 4,35 | – | – | – | – | – | – |
| | crested+unidirectional | 1 | 4,35 | – | – | 1 | 14,29 | – | – |
| | crested+bidirectional | 1 | 4,35 | – | – | – | – | – | – |
| | orthogonal | 4 | 17,39 | – | – | – | – | – | – |
| | semi-crossed | 1 | 4,35 | – | – | – | – | – | – |
| | **TOTAL:** | **23** | 100,00 | **9** | 100,00 | **7** | 100,00 | **3** | 100,00 |
| HORIZON 2c, PIT 1 | cortex | 11 | 7,59 | 1 | 1,96 | – | – | – | – |
| | lateral | 16 | 11,03 | 3 | 5,88 | – | – | 1 | 4,17 |
| | bi-lateral | 1 | 0,69 | 1 | 1,96 | – | – | – | – |
| | unidirectional | 76 | 52,41 | 21 | 41,18 | 33 | 78,57 | 19 | 79,17 |
| | bidirectional | 6 | 4,14 | 7 | 13,73 | 3 | 7,14 | 1 | 4,17 |
| | crested "one side" | – | – | 1 | 1,96 | 1 | 2,38 | 1 | 4,17 |
| | crested "double sides" | – | – | 3 | 5,88 | – | – | – | – |
| | crested+unidirectional | 2 | 1,38 | 6 | 11,76 | – | – | – | – |
| | crested+bidirectional | 1 | 0,69 | 2 | 3,92 | – | – | – | – |
| | crested secondary, unidirectional | 1 | 0,69 | – | – | – | – | 1 | 4,17 |
| | crested secondary, bidirectional | – | – | – | – | 2 | 4,76 | – | – |
| | orthogonal | 28 | 19,31 | 6 | 11,76 | 3 | 7,14 | 1 | 4,17 |
| | semi-crossed | 3 | 2,07 | – | – | – | – | – | – |
| | **TOTAL:** | **145** | 100,00 | **51** | 100,00 | **42** | 100,00 | **24** | 100,00 |
| | unidentifiable | 2 | – | – | – | – | – | – | – |
| HORIZON 2c | cortex | 259 | 9,56 | 27 | 2,12 | 14 | 1,54 | 3 | 0,50 |
| | lateral | 180 | 6,65 | 12 | 0,94 | 13 | 1,43 | 1 | 0,17 |
| | bi-lateral | 17 | 0,63 | 2 | 0,16 | – | – | 1 | 0,17 |
| | unidirectional | 1456 | 53,77 | 768 | 60,24 | 661 | 72,48 | 510 | 84,86 |
| | bidirectional | 116 | 4,28 | 185 | 14,51 | 71 | 7,79 | 25 | 4,16 |
| | bidirectional-crossed | – | – | 1 | 0,08 | 1 | 0,11 | – | – |
| | crested "one side" | 27 | 1,00 | 35 | 2,75 | 20 | 2,19 | 8 | 1,33 |
| | crested "double sides" | 31 | 1,14 | 14 | 1,10 | 5 | 0,55 | – | – |
| | crested alternating | 2 | 0,07 | 2 | 0,16 | 4 | 0,44 | – | – |
| | crested+unidirectional | 76 | 2,81 | 64 | 5,02 | 42 | 4,61 | 18 | 3,00 |
| | crested+bidirectional | 3 | 0,11 | 22 | 1,73 | 7 | 0,77 | 1 | 0,17 |
| | crested secondary, unidirectional | 34 | 1,26 | 49 | 3,84 | 11 | 1,21 | 5 | 0,83 |
| | crested secondary, bidirectional | 5 | 0,18 | 10 | 0,78 | 2 | 0,22 | – | – |
| | orthogonal | 431 | 15,92 | 67 | 5,25 | 55 | 6,03 | 28 | 4,66 |
| | semi-crossed | 42 | 1,55 | 5 | 0,39 | 1 | 0,11 | – | – |
| | crossed | 1 | 0,04 | – | – | – | – | – | – |
| | opposite directional | 28 | 1,03 | 12 | 0,94 | 5 | 0,55 | 1 | 0,17 |
| | **TOTAL:** | **2708** | 100,00 | **1275** | 100,00 | **912** | 100,00 | **601** | 100,00 |
| | unidentifiable | 26 | – | – | – | – | – | – | – |

Table 8-66. Barmaky, western area complex, by horizons and structures: *débitage* dorsal scars (including tools)

| | | flakes | | blades | | bladelets | | micro-blades | |
|---|---|---|---|---|---|---|---|---|---|
| | | # | % | # | % | # | % | # | % |
| HORIZON 2d | cortex | **94** | 9,72 | **10** | 2,45 | **6** | 1,89 | **–** | – |
| | lateral | **80** | 8,27 | **3** | 0,74 | **4** | 1,26 | **1** | 0,70 |
| | bi-lateral | **9** | 0,93 | **1** | 0,25 | **–** | – | **–** | – |
| | unidirectional | **503** | 52,02 | **246** | 60,29 | **228** | 71,70 | **123** | 86,01 |
| | bidirectional | **37** | 3,83 | **46** | 11,27 | **22** | 6,92 | **5** | 3,50 |
| | crested "one side" | **9** | 0,93 | **7** | 1,72 | **11** | 3,46 | **2** | 1,40 |
| | crested "double sides" | **7** | 0,72 | **2** | 0,49 | **2** | 0,63 | **–** | – |
| | crested alternating | **–** | – | **2** | 0,49 | **–** | – | **–** | – |
| | crested+unidirectional | **22** | 2,28 | **24** | 5,88 | **10** | 3,14 | **5** | 3,50 |
| | crested+bidirectional | **2** | 0,21 | **9** | 2,21 | **3** | 0,94 | **1** | 0,70 |
| | crested secondary, unidirectional | **8** | 0,83 | **15** | 3,68 | **3** | 0,94 | **3** | 2,10 |
| | crested secondary, bidirectional | **–** | – | **7** | 1,72 | **3** | 0,94 | **–** | – |
| | orthogonal | **151** | 15,62 | **24** | 5,88 | **21** | 6,60 | **3** | 2,10 |
| | semi-crossed | **31** | 3,21 | **8** | 1,96 | **1** | 0,31 | **–** | – |
| | crossed | **2** | 0,21 | **–** | – | **–** | – | **–** | – |
| | opposite directional | **12** | 1,24 | **4** | 0,98 | **4** | 1,26 | **–** | – |
| | **TOTAL:** | **967** | 100,00 | **408** | 100,00 | **318** | 100,00 | **143** | 100,00 |
| | unidentifiable | 12 | – | – | – | – | – | 2 | – |

Table 8-66. continued.

Straight and concave truncations constitute the **truncated pieces on unidentifiable *débitage*** (Table 8-76). Three variants of retouch combinations were observed: continuous scalar inverse semi-abrupt – 1 item; continuous scalar obverse abrupt – 3 item; partial scalar obverse semi-abrupt – 1 item. The average dimensions are >21.57×>21.07×6.48 mm.

**Notched pieces** are not numerous (Table 8-74; Fig. 8-56, *4*). They were produced on blades (4 items), bladelets (2 items), flakes (8 items), and unidentifiable *débitage* (1 item). Except for regular *débitage*, one crested blade, two primary flakes, one *débordante* flake, and one *Kantenabschlag* served as blanks. Partial scalar inverse semi-abrupt/abrupt retouch shaped eight notches. In addition, different combinations of partial scalar/micro-scalar/sub-parallel obverse semi-abrupt/abrupt retouches were observed. The average dimensions of notched pieces on blades, bladelets, and flakes are 61.90×24.54×8.90, >19.43×8.83×3.55, and 46.63×32.47×6.98 mm, respectively.

The **borer-perforators** are even less numerous than the notched pieces (Table 8-74; Fig. 8-56, *1-3, 7*). They were made on blades (4 items), flake (1 item), burin spall (1 item), and unidentifiable *débitage* (3 items). Most common are pieces with alternatively retouched tips, and were made on two blades, one flake, one burin spall, and one piece of unidentifiable *débitage*. The tips were shaped by partial scalar/sub-parallel alternate flat/semi-abrupt retouch. Tips of other borer-perforators exhibit different combinations of continuous/partial scalar/micro-scalar/sub-parallel obverse semi-abrupt/abrupt retouch. The average dimensions of borer-perforators on blades, flake, burin spall, and unidentifiable *débitage* are 50.97×17.08×4.97, 24.39×68.77×7.58, 58.85×13.82×13.47, and >17.61×>12.18×6.43 mm, respectively.

Convex lateral backing by partial/continuous micro-scalar/scalar obverse semi-abrupt/abrupt retouch formed three **points** on blades (Table 8-74; Fig. 8-56, *5, 6*). The average dimensions are 54.18×20.96×5.86 mm.

| | | | flakes | | blades | | bladelets | | micro-blades | |
|---|---|---|---|---|---|---|---|---|---|---|
| | | | # | % | # | % | # | % | # | % |
| HORIZON 2b | none | 0% | **9** | 39,13 | **4** | 44,44 | **4** | 57,14 | **2** | 66,67 |
| | primary | >75% | **1** | 4,35 | **1** | 11,11 | **–** | – | **–** | – |
| | proximal | 1–25% | **1** | 4,35 | **–** | – | **1** | 14,29 | **–** | – |
| | lateral | 1–25% | **1** | 4,35 | **1** | 11,11 | **–** | – | **–** | – |
| | | 26–50% | **3** | 13,04 | **–** | – | **1** | 14,29 | **–** | – |
| | | 51–75% | **1** | 4,35 | **2** | 22,22 | **1** | 14,29 | **1** | 33,33 |
| | bi-lateral | 51–75% | **1** | 4,35 | **–** | – | **–** | – | **–** | – |
| | distal | 1–25% | **1** | 4,35 | **–** | – | **–** | – | **–** | – |
| | | 51–75% | **1** | 4,35 | **–** | – | **–** | – | **–** | – |
| | distal-lateral | 1–25% | **1** | 4,35 | **–** | – | **–** | – | **–** | – |
| | | 26–50% | **1** | 4,35 | **1** | 11,11 | **–** | – | **–** | – |
| | | 51–75% | **2** | 8,70 | **–** | – | **–** | – | **–** | – |
| | | **TOTAL:** | **23** | 100,00 | **9** | 100,00 | **7** | 100,00 | **3** | 100,00 |
| HORIZON 2c, PIT 1 | none | 0% | **48** | 32,65 | **14** | 27,45 | **26** | 61,90 | **18** | 75,00 |
| | primary | >75% | **11** | 7,48 | **1** | 1,96 | **1** | 2,38 | **–** | – |
| | proximal | 1–25% | **10** | 6,80 | **–** | – | **–** | – | **–** | – |
| | | 26–50% | **1** | 0,68 | **1** | 1,96 | **–** | – | **–** | – |
| | central | 1–25% | **1** | 0,68 | **–** | – | **–** | – | **–** | – |
| | | 26–50% | **–** | – | **–** | – | **1** | 2,38 | **–** | – |
| | | 51–75% | **–** | – | **1** | 1,96 | **–** | – | **–** | – |
| | lateral | 1–25% | **23** | 15,65 | **9** | 17,65 | **6** | 14,29 | **–** | – |
| | | 26–50% | **5** | 3,40 | **10** | 19,61 | **4** | 9,52 | **4** | 16,67 |
| | | 51–75% | **4** | 2,72 | **–** | – | **2** | 4,76 | **–** | – |
| | bi-lateral | 1–25% | **–** | – | **1** | 1,96 | **–** | – | **–** | – |
| | | 26–50% | **–** | – | **2** | 3,92 | **–** | – | **–** | – |
| | | 51–75% | – | – | 1 | 1,96 | – | – | – | – |
| | distal | 1–25% | **14** | 9,52 | **1** | 1,96 | **1** | 2,38 | **2** | 8,33 |
| | | 26–50% | **3** | 2,04 | **–** | – | **–** | – | **–** | – |
| | | 51–75% | **3** | 2,04 | **–** | – | **–** | – | **–** | – |
| | distal-lateral | 1–25% | **5** | 3,40 | **3** | 5,88 | **–** | – | **–** | – |
| | | 26–50% | **3** | 2,04 | **6** | 11,76 | **1** | 2,38 | **–** | – |
| | | 51–75% | **6** | 4,08 | **1** | 1,96 | **–** | – | **–** | – |
| | distal-proximal | 1–25% | **1** | 0,68 | **–** | – | **–** | – | **–** | – |
| | | 26–50% | **7** | 4,76 | **–** | – | **–** | – | **–** | – |
| | | 51–75% | **2** | 1,36 | **–** | – | **–** | – | **–** | – |
| | | **TOTAL:** | **147** | 100,00 | **51** | 100,00 | **42** | 100,00 | **24** | 100,00 |

Table 8–67. Barmaky, western area complex, by horizons and structures: *débitage* primary surfaces placement & percentages (including tools)

| | | | flakes | | blades | | bladelets | | micro-blades | |
|---|---|---|---|---|---|---|---|---|---|---|
| | | | # | % | # | % | # | % | # | % |
| HORIZON 2c | none | 0% | **1206** | 44,11 | **549** | 43,06 | **515** | 56,47 | **423** | 70,38 |
| | primary | >75% | **256** | 9,36 | **26** | 2,04 | **9** | 0,99 | **1** | 0,17 |
| | proximal | 1–25% | **103** | 3,77 | **10** | 0,78 | **12** | 1,32 | **3** | 0,50 |
| | | 26–50% | **4** | 0,15 | **–** | – | **1** | 0,11 | **–** | – |
| | | 51–75% | **5** | 0,18 | **–** | – | **–** | – | **–** | – |
| | central | 1–25% | **3** | 0,11 | **10** | 0,78 | **4** | 0,44 | **4** | 0,67 |
| | | 26–50% | **12** | 0,44 | **3** | 0,24 | **1** | 0,11 | **1** | 0,17 |
| | | 51–75% | **8** | 0,29 | **5** | 0,39 | **–** | – | **1** | 0,17 |
| | lateral | 1–25% | **358** | 13,09 | **250** | 19,61 | **129** | 14,14 | **43** | 7,15 |
| | | 26–50% | **117** | 4,28 | **196** | 15,37 | **126** | 13,82 | **82** | 13,64 |
| | | 51–75% | **69** | 2,52 | **55** | 4,31 | **44** | 4,82 | **19** | 3,16 |
| | bi-lateral | 1–25% | **9** | 0,33 | **4** | 0,31 | **–** | – | **–** | – |
| | | 26–50% | **14** | 0,51 | **7** | 0,55 | **2** | 0,22 | **–** | – |
| | | 51–75% | **5** | 0,18 | **7** | 0,55 | **4** | 0,44 | **–** | – |
| | distal | 1–25% | **178** | 6,51 | **45** | 3,53 | **21** | 2,30 | **10** | 1,66 |
| | | 26–50% | **91** | 3,33 | **9** | 0,71 | **6** | 0,66 | **–** | – |
| | | 51–75% | **29** | 1,06 | **5** | 0,39 | **–** | – | **–** | – |
| | distal-lateral | 1–25% | **71** | 2,60 | **23** | 1,80 | **12** | 1,32 | **3** | 0,50 |
| | | 26–50% | **77** | 2,82 | **41** | 3,22 | **18** | 1,97 | **6** | 1,00 |
| | | 51–75% | **89** | 3,26 | **26** | 2,04 | **7** | 0,77 | **5** | 0,83 |
| | distal-proximal | 1–25% | **15** | 0,55 | **2** | 0,16 | **–** | – | **–** | – |
| | | 26–50% | **11** | 0,40 | **2** | 0,16 | **1** | 0,11 | **–** | – |
| | | 51–75% | **4** | 0,15 | **–** | – | **–** | – | **–** | – |
| | | **TOTAL:** | **2734** | 100,00 | **1275** | 100,00 | **912** | 100,00 | **601** | 100,00 |

Table 8–67. continued 1

There are two ***raclettes*** made of regular flakes (Table 8–74). One of them shows a distally retouched edge (14.65×17.59×2.51 mm), and another is bi-laterally retouched and distally ventrally thinned (>40.60×37.65×6.88 mm). In both cases, the retouch is continuous sub-parallel obverse abrupt.

Two end-scraper-burins make up the **combined tools** (Table 8–74). The first is made on a *débordante* blade and combines a simple-convex distal dorsal end-scraper shaped by sub-parallel obverse abrupt retouch with a single-spall burin on oblique-concave proximal dorsal truncation, shaped by an obverse semi-abrupt single blow (Fig. 8–57, *29*).

The second is made on a regular flake with discontinuous bi-laterally marginal obverse flat retouch on the dorsal side and combines a simple convex distal dorsal end-scraper made by continuous sub-parallel obverse abrupt retouch with a bi-lateral burin on concave proximal dorsal truncation made by continuous scalar obverse abrupt retouch (Fig. 8–57, *28*). Two burin edges exhibit the negatives of two burin spalls. The dimensions of combined tools on the *débordante* blade and flake are 102.90×20.84×16.36 and 52.64×33.34×7.40 mm, respectively.

Laterally backed **microliths** are one of the most numerous tool classes in the western area (Tables 8–74; 8–77; Fig. 8–57, *1–27*; 8–58, *6*). There are two main types of microliths: microgravette points (Fig. 8–57, *2–4, 8, 11, 15, 18, 19–27*) and unfinished pieces (Fig. 8–57, *7, 14*). The high degree of fragmentation is problematic for a typological analysis. The proximal parts with oblique truncation were recorded as points because they are common for complete

| | | | flakes | | blades | | bladelets | | micro-blades | |
|---|---|---|---|---|---|---|---|---|---|---|
| | | | # | % | # | % | # | % | # | % |
| HORIZON 2d | none | 0% | **418** | 42,70 | **194** | 47,55 | **185** | 58,18 | **114** | 78,62 |
| | primary | >75% | **93** | 9,50 | **8** | 1,96 | **4** | 1,26 | **–** | – |
| | proximal | 1–25% | **44** | 4,49 | **2** | 0,49 | **2** | 0,63 | **–** | – |
| | | 26–50% | **3** | 0,31 | **–** | – | **–** | – | **–** | – |
| | | 51–75% | **2** | 0,20 | **–** | – | **–** | – | **–** | – |
| | central | 1–25% | **–** | – | **3** | 0,74 | **2** | 0,63 | **–** | – |
| | | 26–50% | **1** | 0,10 | **2** | 0,49 | **–** | – | **1** | 0,69 |
| | | 51–75% | **2** | 0,20 | **–** | – | **–** | – | **–** | – |
| | lateral | 1–25% | **144** | 14,71 | **73** | 17,89 | **42** | 13,21 | **5** | 3,45 |
| | | 26–50% | **37** | 3,78 | **64** | 15,69 | **49** | 15,41 | **18** | 12,41 |
| | | 51–75% | **37** | 3,78 | **19** | 4,66 | **17** | 5,35 | **7** | 4,83 |
| | bi-lateral | 1–25% | **3** | 0,31 | **1** | 0,25 | **–** | – | **–** | – |
| | | 26–50% | **2** | 0,20 | **2** | 0,49 | **1** | 0,31 | **–** | – |
| | | 51–75% | **3** | 0,31 | **1** | 0,25 | **1** | 0,31 | **–** | – |
| | distal | 1–25% | **54** | 5,52 | **9** | 2,21 | **5** | 1,57 | **–** | – |
| | | 26–50% | **29** | 2,96 | **3** | 0,74 | **–** | – | **–** | – |
| | | 51–75% | **9** | 0,92 | **1** | 0,25 | **–** | – | **–** | – |
| | distal-lateral | 1–25% | **21** | 2,15 | **13** | 3,19 | **5** | 1,57 | **–** | – |
| | | 26–50% | **28** | 2,86 | **8** | 1,96 | **3** | 0,94 | **–** | – |
| | | 51–75% | **34** | 3,47 | **5** | 1,23 | **2** | 0,63 | **–** | – |
| | distal-proximal | 1–25% | **9** | 0,92 | **–** | – | **–** | – | **–** | – |
| | | 26–50% | **4** | 0,41 | **–** | – | **–** | – | **–** | – |
| | | 51–75% | **2** | 0,20 | **–** | – | **–** | – | **–** | – |
| | | **TOTAL:** | **979** | 100,00 | **408** | 100,00 | **318** | 100,00 | **145** | 100,00 |

Table 8-67. continued 2.

microlithic points in Barmaky and Mizyn assemblages (Nuzhnyi 2015: 166-167). Medial parts of broken backed pieces were recorded as unidentifiable (Fig. 8-57, *1, 5, 6, 9, 10, 12, 13, 16, 24*).

There are 12 **microlithic points on bladelets – microgravette points** (Table 8-77; Fig. 8-57, *20, 21, 23, 25-27*; 8-58, *6*), including four complete pieces and one distal fragment One crested and 11 regular bladelets served as blanks. The points on bladelets are straight (10 items) and wavy (2 items) backed. Seven proximally obliquely truncated fragments probably belong to the straight/wavy backed points. The straight/wavy backing was produced by continuous micro-scalar/scalar obverse abrupt retouch; only one item shows a continuous sub-parallel obverse abrupt retouch. All but one proximal oblique truncations were made by continuous scalar/micro-scalar obverse abrupt retouch; the exception is made by continuous scalar inverse semi-abrupt retouch. In addition to lateral backing and proximal truncation, three pieces exhibit extra modifications of the lateral side opposite of the backing: one dorsal notch close to the truncated base and two cases of lateral partial scalar/marginal obverse flat retouch (Fig. 8-57, *20, 21*). Nuzhnyi (2015) proposed to interpret such notches as predetermined breaking points. Several points show clear impact fractures from their use as projectiles (Fig. 8-57, *9, 26*). The average dimensions are 43.03×8.16×3.02 mm.

A relatively large fragment (77.93×10.32×6.33 mm) of a bi-laterally backed microlith on a crested bladelet (Fig. 8-58, *6*) is the only bi-laterally backed piece in the Barmaky, level 2 assemblage, as well as the only microlith of such thickness.

| | | flakes | | blades | | bladelets | | micro-blades | |
|---|---|---|---|---|---|---|---|---|---|
| | | # | % | # | % | # | % | # | % |
| HORIZON 2b | cortex | **2** | 13,33 | **–** | – | **–** | – | **–** | – |
| | plain | **7** | 46,67 | **2** | 50,00 | **–** | – | **1** | 50,00 |
| | linear | **2** | 13,33 | **1** | 25,00 | **1** | 50,00 | **1** | 50,00 |
| | dihedral | **1** | 6,67 | **–** | – | **–** | – | **–** | – |
| | polyhedral | **2** | 13,33 | **–** | – | **–** | – | **–** | – |
| | faceted | **1** | 6,67 | **1** | 25,00 | **1** | 50,00 | **–** | – |
| | **TOTAL:** | **15** | 100,00 | **4** | 100,00 | **2** | 100,00 | **2** | 100,00 |
| | crushed | 3 | – | – | – | – | – | – | – |
| | modified | – | – | 3 | – | – | – | – | – |
| | missing | 5 | – | 2 | – | 5 | – | 1 | – |
| HORIZON 2c, PIT 1 | cortex | **20** | 20,62 | **–** | – | **–** | – | **–** | – |
| | plain | **44** | 45,36 | **16** | 55,17 | **11** | 55,00 | **3** | 100,00 |
| | linear | **6** | 6,19 | **4** | 13,79 | **5** | 25,00 | **–** | – |
| | pointed | **1** | 1,03 | **–** | – | **–** | – | **–** | – |
| | dihedral | **7** | 7,22 | **1** | 3,45 | **2** | 10,00 | **–** | – |
| | polyhedral | **12** | 12,37 | **4** | 13,79 | **1** | 5,00 | **–** | – |
| | faceted | **7** | 7,22 | **4** | 13,79 | **1** | 5,00 | **–** | – |
| | **TOTAL:** | **97** | 100,00 | **29** | 100,00 | **20** | 100,00 | **3** | 100,00 |
| | crushed | 20 | – | 5 | – | 9 | – | 4 | – |
| | modified | – | – | 2 | – | – | – | – | – |
| | unidentifiable | 1 | – | – | – | – | – | – | – |
| | missing | 29 | – | 15 | – | 13 | – | 17 | – |
| HORIZON 2c | cortex | **158** | 9,89 | **20** | 3,85 | **8** | 2,52 | **4** | 2,27 |
| | plain | **803** | 50,25 | **257** | 49,42 | **152** | 47,80 | **66** | 37,50 |
| | linear | **188** | 11,76 | **110** | 21,15 | **92** | 28,93 | **75** | 42,61 |
| | pointed | **14** | 0,88 | **2** | 0,38 | **5** | 1,57 | **6** | 3,41 |
| | dihedral | **200** | 12,52 | **68** | 13,08 | **34** | 10,69 | **14** | 7,95 |
| | polyhedral | **133** | 8,32 | **30** | 5,77 | **10** | 3,14 | **2** | 1,14 |
| | faceted | **101** | 6,32 | **33** | 6,35 | **17** | 5,35 | **9** | 5,11 |
| | en éperon | **1** | 0,06 | **–** | – | **–** | – | **–** | – |
| | **TOTAL:** | **1598** | 100,00 | **520** | 100,00 | **318** | 100,00 | **176** | 100,00 |
| | crushed | 404 | – | 142 | – | 134 | – | 70 | – |
| | modified | 11 | – | 76 | – | 9 | – | 12 | – |
| | unidentifiable | 28 | – | 1 | – | 2 | – | – | – |
| | missing | 693 | – | 536 | – | 449 | – | 343 | – |

Table 8–68. Barmaky, western area complex, by horizons and structures: *débitage* striking platform types (including tools)

| | | flakes | | blades | | bladelets | | micro-blades | |
|---|---|---|---|---|---|---|---|---|---|
| | | # | % | # | % | # | % | # | % |
| HORIZON 2d | cortex | **57** | 10,73 | **3** | 2,01 | **1** | 0,99 | **1** | 4,00 |
| | plain | **280** | 52,73 | **87** | 58,39 | **57** | 56,44 | **12** | 48,00 |
| | linear | **41** | 7,72 | **12** | 8,05 | **23** | 22,77 | **9** | 36,00 |
| | pointed | **2** | 0,38 | **–** | – | **4** | 3,96 | **–** | – |
| | dihedral | **71** | 13,37 | **14** | 9,40 | **5** | 4,95 | **1** | 4,00 |
| | polyhedral | **48** | 9,04 | **18** | 12,08 | **1** | 0,99 | **1** | 4,00 |
| | faceted | **32** | 6,03 | **15** | 10,07 | **10** | 9,90 | **1** | 4,00 |
| | **TOTAL:** | **531** | 100,00 | **149** | 100,00 | **101** | 100,00 | **25** | 100,00 |
| | crushed | 151 | – | 46 | – | 46 | – | 20 | – |
| | modified | 5 | – | 18 | – | 1 | – | 2 | – |
| | unidentifiable | 3 | – | – | – | – | – | – | – |
| | missing | 289 | – | 195 | – | 170 | – | 98 | – |

Table 8–68. continued.

| | | flakes | | blades | | bladelets | | micro-blades | |
|---|---|---|---|---|---|---|---|---|---|
| | | # | % | # | % | # | % | # | % |
| HORIZON 2b | trimmed | **3** | 17,65 | **2** | 50,00 | **–** | – | **1** | 50,00 |
| | untrimmed | **14** | 82,35 | **2** | 50,00 | **2** | 100,00 | **1** | 50,00 |
| | **TOTAL:** | **17** | 100,00 | **4** | 100,00 | **2** | 100,00 | **2** | 100,00 |
| | missing | 5 | – | 2 | – | 5 | – | 1 | – |
| | unidentifiable | 1 | – | 3 | – | – | – | – | – |
| HORIZON 2c, PIT 1 | trimmed | **15** | 13,04 | **12** | 35,29 | **13** | 44,83 | **2** | 50,00 |
| | untrimmed | **100** | 86,96 | **22** | 64,71 | **16** | 55,17 | **2** | 50,00 |
| | **TOTAL:** | **115** | 100,00 | **34** | 100,00 | **29** | 100,00 | **4** | 100,00 |
| | missing | 29 | – | 15 | – | 13 | – | 17 | – |
| | unidentifiable | 3 | – | 2 | – | – | – | 3 | – |
| HORIZON 2c | trimmed | **338** | 17,32 | **299** | 46,28 | **191** | 43,31 | **88** | 37,13 |
| | untrimmed | **1613** | 82,68 | **347** | 53,72 | **250** | 56,69 | **149** | 62,87 |
| | **TOTAL:** | **1951** | 100,00 | **646** | 100,00 | **441** | 100,00 | **237** | 100,00 |
| | missing | 691 | – | 543 | – | 451 | – | 345 | – |
| | unidentifiable | 92 | – | 86 | – | 20 | – | 19 | – |
| HORIZON 2d | trimmed | **112** | 16,89 | **89** | 47,59 | **78** | 56,12 | **18** | 42,86 |
| | untrimmed | **551** | 83,11 | **98** | 52,41 | **61** | 43,88 | **24** | 57,14 |
| | **TOTAL:** | **663** | 100,00 | **187** | 100,00 | **139** | 100,00 | **42** | 100,00 |
| | missing | 292 | – | 201 | – | 170 | – | 99 | – |
| | unidentifiable | 24 | – | 20 | – | 9 | – | 4 | – |

Table 8–69. Barmaky, western area complex, by horizons and structures: *débitage* overhang trimming (including tools)

| | | flakes | | blades | | bladelets | | micro-blades | |
|---|---|---|---|---|---|---|---|---|---|
| | | # | % | # | % | # | % | # | % |
| HORIZON 2b | abrased | **–** | – | **–** | – | **–** | – | **–** | – |
| | unabrased | **17** | 100,00 | **4** | 100,00 | **2** | 100,00 | **2** | 100,00 |
| | **TOTAL:** | **17** | 100,00 | **4** | 100,00 | **2** | 100,00 | **2** | 100,00 |
| | missing | 5 | – | 2 | – | 5 | – | 1 | – |
| | unidentifiable | 1 | – | 3 | – | – | – | – | – |
| HORIZON 2c, PIT 1 | abrased | **1** | 0,87 | **–** | – | **–** | – | **–** | – |
| | unabrased | **114** | 99,13 | **34** | 100,00 | **29** | 100,00 | **4** | 100,00 |
| | **TOTAL:** | **115** | 100,00 | **34** | 100,00 | **29** | 100,00 | **4** | 100,00 |
| | missing | 29 | – | 15 | – | 13 | – | 17 | – |
| | unidentifiable | 3 | – | 2 | – | – | – | 3 | – |
| HORIZON 2c | abrased | **13** | 0,67 | **11** | 1,73 | **3** | 0,69 | **1** | 0,42 |
| | unabrased | **1920** | 99,33 | **625** | 98,27 | **433** | 99,31 | **236** | 99,58 |
| | **TOTAL:** | **1933** | 100,00 | **636** | 100,00 | **436** | 100,00 | **237** | 100,00 |
| | missing | 691 | – | 543 | – | 451 | – | 344 | – |
| | unidentifiable | 110 | – | 96 | – | 25 | – | 20 | – |
| HORIZON 2d | abrased | **1** | 0,15 | **–** | – | **–** | – | **–** | – |
| | unabrased | **662** | 99,85 | **187** | 100,00 | **140** | 100,00 | **42** | 100,00 |
| | **TOTAL:** | **663** | 100,00 | **187** | 100,00 | **140** | 100,00 | **42** | 100,00 |
| | missing | 292 | – | 201 | – | 170 | – | 99 | – |
| | unidentifiable | 24 | – | 20 | – | 8 | – | 4 | – |

Table 8-70. Barmaky, western area complex, by horizons and structures: *débitage* butt abrasion (including tools)

**Microlithic points on micro-blades – micro-gravette points** are the most numerous type of microliths (Table 8-77; Fig. 8-57, *2-4, 8, 11, 15, 18, 19, 22*). Twenty-nine regular and two crested micro-blades served as blanks. Four pieces are preserved completely, 12 as distal fragments, and 15 as proximal fragments with truncated bases. All specimens exhibit straight lateral backing, made by continuous scalar/micro-scalar obverse semi-abrupt/abrupt retouch (n = 22), continuous marginal obverse semi-abrupt/abrupt retouch (n = 5), continuous sub-parallel micro-scalar obverse abrupt retouch (n = 2), and discontinuous/partial micro-scalar obverse semi-abrupt/abrupt retouch (n = 2). The obliquely truncated bases were modified by continuous scalar/micro-scalar obverse abrupt retouch. Additional modifications opposite to the backed edge are observed for three tips in the form of ventral, dorsal, and bi-lateral dorsal scalar flat retouch (Fig. 8-57, *3*). In one case, the edge opposite to the backed side shows a partial scalar obverse flat retouch. The average dimensions are 21.61×4.73×1.98 mm.

The main diagnostic attribute of **unfinished microliths** is partial backing. There are six **unfinished microliths on bladelets** and three on micro-blades (Table 8-77). Two medial and 4 proximal fragments are recorded as unfinished microliths on bladelets (Fig. 8-57, *7, 14*). These unfinished microliths are all made on regular bladelets and reflect the attempts of straight/concave lateral backing by partial scalar/micro-scalar obverse semi-abrupt/abrupt retouch. A partly backed proximal fragment shows a concavely truncated base shaped by continuous scalar obverse abrupt retouch. Another medial piece exhibits a dorsal notch opposite of the backed edge. The widths of backed and unmodified parts of unfinished microlith on one of the bladelets are 5.10 and 7.24 mm, respectively. The average dimensions are >18.47×7.39×2.35 mm.

| | | flakes | | blades | | bladelets | | micro-blades | |
|---|---|---|---|---|---|---|---|---|---|
| | | # | % | # | % | # | % | # | % |
| HORIZON 2b | lipped | **1** | 5,88 | **–** | | **–** | | **–** | – |
| | semi-lipped | **3** | 17,65 | **2** | 50,00 | **1** | 50,00 | **–** | – |
| | unlipped | **13** | 76,47 | **2** | 50,00 | **1** | 50,00 | **2** | 100,00 |
| | **TOTAL:** | **17** | 100,00 | **4** | 100,00 | **2** | 100,00 | **2** | 100,00 |
| | missing | 5 | – | 2 | – | 5 | – | 1 | – |
| | unidentifiable | 1 | – | 3 | – | – | – | – | – |
| HORIZON 2c, PIT 1 | lipped | **6** | 5,88 | **2** | 40,00 | **–** | – | **–** | – |
| | semi-lipped | **8** | 7,84 | **3** | 60,00 | **–** | – | **–** | – |
| | unlipped | **88** | 86,27 | **–** | – | **21** | 100,00 | **4** | 100,00 |
| | **TOTAL:** | **102** | 100,00 | **5** | 100,00 | **21** | 100,00 | **4** | 100,00 |
| | missing | 29 | – | 15 | – | 13 | – | 17 | – |
| | unidentifiable | 16 | – | 31 | – | 8 | – | 3 | – |
| HORIZON 2c | lipped | **64** | 3,76 | **7** | 1,29 | **13** | 3,43 | **5** | 2,42 |
| | semi-lipped | **147** | 8,64 | **59** | 10,85 | **20** | 5,28 | **6** | 2,90 |
| | unlipped | **1491** | 87,60 | **478** | 87,87 | **346** | 91,29 | **196** | 94,69 |
| | **TOTAL:** | **1702** | 100,00 | **544** | 100,00 | **379** | 100,00 | **207** | 100,00 |
| | missing | 691 | – | 543 | – | 450 | – | 344 | – |
| | unidentifiable | 341 | – | 188 | – | 83 | – | 50 | – |
| HORIZON 2d | lipped | **33** | 5,67 | **6** | 3,57 | **5** | 4,20 | **–** | – |
| | semi-lipped | **47** | 8,08 | **17** | 10,12 | **4** | 3,36 | **1** | 2,70 |
| | unlipped | **502** | 86,25 | **145** | 86,31 | **110** | 92,44 | **36** | 97,30 |
| | **TOTAL:** | **582** | 100,00 | **168** | 100,00 | **119** | 100,00 | **37** | 100,00 |
| | missing | 292 | – | 199 | – | 170 | – | 99 | – |
| | unidentifiable | 105 | – | 41 | – | 29 | – | 9 | – |

Table 8-71. Barmaky, western area complex, by horizons and structures: *débitage* butts lipping (including tools)

There are three **unfinished microliths on micro-blades**: two distal and one medial fragment (Table 8-77). Two regular and one *débordante* micro-blades serve as blanks. Partial micro-scalar obverse semi-abrupt/abrupt retouch was applied for the lateral edge modification. The average dimensions are >12.01×5.56×2.33 mm.

Unidentifiable fragmented pieces compose more than half of the total number of microliths (Table 8-77). Proximal (4 items) and medial (5 items) fragments make up the **unidentifiable microliths on bladelets** (Table 8-77; Fig. 8-57, *10, 12, 16, 24*). Eight regular and one *débordante* bladelet served as blanks. One piece shows the clear impact fracture. Continuous scalar/micro-scalar obverse abrupt retouch shaped the backed edges. The average dimensions are >19.31×8.31×2.65 mm.

Two distal, 1 lateral, 37 medial and 6 proximal fragments were recorded as **unidentifiable microliths on micro-blades** (Table 8-77; Fig. 8-57, *1, 5, 6, 9, 13, 17*). All fragments come from regular micro-blades. The backing was made by continuous scalar/micro-scalar obverse semi-abrupt/abrupt retouch. Marginal retouching modified three pieces. Sub-parallel, inverse, and alternating retouch are observed singly. Three pieces show partial marginal obverse/inverse abrupt retouching opposite to the backed edge. The average dimensions are >13.13×5.08×2.19 mm.

**Retouched pieces** were made on blades, bladelets, micro-blades, flakes, natural flakes, and unidentifiable *débitage* (Table 8-78). The 47 regular, 14 crested, 9 *débordantes* and one primary piece served as blanks for about 45 % of **retouched pieces on blades** (Fig. 8-58,

| | | flakes | | blades | | bladelets | | micro-blades | |
|---|---|---|---|---|---|---|---|---|---|
| | | # | % | # | % | # | % | # | % |
| HORIZON 2b | absent | **1** | 5,88 | **–** | – | **–** | – | **–** | – |
| | defused | **4** | 23,53 | **–** | – | **1** | 50,00 | **1** | 50,00 |
| | pronounced | **12** | 70,59 | **4** | 100,00 | **1** | 50,00 | **1** | 50,00 |
| | **TOTAL:** | **17** | 100,00 | **4** | 100,00 | **2** | 100,00 | **2** | 100,00 |
| | missing | 5 | – | 2 | – | 5 | – | 1 | – |
| | unidentifiable | 1 | – | 3 | – | – | – | – | – |
| HORIZON 2c, PIT 1 | absent | **6** | 6,12 | **1** | 3,45 | **–** | – | **–** | – |
| | defused | **23** | 23,47 | **4** | 13,79 | **2** | 9,52 | **1** | 25,00 |
| | pronounced | **69** | 70,41 | **24** | 82,76 | **19** | 90,48 | **3** | 75,00 |
| | **TOTAL:** | **98** | 100,00 | **29** | 100,00 | **21** | 100,00 | **4** | 100,00 |
| | missing | 29 | – | 15 | – | 13 | – | 17 | – |
| | unidentifiable | 20 | – | 7 | – | 8 | – | 3 | – |
| HORIZON 2c | absent | **45** | 2,64 | **5** | 0,92 | **10** | 2,62 | **6** | 2,87 |
| | defused | **340** | 19,94 | **101** | 18,50 | **71** | 18,59 | **55** | 26,32 |
| | pronounced | **1320** | 77,42 | **440** | 80,59 | **301** | 78,80 | **148** | 70,81 |
| | **TOTAL:** | **1705** | 100,00 | **546** | 100,00 | **382** | 100,00 | **209** | 100,00 |
| | missing | 691 | – | 543 | – | 450 | – | 344 | – |
| | unidentifiable | 338 | – | 186 | – | 80 | – | 48 | – |
| HORIZON 2d | absent | **25** | 4,28 | **2** | 1,19 | **3** | 2,50 | **–** | – |
| | defused | **133** | 22,77 | **39** | 23,21 | **23** | 19,17 | **10** | 27,03 |
| | pronounced | **426** | 72,95 | **127** | 75,60 | **94** | 78,33 | **27** | 72,97 |
| | **TOTAL:** | **584** | 100,00 | **168** | 100,00 | **120** | 100,00 | **37** | 100,00 |
| | missing | 292 | – | 199 | – | 170 | – | 99 | – |
| | unidentifiable | 103 | – | 41 | – | 28 | – | 9 | – |

Table 8-72. Barmaky, western area complex, by horizons and structures: *débitage* bulbs (including tools)

*1-5*, *7*) among which laterally retouched pieces dominate (Table 8-78). Laterally retouched blades are represented by 18 complete pieces and 20 distal, 16 medial, 17 proximal fragments with a wide variety of retouch combinations. Dominant (about 50%) is the combination of partial marginal/scalar obverse/inverse flat/semi-abrupt/abrupt retouch. The average dimensions are 51.38×18.61×6.05 mm.

The laterally dorsally retouched pieces prevail in the **retouched bladelet** assemblage (Table 8-78). Nine regular, 1 crested and 3 *débordantes* bladelets served as blanks. Three are completely preserved in addition to 3 distal, 5 medial, and 2 proximal fragments. Among the wide variety of retouch combinations, about 50 % combine partial marginal/scalar obverse/inverse flat/abrupt retouch. The average dimensions are 20.24×9.56×3.37 mm.

Three pieces with lateral dorsal retouch make up the **retouched micro-blades** assemblage (Table 8-78). Distal and medial parts of regular micro-blade and a medial fragment of a *débordante* micro-blade served as blanks. Combinations of continuous/partial irregular/micro-scalar/scalar obverse flat/semi-abrupt retouch modified these pieces. The average dimensions are >21.93×6.39×4.30 mm.

One-third of retouched pieces were made on flakes (Table 8-78; Fig. 8-59, *1, 2, 4, 5*). Laterally retouched pieces dominate the **retouched flake** assemblage. Forty regular, 4 *Kantenabschläge*, 3 crested, 3 *débordantes*, 1 core-tablet, and 2 primary pieces served as blanks. The retouched flakes are represented by 12 distal, 3 lateral, 1 medial, and 5 proximal fragments, and 32 complete flakes. A wide variety of retouch combinations was used.

| | | flakes | | blades | | bladelets | | micro-blades | |
|---|---|---|---|---|---|---|---|---|---|
| | | # | % | # | % | # | % | # | % |
| HORIZON 2b | right | **7** | 46,67 | **3** | 75,00 | **1** | 50,00 | **2** | 100,00 |
| | acute | **8** | 53,33 | **1** | 25,00 | **1** | 50,00 | **–** | – |
| | obtuse | **–** | – | **–** | – | **–** | – | **–** | – |
| | **TOTAL:** | **15** | 100,00 | **4** | 100,00 | **2** | 100,00 | **2** | 100,00 |
| | missing | 5 | – | 2 | – | 5 | – | 1 | – |
| | unidentifiable | 3 | – | 3 | – | – | – | – | – |
| HORIZON 2c, PIT 1 | right | **53** | 54,64 | **21** | 72,41 | **18** | 90,00 | **1** | 33,33 |
| | acute | **44** | 45,36 | **8** | 27,59 | **2** | 10,00 | **2** | 66,67 |
| | obtuse | **–** | – | **–** | – | **–** | – | **–** | – |
| | **TOTAL:** | **97** | 100,00 | **29** | 100,00 | **20** | 100,00 | **3** | 100,00 |
| | missing | 29 | – | 15 | – | 13 | – | 17 | – |
| | unidentifiable | 21 | – | 7 | – | 2 | – | 4 | – |
| HORIZON 2c | right | **1042** | 65,17 | **390** | 74,14 | **245** | 76,80 | **147** | 83,05 |
| | acute | **545** | 34,08 | **135** | 25,67 | **74** | 23,20 | **30** | 16,95 |
| | obtuse | **12** | 0,75 | **1** | 0,19 | **–** | – | **–** | – |
| | **TOTAL:** | **1599** | 100,00 | **526** | 100,00 | **319** | 100,00 | **177** | 100,00 |
| | missing | 691 | – | 543 | – | 450 | – | 344 | – |
| | unidentifiable | 444 | – | 206 | – | 143 | – | 80 | – |
| HORIZON 2d | right | **360** | 68,05 | **109** | 72,67 | **82** | 82,00 | **24** | 88,89 |
| | acute | **165** | 31,19 | **40** | 26,67 | **18** | 18,00 | **3** | 11,11 |
| | obtuse | **4** | 0,76 | **1** | 0,67 | **–** | – | **–** | – |
| | **TOTAL:** | **529** | 100,00 | **150** | 100,00 | **100** | 100,00 | **27** | 100,00 |
| | missing | 292 | – | 199 | – | 170 | – | 99 | – |
| | unidentifiable | 158 | – | 59 | – | 48 | – | 19 | – |

Table 8–73. Barmaky, western area complex, by horizons and structures: *débitage* striking platform angels (including tools)

| | 2b | 2c, pit 1 | 2c | 2d | Σ | % | esse, % |
|---|---|---|---|---|---|---|---|
| **end-scrapers** | – | – | 13 | 4 | **17** | 2,58 | 3,69 |
| **burins** | 2 | 8 | 165 | 39 | **214** | 32,47 | 46,42 |
| **truncated pieces** | 2 | 1 | 62 | 27 | **92** | 13,96 | 19,96 |
| **notched pieces** | – | 1 | 11 | 3 | **15** | 2,28 | 3,25 |
| **borer-perforators** | – | – | 7 | 2 | **9** | 1,37 | 1,95 |
| **points** | – | – | 2 | 1 | **3** | 0,46 | 0,65 |
| **raclettes** | – | – | 2 | – | **2** | 0,30 | 0,43 |
| **combined tools** | – | – | 2 | – | **2** | 0,30 | 0,43 |
| **microliths** | – | 5 | 80 | 22 | **107** | 16,24 | 23,21 |
| **retouched pieces** | 1 | 2 | 113 | 41 | **157** | 23,82 | – |
| **thinned pieces** | – | – | 2 | – | **2** | 0,30 | – |
| **unidentifiable** | – | 4 | 24 | 11 | **39** | 5,92 | – |
| **TOTAL:** | **5** | **21** | **483** | **150** | **659** | 100,00 | 100,00 |

Table 8–74. Barmaky, western area, by horizons and structures: tools

| | 2b | 2c, pit 1 | 2c | 2d | Σ | % | esse,% |
|---|---|---|---|---|---|---|---|
| **BURINS ON TRUNCATED BLADES** | | | | | | | |
| on straight distal dorsal truncation | – | 1 | 2 | 2 | **5** | 2,34 | 2,39 |
| on straight proximal dorsal truncation | – | – | 3 | 1 | **4** | 1,87 | 1,91 |
| on straight proximal ventral truncation | – | – | 1 | – | **1** | 0,47 | 0,48 |
| on oblique distal dorsal truncation | – | 2 | 21 | 6 | **29** | 13,55 | 13,88 |
| on oblique distal ventral truncation | – | – | 2 | – | **2** | 0,93 | 0,96 |
| on oblique proximal dorsal truncation | – | – | 13 | 2 | **15** | 7,01 | 7,18 |
| on oblique-convex distal dorsal truncation | – | – | 11 | 2 | **13** | 6,07 | 6,22 |
| on oblique-convex proximal dorsal truncation | – | 1 | 3 | – | **4** | 1,87 | 1,91 |
| on oblique-concave distal dorsal truncation | – | – | 5 | – | **5** | 2,34 | 2,39 |
| on oblique-concave proximal dorsal truncation | – | – | 3 | 2 | **5** | 2,34 | 2,39 |
| on concave distal dorsal truncation | – | – | 3 | 1 | **4** | 1,87 | 1,91 |
| on concave proximal dorsal truncation | – | – | 1 | – | **1** | 0,47 | 0,48 |
| on concave proximal ventral truncation | – | – | 1 | – | **1** | 0,47 | 0,48 |
| bi-lateral; on straight distal dorsal truncation | – | – | 1 | – | **1** | 0,47 | 0,48 |
| bi-lateral; on straight proximal dorsal truncation | – | – | – | 1 | **1** | 0,47 | 0,48 |
| bi-lateral; on oblique proximal dorsal truncation | – | 1 | – | – | **1** | 0,47 | 0,48 |
| bi-lateral; on oblique-concave proximal dorsal truncation | – | – | 1 | – | **1** | 0,47 | 0,48 |
| bi-lateral; on concave distal dorsal truncation | – | – | 1 | – | **1** | 0,47 | 0,48 |
| opposite; on bi-terminal straight proximal & oblique distal dorsal truncations | – | – | 1 | – | **1** | 0,47 | 0,48 |
| opposite; on bi-terminal straight proximal & oblique distal dorsal truncations; 3-edges | – | – | – | 1 | **1** | 0,47 | 0,48 |
| opposite; on bi-terminal oblique dorsal truncations | 1 | – | – | – | **1** | 0,47 | 0,48 |
| opposite; on bi-terminal oblique proximal & straight distal dorsal truncations | – | – | 1 | – | **1** | 0,47 | 0,48 |
| opposite; on bi-terminal oblique-convex proximal dorsal & oblique-concave distal ventral truncations | – | – | 1 | – | **1** | 0,47 | 0,48 |
| opposite; on bi-terminal oblique-concave dorsal truncations | – | – | 1 | – | **1** | 0,47 | 0,48 |
| opposite; on bi-terminal concave proximal dorsal & oblique-convex distal dorsal truncations | – | – | 1 | – | **1** | 0,47 | 0,48 |
| opposite-alternative; on bi-terminal oblique dorsal truncations | 1 | – | 3 | – | **4** | 1,87 | 1,91 |
| opposite-alternative; on bi-terminal straight proximal & convex distal dorsal truncations | – | – | 1 | – | **1** | 0,47 | 0,48 |
| opposite bi-lateral; on bi-terminal oblique proximal & concave distal dorsal truncations; 4-edges | – | – | 1 | – | **1** | 0,47 | 0,48 |
| **BURINS ON TRUNCATED FLAKES** | | | | | | | |
| on straight proximal dorsal truncation | – | – | – | 2 | **2** | 0,93 | 0,96 |
| on oblique-convex proximal dorsal truncation | – | – | 1 | – | **1** | 0,47 | 0,48 |
| on oblique-concave distal dorsal truncation | – | – | 2 | – | **2** | 0,93 | 0,96 |
| bi-lateral; on straight distal dorsal truncation | – | – | 1 | – | **1** | 0,47 | 0,48 |
| bi-lateral; on concave distal dorsal truncation | – | – | 1 | – | **1** | 0,47 | 0,48 |
| opposite-alternative; on bi-terminal oblique-concave dorsal truncations | – | – | 1 | – | **1** | 0,47 | 0,48 |

Table 8-75. Barmaky, western area, by horizons and structures: burins

| | 2b | 2c, pit 1 | 2c | 2d | Σ | % | esse,% |
|---|---|---|---|---|---|---|---|
| **BURINS ON TRUNCATED UNIDENTIFIABLE *DEBITAGE*** | | | | | | | |
| on straight distal dorsal truncation | – | 1 | 2 | 1 | **4** | 1,87 | 1,91 |
| on straight proximal dorsal truncation | – | – | – | 1 | **1** | 0,47 | 0,48 |
| on oblique distal dorsal truncation | – | – | 5 | – | **5** | 2,34 | 2,39 |
| on oblique proximal dorsal truncation | – | – | 1 | – | **1** | 0,47 | 0,48 |
| on oblique-concave proximal dorsal truncation | – | – | 1 | – | **1** | 0,47 | 0,48 |
| on concave distal dorsal truncation | – | – | 1 | – | **1** | 0,47 | 0,48 |
| on concave proximal dorsal truncation | – | – | 1 | – | **1** | 0,47 | 0,48 |
| **BURINS ON BLADES, ANGLE** | | | | | | | |
| distal | – | – | 5 | 2 | **7** | 3,27 | 3,35 |
| proximal | – | – | 10 | 2 | **12** | 5,61 | 5,74 |
| opposite; | – | – | 1 | – | **1** | 0,47 | 0,48 |
| opposite-alternative | – | – | 1 | – | **1** | 0,47 | 0,48 |
| **BURINS ON BLADELETS, ANGLE** | | | | | | | |
| distal | – | – | 1 | 1 | **2** | 0,93 | 0,96 |
| **BURINS ON FLAKES, ANGLE** | | | | | | | |
| distal | – | – | 4 | – | **4** | 1,87 | 1,91 |
| proximal | – | – | 4 | – | **4** | 1,87 | 1,91 |
| **BURINS ON BLADES, DIHEDRAL** | | | | | | | |
| symmetrical, distal | – | – | 8 | 2 | **10** | 4,67 | 4,78 |
| symmetrical, proximal | – | – | 3 | – | **3** | 1,40 | 1,44 |
| asymmetrical, distal | – | 2 | 7 | 2 | **11** | 5,14 | 5,26 |
| asymmetrical, proximal | – | – | 1 | 1 | **2** | 0,93 | 0,96 |
| bi-terminal: distal symmetrical & proximal asymmetrical | – | – | – | 1 | **1** | 0,47 | 0,48 |
| bi-terminal, asymmetrical | – | – | 2 | – | **2** | 0,93 | 0,96 |
| **BURINS ON FLAKES, DIHEDRAL** | | | | | | | |
| symmetrical, distal | – | – | 2 | – | **2** | 0,93 | 0,96 |
| **BURINS ON UNIDENTIFIABLE *DEBITAGE*, DIHEDRAL** | | | | | | | |
| symmetrical, distal | – | – | 2 | 2 | **4** | 1,87 | 1,91 |
| **BURINS ON BLADES, TRANSVERSAL** | | | | | | | |
| distal | – | – | 1 | – | **1** | 0,47 | 0,48 |
| **BURINS ON FLAKES, TRANSVERSAL** | | | | | | | |
| distal | – | – | 1 | – | **1** | 0,47 | 0,48 |

Table 8-75. continued 1

| | 2b | 2c, pit 1 | 2c | 2d | Σ | % | esse,% |
|---|---|---|---|---|---|---|---|
| **COMBINED BURINS ON BLADES** | | | | | | | |
| on oblique distal dorsal truncation & dihedral-symmetrical, proximal | – | – | – | 1 | **1** | 0,47 | 0,48 |
| on oblique distal dorsal truncation & dihedral-asymmetrical, proximal | – | – | 1 | – | **1** | 0,47 | 0,48 |
| on oblique proximal dorsal truncation & dihedral-symmetrical, distal | – | – | 1 | – | **1** | 0,47 | 0,48 |
| on oblique proximal dorsal truncation & dihedral-asymmetrical, distal | – | – | 1 | – | **1** | 0,47 | 0,48 |
| on oblique-convex distal dorsal truncation & dihedral-asymmetrical, proximal | – | – | – | 1 | **1** | 0,47 | 0,48 |
| on concave distal ventral truncation & angle, double-lateral, proximal | – | – | 1 | – | **1** | 0,47 | 0,48 |
| bi-lateral, on concave distal dorsal truncation & dihedral-asymmetrical, proximal | – | – | 1 | – | **1** | 0,47 | 0,48 |
| opposite, on oblique-convex distal dorsal truncation & angle, proximal | – | – | 1 | – | **1** | 0,47 | 0,48 |
| opposite, on oblique-convex proximal dorsal truncation & angle, distal | – | – | 1 | – | **1** | 0,47 | 0,48 |
| opposite-alternative, on oblique distal dorsal truncation & angle, proximal | – | – | 1 | – | **1** | 0,47 | 0,48 |
| angle, proximal & dihedral-asymmetrical, distal | – | – | 1 | – | **1** | 0,47 | 0,48 |
| dihedral-asymmetrical, proximal & transversal, distal | – | – | 1 | – | **1** | 0,47 | 0,48 |
| **BURINS ON BLADES, UNIDENTIFIABLE** | | | | | | | |
| distal | – | – | – | 2 | **2** | 0,93 | – |
| lateral | – | – | 1 | – | **1** | 0,47 | – |
| proximal | – | – | 1 | – | **1** | 0,47 | – |
| **BURINS ON FLAKES, UNIDENTIFIABLE** | | | | | | | |
| distal | – | – | 1 | – | **1** | 0,47 | – |
| **TOTAL:** | **2** | **8** | **165** | **39** | **214** | 100,00 | 100,00 |

Table 8-75. continued 2.

About half of the flakes were modified by partial scalar/marginal obverse semi-abrupt/abrupt/flat retouch. The average dimensions are 43.10×33.86×9.34 mm.

The laterally retouched pieces dominate the **retouched natural flake** assemblage (Table 8-78). The five retouched pieces comprise nearly all of the possible combinations of retouch: continuous/partial scalar obverse/inverse/alternate flat/semi-abrupt/abrupt. The average dimensions are 45.12×59.67×19.35 mm.

The laterally modified items dominate the **retouched pieces on unidentifiable *débitage*** (Table 8-78). Distal (4), lateral (7), and medial (1) blank fragments make up the retouched pieces on unidentifiable *débitage*. More than half of the retouched pieces were modified by partial marginal/scalar obverse flat/semi-abrupt retouch. The average dimensions are >13.72×15.00×2.85 mm.

Ventrally **thinned pieces** are not numerous (Table 8-74). One item was made on a *débordante* blade: 54.49×22.01×9.25 mm (Fig. 8-59, *3*); another is a lateral fragment (>24.67×>24.38×9.39 mm) of unidentifiable *débitage*. The former is distally ventrally thinned, and the latter is partially thinned by continuous scalar flat retouch.

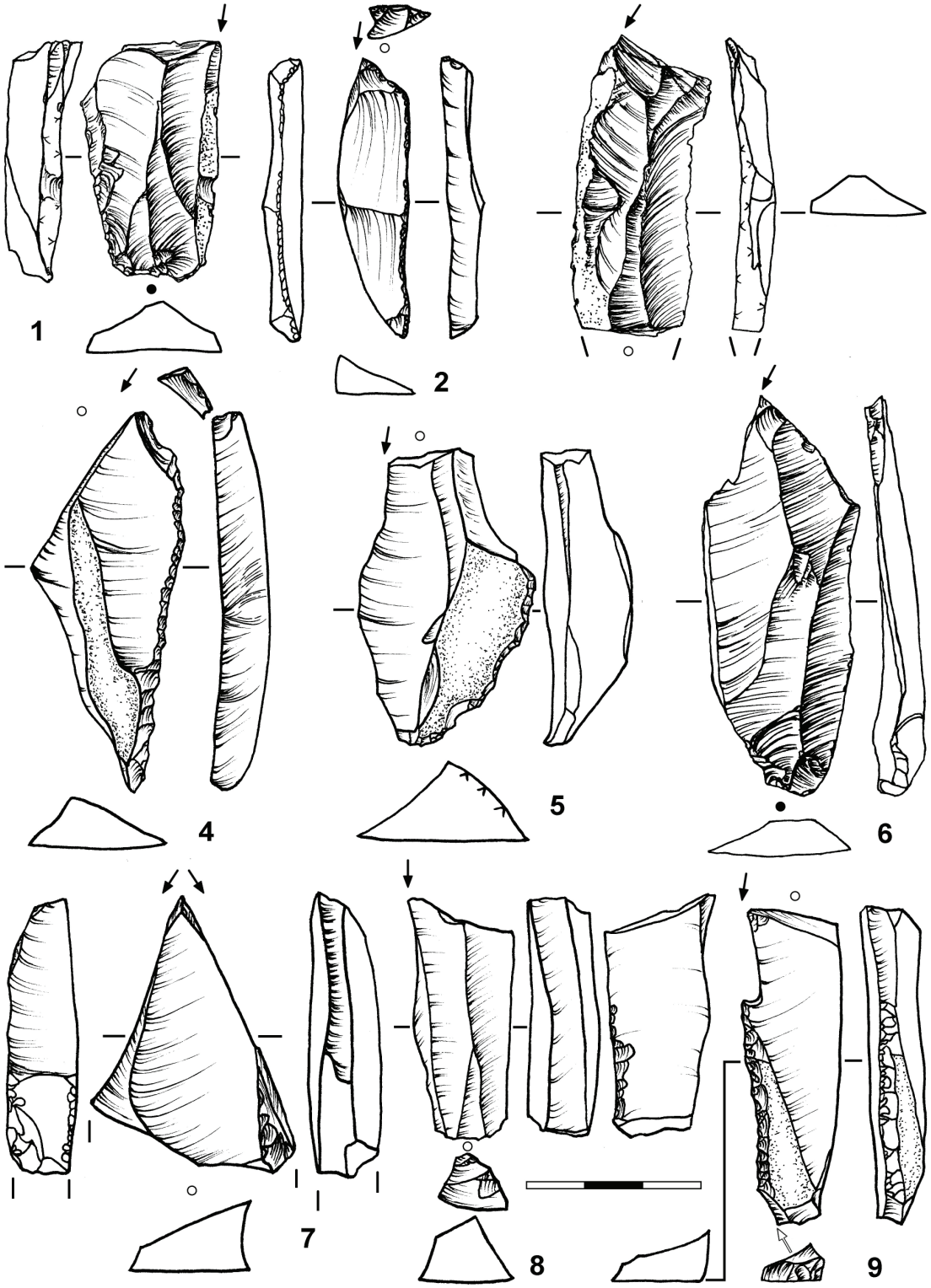


Fig. 8–49. Barmaky, western area complex, horizons 2c (1–5, 7–9) & 2d (6): 1 – angle burin on bi-laterally dorsally retouched blade; 2 – burin on concave, proximal, dorsal truncation, on laterally dorsally retouched unidentifiable *débitage*; 3, 6 – angle burins on blade; 4 – burin on oblique-concave, proximal, dorsal truncation, on laterally dorsally retouched unidentifiable *débitage*; 5 – angle burin on laterally and distally dorsally retouched flake; 7 – dihedral symmetrical burin on laterally dorsally retouched blade; 8 – angle burin on laterally ventrally retouched blade; 9 – angle burin on laterally dorsally retouched and on distally, straightly, dorsally truncated blade. Burin 9 was rejuvenated by truncations.

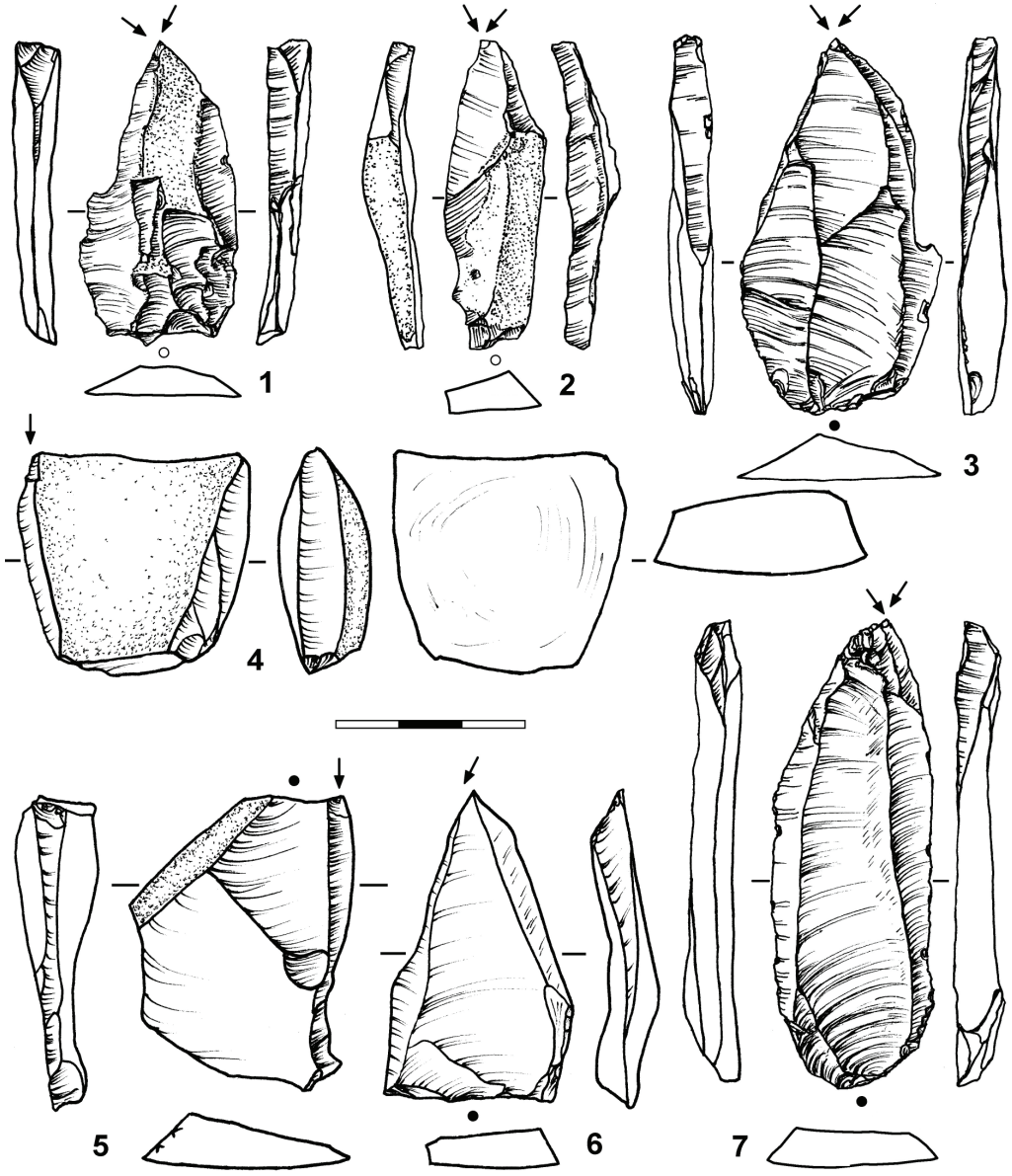


Fig. 8-50. Barmaky, western area complex, horizons 2c (1, 2, 4, 5-7) & 2d (3): 1-3, 7 – dihedral burins on blades, symmetrical, distal; 4, 5, 6 – angle burins on flakes.

**Unidentifiable tools** are represented by heavily fragmented *débitage* pieces with clear traces of secondary modification. One flake, one natural flake, and 37 unidentifiable *débitage* fragments make up the assemblage of unidentifiable tools. About 40 % are modified by continuous scalar obverse abrupt/semi-abrupt retouch. Because of the high degree of fragmentation, there is no reason to mention the average dimensions.

## Flaking instruments

There are two hammer-stones on flint pebbles: one complete (99.98×77.03×58.29 mm), and another fragmented (>25.56×>24.41×>8.54 mm). In addition, there are 670 fragments of sandstone. Among the latter, 2 chips and 29 flakes were observed. The dorsal surfaces of sandstone chips and flakes exhibit parts of the pebble cortex and are interpreted as fragments of hammer-stones.

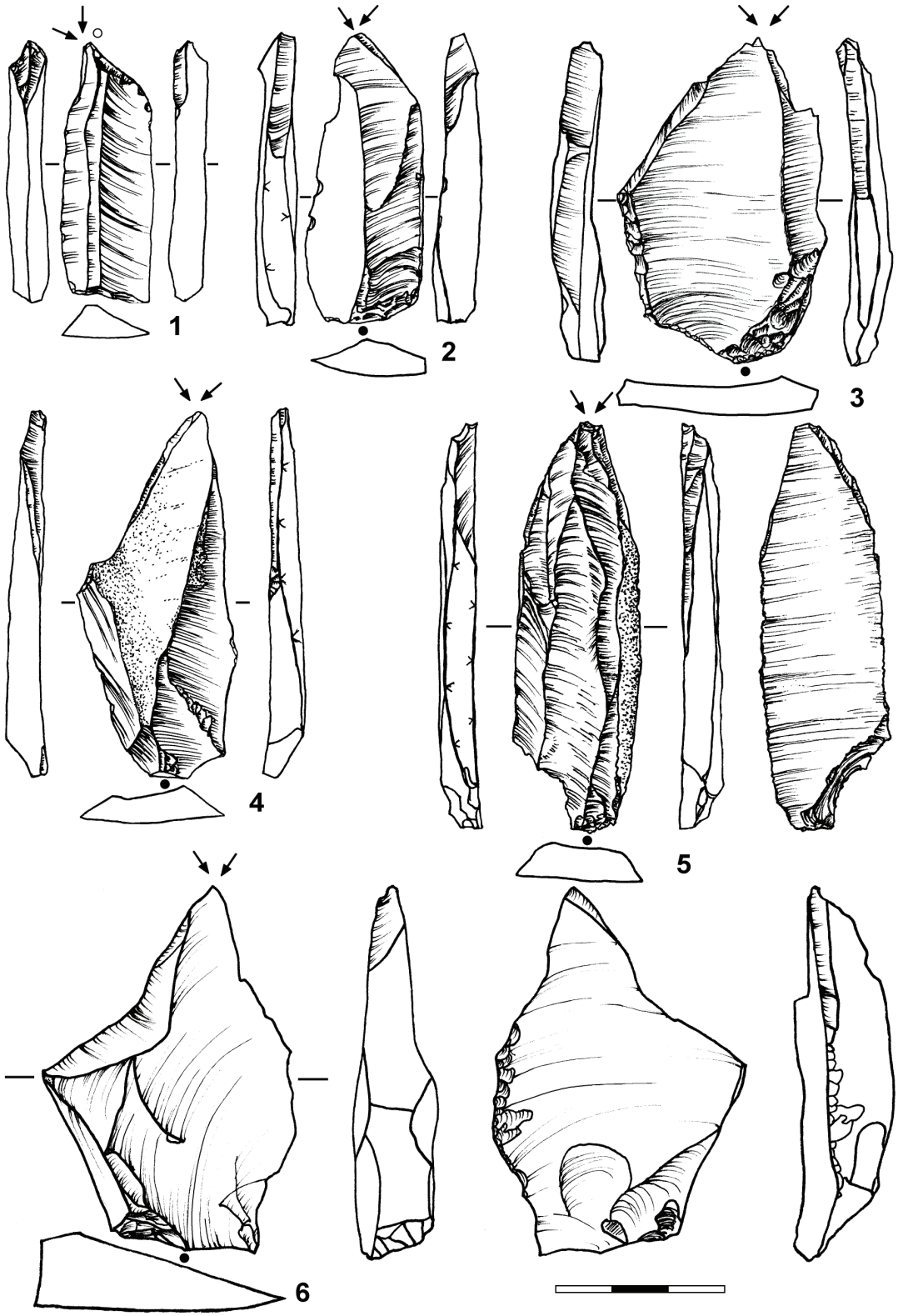


Fig. 8-51. Barmaky, western area complex, horizon 2c: 1 – dihedral asymmetrical burin on the distally dorsally concave-ly truncated blade; 2, 4 – dihedral asymmetrical burins on blades; 3 – dihedral symmetrical burin on laterally dorsally retouched flake; 5 – dihedral symmetrical burin on the proximally ventrally truncated blade; 6 – dihedral symmetrical burin on laterally ventrally retouched flake.

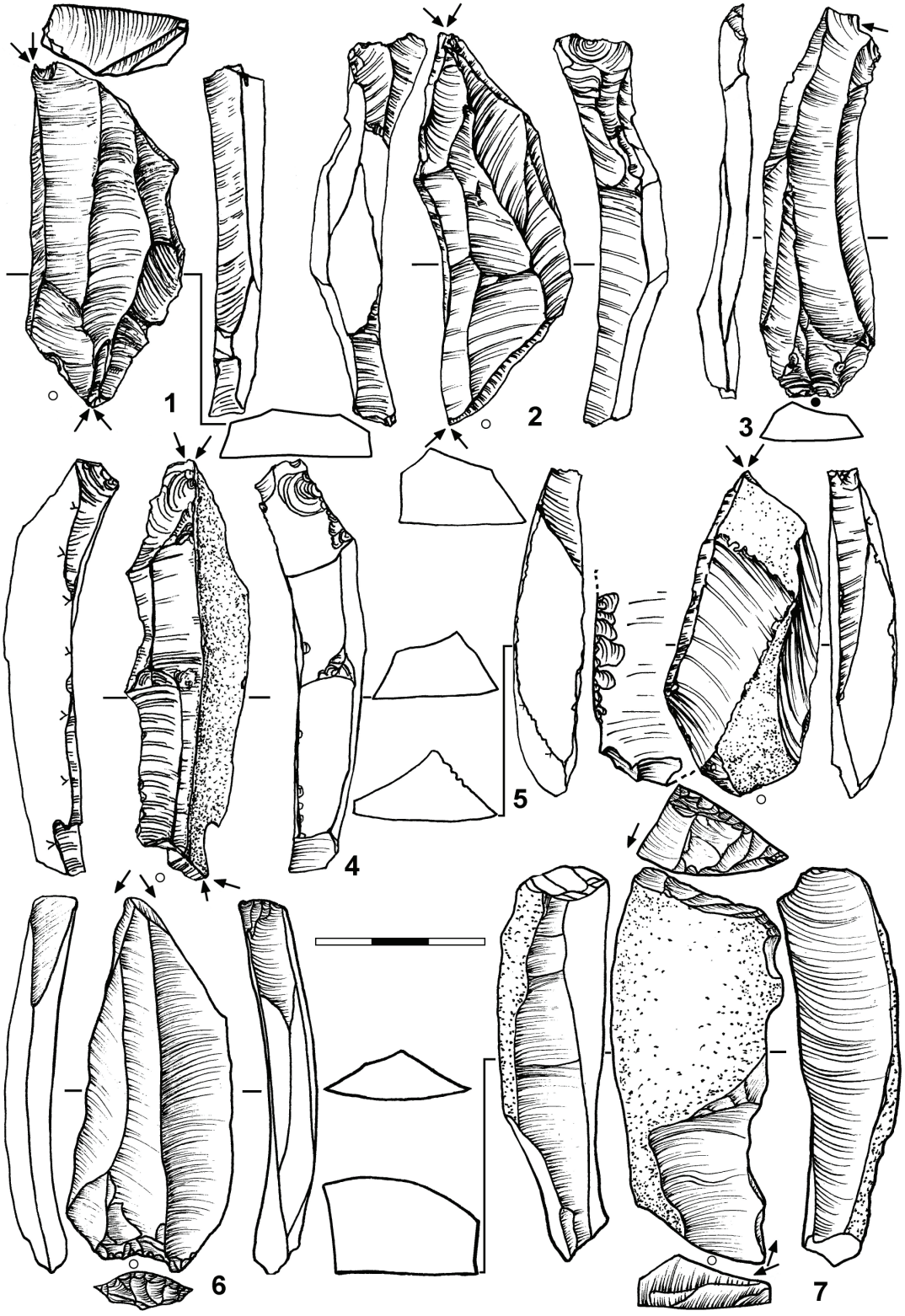


Fig. 8-52. Barmaky, western area complex, horizons 2c (1, 3, 4, 6, 7) & 2d (2, 5), burins: 1, 2 – dihedral-asymmetrical bi-terminal burins on blade; 3 – transversal burin on blade; 4 – dihedral-asymmetrical bi-terminal burin on laterally dorsally retouched blade; 5 – dihedral-asymmetrical burin on laterally and ventrally retouched/thinned-base blade; 6 – dihedral-asymmetrical burin on laterally dorsally retouched and on concavely proximally dorsally truncated blade; 7 – combined burin on blade – on oblique, distal, dorsal truncation & dihedral-asymmetrical, proximal.

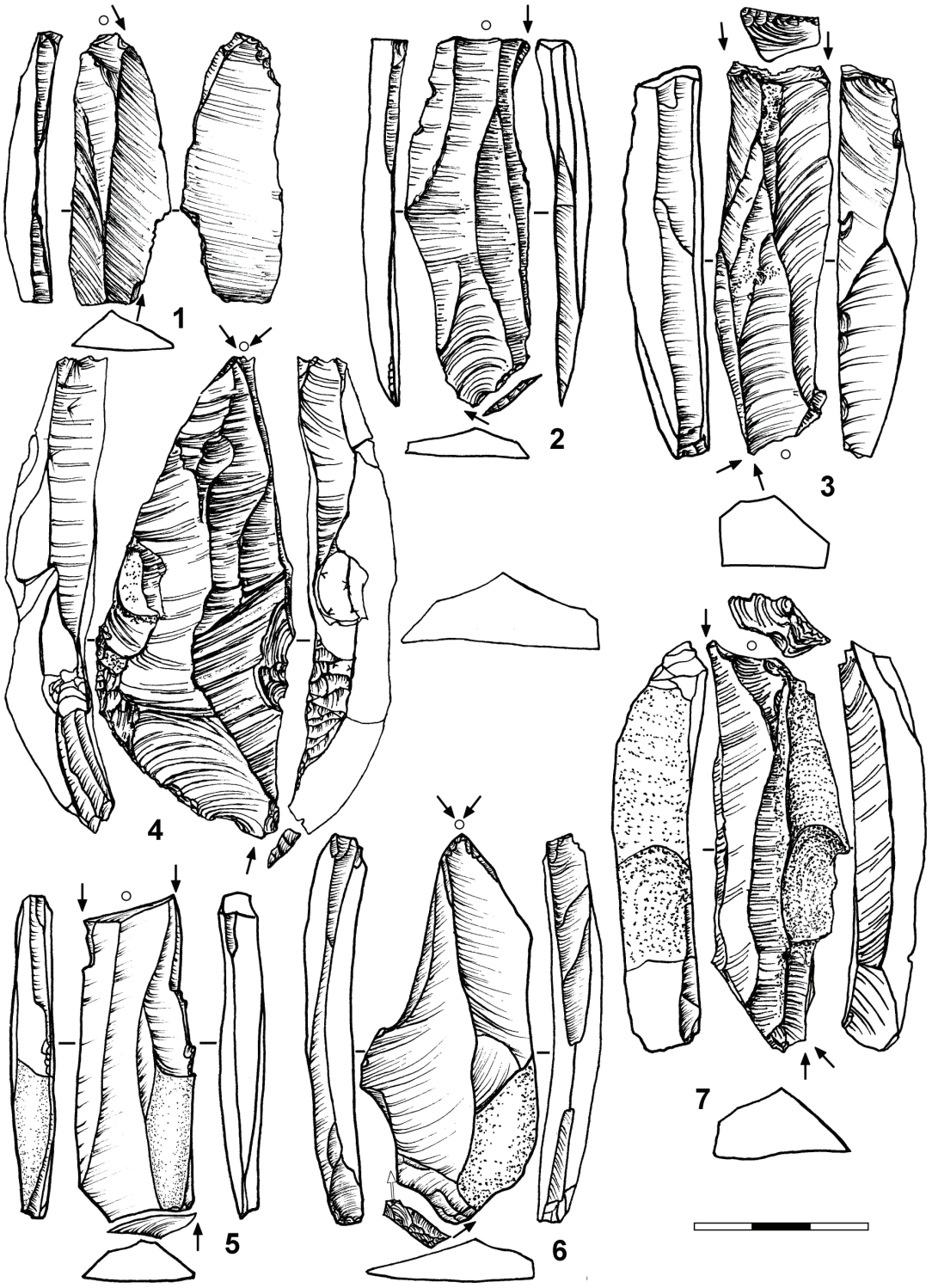


Fig. 8–53. Barmaky, western area complex, horizons 2c (1–3, 5–7) & 2d (4), combined burins on blades: 1 – opposite, on oblique-convex proximal dorsal truncation & angle, distal; 2 – opposite-alternate, on oblique distal dorsal truncation & angle, proximal; 3 – bilateral, on concave distal dorsal truncation & dihedral-asymmetrical, proximal; 4 – on oblique-convex distal dorsal truncation & dihedral-asymmetrical, proximal on bilaterally dorsally retouched piece; 5 – opposite, on concave distal ventral truncation & angle, double-lateral, proximal; 6 – bilateral on oblique proximal dorsal truncation & dihedral-symmetrical, distal; 7 – on oblique proximal dorsal truncation & dihedral-asymmetrical, distal. Burin 6 was rejuvenatet by truncation.

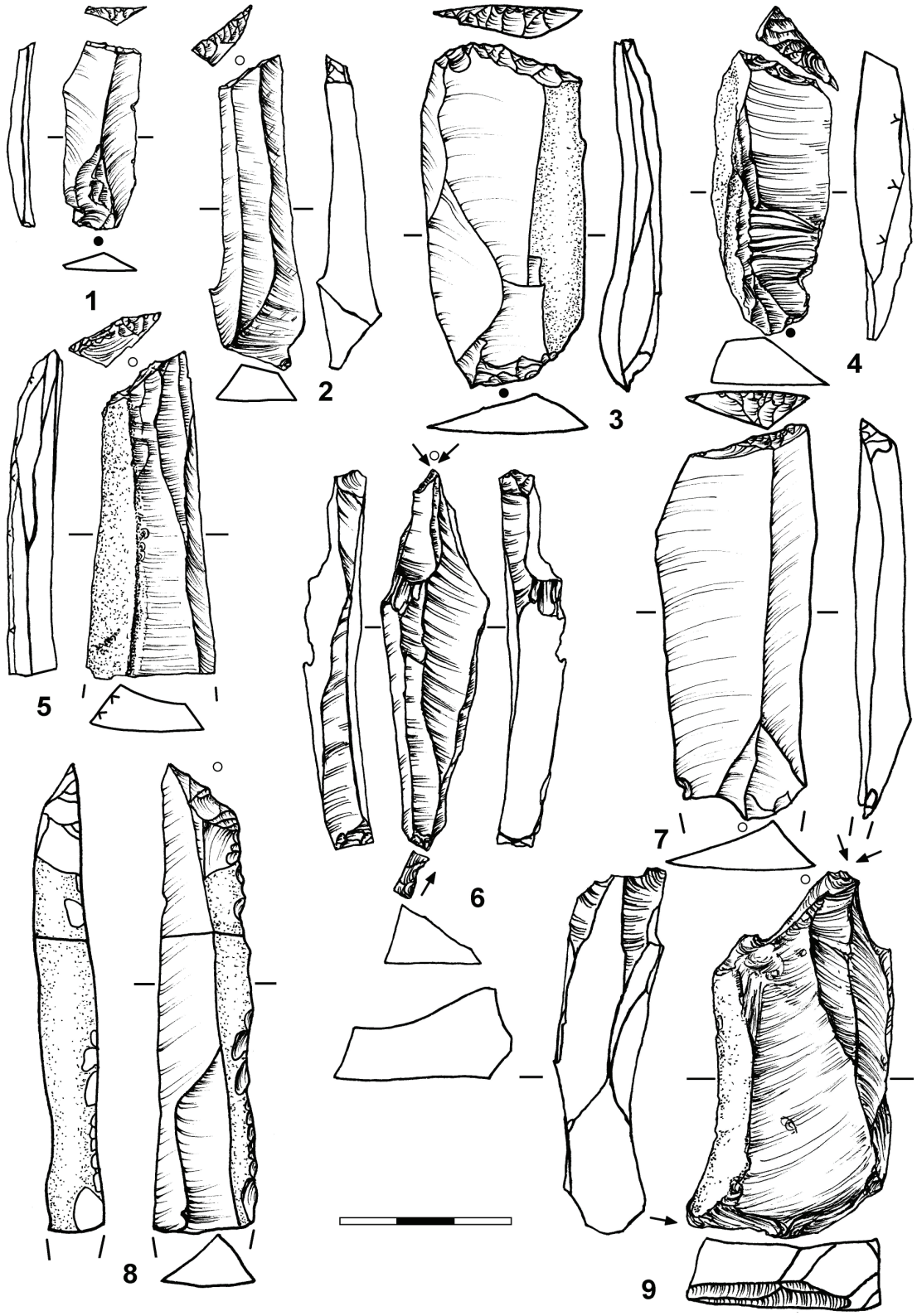


Fig. 8-54. Barmaky, western area complex, horizons 2c (1-5, 7-9) & 2d (6): 1 – truncated blade, straight, distal, dorsal; 2, 5 – truncated blades, oblique, proximal, dorsal; 3 – truncated blade, oblique-convex, distal, dorsal; 4, 7 – truncated blades, oblique, distal, dorsal; 6 – combined burin on blade, on oblique distal dorsal truncation & dihedral-symmetrical, proximal; 8 – truncated blade, oblique, distal, dorsal, on laterally dorsally retouched piece; 9 – combined burin on blade, dihedral-asymmetrical, proximal & transversal, distal.

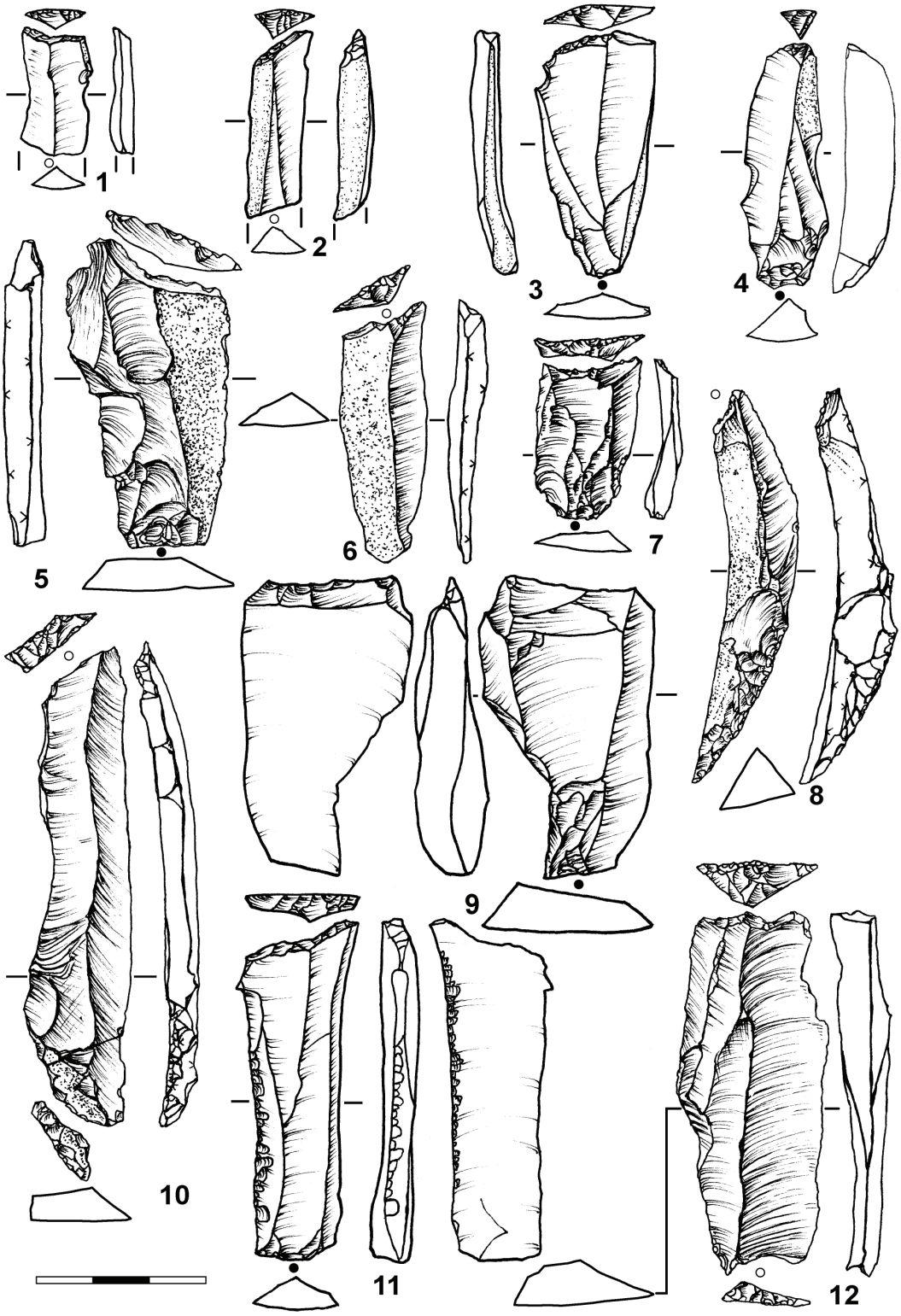


Fig. 8-55. Barmaky, western area complex, horizons 2c (1, 3, 5, 6, 8-12), 2d (2, 7) & pit 1 (4): 1 – truncated bladelet, oblique-concave, distal, dorsal; 2 – truncated bladelet, oblique, distal, dorsal; 3 – truncated blade, oblique-convex, distal, dorsal; 4 – truncated blade, convex, distal, dorsal; 5 – truncated flake, oblique-concave, distal, dorsal; 6, 8 – truncated pieces on blades, oblique-concave, proximal, dorsal; 7 – truncated blade, concave, distal, dorsal; 9 – truncated flake, straight, distal, ventral; 10 – truncated blade, bi-terminal, oblique-convex, dorsal; 11 – truncated blade, oblique-concave, distal, dorsal, on laterally alternative retouched piece; 12 – truncated blade, bi-terminal, concave/wavy, dorsal.

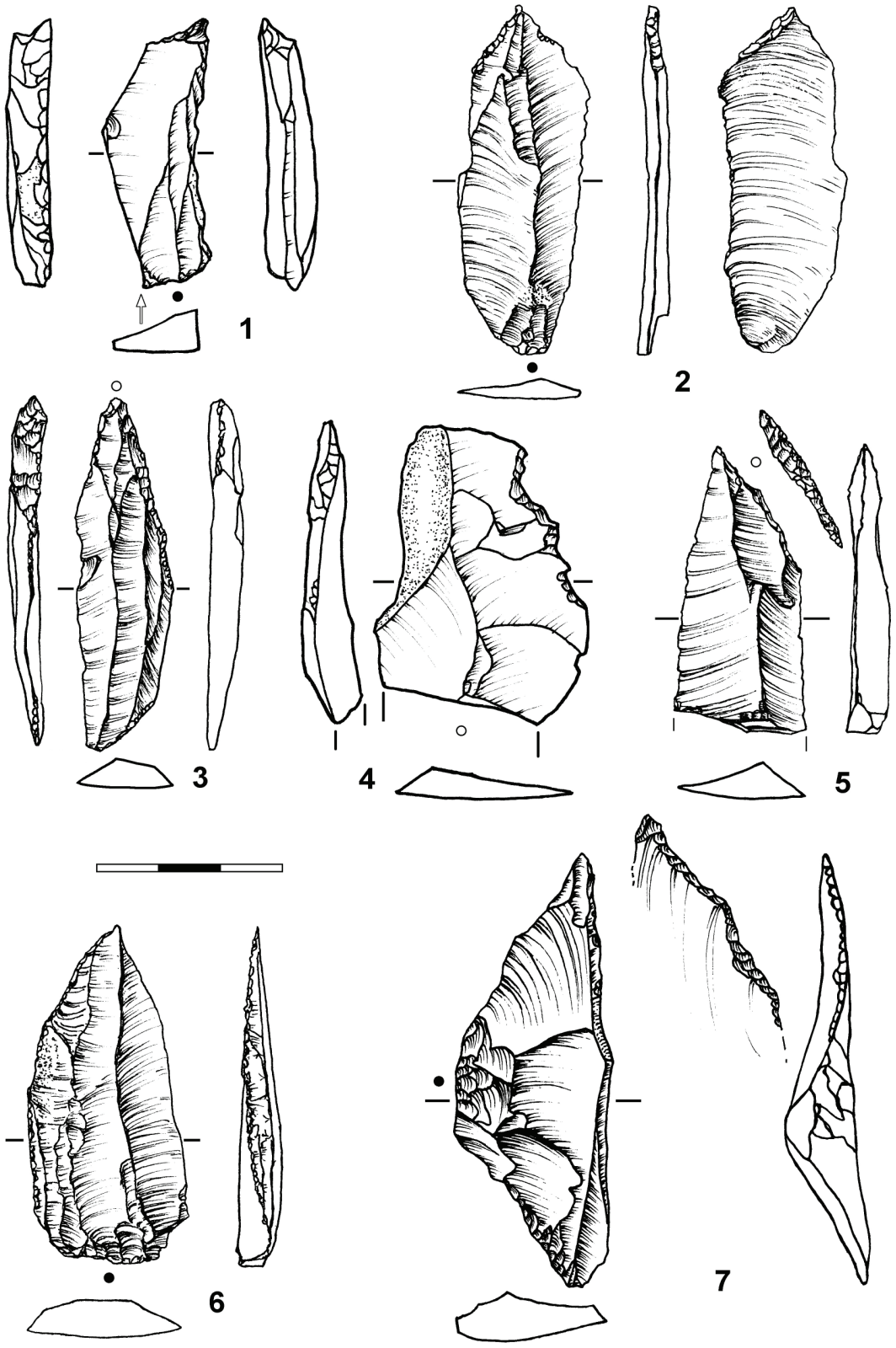


Fig. 8-56. Barmaky, western area complex, horizons 2c (1-4, 6) & 2d (5, 7): 1 – borer-perforator on blade, distal, dorsal; 2 – borer-perforator on blade, distal, alternative; 3 – borer-perforator on blade, proximal, dorsal; with obliquely dorsally truncated/retouched base; 4 – notched piece on flake, lateral, dorsal; 5 – point on blade, proximal, lateral, dorsal; 6 – point on blade, distal, lateral, dorsal; 7 – borer-perforator on *Kantenabschläge*, distal-lateral, alternate.

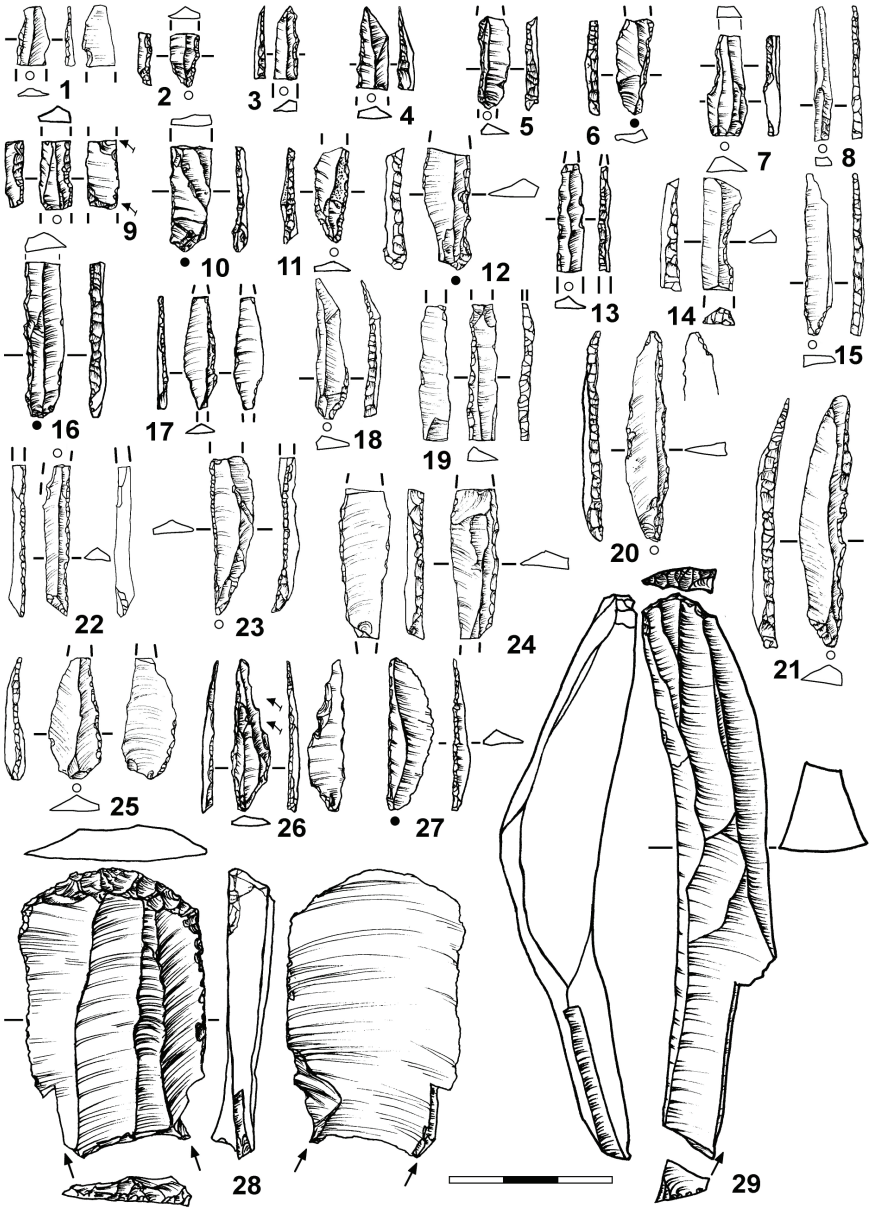

Fig. 8-57. Barmaky, western area complex, horizons 2c (1, 8, 11-15, 18-25, 27-29) & 2d (2-7, 9, 10, 16, 17, 26): 1, 5, 6, 9, 13 – unidentifiable microliths on micro-blades, straightly dorsally backed; 2 – microlithic point on micro-blade, straightly dorsally backed, obliquely dorsally truncated base (broken tip); 3 – microlithic point on micro-blade, straightly dorsally backed, bi-laterally dorsally retouched tip (broken base); 4 – microlithic point on micro-blade, straightly dorsally backed (broken base); 7 – unfinished microlith on bladelet, straightly dorsally backed; 8, 15, 18 – microlithic points on micro-blades, straightly dorsally backed, obliquely dorsally truncated/broken base; 10, 12, 16, 24 – unidentifiable microliths on bladelets, straightly dorsally backed; 11 – microlithic point on micro-blade, straightly dorsally backed, obliquely dorsally retouched base (broken tip); 14 – unfinished microliths on bladelets, concavely dorsally backed, concavely truncated base; 17 – unidentifiable microlith on micro-blade, straightly dorsally backed, laterally ventrally retouched; 19 – microlithic point on micro-blade, straightly dorsally backed (broken tip); 20 – microlithic point on bladelet, straightly dorsally backed, obliquely dorsally truncated base, laterally dorsally retouched; 21 – microlithic point on bladelet, straightly dorsally backed, obliquely dorsally truncated base, distally dorsally retouched tip; 22 – microlithic point, straightly dorsally backed; obliquely dorsally truncated base (broken tip); 23 – microlithic point on bladelet, straightly dorsally backed, obliquely dorsally truncated base (broken tip); 25 – microlithic point on bladelet, straightly dorsally backed, ventrally retouched base; 26, 27 – microlithic points on bladelets, straightly dorsally backed; 28 – combined tool – end-scraper-burin –simple-convex distal end-scraper & bi-lateral burin, on concave, proximal, dorsal truncation, on bi-laterally dorsally retouched flake; 29 – combined tool – end-scraper-burin – simple-convex, distal end-scraper & burin, on oblique-concavely, proximally, dorsally truncated blade.

## ARCHAEOLOGICAL LEVEL 2, COMPARISONS BY HORIZONS & OBJECTS

According to the stratigraphic observations, the artefacts of archaeological level 2 are subdivided into four complexes: 2a; the eastern area; the western area; and pit 2. The material from horizons 2a, 2a1, and 2ab makes up the 2a complex. The eastern area (EA) complex comprises horizons 2c, 2c ash, 2c hearth, and 2d, which originate from the eastern distribution of lithological layer 7a. The western area (WA) complex is documented in horizons 2b, 2c, 2c pit 1, and 2d, which originate from the western distribution of lithological layer 7a. Pit 2 shows no clear stratigraphic connections to the above-mentioned complexes.

### Technological and typological attributes

Despite very different quantities, the Barmaky, level 2 complexes demonstrate a similar technological structure. The main technological feature in all complexes is the prevalence of the sum of bladelets and micro-blades over blades (Tables 8-18; 8-19; 8-37; 8-58).

The importance of bladelet and micro-blade production is underlined by the characteristics of the core-like pieces. Flat and rounded raw volumes are used. The reduction of pre-cores and cores with a narrow flaking surface started with the selection of flat raw volumes. Unidirectional cores with a narrow flaking surface served for bladelet and micro-blade production (Fig. 8-17; 8-18; 8-31, *2*; 8-36, *1*). At the same time, unidirectional cores with sub-cylindrical and cylindrical shape as well as those with a narrow flaking surface were used for blade production (Fig. 8-6, *3*; 8-12, *2, 3*; 8-13; 8-14, *2*; 8-32; 8-33; 8-34; 8-35, *3*). Together, these types dominate the pre-cores and cores (Tables 8-20; 8-38; 8-59). Bidirectional cores show opposite striking platforms and adjacent and alternate flaking (Fig. 8-7, *1*; 8-15, *2*; 8-16, *1, 2*; 8-20, *2, 3*; 8-34). Often one of the opposite platforms is supplemental. Bidirectional cores in the strict sense – i.e., with negatives alternating in opposite directions on one flaking surface – are rare. Generally, overhang trimming and the preparation of crested ridges are also common. The latter were used for flaking surfaces, distal, and backside shaping. The typology of core-like pieces suggests that lamellar products were the only aim of flaking. Based on extensive analytical studies, two discrete reduction strategies were identified: blade and bladelet flaking (Chabai, Dudnyk 2022).

There are no marked differences in the typological structure and dimensions of the *débitage* assemblages of complexes 2a, WA, EA, and pit 2 (Tables 8-21; 8-35; 8-39; 8-60). The percentages of flakes, blades, bladelets, and micro-blades differ to some extent, but show a clear similarity between the same classes of blanks from different complexes. All of the complexes show high numbers of various technical blanks. *Débordante* lamellar pieces dominate the technical blank collections (Fig. 8-1, *9*; 8-4, *4, 6, 7, 10, 12, 17*; 8-8, *1, 2, 7, 8, 11, 12, 14, 15*; 8-21, *1, 3-8, 10-21*; 8-22, *14*; 8-37; 8-38, *1, 3-9, 11, 12*; 8-39, *7, 10, 11, 13, 15*). Crested pieces are more characteristic of blades than of bladelet and micro-blade assemblages (Fig. 8-1, *8*; 8-4, *5, 11, 15, 16;* 8-8, *5, 6, 9 13, 16;* 8-22, *1, 3-7, 8, 9, 13*; 8-23, *1, 5, 6, 8-12*; 8-24, *3*; 8-39, *1-5, 14*; 8-40, *1, 3-8*). Both crested and *débordante* lamellar pieces play the same role in core reduction. This is supported by the presence of crested dorsal scars on *débordante* blades, bladelets, and micro-blades (Fig. 8-8, *10*; 8-21, *2, 9*; 8-22, *2, 8, 11, 12*; 8-23, *2, 3, 4, 7*; 8-24, *10*; 8-38, *2, 10*; 8-39, *6, 12, 16)*. Given the number of cores, it is difficult to explain the low amount of core-tablets. Flakes represent the main primary *débitage* (Tables 8-21; 8-39; 8-60).

The dominance of complete flakes is characteristic of all of the studied complexes, while lamellar blanks are mostly fragmented (Tables 8-22; 8-40; 8-61), probably because of trampling and/or application of hard hammer percussion. Here, the high percentage of broken blanks in the WA complex is noteworthy. When the unidentifiable *débitage* is added, the share of fragmented blanks rises. Broken blanks and unidentifiable *débitage* amount to 59.49 % in the EA complex, and 68.26 %, 69.32 %, and 65.04 % for the WA complex, 2a, and pit 2, respectively.

There is also a high degree of similarity regarding the shapes and axis attributes of lamellar assemblages (Tables 8-23; 8-41; 8-62). Rectangular on-axis pieces dominate,

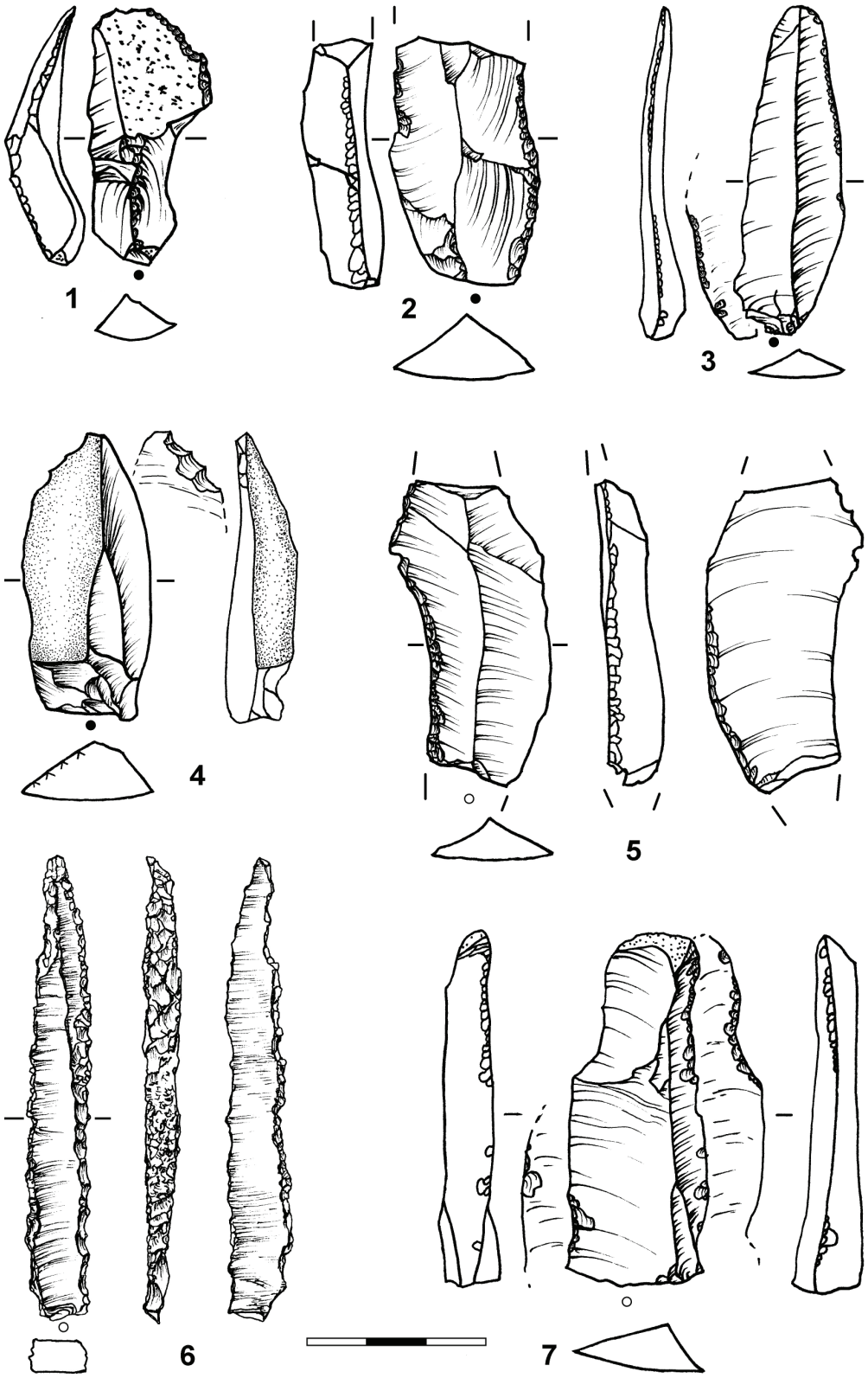


Fig. 8–58. Barmaky, western area complex, hearth (1) & horizons 2c (2–7): 1 – retouched piece on blade, distal, dorsal; 2 – retouched piece on blade, bi-lateral, dorsal; 3 – retouched piece on blade, lateral, alternating; 4 – retouched piece on blade, distal/lateral, ventral; 5, 7 – retouched pieces on blade, bi-lateral, alternate; 6 – microlithic point on bladelet, wavy bi-laterally dorsally backed.

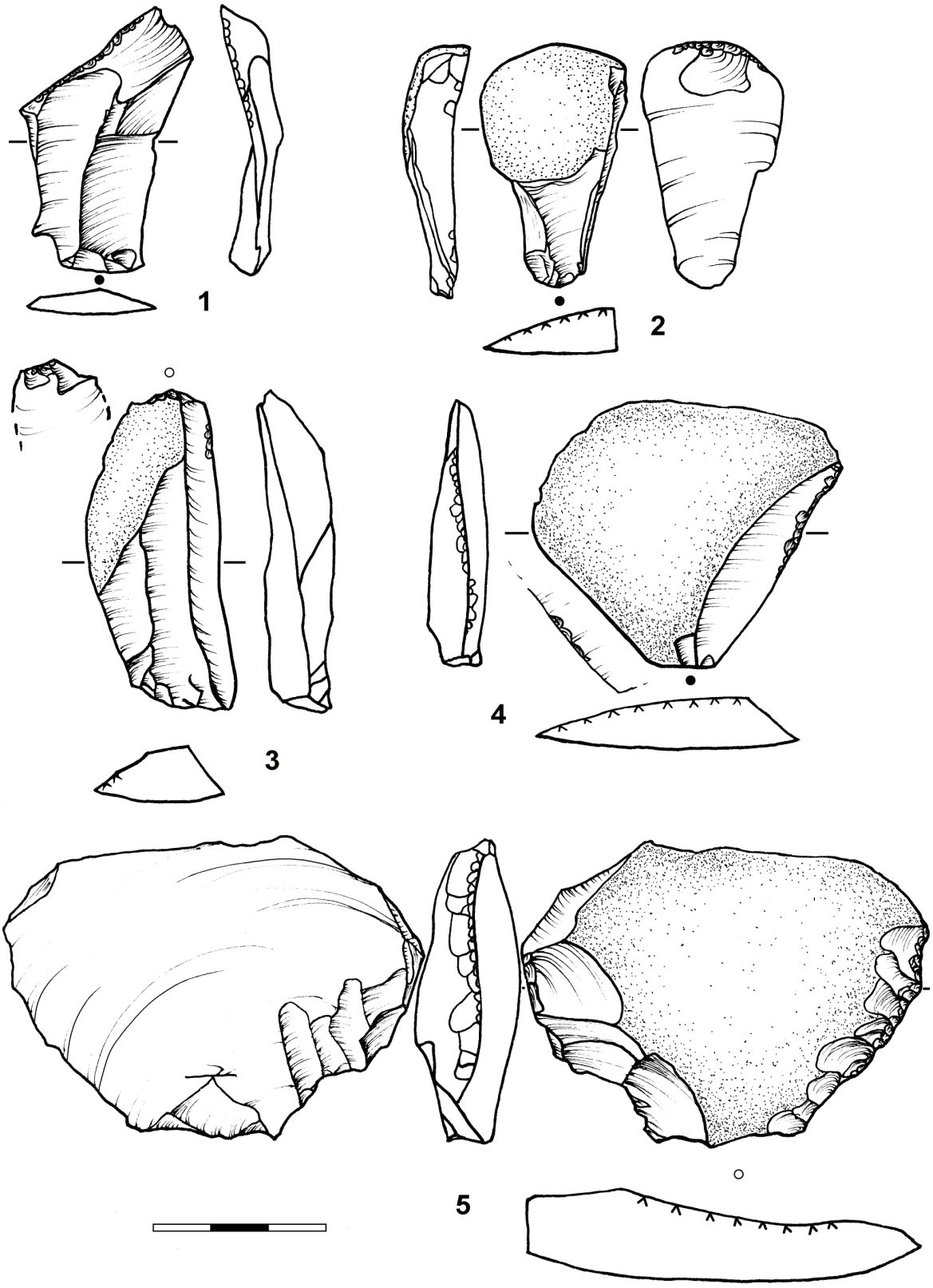


Fig. 8–59. Barmaky, western area complex, horizon 2c: 1 – retouched piece on flake, distal, dorsal; 2 – retouched piece on flake, distal, ventral; 3 – thinned piece on blade, distal, ventral; 4 – retouched piece on flake, lateral, dorsal; 5 – retouched piece on flake, lateral, dorsal, ventrally thinned base.

| | 2b | 2c, pit 1 | 2c | 2d | Σ | % |
|---|---|---|---|---|---|---|
| **TRUNCATED PIECES ON BLADES** | | | | | | |
| straight, distal, dorsal | – | – | 2 | 1 | **3** | 3,26 |
| straight, distal, dorsal; on laterally dorsally retouched piece | – | – | 1 | – | **1** | 1,09 |
| straight, distal, dorsal; on bi-laterally dorsally retouched piece | – | – | | 1 | **1** | 1,09 |
| straight, proximal, dorsal | – | – | 1 | 1 | **2** | 2,17 |
| oblique, distal, dorsal | – | – | 8 | 5 | **13** | 14,13 |
| oblique, distal, dorsal; on laterally dorsally retouched piece | – | – | 1 | 1 | **2** | 2,17 |
| oblique, proximal, dorsal | 1 | – | 7 | 2 | **10** | 10,87 |
| oblique, proximal, dorsal; on bilaterally dorsally retouched piece | – | – | – | 1 | **1** | 1,09 |
| oblique, proximal, ventral | – | – | – | 1 | **1** | 1,09 |
| oblique-convex, distal, dorsal | – | – | 2 | 1 | **3** | 3,26 |
| oblique-convex, distal, dorsal; on laterally dorsally retouched piece | – | – | 2 | – | **2** | 2,17 |
| oblique-convex, proximal, dorsal | – | – | 4 | 1 | **5** | 5,43 |
| oblique-concave, distal, dorsal; on laterally dorsally retouched piece | – | – | 2 | – | **2** | 2,17 |
| oblique-concave, proximal, dorsal | – | – | 2 | – | **2** | 2,17 |
| convex, distal, dorsal | – | 1 | – | 2 | **3** | 3,26 |
| concave, distal, dorsal; on laterally dorsally retouched piece | – | – | 1 | – | **1** | 1,09 |
| concave, proximal, dorsal; on laterally dorsally retouched piece | – | – | 1 | – | **1** | 1,09 |
| bi-terminal, oblique, dorsal | – | – | 2 | – | **2** | 2,17 |
| bi-terminal, oblique / convex, dorsal | – | – | 1 | – | **1** | 1,09 |
| bi-terminal, concave / wavy, dorsal | – | – | 1 | – | **1** | 1,09 |
| **TRUNCATED PIECES ON BLADELETS** | | | | | | |
| straight, distal, dorsal | – | – | – | 2 | **2** | 2,17 |
| straight, distal, dorsal; on laterally dorsally notched piece | – | – | – | 1 | **1** | 1,09 |
| oblique, distal, dorsal | 1 | – | 2 | 1 | **4** | 4,35 |
| oblique, proximal, ventral | – | – | 1 | – | **1** | 1,09 |
| oblique-convex, distal, dorsal | – | – | 2 | – | **2** | 2,17 |
| oblique-concave, distal, dorsal | – | – | 3 | – | **3** | 3,26 |
| **TRUNCATED PIECES ON MICRO-BLADES** | | | | | | |
| oblique, distal, ventral | – | – | 1 | – | **1** | 1,09 |

Table 8-76. Barmaky, western area, by horizons and structures: truncated pieces

| | 2b | 2c, pit 1 | 2c | 2d | Σ | % |
|---|---|---|---|---|---|---|
| **TRUNCATED PIECES ON FLAKES** | | | | | | |
| straight, distal, dorsal | – | – | 1 | – | **1** | 1,09 |
| straight, distal, ventral | – | – | 1 | – | **1** | 1,09 |
| straight, proximal, dorsal | – | – | – | 1 | **1** | 1,09 |
| oblique, distal, dorsal | – | – | 1 | – | **1** | 1,09 |
| oblique, proximal, dorsal | – | – | 2 | – | **2** | 2,17 |
| oblique, proximal, dorsal; on distally / laterally dorsally retouched piece | – | – | 1 | – | **1** | 1,09 |
| oblique, proximal, dorsal; on laterally dorsally retouched piece | – | – | 1 | – | **1** | 1,09 |
| oblique-convex, proximal, dorsal | – | – | 2 | – | **2** | 2,17 |
| oblique-concave, distal, dorsal | – | – | 1 | – | **1** | 1,09 |
| convex, proximal, ventral | – | – | – | 1 | **1** | 1,09 |
| bi-terminal, straight, ventral | – | – | 1 | – | **1** | 1,09 |
| bi-terminal, distally straight / proximally wavy, dorsal | – | – | – | 1 | **1** | 1,09 |
| **TRUNCATED PIECES ON NATURAL FLAKES** | | | | | | |
| straight, ventral | – | – | 1 | – | **1** | 1,09 |
| concave, ventral | – | – | – | 1 | **1** | 1,09 |
| **TRUNCATED PIECES ON UNIDENTIFIABLE *DEBITAGE*** | | | | | | |
| straight, distal, dorsal | – | – | 1 | 1 | **2** | 2,17 |
| straight, proximal, ventral | – | – | 1 | – | **1** | 1,09 |
| concave, distal, dorsal | – | – | 1 | – | **1** | 1,09 |
| concave, proximal, dorsal | – | – | – | 1 | **1** | 1,09 |
| **TOTAL:** | **2** | **1** | **62** | **27** | **92** | 100,00 |

Table 8-76. continued.

but crescent off-axis pieces are important for micro-blades. Trapezoidal off-axis pieces, in contrast, dominate the flake assemblages of all complexes.

At least half of the blades, bladelets, and micro-blades show straight lateral profiles and about one-fifth is curved in the medial part (Tables 8-24; 8-42; 8-63). No significant differences in lateral profile typology of lamellar pieces among the complexes were observed. Among flakes, differently curved profiles make up more than 50 %.

Feathering distal ends are more common in lamellar pieces (≈60-75 %) than in flakes in all complexes (Tables 8-25; 8-43; 8-64). In addition, hinges make up about one-fifth of the lamellar assemblage. The combination of curved lateral profiles in the medial part and hinged distal ends of lamellar pieces are characteristic features of unipolar flaking.

Triangular and trapezoidal cross-sections dominate in all blank types and complexes (Tables 8-26; 8-44; 8-65). In addition, lateral-steep pieces are important, since they reflect the presence of crested and *débordante* pieces. This structure of cross-section types reflects the volumetric hard hammer flaking accompanied by the detachment of crested and *débordante* pieces. Multiple cross-sections, characteristic of pressure and mediator flaking, are rare.

The dorsal scars show the leading role of unipolar knapping and regular application of crested and *débordante* pieces for the trimming of the flaking surface (Tables 8-27; 8-45; 8-66). The dominance of unidirectional scars in both regular and technical blanks is a main characteristic feature of the complexes of archaeological level 2. Technical blanks show a combination of crested unidirectional scars,

| | 2c, pit 1 | 2c | 2d | Σ | % | esse,% |
|---|---|---|---|---|---|---|
| **BACKED POINTS ON BLADELETS** | | | | | | |
| straightly dorsally backed | 1 | – | 1 | **2** | 1,87 | 3,85 |
| straightly dorsally backed (broken tip) | – | 1 | – | **1** | 0,93 | 1,92 |
| straightly dorsally backed; dorsal notch on the opposite edge (broken tip) | – | 1 | – | **1** | 0,93 | 1,92 |
| straightly dorsally backed, obliquely dorsally truncated base (broken tip) | – | 3 | – | **3** | 2,80 | 5,77 |
| straightly dorsally backed, obliquely dorsally truncated base, laterally dorsally retouched | – | 1 | – | **1** | 0,93 | 1,92 |
| straightly dorsally backed, obliquely dorsally truncated base, distally dorsally retouched tip | – | 1 | – | **1** | 0,93 | 1,92 |
| straightly dorsally backed, ventrally retouched base (broken tip) | – | 1 | – | **1** | 0,93 | 1,92 |
| wavy dorsally backed, obliquely dorsally truncated base (broken tip) | – | – | 1 | **1** | 0,93 | 1,92 |
| wavy bi-laterally dorsally backed (broken base) | – | 1 | – | **1** | 0,93 | 1,92 |
| **BACKED POINTS ON MICRO-BLADES** | | | | | | |
| straightly dorsally backed | – | 1 | – | **1** | 0,93 | 1,92 |
| straightly dorsally backed (broken base) | 1 | 2 | 3 | **6** | 5,61 | 11,54 |
| straightly dorsally backed, distally dorsally retouched tip | – | 1 | – | **1** | 0,93 | 1,92 |
| straightly dorsally backed, distally ventrally retouched tip (broken base) | – | 1 | – | **1** | 0,93 | 1,92 |
| straightly dorsally backed, bi-laterally dorsally retouched tip (broken base) | – | 3 | 1 | **4** | 3,74 | 7,69 |
| straightly dorsally backed, obliquely dorsally truncated/broken base | – | 2 | – | **2** | 1,87 | 3,85 |
| straightly dorsally backed; obliquely dorsally truncated base (broken tip) | 1 | 10 | 2 | **13** | 12,15 | 25,00 |
| straightly dorsally backed, obliquely dorsally truncated (broken tip); laterally dorsally retouched | – | 1 | – | **1** | 0,93 | 1,92 |
| straightly dorsally backed, straightly dorsally truncated base (broken tip) | – | 1 | – | **1** | 0,93 | 1,92 |
| straightly dorsally backed, obliquely dorsally retouched base (broken tip) | – | 1 | – | **1** | 0,93 | 1,92 |
| **UNFINISHED BACKED PIECES ON BLADELETS** | | | | | | |
| straightly dorsally backed | – | 2 | 1 | **3** | 2,80 | 5,77 |
| straightly dorsally backed, dorsal notch on the opposite edge | – | 1 | – | **1** | 0,93 | 1,92 |
| concavely dorsally backed | – | 1 | – | **1** | 0,93 | 1,92 |
| concavely dorsally backed, concavely truncated base | – | 1 | – | **1** | 0,93 | 1,92 |
| **UNFINISHED BACKED PIECES ON MICRO-BLADES** | | | | | | |
| straightly dorsally backed | – | 2 | – | **2** | 1,87 | 3,85 |
| concavely dorsally backed | – | 1 | – | **1** | 0,93 | 1,92 |
| **UNIDENTIFIABLE BACKED PIECES ON BLADELETS** | | | | | | |
| straightly dorsally backed | – | 5 | 3 | **8** | 7,48 | – |
| wavy dorsally backed | – | 1 | – | **1** | 0,93 | – |
| **UNIDENTIFIABLE BACKED PIECES ON MICRO-BLADES** | | | | | | |
| straightly dorsally backed | 2 | 31 | 9 | **42** | 39,25 | – |
| straightly dorsally backed; laterally ventrally retouched | – | – | 1 | **1** | 0,93 | – |
| straightly dorsally backed, laterally dorsally notched piece | – | 2 | – | **2** | 1,87 | – |
| straightly ventrally backed | – | 1 | – | **1** | 0,93 | – |
| **TOTAL:** | **5** | **80** | **22** | **107** | 100,00 | 100,00 |

Table 8–77. Barmaky, western area, by horizons and structures: microliths

| | 2b | 2c, pit 1 | 2c | 2d | Σ | % |
|---|---|---|---|---|---|---|
| **RETOUCHED PIECES ON BLADES** | | | | | | |
| distal, dorsal | – | – | 3 | 1 | **4** | 2,55 |
| distal / lateral, dorsal | – | – | 6 | 2 | **8** | 5,10 |
| distal / lateral, ventral | – | – | 2 | – | **2** | 1,27 |
| lateral, dorsal | – | 1 | 19 | 11 | **31** | 19,75 |
| lateral, dorsal, inversely thinned base | – | – | 1 | – | **1** | 0,64 |
| lateral, ventral | – | – | 6 | 2 | **8** | 5,10 |
| lateral, alternating | – | – | 1 | – | **1** | 0,64 |
| bi-lateral, dorsal | – | – | 6 | – | **6** | 3,82 |
| bi-lateral, ventral | – | – | 3 | – | **3** | 1,91 |
| bi-lateral, alternate | – | – | 5 | 1 | **6** | 3,82 |
| bi-lateral, alternating | – | – | 1 | – | **1** | 0,64 |
| **RETOUCHED PIECES ON BLADELETS** | | | | | | |
| lateral, dorsal | – | 1 | 5 | 1 | **7** | 4,46 |
| lateral, ventral | – | – | 2 | 1 | **3** | 1,91 |
| bi-lateral, dorsal | – | – | 2 | – | **2** | 1,27 |
| bi-lateral, alternating | – | – | – | 1 | **1** | 0,64 |
| **RETOUCHED PIECES ON MICRO-BLADES** | | | | | | |
| lateral, dorsal | – | – | 2 | 1 | **3** | 1,91 |
| **RETOUCHED PIECES ON FLAKES** | | | | | | |
| distal, dorsal | – | – | 15 | 4 | **19** | 12,10 |
| distal, ventral | – | – | 1 | – | **1** | 0,64 |
| distal, alternating | – | – | 1 | 1 | **2** | 1,27 |
| distal / lateral, dorsal | – | – | 1 | – | **1** | 0,64 |
| lateral, dorsal | 1 | – | 12 | 7 | **20** | 12,74 |
| lateral dorsal, ventraly thinned base | – | – | 1 | – | **1** | 0,64 |
| lateral, ventral | – | – | 1 | – | **1** | 0,64 |
| lateral, alternating | – | – | – | 1 | **1** | 0,64 |
| bi-lateral, dorsal | – | – | 2 | 1 | **3** | 1,91 |
| bi-lateral, ventral | – | – | 1 | – | **1** | 0,64 |
| bi-lateral, alternate | – | – | 2 | – | **2** | 1,27 |
| bi-lateral, alternate | – | – | – | – | **0** | 0,00 |
| distal-proximal-lateral, alternating | – | – | – | 1 | **1** | 0,64 |
| **RETOUCHED PIECES ON NATURAL FLAKES** | | | | | | |
| distal, dorsal | – | – | 2 | 1 | **3** | 1,91 |
| distal / lateral, alternate | – | – | 1 | – | **1** | 0,64 |
| bi-terminal, ventral | – | – | 1 | – | **1** | 0,64 |
| **RETOUCHED PIECES ON UNIDENTIFIABLE *DEBITAGE*** | | | | | | |
| distal, dorsal | – | – | 2 | 1 | **3** | 1,91 |
| lateral, dorsal | – | – | 5 | 3 | **8** | 5,10 |
| bi-lateral, dorsal | – | – | 1 | – | **1** | 0,64 |
| **TOTAL:** | **1** | **2** | **113** | **41** | **157** | 100,00 |

Table 8-78. Barmaky, western area, by horizons and structures: retouched pieces

as well as a prevalence of unidirectional scars on the dorsal surfaces of *débordante* pieces. The pieces with bidirectional scars (≈15 %) reflect the supplementary role of bipolar knapping, especially for bladelet and micro-blade production. About 10-16 % of the blade and bladelet assemblages belong to the crested pieces. Blades and bladelets with a combination of unidirectional/bidirectional and crested dorsal scars demonstrate the repeated application of crested pieces during the core reduction process.

The location and extent of cortical areas also show a high degree of similarity of the complexes of level 2 (Tables 8-28; 8-46; 8-67). About 10 % of the flakes are primary pieces. The dominant locations of cortex on lamellar pieces are lateral and lateral-distal and can be observed in about 60 % of blades, 42 % of bladelets, and 33 % of micro-blades. This pattern is the result of the unidirectional knapping of flat pieces of raw material for cores with a narrow flaking surface.

The Barmaky, level 2 *débitage*, especially lamellar pieces, also show a high degree of similarity of striking platform preparation and dimensions (Tables 8-29 – 8-35; 8-47 – 8-52; 8-68 – 8-73). Plain and linear types with right angle platforms, pronounced overhang trimming, not abraded, not lipped, but with pronounced bulbs dominate the lamellar assemblages. A specific feature of all blank classes from all complexes is the high percentage of crushed platforms. For the lamellar *débitage*, they are more numerous in the eastern area (33.81 %) than in the western area (26.08 %). Along with the high degree of fragmented lamellar pieces, the relatively large numbers of crushed butts indicate the use of hard hammer percussion.

Burin and truncation spalls represent tool trimming elements. Truncation spalls were not found in the deposits of pit 2. The sum of secondary and multiple burin spalls exceeds primary ones in all complexes (Tables 8-21; 8-39; 8-60; Fig. 8-4, *1, 2, 3, 8*; 8-8, *3, 4*; 8-24, *1, 2, 5, 6-9*; 8-42). About one-third of the burin spalls are preliminary retouched pieces (Fig. 8-4, *1*; 8-42, *4, 12, 18, 21*). The most numerous assemblage of truncation spalls originates from the WA complex (Fig. 8-41, *1-11, 13*). About two-thirds of the truncation spalls reflect the repeated attempt to repair the truncated parts of the truncated pieces and burins (Fig. 8-4, *14*; 8-41, *1, 2, 3, 4, 5, 7, 8, 11, 13*).

Burins, truncated pieces, microliths, and retouched pieces represent the four main tool classes of Barmaky, level 2 complexes (Tables 8-36; 8-53; 8-74). They make up 85-90 % of tool-kits in each complex. End-scrapers, notched pieces, denticulate pieces, borer-perforators, points, combined tools, and thinned pieces, in contrast, are not numerous.

The diversity of tool types depends on the number of artefacts in the complexes and the EA and WA complexes are more diverse than complexes 2a and pit 2. With about 50%, blades are the main blank for tool production. Bladelets and micro-blades served as blanks for 8-9 % and 11-13 %, respectively. About 20 % of the tools were made of flakes. One burin spall is the blank for the borer-perforator. For about 10 % of tool fragments, the blank was not identified. Thus, at least two-thirds of tool blanks are represented by lamellar *débitage*. In addition, 23-27 % of tools were made on technical *débitage*. Among the latter, the crested and *débordante* pieces on blades are used most often.

End-scrapers originate mainly from the WA (Fig. 8-43, *1-7*). Only piece was found in the EA (Fig. 8-25, *4*) and none in 2a and pit 2. End-scrapers thus play a minor role in level 2 (Tables 8-53; 8-74), but are typologically homogenous. The majority is made on blades by distal continuous sub-parallel obverse semi-abrupt/abrupt retouch, several items show also laterally/bilaterally retouch (Fig. 8-43, *5, 7*). A few have oblique-concave/concave proximal obverse truncations (Fig. 8-43, *1, 4*), supposed to be characteristic of the Mizyn Epigravettian industry (Nuzhnyi 2015: 195).

Burins are the most common tool class (Tables 8-36; 8-53; 8-74) with shares between 25 and 50%. Blades, including primary, crested, and *débordante* pieces, make up more than 80 % of burin blanks. About 10 % of burins were made on flakes, including primary, crested, and *débordante* pieces. Natural flakes and bladelets serve as blanks for a few burins, and about 8 % were not identified because of fragmentation. In sum, all types of technical *débitage* served as blanks for one-third of the burins.

Burins on truncated blades (51.20 %) dominate (Tables 8-36; 8-54; 8-75). Single-working edge burins on truncation make up 42.58 % of all burins. Straight and oblique shapes dominate the distal and proximal truncations

(Fig. 8-1, *10, 15*; 8-5; *4, 7, 9*; 8-9, *1, 5, 7*; 8-25, *2, 3, 5, 7-10*; 8-44; 8-45; 8-46, *1, 4-8*; 8-47, *2-6*; 8-48). About a quarter of burins shows lateral/bilateral retouch on terminally truncated pieces (Fig. 8-25, *2, 3, 5, 10*; 8-43, *8, 9*; 8-44, *6*; 8-45, *3, 5*; 8-46, *2*). Angle burins make up about 15 % (Tables 8-54; 8-75). About 60 % of angle burins were made on blades (Fig. 8-25, *6*; 8-49, *1, 3, 6, 8, 9*), and about one-third of angle burins were made on laterally/bilaterally retouched *débitage* (Fig. 8-25, *6*; 8-49, *1, 9*). Dihedral burins also represent about 15 % (Tables 8-54; 8-75). Nearly all of the dihedral burins were made on blades and about 60 % are asymmetrical (Fig. 8-49, *7*; 8-50, *1-3*, *5-7*; 8-51; 8-52, *1, 2, 4-6*) and a quarter was made on laterally retouched pieces (Fig. 8-51, *3, 6*). The combined burins make up 4.76 % of the total number of burins in the WA and are completely absent in the EA, 2a, and pit 2 complexes (Tables 8-54; 8-75). All of them are made on blades. The combination of burins on truncation and dihedral burins (Fig. 8-52, *7*; 8-53, *3, 4, 6, 7*) and the combination of burins on truncation and angle burins (Fig. 8-53, *1, 2, 5*) occur in nearly equal numbers. Laterally retouched blades are uncommon for combined burins. Transversal burins are rare (Tables 8-54; 8-75; Fig. 8-52, *3*).

In essential account, truncated pieces are second numerous together with microliths (Tables 8-36; 8-53; 8-74). The truncated pieces compose about 15 % to 25 % of the total number of tools in general and essential accounts, accordingly. There is no marked difference in the properties of truncated pieces between the complexes. Blades make up two-thirds of the blanks and the technical *débitage* about a quarter. Straight and oblique shapes dominate the distal and proximal truncations (Fig. 8-26, *1, 2, 4, 5, 7, 9*; 8-54, *1-5, 7, 8*; 8-55, *3, 6, 8, 11*). The bi-terminal truncations are not numerous: about 7 % (Fig. 8-26, *10*; 8-55, *10, 12*). The main types of retouch on truncated pieces are continuous scalar/sub-parallel obverse semi-abrupt/abrupt – more than half of all truncations. Single-blow truncations were observed on 6 of 115 pieces.

Microliths were found in all complexes, except pit 2 (Tables 8-36; 8-53; 8-56; 8-74; 8-77) and contribute up to a quarter of the tools in the essential counts. The micro-blade is the main blank for microlith production – 75.76 %. Both technical bladelets and micro-blades are rare. The typological characteristics of microliths of all complexes are very similar. There is only type – dorsally straight-backed micrograveTte points on bladelets/micro-blades with obliquely truncated/retouched base (Fig. 8-5, *3*; 8-27, *3, 4, 5, 8*; 8-57, *2, 8, 15, 18, 20-23*). This type is the characteristic feature of the Mizyn Epigravettian industry (Nuzhnyi 2015: 166; 437). Lateral backing and proximal truncations were produced by obverse scalar/micro-scalar abrupt/semi-abrupt retouch. Out of 132 specimens, one item with alternating and one item with inverse retouches were observed. Geometric microliths and lamelle scalene are absent. The shouldered pieces are not represented, but some fragments of unfinished microliths might indicate their application (Fig. 8-57, *7, 14*). However, in contrast to shouldered pieces, the unfinished microliths show a partial backing of the lateral edge. The difference in width between the retouched and unretouched parts of unfinished microliths is up to 2.14 mm. Thus, the initial blank for a number of microliths were bladelets, whose widths were reduced to micro-blade dimensions through backing. The length, width, and thickness of microliths on bladelets and micro-blades are 34.44×8.04×2.74, and 21.69×5.15×2.14 mm, respectively. The average dimensions are 27.49×5.85×2.28 mm.

Retouched pieces were found in all complexes of Barmaky, level 2 (Tables 8-36; 8-53; 8-57; 8-74; 8-78; Fig. 8-1, *13*; 8-9, *2, 4*; 8-28; 8-58, *1-5, 7*; 8-59, *1, 2, 4, 5*). There are no differences in blank selection and applied retouch combinations between the complexes. Flakes and blades are equally represented among the retouched pieces. In sum, about 80 % of all retouched pieces are retouched blades and flakes, while retouched bladelets and natural flakes are rare. More than a quarter of retouched pieces were made on technical *débitage*. The most characteristic combinations of retouches, which were observed on more than 50 % of the retouched pieces, are partial scalar/marginal obverse/inverse abrupt/semi-abrupt/flat, applied mainly for lateral edge modification.

Denticulate pieces (Fig. 8-26, *8*; 8-27, *13*), notched pieces (Fig. 8-56, *4*), borers-perforators (Fig. 8-1, *16*; 8-56, *1-3, 7*), points on blades (Fig. 8-56, *5, 6*), *raclettes* (Fig. 8-27, *11*), combined tools (Fig. 8-27, *12*; 8-57, *28, 29*), and thinned pieces (Fig. 8-59, *3*) are rare (Tables 8-36; 8-53; 8-74). However, the

characteristic design of borers-perforators is noteworthy, which shows an alternatively retouched tip by partial scalar flat/semi-abrupt retouch. End-scraper-burins represent the combined tools. The combination of a simple end-scraper and burin on proximal oblique/concave truncation is supposed to be a characteristic tool type of the Mizyn industry (Nuzhnyi 2015: 195).

All in all, there are no marked technological and typological differences between 2a, EA, WA, and pit 2 complexes from Barmaky, level 2 assemblage.

## Raw material exploitation

Several attributes suggest intensive on-site core reduction, tool production and rejuvenation, such as the occurrence of a raw material reserve, as well as the presence of pre-cores, cores, technical *débitage*, tool trimming pieces, and flaking instruments. At the same time, differing artefact ratios demonstrate variation in the intensity of raw material exploitation between the complexes.

One of the distinct features concerns the selection of two kinds of raw volumes: rounded nodules and flat pieces (natural flakes, primary flakes, and flint plaquettes). Pieces larger than 50 mm are interpreted as raw material reserve. In sum, flat pieces (14 items) slightly prevail over rounded nodules (12 items). However, knappers in the WA mainly collected rounded nodules (5 flat pieces vs. 10 nodules), while those of the EA preferred the flat pieces (8 flat pieces vs. 1 nodule). On average, the rounded nodules (77.03×54.46×31.32 mm) are somewhat bigger than the flat pieces (72.39×49.28×22.38 mm).

In the EA complex, only flat raw volumes served as blanks for pre-cores while in the WA complex, 4 rounded nodules and 18 flat pieces have been used. Pieces with a narrow flaking surface constitute the pre-core assemblages of the EA, while both pre-cores with a narrow flaking surface and sub-cylindrical pre-cores were observed in the WA complex (Tables 8-38; 8-59). Bidirectional and unidirectional pre-cores are common for both areas.

These approaches to raw material selection and pre-core production influence the core typology. In the WA complex, bladelet cores amount to 12.5 %, while they make up 23.94 % in the EA complex. This difference reflects the significance of cores with narrow flaking surfaces for bladelet production. In the EA and WA complexes, these cores make up 60.87 % and 54.90 %, respectively. Consequently, in the EA and WA complexes, the sum of bladelets and micro-blades compose 60.46 % and 57.44 % of lamellar assemblages, respectively. At first look, the mentioned differences are not very pronounced, but they reflect the peculiarities of the operational chains, which start from raw material selection, continue in pre-core and core typological variability, and end up in bladelet/micro-blades-to-blade ratios. Considering that knappers of Barmaky, level 2 used two distinct methods for producing blades and bladelets/micro-blades, it can be stated that the core reduction approach in the EA was more specialised on the production of narrow lamellar pieces.

The difference in the sizes of pre-cores and cores reflects the intensity of core reduction. In the EA, the average sizes of pre-cores on flat volumes and bladelet cores are 63.29×30.95×57.76 mm and 58.65×22.60×38.15 mm, respectively. In the WA, the average sizes of pre-cores on flat volumes and bladelet cores are 69.63×24.81×64.31 mm and 49.25×20.64×34.01 mm. The core reduction was thus more intense in the WA.

The tools-to-cores ratios reveal more differences between level 2 complexes. The tools-to-cores ratios for the WA and the EA complexes are 7.49 to 1 and 1.41 to 1, respectively. The tools-to-cores ratios for 2a and pit 2 complexes are 12.00 to 1 and 1.27 to 1, respectively. That is, in the frame of the general workshop model, tool production and use are more pronounced in the WA and 2a. In addition, the ratio for pit 1 in the WA is 5.25 to 1 and thus close to the general ratio of the WA complex.

The fragmentation of *débitage* in the WA is somewhat more pronounced than in the EA assemblages. The broken blanks, including unidentifiable *débitage*, in the WA and EA make up 68.30 % and 59.48 %, respectively. Considering the similar core reduction strategies and flaking instruments, it is possible to suggest that the main agent for *débitage* fragmentation is trampling. Thus, trampling was more pronounced in the WA than in the EA.

*Débitage* with completely and partly cortical dorsal surfaces (51-55 %) are nearly similar in all complexes (Tables 8-28; 8-46; 8-67). In

addition, a relatively high amount of primary flakes (up to 10 % of the flake assemblages) was observed for all complexes. Together, they also highlight on-site core reduction.

A number of attributes suggest more intensive burin reduction in the WA complex. The number of multi-edge burins, such as bilateral, bi-terminal, and double dihedral burins is larger in the WA than in 2a, and the EA, and they are absent in pit 2. Combined burins only occur in the WA. The ratio of single-edge to multiple-edge burins in the EA complex is 7.6 to 1, 4.6 to 1 in the WA, and 4.5 to 1 in 2a. The number of burin spall negatives differs between the EA, WA, and 2a complexes. On average, 1.99 and 2 burin spall negatives shape one burin edge in the WA and 2a complexes, while it is somewhat lower in the EA – 1.7 to 1. These findings correlate well with the ratios of primary burin spalls to multiple burin spalls in the EA and WA complexes, namely 1 to 1.37 and 1 to 1.47, respectively.

The EA and pit 2 complexes exhibit no examples of rejuvenated burins. The rejuvenated burins in WA and 2a complexes compose 24 and 1 pieces, respectively. The main method of rejuvenation is the reorientation of the angle of the truncated part towards the opposite lateral side of the blank (Fig. 8-44, *8, 9*; 8-46, *1, 3, 7*; 8-47, *6*; 8-48, *3, 7*; 8-49, *9*). Pit 2 complex contains one bi-terminally truncated blade, whose proximal truncation was made on the burin edge (Fig. 8-9, *6*). One more feature that reflects burin reduction is rejuvenating truncation spalls observed in limited numbers in 2a, EA, and WA complexes (Tables 8-39; 8-60). The average burin dimensions of the EA complex are somewhat higher than those of the WA complex: 63.34×23.2×9.10 and 59.57×22.46×8.21 mm, respectively. Based on these observations, it is possible to state a more intensive burin reduction in the WA complex.

There are no complete microliths in the EA complex. Complete microliths in the WA complex make up 7.48 %. In the EA and WA complexes, distal fragments of microliths are represented by 14.29 % and 16.82 %, respectively. Proximal and medial fragments thus heavily dominate the microliths assemblages. Such a pattern of microlith fragmentation might reflect mainly off-site breakage with the distal parts gone missing during hunting episodes. Both the EA and WA complexes contain unfinished pieces and microliths with projectile impact fractures (Fig. 8-57, *9, 26*). Thus, it is possible to conclude on-site production and off-site use of microlith assemblages. Indeed, it cannot be excluded that parts of the on-site produced microliths leave the site as the hunting equipment.

The available sandstone pieces including flakes and chips reflect the use of relatively soft hammer stones. The nearest outcrop lies about 10 km northwest of the site. In addition, flint pebbles from the local outcrop were used as hard hammer stones.

## ARCHAEOLOGICAL LEVELS 1 & 2: DISCUSSION

Taking into account the significant quantitative difference between archaeological levels 1 and 2 assemblages, detailed technological and typological comparisons are not meaningful. The reconstructed site formation process suggests bioturbation and slope erosion as the main agents responsible for the accumulation of the level 1 assemblage. The source of the artefacts of level 1 is lithological layer 7a, which also contains the artefacts of archaeological level 2. Consequently, there are no obvious technological and typological differences between the artefacts of levels 1 and 2.

The Barmaky, level 2 artefacts assemblage demonstrates close affinities with the Mizyn industry, as described by D. Nuzhnyi (Nuzhnyi 2015). The main characteristic is straight-backed microgravette points with obliquely truncated bases. In the mid-Dnieper basin, such microliths have not been recognised in other Epigravettian industries. The application of discrete methods for blade and bladelet core reduction can be seen as another characteristic feature of the Mizyn type industry (Dudnyk 2024).

All in all, the described characteristics of the artefacts from Barmaky, level 2 suggest both on-site core reduction and tool production, which are based on flint supply from a local source (300 m) and short-distance (10 km) transportation of flaking instruments. At the same time, the EA complex was more oriented toward bladelet production, while the WA knappers produced both blades and bladelets in nearly equal proportions. In the WA complex,

more intensive use of flint is seen in the core and burins reduction, tools ratio, tool type variability, and trampling effect, either indicating a longer or more intense use of the WA. Evidence for the production of mobile art objects on ivory, bone, marl, and perforated fossil snails supports the interpretation of more variable and time-consuming activities in the WA (Chapter 9, this volume). In addition, the faunal exploitation of the WA also seems more time-consuming than in the EA (Chapter 5, this volume). Compared to the WA, activities in the EA were less diverse and rather focused on the production of pre-cores and cores with a narrow flaking surface from flat raw volumes and the production of microlithic insets. In the WA these activities are supplemented by blade production from sub-cylindrical pre-cores and cores made on rounded nodules that serve as blanks for a relatively wide range of tool types required for the variable and time-consuming activities. In sum, the relatively wider range of activities documented in the WA suggests a longer time of settlement occupation.

Despite the statistically insufficient numbers of some artefact categories in complex 2a, the cover of pit 2 shows several similarities with the WA complex. This observation provides indirect evidence for the origin of the material used to cover pit 2, presumably lithological layer 7a. The cover thus contains archaeological material of level 2c with characteristic features of the WA complex, corroborating the stratigraphic observation (Chapter 2, this volume) that pit 2 and its cover, complex 2a, accumulated later than the archaeological horizons of the WA.

# BARMAKY: ARTEFACTS FROM ORGANIC MATERIALS & ADORNMENTS

9

D. STUPAK, V. CHABAI, A. VESELSKY & V. HRYTSENKO

## INTRODUCTION

The non-flint artefacts from Barmaky are not so numerous and variable as in other Middle Dnieper Epigravettian settlements, such as Mizyn, Mezhyrich, Dobranichivka, Gintsi or Yudinovo (Shovkoplias 1965; 1972; Pidoplichko 1976; Grigorieva 1996; Iakovleva 2013; Nuzhnyi 2015).

The field seasons of 1982 and 1990 yielded only a few artefacts from organic materials (Piasetsky 2009: 140, 141; Nuzhnyi 2015: 207, 208). In 1982, a hammer from reindeer antler was found (Piasetsky 2009: 138), and a small fragmented figurine made on mammoth ivory is known from the 1990 campaign (Fig. 9-1, *25*), similar in shape to those from Mizyn (Piasetsky 2009: 138, 140; Iakovleva 2013: 109-110). During the 1990 campaign, fragments of processed mammoth tusks were found. More precisely, a distal end of a mammoth tusk shows traces of intentional cutting, a medial part bears cutting traces that indicate an attempt at dissecting, and a fragment has cutting traces (Piasetsky 2009: 139, 141). In addition, about 200 perforated and non-perforated fossil shells were found by Lupenko and Piasetsky.

While the finds from Piasetsky's and Lupenko's excavations were not accurately documented, the utilitarian and non-utilitarian and organic and inorganic artefacts from Nuzhnyi's field investigations are a reliable source of information (see Chapter 1, this volume). It is necessary to underline that Nuzhnyi's artefact collection originates from 12 square meters, adjacent to those excavated during the 2018 field season. That is, all finds are associated with the Western area of the excavation. Nuzhnyi reported about 368 fossil shells from his excavations (Nuzhnyi 2015: 208). His most remarkable finds are the five fragments of a tusk bracelet with a «herring-like» ornament, a dumbbell-shaped bead, an unfinished example of a similar pendant, and a mammoth figurine made on marl. All of these finds, except one bracelet fragment, originate from square 10Ж (Fig. 9-1, *3-9, 15, 16*) (Nuzhnyi 2015: 208). The tools made from mammoth tusks comprise a medial fragment of a grooved point (Fig. 9-1, *21*), a proximal part of a small spindle-shaped point (Fig. 9-1, *20*), the distal and proximal part of a borer (Fig. 9-1, *24*) and four fragments of needles (Fig. 9-1, *1, 2, 10, 11*). In addition, thirty ivory fragments show traces of processing, mostly unfinished needles, borers and/or points in various stages of production (Fig. 9-1, *12-14, 17-19, 22, 23*) (Nuzhnyi 2003: 15; 2015: 207, 208; Nuzhnyi et al. 2004: 22; 2005: 8). Also, Nuzhnyi mentioned a processed mammoth epiphysis, which resembles the well-known "lamps" from Mezhyrich (Nuzhnyi 2003: 15).

Finds of amber were common during the early investigations. Lupenko, Piasetsky and Nuzhnyi reported numerous pieces from the squares 6Р, 6С, 7С, 10Ж, 11Ж, 12Ж, 103, 113 (Lupenko 1983: 7; Piasetsky, Samoliuk 1990: 8, 9; Nuzhnyi 2003: 7, 15; Nuzhnyi et al. 2004: 22; 2005: 8), the largest (30.0×20.0×7.0 mm) found in pit 1, square 6Л (Piasetsky, Samoliuk 1990: 8).

During the 2018-2020 excavations at Barmaky, 58 organic artefacts were discovered. These are ivory and antler (?) tools, ivory pendants, and ivory fragments with processing traces (Table 9-1). In addition, 340 specimens of perforated and non-perforated fossil molluscs were documented as well as pieces of ochre and amber.

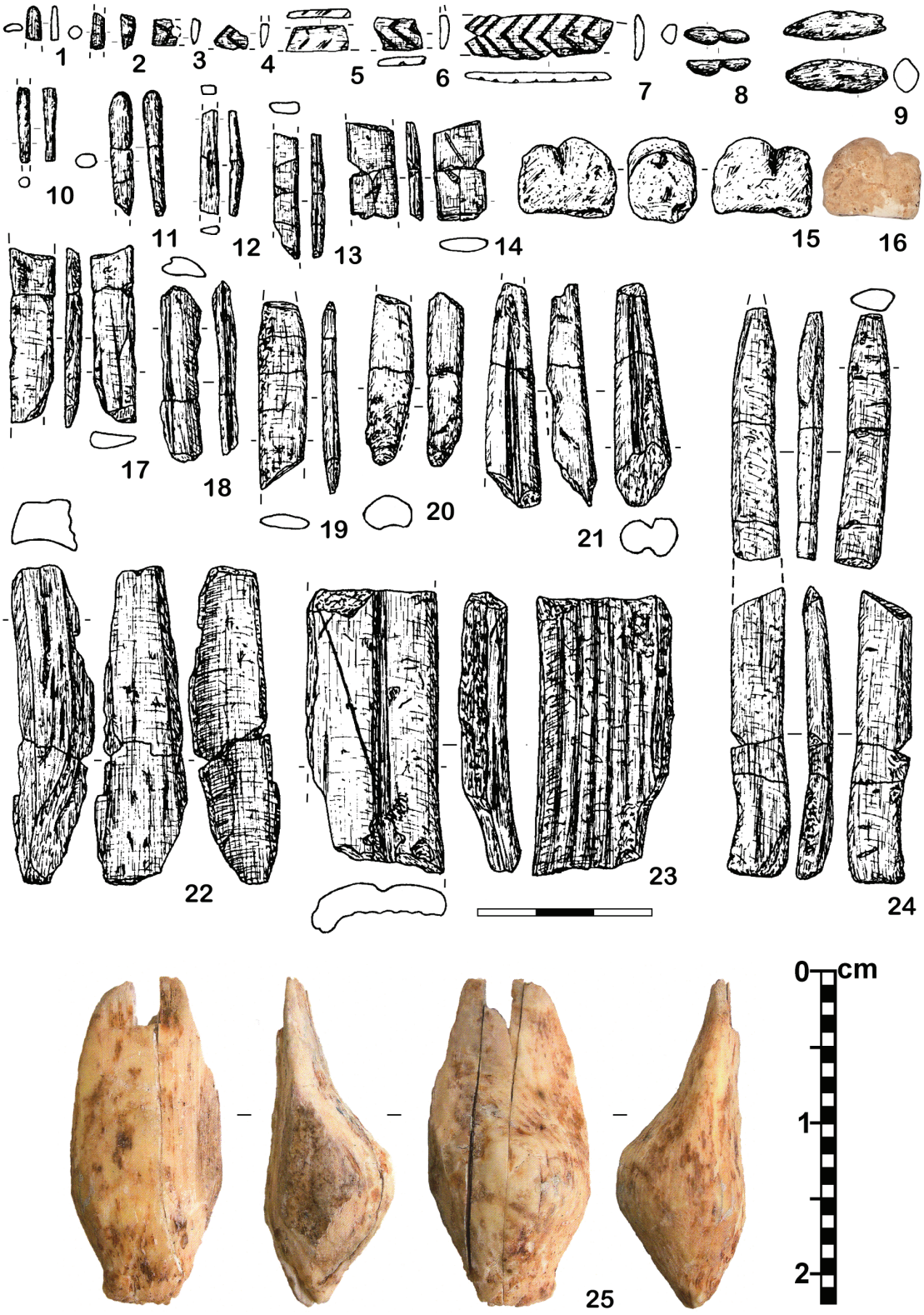


Fig. 9–1. Barmaky, 1990, 2002–2004, level 2: 1, 2, 10, 11 – fragments of needles; 3–7 – fragments of bracelets; 8 – dumbbell-shaped bead; 9 – unfinished dumbbell-shaped bead; 12–14, 17–19, 22, 23 – ivory fragments with traces of processing; 15, 16 – mammoth figurine on marl; 20, 21 – point fragments; 24 – borer; 25 – figurine on ivory; 1–5, 16, 17–24 – after Nuzhnyi 2015: fig. 109; 110; 25 – after Piasetsky 2009: 138.

## MAMMOTH TUSK AND ANTLER TOOLS FROM 2018 – 2020.

**Points.** Two distal fragments of points were found in horizon 2c (Table 9-1), both with a weathered surface. The first comes from square 12Д, is made from ivory and has a length of 47.87 mm and a diameter of 8.56 mm (Fig. 9-2, *10*). The second one is from squares 5-6Л. Probably, it was made on a reindeer antler, which has a length of 38.17 mm and a diameter of 6.37 mm (Fig. 9-2, *9*).

**Fragments of small points, awls / "thick needles".** Thirteen pieces (one distal, twelve medial) of small points, awls or "thick needles" on ivory originate from horizon 2c and are associated with the concentration of the Western area (Table 9-1).

The distal fragment was found in square 12E and has a length of 7.82 mm and a diameter of 2.56 mm (Fig. 9-2, *2*). Five medial fragments originate from the same square with lengths and diameters of 9.36×3.30 mm, 8.80×3.28 mm, 7.00×2.72 mm, 6.04×2.86, and 5.32×3.26 mm.

One more medial fragment was found in squares 6Л and six more in 10e, three of which were probably parts of one artefact (Fig. 9-2, *6-8*), given their specific cross-section, which is not wholly rounded, but slightly flattened on one side. It should be noted that these fragments are the thickest among all fragments of points/borers/ needles; the dimensions of the largest fragment are 13.26×d max 4.74 / d min 3.23 mm; the size of the smallest is 5.59×d max 3.81 / d min 3.19 mm. The lengths and diameters of other medial fragments from squares 10e range between 10.16×3.02 mm, 8.90×3.04 mm, and 8.80×2.93 mm. The fragment from square 6Л is oval in cross-section and 7.19 mm long with a diameter of 2.07×1.70 mm at the distal and 2.75×1.89 mm at the proximal end.

**Needles.** All needle fragments were made from mammoth tusks (Fig. 9-2, *1, 3-5*). Most of them come from squares 12E, 9Д, 8E, 5Л, 6Л in the Western area horizon 2c: one distal and 12 medial fragments (Table 9-1). Another distal fragment from horizon 2d, square 8e is associated with the Western area, too, and a single fragment comes from horizon 2a.

The distal fragment from horizon 2c, square 12E has a length of 4.43 mm and a diameter of 1.65 mm (Fig. 9-2, *1*). Among the six medial fragments from square 6Л, one seems to have preserved a damaged eye. Its length and diameter are 12.44×3.05 mm (Fig. 9-2, *4*). The rest of the medial fragments from horizon 2c, square 6Л have lengths and diameters of 15.58×2.58 mm, 7.16×2.08 mm, 3.47×1.64 mm, 3.25×2.37 mm, and 2.65×1.98 mm.

Further medial fragments of needles from horizon 2c were found in squares 9Д (n=3), 5Л (n=2), and 8E (n=1). Their length and diameters are 14.95×2.21 mm, 9.47×2.28 mm, and 8.21×2.38 mm square 9Д, 13.01× 2.43(d max) /1.86(d min) mm and 4.77×1.85 mm for square 5Л. The specimen from square 8E is 15.90 mm the longest needle fragment in the collection. It is rounded in cross-section and has a diameter of 1.20 mm at the distal and 2.02 mm at the proximal end. The diameter of 1.20 mm is the smallest diameter among all fragments of needles from Barmaky.

The distal fragment from horizon 2d, square 8E has a crescent cross-section and measures: 11.77× 2.40(d max)/1.88(d min) mm (Fig. 9-2, *3*).

| | WA | | | |
|---|---|---|---|---|
| | **2c** | **2d** | **2a** | **Total:** |
| **bracelets** | 1 | 1 | – | 2 |
| **dumbbell-shaped beads** | 15 | 5 | – | 20 |
| **points** | 2 | – | – | 2 |
| **points/borers/massive needles** | 13 | – | – | 13 |
| **needles** | 13 | 1 | 1 | 15 |
| **tusk with slots** | 1 | – | – | 1 |
| **processed tusks** | 5 | – | – | 5 |
| **Total:** | **50** | **7** | **1** | **58** |

Table 9-1. Barmaky, level 2, by horizons: worked tusk and antler

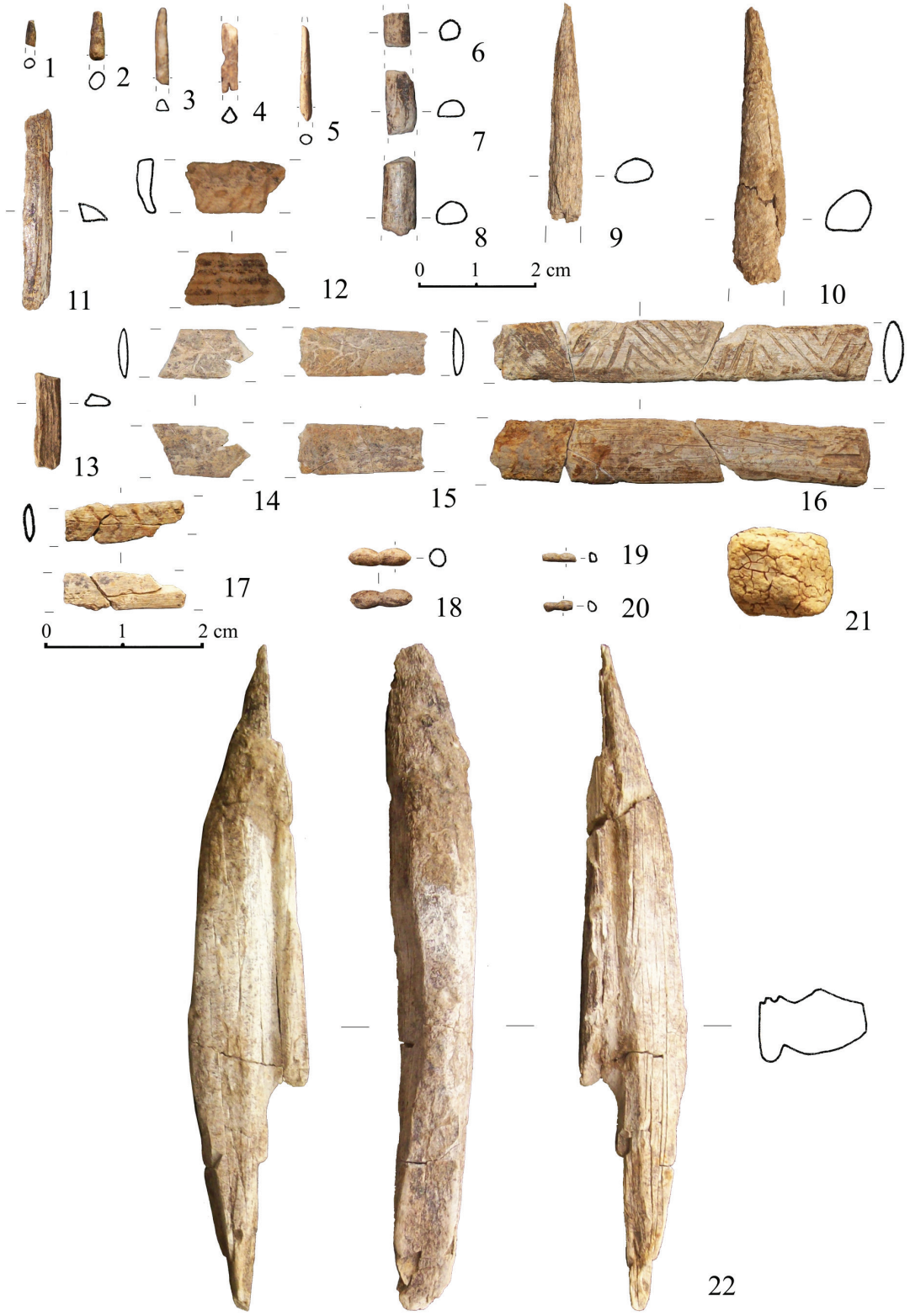


Fig. 9-2. Barmaky, level 2, artefacts from organic materials: 1, 3–5 – fragments of needles; 2, 6–8 – fragments of small points, borers or massive needles; 9, 10 – fragments of points; 11–15 – ivory fragments with traces of processing; 16 – a fragment of a bracelet; 17 – enlarged fragment of a bracelet; 18–20 – dumbbell-shaped beads; 21 – amber; 22 – mammoth tusk with grooves.

A single medial fragment of a needle originates from horizon 2a, square 4O; it measures 10.37 mm in length and 2.43 mm in diameter.

**A fragment of a mammoth tusk with two grooves** measures 112.03×13.08×20.50 mm and comes from intrusive crotovina deposits into horizon 2c, square 8E (Table 9-1), but its association with horizon 2c is very probable. The grooves were made on both sides of the artefact and show widths and depths of 7.42x3.28 mm and 6.39x2.38 mm, respectively (Fig. 9-2, *22*).

**Fragments of mammoth tusk with traces of processing.** The surfaces of five small ivory fragments, all from horizon 2c, squares 9E, 10E and 11E, bear traces of processing (Table 9-1). The dimensions are 34.89×5.01×3.16 mm for the largest (square 11E; Fig. 9-2, *11*) and 16.32×4.89×2.87 mm for the smallest (10E; Fig. 9-2, *13*). The fragment from square 11e has notches which are located obliquely relative to the length of the fragment; its dimensions are 16.66×8.89×3.24 mm (Fig. 9-2, *12*). Two thin, elongated fragments of bladelet-shaped ivory pieces (20.66×8.50×1.45 and 14.54×8.63×1.32 mm) from square 9E might be parts of one artefact (Fig. 9-2, *14, 15*).

## Pendants & Bracelet from Mammoth Tusk

All fragments of bracelets (n=2) and dumbbell-shaped beads (n=15) come from the Western area (Table 9-1). The largest fragment of a bracelet (65.04×11.09×3.57 mm) originates from horizon 2c, square 10E. It has an ornament formed by chevrons arranged in a zigzag pattern (Fig. 9-2, *16*). The second fragment (14.80×4.67×1.03 mm) originates from horizon 2d, square 53 and belongs to a bracelet with a «herring-like» ornament (Fig. 9-2, *17*).

The most numerous organic artefacts are dumbbell-shaped beads. Because of their small size, these pendants were only found during sieving. Two concentrations of these artefacts can be distinguished, differing in number and size. The main concentration is associated with horizon 2c, squares 9E and 10E. One complete bead (10.58×3.19×3.06 mm; Fig. 9-2, *18*) and 13 fragments come from square 9E, and one from 10E. The other concentration was found in horizon 2d, square 6Ж, yielding two complete beads and 3 fragments. With dimensions of 5.73×1.34×1.37 and 5.08×1.86×1.36 mm (Fig. 9-2, *19, 20*), they are all smaller than the beads from the main concentration.

## Shells

Fossil shells are a common feature of the Epigravettian assemblages in the Mid Dnieper basin. Most shells have holes and were likely worn as adornments on clothes or elements of bracelets and necklaces (Iakovleva 2013: 131-156). Samples without holes probably served as a reserve for such ornaments.

Lupenko, Piasetsky and Nuzhnyi reported 35, 167, and 368 shells from Barmaky, respectively (Lupenko 1983: 20; Piasetsky, Samoliuk 1990: fig. 3; Nuzhnyi 2015: 208). During the last field campaign, 340 complete and fragmented shells were found. Neither the shells nor documentation of their origin are available from the excavations by Lupenko and Piasetsky. From Nuzhnyi's 2002-2004 excavations, 239 shells are available and their origin is documented on the site plan in field reports (Nuzhnyi 2003; Nuzhnyi et al. 2004; 2005). The following analysis by Dr. V. Hrytsenko includes these 239 from Nuzhnyi in addition to the 340 shells found during the 2018-2020 field campaign (n=579; Table 9-2). Shells found during excavation have exact coordinates (n=239 and n=302), while those from sieving are only attributed to square meters.

Most shells belong to the marine gastropod genus *Dorsanum* of the family Nassariidae (n=444) and the marine gastropod family Trochidae (n=104). They are supplemented by a small group of the Bivalvia class – 6 items and 25 unidentifiable pieces (Table 9-2; Fig. 9-3; 9-4; 9-5, *1*). The shells of the species *Dorsanum duplicatum* (Sow.) are dominant among representatives of the *Dorsanum* genus. Such species as *Trochus* sp., *Trochus ex gr. Podolicus* (Koles) and *Gibbula podolica* (Montp.) represent the majority of the Trochidae family. Among the class Bivalvia, shells of molluscs are identified as *Mactra* sp. (?) and those assigned to the sub-class Heterodonta (Table 9-2).

These shells originate from the Lower and Middle Sarmatian sediments. Sediments of the Lower Sarmatian ($N_1sm_1$) are composed of sands, clays, and carbonaceous clays with layers of lignin, oolitic limestones and shells and are widely distributed in the Volhynian Upland. Their thickness varies from 2-3 m to 120 m,

| | WA | | EA | | | | Total: | | |
|---|---|---|---|---|---|---|---|---|---|
| | 2c | 2d | 2c | 2d | 2a | pit 2 | # | % | esse,% |
| **DORSANUM** | | | | | | | | | |
| *Dorsanum* sp. | 8 | – | – | 2 | – | 1 | **11** | 1,90 | 1,99 |
| *Dorsanum duplicatum* (Sow.) | 348 | 52 | 1 | 17 | 5 | 3 | **426** | 73,58 | 76,90 |
| *Dorsanum develuinum* (d'Orb.) | 1 | – | – | 1 | – | – | **2** | 0,35 | 0,36 |
| *Dorsanum superabile* (Koles.) | – | – | – | 1 | – | – | **1** | 0,17 | 0,18 |
| *Dorsanum corbianum* (d'Orb.) | 4 | – | – | – | – | – | **4** | 0,69 | 0,72 |
| **TROCHIDAE** | | | | | | | | | |
| *Trochus* sp. | 26 | 2 | 1 | 2 | – | – | **31** | 5,35 | 5,60 |
| *Trochus ex gr. Podolicus* (Koles.) | 15 | 5 | 1 | 2 | – | 1 | **24** | 4,15 | 4,33 |
| *Trochus podolicus* (Dub.) | 4 | – | – | – | 1 | – | **5** | 0,86 | 0,90 |
| *Trochus sulcatopodolicus* (Koles.) | | – | – | 1 | – | – | **1** | 0,17 | 0,18 |
| *Gibbula* sp. | 1 | – | – | – | – | – | **1** | 0,17 | 0,18 |
| *Gibbula insperata* (Koles.) | 2 | – | – | – | – | – | **2** | 0,35 | 0,36 |
| *Gibbula levigatopodolica* (Kolesnikov) | 1 | – | – | – | – | – | **1** | 0,17 | 0,18 |
| *Calliostoma* sp. | 3 | – | – | – | – | – | **3** | 0,52 | 0,54 |
| *Calliostoma beaumontii* (d'Orb.) | 4 | – | – | – | – | – | **4** | 0,69 | 0,72 |
| *Calliostoma podolicoformis* (Kolesnikov) | 6 | – | – | – | – | – | **6** | 1,04 | 1,08 |
| *Gibbula podolica* (Montp.) | 25 | – | – | – | – | – | **25** | 4,32 | 4,51 |
| *Calliostoma pseudohommairei* (Kolesnikov) | 1 | – | – | – | – | – | **1** | 0,17 | 0,18 |
| **BIVALVIA** | | | | | | | | | |
| Bivalve sp. Indeterm. | 1 | – | – | – | – | – | **1** | 0,17 | 0,18 |
| Heterodonta gen. et sp. | – | 1 | – | 1 | – | – | **2** | 0,35 | 0,36 |
| *Mactra* sp. (?) | 3 | – | – | – | – | – | **3** | 0,52 | 0,54 |
| **UNIDENTIFIABLE** | 21 | 3 | – | – | 1 | – | **25** | 4,32 | – |
| **Total:** | **474** | **63** | **3** | **27** | **7** | **5** | **579** | 100,00 | 100,00 |

Table 9–2. Barmaky, level 2, Western (WA) and Eastern (EA) areas, horizon 2a and pit 2: fossil shell, by species

while thicknesses of 40–60 m prevail (Stratigraphy of the Ukrainian SSR 1975). In the limestones and sandy layers of the Lower Sarmatian, the following faunal remains were found: *Tapes vitalianus* Orb., *Ervilia dissita* Eichw., *E. trigonula* Eichw., *Modiola sarmatica* Gat., *Syndesmya reflexa* Eichw., *Cardium lithopodolicum* Dub., *Hydrobia* sp., *Trochus aff. angulatus* Eichw., *Trochus aff. papilla* Eichw., *Buccinum duplicatum* Sow. (=*Dorsanum duplicatum* (Sow.)), *Mactra eichwaldi* Lask.

Most shells from Barmaky, however, originate from the Middle Sarmatian sediments ($N_1sm_2$), which have a much smaller spatial distribution than the Lower Sarmatian deposits and whose thickness does not exceed 30 m. The Middle Sarmatian sediments are overlain by anthropogenic formations. To date, Middle Sarmatian deposits form small elevations on watersheds preserved from erosion, mostly on the watershed of the Ustie and Horyn rivers, on the right bank of the Horyn and the watershed of Wilia and Horyn rivers. Middle Sarmatian sediments are represented by sand-clay formations and shell rocks. The latter is most widely distributed in the northern part near the villages of Antopol, Kolodenka, Taikury, Bila Krynytsia, Khreniv and Bochanytsia (Fig. 9–6).

Fig. 9–3. Barmaky, 2002–2004, level 2, shells: 1–77 – *Dorsanum* genus; 78–81 – Trochidae family; after Nuzhnyi 2015: fig. 111.

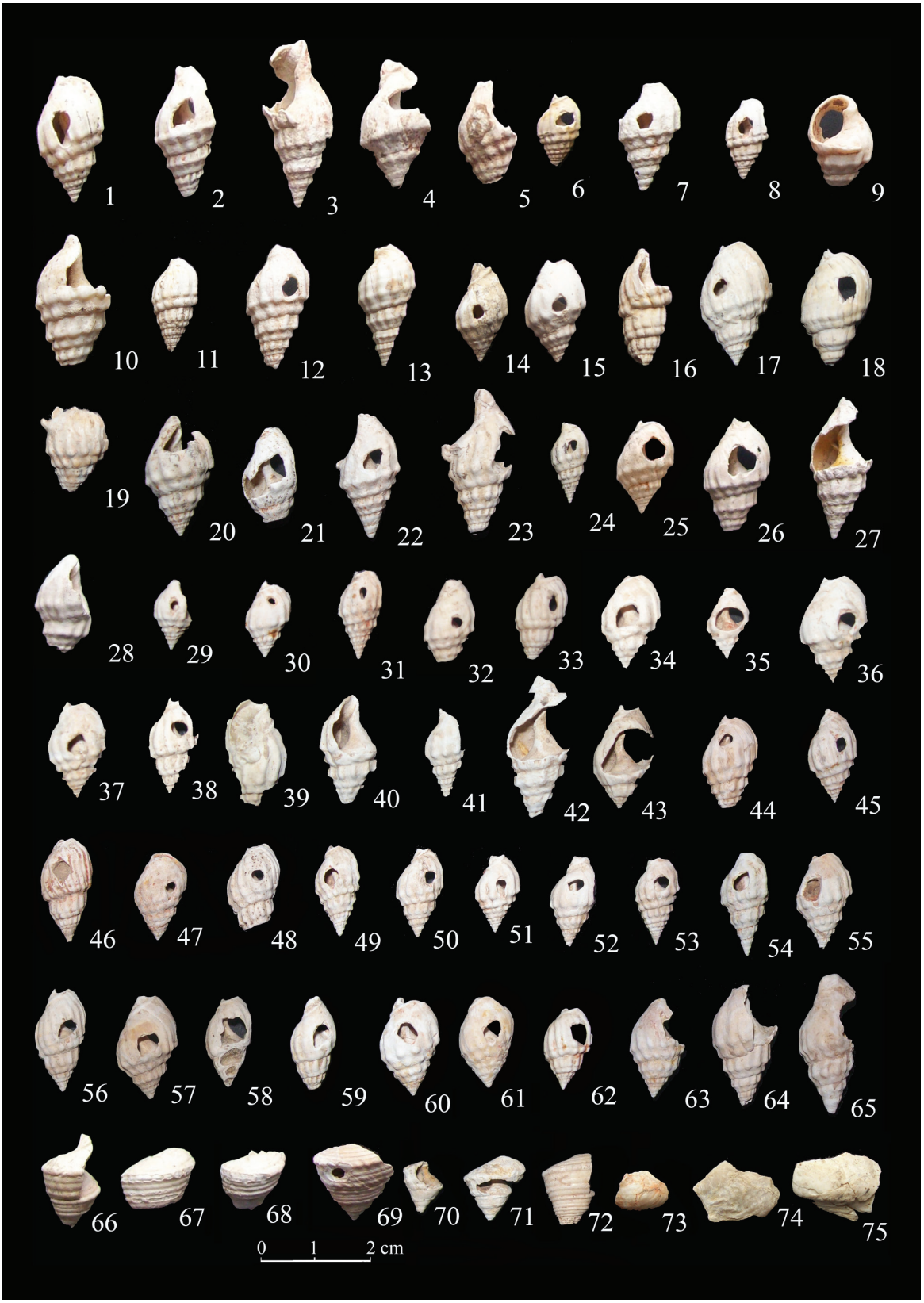


Fig. 9–4. Barmaky site, 2018–2020, level 2: 1–65 – *Dorsanum* genus; 66–72 – Trochidae family; 73–75 – Bivalvia class.

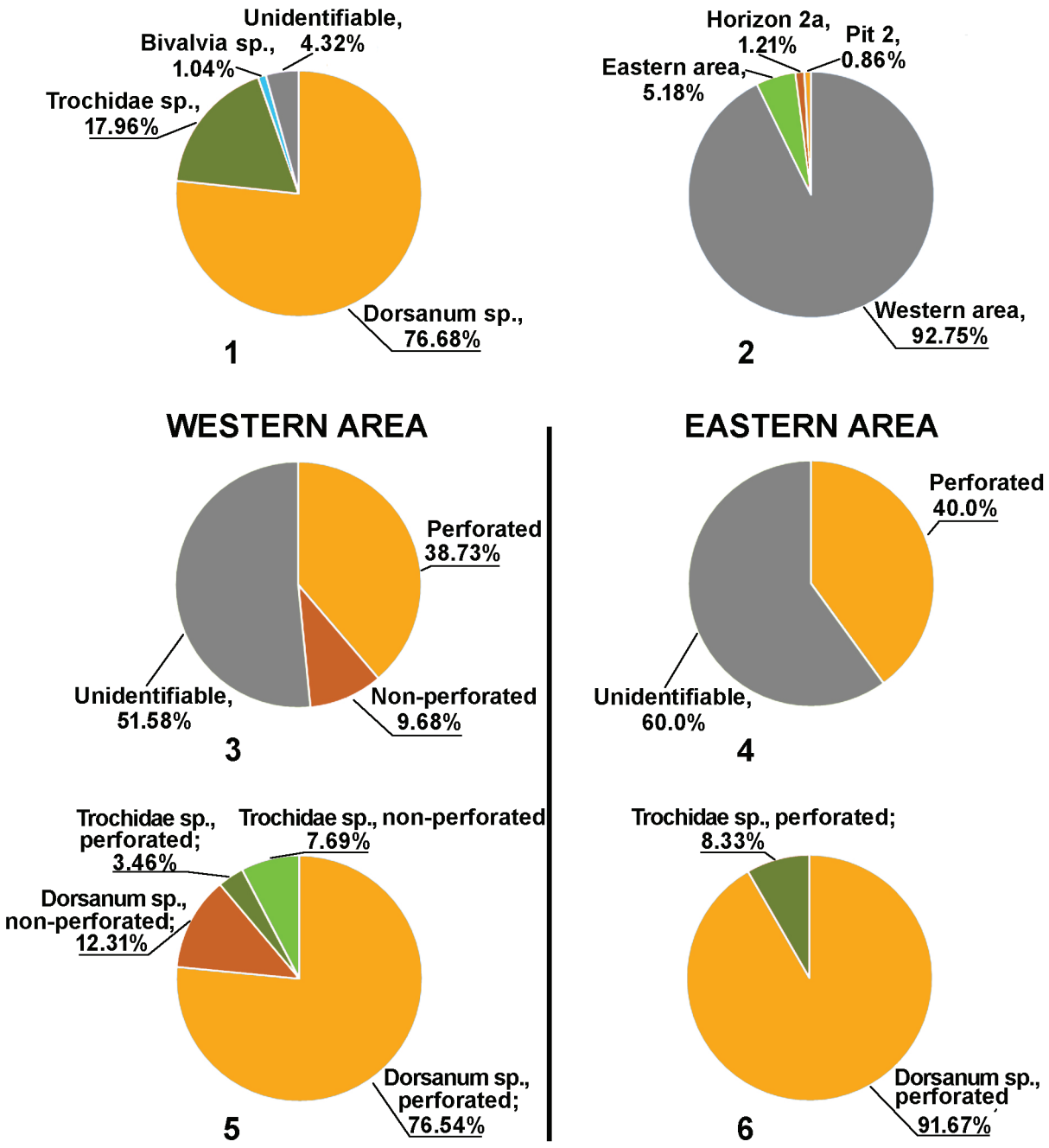


Fig. 9-5. Barmaky, level 2, shells: 1 – shells composition by genus, family and class; 2 – percentages of shells by archaeological units; 3 – Western area, perforated, non-perforated and indistinct shells by percentages; 4 – Eastern area, perforated, non-perforated and indistinct shells by percentages; 5 – Western area, perforated and non-perforated shells by genus and family; 6 – Eastern area, perforated shells by genus and family.

In the southern part, Middle Sarmatian sediments are represented mainly by sands, clays and limestones-shell rocks of greyish-yellow colour. Among a large number of broken shells (detritus) there are well-preserved specimens of *Mactra fabreana* Orb., *Tapes gregaria* Partsch., *Buccinum duplicatum Sowerby* (=*Dorsanum duplicatum* (Sow.)), *Trochus* sp., *T. insperatus* Koles., *T. podolicus* Koles. (= *Trochus ex gr. podolicus* Dub.) (Stratigraphy of the Ukrainian SSR 1975). In the outcrops near the villages of Mykhniv and Shelviv, Middle Sarmatian "pockets" are observed on the surface of Lower Sarmatian sediments. These pockets are filled with Middle Sarmatian limestone shell sediments underlain by a limestone pebble layer. The limestone pebble layer was found in Lower Sarmatian deposits and contains *Ervilia dissita* Eichw., *Cardium lithopodolicum* Dub., *Trochus* aff. *papilla* Eichw. The limestone shell sediments are characterised by *Mactra fabreana* Orb., *Modiola* aff. *sarmatica* Gat., *Tapes gregarius* Goldf., *Ervilia dissita* Eichw., *Cardium guadripartitum* Koles., *Trochus sulcatopodolicum* Koles., *Buccinum superobile* Koles. The noted stratigraphic peculiarity of the Middle/Lower Sarmatian border may described as local disconformity caused by erosion because such pockets are not observed in the rest of the Volhynian-Podilian Upland, where Sarmatian sediments are widespread (Stratigraphy of the Ukrainian SSR 1975).

The fossil shells from Barmaky, level 2 comprise the *Dorsanum* genus, Trochidae family and Bivalve group and are characterised by a clear dominance of *Dorsanum duplicatum* (Sow.) species (Table 9-2). The majority of shells show perforations (Fig. 9-5, *3*) of varying shape and size (Fig. 9-3; 9-4). The sizes of the perforation range between 1-5 mm and it is possible that some of them were not made by humans, but by predatory gastropods. If correct, already perforated shells might have been preferentially collected. Several analyses and experiments on shell perforation and their diagnostic features have been published (Kuhn et al. 2001; Stiner et al. 2013; Tátá et al. 2014; Niţu et al. 2019; Peresani et al. 2019; Álvarez-Fernández et al. 2021). As diagnostic features, the perforated shells from Barmaky show relatively sharp edges, irregular shapes, and small negatives around the perforation on the external surface, indicating the use of direct internal percussion or pressure by thin hard instruments. Nuzhnyi noted that most "holed" shells were "carelessly" internally scrolled or pressured (Nuzhnyi 2003: 16; Nuzhnyi et al. 2004: 22; 2005: 8).

Most shells originate from the Western area (Table 9-2; Fig. 9-5, *2*). The densities of shells and flint artefacts are directly correlated: the higher the number of lithics – the higher the number of shells (Fig. 9-7; 9-8). In all areas, the distribution of *Dorsanum* and Trochidae shells is overlapping (Fig. 9-9). In the Western area, the main concentration of shells was found on 7 square meters: 8E, 9E, 10E, 10Ж, 10З, 11E and 11Ж, containing 308 of 537 items – more than half of the documented specimens (Fig. 9-10; 9-11). The main shell concentration of the Eastern area was identified on squares 4P, 5P and 5C; 16 of 30 items, or about half of the documented specimens (Fig. 9-12; 9-8).

About 10% of shells (n=52) from the Western area do not exhibit perforations, while non-perforated shells are absent in the Eastern area (Fig. 9-5, *3, 4*). There are 277 shells in the Western area and 18 shells in the Eastern area, whose degree of fragmentation does not allow for statements on the presence or absence of perforations.

The small fragments of shells from Western and Eastern areas compose 279 and 18 items, respectively.

There are 208 and 12 **perforated shells** in the Western and Eastern areas, respectively. The perforated shells of the *Dorsanum* genus dominate in both the Western and Eastern areas (Fig. 9-5, *5, 6*). In the Western area, of 199 perforated shells of the *Dorsanum* genus, 198 specimens belong to *Dorsanum duplicatum* (Sow.) and one to *Dorsanum corbianum* (d'Orb.), while the nine perforated Trochidae shells are subdivided into *Gibbula* sp. – 1 item; *Gibbula insperata* (Koles.) – 1; *Calliostoma beaumontii* (d'Orb.) – 1; *Gibbula podolica* (Montp.) – 5; *Calliostoma pseudohommairei* (Kolesnikov) – 1. In the Western area, a concentration of 121 of 208 perforated shells was identified in six neighbouring squares: 10E, 10Ж, 10З, 10К, 11E and 11Ж (Fig. 9-10). In one case, three perforated *Dorsanum* shells were found in a relatively straight line (Fig. 9-13). Nuzhny mentions six perforated shells from square 11Ж, found in a "compact group" with their holes oriented in the same direction, suggesting evidence for them having been threaded (Nuzhnyi 2003: fig. 24, *2*; Nuzhnyi, Piasetsky 2003: 60, fig. 1, 2; Nuzhnyi 2015: fig. 86, *2*).

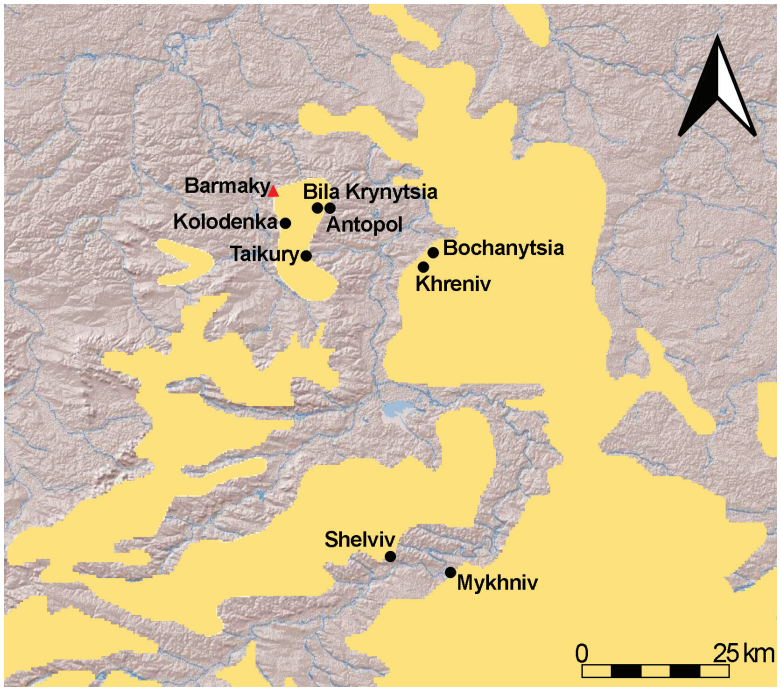


Fig. 9-6. The location of Barmaky to shell deposits.

In the Eastern area, 11 perforated *Dorsanum duplicatum* (Sow.) and one *Trochus sulcatopodolicus* Koles were found. The weak concentration might be identified in square 5P, from where four perforated *Dorsanum duplicatum* (Sow.) originate (Fig. 9-12).

Thus, perforated shells of *Dorsanum duplicatum* (Sow.) were preferred among the *Dorsanum* genus molluscs, while a preference for *Gibbula podolica* (Montp.) among the Trochidae family is not so pronounced: 5 of 10 shells.

In addition, two more perforated *Dorsanum duplicatum* (Sow.) originate from level 2a and pit 2.

**Non-perforated shells** were identified only in the Western area (n=52), from horizon 2a (n=3) and are absent in the Eastern area and pit 2 (Fig. 9-5, *5, 6*). In the Western area, the non-perforated shells belong to the *Dorsanum* genus and Trochidae family, 32 and 20 items respectively. The species of *Dorsanum duplicatum* (Sow.) is dominant – 29 items; one more item belongs to *Dorsanum develuinum* (d'Orb.) and two items to *Dorsanum corbianum* (d'Orb.). The Trochidae family is represented by *Gibbula podolica* (Montp.) and *Calliostoma podolicoformis* (Kolesnikov): 16 and 4 items, respectively. The 39 of 52 non-perforated shells concentrate on 4 square meters: 10Ж – 10 items; 10З – 15 items; 10К – 6 items; and 11Ж – 8 items. A pronounced concentration of non-perforated Trochidae family molluscs originates from 10Ж (9 items) and 10З (6 items) squares; that is 15 of 20 non-perforated Trochidae shells (Fig. 9-11).

In addition, three more non-perforated *Dorsanum duplicatum* (Sow.) originate from level 2a.

Traces of **ochre colouring** on shells were identified on specimens from pit 2 (n=1), the Western area (n=33), and the Eastern area (n=8). As mentioned in Chapter 2, the colour of the archaeological deposits is brownish because of the high ochre content in the sediments, making statements on intentional colouring difficult. The 33 coloured shells from the Western area comprise perforated (n=19), non-perforated (n=2), and indistinct fragments (n=12). Most specimens belong to the species *Dorsanum duplicatum* (Sow.), while three fragmented shells were attributed to *Dorsanum* sp., *Trochus ex gr. Podolicus* (Koles) and *Mactra* sp. (?). The coloured shells are distributed from square line 5 to square line 11 with the highest concentration in square 11E (n=12) with 9 perforated, 1 non-perforated, 2 fragments belonging to Dorsanum duplicatum (Sow.) – 11 pieces and *Dorsanum* sp. – 1 fragmented item.

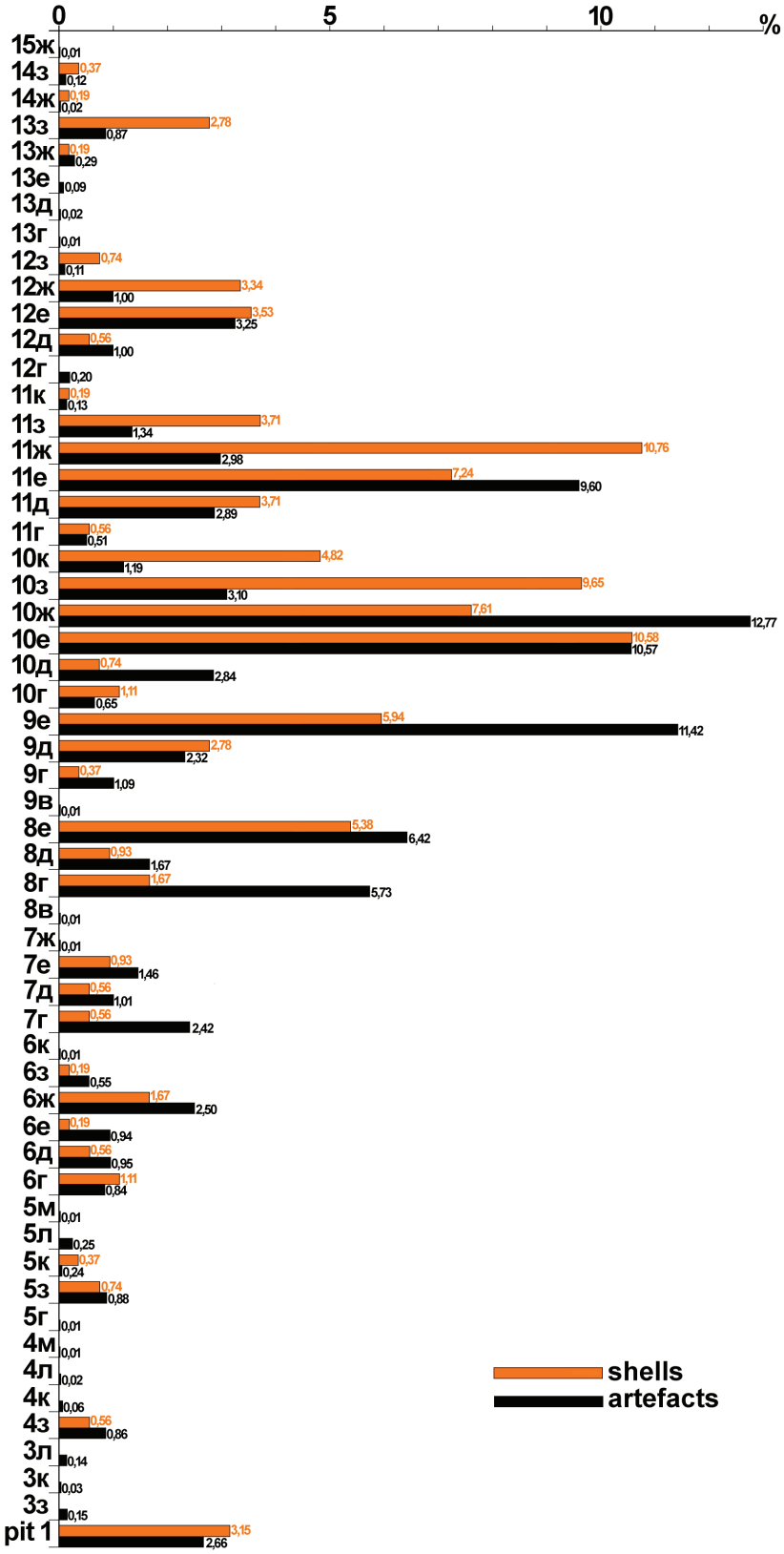


Fig. 9–7. Barmaky, level 2, Western area: artefacts and shells, by squares and percentages.

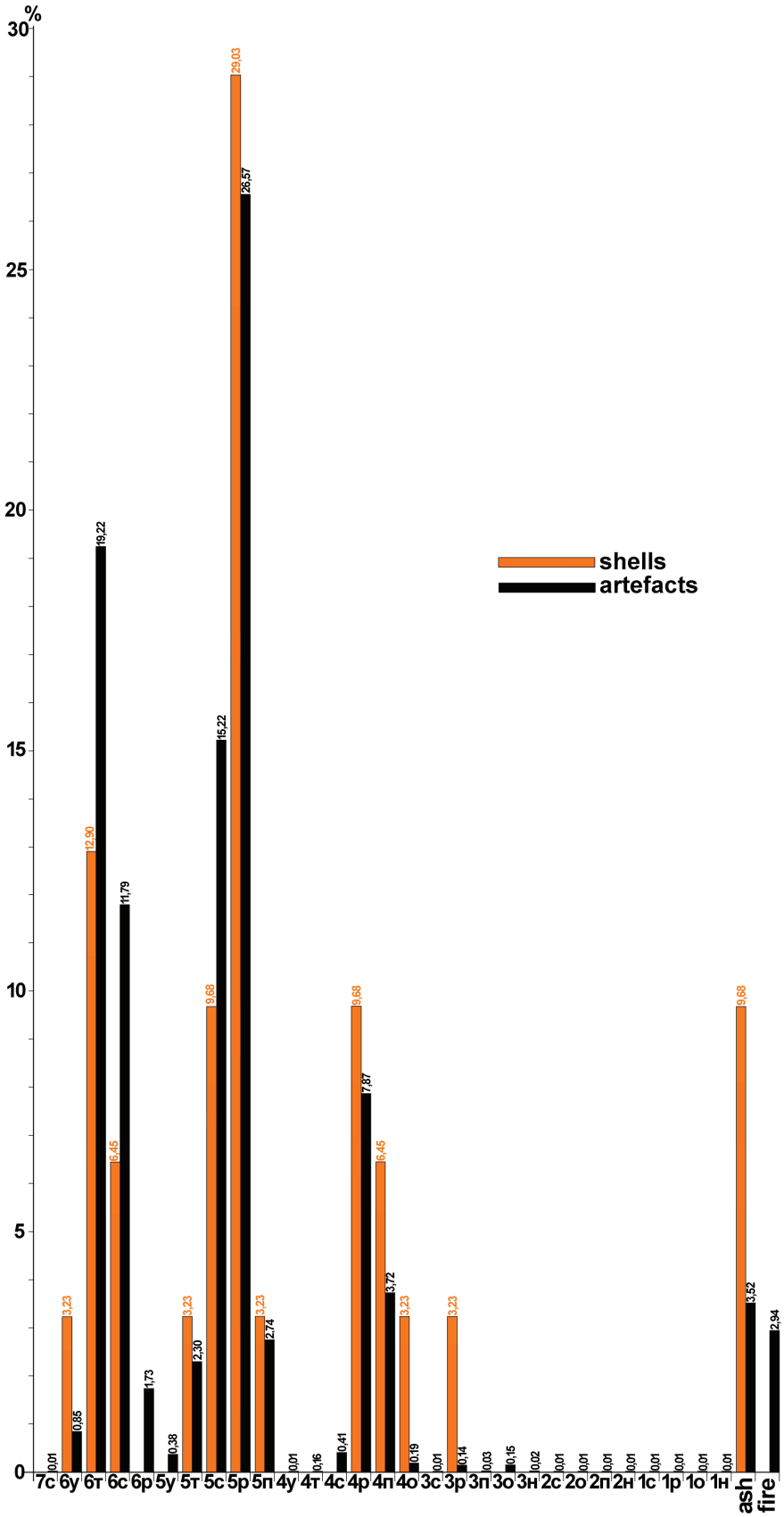


Fig. 9–8. Barmaky, level 2, Eastern area: artefacts and shells, by squares and percentages.

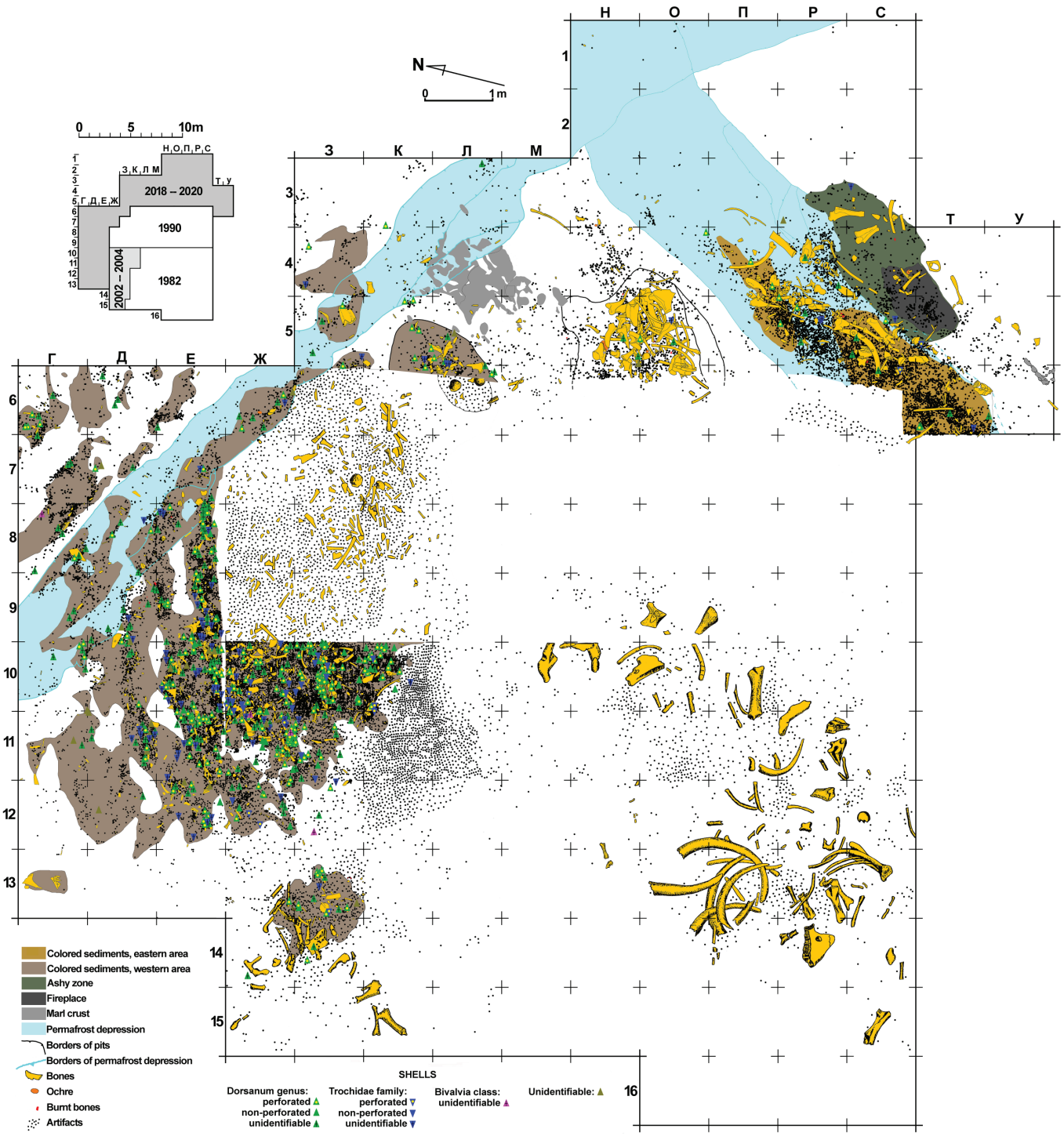


Fig. 9–9. Barmaky, level 2, distribution of shells.

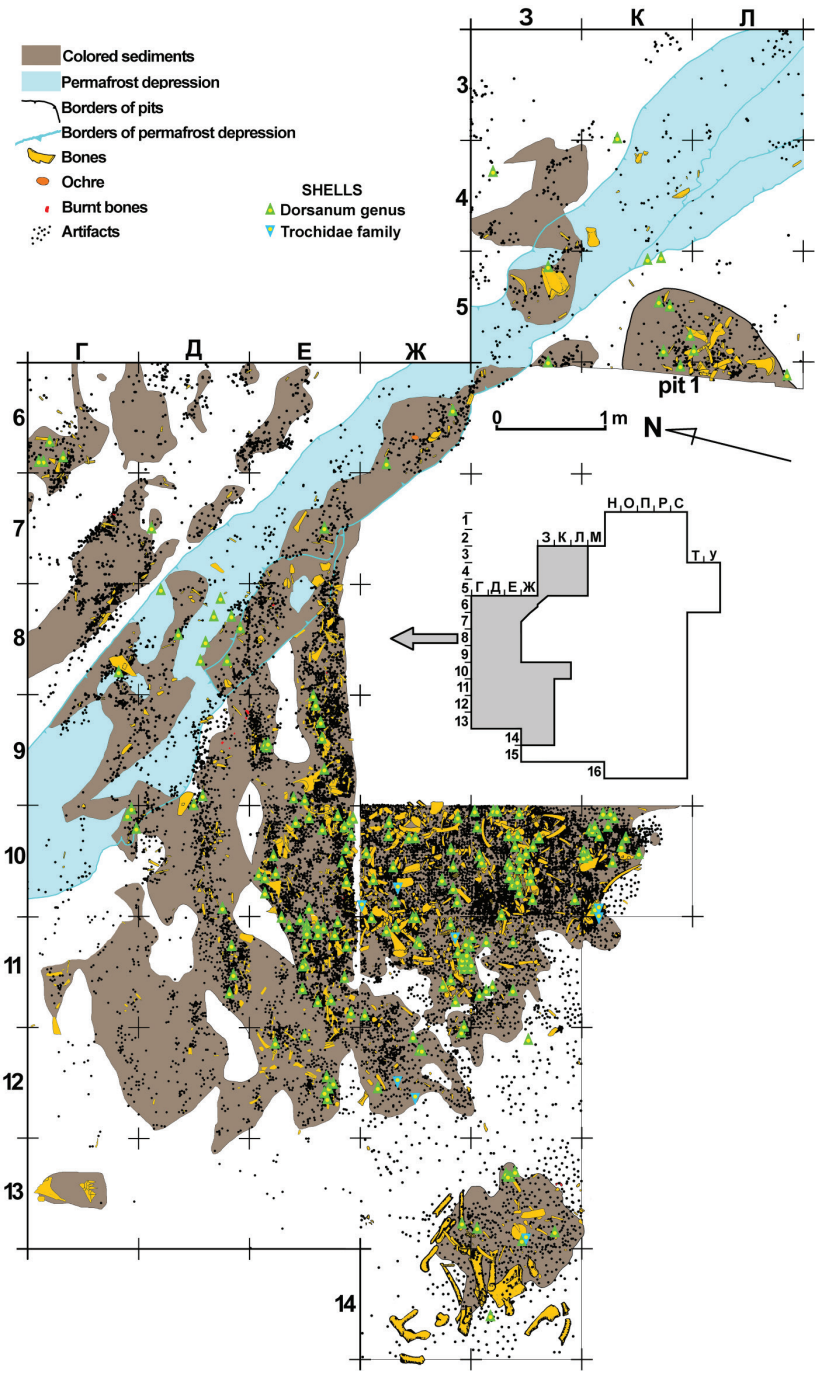


Fig. 9–10. Barmaky, level 2, Western area: distribution of perforated shells.

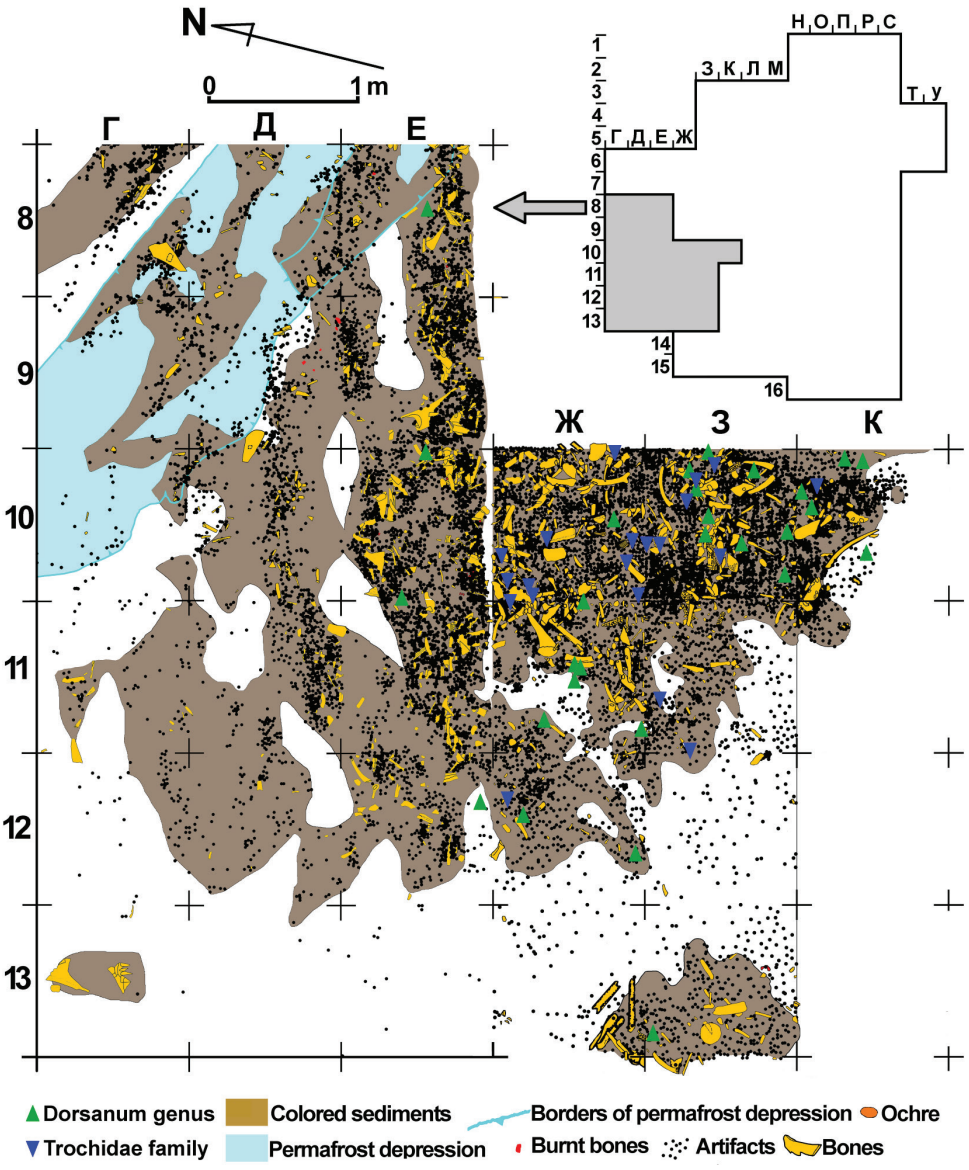


Fig. 9-11. Barmaky, level 2, Western area: distribution of non-perforated shells.

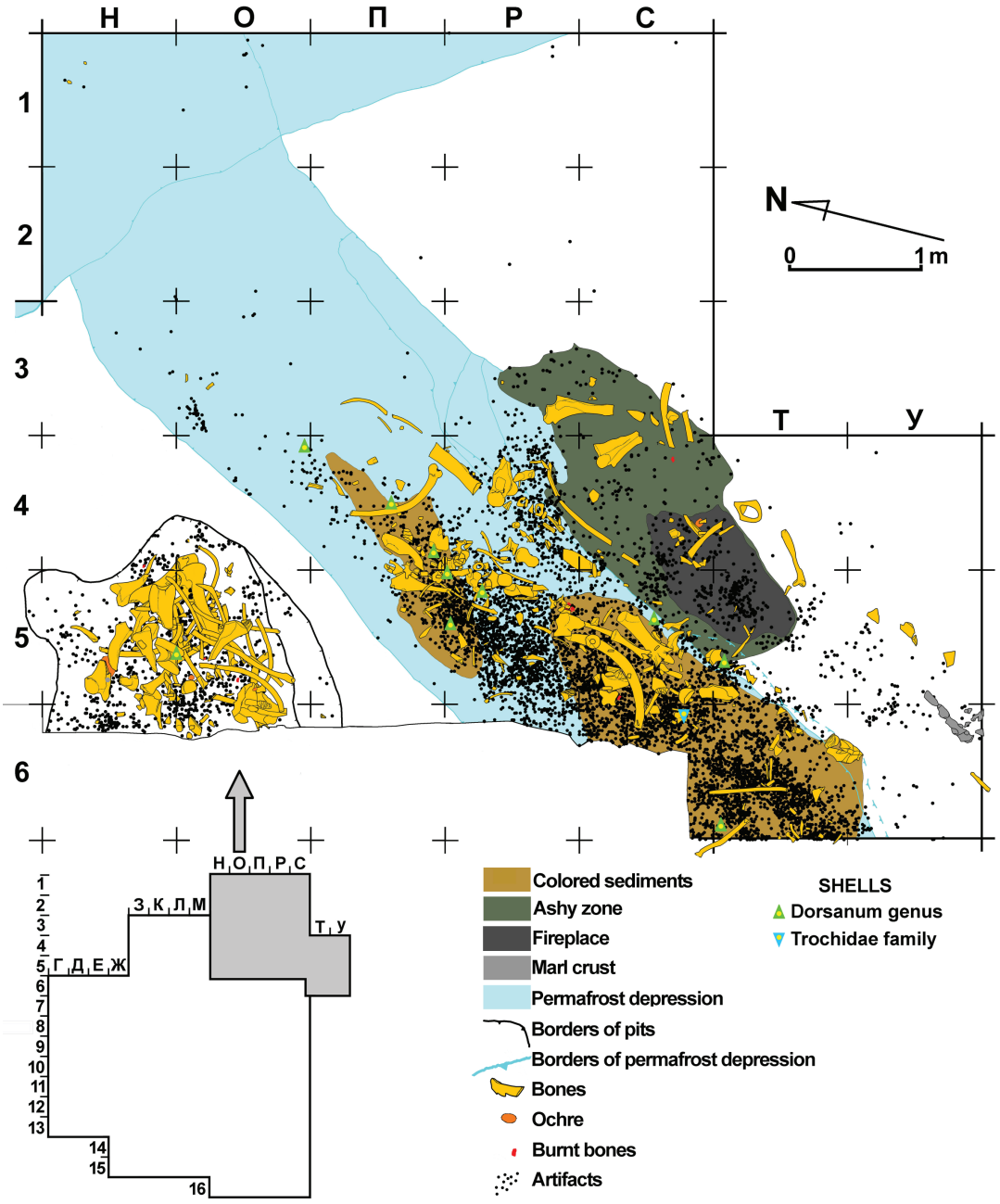


Fig. 9–12. Barmaky, level 2, Eastern area and pit 2: distribution of perforated shells.

In the Eastern area, coloured shells comprise perforated (n=4) and indistinct (n=4) pieces, seven belonging to *Dorsanum duplicatum* (Sow.) and one to *Dorsanum develuinum* d'Orb. Spatially the coloured shells are distributed fairly evenly: square 4П – 2 items, 4Р – 2 items, 5Р – 1 item, 5С – 2 item and 6С – 1 item.

From pit 2 comes one coloured fragment of *Dorsanum duplicatum* (Sow.).

## Ochre

Ochre in various shades of red and less often yellow was used widely, probably being the reason for the brownish colour of the sediments of the cultural layers, mainly in the Western area. Here, small pieces with maximum dimensions of 5 mm originate from squares 8Е – 3 pieces, 9Е – 1 piece, 10Е – 2 pieces and 11Е – 1 piece. In addition, squares 9Е and 10Е contain two ovoid concentrations of ochre powder, 12–18 cm long, 8–10 cm wide, and about 0,2 cm thick (Fig. 2-27, Chapter 2, this volume). The ochre concentration in square 10Е is closely located to a relatively large (5 cm in max dimension) piece of chalk. In the Eastern area, the ochre finds are associated with the potential dwelling structure: single pieces on squares 5Р, 5С, 4Р and a small concentration of ochre powder in the fireplace, square 4С.

## Amber

During the 2018–2020 excavations, a small fragment of amber was found in the filing of pit 2, in square 5О. Its dimensions are 16.30×14.46×12.51 mm (Fig. 9-2, *21*).

Fig. 9-13. Barmaky, level 2, Western area, square 11Е: distribution of perforated *Dorsanum* shells.

# DISCUSSION: INTRA-SITE AND INTER-SITE COMPARISONS

**Intra-site comparison.** The most obvious difference between the Eastern and Western areas consists in the complete absence of artefacts from ivory and antler in the former and rather extensive ivory processing and ivory tool use in the latter (Table 9-1). Moreover, the ivory artefacts and by-products are concentrated in a relatively small zone, limited to the seven squares: 8Е, 9Е, 10Е, 10Ж, 10З, 11Е and 11Ж. In addition, few organic artefacts also originate from the five directly neighbouring squares 9Д, 12Д, 10З, 10К and 11З, as well as the more distant squares 6Ж and 6Л corresponding with pit 1 (Fig. 9-14, *2, 3, 4, 5*).

The finds of ochre (sq. 8Е, 9Е, 10Е, 11Е) and amber (sq. 10Ж, 11Ж, 12Ж and 6Л in pit 1) are associated with the same squares (Fig. 9-14, *1*). In sum, organic artefacts, amber and ochre show a concentration on seven squares in the Western area and occur in a further eight squares in their periphery.

There are single ochre and amber finds in the Eastern area, including ochre powder in the fireplace, and Piasetsky mentioned numerous small pieces of amber in its vicinity (sq. 6Р, 6С, 7С).

Shells are about 18 times more numerous in the Western area compared to the Eastern area (Table 9-2). In the Western area, the main concentration of shells was found on seven square meters: 8Е, 9Е, 10Е, 10Ж, 10З, 11Е and 11Ж (Fig. 9-9; 9-14, *6*). The concentration of perforated shells corresponds to about the same squares 10Е, 10Ж, 10З, 10К, 11Е and 11Ж (Fig. 9-10). The concentration of non-perforated shells is restricted to squares 10Ж, 10З, 10К, and 11Ж (Fig. 9-11; 9-14, *7*), with a cluster of specimens from the Trochidae family in squares 10Ж and 10З and a concentration of coloured shells in the neighbouring square 11Е. So it seems that perforated and presuming worn shells dropped during occupation over the entire area, but especially on sq. 10Е, 10Ж, 10З, 10К, 11Е and 11Ж, whereas non-perforated shells, maybe as a reserve for further production, are restricted to squares 10Ж, 10З, 10К, and 11Ж (Fig. 9-10; 9-11). In the Western area, those squares with the highest density of organic artefacts, ochre and amber also correspond with the highest densities of flints (Fig. 9-7).

There is ample evidence of the extensive activities involving ochre, amber, artefacts and adornments from organic materials, chalk and shells in the Western area (particularly squares 9E, 10E, 10Ж, 103, 11E, 11Ж), but it is unclear whether the finds accumulated during a single stay with a wide variety of activities, or as a palimpsest of several visits with different activities. The Western area workshop zone might be larger, but, unfortunately, there is no reliable information from its neighbouring squares excavated by Lupenko and Piasetsky.

In the Eastern area, the locations with the highest density of artefacts correspond with the highest density of shells: 4P, 5P, 5C, and 6T (Fig. 9-12; 9-14, *6*).

**Inter-site comparison.** Amber appears to be the only material at Barmaky transported over long distances. According to Piasetsky, amber could have been brought to the site from Paleogene deposits in the Horyn River valley, near the village of Berezhnytsia, at a distance of approximately 110 km from the site (Piasetsky, Samoliuk 1990: 12; Piasetsky 1997: 151-161; Piasetsky 2009: 142). In post-LGM sites, Amber processing is commonly attested in the Middle Dnieper region: Mizyn, Dobranichivka, Semenivka 2 and Mezhyrich (Iakovleva 2013: 115, 116).

Ferruginous material, in contrast, is known from local outcrops of chalk/marl deposits, 300 m south of the site, which also contain Turonian flints. This material might be the source of ochre used at Barmaky, a common feature for Epigravettian sites of the Mid Dnieper basin.

Outcrops of *Dorsanum* and Trochidae shells known to date are situated at distances of 5-15 km (Kolodenka, Bila Krynytsia, Antopol, Taikury), about 30 km (Bochanytsia, Khreniv) and 70-75 km (Shelviv, Mykhniv) to the site (Fig. 9-6). These outcrops contain a wide spectrum of fossil shells, including the most popular in Barmaky *Dorsanum duplicatum Sowerby* (=*Buccinum duplicatum* (Sow.)), *Trochus* sp., *Trochus ex gr. Podolicus* (Koles), and *Gibbula podolica* (Montp.) (Table 9-2). However, compared to the variety of shells in natural deposits, the collection found on-site presents a narrow spectrum of species. Such sorting might be an indicator of aesthetic preferences. The quantitative predominance of *Dorsanum duplicatum* (Sow.) among the perforated and coloured shells strongly suggests that it was the most accessible, but likely most valued species for the inhabitants of Barmaky (Table 9-2; Fig. 9-5, *1, 5, 6*). It is worth noting that shells of the *Dorsanum* genus are represented in significant numbers also at the roughly contemporaneous site of Mizyn (Rudenko 1959: 110–113; Iakovleva 2013: 151, 152), in the area where the shells-bearing Sarmatian sediments are absent. Therefore, the presence of a significant number of *Dorsanum* shells at Mizyn might indicate their import from the West.

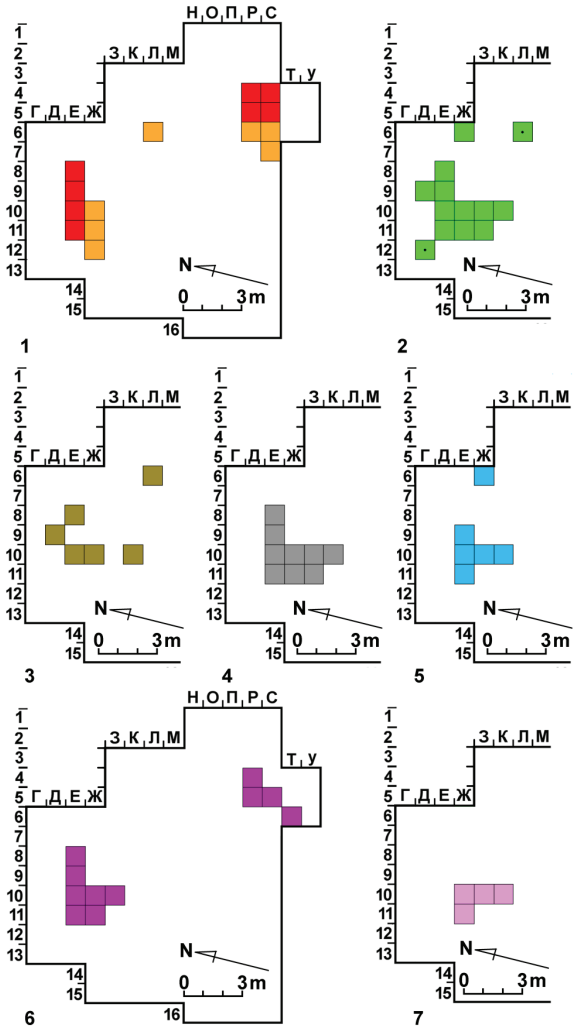


Fig. 9-14. Barmaky, level 2, plans: 1 – ochre and amber distribution; 2 – Western area, artefacts from organic material; 3 – Western area, borers and needles on ivory; 4 – Western area, processed ivory; 5 – Western area, adornments and figurine; 6 – fossil shells concentrations; 7 – Western area, non-perforated shells concentration.

Analogues for the Barmaky mammoth figurine made of marl are known from several pre-LGM and post-LGM sites in Eastern Europe: Kostenki 1, layer 1; Kostenki 4, layer 1; Kostenki 11, layer 2; Yeliseyevichi 1 (Efimenko 1958: 385–388; Rogachev, Anikovich 1982: 79; Rogachev, Popov 1982: 126, 127; Velichko et al. 1997: 137–139; Nuzhnyi et al. 2005: 8; Nuzhnyi 2015: 208).

All in all, the grooved organic points, dumb-bell-shaped beads, bracelets with a «herring-like» ornament, ivory figurine and perforated *Dorsanum* shells from Barmaky are highly similar to the same types of artefacts from Mizyn (Nuzhnyi 2015: 209–210).

# SITE FUNCTION OF BARMAKY: RAW MATERIAL TRANSPORT AND FAUNAL EXPLOITATION

# 10

V. CHABAI, K. PASDA, D. DUDNYK, A. MAIER

## INTRODUCTION

There are two contrasting hypotheses concerning the function and seasonal occupation of sites with larger concentrations of mammoth remains. One hypothesis assumes that mammoth bone structures (interpreted as dwellings) and their associated pits (interpreted as cashes) result from long-term base camps used during winter, while sites without mammoth bone structures and pits were used as short-term summer camps (Levitsky 1949; Shovkoplias 1965; Pidoplichko 1969; Bibikov 1981; Soffer 1985; 1993; Nuzhnyi 2015; Shydlovskyi et al. 2022). Here, sites such as Mezhyrich, Mizyn, Gintsy, Dobranichivka, Yeliseevichy 1, Suponevo and Yudinovo are seen as cold season base camps where variable activities with stone and organic materials for utilitarian and non-utilitarian purposes were carried out. These base camps are thought to comprise several simultaneously used dwellings, occupied by family groups with *"egalitarian economic relationships"* and an *"autonomous economic behaviour"* (Shovkoplias 1965: 90; Klein 1973: 109; Bibikov 1981: 99; Soffer et al. 1997: 61), jointly exploiting resources of flint, fauna, amber, and fossil shells in the site's surroundings. They are thus seen as the remains of a *"prolonged stay"* or even of a *"semi-sedentary lifestyle"*, which is said to be *"similar to that of recent hunter-gatherer residential camps"* (Shovkoplias 1965: 287; Hoffecker 2002: 246). Complementary, sites such as Fastiv and Semenivka 1, 2, and 3 are seen as short-term camps dedicated to hunting or other activities of limited scope conducted during the warm season (Nuzhnyi, Stupak 2001: 72–73; Hoffecker 2002: 241, 246–247; Shydlovskyi et al. 2022: 220). Here, the topographic position of Fastiv and Semenivka 1, 2, and 3 near the top of the loess plateau was a major reasons for this attribution, since wind exposure is said to be uncomfortable during winter, while comfortably decreasing the size of mosquito and gnat swarms during summer (Soffer 1985: 344, 348; Nuzhnyi, Stupak 2001: 73). Accordingly, the composition of the tool kits is also thought to reflect seasonally differentiated activities, with a high ratio of microlithic insets and low ratio of end-scrapers, in summer camps and an opposite pattern during winter (Nuzhnyi & Stupak 2001: 58–62; Chabai et al. 2020c; Shydlovskyi et al. 2022: 219–220). The same reasoning was applied to interpret Barmaky as a camp used during the warm season (see Chapter 1, this volume).

The other hypothesis states that sites both with and without mammoth bone structures were indiscriminately used for short-term stays in the cold and the warm season, based on extensive zoo-archaeological studies of the faunal assemblages of Yeliseevichy 1, Yudinovo, and Mizyn (Demay et al. 2017). In light of recent stratigraphic reviews highlighting the multi-layered character of these sites (for details, see Chapters 3 and 11, this volume), these studies concluded that Yeliseevichy 1 and Mizyn were occupied several times during both the warm and the cold season, while Yudinovo was identified as a winter occupation. Also, the base camp character of Yudinovo and Mizyn has been corroborated, while it was questioned for Yeliseevichy 1, because of the narrow scope of the exploited fauna, which focused on canids and mammoth (Demay et al. 2017: 89–90).

The new excavations at Barmaky and subsequent analyses of data provide an opportunity to contribute to the debate about the seasonal,

topographic, socioecological, and toolkit-related assumptions. Here, the delimitation of a western and eastern area and the question whether Barmaky results from a single settlement event or repeated, temporally and functionally distinct stays is crucial (Fig. 10-1), since the advocates of both hypotheses acknowledge a potential influence of the palimpsest character of the cultural deposits on the proposed seasonal and functional interpretations.

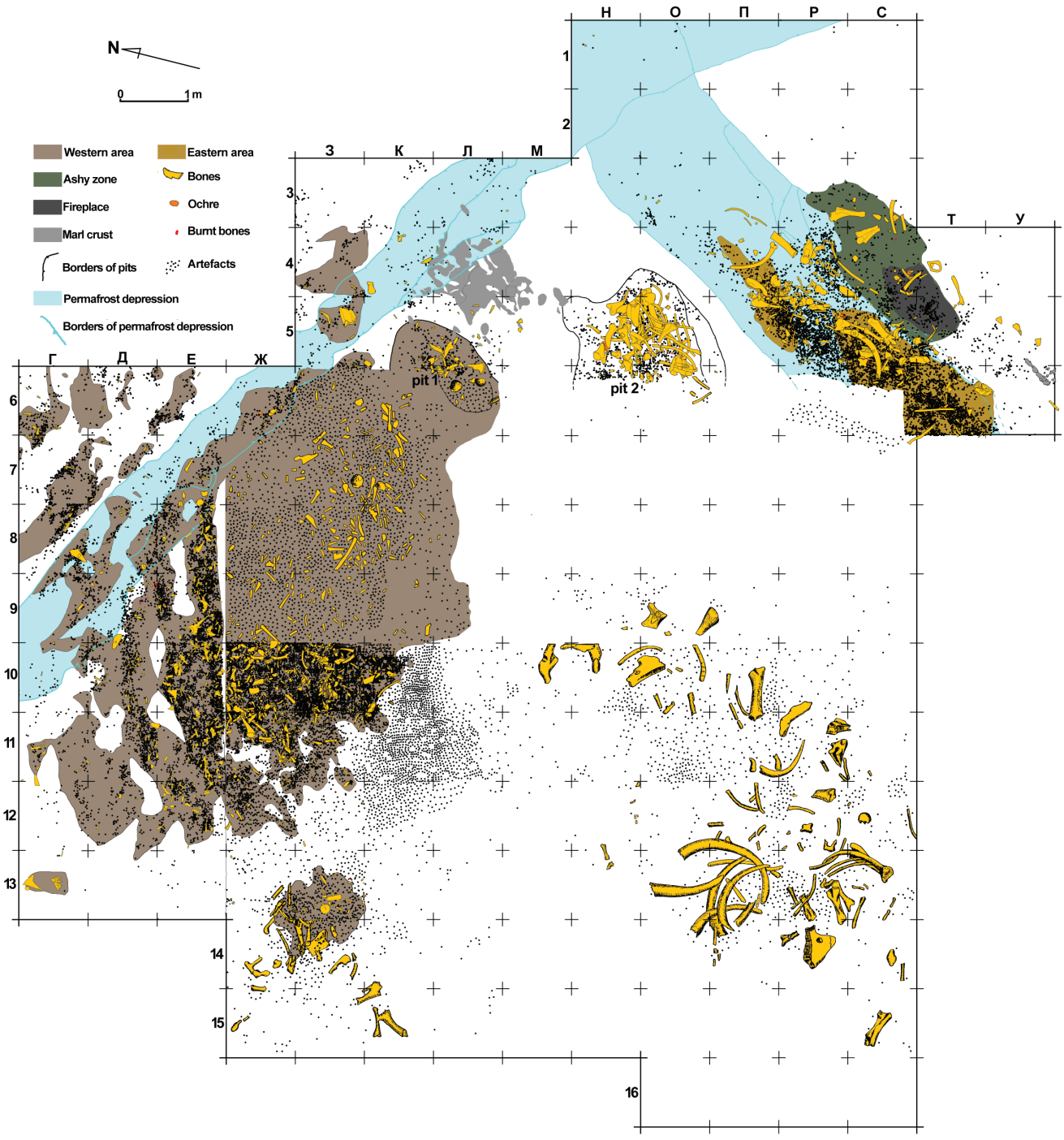


Fig. 10-1. Barmaky, horizons 2b, 2c and 2d: plan showing the Western Area and Eastern Area, pits, and chalk/marl crusts.

## BARMAKY: TOPOGRAPHY AND RESOURCE AVAILABILITY

The cultural deposits at Barmaky have accumulated on the slope of a small hill, at the shore of a water body (Chapter 2, fig. 2-1, 2, and Chapter 4, this volume). The lowest part of the cultural deposits has been observed 4-5 m above the present-day level of Barmatsky Creek and accumulated about 1 m above permafrost deposits. Solifluction lenses suggest the presence of an unstable surface, likely during the warm season. As demonstrated by sondage 4 and excavation area 2, the Epigravettian deposits are widely distributed along the slope and likely represent the remains of distinct localities (Chapter 1, fig. 1-1; Chapter 2, fig. 2-2, 1, this volume).

An extremely rich *in situ* outcrop of high-quality Turonian flint is situated 150-300 m south of the settlements, while the fossil shells originate from the Lower and Middle Sarmatian deposits at distances of 5 to 75 km from Barmaky. The four closest fossil shell outcrops are known from localities 5-10 km south–southeast of the site (Chapter 9, fig. 9-6, this volume). The sandstone pebbles used as hammer-stones are also from the Sarmatian deposits, while ferruginous material, used for ochre powder production, is available in sandy/silty Sarmatian and chalk/marl Turonian deposits. Single pieces of aleurolite (siltstone) and basalt, reported by Piasetsky, originate from the Ustia and Goryn rivers valleys, 34-44 km northeast of Barmaky. According to Piasetsky (2009: 140-141), the closest *in situ* amber sources are situated approximately 110 km northeast in the Goryn River valley. However, amber in a secondary position is known around the Barmaky site (Naumenko, Matsui 2020). Thus, except for the single pieces of basalt and aleurolite, the used resources were available within a one-day foraging radius.

## BARMAKY, LEVEL 2, EASTERN & WESTERN AREAS

The spatial distribution of the archaeological material at Barmaky has a clustered character. Due to the methods of excavating, find labelling, and find mapping employed by Lupenko and Piasetsky, the available information for a spatial analysis of their trenches is very limited (see Chapter 1, this volume). The areas excavated during the 2002-2007 and 2018-2020 field campaigns, however, are a reliable source for activity analyses. Here, the excavated area is subdivided into two parts, a western (WA) and an eastern area (EA). The absence of a stratigraphic connection between the two areas does not allow for an unambiguous statement of their temporal relation (Chapter 2, this volume).

### Structures

In the WA, pit 1 and a chalk/marl crust were found. In the EA, the remnants of a dwelling structure with an internal hearth were excavated. Probably the small chalk/marl crust associates with this dwelling structure (see Chapter 2, this volume). Pit 2 has no stratigraphic connection to either the EA or the WA, so the materials from pit 2 are analysed separately.

### Intensity of occupation

The WA and EA were excavated on 35 and 19 m2, respectively. The difference in areal size is also reflected in the number of finds, which are twice as numerous in the WA – 93,548 lithics and 3,235 bones – than in the EA – 46,783 lithics and 1,187 bones (see Chapter 5, table 5-1a; Chapter 8, tables 8-37, 8-58, this volume). At the same time, the number of squares with high find densities is nearly equal in both areas: squares 8E, 9E, 10E, 9Ж, 10Ж in the WA, and squares 4P, 5P, 4C, 5C, 6T in the EA (Fig. 10-1). In the WA, the most numerous finds originate from square 9E with 13,997 flints and 83 bones, which is very similar to square 5P in the EA with 12,419 flints and 52 bones. Also, there is a direct correlation between bone and flint numbers in all of the excavated squares. Square

5P has a direct spatial connection to the dwelling structure identified in the squares 3P, 3C, 4P, 4C, 5P and 5C. No reliable evidence of a dwelling was found in WA. Despite the hearth feature in the EA, burnt material is extremely rare, a common feature also for the WA as well (Chapter 2, this volume). All other things being equal, the percentage of fragmented *debitage* may reflect trampling, which is more common for the WA (68.30 %) than for the EA (59.48 %) (Fig. 10-2).

## Flint artefacts

In the EA, the production of micro-blades and bladelets was more pronounced than in the WA. This is reflected in the selection of flat raw material blocks, the dominance of narrow surface bladelet cores and pre-cores, and the dominance of bladelets and micro-blades over blades (Fig. 10-3). In the WA, artefact use appears more pronounced, as is indicated by a smaller average size of cores, higher shares of burin and truncation spalls, combined burins, rejuvenated burins, and the ratios of burin spall negatives to burin edges, and primary burin spalls to multiple burin spalls (Fig. 10-2). In addition, the average dimensions of burins are smaller in the WA than in the EA (Fig. 10-2). The tools to cores ratio suggests a more intensive artefact reduction in the WA (Fig. 10-2).

## Artefacts on tusks, antlers and bone

No artefacts on organic materials were found in the EA. Bracelet fragments, dumbbell-shaped beads, points, borers, needles, as well as slotted and processed tusks originated all from the WA (see Chapter 9, table 9-1, fig. 9-14, this volume). Here, the distribution of artefacts from organic materials corresponds with the squares containing also the largest numbers of bones and lithics.

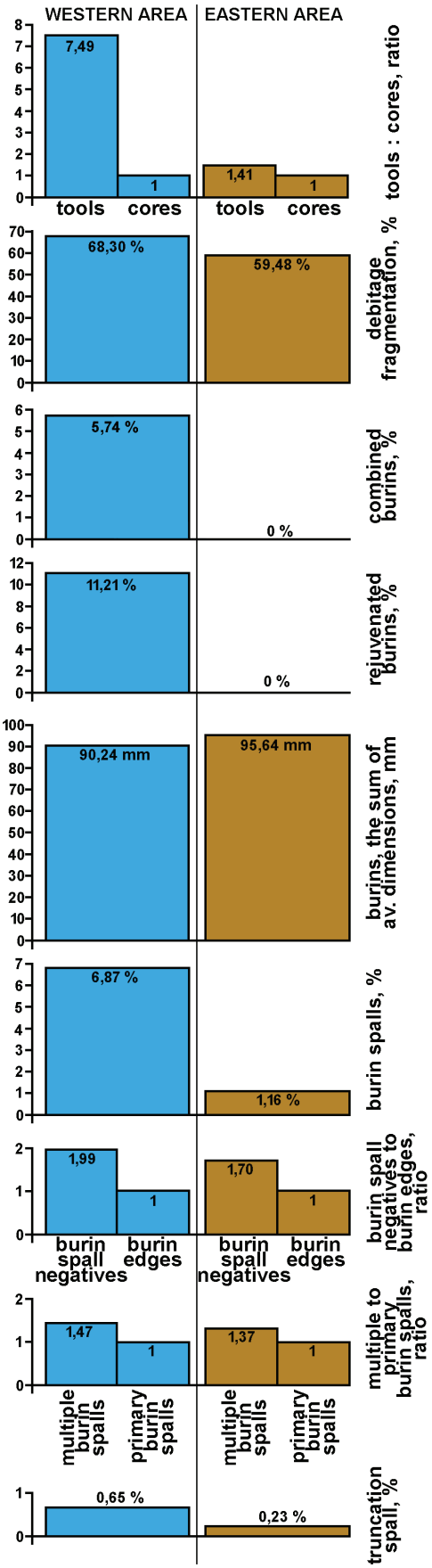


Fig. 10-2. Barmaky, level 2: attributes of tool production and rejuvenation.

## Figurines

The mammoth figurine made of marl originates from square 10Ж in the WA. The small, fragmented female figurine on mammoth tusks, known from the 1990 campaign, was found in squares near the WA (see Chapter 9, fig. 9-1, 15, 16, 25). No figurines are known to exist in the EA.

## Fossil shells

The total number of fossil shells amounts to 537 specimens in the WA and 30 specimens in the EA. The maximum number of shells per square meter in the WA and the EA comprises 57 (sq. 10E) and 9 (sq. 5P) items, respectively. In the WA, the largest number of shells is concentrated on the squares 10E, 10Ж, 10З, 10К, 11E and 11Ж. In both areas, the squares with the highest densities of lithic finds also have the highest number of shells (see Chapter 9, fig. 9-7; 9-8). Most shells belong to the marine gastropod genus *Dorsanum* of the family Nassariidae and the marine gastropod family Trochidae. In the EA, all shells are perforated, while in the WA, 52 of the 208 shells are not perforated, thus probably representing a reserve of 25 %. The non-perforated shells concentrate on four square meters: 10Ж, 10З, 10К, and 11Ж. Hence, in the WA, the concentrations of perforated and non-perforated shells originate from the same squares (see Chapter 9, table 9-2, fig. 9-5, 9-9 – 9-14).

## Ochre

Concentrations of ochre powder were found in squares 9E and 10E of the WA and in the hearth area of square 4C in the EA. In addition, small pieces of ochre originate from squares 8E, 9E, 10E, 11E in the WA and squares 5P, 5C, 4P in the EA (see Chapter 9, fig. 9-14, this volume).

## Amber

In the WA, small pieces of amber were found in the squares 10Ж, 11Ж, and 12Ж. Piasetsky reported finds of the amber pieces from squares 6P, 6C and 7C (Piasetsky, Samoliuk 1990), close to the EA.

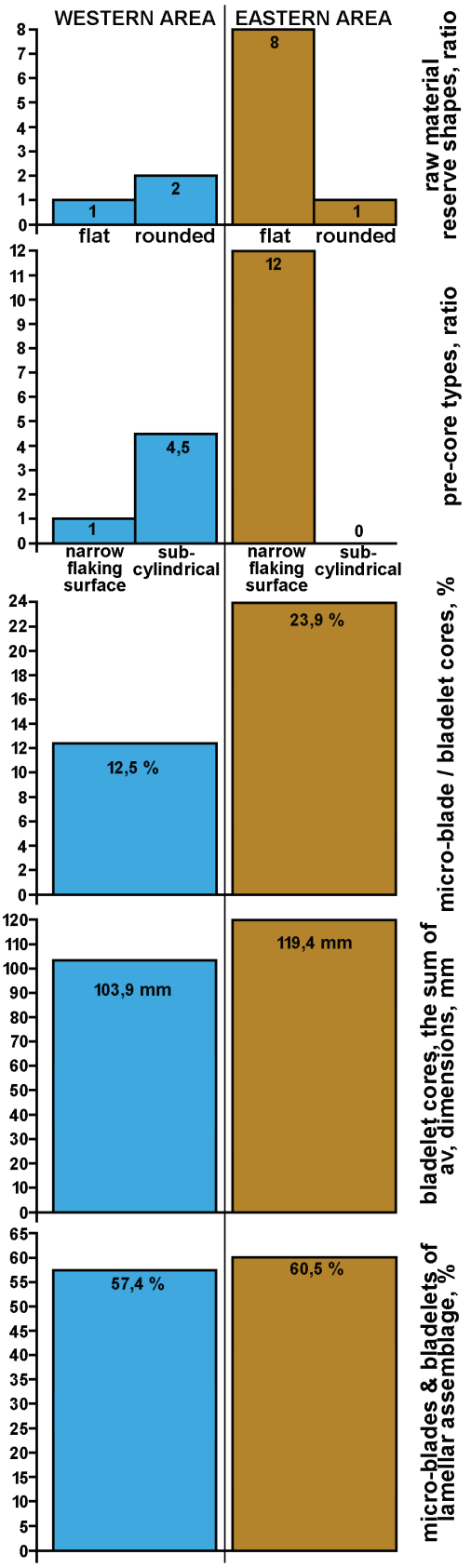


Fig. 10-3. Barmaky, level 2: attributes of core reduction.

### Fauna

Nine mammal and two bird species have been documented in the WA and the EA of the 2018–2020 excavation (see Chapter 5). *Mammoth, Bison, Equus,* and *Rangifer* occur in both areas, although bison and particularly reindeer have higher numbers in the WA, while mammoth has higher numbers in the EA. *Saiga* is only found in the WA, while *Ursus, Lepus* and the two bird species *Larus* and *Phalacrocorax* have only been found in the EA. The EA thus has a markedly higher number of species (n=9) than the WA (n=6), with a complementary occurrence of five species. Looking at the mammoth remains, the age ranges of individuals are similar for both areas, while the minimum number of individuals and the degree of bone fragmentation vary. Here, higher MNIs and larger remains in the EA may point towards dismemberment, while the WA yielded deliberately smashed, smaller fragments, maybe related to narrow extraction.

Based on the remains of the youngest mammoth individuals, the occupation at Barmaky likely took place during the cold season. Judging from the amount of available meat, the stay may have lasted several weeks. The presence of all parts of the body, also from adult mammoths, suggests that there has been only little or even no transportation distance between the place where the animals were killed and the place where they were butchered. This is corroborated by observations on other ungulates, which were presumably also brought to the site as complete animals, suggesting killing spots nearby. The presence of carnivores at the site is likely related to the use of their fur. This is suggested by several paw bones from foxes found in anatomical order, probably as a result of the skinning process.

## BARMAKY, LEVEL 2, PITS 1 AND 2

The assemblages of flint artefacts from the fillings of pits 1 and 2 result from a sediment cover put above the bones. The sediments used for the cover come from around the pits and already contain some cultural remains. The tool to core ratios in pit 1 (5.25 to 1) and pit 2 (1.27 to 1) correspond with those of the WA and the EA, respectively (Fig. 10-2). Unfortunately, the artefacts from both pits are not numerous enough for a quantitative comparison of other attributes. The faunal remains from both pits contain selected parts of mammoth carcasses. Costa and scapula are the most numerous in pit 1, while the costa and cranial bones are prevailing in pit 2 (Chapter 5, tables 5-4 and 5-23, this volume). In pit 1, mandibula fragments probably originate from one juvenile individual. A left maxilla is part of the cranium from pit 2, and the isolated molar found in square 5C of the EA originates from a left maxilla from an animal of about the same age (Chapter 5, this volume). This evidence points towards a closer link between the EA and pit 2.

## VARIATION OF ACTIVITIES IN DIFFERENT SITE AREAS

In sum, five of 20 analysed on-site activities are characteristic for both areas in equal proportions: densities of lithics and bones, intensity of core reduction, season of faunal exploitation, and fur production (Fig. 10-4). The WA shows more intensive activities concerning the production and rejuvenation of lithic and organic tools, production and discard of adornments, mobile art, and cooking/marrow extraction. The EA, on the other hand, is marked by the presence of a dwelling structure, pronounced bladelet production, and intensive carcass dismembering (Fig. 10-4). The range of activities in the WA area is thus more variable and probably time-intensive, especially those connected to the processing of organic materials and fossil shells, also reflected in the high degree of bone and *debitage* fragmentation, at least partly as a result of trampling.

The question thus remains whether the WA and the EA are functionally complementary parts of a single settlement event or represent two distinct occupation events.

Arguments in favour of the latter come from the observation that the EA and WA are spatially clearly separated from one another. However, this observable separation results in larger parts from the use of cultural deposits around the pits to build their covers. In case of repeated occupation events, one may expect evidence of a dwelling structure also in the WA,

| | | EA | WA |
|---|---|---|---|
| 1 | dwelling structure, hearth | ■ | |
| 2 | meat storage | ? | ■ |
| 3 | density of artefacts per sq. m | ■ | ■ |
| 4 | density of bones per sq. m | ■ | ■ |
| 5 | trampling effect, debitage fragmentation | ▒ | ■ |
| 6 | trampling effect, fauna fragmentation | ▒ | ■ |
| 7 | core reduction | ■ | ■ |
| 8 | bladelet production | ■ | ▒ |
| 9 | tool production | ▒ | ■ |
| 10 | tool rejuvenation | ▒ | ■ |
| 11 | artefacts on tusk, antler and bone | | ■ |
| 12 | pieces of mobile art on tusk and marl | | ■ |
| 13 | fossil shells, not perforated | | ■ |
| 14 | fossil shells, perforated | ▒ | ■ |
| 15 | ochre powder concentrations | | ■ |
| 16 | ochre and amber pieces | ▒ | ▒ |
| 17 | fauna, seasonality | winter | winter |
| 18 | fauna, dismembering | ■ | ▒ |
| 19 | fauna, consumption | ▒ | ■ |
| 20 | fauna, fur | ■ | ■ |

| | |
|---|---|
| pronounced | ■ |
| available | ▒ |
| absent | |

Fig. 10-4. Barmaky, level 2, attributes of site structures, as well as flint and faunal exploitation by areas.

potentially signalled by pit 1 and the chalk/marl crust, which may either have not been recorded because of the excavation methods applied during the field campaign of 1990, or may have become invisible because of the intensive occupation (trampling). For now, the arguments supporting a single settlement event seem more convincing:

1. The presence of a dwelling structure in the EA and the absence of respective conclusive evidence in the WA
2. The similar age range of mammoth individuals in both areas is compatible with a single group of animals killed at the same time
3. The complementary character of the activities documented for the WA and the EA

If both areas represent a single occupation event, Barmaky, level 2 can be classified as a cold-season residential camp with a wide range of utilitarian and non-utilitarian activities, based on the exploitation of mostly local resources. According to the faunal analysis, this camp might have been in use for several weeks by a relatively small group of inhabitants (see Chapter 5, this volume). This conclusion contrasts with the three commonly adopted assumptions that (1) mammoth bones dwelling constitute a necessary attribute of cold-season base camps, (2) these camps are aggregations of several family groups, and (3) that winter-camp tool-kits have high numbers of end-scrapers and low numbers of microlithic insets (see Chapter 8, this volume). Also, the topographic description of Barmaky as being on "high" elevation is a clear overstatement, and we refrain from speculating on the comfortable or uncomfortable character of seasonal winds. Probably much more important may have been the seasonal surface stability. Here, solifluction lenses have wrinkled up the cultural deposits, suggesting muddy and slippery conditions of the living floor surface during the warm season, which likely makes the landscape "uncomfortable" for both humans and animals.

## DISCUSSION AND CONCLUSION: TRANSPORT DISTANCES & SUBSISTENCE STRATEGIES

### Barmaky

The Epigravettian winter base camp of Barmaky, level 2, was located at the shore of a water body and most resources, such as flint, sandstone pebbles, fossil shells, ferruginous concretions, and animals were available within a foraging radius of a one-day trip. In terms of Tarriño et al. (2015: 95-96), day-to-day resources, such as water, fauna, and flint could be obtained locally or *"Near Local, < 15 km"*, while others, such as basalt or siltstone, were found *"Near Regional, 30-60 km"*. Only amber may have been gathered *"Distant Regional, 60-120 km"*, if it was retrieved from the known *in-situ* outcrops (Fig. 10-5).

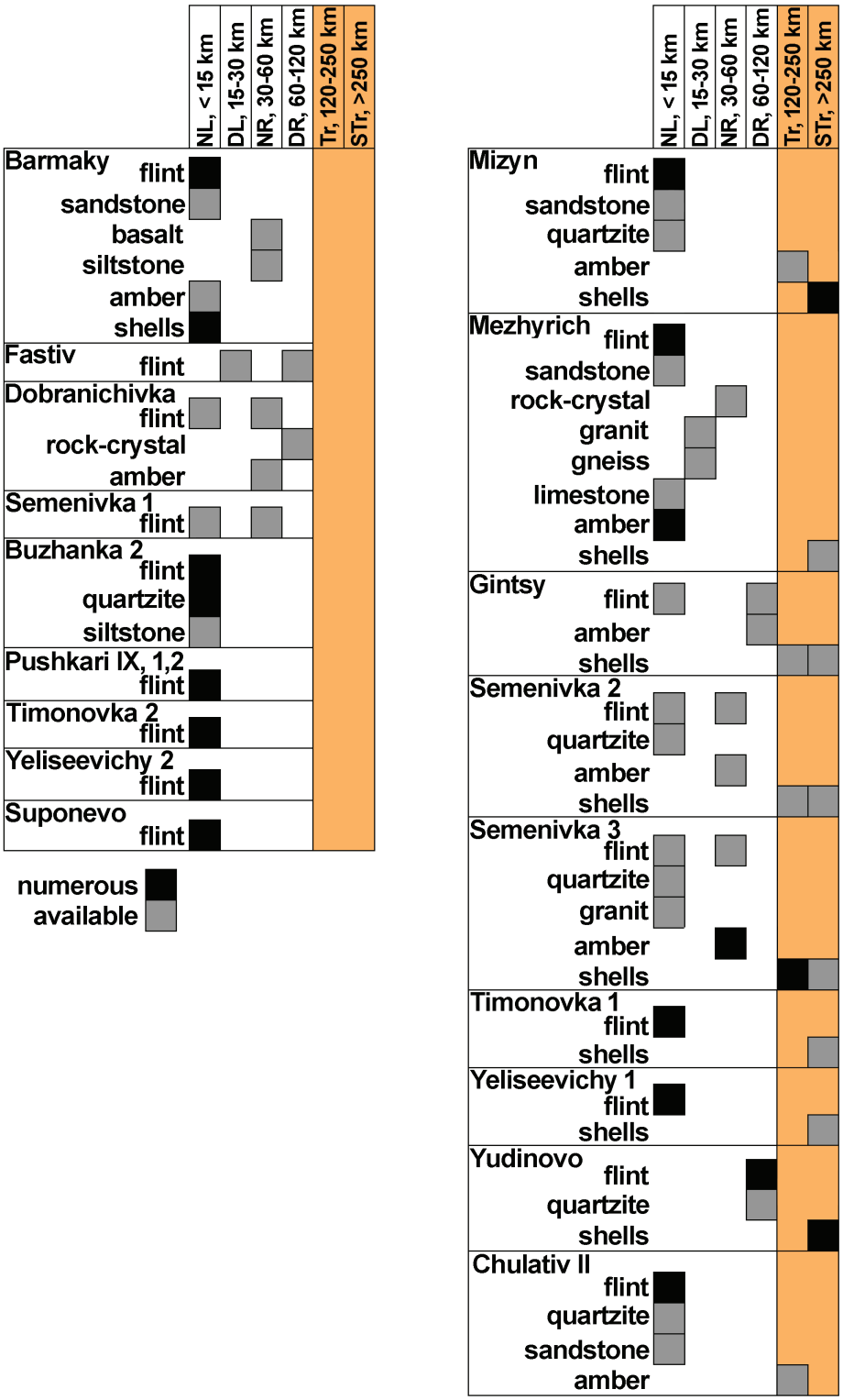


Fig. 10–5. Mid-Dnieper Epigravettian: distances to sources of lithic raw materials, amber and shells; NL – near local; DL – distant local; NR – near regional; DR – distant regional; Tr – tracer; STr – super tracer (sensu Tarriño et al. 2015).

The available amount of meat would be sufficient to feed a smaller group of people during repeated occupations for several weeks (see Chapter 5, this volume). At least one meat-cash was prepared, maybe for a planned but eventually not realised return. Here, the finds from excavation area 2 and sondage 4 may reflect specialised locations in the nearer surroundings of the base camp (see Chapters 1, 2 and 5, this volume; Piasetsky, Samoliuk 1990; Vasyliev et al. 2019). This is reminiscent of the situation at the Semenivka settlement complex, which was interpreted as summer base camps with adjacent killing-butchering activities (Nuzhnyi, Stupak 2001), but it needs to be stressed that the seasonal interpretation is not based on faunal analyses.

The observations from Barmaky are in accord with the findings by Demay et al. (2017) that residential camps with mammoth bone dwellings, such as Mizyn, were periodically occupied during both the warm and cold seasons. They are, however, at odds with claims regarding connections between the season of occupation and a site's topographic position or artefact ratios, as well as necessary connections between cold season base camps and mammoth bone dwellings, or base camps and aggregations of several family groups.

## Mid-Dnieper

In the following, we will compare the findings from Barmaky with those from the Mid-Dnieper region, particularly regarding distance to resources, namely water, fauna, lithics, amber, and shells.

## Water

No Epigravettian site of the Mid-Dnieper Basin is located more than 4 km away from a first to third order tributary to the main stream. It is even the case that the vast majority of the sites along the Desna River – including Mizyn, Pushkari IX, Chulativ I and II, Timonovka 1 and 2, Yudinovo, Yeliseevichi 1 and 2, and Suponevo – are located just 100 to 500 m away from the present-day riverbank (Shovkoplias 1965: 17–29; Khlopachev 2014: 81; Pidoplichko 1940: 65; Voevodsky 1952: 101; Voevodsky 1929: 59; Mirchink 1929; Abramova, Grigoreva 1997: 84; Velichko et al. 1997: 5; Shovkoplias 1950: 177). An exception is Buzhanka 2, which lies approximately 1 km away (Stupak 2014: 538). Similarly, all sites associated with the Ovruch industry (Sholomky 1, Zbranky, Dovhynychi) are found within 100–200 m of the Noryn River, a tributary of the Uzh in the Prypiat Basin (Nuzhnyi 2015: 134, 139, 143).

Sites of the Mezhyrich industry are positioned slightly farther, at a distance of 1–2 km from the present-day riverbank: Mezhyrich from the Ros River; Semenivka 1, 2, and 3 from the Trubizh River; Gintsi from the Uday River and Fastiv from the Unava River (Nuzhnyi 2015: 211, 274, 279, 291, 321, 325). The site of Dobranichivka is approximately 2.5–3 km away from the Supii River (Nuzhnyi 2015: 235).

In addition to rivers, other types of water sources, such as lakes, ponds, and oxbow formations, could have served as important water sources. At Barmaky, the presence of the freshwater molluscs *Radix sp., Galba truncatula* and *Planorbis planorbis* (see Chapter 4) and the water-related bird species *Larus argentatus* and *Phalacrocorax aristotelis* (see Chapter 5) strongly suggests that the site was located on the banks of a standing water reservoir. Proximity to such water resources is also indicated by the presence of freshwater molluscs *Unio sp.* at Mezhyrich, Gintsi and Semenivka 3 and hygrophilous terrestrial molluscs *Succinea sp.* at the Gintsi site (Iakovleva 2013: 147–156).

## Fauna

No evidence for long-distance transport of faunal resources has been recorded for the Epigravettian sites of the Mid-Dnieper Basin. Instead, much like for Barmaky (see Chapter 5), the analyses indicate minimal or no transportation distance between kill and butchery locations. At Yeliseevichi 1, the preservation of all anatomical parts of a mammoth carcass indicates that the animal likely died in immediate proximity to the site (Demay et al. 2017: 85). Similarly, the discovery of complete mammoth skulls, scapulae, humeri, pelvises, femora, ribs, and tusks at Mizyn points to on-site butchering. The meat-bearing postcranial elements of reindeer and bison have also been found at Mizyn, supporting this interpretation (Shovkoplias 1965: 39–50, 67–70, 73, 84–92, 97, 100). Comparable finds of meat bearing mammoth

skeletal parts have been recorded at Mezhyrich, Gintsi, Dobranichivka, Semenivka 1, 2, and 3, Fastiv, Buzhanka 2, Timonovka 1, and Yudinovo (Pidoplichko 1976: 89–91; Iakovleva, Djindjian 2018; Nuzhnyi 2015: 239–240, 276, 291, 295–296, 327; Stupak 2014; Voevodsky 1929: 62; Abramova et al. 1996: 133–134). Notably, Semenivka 1 is the only site in the region where the on-site butchering of Ursus is attested, while mammoth bones seem to have been collected (Nuzhnyi 2015: 276, 415–416).

## Lithics

Epigravettian sites in the Mid-Dnieper Basin are usually located not farther than 15 km to the next flint outcrops, observable for instance in the case of Mizyn, Mezhyrich, Buzhanka 2, Pushkari IX, 1, 2, Chulativ II, Timonovka 1, 2, Yeliseevichi 1, 2, or Suponevo (Voevodsky 1929: 62; 1952; Galych 1941: 150; Shovkoplias 1950: 179–180; 1965: 115; Velichko et al. 1997: 122, 145; Shydlovskyi 2005; Stupak 2013: 145; Khlopachev 2014: 90). Evidences of long-distance transport of stones, in contrast, is rare. The furthest transportation distances of flint are reported for Gintsy and Fastiv with roughly 100 km, and Yudinovo with 80 km (Shydlovskyi 2005: 33; Nuzhnyi 2015: 327; Abramova, Grigorieva 1997: 84). Transportation distances of 40–60 km are assumed for a relatively compact group of sites on the left bank of the Dnieper (namely Dobranichivka, Semenivka 1, 2 and 3), but a use of the local moraine flint is not excluded (Shovkoplias 1955; Nuzhnyi 2015: 241, 307) and in-depth raw material analyses from these sites are still missing.

At Buzhanka 2, local quartzite from deposits within 1 and 6 km distance to the site has been used intensively (Stupak 2013: 145). Rare finds of various rocks are known from Mizyn (quartzite, sandstone, belemnites), Chulativ II (quartzite, sandstone), Mezhyrich (granite, gneiss, sandstone, limestone), Semenivka 2 and Yudinovo (quartzite), Semenivka 3 (quartzite, granite), and Buzhanka (argillite), all foraged at "Near Local" sources (sensu Tarriño et al. 2015) at distances of less than 15 km (Galych 1941: 150; Shovkoplias 1965: 110, 115; Pidoplichko 1969: 150–151; Abramova et al. 1996: 72; Stupak 2013: 145; Nuzhnyi 2015: 281, 307, 319). Few artefacts made of rock crystal are reported from Mezhyrich and Dobranichivka, originating from deposits at a distance of 50 and 90 km to the west, respectively (Pidoplichko 1969: 145), i.e. "Near Regional" and "Distant Regional" sensu Tarriño et al. (2015: 95–96) (Fig. 10-5).

## Amber

Finds of amber at Epigravettian sites in the Mid-Dnieper basin are reported from Mizyn, Chulativ II, Mezhyrich, Gintsy, Dobranichivka, and Semenivka 2 and 3 (Voevodsky 1952: 104; Shovkoplias 1955: 45; 1965: 112–113; Pidoplichko 1976: 154–157; Soffer 1985: 370–371; Nuzhnyi 2015: 290, 319) and said to originate from sources located at distances of less than 15 km to roughly 250 km (Fig. 10-5). It needs to be stressed, however, that these statements are not based on geochemical analyses, and amber deposits in secondary contexts have been documented along both banks of the Mid-Dnieper basin, especially around Mezhyrich (Naumenko, Matsui 2020). Mezhyrich stands out with over 300 recorded pieces of amber, making it the richest site in amber finds of the region (Soffer, 1985: 142), while shells are rather rare (see below). The outcrops around Mezhyrich are seen as a likely source for amber found at Dobranichivka (45 km), Semenivka 2 and 3 (55 km) and Gintsy (100 km). The source for the amber found at Mizyn and Chulativ II is assumed to be located at a distance of about 250 km in the Dnieper valley (Shovkoplias 1965: 112–113).

## Shells

Unquestionable evidence of long-distance transport is provided by fossil and sub-recent specimens of marine shells. The Black Sea species *Nassa reticulata, Theodoxus sp.,* and *Cyclope neritea* were found in Semenivka 2 and 3, transported over a minimum distance of 470 km. The mollusc assemblage of Semenivka 2 and 3 also contains the fossil species *Dorsanum sp.*, with the closest known outcrop at about 200 km west of the site (Nuzhnyi, Stupak 2001: 64; Shydlovskyi et al. 2006: 384; Nuzhnyi 2015: 290, 298). Specimens of *Nassa reticulata* are also known from Mezhyrich, about 450 km north of the Black Sea shore (Pidoplichko 1969: 130). The Black Sea mollusc *Cerastoderma*

*glaucum cf. umbonatum* (Wood, 1850) and the fossil species *Dorsanum sp.* are reported from Gintsy, procured at distances of about 450 km to the south and 250 km to the west, respectively (Iakovleva 2013: 144). Black Sea species are also reported from sites along the Desna, such as Mizyn and Timonovka I (*Nassa reticulata*), Yeliseevichy 1 (Annelids), and Yudinovo (*Nucula, Cerastoderma, Steromphala, Tritia, Cerithium* and *Melarhaphe*) (Rudenko 1959, Shovkoplias 1965: 106; Velichko et al. 1997: 135; Iakovleva 2013: 150–152; Demay et al. 2017: 83; Kijashko, Khlopachev 2022). The minimum distances from Mizyn and Yudinovo to the Black Sea shore are about 700 and 800 km, respectively. The fossil species found at Mizyn (*Buccinum sp. = Dorsanum sp.*) probably originates from Volhynia at a distance of about 500 km (Fig. 10–5). All in all, the transport distances of shells found at Mizyn, Mezhyrich, Gintsy, Semenivka 1 and 2, Timonovka 1, and Yudinovo fall within the categories of "Tracer, 120–250 km" and "Super-Tracer, > 250 km" sensu Tarriño et al. (2015). This list may be expanded by Chulativ II, but the species identification of *"a few shell fragments"* has not been done yet (Voevodsky 1941: 45).

In Mizyn, the minimum numbers of specimens from *Nassa reticulata* and *Buccinum sp.* are 37 and 150 pieces, respectively (Iakovleva 2013: 151–152). In Yudinovo, shells from the Black Sea amount to 239 specimens (Kijashko, Khlopachev 2022: 109). These numbers suggest at least non-accidental – if not regular – long-distance connections to the west and the south.

## Conclusion

At Barmaky, the exploitation of mostly locally available resources speaks in favour of a residentially rather than a logistically organised subsistence practice. And although Barmaky currently marks the oldest known occupation in north-western Ukraine after the LGM, it seems that its inhabitants already had good knowledge about the available resources in the landscape. This indicates at least some familiarity acquired during previous stays and together with the substantial character of the occupation are not in line with ideas of pioneering groups travelling quickly and light towards the north during ephemeral exploration trips (Pedersen et al. 2018). In favour of a repeated presence of people in Volhynia and long-distance contacts at least towards the east is also the finding that materials for adornments, such as amber and especially fossilised marine shells found at sites in other parts of Ukraine, such as Mizyn, Mezhyrich, Gintsy, Semenivka 2 and 3, Timonovka 1, Yudinovo and Chulativ II, likely originate from the region, thus indicating contact, possibly in the form of visits (Binford 1982: 8).

These findings add more tesserae to the emerging picture of the recolonisation process of Central and Eastern Europe after the Last Glacial Maximum. Shortly after the Epigravettian occupation at Barmaky, Maszycka Cave testifies a Magdalenian presence with a western genetic signal in southern Poland (Kozłowski et al. 2017; Maier et al. 2020; Posth et al. 2023). How these early occupations relate to one another needs further clarification in the future.

# EASTERN EUROPE AFTER THE LAST GLACIAL MAXIMUM AND THE ORIGIN OF EPIGRAVETTIAN INDUSTRIES NORTH OF 50° LATITUDE

11

V. CHABAI, A. MAIER & D. DUDNYK

## INTRODUCTION

There is a long-standing debate about the emergence of Epigravettian industries in Eastern Europe and possible cultural continuities and discontinuities that went along with the environmental changes and demographic dynamics of the Last Glacial Maximum (LGM). Sites dated to the pre-LGM, LGM, and post-LGM are not distributed evenly throughout the Eastern European Plane, but form spatially distinct concentrations (Fig. 11-1). Previously, this spatial pattern has been interpreted as reflecting so-called historical-cultural habitats (HCHs), i.e. areas with similarities in subsistence strategies, specific elements of dwelling constructions, mobile art objects, and specific lithic tool types (Anikovich 1998).

The westernmost concentration of sites is located between the Carpathian Mountains and the Dniester basin and corresponds to the Dniester HCH of reindeer hunters after Anikovich (1998). Here, a continuous record of Upper Palaeolithic occupations without any noteworthy chronological gaps has been documented (Noiret 2009; Anghelinu et al. 2021). Another concentration with a comparatively loose distribution of sites is distributed along the northern shores of the Black Sea and Azov Sea, corresponding to Anikovich's steppe HCH of bison hunters. Here, reliable evidence of pre-LGM occupations is absent, while LGM and post-LGM sites are attested (Sapozhnikov 2003; Demidenko 2008; Demidenko et al. 2019; Olenkovsky 2008; Krotova 2013).

A third concentration is located in the Mid Dnieper basin, which consists of two clusters, one around Kyiv at around 50° N latitude, and another one along the Desna and Seim rivers, between 51° and 53° N latitude. The fourth and easternmost concentration is situated in the Upper to Mid Don basin, between 50° and 53° N latitude. Both concentrations in the Mid Dnieper and Upper to Mid Don basin correspond to the Dnieper-Don HCH of mammoth hunters according to Anikovich (1998) and contain numerous Gravettian and Epigravettian sites. However, these areas were also particularly affected by the periglacial conditions south-east of the Scandinavian Ice Sheet, especially during the LGM, and the relation between pre-LGM and post-LGM groups regarding technological as well as stylistic breaks and continuities is debated. Anikovich postulates the existence of a continuous population, but sees neither evidence for "genetic connections" between the pre-LGM and post-LGM sites in the Dnieper-Don HCH, nor "migration evidence" to explain the appearance of the post-LGM industries in the region, underlining their autochthonous character (Anikovich 1998: 56). A different stance is taken by Gavrilov (2016; 2023), who developed so-called economic-cultural types (ECTs) from the HCH concept and states a continuous evolution from the Gravettian to the Epigravettian in the Mid-Dnieper basin. Nuzhnyi (2015) supports the idea of continuous Gravettian-Epigravettian evolution in the Mid-Dnieper basin, but is sceptical of both the HCH and ECT concept.

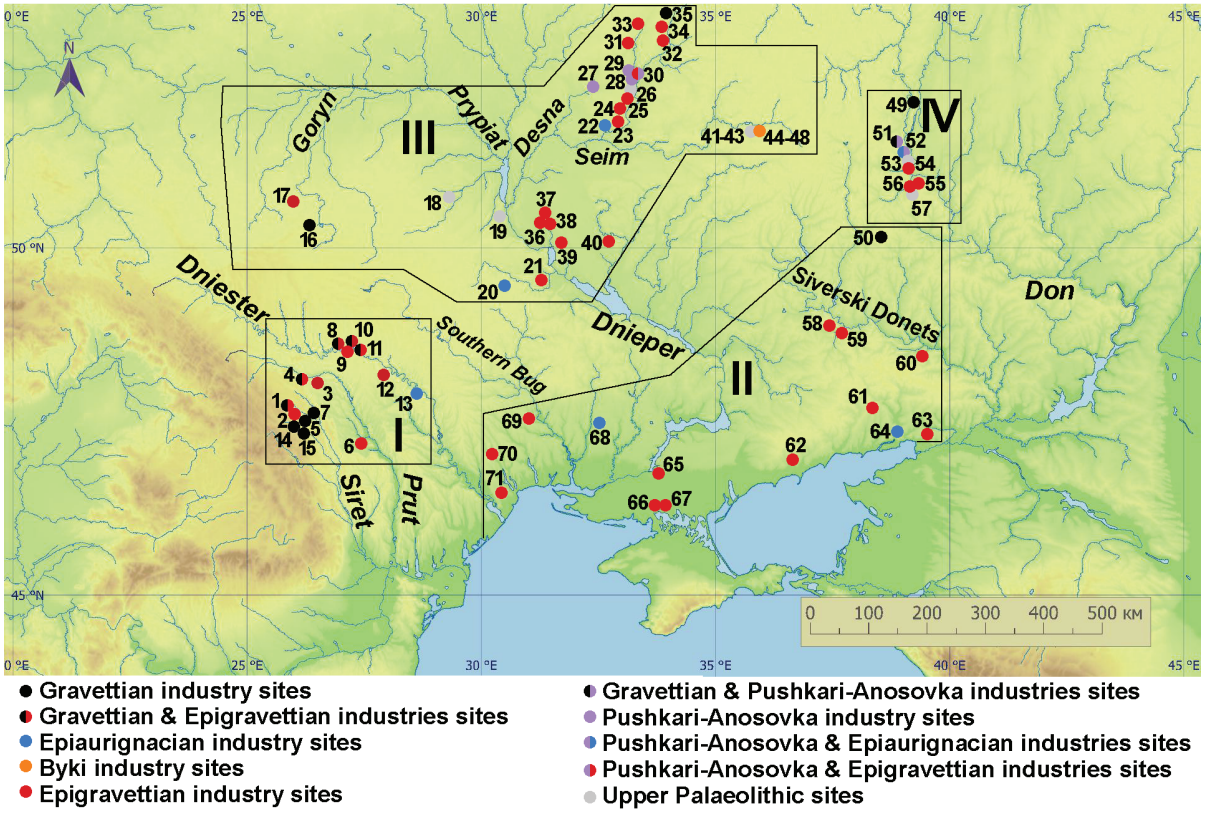


Fig. 11-1. Distribution of pre-LGM, LGM, and post-LGM occupations in Eastern Europe mentioned in the text. Regions: I – Prut-Dniester; II – Northern Black and Azov Seas; III – Mid-Dnieper; IV – Upper Don. Sites: 1 – Bistricioara-Lutărie I, II, III; 2 – Bistricioara-Lutărie 'La Mal'; 3 – Crasnaleuca-Stanişte; 4 – Cotu-Miculinţi; 5 – Poiana Cireşului; 6 – Lespezi; 7 – Cetăţica I; 8 – Molodova V, 7; 9 – Molodovo I, upper layer; 10 – Korman IV; 11 – Korman 9, I; 12 – Kosauşi; 13 – Raşkov VII; 14 – Podiş; 15 – Dârţu; 16 – Zbytenka; 17 – Barmaky; 18 – Radomyshl; 19 – Kyrylivska; 20 – Gordashivka; 21 – Mezhyrich; 22 – Obolonnya; 23 – Buzhanka 2; 24 – Mizyn; 25 – Chulativ I and II; 26 – Novgorod-Siverska; 27 – Kliusy; 28 – Pushkari I; 29 – Pushkari VIII; 30 – Pushkari IX; 31 – Yudinovo; 32 – Suponevo; 33 – Yeliseevichi I and II; 34 – Timonovka 1 and 2; 35 – Khotylevo 2; 36 – Semenivka 1; 37 – Semenivka 2; 38 – Semenivka 3; 39 – Dobranichivka; 40 – Gintsy; 41-43 – Byki 5, Byki 7, II, Byki 8; 44-48 – Byki 1, Byki 2, Byki 3, Byki 4 (Peny), Byki 7, I, Ib, Ia, Ic; 49 – Gagarino; 50 – Yamy; 51 – Kostenki 21, III; 52 – Kostenki 11, I, II; 53 – Borschevo 1; 54 – Borschevo 2; 55 – Divnogorie 9; 56 – Divnogorie 1; 57 – Samotoevka; 58 – Mynievski Yar; 59 – Vysla Balka; 60 – Govorukha; 61 – Amvrosiivka; 62 – Fedorivka, layer 2; 63 – Kamennaya Balka II, II; 64 – Muralovka; 65 – Dmytrivka; 66 – Voznesenka; 67 – Novovolodymyrivka II; 68 – Sagaidak; 69 – Anetovka 2; 70 – Kamianka; 71 – Velyka Akkarzsha.

A crucial factor in the arguments supportive of a chronological and/or stylistic continuity is an unselective use of the available radiocarbon dates, which results, for instance, in statements such as that the age of the Willendorf-Pavlov-Kostenki industry documented at the site of Zaraiskaia dates between 27/26-23/19 ka calBP (23/22-19/16 ka uncalBP) and is thus partly overlapping (i.e. contemporaneous) with the dates for Epigravettian sites, such as Barmaky (see Chapter 3; Anikovich 2019a: 154; 2019b: 195). If a more selective approach to the available radiocarbon dates is chosen (Maier 2020), a different and more articulated picture emerges for the sites in the Mid Dnieper and Upper to Mid Don basins, revealing a chronological and cultural hiatus, which corresponds to the LGM *sensu lato* (Soffer 1985; Hoffecker 2002; Lisitsyn 2019; Lisitsyn, Dudin 2019; Chabai et al. 2020b; 2022. This finding highlights a discontinuous development north of 50° N latitudes (Maier et al. 2020), which is a stark contrast to the continuous evolution documented between the Carpathian Mountains and Dniester basin, and also raises questions as to the post-LGM resettlement process.

Another problem for the understanding of the differences between regional cultural developments and population dynamics is a lack of high-resolution environmental data. For the Mid Dnieper and Upper to Mid Don basins, the rarity of long and well-studied geoscientific and archaeological stratigraphies containing pre-LGM, LGM and post-LGM deposits is a major problem in this regard. In want of such long sequences, environmental reconstructions usually rely on correlating several shorter stratigraphies (Gribchenko 2011). The chronological model of these correlations, however, is usually based on the available radiometric data (Velichko et al. 1997; Velichko, Gribchenko, Kurenkova 1997). Here, the problem of an unselective treatment of these dates reoccurs, plaguing several of these correlations. The latest studies show a more critical and strict analysis of the available radiocarbon dates from the Mid Dnieper basin, allowing for increased precision in the correlation of environmental changes and archaeological events (Khlopachev, Gribchenko 2012; Khlopachev et al. 2017; Haesaerts et al. 2015; Chabai et al. 2020b; 2022; Chabai, Vasyliev 2021a).

Further complicating matters in the debates about cultural continuities and discontinuities during the LGM are varying definitions of the chronological extent of this period (Maier, Mayr, Peresani 2021). The most widespread chronological definitions are: 23–19 or 24–18 ka calBP (Mix et al. 2001), 26–21 ka calBP (Peltier and Fairbanks 2006), 26.5–20/19 ka calBP (Clark et al. 2009), and 27.5–23.3 ka calBP (Hughes, Gibbard 2015). Svensson et al. (2005) use a subdivision into the LGM *sensu stricto* (GS-3) and the LGM *sensu lato* (GS-3, GS-2, GS-2c, and GS-2b), which is in rough agreement with the definition of Clark et al. (2009).

In the eastern part of Central Europe, the definitions of Mix et al. (2001), Svensson et al. (2005), and Clark et al. (2009) are applied most often (Połtowicz-Bobak 2013; Demidenko et al. 2019; Połtowicz-Bobak, Bobak 2020). In line with the definition of Clark et al. (2009), Lengyel et al. (2021) suggest the following subdivision: initial LGM (ILGM) (26.5–24.0 ka), local LGM (LLGM) (24.0–20.0 ka), and post-LGM (PLGM) (20.0–14.7 ka).

For Eastern Europe, there are no strict and generally accepted chronological definitions of LGM. Rather, depositional characteristics such as ice wedges and sandy aeolian deposits are used as signs of LGM environmental conditions and its corresponding dust peak (see sections Final Gravettian, Pushkari-Anosovka industry, Epiaurignacian). On the other hand, the stratigraphic evidence of permafrost degradation is considered to mark the beginning of the post-LGM period. At present, the available chronological and geological information is not sufficient to define a precise beginning of the LGM in Eastern Europe, which should be seen some time after 27 ka calBP. With reference to the site of Byki 7 (see below), the end of the LGM in Eastern Europe takes place between 21–19 ka cal BP. Eventually, these boundaries are fairly consistent with the definition by Clark et al. (2009) of 26.5–20/19 ka cal BP.

For a better understanding of the cultural Evolution in the Eastern European Plain and its relation to environmental change, particularly the regional development from pre-LGM/LGM to post-LGM industries in the Mid Dnieper and Upper to Mid Don basins, a thorough review of the available archaeological and geoscientific data is needed. In the following, we therefore evaluate environmental data, stone artefact assemblages, and 313 radiocarbon dates from 39 sites. All radiocarbon dates were calibrated using OxCal v4.4.4 (Bronk Ramsey 2021) and are given with 2Σ confidence. Selection criteria follow Maier et al. (2020).

## VARIABILITY OF PRE-LGM AND LGM ENVIRONMENTS AND LITHIC INDUSTRIES

Archaeologically, the pre-LGM period is associated with the spatially and temporally large-scale taxonomic terms 'Late Gravettian' and 'Final Gravettian'. At the next lower scale level, these terms comprise chronologically and spatially smaller sub-units, called *industries* or *complexes* (Table 11-1). The Late Gravettian in the Upper to Mid Don Valley, for instance, is represented by the Willendorf-Kostenki complex, also known as the Kostenki-Avdeevo complex, while the Final Gravettian is represented by the Gmelin complex (Lisitsyn and

| | Taxonomic units | Mid Dnieper Basin | Don Basin | Dniester / Prut basins | Black/Azov Sea area |
|---|---|---|---|---|---|
| post-LGM | **Late Epigravettian** | Suponevo<br>Yeliseevichi<br>Yudinovo industry<br>Mezhyrich industry<br>Mizyn industry | Divnogorie 1<br>Borschevo 2, I<br>Divnogorie 9 | Molodovo I, upper layer<br>Molodovo V, 1a-3<br>Bistricioara-Lutărie Mal | Voznesenka<br>Dmytrivka<br>Fedorivka, 2<br>Novovolodymyrivka<br>Kamennaya Balka II, II |
| | **Byki culture** | Byki 1 & Byki 7 | Samotoevka (?) | | |
| pre-LGM / LGM | **Early Epigravettian** | | | Bistricioara-Lutărie III<br>Lespezi<br>Korman 9, I<br>Kosăuţi | Anetovka 2<br>Amvrosiivka<br>Velyka Akkarzsha |
| | **Epiaurignacian** | Gordashivka<br>Obolonnya | Kostenki 11, Ia/3 | Raşkov VII | Muralovka<br>Sagaidak |
| | **Final Gravettian** | **Pushkari / Anosovka complex**<br>Pushkari I<br>Pushkari IX, 3<br>**Gmelin complex**<br>Khotylevo 2 | **Pushkari / Anosovka complex**<br>Kostenki 21, III,dwellings<br>Kostenki 11, II<br>**Gmelin complex**<br>Gagarino<br>Kostenki 21, III, prod.area | Cetăţica I<br>Podiş<br>Dârţu<br>Bistricioara-Lutărie II<br>Bistricioara-Lutărie I<br>Poiana Cireşului<br>Molodovo V, 7 | |

Table 11-1. Taxonomic units and important assemblages of Eastern Europe during the pre-LGM, LGM and post-LGM according to major areas of site concentrations.

Dudin 2019; Lisitsyn 2019). In the Mid Dnieper Valley, the pre-LGM / LGM period is represented by the Pushkari industry (also called Anosovka complex). The Epiaurignacian occurs during the LGM in the Dnieper, Don, and Black Sea region and is not further subdivided (Table 11-1).

## Final Gravettian, Gmelin complex

According to Lisitsyn, the assemblages of Khotylevo 2, Kostenki 21, layer III, and Gagarino represent the Final Gravettian or Gmelin complex (Reynolds et al. 2019; Lisitsyn 2019, 2021; Lisitsyn, Dudin 2019: table 1). Nuzhnyi (2009: 173) underlines the technological and typological similarities between Khotylevo 2 (Desna valley) and Molodovo V, layer VII (Dniester valleys) and states that these assemblages are *"closely linked"* with the Central European complexes of Dolní Věstonice I and II.

### *Environment*

The cultural deposits of Khotylevo 2 likely developed under permafrost conditions (Velichko et al. 1999: 26), with ice wedges affecting both the cultural layer but also the overlying loess deposits (Gavrilov 2008: 25). The faunal remains are heavily dominated by mammoth and polar fox. The arboreal and shrub pollen constitutes 9-24 % and is represented by boreal and arctic-boreal species, such as *Pinus silvestris, Betula sect. alba, Betula nana, Alnus incana,* and *Alnaster fruticosus.* The NAP comprise a diverse spectrum of boreal, steppe and semi-desert taxa, namely *Artemisia*, Asteraceae, Chenopodiaceae, Gramineae, *Boctrychium boreale, Saxifraga sp., Scabiosa, Ephedra,* and *Atriplex patula* (Velichko et al. 1999: 26).

In Gagarino, ice wedges affected the cultural deposits after their accumulation (Tarasov 1979: 20). The most numerous faunal remains belong to *Mammuthus primigenius* and *Alopex lagopus*, exceeding those of *Coelodonta antiquitatis, Boss sp., Rangifer tarandus, Vulpes vulpes, Lepus sp.,* and *Marmota bobac* were

identified (Tarasov 1979: 31–33). The samples connected with cultural deposits contain pollen of *Pinus silvestris, Betula sect. alba / Betula nana, Gramineae, Cyperaceae,* and *Artemisia*, indicating an accumulation during the *"onset of the last Würm cooling"* (Tarasov 1979: 35).

Post-depositional cryoturbation and ice wedges disturb the deposits of cultural layer III at Kostenki 21 (Reynolds et al. 2019: 165), where two-thirds of identified bones in the southern part belong to *Mammuthus primigenius*. Another 20 % comprise *Lepus sp., Equus ferus,* and *Alopex lagopus*, while large canids and large bovids were also recognised (Reynolds et al. 2019: 178–183).

### *Artefacts*

The main technological and typological features of the Gmelin complex are (1) the production of blade and bladelet with soft-hammer percussion (lipped platforms), (2) the presence of Gravette and Micrograveтte points, rectangles, shouldered points, and shouldered blades/bladelets (shoulder ≈ ½ length of a lateral side), as well as (3) the dominance of angle and dihedral burins over burins on truncations (Fig. 11-2) (Tarasov 1979: 126, 128; Nuzhnyi 2009; Gavrilov 2016; Reynolds et al. 2019; Lisitsyn 2019).

### *Chronology*

Generally, there is a common opinion that the Final Gravettian ends before 26.5 ka calBP (Gavrilov 2008; Nuzhnyi 2009; Lisitsyn 2019; Lisitsyn, Dudin 2019), i.e. before the onset of LGM *sensu* Clark et al. (2009).

The occupation at Khotylevo 2 can be dated to between 27.3–27.2 ka calBP, when only AMS dates with a standard deviation of less than 1.5% of the measured $^{14}$C-age are considered (Table 11-2; Fig. 11-3). At Kostenki 21, III-production areas, a weighted average of one AMS and two conventional dates results in an age estimate of 26.9–26.4 ka calBP), which is well within the age range of 27.5–24.5 ka calBP expected by Reynolds et al. (2019: 166). The nine available conventional dates from Gagarino are all made on mammoth, except for one date on a burned bone without species determination. Only pairs of two dates can be combined into weighted averages, spanning a period from 26–21.6 ka calBP (Table 11-2; Fig. 11-3). Mammoth remains might have been gathered in the landscape and may thus be considerably older than the human occupation of the site, suggesting a preference for the younger dates. The observation of ice wedges affecting the cultural deposits (Tarasov 1979: 20–23), on the other hand, may suggest their formation prior to or at the onset of the LGM, thus emphasizing the older dates. According to Tarasov (1979: 35), environmental data (pollen and fauna) suggest an occupation at the beginning of the LGM, which he sees best reflected by the burnt bone (ГИН-1872) from the dwelling area dated to 27–25.6 ka calBP (Tarasov 1979: 150).

## Pushkari industry – Anosovka complex

The Pushkari industry or Anosovka complex comprises the assemblages from Desna (Pushkari I, Pushkari VIII, Pushkari IX, layer 3, Kliusy) and Don (Kostenki 21, III-dwellings and Kostenki 11, II) basins (Nuzhnyi 2009, 2015; Khlopachev 2014; Sinitsyn 2014; Vasyliev 2014, 2018, 2019; Gavrilov 2016; Reynolds et al. 2019; Lisitsyn 2019; Demay et al. 2021). Radomyshl I is described as a separate unit, but still part of the Gravettian techno-complex and with typological similarities to Pushkari I and Kliusy (Shovkoplias 1965; Nuzhnyi 2015; Kononenko 2021).

### *Environment*

In Pushkari IX, layer 3, arboreal pollen amounts to 20–40 %, comprising *Pinus silvestris, Pinus sibirica,* and *Betula sect. alba*, while NAP comprise Gramineae and Cyperaceae, and Ranunculaceae. Among the faunal remains, mammoth, polar fox, and wolf were identified (Khlopachev 2011: 192). The occupation likely took place under permafrost conditions (Gribchenko, Kurenkova 2014: 112), indicated by a net of small ice cracks on the surface of the cultural layer.

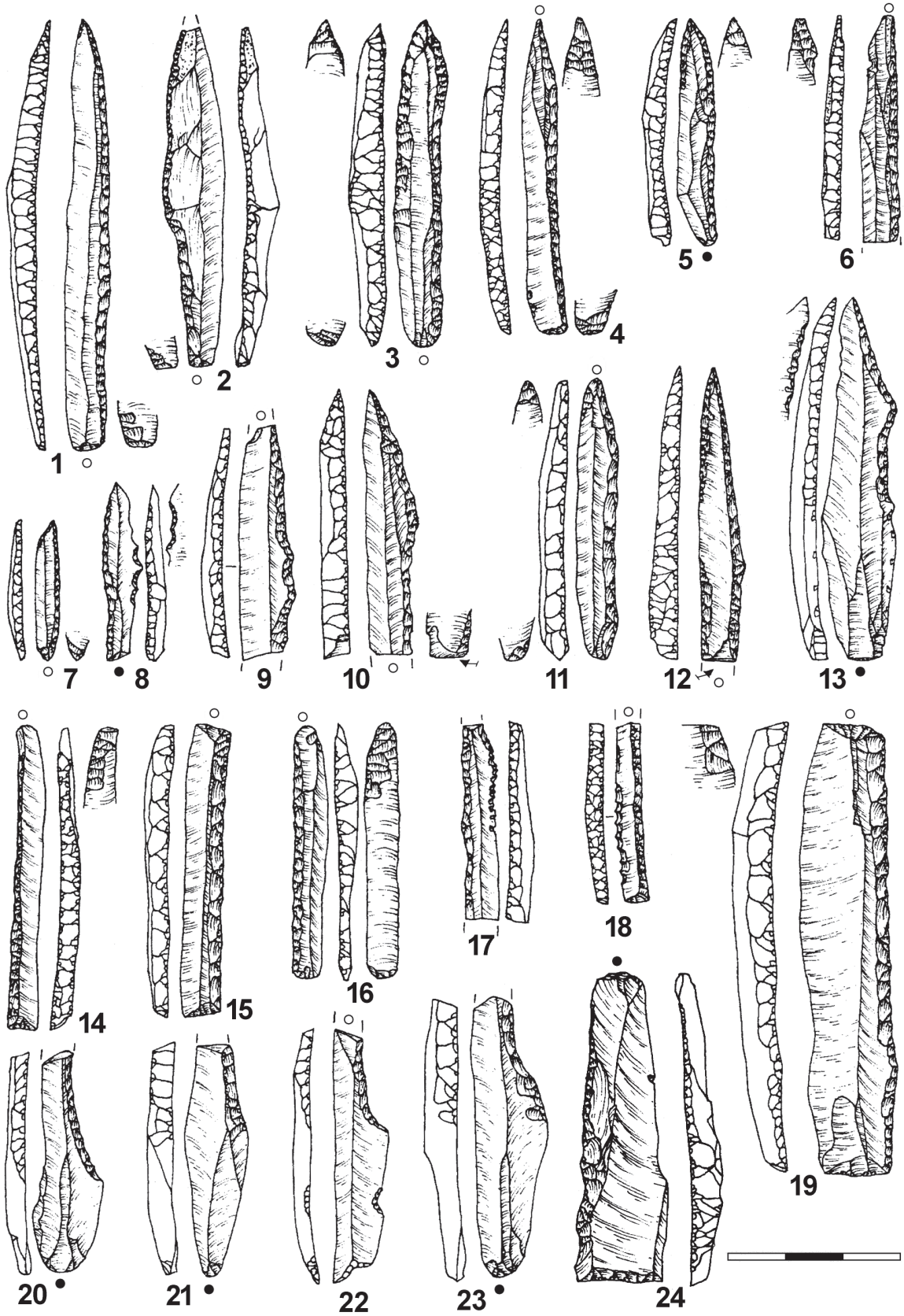


Fig. 11–2. Final Gravettian artefacts of Khotylevo 2 (1–23) and Zbytenka (24): 1–13 – points; 14–16, 19, 24 – rectangles; 17, 18 – *lamelle à dos denticulée*; 20–23 – shouldered pieces; after Nuzhnyi 2015, fig. 31, 34.

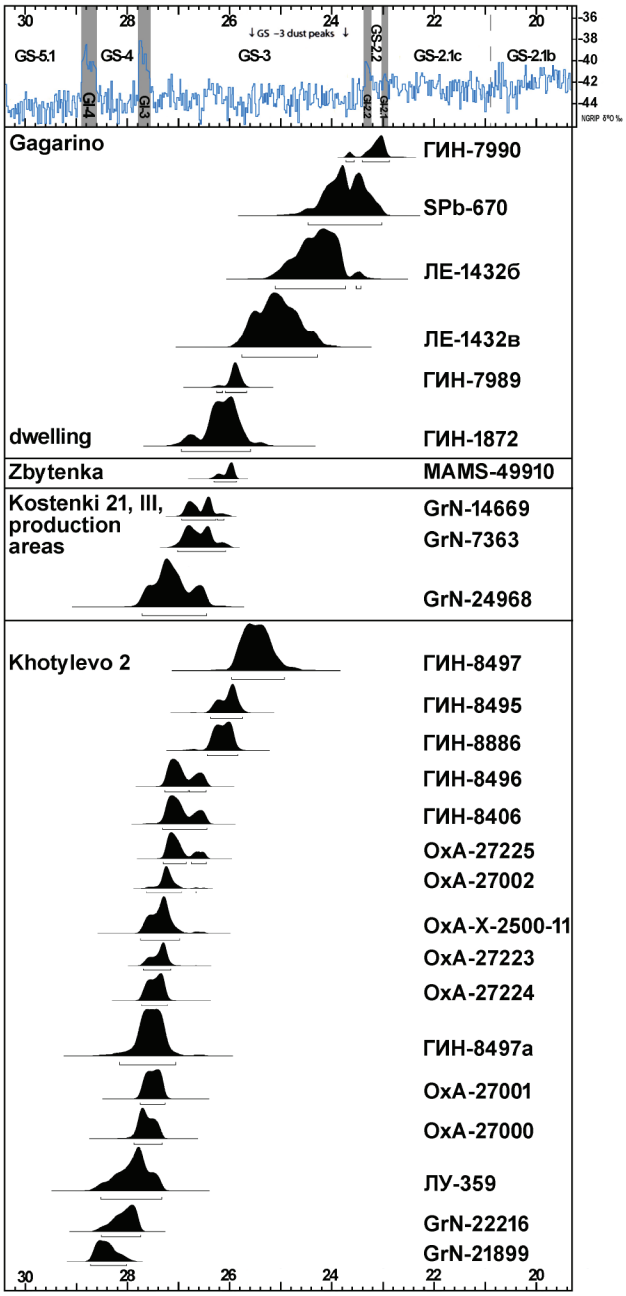


Fig. 11-3. Chronology of the Final Gravettian.

The cultural deposits of Pushkari I accumulated on a surface stabilised by permafrost in the ground and only later became disturbed by the formation of ice wedges (Gribchenko, Kurenkova 2014: 112). During the formation of the cultural layer, bones, artefacts, and artificial pits were covered by sandy lenses of aeolian origin. The dusty winds are thought to be the main reason for the abandonment of the camp (Belyaeva 2009b: 183–184). Remains of *Mammuthus primigenius, Rangifer tarandus, Equus sp., Alopex lagopus,* and *Canis lupus* make up the fauna assemblage (Demay et al. 2016). Scavenging activity is supposed to be one of the main reasons for mammoth bone accumulation (Sablin 1997; Demay et al. 2021). Arboreal pollen constitutes less than 10 % of the entire spectrum and comprises *Pinus silvestris, Pinus sibirica, Betula sect. alba, Betula nana, Alnus incana,* and *Alnaster fruticosus* (Velichko et al. 1999: 29–30).

No evidence of cryoturbation processes was found in Kostenki 11, II. The faunal assemblage is dominated by mammoth and polar fox, woolly rhinoceros, red deer, horse, wolf, wolverine, cave lion, hare and beaver also occur (Rogachev, Popov 1982). The identification of *Cervus elaphus*, however, does not match well with the dominance of mammoth and polar fox.

Kostenki 21, III, (northern) dwelling complex shows traces of post-depositional disturbance by ice cracks. More than 70 % of the bones belong to *Mammuthus primigenius. Alopex lagopus,* large canids*, Ursus arctos, Lynx lynx, Equus ferus, Coelodonta antiquitatis, Rangifer tarandus,* large bovids and *Saiga tatarica* are also present (Reynolds et al. 2019: 184–185).

## *Artefacts*

Technologically, the Pushkari-Anosovka industry is characterised by blade production, while bladelets and micro-blades are not abundant. A few carinated end-scrapers, i.e. scraper-like cores-on-flake, were noticed in Radomyshl (Kononenko 2015; Nuzhnyi 2015). Among the tools, backed points on blades are a common feature, but are absent in Radomyshl I, where points on blades and flakes with flat and semi-abrupt retouch occur (Kononenko 2009: 171).

The so-called Anosovka points are characteristic for all of assemblages of the Pushkari-Anosovka industry. Anosovka points are made on blades and have a lanceolate shape, a retouched back, and a straight or convex base form through a dorsal or ventral retouch or truncation. Anosovka points are also called Azilian points, Federmesser points, thick lanceolate point with retouched base, or Gravettian points with truncated base (Belyaeva

| Site, layer / level, structure | samples | methods | lab. # | uncalBP | Std | Std% | calBP; 95,4% | P % | wuncalBP | wStd | wcalBP (ka) | R | References | Comments |
|---|---|---|---|---|---|---|---|---|---|---|---|---|---|---|
| Gagarino | *Mammuthus primigenius*, tusk | Conv | ГИН-7991 | 17900 | 120 | 0,67 | 22089 - 21390 | * | | | | | Sinitsyn et al. 1997 | Final Gravettian |
| Gagarino | *Mammuthus primigenius*, tooth | Conv | ЛЕ-1432а | 17930 | 100 | 0,55 | 22071 - 21430 | * | | | | | Svezhentsev 1993 | Final Gravettian |
| | | | | | | | | *84.8 | 17918 | 77 | 21.9 - 21.6 | | | |
| Gagarino | *Mammuthus primigenius*, tusk | Conv | ГИН-7990 | 19160 | 130 | 0,68 | 23405 - 22874; 87,1% | * | | | | | Sinitsyn et al. 1997 | Final Gravettian |
| Gagarino | *Mammuthus primigenius*, bone | Conv | SPb-670 | 19742 | 290 | 1,47 | 24465 - 23034 | * | | | | | Khlopachev 2016 | Final Gravettian |
| | | | | | | | | *6.7 | 19257 | 119 | 23.6 - 23.1 | | | |
| Gagarino | *Mammuthus primigenius*, tooth | Conv | ЛЕ-1432Б | 20150 | 300 | 1,49 | 25112 - 23729; 94,1% | * | | | | | Svezhentsev 1993 | Final Gravettian |
| Gagarino | *Mammuthus primigenius*, tooth | Conv | ЛЕ-1432В | 20820 | 300 | 1,44 | 25758 - 24288 | * | | | | | Sinitsyn et al. 1997 | Final Gravettian |
| | | | | | | | | *11.4 | 20485 | 212 | 24.9 - 24.3 | | | |
| Gagarino | *Mammuthus primigenius*, tusk | Conv | ГИН-7989 | 21600 | 140 | 0,65 | 26092 - 25669; 91,7% | * | | | | | Sinitsyn et al. 1997 | Final Gravettian |
| Gagarino, dwelling | burned bone | Conv | ГИН-1872 | 21800 | 300 | 1,38 | 26952 - 25595 | * | | | | | Boriskovsky 1984 | Final Gravettian |
| | | | | | | | | *54.6 | 21636 | 127 | 26.0 - 25.8 | | | |
| Gagarino | *Mammuthus primigenius*, tooth | Conv | ИГАН-83 | 30000 | 1900 | 6,33 | 40331 - 31094 | | | | | 1 | Svezhentsev 1993 | Final Gravettian |
| Gordashivka | bone | Conv | Ki-11680 | 15800 | 250 | 1,58 | 19646 - 18651; 93,6% | | | | | 1 | Gladkikh et al. 2010 | Epiaurignacian |
| Gordashivka | bone | Conv | Ki-11677 | 20370 | 180 | 0,88 | 25030 - 23999 | | | | | | Gladkikh et al. 2010 | Epiaurignacian |
| Khotylevo 2 | *Mammuthus primigenius*, tooth | Conv | ГИН-8497 | 21170 | 260 | 1,23 | 25964 - 24928 | * | | | | | Gavrilov 2008 | Final Gravettian |
| Khotylevo 2 | *Mammuthus primigenius*, tooth | Conv | ГИН-8495 | 21720 | 170 | 0,78 | 26360 - 25746 | * | | | | | Gavrilov 2008 | Final Gravettian |
| Khotylevo 2 | burnt bone | Conv | ГИН-8886 | 21850 | 170 | 0,77 | 26436 - 25835 | * | | | | | Gavrilov 2008 | Final Gravettian |
| | | | | | | | | *8.6 | 21677 | 109 | 26.0 - 25.9 | | | |

Table 11-2. Age estimates of pre-LGM and LGM assemblages of the Mid Dnieper and Upper Don basins. Weighted averages calculated with CalPal-Beyond the Ghost, Version 2020.11, https://zenodo.org/records/11104437 (Weninger and Jöris, 2008);

| Site, layer / level, structure | samples | methods | lab. # | uncalBP | Std | Std% | calBP; 95,4% | P % | wuncalBP | wStd | wcalBP (ka) | R | References | Comments |
|---|---|---|---|---|---|---|---|---|---|---|---|---|---|---|
| Khotylevo 2 | *Mammuthus primigenius*, tooth | Conv | ГИН-8496 | 22660 | 170 | 0,75 | 27270 - 26801; 67,8% | * | | | | | Gavrilov 2008 | Final Gravettian |
| Khotylevo 2 | *Mammuthus primigenius*, tooth | Conv | ГИН-8406 | 22700 | 200 | 0,88 | 27315 - 26444 | * | | | | | Gavrilov 2008 | Final Gravettian |
| Khotylevo 2 | *Mammuthus primigenius*, tooth | Conv | ГИН-8497A | 23300 | 300 | 1,29 | 28150 - 27055 | * | | | | | Gavrilov 2008 | Final Gravettian |
| | | | | | | | | *16 | 22775 | 119 | 27.2 - 27.0 | | | |
| Khotylevo 2 | bone | Conv | ЛУ-359 | 23660 | 270 | 1,14 | 28520 - 27333 | * | | | | | Sinitsyn et al. 1997 | Final Gravettian |
| Khotylevo 2 | bone, fragment #2 | Conv | GrN-22216 | 23870 | 160 | 0,67 | 28502 - 27732 | * | | | | | Gavrilov 2008 | Final Gravettian |
| Khotylevo 2 | bone, fragment #1 | Conv | GrN-21899 | 24220 | 110 | 0,45 | 28772 - 28006 | * | | | | | Gavrilov 2008 | Final Gravettian |
| | | | | | | | | *5.7 | 24062 | 86 | 28.4 - 28.0 | | | |
| Khotylevo 2 | *Mammuthus primigenius*, tooth | Conv | ИГАН-73 | 24960 | 400 | 1,60 | 30076 - 28377 | | | | | 1 | Gavrilov 2008 | Final Gravettian |
| Khotylevo 2, point A, sector 13 | *Mammuthus primigenius*, bone | AMS | OxA-27001 | 23240 | 160 | 0,69 | 27745 - 27260 | | | | | | Gavrilov et al. 2015. | Final Gravettian |
| Khotylevo 2, point B, sector A | Large mammal, bone | AMS | OxA-27000 | 23470 | 170 | 0,72 | 27873 - 27320 | | | | | | Gavrilov et al. 2015. | Final Gravettian |
| Khotylevo 2, point B, sector Б | Large mammal, bone | AMS | OxA-27225 | 22720 | 150 | 0,66 | 27308 - 26851; 77,8% | * | | | | | Gavrilov et al. 2015. | Final Gravettian |
| Khotylevo 2, point B, sector Б | *Rangifer tarandus*, bone | AMS | OxA-X-2500-11 | 23020 | 210 | 0,91 | 27747 - 26978 | * | | | | | Gavrilov et al. 2015. | Final Gravettian |
| Khotylevo 2, point B, sector Б | *Canis lupus*, bone | AMS | OxA-27223 | 23050 | 150 | 0,65 | 27684 - 27150 | * | | | | | Gavrilov et al. 2015. | Final Gravettian |
| Khotylevo 2, point B, sector Б | Bird, bone | AMS | OxA-27224 | 23160 | 160 | 0,69 | 27721 - 27222 | * | | | | | Gavrilov et al. 2015. | Final Gravettian |
| | | | | | | | | ***21** | **22977** | **81** | **27.3 - 27.2** | | | |
| Khotylevo 2, point Б, sector 1 | *Canis lupus*, bone | AMS | OxA-27002 | 22900 | 150 | 0,65 | 27632 - 26938; 95,1% | | | | | | Gavrilov et al. 2015. | Final Gravettian |
| Kostenki 11/I | *Mammuthus primigenius*, bone | Conv | ЛЕ-1403 | 12000 | 100 | 0,84 | 14082 - 13732; 86,5% | | | | | | Rogachev, Popov 1982 | Epiaurignacian |
| Kostenki 11/I | *Mammuthus primigenius*, bone | Conv | ЛЕ-1637 | 14610 | 120 | 0,83 | 18194 - 17458 | | | | | | Rogachev, Popov 1982 | Epiaurignacian |

Table 11-2. continued 1;

| Site, layer / level, structure | samples | methods | lab. # | uncalBP | Std | Std% | calBP; 95,4% | P % | wuncalBP | wStd | wcalBP (ka) | R | References | Comments |
|---|---|---|---|---|---|---|---|---|---|---|---|---|---|---|
| Kostenki 11/I | bone | Conv | ЛЕ-1704А | 16040 | 120 | 0,75 | 19605 - 19025 | | | | | | Rogachev, Popov 1982 | Epiaurignacian |
| Kostenki 11/I | bone | Conv | ЛЕ-1704 | 16610 | 150 | 0,90 | 20430 - 19619 | | | | | | Bessudnov 2013* | Epiaurignacian |
| Kostenki 11/I | bone | Conv | ЛЕ-1704Бb | 17310 | 280 | 1,62 | 21827 - 20280 | | | | | 1 | Rogachev, Popov 1982 | Epiaurignacian |
| Kostenki 11/I | *Mammuthus primigenius*, bone | Conv | ГИН-8079 | 18700 | 80 | 0,43 | 22901 - 22423 | | | | | | Sinitsyn et al. 1997 | Epiaurignacian |
| Kostenki 11/I | burnt bone | Conv | ГИН-2532 | 19900 | 350 | 1,76 | 24895 - 23095 | | | | | 1 | Rogachev, Popov 1982 | Epiaurignacian |
| Kostenki 11/Ia | *Mammuthus primigenius*, bone | Conv | ЛЕ-1645 | 14610 | 150 | 1,03 | 18210 - 17424 | | | | | | Bessudnov 2013* | Epiaurignacian |
| Kostenki 11/Ia, complex 3 | burnt bone | Conv | NSKA-00892 | 13854 | 139 | 1,01 | 17136 - 16356; 93,7 % | | | | | | Dudin, Fedyunin 2019 | Epiaurignacian |
| Kostenki 11/Ia, complex 3 | *Mammuthus primigenius*, scapula | Conv | NSKA-00888 | 18147 | 3592 | 19,80 | 49225 - 15133 | | | | | 1 | Dudin, Fedyunin 2019 | Epiaurignacian |
| Kostenki 11/Ia, complex 3 | burnt bone | Conv | NSKA-00885 | 19514 | 257 | 1,32 | 24049 - 22960 | b | | | | | Dudin, Fedyunin 2019 | Epiaurignacian |
| Kostenki 11/Ia, complex 3 | bone | Conv | NSKA-00889 | 20006 | 319 | 1,60 | 24997 - 23289 | b | | | | 1 | Dudin, Fedyunin 2019 | Epiaurignacian |
| Kostenki 11/Ia, complex 3 | charcoal | AMS | CURL-21043 | 20360 | 150 | 0,74 | 24976 - 24078 | *, b | | | | | Dudin, Fedyunin 2019 | Epiaurignacian |
| Kostenki 11/Ia, complex 3 | charcoal | AMS | CURL-22804 | 20620 | 150 | 0,73 | 25208 - 24329 | *, b | | | | | Dudin, Fedyunin 2019 | Epiaurignacian |
| Kostenki 11/Ia, complex 3 | charcoal | AMS | CURL-21040 | 20670 | 160 | 0,78 | 25279 - 24339 | *, b | | | | | Dudin, Fedyunin 2019 | Epiaurignacian |
| | | | | | | | | ***30.4** | **20545** | **88** | **24.9 - 24.6** | | | |
| Kostenki 11/Ia, complex 3 | bone | Conv | NSKA-00886 | 20728 | 316 | 1,52 | 27730 - 24190 | b | | | | 1 | Dudin, Fedyunin 2019 | Epiaurignacian |
| Kostenki 11/Ia, complex 3 | bone | Conv | NSKA-00890 | 20838 | 519 | 2,49 | 26081 - 23834 | b | | | | 1 | Dudin, Fedyunin 2019 | Epiaurignacian |
| Kostenki 11/Ia, complex 3 | bone | Conv | NSKA-00891 | 23258 | 446 | 1,91 | 28559 - 26840 | | | | | 1 | Dudin, Fedyunin 2019 | Epiaurignacian |
| | | | | | | | | b0.3 | 20437 | 77 | 24.7 - 24.4 | | | |

*in Bessudnov 2013 this date mentioned with reference on Sinitsyn et al.1997; in Sinitsyn et al. 1997 this date is absent.

Table 11-2. continued 2;

| Site, layer / level, structure | samples | methods | lab. # | uncalBP | Std | Std% | calBP; 95,4% | P % | wuncalBP | wStd | wcalBP (ka) | R | References | Comments |
|---|---|---|---|---|---|---|---|---|---|---|---|---|---|---|
| Kostenki 11/II | bone | Conv | TA-34 | 15200 | 300 | 1,98 | 19154 - 17835 | | | | | 1 | Rogachev, Popov 1982 | Pushkari industry |
| Kostenki 11/II | burnt bone | Conv | ГИН-2531 | 21800 | 200 | 0,92 | 26452 - 25735 | | | | | | Rogachev, Popov 1982 | Pushkari industry |
| Kostenki 21/III, dwellings | *Mammuthus primigenius*, bone | AMS | ГИН-9668 | 21780 | 90 | 0,42 | 26305 - 25865 | | | | | | Sinitsyn 2014 | Pushkari industry |
| Kostenki 21/III, dwellings | charcoal | Conv | GrN-10513 | 21260 | 340 | 1,60 | 26306 - 24784 | | | | | 1 | Praslov, Ivanova 1982 | Pushkari industry |
| Kostenki 21/III, dwellings | charcoal | Conv | ЛЕ-1043 | 16960 | 300 | 1,77 | 21435 - 19809; 94,2% | | | | | 1 | Praslov, Ivanova 1982 | Pushkari industry |
| Kostenki 21/III | burnt clay, hearth | TL | TA-151 | 26765 | 2000 | 7,47 | 37752 - 27367 | | | | | 1 | Praslov, Ivanova 1982 | Pushkari industry |
| Kostenki 21, III-production areas | charcoal | AMS | GrN-14669 | 22230 | 100 | 0,45 | 26940 - 26262; 91,4% | * | | | | | Lisitsyn, Dudin 2019 | Final Gravettian |
| Kostenki 21, III-production areas | charcoal | Conv | GrN-7363 | 22270 | 150 | 0,68 | 27019 - 26085 | * | | | | | Praslov, Ivanova 1982 | Final Gravettian |
| Kostenki 21, III-production areas | charcoal | Conv | GrN-24968 | 22860 | 320 | 1,40 | 27711 - 26439 | * | | | | | Lisitsyn, Dudin 2019 | Final Gravettian |
| | | | | | | | | ***17** | **22281** | **81** | **26.9 - 26.4** | | | |
| Kyrylivska | *Mammuthus primigenius*, tooth | AMS | OXA-718 | 19200 | 250 | 1,30 | 23774 - 22600 | | | | | 8 | Svezhentsev, Popov 1993 | UP |
| Novgorod-Siverska | *Mammuthus primigenius*, tooth | Conv | OXA-698 | 19800 | 350 | 1,77 | 24723 - 22999 | | | | | 1 | Svezhentsev, Popov 1993 | UP |
| Obolonnya | *Mammuthus primigenius*, bone | AMS | SPb-442 | 15200 | 200 | 1,32 | 18880 - 18181 | | | | | 8 | Stupak et al. 2014 | Epiaurignacian |
| Obolonnya | *Mammuthus primigenius*, bone | AMS | OXA-28035 | 20730 | 120 | 0,58 | 25275 - 24615 | | | | | | Stupak et al. 2014 | Epiaurignacian |

Table 11-2. continued 3;

| Site, layer / level, structure | samples | methods | lab. # | uncalBP | Std | Std% | calBP; 95,4% | P % | wuncalBP | wStd | wcalBP (ka) | R | References | Comments |
|---|---|---|---|---|---|---|---|---|---|---|---|---|---|---|
| Pushkari I | burnt bone | Conv | QC-899 | 16775 | 605 | 3,61 | 21955 - 18954 | | | | | 1 | Svezhentsev, Popov, 1993 | Pushkari industry |
| Pushkari I, area V | burnt bone | Conv | AA-1389 | 19010 | 220 | 1,12 | 23392 - 22432; 90,7% | | | | | | Gribchenko, Kurenkova 2014 | Pushkari industry |
| Pushkari I, area V | bone | Conv | ГИН-11311Б | 20500 | 500 | 2,44 | 25882 - 23735; 94,9% | * | | | | 1 | Gribchenko, Kurenkova 2014 | Pushkari industry |
| Pushkari I, area V | *Mammuthus primigenius*, tooth | Conv | ГИН-8529 | 20600 | 1200 | 5,83 | 27676 - 22420 | * | | | | 1 | Gribchenko, Kurenkova 2014 | Pushkari industry |
| Pushkari I, area V | *Mammuthus primigenius*, tooth | Conv | ГИН-8529А | 20700 | 500 | 2,42 | 25932 - 23824 | * | | | | 1 | Gribchenko, Kurenkova 2014 | Pushkari industry |
| Pushkari I, area V | bone | Conv | ГИН-11311А | 20900 | 900 | 4,31 | 26424 - 23799 | * | | | | 1 | Gribchenko, Kurenkova 2014 | Pushkari industry |
| Pushkari I, area V | bone | Conv | ГИН-3382 | 21000 | 400 | 1,91 | 26009 - 24235 | * | | | | 1 | Gribchenko, Kurenkova 2014 | Pushkari industry |
| Pushkari I, area V | burnt bone | Conv | ГИН-3381 | 21100 | 400 | 1,90 | 26090 - 24308; 94,6% | * | | | | 1 | Gribchenko, Kurenkova 2014 | Pushkari industry |
| | | | | | | | | *94.9 | 20867 | 211 | 25.5 - 24.8 | | | |
| Pushkari I, area V | burnt bone | Conv | ГИН-11307 | 22350 | 150 | 0,67 | 27120 - 26318 | | | | | | Gribchenko, Kurenkova 2014 | Pushkari industry |
| Pushkari I, area VII | Equid, bone | Conv | Ki-11901 | 19500 | 240 | 1,23 | 23959 - 22960 | | | | | | Gribchenko, Kurenkova 2014 | Pushkari industry |
| Pushkari I, area VII | burnt bone | Conv | ГИН-11310 | 20160 | 180 | 0,89 | 24713 - 23808 | *,b | | | | | Gribchenko, Kurenkova 2014 | Pushkari industry |
| Pushkari I, area VII | burnt bone | Conv | ГИН-10195 | 20350 | 180 | 0,88 | 25000 - 23966 | *,b | | | | | Gribchenko, Kurenkova 2014 | Pushkari industry |
| Pushkari I, area VII | *Mammuthus primigenius*, tooth | Conv | ГИН-11311 | 20500 | 500 | 2,44 | 25882 - 23735; 94,9% | b | | | | 1 | Gribchenko, Kurenkova 2014 | Pushkari industry |
| Pushkari I, area VII | burnt bone | Conv | ГИН-11309 | 20840 | 190 | 0,91 | 25662 - 24609 | *,b | | | | | Gribchenko, Kurenkova 2014 | Pushkari industry |
| Pushkari I, area VII | *Mammuthus primigenius*, tooth | Conv | ГИН-11311А | 20900 | 600 | 2,87 | 26424 - 23799 | b | | | | 1 | Gribchenko, Kurenkova 2014 | Pushkari industry |
| | | | | | | | | ***2.9** | **20436** | **106** | **24.8 - 24.4** | | | |
| | | | | | | | | b10.4 | 20452 | 102 | 24.8 - 24.4 | | | |

Table 11-2. continued 4;

| Site, layer / level, structure | samples | methods | lab. # | uncalBP | Std | Std% | calBP; 95,4% | P % | wuncalBP | wStd | wcalBP (ka) | R | References | Comments |
|---|---|---|---|---|---|---|---|---|---|---|---|---|---|---|
| Pushkari VIII | bone | Conv | ЛУ-361 | 18690 | 770 | 4,12 | 24633 - 20831 | | | | | 1 | Sulerzhytsky 2004 | Pushkari industry |
| Pushkari IX, 3 | bone | Conv | ГИН-10193 | 22300 | 300 | 1,35 | 27194 - 25985 | * | | | | | Sulerzhytsky 2004 | Pushkari industry |
| Pushkari IX, 3 | femur | Conv | ГИН-10194 | 22500 | 450 | 2,00 | 27624 - 25954 | * | | | | 1 | Sulerzhytsky 2004 | Pushkari industry |
| Pushkari IX, 3 | rib | Conv | ГИН-11315 | 23800 | 700 | 2,94 | 29868 - 26909; 95,3% | * | | | | 1 | Sulerzhytsky 2004 | Pushkari industry |
| Pushkari IX, 3 | bone | Conv | ГИН-11312 | 24000 | 1200 | 5,00 | 31033 - 26235; 94,9% | * | | | | 1 | Sulerzhytsky 2004 | Pushkari industry |
| | | | | | | | | *14.8 | 22578 | 231 | 27.1 - 26.5 | | | |
| Radomyshl, 0,6-0,8 m | *Mammuthus primigenius*, tooth | AMS | OxA-697 | 19000 | 300 | 1,58 | 23464 - 22388; 85,6% | | | | | 1 | Soffer 1985 | Pushkari industry |
| Yamy | bone | Conv | Ki-10356 | 19300 | 180 | 0,93 | 23730 - 22960 | | | | | | Krotova 2013 | Final Gravettian (?) |
| Zbytenka | bone | AMS | MAMS-49910 | 21770 | 90 | 0,41 | 26298 - 25858 | | | | | | Chabai, Vasyliev 2021b | Final Gravettian (?) |



Table 11-2. continued 5.

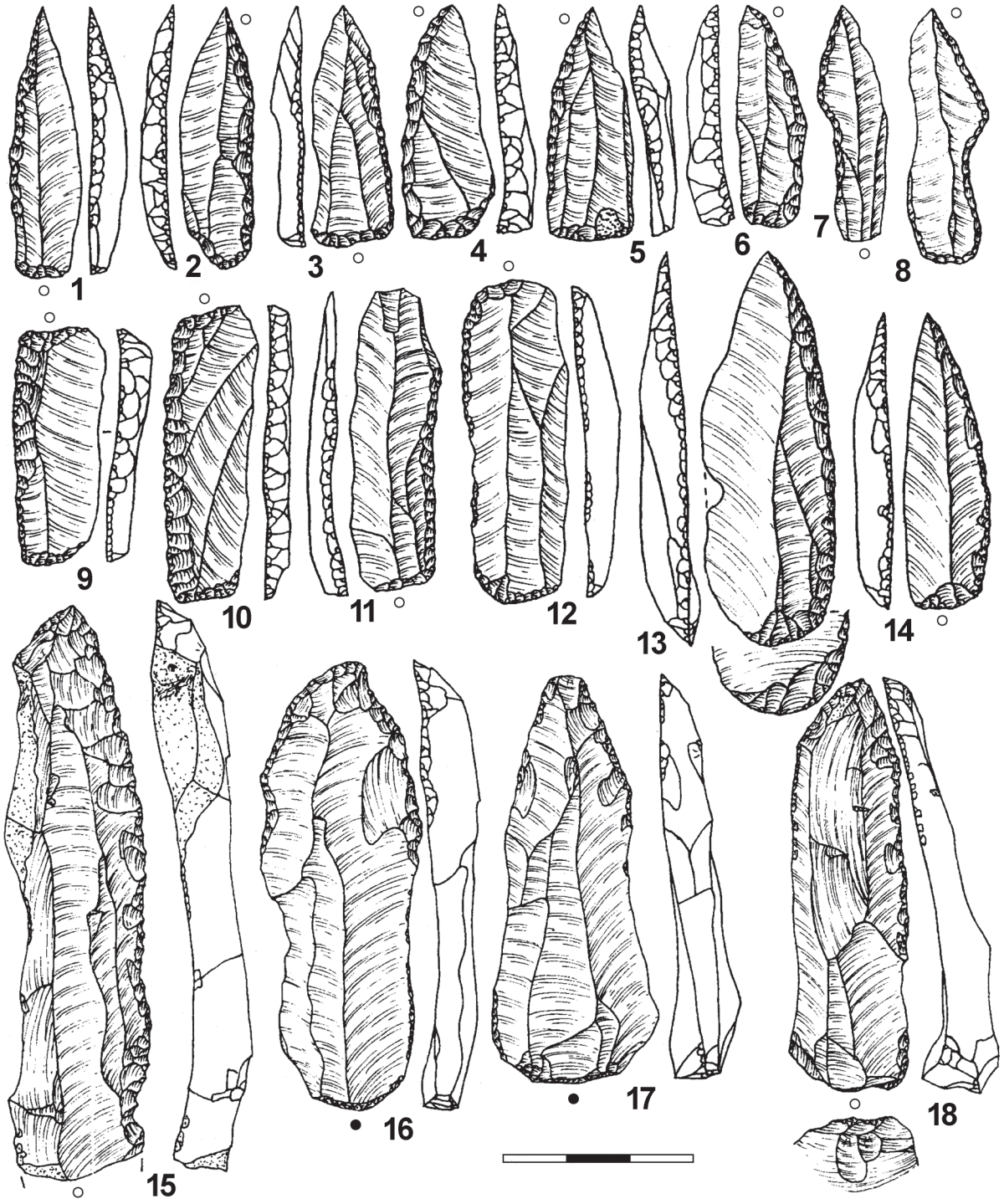


Fig. 11–4. Pushkari–Anosovka industry, artefacts from Pushkari I: 1–6, 13, 14 – Anosovka points; 7, 8 – shouldered point on blades; 9–12 – rectangles on blades; 15–18 – Pavlov points; after Nuzhnyi 2015, fig. 41, 42, 43.

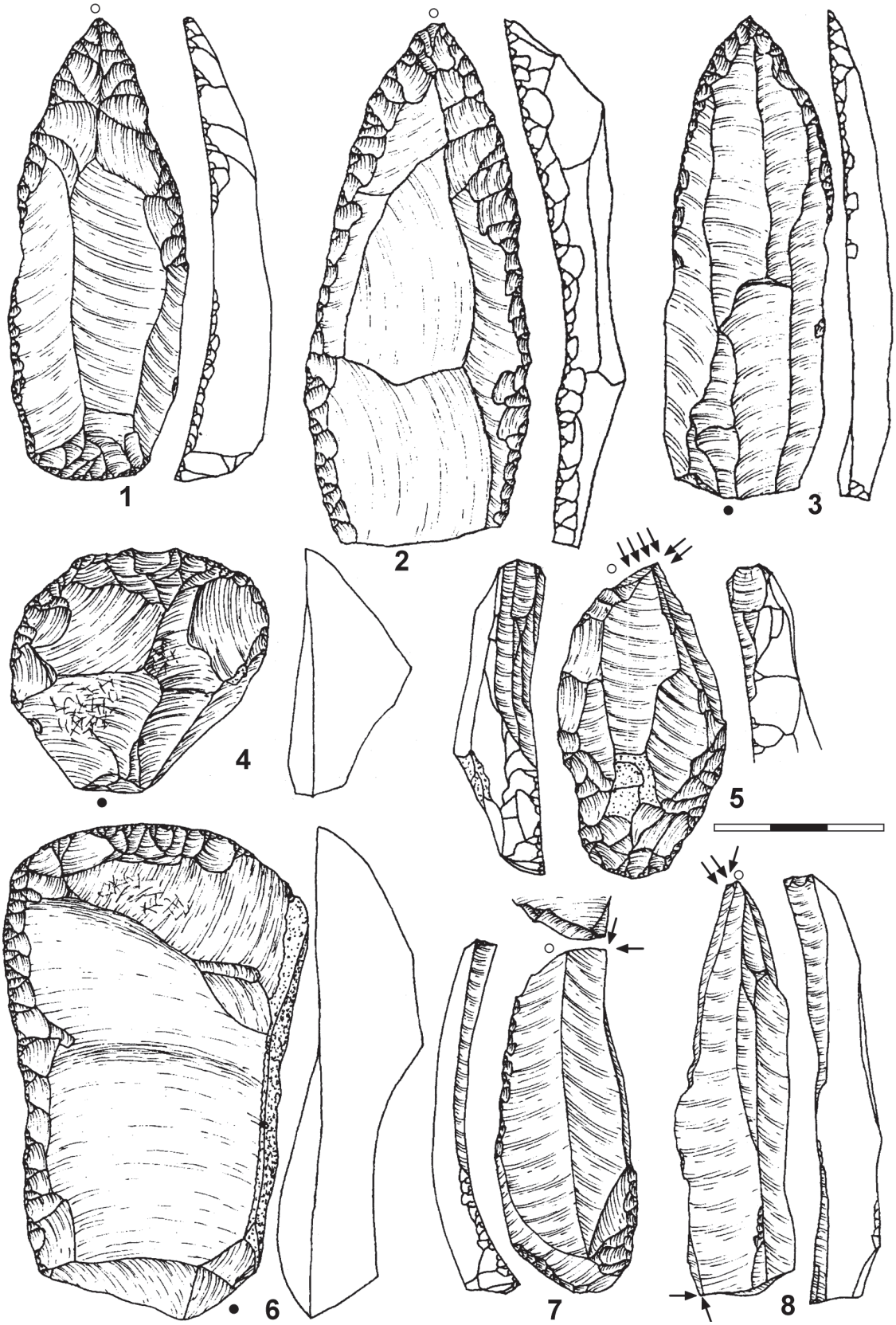


Fig. 11–5. Artefacts from Radomyshl: 1–3 Pavlov points; 4, 6 – end-scrapers; 5, 7, 8 – dihedral burins; after Nuzhnyi 2015, fig. 38, 39.

2002a: 136; Sinitsyn 2014: 237; Nuzhnyi 2015: 73; Vasyliev 2019: 130). They are also attested at Pushkari I, Kliusy, Kostenki 11, II and Kostenki 21, III, but are absent in Radomyshl (Lisitsyn, Dudin 2019: 77; Kononenko 2015).

In addition to the widespread Anosovka points, three other types of points occur in some of the mentioned assemblages of this taxonomic unit. Pavlov points are made on relatively wide blades and have symmetrical or asymmetrical shape, formed by flat to semi-abrupt or scalar to sub-parallel dorsal retouch. They are rare in Kostenki 11, II and Kostenki 21, III assemblages, but are common at Radomyshl, Pushkari I and Kliusy (Fig. 11-4, *15-18*; 11-5, *1-3*) (Nuzhnyi 2015: 68, 78, 79). Leaf-shaped points with their back and/or base thinned by alternating retouch are known from Kostenki 11, II and Kostenki 21, III. Shouldered points occur at Pushkari I, although only in very small numbers.

Rectangles on blades are another important component of many assemblages of the Pushkari-Anosovka industry (Fig. 11-4, *9-12*), but not for Radomyshl I (Kononenko 2015; Nuzhnyi 2015). The spectrum of burins is dominated by dihedral and angled types in the mentioned collections, including Radomyshl I (Fig. 11-5, *5, 7, 8*). On the other hand, burins on truncated blades are common in Kostenki 11, II and Kostenki 21, III-dwellings (Lisitsyn, Dudin 2019: 77, 80). Simple end-scrapers are made on flakes and blades.

## *Pushkari Industry / Anosovka Complex – Taxonomic attribution*

The high variability in tool morphologies is also reflected in the high number of proposed taxonomic terms. The highest number of controversial taxonomic terms can be found for Radomyshl I, which has been named "Aurignacoid character industry" (Anikovich 1998); Aurignacian, Early Upper Palaeolithic (Cohen, Stepanchuk 2001); Epiaurignacian (Demidenko 2004); and Late Gravettian, "similar to Eastern Gravettian" (Kononenko 2021). The assemblages of Pushkari I, in contrast, have been attributed to "the initial stage of Magdalenian" (Belyaeva 2002a) and the Late Gravettian of the "LGM peak" (Vasyliev 2019; Demay et al. 2021). The toolkit of Pushkari IX, layer 3, is with three backed blades and one retouched blade fragment too small for a taxonomic attribution (Khlopachev 2011: 192).

According to Lisitsyn and Dudin, the Anosovka complex is attributed to a "pre-LGM Early Epigravettian" and comprises the assemblages of Pushkari I, Kliusy, and Kostenki 11, II, as well as the recently re-evaluated assemblage from Kostenki 21, layer III-dwelling (Lisitsyn 2019; Lisitsyn, Dudin 2019: 77). According to Nuzhnyi (2015: 91), the Pushkari industry comprises Pushkari I, Kliusy and Kostenki 11, layer II assemblages, which he sees closely linked to the preceding complex of Radomyshl I. The two perspectives of Nuzhnyi and Lisitsyn differ in their view of the assemblages from Radomyshl I and Kostenki 21, layer III-dwellings, but are in accord regarding the characteristics of the assemblages from Pushkari I, Kliusy, and Kostenki 11, layer II. In his attribution, Nuzhnyi (2015) emphasizes the material culture, but does not pay much attention to the chronological positions of the assemblages in question. Sinitsyn and Lisitsyn, by contrast, stress the chronological and typological proximity of Kostenki 11, II, Kostenki 21, III-dwellings, and Pushkari I (Sinitsyn 2014; Lisitsyn 2019), while Lisitsyn and Dudin point out the high uncertainty regarding the attribution of Pushkari I to the Epigravettian (Lisitsyn, Dudin 2019: 95).

Unlike other assemblages traditionally attributed to the Eastern European Epigravettian, the Anosovka complex does not show evidence of a bladelet or micro-blade production and is thus characterised by the absence of backed bladelets or micro-blades and micro-gravette points. Sinitsyn (2014: 239), underlining the specific technology and typology of the Anosovka complex, proposed to rather search for differences than similarities between traditionally recognised Gravettian assemblages on the one hand, and Pushkari I, Kliusy, Kostenki 11, II and Kostenki 21, III, on the other. In this regard, the assemblages of Pushkari I and Kliusy do show similarities to the Gravettian, namely a technology based on blade core reduction, a dominance of dihedral and angle burins, and the presence of Pavlov points and rectangles on blades. Kostenki 11, II and Kostenki 21, III, in contrast, lack Pavlov points and show a dominance of burins on truncation over dihedral and angle ones. The dominance of burins on truncation is rather in line with an Epigravettian than Gravettian assemblage composition.

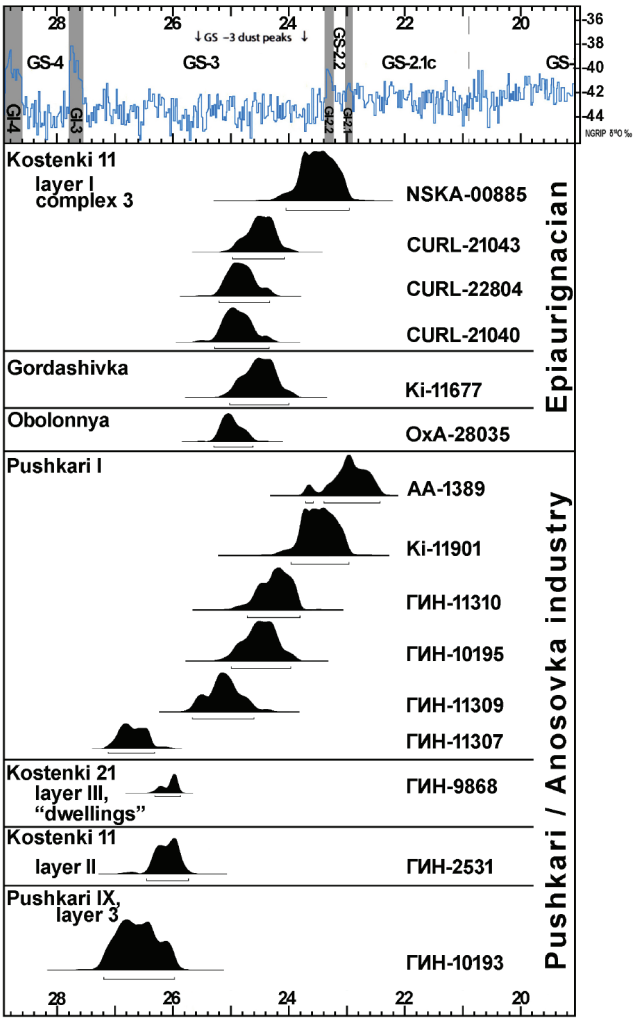


Fig. 11-6. Chronology of the Pushkari–Anosovka industry and the Epiaurignacian.

Eventually, the assemblages combined in the taxonomic units Pushkari industry / Anosovka complex are rather heterogeneous in their typological composition. It appears that the least common denominator is the occurrence of Anosovka points, which, however, are not characteristic of the “closely linked Radomyshl assemblage”. Therefore, any attribution of the Pushkari industry / Anosovka complex to the Final Gravettian or Early Epigravettian does not seem warranted. A little more accord can be observed in the chronological position of the assemblages of the Pushkari industry / Anosovka complex.

### *Chronology*

For Kostenki 11, II, two inconsistent dates are available, of which the older one seems more reliable and places the occupation between 26.5 and 25.7 ka calBP. For Kostenki 21, III-dwellings, three dates on charcoal give a weighted average between 26.9 and 26.4 ka calBP (Table 11-2; Fig. 11-6). The available radiocarbon dates for Pushkari I come from two areas V and VII. Six of the eight radiocarbon dates from area V (most of which have a high standard deviation) can be integrated in a weighted average with high probability (94.9%), resulting in an age estimate of between 25.5 and 24.8 ka calBP. The weighted average for the dates from area VII places this occupation between 24.8 and 24.4 ka calBP. Three of the four dates from Pushkari IX, 3 have high standard deviations, but all can be integrated in a weighted average between 27.1 and 26.5 ka calBP, which is in good agreement with the ages from Kostenki 21, III-dwellings (Table 11-2; Fig. 11-6). These age estimates are also in line with the observations of ice cracks and aeolian sediments at Pushkari I and Pushkari IX, 3 (Belyaeva 2009: 183–184; Khlopachev 2011: 192), indicating an accumulation of the cultural deposits under cold and arid conditions connected to the LGM (Belyaeva 2002b; Vasyliev 2019; Demay et al. 2021). There is a single date on a mammoth tooth from Radomyshl 1 (23.5–22.4 ka calBP), which has always been considered unreliable. No dates are available for Kliusy. In sum, it is thus possible to place the assemblages of the Pushkari industry / Anosovka complex within the LGM (Fig. 11-6).

## Epiaurignacian

Another archaeological taxonomic unit during the LGM in Eastern Europe is the so-called Epiaurignacian. Assemblages attributed to this unit are Kostenki 11, layer Ia, complex 3; Obolonnya and, probably, Gordashivka (Lisitsyn, Dudin 2019; Chabai, Vasyliev 2021a). Initially, the first cultural layer of Kostenki 11 was subdivided into two levels Ia and 1б (Rogachev, Popov 1982). However, this subdivision was later revoked due to a lack of evidence. In recent publications, the terms ‘layer Ia’, ‘layer

16' and 'layer I' are used as synonyms (Lisitsyn, Dudin 2019: 83; Dudin, Fedyunin 2019). Kostenki 11, Ia is known for its earthen-bone dwelling complexes, the most recently excavated and published of which is complex 3, which is also surrounded by pits. Traditionally, Kostenki 11, Ia – alongside Kostenki 2, 3, and 19 – has been attributed to the Zamiatnin culture, which is seen as having no discernible link with pre- and succeeding units of the area, and forms the second phase of Dnieper-Don HCH (Anikovich 1998: 58). Recent studies have demonstrated mixing of archaeological material in the assemblages of Kostenki 2 and 3, and underlined the small number of finds at Kostenki 19, calling into question the taxonomic consistency and integrity of the Zamiatnin culture (Lisitsyn, Dudin 2019: 82-87). At the same time, recent excavations shed new light on the stratigraphic and chronological position as well as typological peculiarities of Kostenki 11, Ia. The artefacts and faunal material of layer Ia originate from the upper part of the loess sequence and the base of the transition from the loess to the modern soil (Dudin, Fedyunin 2019: 225).

## *Environment*

Neither in Kostenki 11, Ia nor in Gordashivka traces of cryoturbation processes were observed. In the Obolonnya, by contrast, the cultural layer accumulated in aeolian sands and shows clear signs of cryoturbation (Stupak et al. 2014: 12). Here, cold and arid conditions are also reflected by the pollen analysis from the cultural deposits, which indicates a park tundra to periglacial steppe vegetation (Stupak et al. 2014: 14), where non-arboreal pollen dominate with 73 % (*Armeria, Artemisia, Dryas octopetala*), followed by spores (15 %) and arboreal pollen with 12 % (*Pinus silvestris, Betula sect. alba, Betula nana, Salix*; Stupak et al. 2014: 13). The faunal remains at Obolonnya comprise *Mammuthus primigenius, Ursus arctos, Canis lupus, Alopex lagopus, Lepus timidus* (Stupak et al. 2014: 15). At Gordashivka, mammoth, bison, horse and an unidentifiable bird were documented (Gladkikh et al. 2010: 98). Mammoth is the dominant species of the faunal assemblage in Kostenki 11, Ia complemented by few bones of reindeer, wolf and hare (Rogachev, Popov 1982: 125).

## *Artefacts*

The toolkit of Kostenki 11, Ia, complex 3 is characterised by numerous dihedral and angle burins on blades and simple end-scrapers on flakes and blades. Points on micro-blades and bladelets made by a marginal, dorsal (probably abrasion) retouch at the lateral and/or distal edges are not numerous, in contrast (Dudin, Fedyunin 2019: 231-233). The analysis of the entire collection of layer I (levels Ia and 16, see above) shows some differences and additions. Among the blade and bladelet cores, burin-like and scraper-like cores-on-flakes are reported, and marginally retouched, curved micro-blades and bladelets are the dominant tool type. Splintered pieces on flakes and fragmented blades are the second most numerous tool class. Dihedral burins, angle burins, and burins on truncated blades occur in nearly equal proportions (Lisitsyn, Dudin 2019: 84). Grounded on a recent analysis of the materials from Kostenki 11, I and with reference to specific types of insets analogous to specimens found in assemblages of steppe region (Demidenko et al. 2019), Lisitsyn and Dudin attribute Kostenki 11, I to the Epiaurignacian.

In Obolonnya, the production of lithic artefacts is based on the reduction of uni- and bidirectional blade cores (Stupak et al. 2014: 16). The toolkit is characterised by thick and thick-shouldered end-scrapers, a predominance of angle and dihedral burins over those on truncated blades, as well as blades and bladelets with marginal flat or semi-abrupt inverse/obverse retouch (Fig. 11-7; Stupak et al. 2014: 17-26). In addition, two fragments of ivory points of the Isturitz type and one ornamented tusk were found (Stupak et al. 2014: 28, fig. 16; 17; 18).

The Gordashivka assemblage is characterised by uni- and bidirectional blade and flake cores as well as multi-platform flake cores, the presence of thick end-scrapers, angle and dihedral burins, and a variety of obversely, inversely alternating, and marginally alternating retouched blades (Gladkikh et al. 2010).

## *Chronology*

There is a number of carefully selected samples from bone (conventional, NSKA lab-numbers) and charcoal (AMS, CURL lab-numbers) from

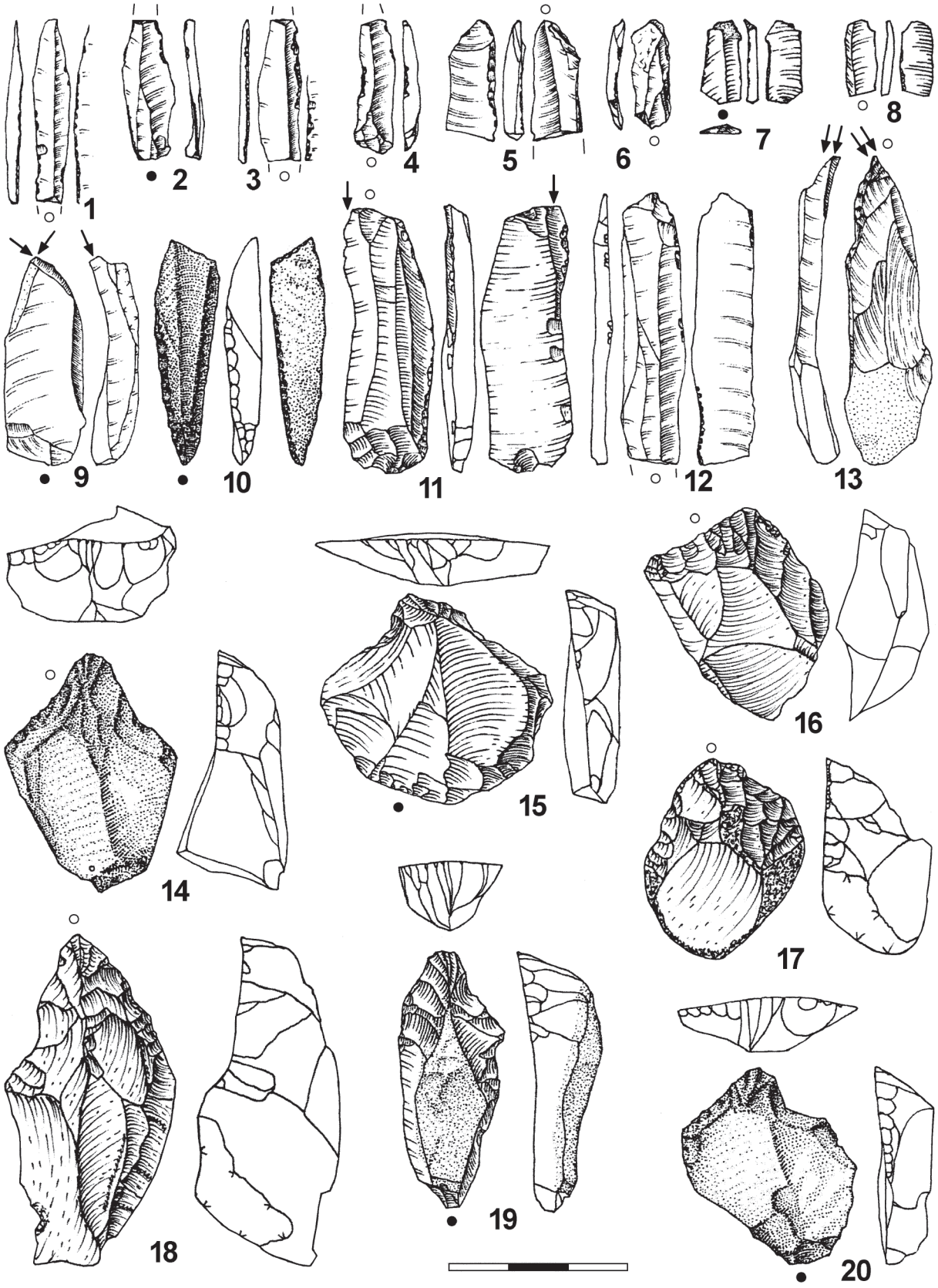


Fig. 11–7. Epiaurignacian artefacts from Obolonnya: 1–8 – bladelets with partial marginal semi-abrupt / abrupt retouches; 9, 11, 13 – burins; 10, 12 – retouched blades; 14–20 – end-scrapers; after Stupak et al. 2014.

Kostenki 11, Ia, complex 3. A weighted average of the only three AMS dates on charcoal result in an age estimate between 24.9 and 24.6 ka calBP (Table 11-2; Fig. 11-6). This is in line with the age estimate of 25063-24490 calBP suggested by Pryor and co-authors, which correlates with *"the onset of the last Glacial Maximum in Greenland-Stadial 3"* (Pryor et al. 2020: 8).

There are two dates on the mammoth bone from Obolonnya. Sample OxA-28035, originates from the excavation area and give an age range between 25.3 and 24.6 ka calBP (Table 11-2; Fig. 11-6), while sample SPb-442 is dated to 18.9-18.2 ka calBP, but was found in the backdirt of a builders' pit close to the excavated area (Stupak et al. 2014: 15, 29) and thus cannot be considered reliable. The latter date, however, gave rise to reflections on chronological and typological affinities to the Franco-Cantabrian Magdalenian (Demidenko 2020: 231).

There are two conventional and inconsistent dates on bone from Gordashivka. Here, we give preference to the one with a comparatively small standard deviation, which has an age estimate of 25 to 24 ka calBP (Table 11-2; Fig. 11-6).

### Kyrylivska, Novgorod-Siverska, Yamy and Zbytenka sites

The two sites of Kyrylivska and Novgorod-Siverska, located in the Mid Dnieper Basin, are frequently mentioned in the Gravettian and Epigravettian debates (Gavriliov 2023). However, recent investigations demonstrate the inhomogeneous character of these assemblages and point out the uncertain origins of the samples used for dating (Table 11-2) (Shydlovskyi 2012; Demay, Stupak 2021).

Krotova (2013: 197) stresses that the assemblage of the site of Yamy in the Donets River basin, a western tributary to the Don River, is similar to Gagarino. The cultural layer at Yamy is found in the pre-LGM "Bryansk soil", and described as affected by post-depositional ice-wedge cryoturbation. Bison and reindeer make up the fauna assemblage, while mammoth is not attested (Krotova 2003: 190-191; 2021a). For the cultural deposits at Yamy, Krotova (2021a) suggests a pre-LGM age based on stratigraphic observations (Bryansk soil and post-depositional ice wedges) despite a single and relatively late radiocarbon age of around 23 ka calBP (Table 11-2). Typologically, the assemblage of Yamy is characterised by a dominance of burins on truncated blades, Gravette points and rectangles on bladelets. In addition, two *"atypical shouldered points"* were found (Krotova 2013: 197). Thus, the Yamy assemblage differs from those of the Gmelin complex by both the absence of "typical" shouldered points and a dominance of burins on truncated blades, calling for further techno-typological and chronological studies.

At the site of Zbytenka, situated on the high terrace of the left bank of the Zbytenka River (Volyhnian Upland, Mid Dnieper basin), a single occupation has been documented within about 4 m thick loess deposits. No traces of cryoturbation were observed in the deposits. The faunal assemblage contains remains of mammoth and woolly rhino. The small assemblage from Zbytenka comprises sub-cylindrical cores, blanks with lipped platforms, a backed point with truncated base, an "atypical" rectangle, and an angle burin (Nuzhnyi 2009: 166, 171). The very limited artefact assemblage does not provide a sufficient clue for a technological or typological attribution. A single date from Zbytenka (26.3-25.9 ka calBP, Table 11-2) is in line with the chronology of both the Gmelin complex and the Pushkari-Anosovka industry.

## THE TECHNOLOGICAL, TYPOLOGICAL AND CHRONOLOGICAL VARIABILITY OF THE POST-LGM OCCUPATIONS

During the last decades, the post-LGM industrial variability of the Mid Dnieper and Upper Don basins has been the subject of continuous debates. The most recent versions are represented by two main approaches. The first approach is based on the analysis of morphological peculiarities of all types of tool assemblage (Anikovich 1998; Bessudnov 2013; Gavrilov 2016; Akhmetgaleeva 2019; Lisitsyn 2019; Demidenko 2020). The second approach, in

contrast, emphasises the differences and similarities in microlithic insets morphology, while the typology of burins, end-scrapers and other tool types is seen as attributes of secondary importance for a taxonomic allocation (Nuzhnyi 2006, 2008b, 2015). Neither of these approaches uses chronological and technological characteristics. Despite the long history of research, technological analyses were only performed for three assemblages, namely Mezhyrich, Barmaky and Mizyn (Lozovski, Lozovskaya 2014; Nuzhnyi et al. 2017; Chabai, Dudnyk 2022; Dudnyk 2024).

To date, four archaeological sub-units, called industries, of the Epigravettian techno-complex in Ukraine have been described. These are the Mizyn, Mezhyrich, Yudinovo, and Ovruch industries. In addition, the assemblages of Suponevo and Yeliseevichy are also attributed to the Epigravettian, but are not attributed to distinctive sub-units. The absence of faunal material at the sites of Ovruch industry prevents a more detailed environmental or chronological characterisation (Nuzhnyi 1998; 2015; Zaliznyak 2017). Therefore, the Ovruch industry will not be considered in the following discussion.

So, the highest number of taxonomic units, which are also chronologically often overlapping, can be observed in the Mid Dnieper Basin. The Mizyn industry is represented by two relatively distant (about 450 km) assemblages: Barmaky and Mizyn. Sites with assemblages attributed to the Yudinovo industry are restricted to the Desna Valley, and the Mezhyrich industry is known from both the Desna and the Dnieper valleys. The only non-Epigravettian industry – "Byki culture" (see below) – is reported from a few sites in the Seim valley and probably the Don valley. This pronounced taxonomic variability might reflect limited communication between different regional groups in combination with a low population density.

## Byki industry

The Byki industry is spatially restricted to a group of assemblages in the Seim River valley, a tributary to the Desna and thus the Dnieper system. These assemblages are subdivided into two chronological groups. The early group comprises Byki 5, 7-II, and 8, while the late group comprises (Byki 1, 2, 3, 4 (also called Peny), 7-I, 7-Ib, 7-Ia, and 7-Ic). The relatively few finds of the early assemblages were generally attributed to the Upper Palaeolithic. The material of the late group is labelled as "Byki culture" (Akhmetgaleeva 2004; 2019). The most extensively studied site is Byki 7, whose stratigraphic sequence spans about 1,5 m of sediments. The excavation area of roughly 300 m² yielded 4000 bones and more than 3000 artefacts from layers I, Ib, Ia, and Ic.

### *Environment*

At Byki 7, permafrost cracks disturbed the accumulation of the cultural deposits in layer II, while layers I, Ib, Ia, and Ic show traces of "permafrost degradation" (Akhmetgaleeva 2019: 22; 2011: 346). This indicates that the earliest occupation, manifest in layer II, accumulated before the appearance of permafrost cracks, while the layers I, Ib, Ia, and Ic accumulated *"after the end of degradation and complete disappearance of permafrost"* in the region (Akhmetgaleeva 2019: 22). *Equus ferus* and *Rangifer tarandus* dominate the faunal assemblage of all cultural layers. The remains of *Lepus tanaiticus* and *Vulpes lagopus* are likewise numerous (Akhmetgaleeva 2019: 23), while mammoth bones are rare. According to Akhmetgaleeva, the faunal composition reflects the geographic position of Byki at the edge of tundra-steppe and steppe environments (Akhmetgaleeva 2014: 222). In the rodent assemblage, typical tundra species are present in small quantities, whereas steppe species dominate and forest species are absent (Markova, Puzachenko 2022).

### *Artefacts*

The technological spectrum comprises both blade and flake cores. The toolkit is characterised by triangular geometrical microliths (Fig. 11-8, *1-16*), dihedral burins, which are more numerous than angle bruins and burins on truncations, end-scrapers on flakes with lateral retouch, including double forms (Fig. 11-8, *17-19*), and borer-perforators (Fig. 11-8, *20-24*) with variable morphology (Akhmetgaleeva 2019: 28). Taxonomically, the Byki industry is

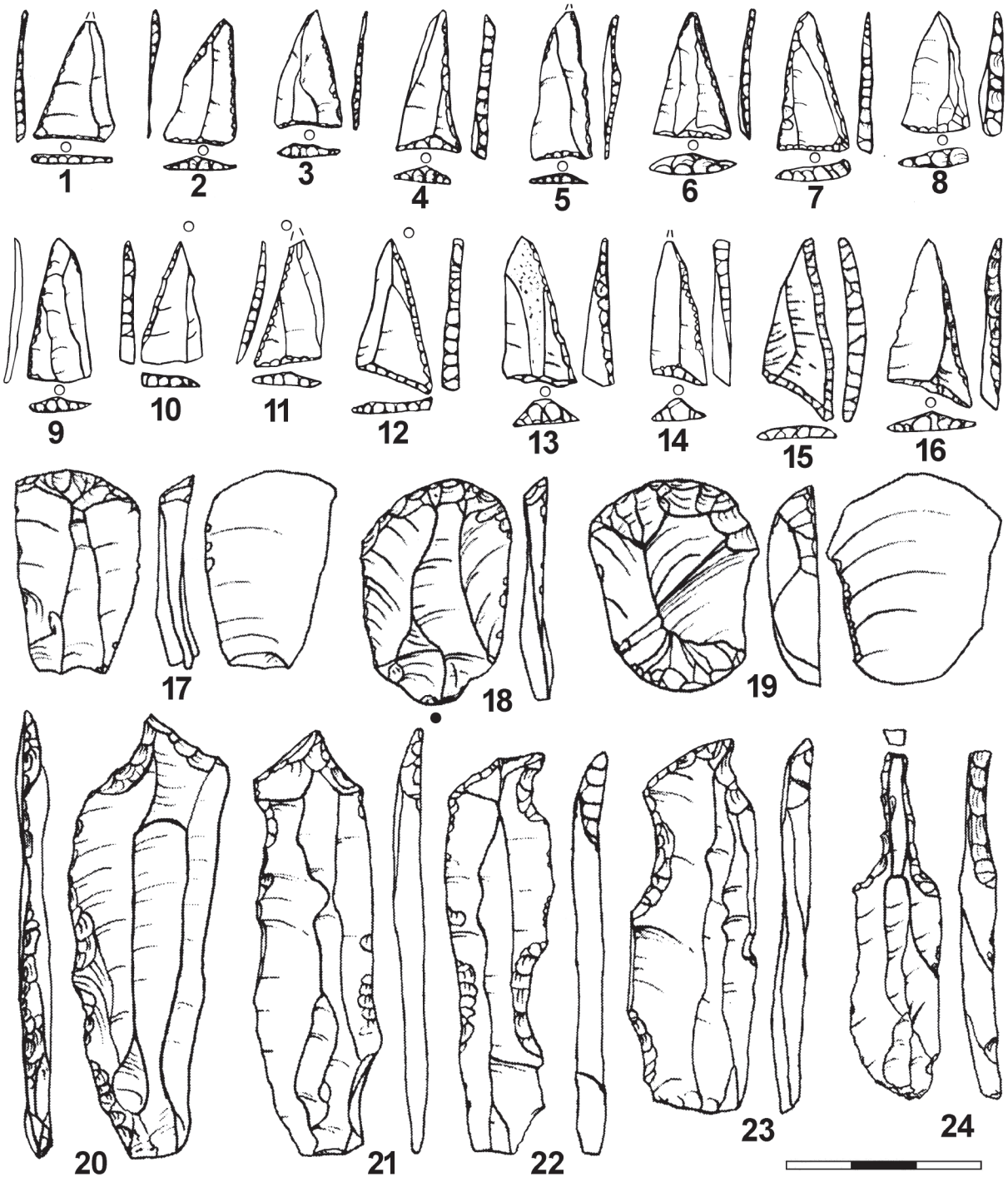


Fig. 11–8. Byki industry, artefacts from Byki 7: 1–16 – triangles; 17–19 – end-scrapers; 20–24 – borers / perforators; after Akhmetgaleeva 2004, fig. 4, 5, 7.

discussed as a manifestation of the Magdalenian in Eastern Europe, a part of the Epigravettian of the Desna basin, or part of the Mizyn industry (Chubur 2001; Grigoriev 2008; Gavrilov 2016; Demidenko 2020). Akhmetgaleeva (2019), however, underlines the marked technological and typological differences between the Byki assemblages and all other mentioned archaeological units and proposes to use the term "Byki culture" instead, stressing that there are no obvious links with older or younger industries in the wider region. At the same time, she mentions that the Byki triangles artefacts found in the Samotoevka assemblage, potentially reflecting cultural connections.

### *Chronology*

Radiocarbon dates are available for Byki 1, Byki 4 (Peny) and Byki 7. Three conventional and inconsistent dates on mammoth bones are available for Byki 4 (Peny) (Table 11-3). Given the possibility of gathered and thus older material, the youngest estimate of between 26.6 and 26 ka calBP should be given preference – if considered at all. Two dates from Byki 1 can be combined to a weighted average and place the occupation between 21.4 and 21.2 ka calBP (Table 11-3; Fig. 11-9). The main problem with the age determination of layers Ia, Ib, and I from Byki 7 is the use of bulk samples of horse and reindeer bones (Table 11-3). Here, one date per layer has an acceptably large standard deviation. If these dates are taken for an age estimate, the respective occupations probably took place between 20.8 to 19 ka calBP (Table 11-3; Fig. 11-9). In sum, the datable occupations of the Byki 1 and 7 took place after the end of the LGM, which is in line with the observations on permafrost degradation events. At the same time, the Byki sites are situated at the most distant location from the edge of the Scandinavian Ice Sheet in the Mid Dnieper basin. Considering the dating of 20-19 ka calBP, the area of Byki might have experienced an earlier beginning of the permafrost degradation and a concomitant relative rarity of tundra species compared to more north-western locations.

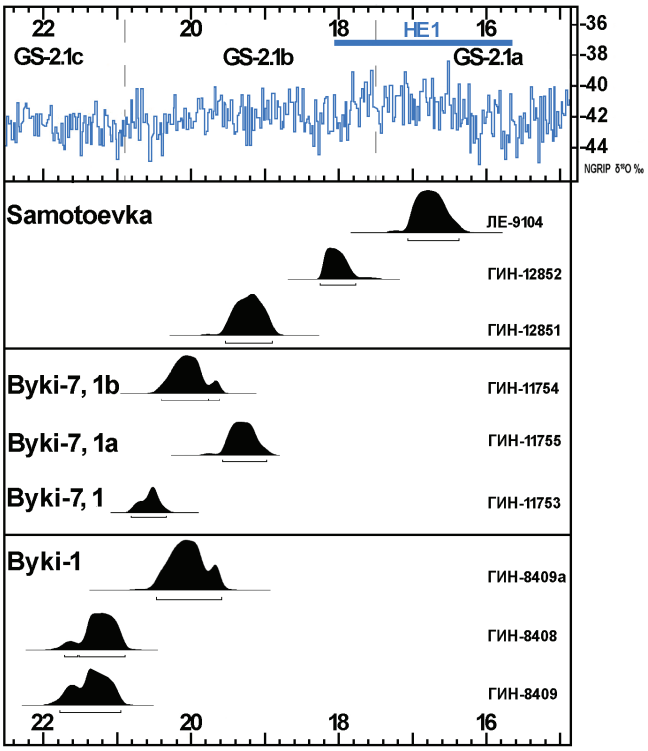


Fig. 11-9. Chronology of the Byki industry and Samotoevka.

## Samotoevka industry

The site of Samotoevka was discovered in the valley of the Chernaya Kalitva River, which belongs to the Don Drainage system. A single archaeological occupation includes a dwelling structure with an internal hearth surrounded by limestone concentration and external pits (Bessudnov, Bessudnov 2012).

### *Environment*

No evidence for cryoturbation has been documented at the site. Horse bones dominate the faunal assemblage, while remains of elk, bovids, beaver, and hair are also common. Noteworthy is the complete absence of mammoth bones (Bessudnov, Bessudnov 2012).

| Site, layer / level, structure | samples | methods | lab. # | uncalBP | Std | Std% | calBP; 95,4% | P % | wuncalBP | wStd | wcalBP (ka) | R | References | Comments |
|---|---|---|---|---|---|---|---|---|---|---|---|---|---|---|
| Barmaky | bone | Conv | KI-11087 | 14300 | 220 | 1,54 | 18154 - 16906 | | | | | 1 | Nuzhnyi 2008b | Mizyn industry |
| Barmaky, 2 | bone | AMS | OxA-38249 | 15610 | 80 | 0,51 | 19062 - 18760 | * | | | | | Chabai et al. 2019b | Mizyn industry |
| Barmaky, 2 | bone | AMS | OxA-X-2804-40 | 15720 | 80 | 0,51 | 19154 - 18838 | * | | | | | Chabai et al. 2019b | Mizyn industry |
| Barmaky, 2 | bone | AMS | MAMS-49912 | 15770 | 50 | 0,32 | 19146 - 18904 | * | | | | | Chabai, Vasyliev 2021b | Mizyn industry |
| Barmaky, 2 | bone | AMS | OxA-38250 | 15850 | 80 | 0,51 | 19379 - 18924 | * | | | | | Chabai et al. 2019b | Mizyn industry |
| | | | | | | | | ***17.8** | **15747** | **34** | **19.1 - 18.9** | | | |
| Borschevo 1 | shell | Conv | ICFN-903 | 9900 | 70 | 0,71 | 11510 - 11196; 83,6% | | | | | 8 | Sinitsyn et al. 1997 | Borschevo 1 complex |
| Borschevo 1 | *Mammuthus primigenius*, bone | Conv | ГИН-11197 | 15140 | 100 | 0,66 | 18674 - 18244 | * | | | | | Sinitsyn et al. 1997 | Borschevo 1 complex |
| Borschevo 1 | *Mammuthus primigenius*, bone | Conv | ГИН-11198 | 15200 | 100 | 0,66 | 18715 - 18260 | * | | | | | Sinitsyn et al. 1997 | Borschevo 1 complex |
| Borschevo 1 | *Mammuthus primigenius*, bone | Conv | ГИН-11199 | 15200 | 200 | 1,32 | 18880 - 18181 | * | | | | | Sinitsyn et al. 1997 | Borschevo 1 complex |
| | | | | | | | | ***90.5** | **15173** | **67** | **18.6 - 18.3** | | | |
| Borschevo 1 | *Mammuthus primigenius*, bone | Conv | ГИН-8085 | 15600 | 70 | 0,45 | 19024 - 18763 | | | | | | Sinitsyn et al. 1997 | Borschevo 1 complex |
| Borschevo 1 | *Mammuthus primigenius*, bone | Conv | ЛЕ-3727 | 17120 | 110 | 0,64 | 20913 - 20447 | | | | | | Sinitsyn et al. 1997 | Borschevo 1 complex |
| Borschevo 2, gittia | gyttja | Conv | ГИН3261 (3268) | 12550 | 200 | 1,59 | 15457 - 14084 | | | | | 1 | Sinitsyn et al. 1997 | Don Epigravettian |
| Borschevo 2, I | humus | Conv | МО-636 | 11760 | 240 | 2,04 | 14250 - 13155; 95,1% | | | | | 1 | Sinitsyn et al. 1997 | Don Epigravettian |
| Borschevo 2, I | soil | Conv | ГИН-88 | 12300 | 100 | 0,81 | 14867 - 14039 | * | | | | | Boriskovsky, Dmitrieva 1982 | Don Epigravettian |
| Borschevo 2, I | charcoal | Conv | ЛУ-742 | 13210 | 270 | 2,04 | 16723 - 15100 | | | | | 1 | Boriskovsky, Dmitrieva 1982 | Don Epigravettian |
| Borschevo 2, I/1 | humus | Conv | ЛЕ-4866 | 9330 | 390 | 4,18 | 11756 - 9542; 95,2% | | | | | 1 | Sinitsyn et al. 1997 | Don Epigravettian |
| Borschevo 2, I/1 | humus | Conv | ЛЕ-4865 | 9520 | 300 | 3,15 | 11838 - 10122; 94,6% | | | | | 1 | Sinitsyn et al. 1997 | Don Epigravettian |
| Borschevo 2, I/1 | charcoal | AMS | GrA-9249 | 12720 | 140 | 1,10 | 15636 - 14793; 87,4% | * | | | | | Sinitsyn et al. 1997 | Don Epigravettian |

Table 11-3. Age estimates of post-LGM assemblages of the Mid Dnieper and Upper Don basins. Weighted averages calculated with CalPal-Beyond the Ghost, Version 2020.11, https://zenodo.org/records/11104437 (Weninger and Jöris, 2008);

| Site, layer / level, structure | samples | methods | lab. # | uncalBP | Std | Std% | calBP; 95,4% | P % | wuncalBP | wStd | wcalBP (ka) | R | References | Comments |
|---|---|---|---|---|---|---|---|---|---|---|---|---|---|---|
| Borschevo 2, I? | *Equid*, burt bones | Conv | ГИН-8084 | 10400 | 200 | 1,92 | 12742 - 11606; 93,8% | | | | | 1 | Sinitsyn et al. 1997 | Don Epigravettian |
| Borschevo 2, I? | *Equid*, burt bones | Conv | ГИН-8415 | 10900 | 300 | 2,75 | 13443 - 11998 | | | | | 1 | Sinitsyn et al. 1997 | Don Epigravettian |
| Borschevo 2, II | bone | AMS | SPb-776 | 12590 | 150 | 1,19 | 15382 - 14196 | * | | | | | Khlopachev 2016 | Don Epigravettian |
| Borschevo 2, II | charcoal | Conv | ЛЕ-4837 | 13480 | 720 | 5,34 | 18235 - 14130 | | | | | 1 | Sinitsyn et al. 1997 | Don Epigravettian |
| Borschevo 2, III | charcoal | Conv | ЛЕ-4834 | 13540 | 300 | 2,22 | 17159 - 15542; 93,9% | | | | | 1 | Sinitsyn et al. 1997 | Don Epigravettian |
| | | | | | | | | ***3.5** | **12476** | **72** | **14.9 - 14.4** | | | |
| Buzhanka 2, upper layer | *Canis Lupus*, bone | AMS | GifA-80178/ SacA-12043 | 13500 | 80 | 0,59 | 16541 - 16021 | | | | | | Stupak 2014 | Mezhyrich industry |
| Buzhanka 2, upper layer, pit 1 | *Mammuthus primigenius*, bone | AMS | GrA-38555 | 14350 | 60 | 0,42 | 17813 - 17300 | | | | | | Stupak 2014 | Mezhyrich industry |
| Byki 7, I | mammalian & birds bones | Conv | ГИН-13084 | 15600 | 400 | 2,56 | 19929 - 18165 | | | | | 1 | Akhmetgaleeva 2019 | Byki culture |
| Byki 7, I | horse and reindeer bones | Conv | ГИН-11753 | 17000 | 90 | 0,53 | 20812 - 20332 | | | | | | Akhmetgaleeva 2019 | Byki culture |
| Byki 7, Ia | mammalian & birds bones | Conv | ГИН-13082 | 14300 | 370 | 2,58 | 18288 - 16363 | | | | | 1 | Akhmetgaleeva 2019 | Byki culture |
| Byki 7, Ia | horse and reindeer bones | Conv | ГИН-11755 | 16000 | 130 | 0,81 | 19579 - 18979 | | | | | | Akhmetgaleeva 2019 | Byki culture |
| Byki 7, Ia | polar fox and hair bones | Conv | ЛЕ-7794 | 17320 | 640 | 3,69 | 22585 - 19480 | | | | | 1 | Akhmetgaleeva 2019 | Byki culture |
| Byki 7, Ib | mammalian & birds bones | Conv | ГИН-13083 | 14600 | 250 | 1,71 | 18293 - 17102 | | | | | 1 | Akhmetgaleeva 2019 | Byki culture |
| Byki 7, Ib | horse and reindeer bones | Conv | ГИН-11754 | 16600 | 140 | 0,84 | 20408 - 19619 | | | | | | Akhmetgaleeva 2019 | Byki culture |
| Byki 7, Ib | *Equus ferus*, scapula | Conv | ЛЕ-11703 | 17600 | 300 | 1,71 | 22115 - 20565 | | | | | 1 | Akhmetgaleeva 2019 | Byki culture |
| Byki 1 | *Bison priscus*, bone | Conv | ГИН-8409A | 16600 | 180 | 1,08 | 20468 -19585 | | | | | | Abramova et al. 2001 | Byki culture |
| Byki 1 | *Mammuthus primigenius*, bone | Conv | ГИН-8408A | 17200 | 300 | 1,74 | 21759 - 20071 | | | | | 1 | Abramova et al. 2001 | Byki culture |
| Byki 1 | *Rangifer tarandus*, bone | Conv | ГИН-8408 | 17570 | 120 | 0,68 | 21517 - 20899 | * | | | | | Abramova et al. 2001 | Byki culture |
| Byki 1 | *Coelodonta antiquitatis*, bone | Conv | ГИН-8409 | 17640 | 130 | 0,74 | 21815 - 20943 | * | | | | | Abramova et al. 2001 | Byki culture |
| | | | | | | | | ***69.2** | **17602** | **88** | **21.4 - 21.1** | | | |

Table 11-3. continued 1;

| Site, layer / level, structure | samples | methods | lab. # | uncalBP | Std | Std% | calBP; 95,4% | P % | wuncalBP | wStd | wcalBP (ka) | R | References | Comments |
|---|---|---|---|---|---|---|---|---|---|---|---|---|---|---|
| Byki 4 (Peny) | *Mammuthus primigenius*, bone | Conv | ЛЕ-1434А, idem ЛЕ-1434Б, ЛЕ1434В | 21600 | 50 | 0,24 | 25990 - 26593 | | | | | 5; 8 | Akhmetgaleeva 2019 | Byki culture |
| Byki 4 (Peny) | *Mammuthus primigenius*, bone | Conv | ЛЕ-1434Б, idem ЛЕ-1434А, ЛЕ1434В | 23100 | 280 | 1,22 | 27951 - 26593 | | | | | 5; 8 | Akhmetgaleeva 2019 | Byki culture |
| Byki 4 (Peny) | *Mammuthus primigenius*, bone | Conv | ЛЕ-1434В, idem ЛЕ-1434Б, ЛЕ1434А | 25200 | 350 | 1,39 | 30106 - 28776 | | | | | 5; 8 | Akhmetgaleeva 2019 | Byki culture |
| Chulativ I | *Mammuthus primigenius*, tooth | AMS | OxA-715 | 14700 | 250 | 1,70 | 18643 - 17312 | | | | | 1 | Svezhentsev, Popov 1993 | Epigravettian |
| Divnogorie 1 | horse bones | Conv | ЛЕ-8649 | 12050 | 170 | 1,41 | 14527 - 13576; 90,8% | | | | | | Bessudnov et al. 2012 | Don Epigravettian |
| Divnogorie 1 | horse bones | Conv | ЛЕ-8648 | 13380 | 220 | 1,64 | 16856 - 15500 | | | | | 1 | Bessudnov et al. 2012 | Don Epigravettian |
| Divnogorie 1 | horse bones | | AA-no number | 13430 | 130 | 0,97 | 16575 - 15782 | | | | | | Bessudnov 2013 | Don Epigravettian |
| Divnogorie 9, Bolling soil, upper | charcoal | AMS | ГИН-14547 | 11880 | 140 | 1,18 | 14061 - 13482 | * | | | | | Bessudnov et al. 2013 | Don Epigravettian |
| Divnogorie 9, Bolling soil, upper | charcoal | Conv | ИГАН-4247 | 12060 | 80 | 0,66 | 14105 - 13773 | * | | | | | Bessudnov et al. 2013 | Don Epigravettian |
| Divnogorie 9, Bolling soil, lower | charcoal | AMS | ГИН-14548 | 12090 | 100 | 0,83 | 14299 - 13759 | * | | | | | Bessudnov et al. 2013 | Don Epigravettian |
| | | | | | | | | ***44.5** | **12040** | **57** | **14.0 - 13.8** | | | |
| Divnogorie 9, I | horse bones | Conv | ЛЕ-8137 | 11400 | 120 | 1,05 | 13489 - 13098 | | | | | | Bessudnov et al. 2012 | Don Epigravettian |
| Divnogorie 9, I | horse bones | Conv | ЛЕ-8135 | 12980 | 180 | 1,39 | 16075 - 15020 | | | | | | Bessudnov et al. 2012 | Don Epigravettian |
| Divnogorie 9, I | horse bones | Conv | ЛЕ-8136 | 13150 | 200 | 1,52 | 16360 - 15206 | | | | | 1 | Bessudnov et al. 2012 | Don Epigravettian |
| Divnogorie 9, II | horse bones | Conv | ЛЕ-8134 | 13100 | 200 | 1,53 | 16295 - 15150 | | | | | 1 | Bessudnov et al. 2012 | Don Epigravettian |
| Divnogorie 9, II | horse bones | Conv | ЛЕ-8130 | 13370 | 240 | 1,79 | 16885 - 15416 | | | | | 1 | Bessudnov et al. 2012 | Don Epigravettian |
| Divnogorie 9, II | horse bones | AMS | AA-90650 | 13430 | 130 | 0,97 | 16575 - 15782 | | | | | | Lavrushin et al. 2010 | Don Epigravettian |
| Divnogorie 9, II | horse bones | Conv | ЛЕ-8131 | 13560 | 240 | 1,77 | 17065 - 15703 | | | | | 1 | Bessudnov et al. 2012 | Don Epigravettian |
| Divnogorie 9, III | horse bones | Conv | ЛЕ-8955 | 12250 | 350 | 2,86 | 15491 - 13487 | | | | | 1 | Bessudnov et al. 2012 | Don Epigravettian |
| Divnogorie 9, III | horse bones | AMS | ГИН-13192 | 12350 | 200 | 1,62 | 15152 - 13979 | | | | | 1 | Bessudnov et al. 2012 | Don Epigravettian |
| Divnogorie 9, III | horse bones | Conv | ЛЕ-9250 | 13820 | 130 | 0,94 | 17090 -16340 | * | | | | | Bessudnov et al. 2013 | Don Epigravettian |
| Divnogorie 9, III | horse bones | AMS | AA-90652 | 13870 | 140 | 1,01 | 16575 - 15782 | * | | | | | Lavrushin et al. 2010 | Don Epigravettian |
| | | | | | | | | ***79.4** | **13843** | **95** | **16.9 - 16.6** | | | |

Table 11-3. continued 2;

| Site, layer / level, structure | samples | methods | lab. # | uncalBP | Std | Std% | calBP; 95,4% | P % | wuncalBP | wStd | wcalBP (ka) | R | References | Comments |
|---|---|---|---|---|---|---|---|---|---|---|---|---|---|---|
| Divnogorie 9, IV | horse bones | Conv | ЛЕ-8956 | 13200 | 300 | 2,27 | 16848 – 15009 | | | | | 1 | Bessudnov et al. 2012 | Don Epigravettian |
| Divnogorie 9, IV | horse bones | AMS | ГИН-14540 | 13650 | 320 | 2,34 | 17407 – 15604 | | | | | 1 | Bessudnov et al. 2013 | Don Epigravettian |
| Divnogorie 9, IV | horse bones | AMS | AA-90653 | 13830 | 150 | 1,08 | 17146 – 16342; 92,5% | | | | | | Lavrushin et al. 2010 | Don Epigravettian |
| Divnogorie 9, V | horse bones | AMS | ГИН-14541 | 12600 | 250 | 1,98 | 15674 – 14060 | | | | | 1 | Bessudnov et al. 2013 | Don Epigravettian |
| Divnogorie 9, V | horse bones | Conv | ЛЕ-8957 | 13100 | 500 | 3,82 | 17130 – 14070 | | | | | 1 | Bessudnov et al. 2012 | Don Epigravettian |
| Divnogorie 9, V | horse bones | Conv | ЛЕ-8932 | 13270 | 630 | 4,75 | 17833 – 14068 | | | | | 1 | Bessudnov et al. 2012 | Don Epigravettian |
| Divnogorie 9, V | horse bones | AMS | AA-90654 | 13900 | 140 | 1,01 | 17315 – 16457 | | | | | | Lavrushin et al. 2010 | Don Epigravettian |
| Divnogorie 9, VIA | horse bones | AMS | ГИН-14544 | 12540 | 470 | 3,75 | 17833 – 14068 | | | | | 1 | Bessudnov et al. 2013 | Don Epigravettian |
| Divnogorie 9, VI | horse bones | AMS | ГИН-14543 | 12140 | 300 | 2,47 | 15190 – 13461 | | | | | 1 | Bessudnov et al. 2013 | Don Epigravettian |
| Divnogorie 9, VI | horse bones | Conv | ЛЕ-9620 | 13100 | 600 | 4,58 | 17422 – 13980 | | | | | 1 | Bessudnov et al. 2013 | Don Epigravettian |
| Divnogorie 9, VI | horse bones | Conv | ЛЕ-9619 | 13800 | 150 | 1,09 | 17122 – 16252 | * | | | | | Bessudnov et al. 2013 | Don Epigravettian |
| Divnogorie 9, VI | horse bones | Conv | ЛЕ-8958 | 13920 | 175 | 1,26 | 17366 – 16385 | * | | | | | Bessudnov et al. 2013 | Don Epigravettian |
| Divnogorie 9, VI | horse bones | Conv | ЛЕ-9102 | 13940 | 180 | 1,29 | 17390 – 16383 | * | | | | | Bessudnov et al. 2013 | Don Epigravettian |
| Divnogorie 9, VI | horse bones | Conv | ЛЕ-9618 | 14080 | 190 | 1,35 | 17763 – 16563 | * | | | | | Bessudnov et al. 2013 | Don Epigravettian |
| Divnogorie 9, VI | horse bones | AMS | AA-90655 | 14430 | 160 | 1,11 | 18099 – 17129 | * | | | | | Bessudnov et al. 2013 | Don Epigravettian |
| | | | | | | | | ***5.4** | **14032** | **76** | **17.2 – 16.9** | | | |
| Dobranichivka | *Mammuthus primigenius*, tooth | AMS | OxA-700 | 12700 | 200 | 1,57 | 14245 – 15705 | | | | | 1 | Svezhentsev, Popov 1993 | Mezhyrich industry |
| Dobranichivka | *Ursus sp.*, calcaneum bone | AMS | OxA-12108, idem GrA-22472 | 13990 | 90 | 0,64 | 17330 – 16706 | * | | | | | Haesaerts et al. 2015 | Mezhyrich industry |
| Dobranichivka | *Ursus sp.*, calcaneum bone | AMS | GrA-22472, idem OxA-12108 | 14355 | 90 | 0,62 | 17855 – 17146 | * | | | | | Haesaerts et al. 2015 | Mezhyrich industry |
| | | | | | | | | ***0.4** | **14173** | **64** | **17.3 – 17.1** | | | |
| Gintsy, pit 9 | burnt bone | Conv | ISGS-1740 | 13200 | 270 | 2,05 | 16709 – 15085 | | | | | 1 | Svezhentsev, Popov 1993 | Mezhyrich industry |
| Gintsy, pit 9 | burnt bone | Conv | QC-898 | 13400 | 185 | 1,38 | 16734 – 15602 | * | | | | | Boriskovsky 1984 | Mezhyrich industry |
| Gintsy, pit 9 | burnt bone | Conv | ГИН-8410 | 13700 | 100 | 0,73 | 16948 – 16289 | * | | | | | Sinitsyn et al. 1997 | Mezhyrich industry |
| | | | | | | | | *15.4 | 13632 | 88 | 16.6 – 16.3 | | | |

Table 11-3. continued 3;

| Site, layer / level, structure | samples | methods | lab. # | uncalBP | Std | Std% | calBP; 95,4% | P % | wuncalBP | wStd | wcalBP (ka) | R | References | Comments |
|---|---|---|---|---|---|---|---|---|---|---|---|---|---|---|
| Gintsy, lower layer | bone | AMS | OxA-6729 | 14110 | 120 | 0,85 | 17459 - 16795 | *, b | | | | | Iakovleva, Djindjian 2005 | Mezhyrich industry |
| Gintsy, lower layer | antler | AMS | OxA-5934 | 14250 | 110 | 0,77 | 17759 - 17053 | *, b | | | | | Iakovleva, Djindjian 2005 | Mezhyrich industry |
| Gintsy, lower layer | *Mammuthus primigenius*, bone | AMS | OxA-7609 | 14420 | 100 | 0,69 | 17934 - 17308 | b | | | | | Iakovleva, Djindjian 2005 | Mezhyrich industry |
| Gintsy, lower layer | *Mammuthus primigenius*, bone | AMS | OxA-6142 | 14670 | 110 | 0,75 | 18225 - 17540 | b | | | | | Iakovleva, Djindjian 2005 | Mezhyrich industry |
| | | | | | | | | *39 | 14186** | 81 | 17.3 - 17.1 | | | |
| | | | | | | | | b0.4 | 14375 | 55 | 17.7 - 17.4 | | | |
| Gintsy, upper layer | *Mammuthus primigenius*, bone | AMS | OxA-7387 | 14120 | 90 | 0,64 | 17398 - 16986 | * | | | | | Iakovleva, Djindjian 2005 | Mezhyrich industry |
| Gintsy, upper layer | *Mammuthus primigenius*, bone | AMS | OxA-8409 | 14280 | 110 | 0,77 | 17789 - 17073 | * | | | | | Iakovleva, Djindjian 2005 | Mezhyrich industry |
| Gintsy, upper layer | *Mammuthus primigenius*, bone | AMS | OxA-8368 | 14620 | 100 | 0,68 | 18190 - 17494 | * | | | | | Iakovleva, Djindjian 2005 | Mezhyrich industry |
| | | | | | | | | *0.1 | 14327** | 57 | 17.6 - 17.4 | | | |
| Gintsy, ashy area U21 | burnt bone | Conv | ISGS-1739 | 14350 | 190 | 1,32 | 18093 - 17035 | * | | | | | Svezhentsev, Popov 1993. | Mezhyrich industry |
| Gintsy, ashy area U21 | tooth | AMS | OxA-717 | 14600 | 200 | 1,37 | 18265 - 17314 | * | | | | | Svezhentsev, Popov 1993 | Mezhyrich industry |
| | | | | | | | | *36.5 | 14469** | 138 | 17.9 - 17.5 | | | |
| Gintsy, dump from dwelling #1 | bone | AMS | OxA-6601 | 14180 | 110 | 0,78 | 17697 - 16963 | * | | | | | Iakovleva, Djindjian 2005 | Mezhyrich industry |
| Gintsy, dump from dwelling #1 | bone | AMS | OxA-6602 | 14590 | 120 | 0,82 | 18181 - 17442 | * | | | | | Iakovleva, Djindjian 2005 | Mezhyrich industry |
| | | | | | | | | *1.2 | 14367** | 81 | 17.7-17.4 | | | |
| Gintsy, dwelling 1, pit 10 | *Mammuthus primigenius*, bone | AMS | OxA-5933 | 14400 | 110 | 0,76 | 17940 - 17154 | * | | | | | Iakovleva, Djindjian 2005 | Mezhyrich industry |
| Gintsy, dwelling 1, pit 10 | *Mammuthus primigenius*, tooth | AMS | OxA-5932 | 14550 | 150 | 1,03 | 18187 - 17380 | * | | | | | Iakovleva, Djindjian 2005 | Mezhyrich industry |
| | | | | | | | | *42 | 14452** | 89 | 17.8 - 17.5 | | | |
| | | | | | | | | **18.3 | 14337 | 36 | 17.5 - 17.4 | | | |

Table 11-3. continued 4;

| Site, layer / level, structure | samples | methods | lab. # | uncalBP | Std | Std% | calBP; 95,4% | P % | wuncalBP | wStd | wcalBP (ka) | R | References | Comments |
|---|---|---|---|---|---|---|---|---|---|---|---|---|---|---|
| Mezhyrich | burnt bone | Conv | ГИН-2597 | 11700 | 800 | 6,84 | 16409 - 11818 | | | | | 1 | Sinitsyn et al. 1997 | Mezhyrich industry |
| Mezhyrich | *Mammuthus primigenius*, bone | AMS | OxA-709 | 12900 | 200 | 1,55 | 16070 - 14591 | | | | | 1 | Svezhentsev, Popov 1993 | Mezhyrich industry |
| Mezhyrich, cultural layer (?) | burnt bone | Conv | QC-900 | 15245 | 1080 | 7,08 | 21743 - 15980 | | | | | 1 | Svezhentsev, Popov 1993 | Mezhyrich industry |
| Mezhyrich, cultural layer (?) | burnt bone | Conv | Ki-1055 | 18020 | 600 | 3,33 | 23278 - 20408 | | | | | 1 | Sinitsyn et al. 1997 | Mezhyrich industry |
| Mezhyrich, cultural layer (1976) | burnt bone | Conv | Ki-1056 | 18470 | 550 | 2,98 | 23741 - 21050 | | | | | 1 | Sinitsyn et al. 1997 | Mezhyrich industry |
| Mezhyrich, dwelling #1 | обпалена кістка | Conv | QC-897 | 14320 | 270 | 1,88 | 18211 - 16771 | | | | | 1 | Soffer 1985 | Mezhyrich industry |
| Mezhyrich, dwelling #1 | *Vulpes lagopus*, tibia | AMS | SacA-14982 | 14400 | 90 | 0,63 | 17886 - 17312 | * | | | | | Haesaerts et al, 2015 | Mezhyrich industry |
| Mezhyrich, dwelling #1 | *Canis Lupus*, femur | AMS | GrA-22501 | 14450 | 90 | 0,62 | 17923 - 17352 | * | | | | | Haesaerts et al, 2015 | Mezhyrich industry |
| Mezhyrich, dwelling #1 | burnt bone | Conv | Ki-1057 | 19100 | 500 | 2,61 | 24263 - 22050 | | | | | 1 | Sinitsyn et al. 1997 | Mezhyrich industry |
| Mezhyrich, dwelling #1 | *Mammuthus primigenius*, bone | Conv | Ki-1058 | 19280 | 600 | 3,11 | 24893 - 22090 | | | | | 1 | Sinitsyn et al. 1997 | Mezhyrich industry |
| | | | | | | | | ***69.4** | **14425** | **64** | **17.7 - 17.5** | | | |
| Mezhyrich, dwelling #2 | *Canis Lupus*, femur | AMS | OxA-13044, idem GrA-22094 | 14380 | 60 | 0,42 | 17815 - 17337 | * | | | | | Haesaerts et al. 2015 | Mezhyrich industry |
| Mezhyrich, dwelling #2 | *Mammuthus primigenius*, bone | AMS | OxA-712 | 14400 | 250 | 1,74 | 16988 - 18225 | | | | | 1 | Svezhentsev, Popov 1993 | Mezhyrich industry |
| Mezhyrich, dwelling #2 | burnt bone | Conv | ГИН-2595 | 14530 | 300 | 2,06 | 16982 - 18619 | | | | | 1 | Sinitsyn et al. 1997 | Mezhyrich industry |
| Mezhyrich, dwelling #2 | *Canis Lupus*, femur | AMS | GrA-22094, idem OxA-13044 | 14600 | 110 | 0,75 | 18181 - 17461 | * | | | | | Haesaerts et al, 2015 | Mezhyrich industry |
| | | | | | | | | ***7.9** | **14430** | **53** | **17.7 - 17.5** | | | |
| Mezhyrich, dwelling #3 | bone | AMS | AA-1317 | 14420 | 190 | 1,32 | 18138 - 17097 | | | | | | Sinitsyn et al. 1997 | Mezhyrich industry |
| Mezhyrich, dwelling #3 | *Mammuthus primigenius*, tooth | Conv | ГИН-2593 | 14700 | 500 | 3,40 | 19056 - 16611 | | | | | 1 | Sinitsyn et al. 1997 | Mezhyrich industry |

Table 11-3. continued 5;

| Site, layer / level, structure | samples | methods | lab. # | uncalBP | Std | Std% | calBP; 95,4% | P % | wuncalBP | wStd | wcalBP (ka) | R | References | Comments |
|---|---|---|---|---|---|---|---|---|---|---|---|---|---|---|
| Mezhyrich, dwelling #4 | burnt bone | Conv | ГИН-2596 | 14300 | 300 | 2,09 | 18221 - 16641 | | | | | 1 | Soffer 1985 | Mezhyrich industry |
| Mezhyrich, dwelling #4 | *Mammuthus primigenius*, femur | Conv | GrN-29876 | 14550 | 70 | 0,48 | 18059 - 17435 | * | | | | | Haesaerts et al. 2015 | Mezhyrich industry |
| Mezhyrich, dwelling #4 | *Mammuthus primigenius*, femur | Conv | GrN-29877, idem OxA-15587 | 14560 | 70 | 0,48 | 18083 - 17450 | * | | | | | Haesaerts et al. 2015 | Mezhyrich industry |
| Mezhyrich, dwelling #4 | *Mammuthus primigenius*, femur | AMS | OxA-15587 | 14790 | 60 | 0,41 | 18245 - 17928 | * | | | | | Haesaerts et al. 2015 | Mezhyrich industry |
| Mezhyrich, dwelling #4 | *Canis Lupus*, femur | AMS | SacA-14981 | 15210 | 130 | 0,86 | 18763 - 18252 | | | | | | Haesaerts et al. 2015 | Mezhyrich industry |
| Mezhyrich, dwelling #4 / cultural layer (?) | burnt bone | Conv | Ki-1054 | 17855 | 950 | 5,32 | 24115 - 19489 | | | | | 1 | Sinitsyn et al. 1997 | Mezhyrich industry |
| | | | | | | | | ***1** | **14650** | **38** | **18.1 - 17.9** | | | |
| Mezhyrich, pit #6 | charcoal | AMS | SacA-11487 | 14600 | 60 | 0,41 | 18149 - 17540 | * | | | | | Haesaerts et al. 2015 | Mezhyrich industry |
| Mezhyrich, pit #6 | charcoal | AMS | SacA-11486, idem SacA-11176, GrA-38787 | 14610 | 60 | 0,41 | 18162 - 17571 | * | | | | | Haesaerts et al. 2015 | Mezhyrich industry |
| Mezhyrich, pit #6 | *Mammuthus primigenius*, bone | AMS | GrA-38810, idem SacA-11777 | 14750 | 50 | 0,34 | 18222 - 17907 | * | | | | | Haesaerts et al. 2015 | Mezhyrich industry |
| Mezhyrich, pit #6 | *Mammuthus primigenius*, bone | AMS | SacA-11177, idem GrA-38810 | 14810 | 90 | 0,61 | 18266 - 17884 | * | | | | | Haesaerts et al. 2015 | Mezhyrich industry |
| Mezhyrich, pit #6 | *Canis Lupus*, bone | AMS | SacA-12040 | 15320 | 90 | 0,59 | 18820 - 18290 | | | | | | Haesaerts et al. 2015 | Mezhyrich industry |
| | | | | | | | | ***6.6** | **14682** | **30** | **18.1 - 17.9** | | | |
| Mezhyrich, trampling zone 3B, upper level | *Mammuthus primigenius*, bone | AMS | GrA-66076 | 14660 | 70 | 0,48 | 18212 - 17746 | * | | | | | Tsvirkun, Shydlovskyi 2022 | Mezhyrich industry |
| Mezhyrich, trampling zone 3A, upper level | *Mammuthus primigenius*, bone | AMS | GrA-66078 | 14730 | 70 | 0,48 | 18221 - 17858 | * | | | | | Tsvirkun, Shydlovskyi 2022 | Mezhyrich industry |
| | | | | | | | | ***48** | **14695** | **49** | **18.1 - 17.9** | | | |
| Mezhyrich, pit #7 | *Mammuthus primigenius*, femur | AMS | GrA-38787, idem SacA-11176, 14986 | 14590 | 60 | 0,41 | 18130 - 17515 | | | | | | Haesaerts et al. 2015 | Mezhyrich industry |
| Mezhyrich, pit #7 | *Mammuthus primigenius*, femur | AMS | SacA-11176, idem SacA-14986, GrA-38787 | 15030 | 90 | 0,60 | 18647 - 18191 | | | | | | Haesaerts et al. 2015 | Mezhyrich industry |
| Mezhyrich, pit #7 | *Mammuthus primigenius*, femur | AMS | SacA-14986, idem SacA-11176, GrA-38787 | 15430 | 90 | 0,58 | 18898 - 18337 | | | | | | Haesaerts et al. 2015 | Mezhyrich industry |

Table 11-3. continued 6;

| Site, layer / level, structure | samples | methods | lab. # | uncalBP | Std | Std% | calBP; 95,4% | P % | wuncalBP | wStd | wcalBP (ka) | R | References | Comments |
|---|---|---|---|---|---|---|---|---|---|---|---|---|---|---|
| Mezhyrich, pit #8 | *Mammuthus primigenius*, bone | AMS | SacA-12041, idem SacA-14984, 12259 | 14830 | 90 | 0,61 | 18277 - 17891 | * | | | | | Haesaerts et al. 2015 | Mezhyrich industry |
| Mezhyrich, pit #8 | *Mammuthus primigenius*, bone | AMS | SacA-14984, idem SacA-12041,12259 | 14920 | 90 | 0,60 | 18620 - 17985 | * | | | | | Haesaerts et al. 2015 | Mezhyrich industry |
| Mezhyrich, pit #8 | *Mammuthus primigenius*, bone | AMS | SacA-12259, idem SacA-12041,14984 | 14970 | 90 | 0,60 | 18642 - 18106 | * | | | | | Haesaerts et al. 2015 | Mezhyrich industry |
| | | | | | | | | ***53.7** | **14907** | **52** | **18.3 - 18.2** | | | |
| Mizyn | bone | AMS | MAMS-49908 | 14170 | 60 | 0,42 | 17383 - 17066 | | | | | | Chabai et al. 2022 | Mizyn industry |
| Mizyn | *Canis Lupus*, bone | AMS | OxA-13825 | 14450 | 70 | 0,48 | 17874 - 17383 | * | | | | | Germonpre et al. 2017 | Mizyn industry |
| Mizyn | bone | AMS | MAMS-49907 | 14540 | 60 | 0,41 | 18004 - 17440 | * | | | | | Chabai et al. 2022 | Mizyn industry |
| Mizyn | *Canis Lupus*, calcaneum bone | AMS | GrA-22499 | 14560 | 90 | 0,62 | 18125 - 17437 | * | | | | | Nuzhnyi 2008b | Mizyn industry |
| | | | | | | | | ***52.6** | **14514** | **41** | **17.8 - 17.6** | | | |
| Mizyn | *Mammuthus primigenius*, tooth | Conv | OxA-719 | 15100 | 200 | 1,32 | 18825 - 18021 | * | | | | 9 | Sviezhentsev, 1993 | Mizyn industry |
| Mizyn | bone | AMS | SPb-662 | 15340 | 300 | 1,95 | 18083 - 19375 | * | | | | 1 | Khlopachev 2016 | Mizyn industry |
| Mizyn | *Canis Lupus*, mandible | AMS | Ki-11084 | 15600 | 250 | 1,60 | 18291 - 19481 | * | | | | 1 | | Nuzhnyi 2008b |
| | | | | | | | | *29.3 | 15305 | 139 | 18.7 - 18.5 | | | |
| Mizyn | *Mammuthus primigenius*, tooth | Conv | ГИН-4 | 21600 | 2200 | 10,19 | 21425 - 33992 | | | | | 1 | Soffer 1985 | Mizyn industry |
| Mizyn | *Mammuthus primigenius*, tooth | Conv | KI-1051 | 27500 | 800 | 2,91 | 30248 - 33853 | | | | | 1 | Soffer 1985 | Mizyn industry |
| Mizyn | shells | Conv | KI-1052 | 29100 | 700 | 2,40 | 31732 - 35047 | | | | | 1 | Soffer 1985 | Mizyn industry |
| Mizyn | shells | Conv | KI-1053 | 29700 | 800 | 2,69 | 32119 - 35919 | | | | | 1 | Soffer 1985 | Mizyn industry |
| Pushkari IX, 1 | *Ovibos moschatus*, tooth | Conv | KI-13078 | 11060 | 140 | 1,27 | 12743 - 13228 | | | | | | Khlopachev 2011. | Yudinovo industry |
| Pushkari IX, 1 | *Mammuthus primigenius*, tooth | Conv | ЛЕ-6961 | 11500 | 400 | 3,48 | 12700 - 14819 | | | | | 1 | Khlopachev 2011. | Yudinovo industry |
| Pushkari IX, 1 | *Mammuthus primigenius*, tooth | Conv | KI-13079 | 11700 | 250 | 2,14 | 13093 - 14181 | | | | | 1 | Khlopachev 2011. | Yudinovo industry |
| Pushkari IX, 1 | *Mammuthus primigenius*, tooth | Conv | KI-11900 | 17200 | 250 | 1,45 | 20128 - 21656 | | | | | 5 | Khlopachev 2011. | Yudinovo industry |

Table 11-3. continued 7;

| Site, layer / level, structure | samples | methods | lab. # | uncalBP | Std | Std% | calBP; 95,4% | P % | wuncalBP | wStd | wcalBP (ka) | R | References | Comments |
|---|---|---|---|---|---|---|---|---|---|---|---|---|---|---|
| Pushkari IX, 2 | *Ovibos moschatus*, tooth | AMS | Hela-1517 | 14770 | 115 | 0,78 | 18282 – 17751 | * | | | | | Khlopachev 2011. | Yudinovo industry |
| Pushkari IX, 2 | *Mammuthus primigenius*, tooth | AMS | OxA-17799 | 14820 | 60 | 0,41 | 18258 – 17961 | * | | | | | Khlopachev 2011. | Yudinovo industry |
| | | | | | | | | ***70** | **14809** | **53** | **18.2 – 18.1** | | | |
| Samotoevka | bones | Conv | ЛЕ-8566 | 13800 | 350 | 2,53 | 17801 – 15760 | | | | | 1 | Bessudnov, Bessudnov 2012 | Samotoevka |
| Samotoevka | mammalian bones | Conv | ЛЕ-9104 | 13820 | 120 | 0,87 | 17071 – 16378 | | | | | | Bessudnov, Bessudnov 2012 | Samotoevka |
| Samotoevka | horse bones | AMS | ГИН-12852 | 14730 | 100 | 0,68 | 18252 – 17771 | | | | | | Bessudnov, Bessudnov 2012 | Samotoevka |
| Samotoevka | mammalian bones | Conv | ЛЕ-8657***** | 15600 | 550 | 3,52 | 20420 – 17782 | | | | | 1 | Bessudnov, Bessudnov 2012 | Samotoevka |
| Samotoevka, hearth | sediments with charcoal | AMS | ГИН-12851 | 15900 | 150 | 0,94 | 19527 –18889 | | | | | | Bessudnov, Bessudnov 2012 | Samotoevka |
| Semenivka 1 | *Ursus arctos*, femur | AMS | GrA-22469, idem Ki-5510 | 13440 | 90 | 0,67 | 16485 – 15897 | * | | | | | Nuzhnyi 2015 | Mezhyrich industry |
| Semenivka 1 | *Ursus arctos*, femur | Conv | KI-5510, idem GrA-22469 | 13600 | 160 | 1,18 | 16971 – 15984 | * | | | | | Nuzhnyi 2015 | Mezhyrich industry |
| | | | | | | | | ***38.3** | **13478** | **78** | **16.4 – 16.1** | | | |
| Semenivka 2 | *Mammuthus primigenius*, rib | Conv | KI-5509 | 14200 | 180 | 1,27 | 17885 – 16778 | | | | | 6 | Nuzhnyi 2015 | Mezhyrich industry |
| Semenivka 3 | *Cervidae*, bone | AMS | GrA-22471 | 13690 | 90 | 0,66 | 16915 – 16291 | | | | | 6 | Nuzhnyi 2015 | Mezhyrich industry |
| Suponevo | *Mammuthus primigenius*, tooth | Conv | ГИН-3381 | 13500 | 100 | 0,74 | 16601 – 15968 | | | | | | Sinitsyn et al. 1997 | Suponevo industry |
| Suponevo | *Mammuthus primigenius*, bone | Conv | ГИН-7729А | 13920 | 140 | 1,01 | 17332 – 16490 | | | | | | Sinitsyn et al. 1997 | Suponevo industry |
| Suponevo | *Mammuthus primigenius*, tooth | Conv | ГИН-3719 | 14260 | 120 | 0,84 | 17792 – 17052 | | | | | | Sinitsyn et al. 1997 | Suponevo industry |
| Timonovka 1 | *Mammuthus primigenius*, tooth | Conv | ИГАН-86 | 12200 | 300 | 2,45 | 15248 – 13501 | | | | | 1 | Abramova et al. 2001 | Yudinovo industry |
| Timonovka 1 | *Mammuthus primigenius*, tooth | Conv | ГИН-8414 | 14530 | 120 | 0,82 | 18138 – 17391 | * | | | | | Abramova et al. 2001 | Yudinovo industry |
| Timonovka 1 | *Mammuthus primigenius*, tooth | Conv | ГИН-8413 | 14750 | 120 | 0,81 | 18275 – 17586 | * | | | | | Abramova et al. 2001 | Yudinovo industry |
| Timonovka 1 | burnt bone | Conv | ГИН-2003 | 15300 | 700 | 4,58 | 20461 – 17005 | | | | | 1 | Abramova et al. 2001 | Yudinovo industry |
| | | | | | | | | ***19.5** | **14640** | **85** | **18.1 – 17.8** | | | |

Table 11-3. continued 8;

| Site, layer / level, structure | samples | methods | lab. # | uncalBP | Std | Std% | calBP; 95,4% | P % | wuncalBP | wStd | wcalBP (ka) | R | References | Comments |
|---|---|---|---|---|---|---|---|---|---|---|---|---|---|---|
| Timonovka II | bone | Conv | ЛУ-358 | 15110 | 530 | 3,51 | 19610 – 17065 | | | | | 1 | Velichko et al. 1997 | Yudinovo industry |
| Yeliseevychi I, bone concentration 5 | *Mammuthus primigenius*, tooth | Conv | ЛУ-360 | 17340 | 170 | 0,98 | 21414 – 20510 | | | | | 8 | Svezhentsev, Popov 1993 | Yeliseevychi industry |
| Yeliseevychi I, permafrost wedge ("passage") | *Mammuthus primigenius*, rib | AMS | SPb-1766 | 12239 | 150 | 1,22 | 14901 – 13801 | | | | | 8 | Khlopachev et al. 2017 | Yeliseevychi industry |
| Yeliseevychi I, permafrost wedge | *Mammuthus primigenius*, bone | AMS | SPb-1767 | 13300 | 200 | 1,50 | 16599 – 15380 | | | | | 8 | Khlopachev et al. 2017 | Yeliseevychi industry |
| Yeliseevychi I, pit 1 | *Mammuthus primigenius*, tooth | Conv | ГИН-4137 | 12630 | 360 | 2,85 | 16011 – 13805 | | | | | 1; 5 | Velichko et al. 1997 | Yeliseevychi industry |
| Yeliseevychi I, pit 1 | *Mammuthus primigenius*, tooth | Conv | ГИН-4138 | 16850 | 120 | 0,71 | 20696 – 20026 | | | | | 5 | Velichko et al. 1997 | Yeliseevychi industry |
| Yeliseevychi I, pit 2 | *Mammuthus primigenius*, tooth | AMS | ИГАН-1134 | 15370 | 195 | 1,27 | 18250 – 19008 | | | | | 8 | Khlopachev et al. 2017 | Khlopachev et al. 2017 |
| Yeliseevychi I, pit 3 | *Mammuthus primigenius*, tooth | AMS | ИГАН-1133 | 13100 | 330 | 2,52 | 16827 – 14510 | | | | | 1 | Khlopachev et al. 2017 | Yeliseevychi industry |
| Yeliseevychi I, ashy zone | burnt bone | Conv | ГИН-4135 | 14080 | 70 | 0,50 | 17359 – 16982 | * | | | | | Velichko et al. 1997 | Yeliseevychi industry |
| Yeliseevychi I, ashy zone | *Mammuthus primigenius*, tooth | AMS | ГИН-4139 | 14100 | 400 | 2,84 | 18225 – 16091 | | | | | 1 | Velichko et al. 1997 | Yeliseevychi industry |
| Yeliseevychi I, ashy zone | *Ursus sp.*, bone | AMS | SPb-1931 | 14113 | 120 | 0,85 | 17464 – 16798 | *, b | | | | | Khlopachev et al. 2017 | Yeliseevychi industry |
| Yeliseevychi I, ashy zone | *Canis Lupis*, bone | AMS | SPb-1932 | 14622 | 150 | 1,03 | 18216 – 17432 | *, b | | | | | Khlopachev et al. 2017 | Yeliseevychi industry |
| | | | | | | | | *0.4 | 14163 | 56 | 17.3 – 17.1 | | | |
| Yeliseevychi I, churingas storage | *Mammuthus primigenius*, bone | AMS | SPb-1933 | 13384 | 150 | 1,12 | 16569 – 15678 | | | | | | Khlopachev et al. 2017 | Yeliseevychi industry |
| Yeliseevychi I, churinga and figurine pit | *Canidae*, tooth | AMS | KIA-18760 | 13905 | 55 | 0,40 | 17058 – 16675 | b | | | | | Sablin, Khlopachev 2002 | Yeliseevychi industry |
| Yeliseevychi I, main layer (?) | *Mammuthus primigenius*, bone | AMS | SPb-1664 (664) | 14435 | 150 | 1,04 | 18115 – 17137 | | | | | 8 | Khlopachev et al. 2017 | Yeliseevychi industry |
| Yeliseevychi I, sq. 68-69 | burnt bone | AMS | ГИН-5475 | 14240 | 120 | 0,84 | 17774 – 17037 | b | | | | 8 | Velichko et al. 1997 | Yeliseevychi industry |
| Yeliseevychi I, sq. У,Т-73 | *Mammuthus primigenius*, tooth | Conv | ГИН-4186 | 14590 | 140 | 0,96 | 18195 – 17420 | | | | | 8 | Velichko et al. 1997 | Yeliseevychi industry |
| Yeliseevychi I, sq. 72 | bone | Conv | QC-889 | 15600 | 1350 | 8,65 | 22980 – 15816 | | | | | 1; 8 | Svezhentsev, Popov 1993 | Yeliseevychi industry |
| | | | | | | | | b2.9 | 14014 | 39 | 17.1 – 17.0 | 43 | | |

Table 11-3. continued 9;

| Site, layer / level, structure | samples | methods | lab. # | uncalBP | Std | Std% | calBP; 95,4% | P % | wuncalBP | wStd | wcalBP (ka) | R | References | Comments |
|---|---|---|---|---|---|---|---|---|---|---|---|---|---|---|
| Yeliseevychi I, unknown location | burnt bone | Conv | ЛУ-102 | 12970 | 140 | 1,08 | 15938 - 15131 | | | | | 8 | Svezhentsev, Popov 1993 | Yeliseevychi industry |
| Yeliseevychi I, unknown location | *Canis Lupus*, skull | AMS | Beta-192417 | 13370 | 70 | 0,52 | 16309 - 15851 | | | | | 8 | Khlopachev et al. 2013 | Yeliseevychi industry |
| Yeliseevychi I, unknown location | *Mammuthus primigenius*, tooth | Conv | ЛУ-126 | 14470 | 100 | 0,69 | 17995 - 17351 | | | | | 8 | Svezhentsev, Popov 1993 | Yeliseevychi industry |
| Yeliseevychi I, unknown location | *Mammuthus primigenius*, tooth | Conv | ГИН-4136, the same as ГИН-4186 | 14590 | 140 | 0,95 | 18195 - 17420 | | | | | 8 | Abramova et al. 2001 | Yeliseevychi industry |
| Yeliseevychi I, unknown location | *Mammuthus primigenius*, bone | AMS | SPb-1934 | 15995 | 120 | 0,75 | 19564 - 19005 | | | | | 8 | Khlopachev et al. 2017 | Yeliseevychi industry |
| Yeliseevychi I, unknown location | burnt bone | Conv | ЛЕ-450 | 20570 | 430 | 2,09 | 25737 - 23836 | | | | | 1; 8 | Abramova et al. 2001 | Yeliseevychi industry |
| Yeliseevychi I, unknown location | wood fragmnet | Conv | ГИН-80 | 33000 | 400 | 1,21 | 39073 - 36576 | | | | | 8; 9 | Iakovleva, Djindjian 2005 | Yeliseevychi industry |
| Yeliseevychi II | *Mammuthus primigenius*, tooth | Conv | ИГАН-556 | 15620 | 200 | 1,28 | 19432 - 18330 | | | | | 6 | Velichko et al. 1997 | Epigravettian |
| Yudinovo | burnt bone | AMS | AA-4803 the same as AA-4801 | 14470 | 160 | 1,11 | 18182 - 17167 | | | | | | Abramova et al. 2001 | |
| Yudinovo | *Mammuthus primigenius*, skull | AMS | SPb-775 | 15813 | 200 | 1,26 | 19556 - 18760 | | | | | 9 | Khlopachev 2016 | Yudinovo industry |
| Yudinovo | burnt bone | Conv | ЛЕ-3401**** | 18630 | 320 | 1,71 | 21870 - 23323 | | | | | 1 | Svezhentsev, Popov 1993; Khlopachev 2019b | Yudinovo industry |
| Yudinovo, upper layer | *Mammuthus primigenius*, tooth | AMS | SPb-2855 | 12060 | 135 | 1,12 | 14790 - 13528 | * | | | | | Khlopachev 2019b | Yudinovo industry |
| Yudinovo, upper layer | *Mammuthus primigenius*, tooth | AMS | SPb-2913 | 12070 | 120 | 0,99 | 14315 - 13606 | * | | | | | Khlopachev 2019b | Yudinovo industry |
| Yudinovo, upper layer | *Mammuthus primigenius*, tooth | AMS | SPb-2912 | 12157 | 120 | 0,99 | 14817 - 13771 | * | | | | | Khlopachev 2019b | Yudinovo industry |
| Yudinovo, upper layer | *Mammuthus primigenius*, bone | AMS | SPb-105 | 12200 | 200 | 1,63 | 15000 - 13612 | | | | | 1 | Khlopachev, Gribchenko 2012 | Yudinovo industry |
| Yudinovo, upper layer | *Mammuthus primigenius*, tooth | AMS | SPb-2893 | 12200 | 100 | 0,82 | 14812 - 13802 | * | | | | | Khlopachev 2019b | Yudinovo industry |
| Yudinovo, upper layer | *Mammuthus primigenius*, bone | AMS | SPb-537 | 12239 | 100 | 0,82 | 14837 - 13813 | * | | | | | Khlopachev 2019b | Yudinovo industry |
| Yudinovo, upper layer | *Mammuthus primigenius*, bone | AMS | SPb-573 | 12240 | 100 | 0,82 | 14838 - 13814 | * | | | | | Khlopachev 2019b | Yudinovo industry |

Table 11-3. continued 10;

| Site, layer / level, structure | samples | methods | lab. # | uncalBP | Std | Std% | calBP; 95,4% | P % | wuncalBP | wStd | wcalBP (ka) | R | References | Comments |
|---|---|---|---|---|---|---|---|---|---|---|---|---|---|---|
| Yudinovo, upper layer | burnt bone | AMS | OxA-696 | 12300 | 200 | 1,62 | 15096 - 13798 | | | | | 1 | Svezhentsev, Popov 1993; Khlopachev 2019b | Yudinovo industry |
| Yudinovo, upper layer | *Mammuthus primigenius*, кістка | AMS | SPb-107 | 12350 | 80 | 0,65 | 14856 - 14090 | * | | | | | Khlopachev, Gribchenko 2012; Khlopachev 2019b | Yudinovo industry |
| Yudinovo, upper layer | *Mammuthus primigenius*, кістка | AMS | SPb-106 | 12500 | 95 | 0,76 | 15125 - 14264 | * | | | | | Khlopachev, Gribchenko 2012; Khlopachev 2019b | Yudinovo industry |
| | | | | | | | | ***6.0** | **12259** | **36** | **14.3 - 14.1** | | | |
| Yudinovo, lower layer | burnt bone | AMS | ЛЕ-5518 | 12850 | 200 | 1,56 | 15997 - 14497 | | | | | 1 | Khlopachev 2019b | Yudinovo industry |
| Yudinovo, lower layer | *Mammuthus primigenius*, bone | AMS | SPb-104 | 12900 | 200 | 1,55 | 16070 - 14591 | | | | | 1 | Khlopachev 2019b | Yudinovo industry |
| Yudinovo, lower layer | *Mammuthus primigenius*, bone | AMS | SPb-1768*** | 12943 | 100 | 0,77 | 15774 - 15191 | | | | | | Khlopachev 2019b | Yudinovo industry |
| Yudinovo, lower layer | *Mammuthus primigenius*, bone | AMS | SPb-103 | 12943 | 140 | 1,08 | 15898 - 15094 | | | | | | Khlopachev 2019b | Yudinovo industry |
| Yudinovo, lower layer | *Mammuthus primigenius*, bone | AMS | SPb-1768 | 12950 | 140 | 1,08 | 15909 - 15105 | | | | | | Khlopachev 2019b | Yudinovo industry |
| | | | | | | | | ***99.9** | **12945** | **70** | **15.6 - 15.4** | | | |
| Yudinovo, lower layer | burnt bone | AMS | ЛЕ-5519 | 13200 | 200 | 1,52 | 16435 - 15265 | | | | | 1 | Khlopachev 2019b | Yudinovo industry |
| Yudinovo, lower layer | burnt bone | AMS | OxA-695 | 13300 | 200 | 1,50 | 16599 - 15380 | * | | | | | Svezhentsev, Popov 1993; Khlopachev 2019b | Yudinovo industry |
| Yudinovo, lower layer | *Mammuthus primigenius*, tooth | Conv | ЛУ-153 | 13650 | 200 | 1,47 | 17074 - 15922 | * | | | | | Boriskovsky 1984; Khlopachev 2019b | Yudinovo industry |
| Yudinovo, lower layer | burnt bone | Conv | ЛЕ-3303 ** | 13720 | 210 | 1,53 | 17277 - 15999 | | | | | 1 | Svezhentsev, Popov 1993; Khlopachev 2019b | Yudinovo industry |
| Yudinovo, lower layer | bone | AMS | SPb-1770 | 13720 | 120 | 0,88 | 17003 - 16278 | * | | | | | Khlopachev 2019b | Yudinovo industry |
| Yudinovo, lower layer | burnt bone | Conv | ЛУ-103 | 13830 | 850 | 6,15 | 18932 - 14231 | | | | | 1 | Boriskovsky 1984; Khlopachev 2019b | Yudinovo industry |
| Yudinovo, lower layer | *Mammuthus primigenius*, tooth | AMS | SPb-1769 | 13835 | 100 | 0,72 | 17061 - 16466 | * | | | | | Khlopachev 2019b | Yudinovo industry |
| Yudinovo, lower layer | *Mammuthus primigenius*, bone | Conv | ISGS-2085 | 13980 | 110 | 0,79 | 17338 - 16644 | * | | | | | Abramova et al. 2001. | Yudinovo industry |
| Yudinovo, lower layer | burnt bone | AMS | ИГАН-1266 | 13980 | 180 | 1,29 | 17432 - 16405 | * | | | | | Khlopachev, Gribchenko 2012; Khlopachev 2019b | Yudinovo industry |
| | | | | | | | | ***5.1** | **13806** | **55** | **16.9 - 16.6** | | | |

Table 11-3. continued 11;

| Site, layer / level, structure | samples | methods | lab. # | uncalBP | Std | Std% | calBP; 95,4% | P % | wuncalBP | wStd | wcalBP (ka) | R | References | Comments |
|---|---|---|---|---|---|---|---|---|---|---|---|---|---|---|
| Yudinovo, lower layer | *Mammuthus primigenius*, tooth | AMS | ИГАН-1270 | 14010 | 230 | 1,64 | 17759 - 16354 | | | | | 1 | Khlopachev, Gribchenko 2012; Khlopachev 2019b | Yudinovo industry |
| Yudinovo, lower layer | burnt bone | Conv | ISGS-2084 | 14300 | 110 | 0,77 | 17808 - 17085 | * | | | | | Abramova et al. 2001; Khlopachev 2019b | Yudinovo industry |
| Yudinovo, lower layer | bone | AMS | AA-4801 | 14470 | 160 | 1,11 | 18182 - 17167 | * | | | | | Abramova et al. 2001; Khlopachev 2019b | Yudinovo industry |
| Yudinovo, lower layer | burnt bone | AMS | Beta-199779 | 14480 | 80 | 0,55 | 17935 - 17382 | * | | | | | Khlopachev, Gribchenko 2012; Khlopachev 2019b | Yudinovo industry |
| Yudinovo, lower layer | burnt bone | Conv | ГИН-5588 | 14500 | 200 | 1,38 | 18214 - 17137 | * | | | | | Abramova et al. 2001; Khlopachev 2019b | Yudinovo industry |
| Yudinovo, lower layer | burnt bone | Conv | ГИН-5661 | 14610 | 60 | 0,41 | 18162 - 17571 | * | | | | | Abramova et al. 2001; Khlopachev 2019b | Yudinovo industry |
| Yudinovo, lower layer | burnt bone | AMS | AA-4802 | 14650 | 105 | 0,72 | 18212 - 17526 | * | | | | | Abramova et al. 2001; Khlopachev 2019b | Yudinovo industry |
| | | | | | | | | *15.7 | 14535 | 39 | 17.9 - 17.6 | | | |
| Yudinovo, lower layer | *Mammuthus primigenius*, bone | AMS | OxA-21004 | 14715 | 65 | 0,44 | 18212 - 17851 | * | | | | | Khlopachev 2019b | Yudinovo industry |
| Yudinovo, lower layer | *Mammuthus primigenius*, bone | AMS | SPb-777 | 14800 | 120 | 0,81 | 18576 - 17774 | * | | | | | Khlopachev 2019b | Yudinovo industry |
| Yudinovo, lower layer | *Mammuthus primigenius*, tooth | AMS | OxA-21033 | 14820 | 60 | 0,41 | 18258 - 17961 | * | | | | | Khlopachev 2019b | Yudinovo industry |
| Yudinovo, lower layer | *Mammuthus primigenius*, tooth | AMS | OxA-21005 | 14840 | 65 | 0,44 | 18269 - 17970 | * | | | | | Khlopachev 2019b | Yudinovo industry |
| Yudinovo, lower layer | *Mammuthus primigenius*, tooth | Conv | ЛЕ-3835 | 14870 | 150 | 1,01 | 18645 - 17790 | * | | | | | Abramova et al. 2001; Khlopachev 2019b | Yudinovo industry |
| Yudinovo, lower layer | *Mammuthus primigenius*, tooth | AMS | OxA-21006 | 14910 | 65 | 0,44 | 18589 - 18069 | * | | | | | Khlopachev 2019b | Yudinovo industry |
| Yudinovo, lower layer | *Mammuthus primigenius*, tooth | AMS | OxA-21007 | 14955 | 65 | 0,44 | 18611 - 18160 | * | | | | | Khlopachev 2019b | Yudinovo industry |
| | | | | | | | | *22.3 | 14845 | 27 | 18,2 | | | |
| Yudinovo, lower layer | *Mammuthus primigenius*, bone | Conv | ЛУ-127 | 15660 | 180 | 1,15 | 19445 - 18651 | | | | | 9 | Boriskovsky 1984; Khlopachev 2019b | Yudinovo industry |
| Yudinovo, lower layer | bone | Conv | ЛЕ-3301 | 15790 | 320 | 2,03 | 19896 - 18306 | | | | | 1 | Svezhentsev, Popov 1993; Khlopachev 2019b | Yudinovo industry |
| Yudinovo, lower layer | burnt bone | Conv | ЛЕ-3302* | 17800 | 810 | 4,55 | 23735 - 19631 | | | | | 1 | Svezhentsev, Popov 1993; Khlopachev 2019b | Yudinovo industry |

Table 11-3. continued 12; see *notes on the next page.

Table 11-3. *notes.

* in Khlopachev 2019b, ЛЕ-3302 is mentioned as the date for Yudinovo, lower layer with the value 14980±110

** in Khlopachev 2019b, ЛЕ-3303 is mentioned as the date for Yudinovo lower layer with the value 13380±160

*** in Khlopachev 2019b, two different values are mentioned under this lab number: 12950±140 and 12943±100

**** in Khlopachev 2019b, ЛЕ-3401 is mentioned as the date for Yudinovo, lower layer with the value 12980±320

***** in Bessudnov 2013, the lab number ЛЕ-8657 is mentioned as ЛЕ-8567

### *Artefacts*

In the artefact assemblage, multiple transversal and dihedral burins play the main role. In addition, there are simple end-scrapers on blade and rounded end-scrapers on flakes. Interestingly, geometrical microliths resembling the triangles from Byki are also present (Bessudnov 2013: 134).

### *Chronology*

The five available radiocarbon dates are made on bulk samples (Table 11-3). They cannot be aggregated to a weighted average and if those with comparatively small standard deviation are selected range between 19.5 and 16.4 ka calBP (Table 11-3; Fig. 11-9). Bessudnov preferred an age range between 19-18 ka calBP. The absence of backed bladelets or micro-blades, microgravette points, and burins on truncated blades on the one hand, and the presence of triangles and a dominance of marginally irregularly retouched items on the other, set the assemblage of Samotoevka apart from the other complexes traditionally assigned to the Epigravettian in Eastern Europe.

## Mizyn industry

The taxonomic unit Mizyn industry comprises, besides the eponymous site, also Barmaky. The taxonomic definition of the Borschevo 1 assemblage is debatable. Straight-backed microgravette points, often in combination with a dorsally oblique retouch or truncated base, are the most characteristic tool type of this industry (Fig. 11-10, 1-39). For Barmaky, four recently obtained dates can be integrated in a weighted average and give an age estimate between 19.1-18.9 ka calBP (Table 11-3; Fig. 11-11; see Chapters 2 and 3 of this volume for a detailed description of stratigraphy and dates).

## Mizyn

Mizyn is situated in a gorge intersecting the loess plateau on the right bank of the Desna River. The maximum thickness of the loess deposits is about 6 m (Shovkoplias 1965: 27). The site was excavated on more than 1200 m² and two archaeological horizons, an upper and a lower one, were identified, which accumulated on a slope with 7-20° inclination. The upper horizon (about 10 cm thick) was documented in the entire excavated area and subdivided into five "household complexes". Each household complex is represented by a mammoth bones dwelling, internal and external fire-places, pits, and "production areas", characterised by concentrations of archaeological material (Shovkoplias 1965: 35-76). The lower horizon was observed in the western part of the site below the first household complex. The remains of the lower horizon were subdivided into pits I-V and concentration VII. In the area of the pits, the lower and upper horizons are separated by 15-25 cm sterile sediments of "striated loess" (Shovkoplias 1959; 1965: 81-92). The "striated loess" in the section of pit III (Shovkoplias 1965: 90, fig. 48) resembles solifluction lenses. Above the lower horizon in the area of pits I-IV, the "deepened hearths" of the upper horizon were found. Concentration VII is a 3-5 cm thick scatter of bones and lithic artefacts, separated from the upper horizon by 60 cm of sterile striated loess (Shovkoplias 1965: 81-90). According to Shovkoplias (1965: 90-92), the settlement of the lower horizon has been partly eroded.

### *Environment*

No traces of cryoturbation were observed at the site. The reported "striated loess" (Shovkoplias 1965: 90, fig. 48), however, likely signals episodes of solifluction. Archaeological evidence on vegetation comes from analysed charcoal from fire-places and indicates the presence of coniferous trees, willow, and even

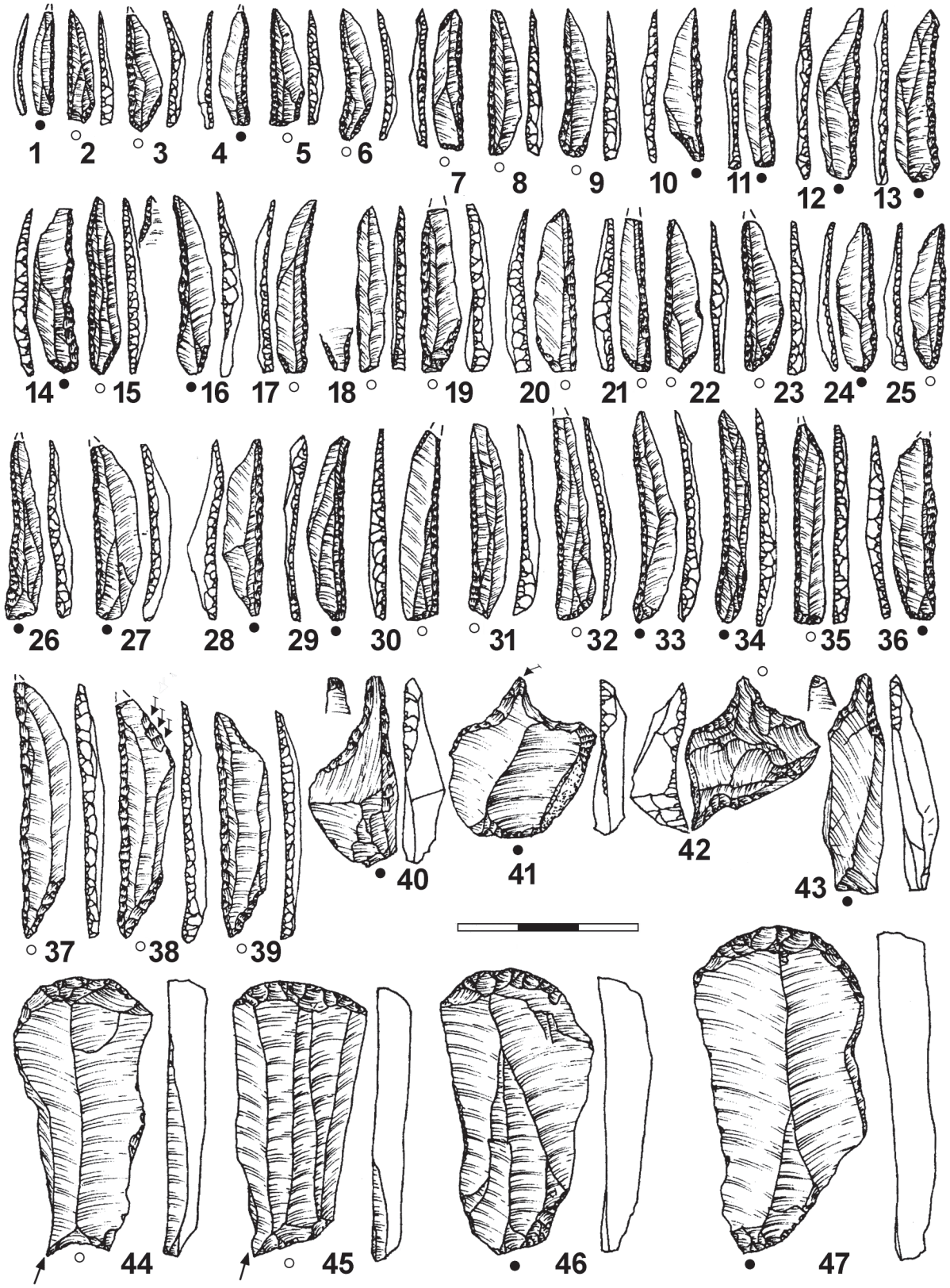


Fig. 11–10. Mizyn industry, artefacts from Mizyn: 1–39 – straight back microgravette points; 40–42 – borer / perforator on flakes; 43 – borer / perforator on blade; 44, 45 – end-scraper-burin on blades; 46–47 – end-scraper on blades; after Nuzhnyi 2015, fig. 113, 113-A, 115, 116.

oak in probably ecologically diverse landscapes with elements of tundra, steppe and scattered trees (Shovkoplias 1965: 104, 111). Despite the presence of two archaeological horizons, the fauna was published as a single complex. The faunal assemblage comprises mammoth (20% of identifiable bones), horse (19%), polar fox (19%), reindeer (14%), and wolf (10%). In addition, *Bison priscus, Ovibos moscatus, Ursus arctos, Gulo gulo, Lepus, Marmota bobak,* and *Dicrostonyx torquatus* are attested (Shovkoplias 1965: 97–101; Demay et al. 2017).

### *Artefacts*

An exceptionally rich collection of lithic and organic artefacts, figurines, adornments and perforated fossil shells, and potential music instruments was recovered from the site (Rudenko 1959; Shovkoplias 1965; Bibikov 1981; Iakovleva 2013: 63–65, 80–100; 121–127; Nuzhnyi 2015: 195–206). However, just as the faunal assemblage, the artefacts were also published as a single assemblage, without reference to the two horizons. Technologically, the blank production is based on two discrete reduction strategies, one for blades and another for bladelet and micro-blade production (Dudnyk 2024). The most characteristic tool types are straight-backed microgravette points with obliquely truncated bases, burins on obliquely truncated blades, simple end-scrapers on blades and flakes, frequently combined with burins on truncations and typologically variable perforators (Fig. 11-10).

### *Chronology*

Samples selected for radiocarbon dating are plagued with the problem that information about their stratigraphic and spatial origin is not available. Also, six of eleven samples have a comparatively high standard deviation (Table 11-3; Fig. 11-11). Three AMS-dates can be combined in a weighted average with an age estimate of between 17.8–17.6 ka calBP. One conventional and two AMS dates with large standard deviations, in contrast, give a weighted average between 18.7 and 18.5 ka calBP. These differences might reflect the site's multi-layered character

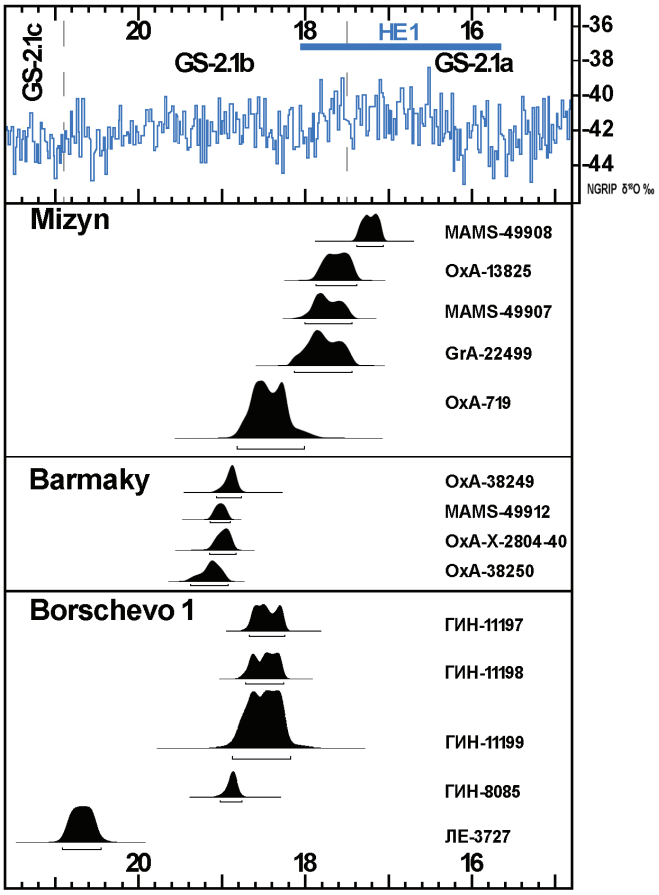


Fig. 11-11. Chronology of the Mizyn industry and Borschevo 1.

## Borschevo 1 debates

The site was found on the slope of a small ravine of the Don River drainage system. This slope contains the remnants of 1st and 2nd river terraces. Borschevo 1 was excavated through about 40 sondages with a total area of about 400 m², but without establishing a correlation between the observed cultural deposits in the different trenches (Rogachev, Kudryashov 1982: 211; Lisitsyn, Dudin 2019: 90). The roughly 5000 artefacts originate from the contact zone between the modern soil and silty loess sediments, making the *in situ* status of this assemblage highly questionable (Lisitsyn, Dudin 2019: 90). The faunal assemblage is composed of horse, mammoth, wolf, woolly rhinoceros, marten, lynx, and also red deer, a rather temperate species (Rogachev, Kudryashov 1982: 216).

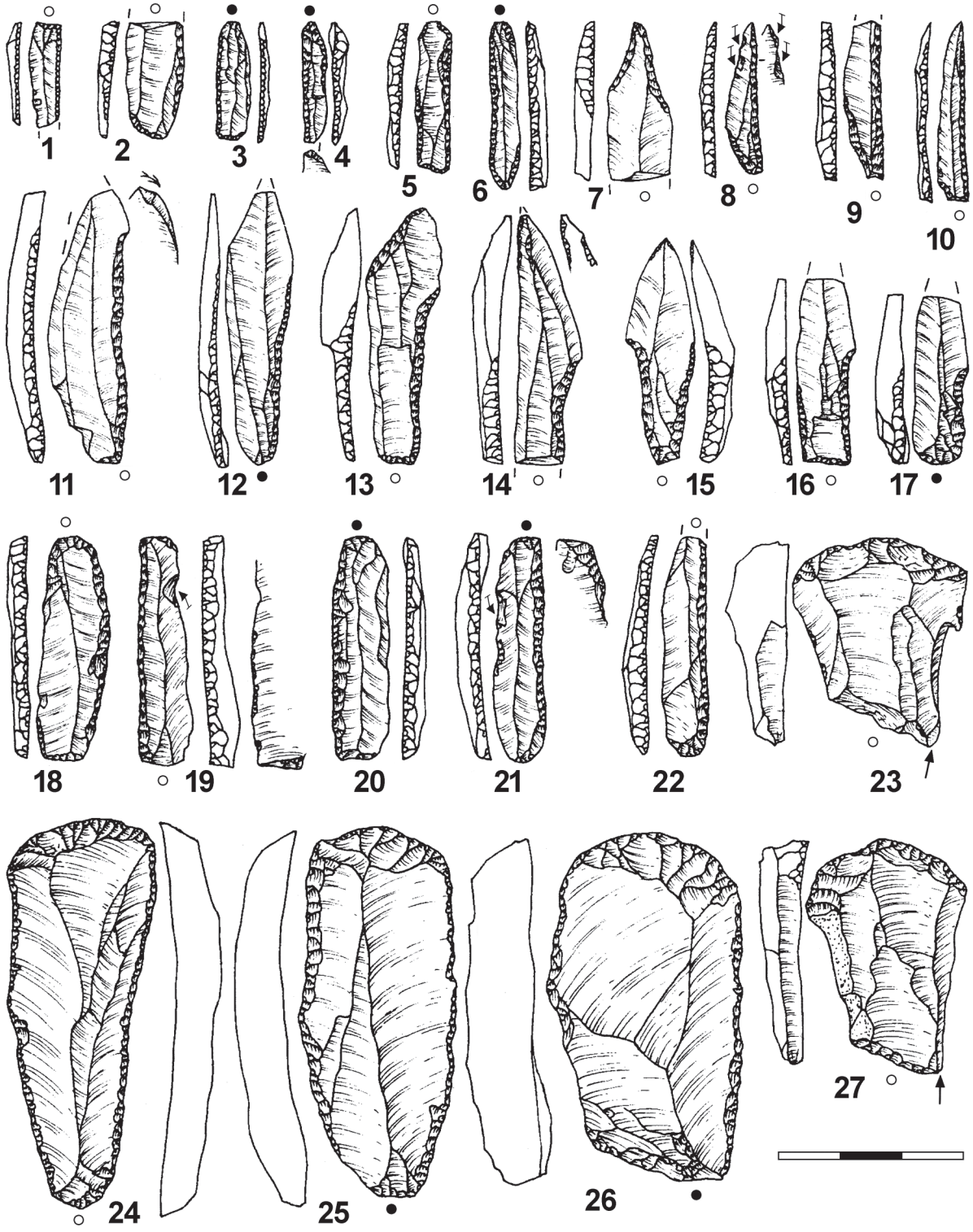


Fig. 11–12. Artefacts from Borschevo 1: 1–6, 18–22 – rectangles; 7 – borer/perforator on bladelet; 8–10 – straightly backed microgravette points with obliquely truncated base; 11–17 – shouldered points; 23, 27 end-scraper-burins; 24–26 – end-scrapers; after Nuzhnyi 2015, fig. 198, 201.

### *Artefacts and taxonomic attribution*

Anikovich (1998) pools the assemblages of Mizyn and Borschevo 1 under the term "Mizyn culture", based on the typological similarities, namely the presence of double burins on bi-terminally truncated blades, combined burins and end-scrapers, backed bladelets, rectangles on bladelets, straight-backed microgravette points with a truncated base, so-called "Chatelperronian knives" and shouldered points (Fig. 11-12). Later, Lisitsyn and Dudin (2019: 92) convincingly demonstrate that double burin types and combined burins and end-scrapers are related to tool rejuvenation processes, but should not be used as attributes for taxonomic differentiation of assemblages. Moreover, "Chatelperronian knives" (i.e. lanceolate backed points on blades), shouldered points, and rectangles are not characteristic for the assemblage from Mizyn (Nuzhnyi 2015: 207, 210). Shouldered points are, in contrast, the characteristic type of the Gmelin complex (Lisitsyn, Dudin 2019: 92). The only diagnostic typological element the two assemblages have in common is straight-backed microgravette points with a truncated base. In sum, the assemblage of Borschevo 1 does not originate from an *in situ* position, but comes from different topographic locations and contains a mixture of stylistically different artefacts. Therefore, it cannot be assigned to any taxonomic unit (Lisitsyn, Dudin 2019: 89-92).

### *Chronology*

Most of the available, conventional radiocarbon dates on mammoth bones align with the Mizyn industry chronology, except for the sample ЛЕ-3727 (Table 11-3; Fig. 11-11). A weighted average of three dates results in an age estimate between 18.6 and 18.3 ka calBP.

## Mezhyrich industry

The industry is named after its eponymous site Mezhyrich, currently the best analysed assemblage among the Epigravettian localities in the Mid-Dnieper basin and famous for its dwelling structures. Other important sites associated with this industry are Semenivka 1-3, Dobranichivka, Buzhanka 2, and Gintsy. Characteristic lithic tools are lanceolate microgravette points and rectangles on bladelets and micro-blades, and, like in the Yudinovo industry (see below), and this is a less distinctive short double and rounded end-scrapers.

## Mezhyrich

The site is situated on a promontory between the Ros and Rosava river valleys, which form the local drainage system on the right bank of the Dnieper. Here, the loess deposits reach about 3 m in thickness (Haesaerts et al. 2015). Although the site was initially excavated as one cultural layer. Four dwelling structures from mammoth bones and their corresponding zones of household activities with "trampling areas", pits, as well as internal and external hearths were documented (Nuzhnyi 2015: 211-213; Shydlovskyi et al. 2022). Recently, a complex multi-level stratigraphy has been established, encompassing strata inside and outside of the dwelling structures (Komar et al. 2003; Shydlovskyi et al. 2019; Tsvirkun, Shydlovskyi 2022).

### *Environment*

A pattern of small polygons originates from microfractures and is indicative of cryogenic deformations (Velichko et al. 1999; Komar et al. 2003; Haesaerts et al. 2015). Arboreal pollen amounts to 19-36 % and the non-arboreal pollen to 32-57 %. *Pinus silvestris* and *Betula sect. alba* dominate among the tree pollen, but broad-leaf species, such as *Quercus, Alnus, Corylus avellana, Ulmus,* and *Carpinus betulus* were also observed. The herbaceous pollens mainly originate from Cyperaceae, Cichoriaceae, Ranunculaceae and *Artemisia* (Komar 2015). The palynological analysis thus suggests a vegetation with a mosaic character. In addition to a predominance of herbaceous plants characteristic of periglacial steppe environments, some trees were probably growing on protected southern slopes of the river valleys, providing refugial conditions in the meadows (Prisiazhniuk 2015; Komar 2015). The analy-

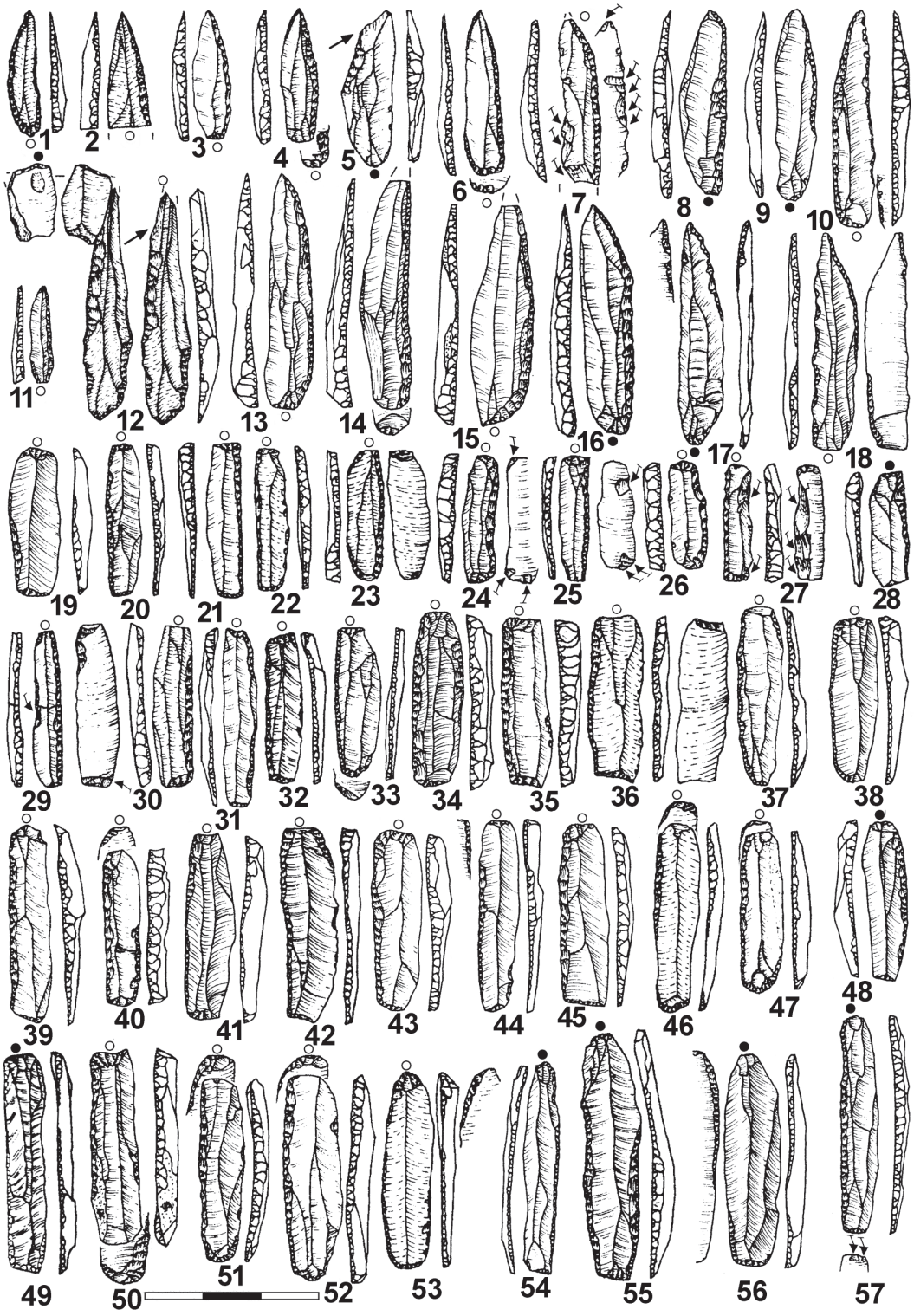

Fig. 11–13. Mezhyrich industry, artefacts from Semenivka 2 (1, 4, 12, 22, 23, 30, 40), Semenivka 3 (2, 3, 5, 6, 26, 27, 33, 35, 36, 46, 47, 50, 51, 52, 53), Dobranichivka, HHC 3 (7), Mezhyrich, dwelling 1 (8, 9, 10, 11, 13, 14, 15 18, 19, 34, 38, 41, 43, 44, 45, 48, 54, 56, 57), Dobranichivka, HHC 1 (16), Mezhyrich, HHC 1 (17, 20, 32), Gintsi, horizon K′ (21, 24, 25, 28, 29), Mezhyrich, dwelling 2 (31, 37, 39), Dobranichivka, HHC 4 (42, 55) and Mezhyrich, HHC 4 (49): 1–18 – lanceolate microgravette points; 19–57 – rectangles; after Nuzhnyi 2015, fig. 118, 122, 124, 129–131, 135, 145, 179, 155–158, 164–168.

sis of rodents, avifauna, charcoal, terrestrial and aquatic molluscs supports this conclusion (Komar et al. 2003; Péan 2015; Péan et al. 2015; Prisiazhniuk 2015; Marquer et al. 2015). The assemblage of the larger fauna is quite variable and comprises *Mammuthus primigenius, Bison priscus, Rangifer tarandus, Sus scrofa, Equus sp.* or *E. latipes, Ursus arctos, Canis lupus, Alopex lagopus, Vulpes vulpes, Vulpes corsac, Panthera leo spelaea, Gulo gulo, Lepus europaeus/Lepus sp.* (Péan 2015). Here, mammoth and hare are the dominant species both for the number of identified bones and the estimated minimum number of individuals.

### *Artefacts*

Numerous flint and organic artefacts were discovered (Nuzhnyi 2015: 214–234; Nuzhnyi, Shydlovskyi 2015; Péan 2015). Technologically, a continuous blade-bladelet reduction strategy, involving extensive abrasion of the cores' striking platform, is characteristic (Lozovski, Lozovskaya 2014; Nuzhnyi et al. 2017). The typological spectrum is marked by lanceolate microgravette points and rectangles on bladelets and micro-blades, simple end-scrapers on blades and flakes, and burins on truncated blades (Fig. 11-13, *8–11, 13–15, 17–20, 31, 32, 34, 37–39, 41, 43–45, 48, 49, 54, 56, 57*; 11-14, *5, 9, 14–20, 22, 23*; Nuzhnyi 2015). In addition, various artefacts and adornments made from tusk, antler, and bone are described (Pidoplichko 1976).

### *Chronology*

Haesaerts et al. (2015) propose four chronological settlement phases (1, 2, 2-3 and 3) based on selected radiocarbon dates, with priority given to newly obtained AMS dates. The first and earliest phase is associated with the samples SacA-12041, SacA-14984 and SacA-12259 from pit 8 and dates between. 18.3-18.2 ka calBP. Phase 2 is correlated with the samples GrN-29876, GrN-29877, GrN-38810, OxA-15587, and SacA-11177 from dwelling 4 and pit 6 and dates between 18.1-17.9 ka cal BP. The same date range is found for a weighted average of the trampling zone. Phase 2-3 is based on a femur of *Canis Lupus* from dwelling 2, analysed in two labs (OxA-13044; GrA-22094) and dated between 17.7-17.5 ka calBP. Phase 3 eventually is associated with the samples GrA-22501 and SacA-14982 from dwelling 1. When the weighted average is calculated, the expected age range is 17.7– 17.5 ka calBP, the same as for Phase 2-3 (Table 11-3, Fig. 11-15). In sum, the maximum time of occupation documented at Mezhyrich covers 800 years, roughly between 18.3-17.5 ka calBP. Other models for the Mezhyrich settlement as a whole and specific site features do not differ much and generally support Haesaerts' et al. approach (Chabai et al. 2020b; 2022; Chabai, Vasyliev 2021b; Tsvirkun, Shydlovskyi 2022; Shydlovskyi et al. 2023).

## Semenivka settlement complex

Three sites located in close proximity to one another form the Semenivka settlement complex. They are situated on a gentle hill close to the watershed plateau at a small valley connected to the Trubezh River, a right tributary of the Dnieper. The archaeological material originates from the upper part of the loess section, which underlies the about 1.5 m thick Holocene soil. The sediments of all Semenivka locations were heavily reworked by animal borrow tunnels (Nuzhnyi 2015: 275, 279–280, 292–293). According to Nuzhnyi and Stupak, the Semenivka settlement complex accumulated during the warm season and consists of a short-term hunting camp, Semenivka 1, and two base camps, Semenivka 2 and 3 (Nuzhnyi, Stupak 2001).

## Semenivka 1

Semenivka 1 was excavated on 59 m², yielding two separate bone concentrations and four lithic artefacts. A concentration of 21 bones from *Ursus arctos* is associated with a flake, an angle burin on the blade, and the distal part of a microgravette point on the bladelet. In the second concentration, one blade was found between 39 bones of *Mammuthus primigenius* (Nuzhnyi 2015: 275–276). Two AMS dates on the same bear femur give a weighted average of 16.4–16.1 ka calBP (Table 11-3; Fig. 11-15).

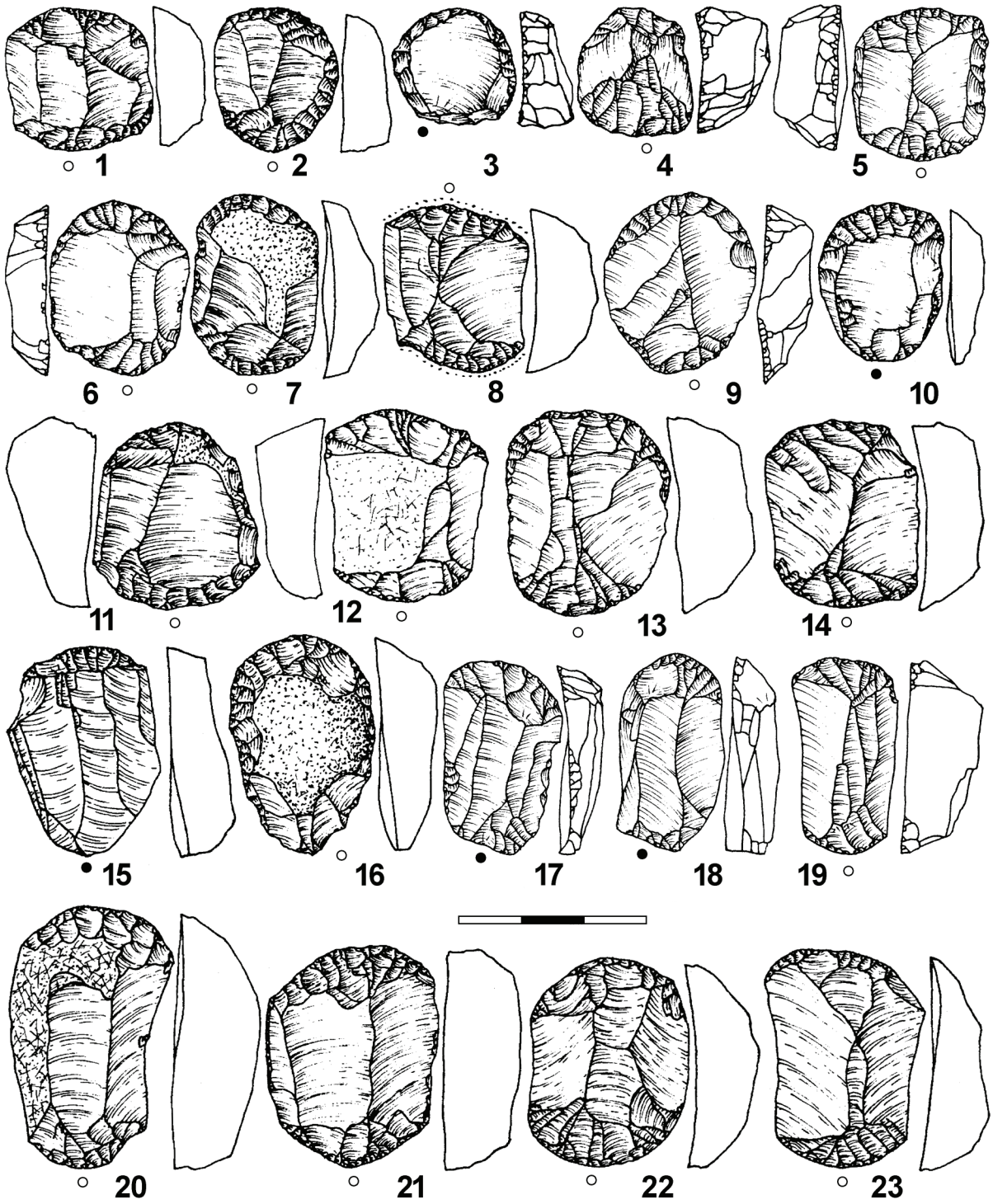


Fig. 11–14. Mezhyrich industry, artefacts from Dobranichivka, HHC 4 (1, 2, 3, 7, 8, 11, 21), Gintsi, horizon K' (4, 6, 10), Mezhyrich, dwelling 1 (5, 9, 17, 18, 19), Dobranichivka, HHC 3 (12, 13), Mezhyrich, dwelling 2 (14, 20, 22, 23) and Mezhyrich, HHC 4 (15, 16): 1–17, 20–23 – end-scrapers on flakes; 18, 19 – end-scrapers on blades; after Nuzhnyi 2015, fig. 118, 128, 131, 144, 148, 179, 180.

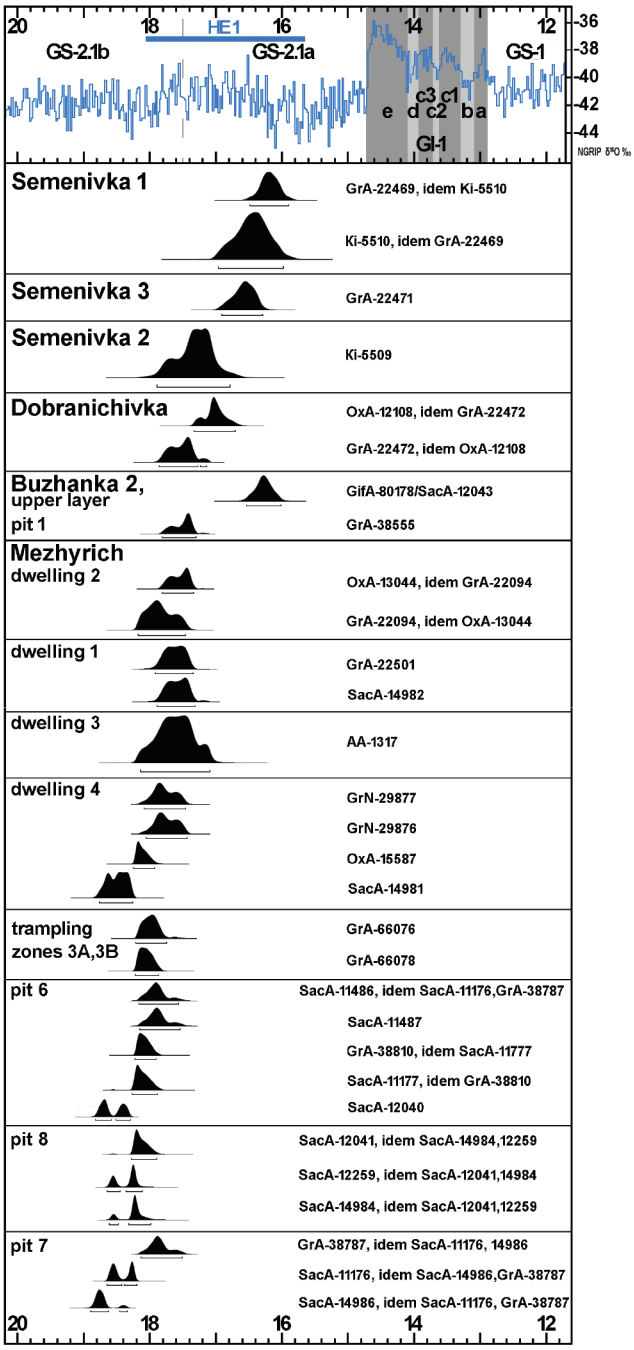


Fig. 11-15. Chronology of the Mezhyrich industry: Mezhyrich, Buzhanka 2, Dobranichivka, Semenivka 1, 2, 3.

## Semenivka 2

Semenivka 2 is situated about 200 m southeast of Semenivka 1. On about 150 m², a relatively dense concentration of 79 mammoth bones, 3500 artefacts and a number of freshwater, sea and fossil shells were documented. The toolkit is dominated by burins on truncated blades, followed by lanceolate microgravette points and rectangles (Fig. 11-13, *1, 4, 12, 22, 23, 30, 40*). Other types only occur in low numbers. The micro-burin technique was used for the production of the microgravette points (Fig. 11-13, *12*; Nuzhnyi 2015: 289). In addition, there is an amber pendant with a bi-conically drilled hole (Nuzhnyi 2015: 279-291). There is only one radiocarbon date on a mammoth rib, which gives a brought age range of between 17.9-16.8 ka calBP (Table 11-3; Fig. 11-15).

## Semenivka 3

Semenivka 3 is situated about 60 m east of Semenivka 2. On 132 m², more than 327 bones and 100 specimens of freshwater, sea and fossil shells, and 7000 artefacts were documented. Cervidae*, Rangifer tarandus, Saiga tatarica, Ursus arctos,* and *Canis lupus* complement the dominating mammoth remains. The microliths – lanceolate microgravette points and rectangles – make up nearly 40 % of the toolkit (Fig. 11-13, *2, 3, 5, 6, 26, 27, 33, 35, 36, 46, 47, 50-53*) and the micro-burin technique for the production of microgravette points was identified (Fig. 11-13, *5*). Burins (33 %), especially those on truncated blades, are the second most numerous tool types. The end-scrapers and perforators are not numerous (Nuzhnyi 2015: 309-311). Besides flint artefacts, fragments of grooved points on mammoth tusks and a tube-like needle container on *Rangifer tarandus metatarsus* were found (Nuzhnyi 2015: 279-291). Perforated shells comprise fossil specimens of *Dorsamum sp.*, the freshwater taxon *Theodoxus sp.*, and the quaternary Black Sea shells *Cyclope neritea L.* (Nuzhnyi 2015: 298). A single available date on a cervid bone gives an age estimate of between 16.9-16.2 ka calBP, thus overlapping with the date of Semenivka 1 (Table 11-3; Fig. 11-15).

## Dobranichivka

Dobranichivka is situated on a promontory of the second terrace of the Supoi River, an eastern tributary to the Dnieper (Shovkoplias 1972). Within loess deposits of about 4 m thickness, a single cultural layer was observed at a depth of 1.75-2.00 m, above a dark, humic horizon

(3.00–3.10 m depth), most likely a buried soil. With an excavated area of roughly 1300 m², the extent of the site has probably been covered completely, and four "household complexes", each consisting of mammoth bone structure, internal and external hearths, and storage pits, were documented (Shovkoplias 1972; 1992).

### *Environment*

No traces of cryoturbation were found at the site, but the pollen spectrum (arboreal pollen ≈ 33 %) is similar to the one described for Mezhyrich (Velichko et al. 1999:40–41). The faunal assemblage is clearly dominated by mammoth remains, but also comprises *Bison priscus, Rangifer tarandus, Ovibos moschatus* and a number of carnivores, namely *Ursus arctos, Gulo gulo, Canis lupus, Vulpes vulpes* and *Alopes lagopus.*

### *Artefacts*

To date, more than 12,000 artefacts are available in several museum collections (Nuzhnyi 2015: 241, 255, 274). Characteristic tool types are burins on truncated blades, short and circular end-scrapers on flakes, lanceolate microgravette points, and rectangles on bladelets and micro-blades (Fig. 11-13, *7, 16, 42, 55*; 11-14, *1-3, 7, 8, 11, 21*). Numerous awls on bones, hammers on reindeer antlers, unfinished artefacts on mammoth tusks, and a figurine are also reported (Nuzhnyi 2015: 237–274).

### *Chronology*

Two AMS dates on a calcaneus bone of *Ursus* give a weighted average of 17.3–17.1 ka calBP (Table 11-3; Fig. 11-15).

## Buzhanka 2

Buzhanka 2 is situated relatively low on the right bank of the Desna River. Within lithologically homogeneous loess sediments of about 1.5 m thickness, three cultural layers, named upper layer 1, upper layer, and lower layer, were observed (Stupak 2013: 145–145), separated by 10 to 30 cm thick, sterile sediments. Traces of cryoturbation were not observed. Mammoth, reindeer, polar fox, wolf and bear mark the faunal assemblages. A pit filled with mammoth bones is associated with the upper layer. The largest collection of artefacts comprises roughly 6,000 pieces and comes from the upper layer. The toolkit is characterised by microgravette points and rectangles (Stupak 2009). Although much lower in numbers, the assemblages of the upper layer 1 and the lower layer show similar techno-typological features (Stupak 2013; 2014). Two AMS dates are available on bones of wolf (16.6–16.0 ka calBP) and mammoth (17.8–17.3 ka calBP) for the upper layer and upper layer, pit 1, respectively (Table 11-3; Fig. 11-15). Since the mammoth bone might be older than human activity on the upper layer, preference should be given to the date on the wolf bone.

## Gintsy

The site is situated on a promontory of the second terrace of the Udai River, a right tributary to the Dnieper. Despite a long history of investigations, thousands of excavated square meters, and numerous bones and artefacts, the available information about the stratigraphy, fauna, and finds is limited (Levytsky 1949; Gavrylenko 2003; Nuzhnyi 2015: 319–325; Sergin 2024). What is known is that there is a more than 4-meter-thick sequence of silty loess deposits that contains two separate archaeological occupations, from which a number of mammoth bone concentrations, including dwelling structures and pits, are reported (Sergin 1981; Iakovleva, Djindjian 2001; 2018). According to Nuzhnyi, the upper layer (horizon K′) from Levytsky's 1935 field campaign shows evidence of a micro-blade core reduction strategy. Among the tools, rectangles and microgravette points on micro-blades, simple and double end-scrapers on blades and flakes, as well as burins on truncated blades are common (Fig. 11-13, *21, 24, 25, 28, 29*; 11-14, *4, 6, 10*; Nuzhnyi 2015: 322–325). The available age estimates for most of the structures (Iakovleva, Djindjian 2005) of both the upper and lower layer are fairly consistent and mainly range between 17.9 and 17.4 ka calBP. Only a weighted average of dates from pit 9 are younger and range between 16.6–16.3 ka calBP (Table 11-3; Fig. 11-16).

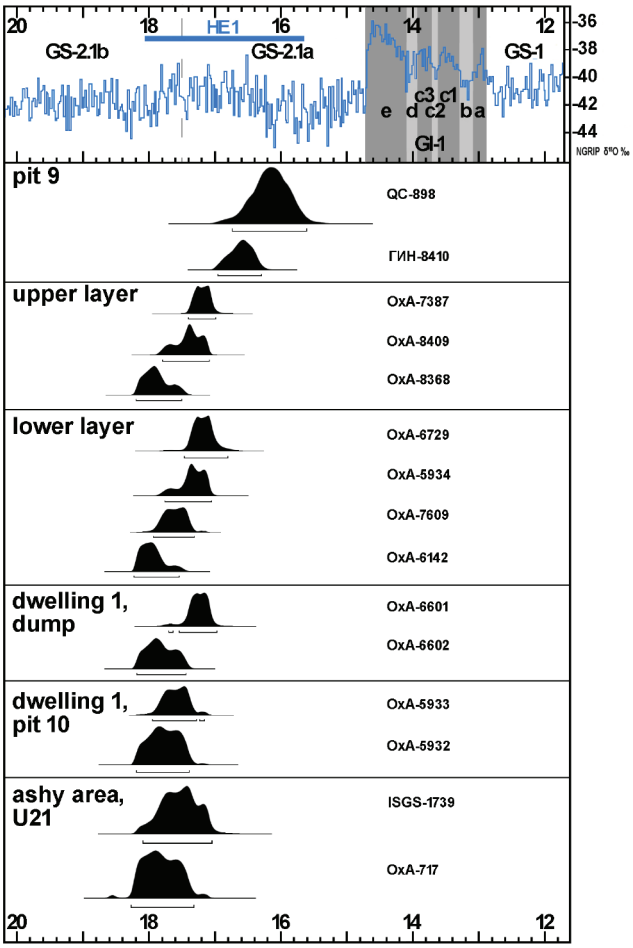


Fig. 11-16. Chronology of the Mezhyrich industry: Gintsi.

## Yudinovo industry

Apart from the eponymous site of Yudinovo, the assemblages of Pushkari IX, layers 1 and 2, Timonovka 1 and 2, and Chulativ I and II are comprised in the taxonomic unit of the Yudinovo industry. The common denominator in the material culture of these assemblages is the occurrence of lanceolate points on blades and bladelets (some with proximal retouch resembling the Anosovka points) and specific atypical rectangles without right angles between the distal and/or proximal extremities and the lateral sides of the blade or bladelet used as blank. In addition, short double and rounded end-scrapers are common (Fig. 11-17).

## Yudinovo

Yudinovo lies on the lowest terrace of the right bank of Sudost River, a right tributary of the Desna and shows a roughly 3 m thick section of silty sediments which accumulated over alluvial deposits. With a location at 8-10 m above the water level, Yudinovo currently takes the lowest position regarding river terraces in the Mid Dnieper basin, which is seen as an argument for a relatively late age (Velichko et al. 1999: 32-33; Gribchenko, Kurenkova 2014).

The site was excavated on more than 1000 m². Five dwelling structures made from mammoth bones, several pits, as well as flint knapping and tusk processing areas were identified (Abramova 1995; Abramova, Grigorieva, Christensen 1996; Abramova, Grigorieva 1997; Khlopachev 2018; 2019a). Until recently, the site was though to consist of a single cultural layer, but multidisciplinary studies proved the presence of an upper and a lower cultural layer of 0.10-0.15 m and 0.10-0.45 m maximum thickness, respectively, separated by up to 0.35 m of sterile sediments (Khlopachev, Gribchenko 2012; Khlopachev 2018; 2019a). The lower and main cultural layer presents a complex, non-homogeneous lithologic situation and consists of three lens-like horizons (Khlopachev 2019b: 163-164). Differences in artefacts and faunal structures between the two layers have not yet been studied.

### *Environment*

The cultural deposits at Yudinovo accumulated under permafrost conditions. A polygonal system of small ice cracks is connected with the main cultural layer (Velichko et al. 1999: 34), and traces of post-depositional depressions, caused by the ice melting during permafrost degradation, were identified (Gribchenko, Kurenkova 2014: 107). The fauna assemblage is represented by the mammoth complex, well-known for the Desna Valley. Here, bones of *Mammothus primigenius* and *Alopex lagopus* heavily dominate, while *Lepus tanaiticus, Marmota bobak, Vulpes vulpes, Canis lupus, Ursus arctos, Panthera spelaea, Equus latipes, Rangifer tarandus, Saiga borealis* and *Ovibus pallantis* are also present (Sablin 2014). The spectrum of terrestrial and

freshwater molluscs indicates rich grassland near the floodplains with lakes and/or slow-flow, low-energy rivers, complemented by sparse stands of coniferous and deciduous trees (Kijasko, Khlopachev 2022: 127). The pollen spectra, analysed individually for the lower and upper layer, show subtle differences. In general, the landscapes are characterized by xerophytic and mesophytic grasslands with sparse patches of trees. The lower layer is characterised by herbaceous pollen (about 80%) of Chenopodiaceae, Cichoriaceae, Ranunculaceae, Asteraceae and *Artemisia,* supplemented by 10 % arboreal pollen (*Pinus, Betula, Alnus, Alnaster, Salix*). The main difference in the upper level of pollen spectra is the presence of *Picea* (Sapelko 2014: 118- 123).

### *Artefacts*

The lithic artefact assemblage is marked by the dominance of burins on truncated blades, the presence of lanceolate backed points and "atypical" rectangles on blades and bladelets, and variable, often rounded end-scrapers on flakes and blades (Abramova et al. 1996: 5-75). According to Nuzhnyi, the microlithic complex of Yudinovo is very similar to those from Mezhyrich and Dobranichivka (Nuzhnyi 2015: 404). Unfortunately, this similarity was not specified. The morphologically highly variable artefacts from bone and tusk are often ornamented and include hunting weapons, tools and adornments (Abramova et al. 1996: 76-137).

### *Chronology*

Khlopachev subdivides the 44 available radiocarbon dates into two periods, corresponding to the two cultural layers (Table 11-3). However, the association of these dates with specific structures has not been published. All dates with species identification were made on mammoth remains. For the upper layer, the available dates can be integrated in a weighted average of between 14.3 and 14.1 ka calBP, placing the occupation in the Bølling period. The lithological non-homogenous character of the lower cultural layer, in contrast, is reflected also in the distribution of radiocarbon dates, which can be divided into four clusters based on weighted averages, namely 1st phase – 18.2 ka calBP, 2nd phase – 17.9-17.6 ka calBP, 3rd phase – 16.9-16.6 ka calBP, and 4th phase – 15.6-15.4 ka calBP (Fig. 11-18; Table 11-3).

## Pushkari IX, layers 1 and 2

Pushkari IX is situated on a promontory at the right bank of the Desna River. The stratigraphic sequence spans about 2.5 m of Pleistocene sediments and three archaeological layers, separated by pronounced sterile deposits. Pushkari IX, layer 1, the main cultural horizon, is also known as the Bugorok site. Layer 2 is also often referred to as Bugorok or Bugorok, lower horizon of the main cultural layer. Pushkari IX, layer 3 is also named Pogon, as is the single occupation of Pushkari VIII (Vasyliev 2014; Khlopachev 2011; 2014). Both Pushkari IX, layer 3 and Pushkari VIII, however, contain artefacts characteristic of the Pushkari-Anosovka industry (Khlopachev 2011; Vasyliev 2014; 2018), which is consistent with the available radiocarbon dates (Table 11-2; Fig. 11-6).

### *Environment*

The surfaces of both layers 1 and 2 at Pushkari IX were partly disturbed by permafrost depressions as a result of underground ice melting (Khlopachev 2011: 189), indicating that both layers accumulated under permafrost conditions. This is in line with the faunal assemblage of *Mammuthus primigenius, Ovibos moschatus* and *Alopex lagopus* (Gvozdover 1947: 93; Khlopachev 2014: 88). The vegetation, in contrast, indicates a periglacial forest-steppe, characteristic of the Allerød period (Sapelko 2014: 130) with abundant pollen of Chenopodiaceae, Cichoriaceae, and Poaceae and 53 % arboreal pollen of *Pinus, Betula, Alnus,* and *Picea* (Khlopachev 2014; Sapelko 2014).

### *Artefacts*

The lithic artefacts of Pushkari IX, layers 1 and 2 constitute a relatively small collection with short double end-scrapers on flakes, a dominance of burins on truncated blades, truncated blades, lanceolate points on blades and bladelets, and backed bladelets and rectan-

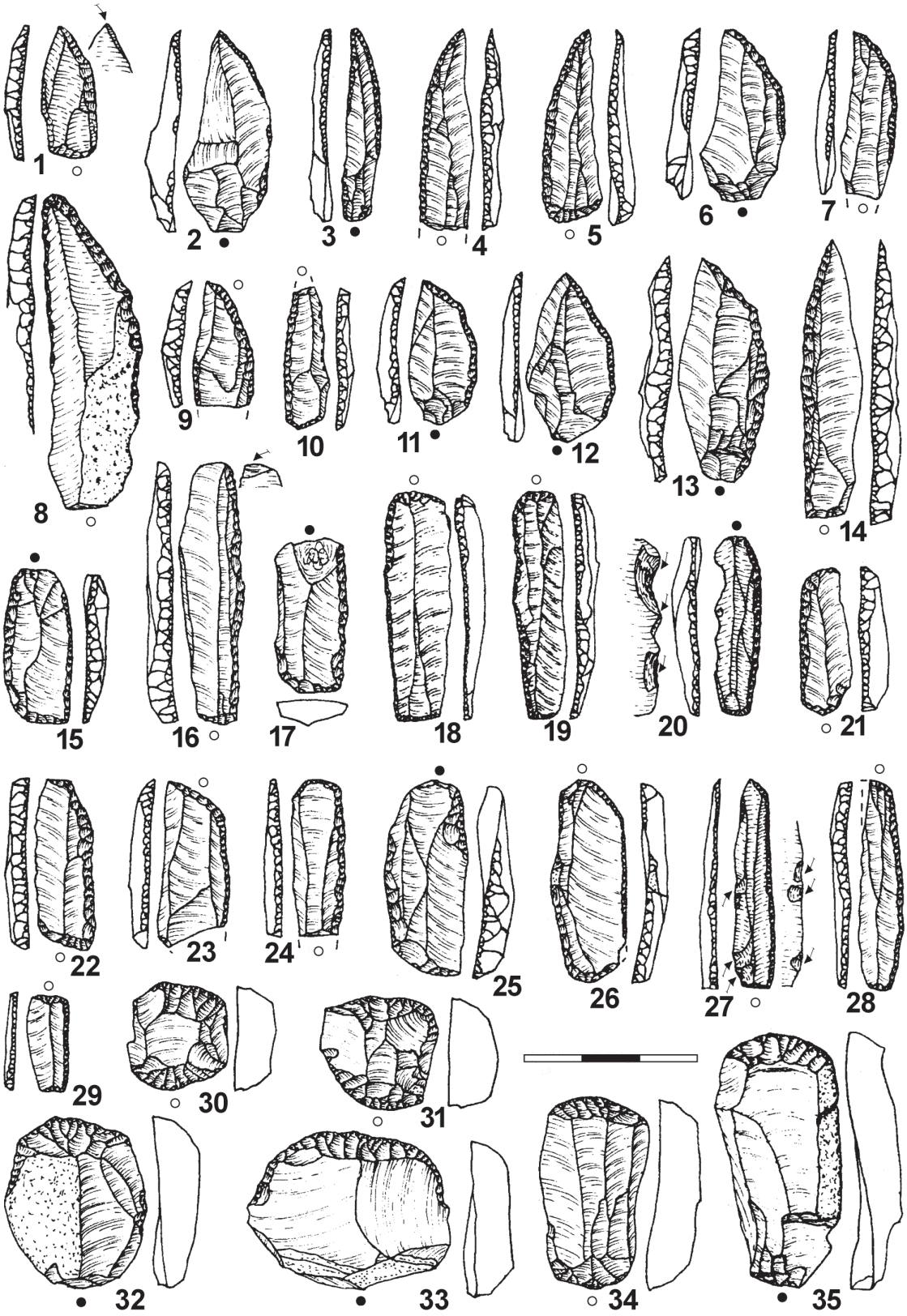

Fig. 11–17. Yudinovo industry, artefacts from Pushkari IX, 2 (1, 8, 18, 19, 20, 27, 35) and Timonovka I (2–7, 9–17, 21–26, 28–34): 1–14 – lanceolate points; 15–29 – rectangles; 30–35 – end-scrapers; after Nuzhnyi 2015, fig. 190–195.

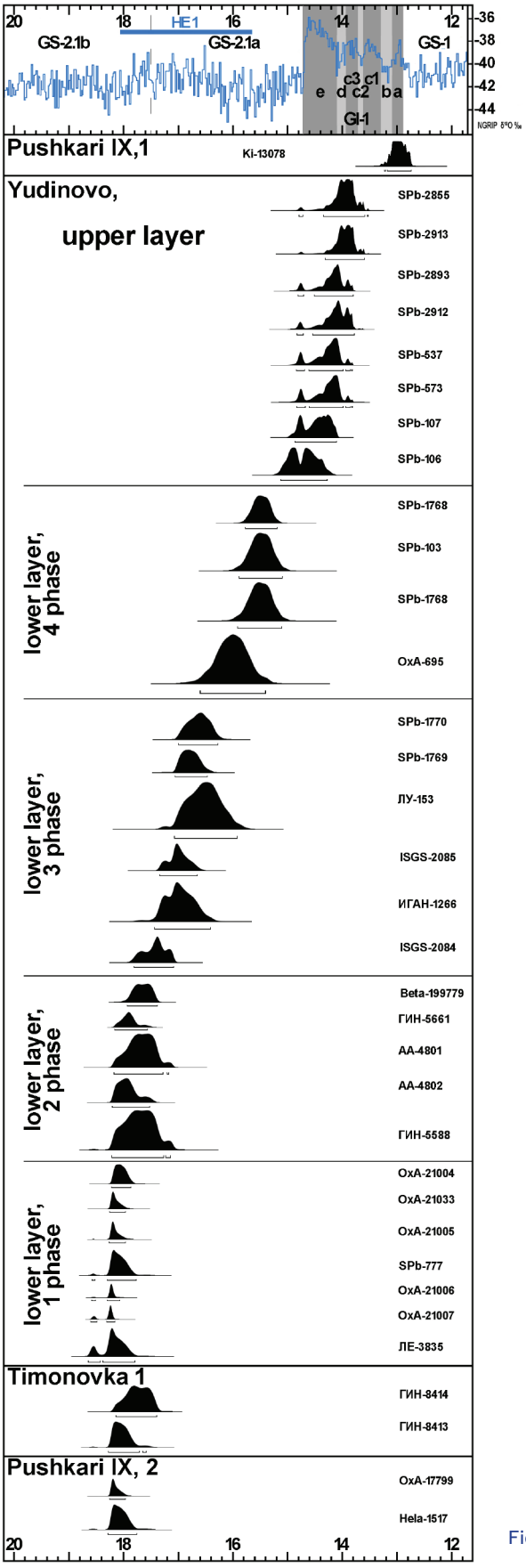


Fig. 11-18. Chronology of the Yudinovo industry.

gles on blades and bladelets as characteristic features (Fig. 11-17, *1, 8, 18-20, 27, 35*) (Nuzhnyi 2015: 360-366).

### *Chronology*

A single reliable date on a musk ox tooth places layer 1 between 13.2 and 12.7 ka calBP, i.e. in the Allerød interstadial, in line with the pollen data from this layer (Khlopachev 2014: 83-89). The two available dates from layer two, one on a mammoth, the other on a musk ox tooth, can be integrated in a weighted average of 18.2-18.1 ka calBP (Table 11-3; Fig. 11-18).

## Timonovka 1 and 2

Timonovka 1 site is situated at a promontory on the eroded right bank of the Desna River at 25-30 m above the water level (Mirchink 1929). The 15-7 cm thick cultural deposits, whose upper part was truncated by agricultural activities, were embedded in silty sediments (Voevodsky 1929). Gorodtsov excavated 1178 m² and defined three "household zones" consisting of deepened dwellings, "workshops", hearths, storage pits, faunal remains and concentrations of in total more than 100,000 lithic artefacts. Bone awls and ornamented mammoth ribs and tusks were also found (Gorodtsov 1935; Velichko et al. 1997: 102, 106-107). Later, it turned out that most of the deepened structures are the result of post-depositional permafrost depressions (Velichko et al. 1997: 100). Timonovka 2 was discovered 240 m southwest of Timonovka 1 in comparable topographic and stratigraphic conditions and highly similar techno-typological characteristics (Velichko et al. 1997: 86-110).

### *Environment*

The mentioned post-depositional permafrost depressions observed at both sites indicate that the cultural layers accumulated before permafrost degradation. Pollen analysis from the cultural layer at Timonovka 2 shows a

dominance of grasses (up to 75 %) and xerophytes, while arboreal pollen demonstrates the typical composition for the Late Pleistocene in the Desna Valley with *Pinus, Betula,* and *Alnus*. Hence, an open and dry steppe with patchy stands of trees characterised the surrounding landscape (Velichko et al. 1977: 77). The faunal assemblage of both sites is characterised by the dominance of *Mammuthus primigenius* over *Rangifer tarandus, Alopex lagopus, Canis sp., Gulo gulo, Ursus sp.,* and *Lepus timidus* (Velichko et al. 1977: 85).

### *Artefacts*

A part of the Timonovka 1 artefact collection was studied by C. Gavrilov and D. Nuzhnyi (Gavrilov 1994; Nuzhnyi 2015: 367–379). The characteristic features of the toolkit are a dominance of burins on obliquely truncated blades, simple end-scrapers on blades and flakes, and lanceolate backed points as well as typical and atypical rectangles on blades and bladelets (Fig. 11–17, *2–7, 9–17, 21–26, 28–34*).

### *Chronology*

Two of the four dates from Timonovka 1 (both on mammoth) result in a weighted average of 18.1–17.8 ka calBP (Table 11–3; Fig. 11–18). The only date available for Timonovka 2 has an unsuitably large standard deviation (Table 11–3).

## Chulativ I and II

The artefact collections from Chulativ I and II are often mentioned as belonging to the Yudinovo industry (Abramova 1997; Nuzhnyi 2015). The sites were studied before and after the Second World War (Pidoplichko 1940; Voevodsky 1952; Boriskovsky 1953; Galych 1941), but the data on stratigraphy, fauna, and artefacts need additional verifications. There is a single radiocarbon date on a mammoth tooth for Chulativ I with an unsuitably large standard deviation (Table 11–3).

## Yeliseevichi industry

Yeliseevichi I is located on the lowest terrace of the right bank of Sudost River, a right tributary to the Desna. The thickness of Pleistocene deposits is about 1.5 m and the cultural deposits are embedded in silty-loess sediments at a depth of 1.3 m. The site was initially excavated as a single cultural layer consisting of an ashy zone and several pits with bone concentrations, including the so-called "churingas storage" and "churinga and figurine pit", sunken features containing artefacts with artistic expressions.

Only later it turned out that the mentioned structures exhibit complex stratigraphic sequences (Velichko et al. 1997: 94–118; Khlopachev et al. 2013; Khlopachev et al. 2017: 44–51), which are not yet correlated. About 20 of the 438 excavated m², associated with the ashy zone, churinga storage, and churinga and figurine pit, contain more than half of the artefact collection (Velichko et al. 1997: 89–91). Yeliseevichi II was found during the road construction 300 m northwest of Yeliseevichi I. Partly destroyed by modern anthropogenic activity, the archaeological material originates from 20 m², embedded in silty-loess sediments at a depth of 0.6–0.8 m (Velichko et al. 1997: 140–141). An also attested concentration of mammoth bones is redeposited (Ibid: 141–144).

### *Environment*

The accumulation of cultural deposits at Yeliseevichy I took place under permafrost conditions. Permafrost degradation later caused post-depositional deformations of the cultural deposits (Velichko et al. 1997: 72; 1999: 30; Gribchenko, Kurenkova 2014: 104). Khlopachev et al. (2013; 2017) postulate the presence of a main lower layer (about 17 ka calBP) and an upper layer (15–14 ka calBP; Older Dryas to Bølling) at Yeliseevichy I. In the lower layer, non-arboreal pollen amount to 85 % dominated by Chenopodiaceae, Cichoriaceae, and Poaceae, while pollen of *Pinus, Betula, Alnus,* and *Alnaster* hint at a sparse arboreal component (Sapelko 2014: 128–129) in a periglacial steppic landscape (Velichko et al. 1997: 84). The upper layer shows an increase in arboreal pollen of up

to 45% with a noticeable prevalence of Betula and Alnus (Sapelko 2014: 128–129), which is in line with other geoscientific indices of a warming episode (Khlopachev et al. 2017: 53). According to Khlopachev, some of the available radiocarbon dates (see below) point towards on occupation of the upper cultural layer during either the Older Dryas or the Bølling interstadial, (Khlopachev et al. 2017: 54–55). The available faunal data of the lower layer might indicate some intrusions from the upper layer. On the one hand, it is dominated by the remains of *Mammuthus primigenius, Alopex lagopus* and *Canis lupus, while Ursus arctos, Lemmus cf. obensis,* and *Cricetus sp.* are also well represented. Some species are only attested by a few bones, such as *Rangifer tarandus, Equus sp.,* and *Alces alces* (Velichko et al. 1997: 85–88; Demay et al. 2017: 84–86). The presence of elk, however, is not characteristic of the periglacial vegetation in the Desna Valley, but rather of the more forested landscapes of the Bølling.

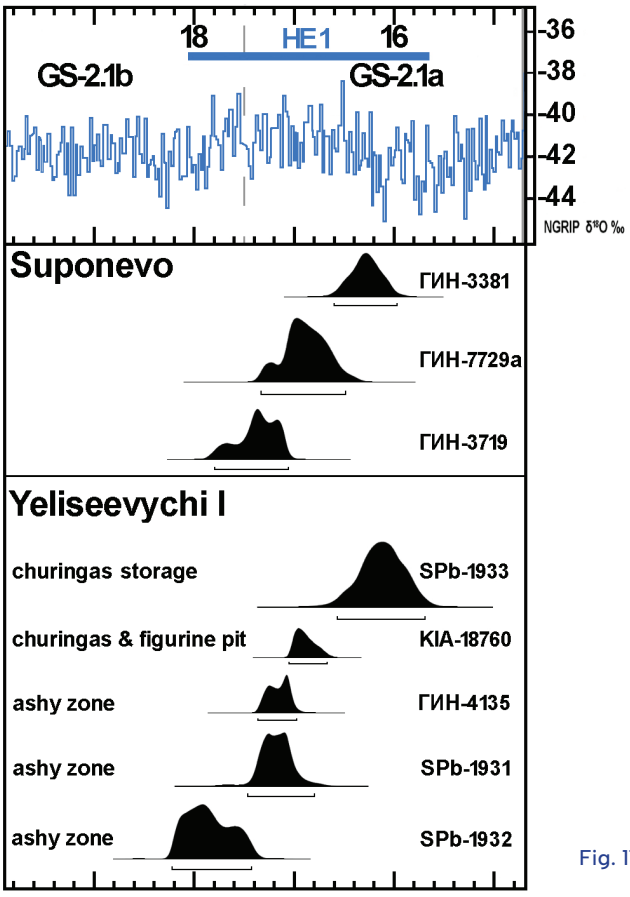


Fig. 11–19 Chronology of Suponevo and Yeliseevichy 1.

## *Artefacts*

Burins on obliquely truncated blades dominate the tool assemblage of Yeliseevichi I, followed by backed bladelets. Simple types of end-scrapers were made on blades and bladelets (Velichko et al. 1997: 124–132). The backed bladelets include specimens with alternating retouch, which are the distinct markers used to separate the Yeliseevichi industry from other taxonomic sub-units of the Mid Dnieper Epigravettian (Nuzhnyi 2008a). The small artefact assemblage from Yeliseevichi II is characterised by backed bladelets, rectangles and truncated blades (Velichko et al. 1997: 145).

## *Chronology*

A number of radiocarbon dates available for Yeliseevichy I, grouped into three chronological intervals by Velichko et al. (1997: 76), namely early (~17.0 ka uncalBP), middle (14.5–14.0 ka uncalBP), and late (~13.0 ka uncalBP). Later, Khlopachev et al. (2017: 55–56) proposed a revised chronological structure – based on a multidisciplinary study and suggesting a natural origin of pit 1 and its filling and an unclear origin for bone accumulation 5 – with a lower (17.0–15.0 ka uncalBP), main (14.5–13.0 ka uncalBP), and upper (~12.0 ka uncalBP) chronological interval, from which the youngest is the most uncertain.

Most of the dates are made on mammoth remains. Since these remains could have been gathered in the landscape, they will not be used for the following chronological reflections. The only other determined species used for dating are *Canis lupus* (Canidae) and *Ursus sp.* The only context from which a weighted average could be calculated is the so-called ashy zone with an age estimate between 17.3 and 17.1 ka calBP. If different contexts are considered, a date on a Canidae tooth from the churinga and figurine pit (KIA-18760) and an undetermined burned bone from sq. 68–69 and thus out of the main concentration (ГИН-5475) can be integrated with

two dates from the ashy zone into a weighted age estimate of between 17.1 and 17.0 ka calBP (Table 11-3; Fig. 11-19). Three dates with ages around 15.5 and 14.0 ka calBP are discussed to indicate a chronological attribution of the upper layer to the Older Dryas or Bølling interstadial. One of these samples (SPb-1766) originates from the permafrost wedge, two more samples from pit 1 (ГИН-4137) and pit 3 (ИГАН-1133) show a rather large standard deviation (Table 11-3). Thus, an attribution of the upper layer to the Older Dryas or Bølling needs additional chronological arguments. In addition, at Pushkari IX, 1, Yudinovo, upper layer, and Divnogorie 9, the Bølling / Allerød deposits are associated with the presence of Picea pollen, which is not the case at Yeliseevichy I (Khlopachev et al. 2013: 88-89; Khlopachev et al. 2017: 50-51, fig. 7).

From Yeliseevichi II, there is only a radiometric date on the mammoth tooth (Table 11-3).

## Suponevo industry

The eponymous site Suponevo is situated at a promontory on the right bank of the second terrace of the Desna River and was partly destroyed by agricultural activities. The maximum elevation of the terrace is about 25 m above the water level. The cultural deposits originate from the lower part of a loess sequence, underlain by a chalk layer. Several concentrations of bones and lithic artefacts could be observed in the excavated area of about 200 m². Shovkoplias documents the observation of a potential dwelling structure, probably intentionally dug into the loess deposits, and reports a 20-25 cm thick sandy lens, which he interprets as the result of a flooding event, subdividing the cultural deposits within the dwelling in two horizons, which formed with only little time between both occupations (Shovkoplias 1951: 128, 138, 141).

### *Environment*

In the faunal assemblage, remains of mammoth and polar fox dominate over those of rhino, horse, reindeer, wolf, wolverine and hair. No traces of cryoturbation were observed.

### *Artefacts*

The excavation unearthed more than 30,000 lithic artefacts alongside organic tools and adornments (Shovkoplias 1950: 79-80), which were not subdivided by horizons. Burins on truncated blades dominate the tool assemblage. Distinctive of the Suponevo industry (Nuzhnyi 2008a) are transversal burins on laterally truncated blades and flakes, so-called Suponevo-type burins (Shovkoplias 1950: 180). End-scrapers were made on short blades and flakes, some of them described as thick (Lisitsyn, Dudin 2019: 89). The lanceolate-backed points, rectangles, and bladelets with marginal retouch characterise the kit of lithic insets. Artefacts made of bone, antler, and mammoth tusks occur together with adornments (Shovkoplias 1950: 177-180). Lisitsyn and Dudin (2019: 89) question the taxonomic independence of the Suponevo industry by stressing the similarities in the toolkits of Suponevo and Kostenki 11, Ia, particularly the occurrence of bladelets with marginal retouch and thick end-scrapers. To date, it remains unclear whether the Suponevo assemblage should be considered mixed or a specific variant of the Epigravettian.

### *Chronology*

There are three radiocarbon dates on mammoth remains available for Suponevo which cannot be averaged into a weighted average and cover the period between 17.8 and 16.0 ka calBP (Table 11-3; Fig. 11-19). Given that mammoth remains could have been gathered in the landscape, the younger end of the date spectrum seems most likely to date the occupation.

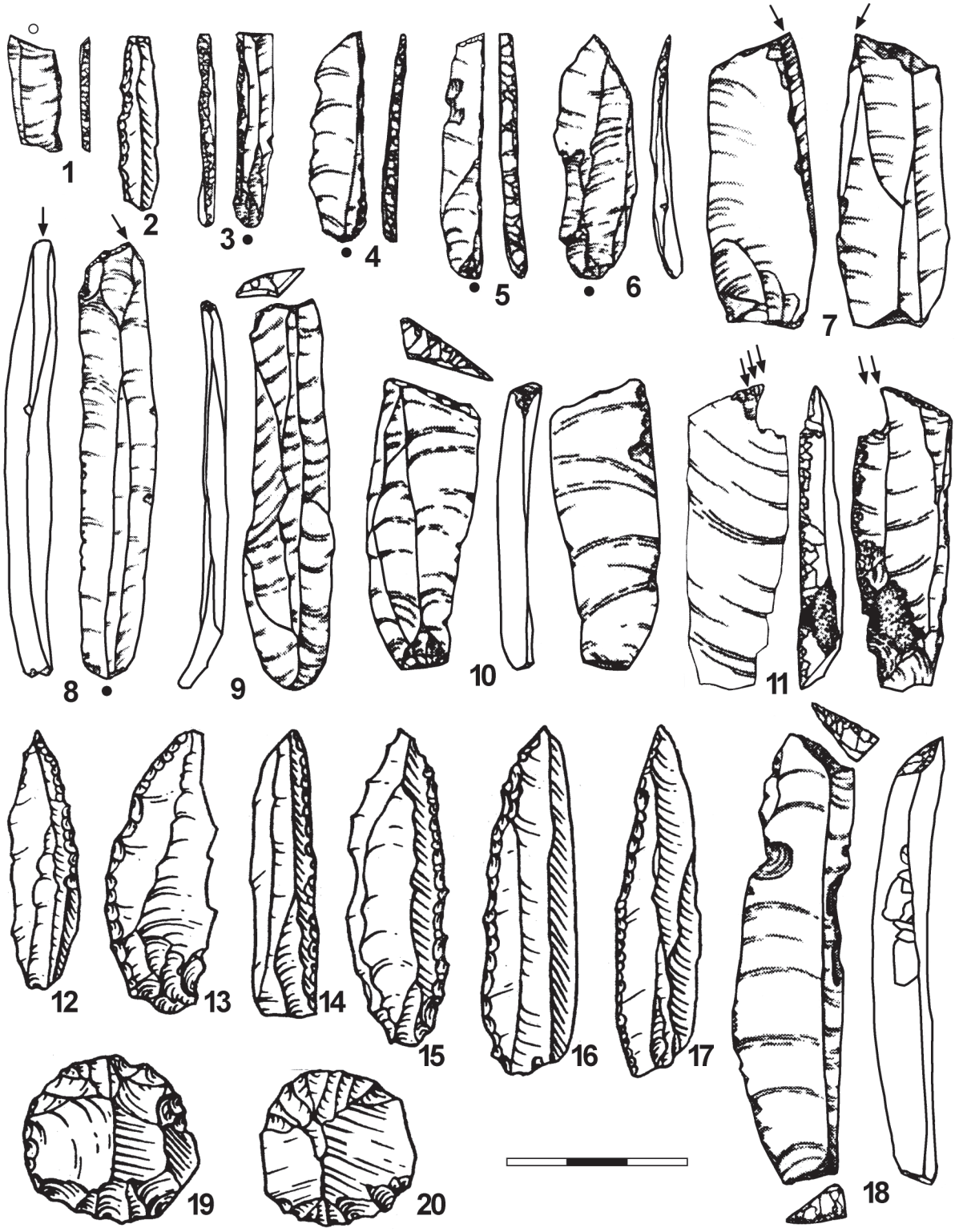


Fig. 11–20. Don Epigravettian, artefacts from Divnogorie 1 (1, 3–6, 8, 11), Divnogorie 9 (7, 9, 10, 18) and Borschevo 2 (2, 12–17, 19, 20): 1, 3, 4 – backed bladelets; 2, 5 – rectangles on bladelets; 7, 8, 11 – burins on truncated blades; 6, 12–17 – points on blades and bladelets; 9, 10, 18 – truncated blades; 19, 20 – rounded end-scrapers; 1–11, 18 –after Bessudnov et al. 2012; 12–17, 19, 20 – after Boriskovsky and Dmitrieva 1982.

## The Epigravettian in the Don Basin

In the Don basin, the Epigravettian is reliably attested at Borschevo 2 as well as Divnogorie 1 and 9.

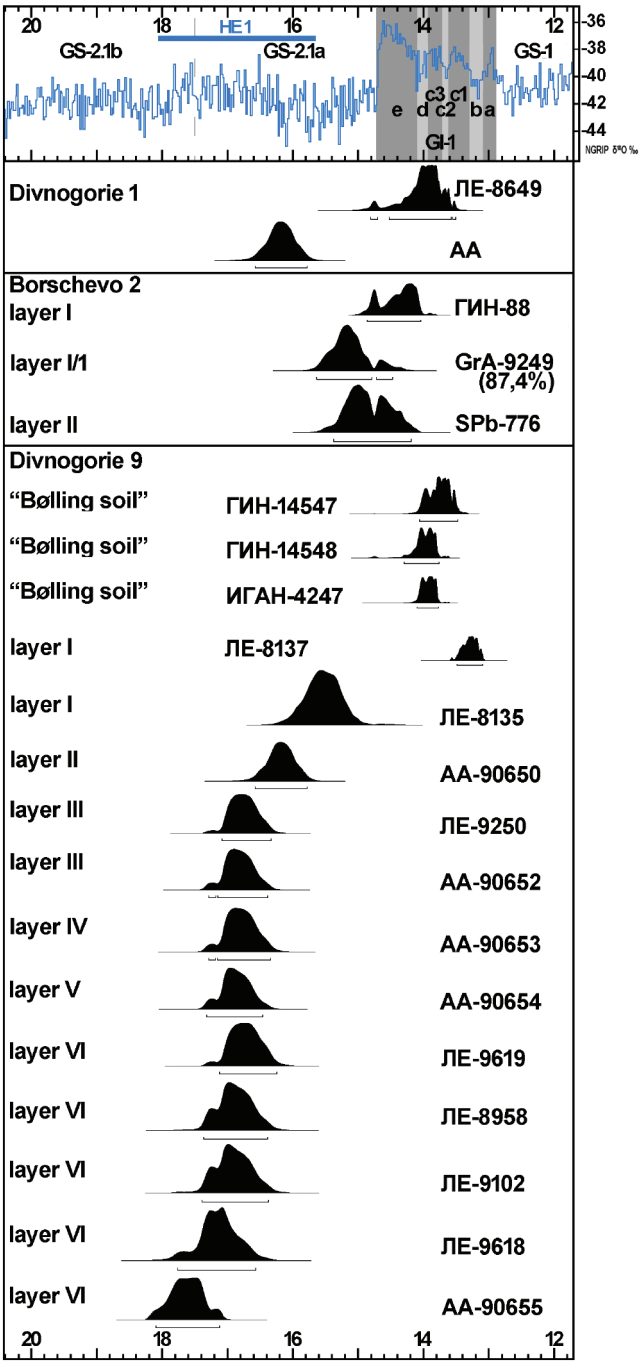


Fig. 11-21. Chronology of the Don Epigravettian.

## Borschevo 2

Borschevo 2 is situated on the lowest terrace of the Don River, which becomes submerged during seasonal flooding. The cultural deposits originate from a 1.5 m thick silt, underlying alluvial sediments. Initially, three cultural layers were reported (Boriskovsky, Dmitrieva 1982: 217), which later were identified as remnants of a single cultural layer, partly disturbed and redeposited by erosional processes (Lisitsyn, Dudin 2019: 92).

### *Environment*

No traces of cryoturbation were observed. Horse is the dominant species in the faunal assemblage and occurs together with reindeer, Bovidae, wolf, fox, elk, hare, and wolverine. Mammoth bones are present, but not numerous (Boriskovsky, Dmitrieva 1982: 219-222).

### *Artefacts*

Technologically, the assemblage contains uni- and bidirectional blade cores. Among the tools, burins on truncated blades prevail in the burin assemblage, and simple, double and rounded end-scrapers occur (Fig. 11-20, *19, 20*). There are numerous lanceolate and straight-backed microgravette points, backed micro-blades and rectangles (Fig. 11-20, *2*). Laterally retouched points on blades and truncated blades are common (Fig. 11-20, *12-17*) (Boriskovsky, Dmitrieva 1982: 219-221; Lisitsyn, Dudin 2019: 93).

### *Chronology*

A number of dates have been taken from all layers initially thought to represent distinct events. Since it has been shown that Borschevo 2 relates to a single occupation, a weighted average from all reliable dates (GrA-9249, SPb-776, and ГИН-88) can be calculated and results in an age estimate of between 14.9 and 14.4 ka calBP (Table 11-3; Fig. 11-21).

## Divnogorie 9

Divnogorie 9 is situated on the right bank of a big ravine connecting with the right bank of the Tikhaya Sosna River, a right tributary to the Don Drainage system. The stratigraphic sequence spans about 13 m and comprises 7 cultural levels, sandwiched between underlying lacustrine sediments and topped by pronounced soils, related to the Bølling and Allerød, lacking both artefacts and faunal remains. No traces of cryoturbation were observed. According to Bessudnov (2013: 135), the site functioned as a kill and butchering site for horses at the shores of a paleo-lake.

### *Environment*

The pollen spectra from the cultural levels are dominated by herbaceous and shrub pollen, with a prevalence of *Artemisia* and Chenopodiaceae, while pine dominates the arboreal species. At the time of the occupation of the site, a periglacial steppe with patches of pine stands thus probably marked the local landscape (Lavrushin et al. 2010; Bessudnov 2013; Bessudnov et al. 2013). During the Bølling, grasses and shrubs dominate, while the spectra from the Allerød soil are dominated by arboreal pollen, particularly spruce (Bessudnov et al. 2012: 147; 2013: 96-97).

*Equus ferus* dominates the faunal assemblage with about 8000 bones, often comprising entire carcasses, supplemented by a few bones of *Gulo gulo* and *Alopex lagopus* (Bessudnov et al. 2012: 147).

### *Artefacts*

The roughly 70 artefacts from the Divnogorie 9 sequence comprise simple end-scrapers, burins on truncations, truncated blades and backed pieces (Fig. 11-20, *7-10, 18*) (Bessudnov et al. 2012: 148; Bessudnov 2013: 135).

### *Chronology*

In general, the dated samples are in good agreement with the stratigraphic sequence. While the lowest level (VI) dates to around 17.2-16.9 ka calBP, level III was probably occupied between 16.9 and 16.6 ka calBP, and the youngest occupation (level I) may have been as late as 15 ka calBP. The Bølling soil is dated to around 14 ka calBP (Table 11-3; Fig. 11-21).

## Divnogorie 1

At a distance of 2.5 km southwest of Divnogorie 9 lies Divnogorie 1 on the lowest terrace of the Tikhaya Sosna River. A single cultural layer, strongly affected by animal burrows, was found at 1.4-1.8 m depth in silty-sandy sediments, which underlie the modern soil (Bessudnov et al. 2012).

### *Environment*

No traces of cryoturbation were observed. Again, *Equus ferus* dominates the faunal assemblage with 789 bones, complemented by 24 bones of *Rangifer tarandus* (Bessudnov et al. 2012: 152).

### *Artefacts*

The roughly 1000 lithic artefacts attest to uni- and bidirectional blade production, and nearly 10% are tools. The toolkit (Fig. 11-20, *1, 3-6, 8, 11*) comprises typologically variable end-scrapers (simple on flakes and blades, small rounded on flakes and inversely laterally retouched), burins on truncated blades, backed micro-blades, backed points on micro-blades, laterally retouched points on blades, and truncated pieces (Bessudnov et al. 2012: 152-153).

### *Chronology*

Three available radiocarbon dates (Table 11-3; Fig. 11-21) span the entire period from 16.5 to 13.5 ka calBP and thus neither support nor contradict Bessudnov's suggestion that Divnogorie 1 is about the same age as Divnogorie 9.

## DISCUSSION AND CONCLUSION

### Pre-LGM and LGM

The environmental conditions during the LGM in the Eastern European Plain were characterised by cold, arid, and continental conditions with minimum winter temperatures between -30 and -40 °C, maximum summer temperatures of +16 °C, and a low annual precipitation between 250 and 350 mm per m² (Velichko et al. 1999: 49). The landscape was characterised by tundra-steppe vegetation with sparse patches of trees and shrubs. Sediment deformations by cryoturbation are regularly observable in LGM deposits as far south as the Mid-Dnieper and Mid-Don valley. In the Mid-Dnieper valley, however, they are not attested at the southernmost site of Gordashivka. In the Mid-Don valley site cluster, permafrost phenomena are attested at both its northern margins in layer III of Kostenki 21 and at Yamy, at its southern fringe. However, no evidence of cryoturbation is reported from Kostenki 11, layer II, indicating that permafrost was probably not a ubiquitous phenomenon, but may have varied also according to local conditions.

The stratigraphic sequence of the Kostenki 11 site suggests a later age of Epiaurignacian (layer Ia) than the Pushkari-Anosovka industry (layer II). The increase of aeolian deposits in Pushkari I (Pushkari-Anosovka industry) and Obolonnya (Epiaurignacian) correlates with "GS-3 dust peaks", which are the result of the global event of aeolian sediment transportation from Asian, European and North African deserts during the LGM (Újvári 2022). In Kostenki 21, layer III, the stratigraphic correlation of "production areas" (Final Gravettian) and "dwellings" (Pushkari-Anosovka industry) is unclear. The distribution of the radiocarbon dates for the Final Gravettian / Gmelin complex (≈27.3-25.6 ka calBP) and Epiaurignacian (≈25.3-24.0 ka calBP) demonstrate a certain sequence. The chronological frame of the Pushkari-Anosovka industry (≈27.1-24.4 ka calBP) partly overlaps with both chrono-cultural units. If so, all of the described industries ended before and/or during GS-3 – the LGM *sensu stricto* (Fig. 11-22; Table 11-4).

The pre-LGM and LGM industries demonstrate discrete technological and typological characteristics and a mammoth-oriented economy. The Final Gravettian / Gmelin complex is characterised by unidirectional and bidirectional blade and bladelet cores, shouldered, Gravette, and microgravette points as well as rectangles. The Pushkari-Anosovka industry, in contrast, is solely characterised by uni-polar and bi-polar blade cores, while respective cores for bladelets are largely absent. Among the tools, Anosovka points, as well as rectangles on blades, are common. A few shouldered points reported from Pushkari I may reflect a probable contemporaneity of the Gmelin and Anosovka complexes (see Reynolds et al. 2019: 171-174 for details). Cores-on-flakes in the form of carinated scrapers and carinated burins are the most characteristic features of the Epiaurignacian, alongside bladelets with a fine, marginal retouch and thick end-scrapers on flakes. In all mentioned industries, dihedral burins are the dominant burin type.

It thus seems that the Pushkari-Anosovka industry is a cultural taxonomic unit spatially restricted to areas north of 50° northern latitude. As such, it is contemporaneous to both the older Final Gravettian / Gmelin complex with shouldered points and the younger Epiaurignacian assemblages with carinated cores, which have a more widespread extent beyond the Mid Dnieper and Upper Don Basins, including the Prut and Dniester basins and the steppe zones north of the Black and Azov Seas (Nuzhnyi 2009; Demidenko et al. 2019).

### Post-LGM

The industry documented at Byki – with its characteristic blade and flake core technology, triangular microliths, and horse hunting at the base of subsistence – shows, apart from a dominance of dihedral burins, no obvious technological and typological connections with either predecessors or successors in Eastern Europe. Also, its exact chronological position is still unclear, it seems that the accumulation of its cultural deposits took place after the beginning of permafrost degradation, probably between 21.5 and 19 ka calBP, i.e. towards the end of the LGM. In contrast to preceding Gmelin and Pushkari-Anosovka units, the "Byki culture" fauna assemblages are based on horse hunting. The closest comparable assemblage to Byki 7, I in terms of its techno-typological characteristics and hunting pattern, is Samo-

toevka. Although the chronological signals from radiocarbon dating vary, the site was probably in use between 19.5 and 16 ka calBP. In any case, there are no other candidates to cover the approximately 5–4 thousand years gap between the latest LGM industries and the earliest manifestation of the Epigravettian in the Mid Dnieper Basin (Fig. 11–22; Table 11–4).

Also, the traces of permafrost are not attested in the southern part of the Mid-Dnieper (Mezhyrich, Gintsy, Semenivka 1–3, Dobranichivka) and the Upper Don basins (Divnogorie 1 and 9, Borschevo 2, I). In addition, the Upper Don settlements show a horse-oriented subsistence (Table 11–4).

The early post-LGM environment in the northern part of the Mid-Dnieper basin is characterised by tundra-steppe vegetation with sparse patches of trees and shrubs, although an increase of arboreal pollen is noticeable. Permafrost deposits are still a characteristic feature of the Epigravettian occupations in the northern part of the Mid Dnieper basin, in line with the attested animal assemblages, which still reflect the mammoth fauna complex. Here, the environmental reconstructions at Yudinovo, upper layer (14.3–14.1 ka calBP) and observations at Yeliseevichy, upper layer, Pushkari IX, 1 suggest the continuation of permafrost conditions and the presence of mammoths even until the Greenland-Interstadial 1e (Bølling), at least in the mid-part of the Desna River basin.

The earliest cultural phenomenon of clearly post-LGM age in Eastern Europe north of 50° northern latitude is the Epigravettian, and the earliest manifestation of the Epigravettian north of 50° northern latitude is currently attested at the site of Barmaky (Tables 11-3; 11-4; Fig. 11-11; 11-22). Concerning its material culture, the Barmaky assemblage shows characteristics of both the Early and Late Epigravettian. Characteristic of the Early Epigravettian is the use of two discrete core reduction methods for blades and bladelets, while the abundance of microliths is common for the Late Epigravettian (Naudinot et al. 2017; Lengyel et al. 2021). The Mizyn industry combines these features and shows a dominance of burins on truncated blades and straight-backed microgravette points.

All other post-LGM assemblages of the Mid Dnieper and Upper Don basin (Mezhyrich industry and Yudinovo industry as well as Suponevo and Yeliseevichy assemblages) belong to the Late Epigravettian complexes. Technologically, they are characterised by a continuous, unidirectional blade-bladelet core reduction with direct percussion using mineral hammers. The tool spectrum is marked by the presence of lanceolate microgravette points and rectangles on bladelets, as well as a dominance of burins on truncated blades. Another characteristic feature of the Late Epigravettian in the Mid Dnieper basin is the appearance of short double and/or rounded end-scrapers and rectangles on bladelets, unknown from the preceding Mizyn industry. In contemporaneous assemblages of the Upper Don, but backed bladelets, including pointed pieces and rectangles, burins on truncated blades, and short rounded and double end-scrapers are known (Fig. 11–22). The latest manifestations of the Epigravettian are observed in the Upper Don Basin and assemblages of the Yudinovo industry (Table 11–4; Fig. 11–18; 11–21; 11–22).

## The origin of post-LGM industries north of 50° latitudes

In the Mid Dnieper and Upper Don basins, a chronological gap of about 4–5 thousand years is observable between pre-LGM/LGM industries on the one hand and post-LGM industries on the other (Table 11–4; Fig. 11–22). This marked hiatus renders a continuous cultural evolution north of 50° latitudes doubtful and calls for a search of the sources of the Late Epigravettian population and its techno-typological characteristics. Since the spatially and chronologically closest potential source, the Byki industry (Fig. 11–22), shows only little technological and typological similarities, it seems advisable to widen the perspective and to look at the Early Epigravettian of the Black and Azov Sea area and the Dniester and Prut basins.

The Early Epigravettian at the northern shores of the Black Sea and Azov Sea (23/22–19/18 ka calBP) comprises the assemblages of Amvrosiivka, Anetovka 2, Velyka Akkarzsha, Novovolodymyrivka, Fedorivka, layer 2, Dmytrivka, Voznesenka, lower and middle layers, and Kamenaya Balka II, II (Krotova 2013: 203). A specific typological component of these assemblages – alongside Epigravettian microliths

| Climate | Cryoturbation evidences | wcalBP (ka) | Sites | Taxonomic units | |
|---|---|---|---|---|---|
| Allerød | permafrost conditions | 13,2–12,7* | Pushkari IX, layer 1 | Yudinovo industry | Late Epigravettian, ≈19,0–13,0 ka calBP |
| Bølling | **not observed** | **14,0–13,8** | **Divnogorie 9, upper soil** | **no artefacts** | |
| | **permafrost conditions** | **14,3–14,1** | **Yudinovo, upper layer** | **Yudinovo industry** | |
| post-LGM | **not observed** | **14,9–14,4** | **Borschevo 2** | **Don Epigravettian** | |
| | **permafrost conditions, ice cracks** | **15,6–15,4** | **Yudinovo, lower layer, 4 phase** | **Yudinovo industry** | |
| | not observed | ≈15,0 | Divnogorie 9, I | Don Epigravettian | |
| | **not observed** | **16,4–16,1** | **Semenivka 1** | **Mezhyrich industry** | |
| | not observed | ≈16,5–13,5 | Divnogorie 1 | Don Epigravettian | |
| | not observed | 16,6–16,0* | Buzhanka 2 | Mezhyrich industry | |
| | **not observed** | **16,6–16,3** | **Gintsy, pit 9** | **Mezhyrich industry** | |
| | **not observed** | **16,9–16,6** | **Divnogorie 9, III** | **Don Epigravettian** | |
| | not observed | 16,9–16,2* | Semenivka 3 | Mezhyrich industry | |
| | **permafrost conditions, ice cracks** | **16,9–16,6** | **Yudinovo, lower layer, 3 phase** | **Yudinovo industry** | |
| | **not observed** | **17,2–16,9** | **Divnogorie 9, VI** | **Don Epigravettian** | |
| | **permafrost** | **17,3–17,1** | **Yeliseevichi I** | **Yeliseevichi industry** | |
| | **not observed** | **17,3–17,1** | **Dobranichivka** | **Mezhyrich industry** | |
| | **small polygons; microfractures** | **17,7–17,5** | **Mezhyrich, phase 3** | **Mezhyrich industry** | |
| | **small polygons; microfractures** | **17,7–17,5** | **Mezhyrich, phase 2–3** | **Mezhyrich industry** | |
| | not observed | ≈17,8–16,0 | Suponevo | Suponevo industry | |
| | solifluction (?) | 17,8–17,6 | Mizyn | Mizyn industry | |
| | not observed | 17,9–16,8* | Semenivka 2 | Mezhyrich industry | |
| | not observed | 17,9–17,4 | Gintsy, upper & lower layers | Mezhyrich industry | |
| | **permafrost conditions, ice cracks** | **17,9–17,6** | **Yudinovo, lower layer, 2 phase** | **Yudinovo industry** | |
| | **permafrost conditions** | **18,1–17,8** | **Timonovka 1** | **Yudinovo industry** | |
| | **small polygons; microfractures** | **18,1–17,9** | **Mezhyrich, phase 2** | **Mezhyrich industry** | |
| | **permafrost conditions** | **18,2–18,1** | **Pushkari IX, layer 2** | **Yudinovo industry** | |
| | **permafrost conditions, ice cracks** | **18,2** | **Yudinovo, lower layer, 1 phase** | **Yudinovo industry** | |
| | **small polygons; microfractures** | **18,3–18,2** | **Mezhyrich, phase 1** | **Mezhyrich industry** | |
| | **solifluction (?)** | **18,7–18,5** | **Mizyn** | **Mizyn industry** | |
| | **permafrost conditions, solifluction** | **19,1–18,9** | **Barmaky, 2** | **Mizyn industry** | |
| | not observed | ≈19,5–16,4 | Samotoevka | **Byki culture, ≈21,4–19,0 ka calBP** | |
| | after permafrost degradation | ≈20,8–19,0 | Byki 7, I, Ib, Ia | | |
| | **not observed** | **21,4–21,1** | **Byki 1** | | |
| LGM | **not observed** | **24,9–24,6** | **Kostenki 11, Ia, complex 3** | **Epiaurignacian, ≈25,3–24,0 ka calBP** | |
| | not observed | 25,0–24,0* | Gordashivka | | |
| | net of ice cracks; dust events | 25,3–24,6* | Obolonnya | | |
| | **ice wedges; dust events** | **24,8–24,4** | **Pushkari I, VII** | **Pushkari industry / Anosovka complex, ≈27,1–24,4 ka calBP** | |
| | **ice wedges; dust events** | **25,5–24,8** | **Pushkari I, V** | | |
| | not observed | 26,5–25,7* | Kostenki 11, II | | |
| | **ice wedges** | **26,9–26,4** | **Kostenki 21, III–dwellings** | | |
| | **net of ice cracks** | **27,1–26,5** | **Pushkari IX, 3** | | |
| LGM / pre-LGM | before (?) ice wedges | 26,9–25,6* | Gagarino | **Final Gravettian / Gmelin complex, ≈27,3–25,6 ka calBP** | |
| | **before (?) ice wedges** | **26,9–26,4** | **Kostenki 21, III–production areas** | | |
| pre-LGM | **before ice wedges** | **27,3–27,2** | **Khotylevo 2** | | |

Table 11–4. Eastern European assemblages north of 50° latitude: environment, chronology, taxonomy; *single date, ≈ estimated radiocarbon age. For dates and weighted averages, see Tables 11–2 and 11–3.

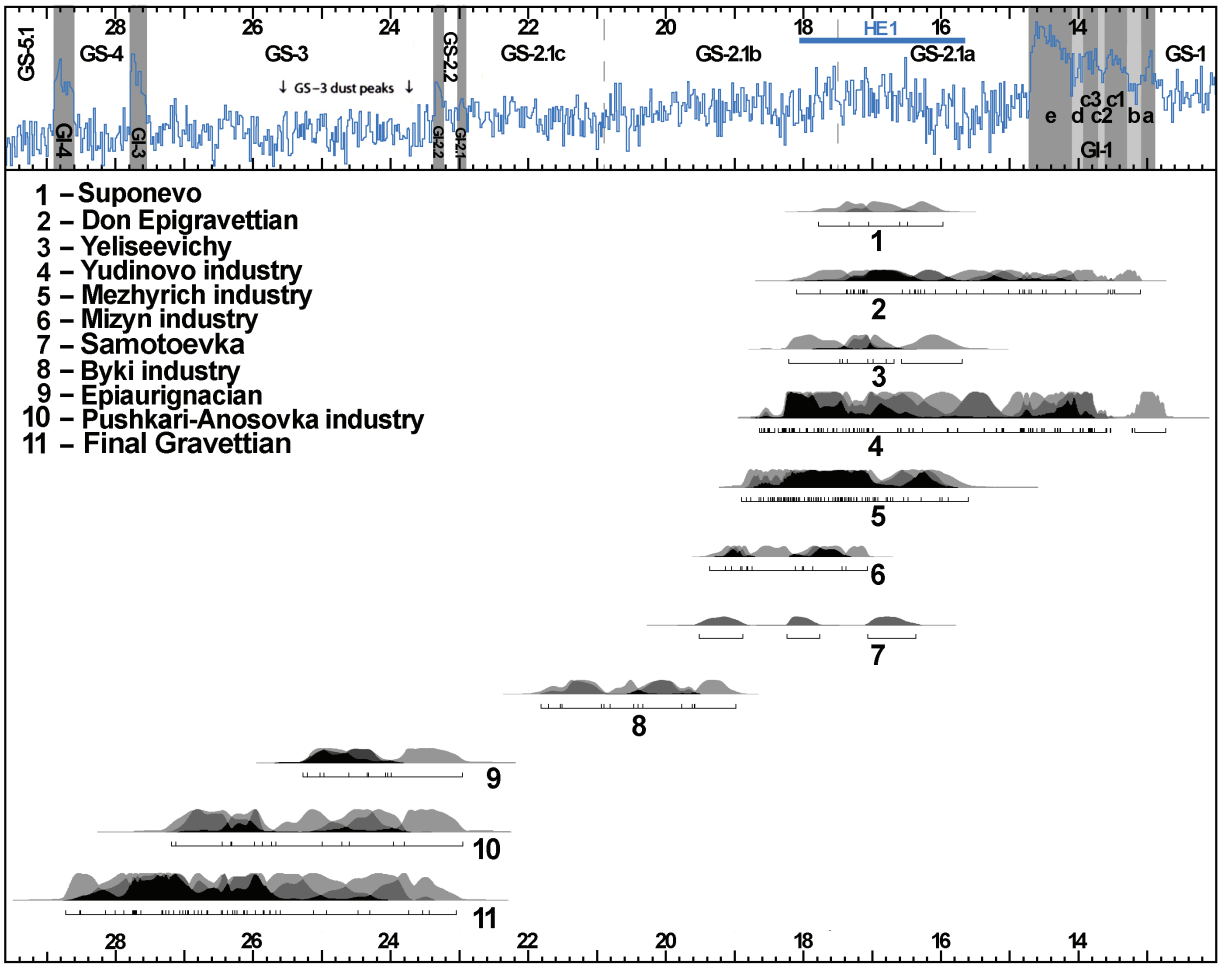


Fig. 11-22. Chronology of pre-LGM, LGM and post-LGM industries above 50° northern latitude in Eastern Europe.

(backed bladelets and micro-blades, including points and rectangles) – is the presence of cores-on-flakes in the form of carinated burins and carinated scrapers, slightly twisted micro-blades with light marginal retouch, thick end-scrapers, and the dominance of dihedral burins (Stanko et al. 1989; Krotova 2013: 203-208; Sapozhnikov 2003: 230; Olenkovsky 2008: 191, 203, 228). Since this component is similar to the characteristics of the Epiaurignacian, a genealogical descent or co-existence of the two is debated. Zaliznyak (2005: 36; 2021) suggested a migration of people with "Gravettian-like industries" (Pushkari I, Khotylevo 2) from the Desna basin into the region of the northern Black Sea and Azov Sea, where they mixed with the local Epiarignacian population and together formed the Early Epigravettian. However, this hypothesis could so far not be corroborated by chronological analyses or technological and typological studies. The characteristic elements of northern pre-LGM and LGM assemblages, namely Pavlov, Anosovka, and shouldered points, are not observed in the Early Epigravettian of the northern Black Sea and Azov Sea area. Straight-backed points observed in some Epigravettian assemblages of the Black and Azov Sea area (Govorukha, Mynievski Yar, Vysla Balka and Kamianka) are also discussed as a possible analogy to the microliths of the Mizyn industry (Krotova 2021b). Unfortunately, these assemblages are not well-dated.

The Early Epigravettian (24-20 ka calBP) of eastern Central Europe (Austria, Moravia and the Carpathian basin) is characterised

by a relative scarcity of backed pieces and a dominance of domestic tools over the armatures (Lengyel et al. 2021). Another specific feature is the presence of carinated scrapers and small, marginally retouched bladelets at Kammern-Grubgraben and Mohelno-Plevovce, leading to debates about the taxonomic attribution of these assemblages to the Badegoulien and/or Epiaurignacian (Demidenko et al. 2019; Händel et al. 2020; Lengyel et al. 2021). The Late Epigravettian (20–15 ka calBP) sees a northward expansion into southern Poland after the LGM (Wiśniewski et al. 2017; Bobak, Połtowicz-Bobak 2018; Połtowicz-Bobak, Bobak 2020; Lengyel et al. 2021), with a toolkit characterised by numerous backed pieces on bladelets, inducing points, rectangles and trapezes (Lengyel et al. 2021: 10).

One of the few places where a continuous evolution from Early to the Late Epigravettian between 27/25–19/18 ka calBP becomes observable is the area around the Dniester and Prut basins, most notably in the stratigraphic and cultural sequences of Molodova V, Korman IV, Cotu-Miculinţi, Poiana Cireşului, Crasnaleuca-Stanişte, Bistricioara-Lutărie III, Kosăuţi, Bistricioara-Lutărie 'La Mal', Korman 9 (Haesaerts et al. 2004; Borziac et al. 2006; Noiret 2009; Nuzhnyi 2015; Anghelinu et al. 2012; 2022; Kulakovska et al. 2021). Here, the earliest manifestation of the Epigravettian occurs during the LGM without a discernible hiatus (Anghelinu et al. 2012: 26). Common features linking the Gravettian to the Epigravettian are microgravette points and rectangles. Otherwise, the technological and typological alterations from the Early to the Late Gravettian appear gradually and are mainly marked by a microlithisation of the toolkit and the disappearance of shouldered pieces (Anghelinu et al. 2012: 26; Nuzhnyi 2015: 430; Niţă et al. 2021).

Further clarification is needed to see how far the material culture evolution observable in the sites of the Dniester and Prut basins is transferable for a better understanding of the punctuated processes to the Mid Dnieper and Upper Don regions and the source regions for the post-LGM resettlement. The Final Gravettian (Gmelin complex) of the Mid Dnieper and Upper Don shows techno-typological affinities to Molodovo V, layer 7 in the Dniester valley (Nuzhnyi 2009: 173; Nuzhnyi 2015: 66). On the other hand, the Early Epigravettian from the regions north of the Black Sea and Azov Sea shares neither common techno-typological features with contemporaneous assemblages in the Dniester and Prut basins, nor with assemblages of the chronologically older Final Gravettian Gmelin and Pushkari-Anosovka complexes, but show technological and typological elements characteristic of the Epiaurignacian.

For now, the most appropriate scenario of the transition from the Gravettian to the Epigravettian north of 50° northern latitudes of Eastern Europe is a depopulation of the Mid Dnieper and Upper Don basins during the LGM (26,5–20/19 ka calBP, after Clark et al. 2009) and a subsequent recolonisation from about 19 ka calBP. The Early Epigravettian populations of eastern Central Europe, the Dniester and Prut basins, and the Black Sea and Azov Sea region are potential source areas for the recolonisation. Given the geographical and chronological positions of the site of Barmaky, the most likely sources of its inhabitants are the Dniester-Prut region and eastern Central Europe.

# BIBLIOGRAPHY


*Abramova 1995.* Абрамова, З. А. 1995. *Верхнепалеолитическое поселение Юдиново. Выпуск 1.* Санкт-Петербург: ИИМК РАН.

Abramova, Z. A. 1995. *The Upper Palaeolithic site Yudinovo.* Vol. 1. Saint-Petersburg: IIMK RAN. (In Russian).

*Abramova et al. 1996.* Абрамова, З. А., Григорьева, Г. В., Кристенсен, М. 1996. *Верхнепалеолитическое поселение Юдиново.* Выпуск 2. Санкт-Петербург: ИИМК РАН.

Abramova, Z. A., Grigoreva, G. V. Christensen, M. 1996. *The Upper Palaeolithic site Yudinovo.* Vol. 2. Saint-Petersburg: IIMK RAN. (In Russian).

*Abramova et al. 2001.* Abramova, Z. A., Grigorieva, G. A., Zaitseva, G. I. 2001. The age of Upper Paleolithic sites in the Middle Dnieper River basin of Eastern Europe. *Radiocarbon*, 43 (2B), p. 1077–1084.

*Abramova, Grigoreva 1997.* Абрамова, З. А., Григорьева, Г. В. 1997. *Верхнепалеолитическое поселение Юдиново.* Выпуск 3. Санкт-Петербург: ИИМК РАН.

Abramova, Z. A., Grigoreva, G. V. 1997. *The Upper Palaeolithic site Yudinovo.* Vol. 3. Saint-Petersburg: IIMK RAN. (In Russian).

*Akhmetgaleeva 2004.* Ахметгалеева, Н. Б. 2004. Кремневый комплекс стоянки *Быки-7.* В: Амирханов, Х. А. (ред.). *Проблемы каменного века Русской равнины.* Москва: Научный мир, с. 285-298.

Akhmetgaleeva, N. B. 2004. The flint complex of the Byki-7 site. In: Amirkhanov, H. A. (Ed.). *The problems of the Stone Age of Russian Plane.* Moscow: Nauchnyi mir, p. 285–298. (In Russian).

*Akhmetgaleeva 2011.* Ахметгалеева, Н. Б. 2011. Нижний культурный слой стоянки Быки-7: проблемы и перспективы исследований. В: Гаврилов, К. (ред.). *Палеолит и мезолит Восточной Европы.* Москва: Институт археологии РАН, с. 443-455.

Akhmetgaleeva, N. B. 2011. The Lower Cultural Layer of the Byki-7 Site: Problems and Perspectives of Investigation. In: Gavrilov, C. (Ed.). *The Palaeolithic and Mesolithic of the Eastern Europe.* Moscow: Institute of Archaeology RAS, p. 443–455. (In Russian).

*Akhmetgaleeva 2014.* Ахметгалеева, Н. Б. 2014. К вопросу о расселении первобытного человека в Посеймье на заключительных этапах последнего оледенения. В: Васильев, С. А., Ткач, Е. С. (ред.). *Верхний палеолит Северной Евразии и Америки: памятники, культуры, традиции.* Санкт-Петербург: ИИМК РАН, с. 217-227.

Akhmetgaleeva, N. B. 2014. To the question of the resettlement of Prehistoric Humans in the Seim basin during the final stage of the Last Glacial. In: Vasiliev, S., Tkach, Ye. (Eds.). *The Upper Paleolithic of Northern Eurasia and America: sites, cultures, traditions.* Sankt-Petersburg: Institute of the History of Material Culture, p. 217–227. (In Russian).

*Akhmetgaleeva 2019.* Ахметгалеева, Н. Б. 2019. Стоянки позднего палеолита Быки в центре Русской Равнины: культурная составляющая. *Camera Prehistorica*, 1 (2), с. 18–35.

Akhmetgaleeva, N. B. 2019. The Upper Palaeolithic sites Byki in the centre of the Russian Plain: cultural definition. *Camera Prehistorica,* 1 (2), p. 18–35. (In Russian).

*Alexandrowicz 1987.* Alexandrowicz, S. W. 1987. Analiza malakologiczna w badaniach osadów czwartorzedowych. *Geologia,* 13 (1–2), p. 3–240.

*Alexandrowicz et al. 2014.* Alexandrowicz, P. W., Lanczont, M., Boguckyj, A. B., Kulesza, P., Dmytruk, R. 2014. Molluscs and ostracods of the Pleistocene loess deposits in the Halych site (Western Ukraine) and their significance for palaeoenvironmental reconstructions. *Quaternary Science Reviews*, 105, p. 162–180.

*Almeida 2000.* Almeida, F. J. N. 2000. *The Terminal Gravettian of Portuguese Estremadura: Technological Variability of the Lithic Industries.* PhD. thesis. Dedman College of Southern Methodist University, Dallas. doi:10.13140/RG.2.2.23479.32169

*Álvarez-Fernández et al. 2021.* Álvarez-Fernández, E., Martin-Jarque, S., Tarriño, A. 2021. Flint & shell: raw material as evidence of long-distance contacts in Cantabrian Spain during Magdalenian. In: Gaudzinski-Windheuser, S. and Jöris, O. (Eds.). *The Beef behind all Possible Pasts. The tandem-Festschrigt in honour of Elaine Turner and Martin Street. Volume 1.* Monographien des RGZM 157. Heidelberg: Propylaeum, p. 307–323.

*Ambrose 1990.* Ambrose, S. H. 1990. Preparation and characterization of bone and tooth collagen for isotopic analysis. *Journal of Archaeological Science 17,* p. 431–451.

*Ambrose & Norr 1993.* Ambrose, S. H. & Norr, L. 1993.Experimental evidence for the relationship of the carbon isotope ratios of whole diet and dietary protein to those of bone collagen and carbonate. In: Lambert J, Grupe G. (Eds.). *Prehistoric Human Bone, Archaeology at the Molecular Level,* Springer: Berlin, Heidelberg, p. 1–37.

*Amirkhanov 2000.* Амирханов, Х. А. 2000. *Зарайская стоянка.* Москва: Научный мир.
Amirkhanov, H. A. 2000. *Zaraiskaya site.* Moscow: Nauchnyi mir. (In Russian).

*Amirkhanov 2009.* Амирханов, Х. А. 2009. Стоянка Зарайск А: характеристика объектов третьего культурного слоя. В: Амирханов, Х. А. (ред.). *Исследования палеолита в Зарайске. 1999-2005.* Москва: Палеограф, с. 15-36.
Amirkhanov, H. A. 2000. Zaraisk A site: the characteristics of the objects of the third cultural layer. In: Amirkhanov, H. (Ed.). *Palaeolithic studies in Zaraisk.* 1999–2005. Moscow: Paleograf, p. 15–36. (In Russian).

*Anghelinu et al. 2012.* Anghelinu, M., Niță, L., Steguweit, L. 2012. Not that original after all: the chrono-cultural framework of the Upper Paleolithic on the Bistrita valley. *Arheologia Moldovei,* XXXV, p. 7–46.

*Anghelinu et al. 2021.* Anghelinu, M., Händel, M., Niță, L., Cordoș, C., Veres, D., Hambach, U., .Murătoreanu, G., Ciornei, A., Schmidt, Ch., Sava, T., Mănăilescu, C., Ilie, M., Demay, L., & Georgescu, V. (2021). From Gravettian to Epigravettian in the Eastern Carpathians: Insights from the Bistricioara-Lutărie III archaeological site. *Quaternary International, 587,* 210–229.

*Anghelinu et al. 2022.* Anghelinu, M., Händel, M., Niță, L., Cordoș, Ch., Veres, D., Hambach, U., Ciornei, A., Buchinger, N. 2022. New Research on the Upper Paleolithic site at Bistricioara-Lutărie III (Eastern Romanian Carpathians). *Varia Archaeologica,* II, p. 11–29.

*Anikovich 1998.* Аникович, М. В. 1998. Днепро-Донская историко-культурная область охотников на мамонтов: от «восточного граветта» к «восточному эпиграветту». В: Амирханов, Х. А. (ред.). *Восточный граветт.* Москва: Научный мир, с. 35-66.
Anikovich, M. V. 1998. The Dnieper-Don historical-cultural region of mammoth hunters: from Eastern Gravettian to Eastern Epigravettian. In: Amirkhanov, H. (Ed.). *The Eastern Gravettian.* Moscow: Nauchnyi mir, p. 35–66. (In Russian).

*Anikovich 2019a.* Аникович, М. В. 2019. Днепро-Донская историко-культурная область: Виллендорфско-Павловско-Костёнковское единство в Восточной Европе. *Труды Костёнковско-Борщёвской археологической экспедиции ИИМК РАН,* 8/II, с. 11-156.
Anikovich, M. V. 2019. Dnieper-Don historical and cultural entity: Willendorf-Pavlov-Kostenki cultural entity in Eastern Europe. *The Proceedings of the Kostenki-Borschevo archaeological expedition,* 8/II, p. 11–156. (In Russian).

*Anikovich 2019b.* Аникович, М. В. 2019. Второй этап функционирования Днепро-Донской ИКО: основные проблемы. *Труды Костёнковско-Борщёвской археологической экспедиции ИИМК РАН,* 8/II, с. 194-196.
Anikovich, M. V. 2019. The second stage of the Dnieper-Don HCH existence: key issues. *The Proceedings of the Kostenki-Borschevo archaeological expedition,* 8/II, p. 194–196. (In Russian).

*Baumann 2023.* Baumann, C. 2023. The paleo-synanthropic niche: a first attempt to define animal's adaptation to a human-made micro-environment in the Late Pleistocene. *Archaeological and Anthropological Sciences 15,* p. 1–13.

*Baumann et al. 2020.* Baumann, C., Starkovich, B. M., Drucker, D. G., Münzel, S. C., Conrad, N. J. & Bocherens, H. 2020: Dietary niche partitioning among Magdalenian canids in southwestern Germany and Switzerland. *Quaternary Science Reviews 227,* 106032.

*Beijersbergen et al. 2021.* Beijersbergen, L. M. T., Fernandes, R., Mørkved, P. T., & Hufthammer, A. K. 2021. Temporal and spatial variability of bone collagen stable carbon and nitrogen isotopic ratios of Norwegian reindeer. *Journal of Archaeological Science: Reports, 37,* 102890.

*Belyaeva 2002a.* Беляева, В. И. 2002. Кремневая индустрия Пушкарей I. В: Праслов, Н. Д. (ред.). *Верхний палеолит – Верхний плейстоцен: динамика природных событий и периодизация археологических культур.* Санкт-Петербург: ИИМК, с. 132-137.
Belyaeva, V. I. 2002. Flint industry of Pushkari I. In: Praslov, N. D. (Ed.). *The Upper Paleolithic – Upper Pleistocene: dynamics of natural events and periodization of archaeological cultures.* Saint-Petersburg: Institute of Material Culture History, p. 132–137. (In Russian).

*Belyaeva 2002b.* Беляева, В. И. 2002. *Палеолитическая стоянка Пушкари I (характеристика культурного слоя).* Санкт-Петербург: Санкт-Петербургский государственный Университет.

Belyaeva, V. I. 2002. *The Palaeolithic site Pushkari I (the characteristics of the cultural layer).* Sankt-Petersburg: S.-Petersburg State University. (In Russian).

*Bessudnov 2013.* Бессуднов, А. А. 2013. Палеолитические памятники конца плейстоцена в бассейне Верхнего и Среднего Дона. В: Синицына, Г. В. (ред.). *Проблемы заселения северо-запада Восточной Европы в верхнем и финальном палеолите (культурно-исторические процессы).* Санкт-Петербург: ЭлекСис, с. 127-151.

Bessudnov, A. A. 2013. The Palaeolithic sites of the Late Pleistocene in the Upper and Mid Don basin. In: Sinitsyna, G. V. (Ed.). *The problems of populating of the north-western Eastern Europe in Upper and Final Palaeolithic (the cultural and historical processes).* Sankt-Petersburg: ElekSis, p. 127-151. (In Russian).

*Bessudnov et al. 2012.* Бессуднов, А. Н., Бессуднов, А. А., Бурова, Н. Д., Лаврушин, Ю. А., Спиридонова, Е. А. 2012. Некоторые результаты исследований палеолитических памятников у хутора Дивногорье на Среднем Дону (2007-2011 гг.). *Краткие сообщения Института археологии РАН,* 227, с. 146-156.

Bessudnov, A. N., Bessudnov, A. A., Burova, N. D., Lavrushin, Yu. A., Spiridonova, E. A. 2012. Some results of the investigations of Palaeolithic sites near the farm Divnogorie on the Mid Don (2007-2011). *The short reports of the Institute of Archaeology RAS*, 227, p. 146-156. (In Russian).

*Bessudnov et al. 2013.* Bessudnov, A. N., Sycheva, S. A., Bessudnov, A. A., Lavrushin, Yu. A., Chepalyga, A. L., Sadchikova T. A. 2013. Geoarchaeological sites Divnogorie 9 & 1 (Paleosols and Sediments MIS 2). In: Kovda, I. V. (Ed.). *Guidebook for Field Excursions XIIth International Symposium and Field Seminar on Paleopedology, 10-15 August, 2013, Kursk, Russia.* Moscow: Institute of Geography, p. 89-104.

*Bessudnov, Bessudnov 2012.* Бессуднов, А. Н., Бессуднов, А. А. 2012. Позднепалеолитическая стоянка Самотоевка в бассейне Черной Калитвы (предварительное сообщение). В: Отрощенко, В. В. (ред.). *Проблеми дослідження пам'яток археології Східної України. Матеріали III Луганської міжнародної історико-археологічної конференції, присвяченої пам'яті С. Н. Братченка.* Луганськ (б. в.), с. 37-45.

Bessudnov, A. N., Bessudnov A. A. 2012. The Upper Palaeolithic site Samotoevka in the Basin of the Chernaya Kalitva River. In: Otroschenko, V. V. (Ed.). *The Problems of Investigating Archaeological Sites in Eastern Ukraine. The papers of the Third Lugansk International Conference devoted to the memory of S. N. Bratchenko.* Lugansk, p. 37-45. (In Russian).

*Bibikov 1981.* Бибиков, С. Н. 1981. *Древнейший музыкальный комплекс из костей мамонта.* Киев: Наукова думка.

Bibikov, S. N. 1981. *The oldest musical complex made on mammoth bones.* Kyiv: Naukova dumka. (In Russian).

*Binford 1982.* Binford, L. R. 1982. The archaeology of place. *Journal of Anthropological Archaeology, 1,* p. 5–31.

*Bobak, Połtowicz-Bobak 2018.* Bobak, D., Połtowicz-Bobak, M. 2018. Between Magdalenian and Epigravettian. A contribution to the study of the Palaeolithic on the Polish-Ukrainian border. *Матеріали і дослідження з археології Прикарпаття і Волині,* 22, p. 42-53.

*Bocherens 2003.* Bocherens, H. 2003. Isotopic biogeochemistry and the palaeoecology of the mammoth steppe fauna. *Deinsea 9,* p. 57–76.

*Bocherens & Drucker 2003.* Bocherens, H. & Drucker, D. 2003. Trophic level isotopic enrichment of carbon and nitrogen in bone collagen: Case studies from recent and ancient terrestrial ecosystems. *International Journal of Osteoarchaeology 13,* p. 46–53.

*Bocherens et al. 1991.* Bocherens, H., Fizet, M., Mariotti, A., Lange-Badre, B., Vandermeersch, B., Borel, J. P. & Bellon, G. 1991. Isotopic biogeochemistry ($^{13}C$,$^{15}N$) of fossil vertebrate collagen: application to the study of a past food web including Neandertal man. *Journal of Human Evolution 20*, p. 481–492.

*Bocherens et al. 1994.* Bocherens, H., Fizet, M., Mariotti, A., Gangloff, R. A. & Burns, J. A. 1994. Contribution of isotopic biogeochemistry $^{13}C$, $^{15}N$, $^{18}O$ to the paleoecology of mammoths *(Mammuthus primigenius). Historical Biology 7,* p. 187–202.

*Bocherens et al. 1997.* Bocherens, H., Billiou, D., Patou-Mathis, M., Bonjean, D., Otte, M., Mariotti, A. 1997. Paleobiological Implications of the isotopic Signatures $^{13}C$, $^{15}N$) of Fossil Mammal Collagen in Scladina Cave (Sclayn, Belgium). *Quaternary Research,* 48, p. 370-380.

*Bocherens et al. 2001.* Bocherens, H., Billiou, D., Mariotti, A., Toussaint, M., Patou-Mathis, M., Bonjean, D., Otte, M. 2001. New isotopic evidence for dietary habits of Neandertals from Belgium. *Journal of Human Evolution*, 40, p. 497-505.

*Bocherens et al. 2011.* Bocherens, H., Drucker, D. G., Bonjean, D., Bridault, A., Conard, N. J., Cupillard, Ch., Germonpré, M., Höneisen, M., Münzel, S. C., Napierala, H., Patou-Mathis, M., Stephan, E., Uerpmann, H.-P., Ziegler, R. 2011. Isotopic evidence for dietary ecology of cave lion (Panthera spelaea) in North-Western Europe: Prey choice, competition and implications for extinction. *Quaternary International,* 245 (2), p. 249–261. https://doi.org/10.1016/j.quaint.2011.02.023

*Bocherens et al. 2015.* Bocherens, H., Drucker, D. G., Germonpré, M., Lázničková-Galetová, M., Naito, Y. I., Wissing, C., Brůžek, J. & Oliva, M. 2015. Reconstruction of the Gravettian food-web at Předmostí I using multi-isotopic tracking $^{13}C$, $^{15}N$, 34S of bone collagen. *Quaternary International 359–360*, p. 211–228.

*Bonafini et al. 2013.* Bonafini, M., Pellegrini, M., Ditchfield, P. & Pollard, A. M. 2013. Investigation of the 'canopy effect' in the isotope ecology of temperate woodlands. *Journal of Archaeological Science 40,* p. 3926–3935.

*Boriskovsky 1953.* Борисковский, П. И. 1953. *Палеолит Украины.* Москва-Ленинград: Наука.

Boriskovsky, P. I. 1953. *The Palaeolithic of Ukraine.* Moscow-Leningrad: Nauka. (In Russian).

*Boriskovsky 1984.* Борисковский, П. И. 1984. Радиоуглеродные даты. В: Борисковский, П. И. (ред.). *Палеолит СССР.* Москва: Наука, с. 356-359.

Boriskovsky, P. I. 1984. The radiocarbon dates. In: Boriskovsky, P. I. (Ed.). *The Palaeolithic of the USSR.* Moscow: Nauka, p. 356–359. (In Russian).

*Boriskovsky, Dmitrieva 1982.* Борисковский, П. И., Дмитриева, Т. Н. 1982. Борщево 2. В: Праслов, Н. Д., Рогачев, А. Н. (ред.). *Палеолит Костенковско-Борщевского района на Дону, 1879-1979.* Ленинград: Наука, с. 217-222.

Boriskovsky, P. I., Dmitrieva T. N. 1982. Borschevo 2. In: Praslov, N. D. and Rogachev, A. N. (Eds.). *Palaeolithic of the Kostenki-Borshchevo area on the River Don, 1979–1989.* Leningrad: Nauka, p. 217–222. (In Russian).

*Borziac et al. 2006.* Borziac, I., Chirica, V., Văleanu, M.-C. 2006. *Culture et sociétés pendant le Paléolithique Supérieur à travers l'espace Carpato-Dniestréen.* Iaşi, Bibliotheca archaeologica Moldaviae VI.

*Bösl et al. 2006.* Bösl, C., Gruppe, G. & Peters, J. 2006. A Late Neolithic vertebrate food web based on stable isotope analyses. *International Journal of Osteoarchaeology 16*, p. 296–315.

*Bronk Ramsey 2021.* Bronk Ramsey, C. 2021. OxCal version 4.4.4. *The Oxford Radiocarbon Accelerator Unit,* University of Oxford. http://c14.arch.ox.ac.uk/oxcal/OxCal.html

*Brandl 2016.* Brandl, M. 2016. The Multi Layered Chert Sourcing Approach (MLA). Analytical Provenance Studies of Silicite Raw Materials. *Archeometriai Műhely XIII/3*, p. 145–156.

*Brandl et al. 2018.* Brandl, M., Martinez, M. M., Hauzenberger, C., Filzmoser, P., Nymoen, P. & Mehler, N. 2018. A multi-technique analytical approach to sourcing Scandinavian flint: Provenance of ballast flint from the shipwreck aLeirvigen 1°, Norway. *PLoS ONE 13(8)*: e0200647.

*Bump et al. 2007.* Bump, J. K., Fox-Dobbs, K., Bada, J. L., Koch, P. L., Peterson, R. O., & Vucetich, J. A. 2007. Stable isotopes, ecological integration and environmental change: wolves record atmospheric carbon isotope trend better than tree rings. *Proceedings of the Royal Society B: Biological Sciences 274,* p. 2471–2480.

*Chabai et al. 2019a.* Чабай, В. П., Ступак, Д. В., Весельський, А. П., Вотякова, О. Л., Маєр, А., Пазда, К., Дудник, Д. В. 2019. *Дослідження Волинської палеолітичної експедиції на верхньопалеолітичній стоянці Бармаки у місті Рівне в 2018 році.* Науковий архів ІА НАНУ, ф. е., 2018/18. Київ: Інститут археології.

Chabai, V. P., Stupak, D. V., Veselsky, A. P., Votiakova, O. L., Maier, A., Pasda, K., Dudnyk, D. V. 2019. *Research of the Volhynian Palaeolithic Expedition at the Upper Palaeolithic site of Barmaky in Rivne in 2018.* The scientific archive of the Institute of Archaeology, fund of the expeditions, 2018/18. Kyiv: Institute of Archaeology. (In Ukrainian).

*Chabai et al. 2019b.* Чабай, В. П., Ступак, Д. В., Весельський, А. П., Дудник, Д. В. 2019. Характеристика процесу акумуляції другого культурного шару верхньопалеолітичної стоянки Бармаки. В: Чабай, В. П. (ред.). *І Всеукраїнський археологічний з'їзд: матеріали роботи.* Київ: ІА НАН України, с. 213-225.

Chabai, V., Stupak, D., Veselsky, A., Dudnyk, D. 2019. The characteristics of the accumulation process of the Upper Palaeolithic site Barmaky, second cultural layer. In: Chabai, V. (Ed.). *The I$^{st}$ Ukrainian archaeological congress.* Kyiv: Institute of Archaeology, p. 213–225. (In Ukrainian).

*Chabai et al. 2020a.* Чабай, В. П., Ступак, Д. В., Весельський, А. П., Вотякова, О. Л., Маєр, А., Пазда, К., Дудник, Д. В. 2020. *Дослідження Волинської палеолітичної експедиції на верхньопалеолітичній стоянці Бармаки у місті Рівне в 2019 році.* Науковий архів ІА НАНУ, ф. е., 2019/50. Київ: Інститут археології.

Chabai, V. P., Stupak, D. V., Veselsky, A. P., Votiakova, O. L., Maier, A., Pasda, K., Dudnyk, D. V. 2019. *Research of the Volhynian Palaeolithic Expedition at the Upper Palaeolithic site of Barmaky in Rivne in 2019.* The scientific archive of the Institute of Archaeology, fund of the expeditions, 2019/50. Kyiv: Institute of Archaeology (In Ukrainian).

*Chabai et al. 2020b.* Чабай, В. П., Ступак, Д. В., Весельський, А. П., Дудник, Д. В. 2020. Культурно-хронологічна варіабельність епіграветy Середнього Подніпров'я. *Археологія,* 2, с. 5-31.

Chabai, V., Stupak, D., Veselsky, A., Dudnyk, D. 2020. The cultural and chronological variability of the Epigravettian of the Middle Dnieper basin. *Arheologia,* 2, p. 5–31. (In Ukrainian).

*Chabai et al. 2020c.* Чабай, В. П., Ступак, Д. В., Весельський, А. П., Дудник, Д. В. 2020. Стоянка Бармаки в контексті епіграветy Середнього Подніпров'я. *Археологія і давня історія України,* 4, с. 107-125.

Chabai, V. P., Stupak, D. V., Veselsky, A. P., Dudnyk, D. V. Barmaky site in the context of Epigravettian of the Middle Dnieper Basin. *The Archaeology and Ancient History of Ukraine*, 4, p. 107–125. (In Ukrainian).

*Chabai et al. 2021.* Чабай, В. П., Дудник, Д. В., Ступак, Д. В., Весельський, А. П., Васильєва М. А. 2021. *Розкопки Волинської палеолітичної експедиції верхньопалеолітичної стоянки Бармаки у місті Рівне у 2020 році.* Науковий архів ІА НАНУ, ф. е., 2020/1. Київ: Інститут археології.

Chabai, V. P., Dudnyk, D. V., Stupak, D. V., Veselsky, A. P., Vasylieva, M. A. 2021. *Excavations of the Volhynian Palaeolithic Expedition at the Upper Palaeolithic site of Barmaky in Rivne in 2020.* The scientific archive of the Institute of Archaeology, fund of the expeditions, 2020/1. Kyiv: Institute of Archaeology (In Ukrainian).

*Chabai et al. 2022.* Chabai, V., Dudnyk, D., Pasda, K., Brandl, M. & Maier, A. 2022. Investigations at the Epigravettian site of Barmaky in Volhynia, north-west Ukraine: analyses and taxonomic reflections. *Quartär*, 69, p. 105–144.

*Chabai, Demidenko 1998.* Chabai, V. P., Demidenko, Yu. E. 1998. The classification of flint artifacts. In: Marks, A., Chabai, V. (Eds.). *The Middle Paleolithic of Western Crimea*, vol. 1. Études et Recherches Archéologiques de L'Université de Liège, 84. Liege: University of Liege, p. 31–51.

*Chabai, Dudnyk 2022.* Chabai, V., Dudnyk, D. 2022. The Barmaky, level 2 Epigravettian assemblage: the core reduction strategies. *The Archaeology and Ancient History of Ukraine,* 4 (45), p. 33–57. https://doi.org/10.37445/adiu.2022.04.02.

*Chabai, Vasyliev 2021a.* Чабай, В. П., Васильєв, П. М., 2021. Культурно-хронологічні особливості еволюції палеоліту Середнього Подніпров'я. *Кам'яна доба України,* 12, с. 77-114.

Chabai, V., Vasyliev, P. 2021. The cultural and chronological peculiarities of the Paleolithic evolution at the Middle Dnieper basin. *The Stone Age of Ukraine,* 12, p. 77–114. (In Ukrainian).

*Chabai, Vasyliev 2021b.* Чабай, В. П., Васильєв, П. М., 2021. Культурно-хронологічні особливості еволюції верхнього палеоліту Волині. *Археологічні зошити з Пересопниці,* 8, с. 10-22.

Chabai, V., Vasyliev, P. 2021. The cultural and chronological peculiarities of the Volhynian Upper Palaeolithic evolution. *The archaeological papers from Peresopnitsa,* 8, p. 10–22. (In Ukrainian).

*Chubur 2001.* Чубур, А. А. 2001. *Быки. Новый палеолитический микрорегион и его место в верхнем палеолите Русской равнины.* Брянск: Брянск сегодня.

Chubur, A. A. 2001. *Buki. The new Palaeolithic micro-region and its significance in the Upper Palaeolithic of the Russian Plane.* Bryansk: Bryansk segodnia. (In Russian).

*Clark et al. 2009.* Clark, P. U., Dyke, A. S., Shakun, J. D., Carlson, A. E., Clark, J., Wohlfarth, B., Mitrovica, J. X., Hostetler, S. W., McCabe, A. M. 2009. The Last Glacial Maximum. *Science*, 325, p. 710–714.

*Cohen, Stepanchuk 2001.* Коен, В. Ю., Степанчук, В. М. 2001. Переход от среднего к верхнему палеолиту в Восточной Европе: проблемы таксономии и хроностратиграфии. *Vita Antiqua*, 3-4, с. 78-107.

Cohen, V. Yu, Stepanchuk, V. N. 2001. The transition from Middle to Upper Palaeolithic in Eastern Europe: the problems of taxonomy, chronology and stratigraphy. *Vita Antiqua*, 3–4, p. 78–107. (In Russian).

*Coltrain et al. 2004.* Coltrain, J. B., Harris, J. M., Cerling, T. E., Ehleringer, J. R., Dearing, M. D., Ward, J. & Allen, A. 2004. Rancho La Brea stable isotope biogeochemistry and its implications for the palaeoecology of late Pleistocene, coastal southern California. *Palaeogeography, Palaeoclimatology, Palaeoecology 205,* p. 199–219.

*Coplen 2011.* Coplen, T. B. 2011. Guidelines and recommended terms for expression of stable-isotope-ratio and gas-ratio measurement results. *Rapid Communications in Mass Spectrometry 25,* p. 2538–2560.

*Demars, Laurent 1992.* Demars, P.-Y., Laurent, P. 1992. *Types d'outils lithiques du paléolithique supérieur en Europe.* 2nd edition, Paris: Presses du CNRS.

*Demay et al. 2016.* Demay, L., Péan, S., Belyaeva, V. I., Vasil'ev, P. M., Patou-Mathis, M. 2016. Zooarchaeological study of an Upper Palaeolithic site with mammoth remains, Pushkari I – excavation VII (Chernigov oblast, Ukraine). *Quaternary International,* 406 (part B), p. 183–201.

*Demay et al. 2017.* Demay, L., Patou-Mathis, M., Péan, S., Khlopachev, G. A., Sablin, M. V. 2017. From mammoth to fox: functional identification of Eliseevichi 1 within Upper Pleniglacial settlements of the Desna valley. *Vita Antiqua,* 9, p. 81–106.

*Demay et al. 2020.* Demay, L., Vasylev, P. M., Koulakovska, L. V., Stupak, D. V., Shydlovskyi, P. S., Belyaeva, V. I. 2020. Palaeolithic Human societies during the Upper Pleniglacial period and their connections with the animal world according the evidence from archaeological sites of Ukraine. *The Archaeology and Ancient History of Ukraine,* 4, p. 82–93.

*Demay et al., 2021.* Demay, L., Vasyliev, P. M., Belyaeva, V. I. 2021. Subsistence activities in the Gravettian occupations of the Pushkari group: Pushkari I and Pushkari VIII (Pogon) (Ukraine). *Quaternary International,* 587–588, p. 291–309.

*Demay, Stupak 2021.* Demay, L., Stupak, D. 2021. New complex investigations of the Novhorod-Siverskyi Upper Palaeolithic site. *Arheologia,* 4, p. 5–34.

*DeNiro 1985.* DeNiro, M. J. 1985. Postmortem preservation and alteration of in vivo bone collagen isotope ratios in relation to palaeodietary reconstruction. *Nature 317,* p. 806–809.

*DeNiro & Epstein 1978.* DeNiro, M. J. & Epstein, S. 1978. Influence of diet on the distribution of carbon isotopes in animals. *Geochimica et Cosmochimica Acta 42,* p. 495–506. https://doi.org/10.1016/0016-70377890199-0

*DeNiro & Epstein 1981.* DeNiro, M. J. & Epstein, S. 1981. Influence of diet on the distribution of nitrogen isotopes in animals. *Geochimica et Cosmochimica Acta 45*, p. 341–351. https://doi.org/10.1016/0016-70378190244-1

*DeNiro & Weiner 1988.* DeNiro, M. J. & Weiner S. 1988. Chemical, enzymatic and spectroscopic characterization of "collagen" and other organic fractions from prehistoric bones. *Geochimica et Cosmochimica Acta 52*, p. 2197–2206.

*Demidenko 2004.* Демиденко, Ю. Э. 2004. Восточная Европа в контексте проблематики ориньяка Европы: прошлые подходы и новые перспективы. *Археологический альманах,* 16, с. 161-193.

Demidenko, Yu. E. 2004. Eastern Europe in the context of the European Aurignacian problematic. *Archaeological Almanac,* 16, p. 161–193. (In Russian).

*Demidenko 2008.* The Early and Mid-Upper Palaeolithic of the north Black Sea region: an overview. *Quartär,* 55, p. 99–114.

*Demidenko 2012.* Demidenko, Yu. E. 2012. The classification and attribute system applied to the Siuren I lithic assemblages. In: Demidenko, Yu., Otte, M., Noiret, P. (Eds.). *The Palaeolithic of Crimea, vol. IV. Siuren I rock-shelter: from Late Middle Palaeolithic and Early Upper Palaeolithic to Epi-Palaeolithic in Crimea.* Études et Recherches Archéologiques de L'Université de Liège, 129. Liege: University of Liege, p. 91–107.

*Demidenko 2020.* Demidenko, Yu. E. 2020. Magdalenian in Eastern Europe: is it reality there? *Anthropologie,* LVIII/2–3, p. 227–249.

*Demidenko, Chabai 2012.* Demidenko, Yu. E., Chabai, V. P. 2012. Unit F: Lithic Artifacts. In: Demidenko, Yu. E., Otte, M., Noiret, P. (Eds.). Suiren I rock-shelter. *From Late Middle Paleolithic and Early Upper Paleolithic to Epi-Paleolithic in Crimea.* Études et Recherches Archéologiques de L'Université de Liège, 129. Liege: University of Liege, p. 213–279.

*Demidenko et al. 2019.* Demidenko, Yu. E., Škrdla, P., Rios-Garaizar, J. 2019. In Between Gravettian and Epigravettian in Central and Eastern Europe: a peculiar LGM Early Late Upper Paleolithic industry. *Přehled výzkumů,* 60–1, p. 11–42.

*Derevianko et al. 2018.* Derevianko, A. P., Markin, S. V., Kolobova, K. A., Chabai, V. P., Rudaya, N. A., Viola, B., Buzhilova, A. P., Mednikova, M. B., Vasiliev, S. K., Zykin, V. S., Zykina, V. S., Zazhigin, V. S., Volvakh, V. O., Roberts, R. G., Jacobs, Z., Bo Li. 2018. *Multidisciplinary studies of Chagyrskaya cave.* Novosibirsk: Institute of Archaeology and Ethnography.

*Dierenfeld et al. 2020.* Dierenfeld, E. S., Han, Y. A. M., Mar, K. U., Aung, A., Soe, A. T., Lummaa, V., Lahdenperä, M. 2020. Milk Composition of Asian Elephants (*Elephas maximus*) in a Natural Environment in Myanmar during Late Lactation. *Animals* (Basel). 2020 Apr; 10(4): 725. Published online 2020 Apr 22. doi: 10.3390/ani10040725, last accessed on 12/1/2024

*Dobberstein et al. 2009.* Dobberstein, R. C., Collins, M. J., Craig, O. E., Taylor, G., Penkman, K. E. H. & Ritz-Timme, S. 2009. Archaeological collagen: Why worry about collagen diagenesis? *Archaeological and Anthropological Sciences 1,* p. 31–42, https://doi.org/10.1007/s12520-009-0002-7

*Drucker 2022.* Drucker, D. G. 2022. The isotopic ecology of the mammoth steppe. *Annual Review of Earth and Planetary Sciences 50,* p. 395–418.

*Drucker & Fontana 2024.* Drucker, D. G. & Fontana, L. 2024. Environmental conditions in the Massif Central during the Upper Palaeolithic using stable isotope tracking ($^{13}C$, $^{15}N$) of bone collagen from large herbivores. *Journal of Quaternary Science,* p. 1–16, https://doi.org/10.1002/jqs.3617

*Drucker et al. 2003.* Drucker, D. G., Bocherens, H. & Billiou, D. 2003. Evidence for shifting environmental conditions in Southwestern France from 33,000 to 15,000 years ago derived from carbon-13 and nitrogen-15 natural abundances in collagen of large herbivores. *Earth and Planetary Science Letters 216,* p. 163–173.

*Drucker et al. 2008.* Drucker, D.G., Bridault, A., Hobson, K.A., Szuma, E. & Bocherens, H., 2008. Can carbon-13 in large herbivores reflect the canopy effect in temperate and boreal ecosystems? *Evidence from modern and ancient ungulates. Palaeogeography, Palaeoclimatology, Palaeoecology 266 (1–2)*, p. 69–82. https://doi.org/10.1016/j.palaeo.2008.03.020

*Drucker et al. 2011.* Drucker, D. G., Kind, C. J. & Stephan, E. 2011. Chronological and ecological information on Late-glacial and early Holocene reindeer from northwest Europe using radiocarbon ($^{14}C$) and stable isotope ($^{13}C$, $^{15}N$) analysis of bone collagen: Case study in southwestern Germany. *Quaternary International 245*, p. 218–224.

*Drucker et al. 2015.* Drucker, D. G., Vercoutere, C., Chiotti, L., Nespoulet, R., Crepin, L., Conard, N. J., Munzel, S. C., van der Plicht, J., Higham, T., Laznickova-Galetova, M., & Bocherens, H. 2015. Tracking possible decline of woolly mammoth during the Gravettian in Dordogne (France) and the Ach Valley (Germany) using multi-isotope tracking ($^{13}C$, $^{14}C$, $^{15}N$, $^{34}S$, $^{18}O$). *Quaternary International*, 359-360, p. 304-317. https://doi.org/10.1016/j.quaint.2014.11.028

*Drucker et al. 2018.* Drucker, D. G., Stevens, R. E., Germonpré, M., Sablin, M. V., Péan, S. & Bocherens, H. 2018. Collagen stable isotopes provide insights into the end of the mammoth steppe in the central East European plains during the Epigravettian. *Quaternary Research 90,* p. 457–469.

*Dudin, Fedyunin 2019.* Дудин, А. Е., Федюнин, И. В. 2019. Третий костно-земляной жилой комплекс стоянки Костёнки 11/Ia. В: Лисицын, С. Н., Платонова, Н. И. (ред.). *Человек и мамонт в Палеолите Европы.* СПб.: Ars longa, с. 221-236.

Dudin, A. E., Fedyunin, I. V. 2019. The third bone-and-earthen dwelling complex of the Kostenki 11/Ia site. In: Lisitsyn, S., Platonova, N. (Eds.). *Man and mammoth in European Palaeolithic.* Sankt-Petersburg: Ars longa, p. 221-236. (In Russian).

*Dudnyk 2024.* Дудник Д. В. 2024. Стратегія нуклеусного розколювання мізинської індустрії епіграветського технокомплексу. *Археологія,* 3, с. 120-148.

Dudnyk, D. V. 2024. The core reduction strategy of the Mizyn industry of the Epigravettian techno-complex. *Arheologia,* 3, p. 120-148. (In Ukrainian).

*Dytham 2011.* Dytham, C. 2011. *Choosing and using Statistics. A biologist's guide.* Third Edition. Wiley Blackwell: West Sussex.

*Efimenko 1958.* Ефименко П. П. 1958. Костенки 1. Москва-Ленинград: Наука. Efimenko, P. P. 1958. *Kostenki 1.* Moscow-Leningrad: Nauka. (In Russian).

*Finstad & Kielland 2011.* Finstad, G. L. & Kielland, K. 2011. Landscape variation in diet and productivity of reindeer in Alaska based on stable isotope analyses. *Artic, Antarctic and Alpine Research 43,* p. 543–554.

*Fizet et al. 1995.* Fizet, M., Mariotti, A., Bocherens, H., Lange-Badré, B., Vandermeersch, B., Borel, J. P. & Bellon, G. 1995. Effect of diet, physiology and climate on carbon and nitrogen stable isotopes of collagen in a late Pleistocene anthropic palaeoecosystem: Marillac, Charente, France. *Journal of Archaeological Science 22,* p. 67–79.

*Fogel 1989.* Fogel, M. L. 1989. Nitrogen isotope tracers of human lactation in modern and archaeological populations. In: *Annual Report of the Director of the Geophysical Laboratory*, Washington: Carnegie Institution, volume 88, p. 111–117.

*Fox-Dobbs et al. 2007.* Fox-Dobbs, K., Bump, J. K., Peterson, R. O., Fox, D. L. & Koch, P. L. 2007. Carnivore-specific stable isotope variables and variation in the foraging ecology of modern and ancient wolf populations: case studies from Isle Royale, Minnesota, and La Brea. *Canadian Journal of Zoology 85,* p. 458–471.

*Fox-Dobbs et al. 2008.* Fox-Dobbs, K., Leonard, J. A. & Koch, P. L. 2008. Pleistocene megafauna from eastern Beringia: paleoecological and paleoenvironmental interpretations of stable carbon and nitrogen isotope and radiocarbon records. *Palaeogeography, Palaeoclimatology, Palaeoecology 261*, p. 30–46.

*Frank 2006.* Frank, C. 2006. *Plio-Pleistozäne und holozäne Mollusken Österreichs.* Mitteilungen der Prähistorischen Kommission, 62 (1–2). Wien: Verlag der Österreichischen Akademie der Wissenschaften.

*Fűköh et al. 1995.* Fűköh, L, Krolopp, E. Sümegi, P. 1995. *Quaternary malacostratigraphy in Hungary.* Malacological Newsletter, suppl. 1. Gyöngyös: Natural Science Section of Mátra Museum.

*Galych 1941.* Галич, Д. З. 1941. Палеолітична стоянка Чулатів II (Робочий Рів). *Палеоліт і неоліт України, 1:* 149-153.

Galych, D. Z. 1941. The Palaeolithic site of Chulativ II. *The Palaeolithic and Neolithic of Ukraine, 1:* 149–153. (In Ukrainian).

*Gavrilov 1994.* Гаврилов, К. Н. 1994. Кремневые комплексы стоянки Тимоновка 1. *Вестник Московского университета,* 8 (История 3), с. 63-76.

Gavrilov, C. N. 1994. The flint complexes of the Timonovka 1 site. *The newsletters of Moscow University,* 8 (History 3), p. 63–76. (In Russian).

*Gavrilov 2008.* Гаврилов, К. Н. 2008. Верхнепалеолитическая стоянка Хотылево 2. Москва: ТАУС.

Gavrilov, C. N. 2008. *The Upper Palaeolithic site Khotylevo 2.* Moscow: TAUS. (In Russian).

*Gavrilov 2016.* Гаврилов, К. Н. 2016. *Верхний палеолит Десны. Преемственность и вариабельность в развитии материальной культуры.* Москва; Санкт-Петербург: Нестор-История.

Gavrilov, C. N. 2016. *The Upper Palaeolithic of Desna basin. Continuity and variability in the evolution of material culture.* Moscow; St. Petersburg: Nestor-Istoria. (In Russian).

*Gavrilov 2023.* Гаврилов, К. Н. 2023. Переход от средней к поздней поре верхнего палеолита в центре Русской равнины: реколонизация или автохтонное развитие? *Первобытная археология. Журнал междисциплинарных исследований,* 1, с. 47-67.

Gavrilov, K. N. 2023. Transition from the Middle to the Late Upper Paleolithic in the Central Russian Plane: recolonization or autochthonous development? *Prehistoric Archaeology. Journal of Interdisciplinary Studies,* 1, p. 47–67. (In Russian).

*Gavrilov et al. 2015.* Gavrilov, K. N., Voskresenskaya, E. V., Maschenko, E. N., Douka, K. 2015. East Gravettian Khotylevo 2 site: Stratigraphy, archeozoology, and spatial organization of the cultural layer at the newly explored area of the site. *Quaternary International*, 359–360, p. 335–346.

*Gavrylenko 2003.* Гавриленко, І. М. 2003. Вадим Щербаківський та дослідження Гінцівської пізньопалеолітичної стоянки. *Кам'яна доба України,* 4, с. 53-81.

Gavrylenko, I. 2003. Vadym Scherbakivsky and the investigations of the Gintsy Upper Palaeolithic site. *The Stone Age of Ukraine,* 4, p. 53–81. (In Ukrainian).

*Germonpre et al. 2017.* Germonpre, M., Fedorov, S., Danilov, P., Galeta, P., Jimenez, E-L., Sablin, M., Losey, R. 2017. Palaeolithic and prehistoric dogs and Pleistocene wolves from Yakutia: Identification of isolated skulls. *Journal of Archaeological Science,* 78, p. 1–19.

*Gladilin 1976.* Гладилин, В. Н. 1976. *Проблемы раннего палеолита Восточной Европы.* Киев: Наукова думка.

Gladilin, V. N. 1976. *The problems of the Early Palaeolithic of Eastern Europe.* Kyiv: Naukova dumka. (In Russian).

*Gladkikh et al. 2010.* Гладких, М. І., Рижов, С. М., Суховий, М. С. 2010. Оріньякоїдна стоянка Гордашівка I на Черкащині. *Кам'яна доба України,* 13, с. 95-112.

Gladkikh, M. I., Ryzhov S. M., Sukhovyj, M. O. 2010. Aurignacoide site of Gordashivka I in Cherkasy region. *The Stone Age of Ukraine,* 13, p. 95–112. (In Ukrainian).

*Glöer 2019.* Glöer, P. 2019. *The freshwater Gastropods of the West-Palaearctic. Volume 1. Fresh- and brackish waters except spring and subterranean snails. Identification key, anatomy, ecology, distribution.* Hetlingen: Biodiversity Research Lab.

*Gorodtsov 1935.* Городцов, В. А. 1935. *Тимоновская палеолитическая стоянка.* Москва-Ленинград: АН СССР.

Gorodtsov, V. A. 1935. *The Timonovka Palaeolithic site.* Moscow–Leningrad: Academy of Sciences of the USSR. (In Russian).

*Gribchenko 2011.* Грибченко, Ю. Н. 2011. Проблемы палеогеографии позднего палеолита Восточно-Европейской равнины. В: Гаврилов, К. Н. (ред.). *Палеолит и мезолит Восточной Европы.* Москва: Таус, с. 100-118.

Gribchenko, Yu. N. 2011. The problems of the palaeogeography of the Upper Palaeolithic of the Eastern-European Plain. In: Gavrilov, C. (Ed.). *The Palaeolithic and Mesolithic of Eastern Europe.* Moscow: Taus, p. 100–118. (In Russian).

*Gribchenko, Kurenkova 2014.* Грибченко, Ю. Н., Куренкова, Е. И. 2014. Палеогеографические особенности основных стоянок позднего палеолита бассейна реки Десны (Хотылево, Елисеевичи, Юдиново, Пушкари). *Археологический Альманах,* 31, с. 99-115.

Gribchenko, Yu. N., Kurenkova, E. I. 2014. The paleogeographical peculiarities of the main Upper Palaeolithic sites from the Desna River basin (Khotylevo, Yeliseevichi, Yudinovo, Pushkari). *Archaeological Almanac,* 31, p. 99–115. (In Russian).

*Grigoriev 2008.* Григорьев, Г. П. 2008. Структура палеолита Десны. *Замятнинский сборник,* 1, с. 48-62.

Grigoriev, G. P. 2008. The structure of the Palaeolithic of Desna. *Zamyatnin papers,* 1, p. 48–62. (In Russian).

*Grigorieva 1996.* Григорьева, Г. В. 1996. Костяная индустрия. В: Абрамова, З. А., Григорьева, Г. В., Кристенсен, М. (ред.). *Верхнепалеолитическое поселение Юдиново. Выпуск 2.* Санкт-Петербург: ИИМК РАН, с. 76-137.

Grigorieva, G. V. 1996. The bone industry. In: Abramova, Z., Grigorieva, G., Christensen, M. (Eds.). *The Upper Palaeolithic settlement of Yudinovo. Vol. 2.* Sankt-Petersburg: IIMK, p. 76–137 (In Russian).

*Grigorieva 2008.* Григорьева, Г. В. 2008. Адаптация к окружающей среде на верхнепалеолитическом Юдиновском поселении. В: Хлопачев, Г. А. (ред.). *Проблемы биологической и культурной адаптации человеческих популяций.* Санкт-Петербург: Наука, с. 53-57.

Grigorieva, G. V. 2008. The adaptation to the environment on the Upper Palaeolithic settlement Yudinovo. In: Khlopachev, G. (Ed.). *The problems of biological and cultural adaptations of Human population.* Sankt-Petersburg: Nauka, p. 53–57. (In Russian).

Grupe et al. 2003. Grupe, G., Mikic, Z., Peters, J. & Manhart, H. 2003. Vertebrate food webs and subsistence strategies of Meso- and Neolithic populations of central Europe. *Documenta Archaeobiologia 1,* p. 193–213.

*Guthrie 2001.* Guthrie, R.D. 2001. Origin and causes of the mammoth steppe: a story of cloud cover, woolly mammal tooth pits, buckles, and inside-out Beringia. *Quaternary Science Reviews 20 (1–3)*, p. 549–574. https://doi.org/10.1016/s0277-3791(00)00099-8

*Gvozdover 1947.* Гвоздовер, М. Д. 1947. Палеолитическая стоянка Бугорок. *Краткие сообщения Института истории материальной культуры,* XV, с. 92-97.

Gvozdover, M. D. 1947. The Palaeolithic site Bugorok. *The short reports of the Institute of the Material Culture,* XV, p. 92–97. (In Russian).

*Haase et al. 2021.* Haase, M., Meng, S., Horsák, M. 2021. Tracking parallel adaptation of shells morphology through geological times in the land snails genus Pupilla (Gastropoda: Stylommatophora: Pupillidae). *Zoological Journal of the Linnean Society,* 191, p. 720–747.

*Haesaerts et al. 2004.* Haesaerts, P., Borziak, I., Chirica, V., Damblon, F., Koulakovska, L. 2004. Cadre stratigraphique et chronologique du Gravettien en Europe Centrale. *The Dolni Vestonice Studies,* 11, p. 33–57.

*Haesaerts et al. 2015.* Haesaerts, P., Péan, S., Valladas, H., Damblon, F., Nuzhnyi, D. 2015. Contribution à la stratigraphie du site paléolithique de Mezhyrich (Ukraine). *L'anthropologie,* 119, p. 364–393.

*Händel et al. 2020.* Händel, M., Simon, U., Maier, A., Brandl, M., Groza-Săcaciu, S. M., Timar-Gabor, A., Einwögerer, T. 2020. Kammern-Grubgraben revisited – First results from renewed investigations at a well-known LGM site in East Austria. *Quaternary International.* https://doi.org/10.1016/j.quaint.2020.06.012

*Haynes 1991.* Haynes, G. 1991. *Mammoths, Mastodonts, & Elephants. Biology, Behavior, and the fossil Record.* Cambridge University Press, Cambridge.

*Haynes 2017.* Haynes, G. 2017. Finding meaning in mammoth age profiles. *Quaternary International 443*, p. 65–78. http://dx.doi.org/10.1016/j.quaint.2016.04.012

*Hedges et al. 2007.* Hedges, R. E. M., Clement, J. G., Thomas, C. D. L. & O'Connell, T. C. 2007. Collagen turnover in the adult femoral mid-shaft: modelled from anthropogenic radiocarbon tracer measurements. *American Journal of Physical Anthropology 133,* p. 808–816.

*Herre 1986.* Herre, W. 1986. Rangifer tarandus (Linnaeus, 1758) – Ren, Rentier. In: Jochen Niethammer & Franz Krapp (Hrsg.), *Handbuch der Säugetiere Europas. Band 2/II, Paarhufer – Artiodactyla (Suidae, Cervidae, Bovidae).* Wiesbaden: AULA-Verlag, p. 198–216.

*Hobson et al. 1993.* Hobson, K. A., Alisauskas, R. T. & Clark, R. G. 1993. Stable-nitrogen isotope enrichment in avian tissues due to fasting and nutritional stress: implications for isotopic analyses of diet. *The Condor 95,* p. 388–394.

*Hoffecker 2002.* Hoffecker, J. F. 2002. *Desolate landscapes. Ice-age settlement in Eastern Europe.* New Brunswick; New Jersey; London: Rutgers University Press.

*Hofreiter et al. 2004.* Hofreiter, M., Serre, D., Rohland, N., Rabeder, G., Nagel, D., Conrad, N., Münzel, S. & Pääbo, S. 2004. Lack of phylogeography in European mammals before the last glaciation. *PNAS 101,* p. 12963–12968, https://doi.org/10.1073/pnas.0403618101

*Horsák et al. 2010.* Horsák, M., Chytrý, M., Pokryszko, B. M., Danihelka, J., Ermakov, N., Hájek, M., Hájková, P., Kintrová, K., Kočı, M., Kubešová, S., Lustyk, P., Otýpková, Z., Pelánková, B. and Valachovič, M. 2010. Habitats of relict terrestrial snails in southern Siberia: lessons for the reconstruction of palaeoenvironments of full-glacial Europe. *Journal of Biogeography,* 37, p. 1450–1462.

*Hughes, Gibbard 2015.* Hughes, P. D., Gibbard, P. L., 2015. A stratigraphical basis for the Last Glacial Maximum (LGM). *Quaternary International 383:* 174–185.

*Iacumin et al. 2000.* Iacumin, P., Nikolaev, V. & Ramigni, M. 2000. C and N stable isotope measurements on Eurasian fossil mammals, 40,000 to 10,000 years BP: Herbivore physiologies and palaeoenvironmental reconstruction. *Palaeogeography, Palaeoclimatology, Palaeoecology 163,* p. 33–47.

*Iacumin et al. 2006.* Iacumin, P., Davanzo, S. & Nikolaev, V. 2006. Spatial and temporal variations in the $^{13}C/^{12}C$ and $^{15}N/^{14}N$ ratios of mammoth hairs: Palaeodiet and palaeoclimatic implications. *Chemical Geology 231,* p. 16–25.

*Iacumin et al. 2010.* Iacumin, P., Di Matteo, A., Nikolaev, V. & Kuznetsova, T.V. 2010. Climate information from C, N and O stable isotope analyses of mammoth bones from northern Siberia. *Quaternary International 212,* p. 206–212.

*Iakovleva 2013.* Яковлева, Л. 2013. *Найдавніше мистецтво України.* Київ: Стародавній Світ.

Iakovleva, L. 2013. *The ancient art of Ukraine.* Kyiv: Starodavniy svit. (In Ukrainian).

*Iakovleva 2016.* Iakovleva, L. 2016. Mezinian landscape system (Late Upper Palaeolithic of Eastern Europe). *Quaternary International,* 412, p. 4–15.

*Iakovleva, Djindjian 2001.* Iakovleva, L., Djindjian, F. 2001. Epigravettian settlement models in the Dniepr basin in the lights of the new excavations of the Gontsy site (Ukraine). In: West, D. (Ed.). *Proceedings of the International Conference on Mammoth Site Studies.* Lawrence: University of Kansas, p. 85–94.

*Iakovleva, Djindjian 2005.* Iakovleva, L., Djindjian, F. 2005. New data on Mammoth bone settlement of Eastern Europe in the light of new excavations of the Gontsy site (Ukraine). *Quaternary International,* 126–128, p. 195–297.

*Iakovleva, Djindjian 2018.* Iakovleva, L., Djindjian, F. 2018. The mammoth bone dwellings of the Upper Palaeolithic settlement of Gontsy (Ukraine: a first synthesis). *Arheologia,* 4, p. 86–94.

*Jackson et al. 2011.* Jackson, A., Inger, R., Parnell, A. C. & Bearhop, S. 2011. Comparing isotopic niche widths among and within communities: SIBER – Stable Isotope Bayesian Ellipses in R. *Journal of Animal Ecology 80,* p. 595–602.

*Jenkins et al. 2001.* Jenkins, S. G., Partridge, S. T., Stephenson, T. R., Farley, S. D. & Robbins, C. T. 2001. Nitrogen and carbon isotope fractionation between mothers, neonates, and nursing offspring. *Oecologia 129,* p. 336–341.

*Kahlke 2001.* Kahlke, R.-D. 2001. Ein Hinweis auf Herbivoren-Osteophagie im Unterpleistozän von Untermassfeld. Sowie Bemerkungen zur Gabelbildung an Knochenenden. In: Kahlke, R.-D. (Ed.), Das Pleistozän von Untermaßfeld bei Meiningen (Thüringen). Teil 3. *Monographien des Römisch-Germanischen Zentralmuseums 40,* 3, 897–903.

*Kaltenthaler 2018.* Kaltenthaler, D.; Lohrer, J.; Kröger, P.; van der Meijden, C.; Granado, E.; Lamprecht, J.; Nücke, F.; Obermaier, H.; Stopp, B.; Baly, I.; Callou, C.; Gourichon, L.; Pöllath, N.; Peters, J.; Schibler, J. 2018. *OssoBook v5.6.2.* München-Basel. http://xbook.vetmEd.uni-muenchen.de/

*Kapustin et al. 1996.* Kapustin, N., Critser, J. K., Olson, D., Malven, P. V. 1996. Nonluteal Estrous Cycles of 3-Week Duration Are Initiated by Anovulatory Luteinizing Hormone Peaks in African Elephants. *Biology of Reproduction 55,* 1996, p. 1147–1154.

*Khlopachev 2011.* Хлопачев, Г. А. 2011. Многослойная палеолитическая стоянка Пушкари IX. В: Гаврилов, К. Н. (ред.). *Палеолит и мезолит Восточной Европы.* Москва: Таус, с. 185-203.

Khlopachev, G. 2011. The multi-layered site Pushkari IX. In: Gavrilov, C. (Ed.). *Palaeolithic and Mesolithic of Eastern Europe.* Moscow: Taus, p. 185–203. (In Russian).

*Khlopachev 2014.* Хлопачев, Г. А. 2014. Абсолютный и относительный возраст стоянки Бугорок: естественно-научные и археологические данные. *Археологический Альманах,* 31, с. 81-98.

Khlopachev, G. 2014. The absolute and relative chronology of Bugorok site: the environmental and archaeological data. *Archaeological Almanac,* 31, p. 81–98. (In Russian).

*Khlopachev 2016.* Хлопачев, Г. А. 2016. Образы, символы, знаки верхнего палеолита: древности археологического собрания МАЭ. В: Хлопачев, Г. А. (ред.). *Верхний палеолит: образы, символы, знаки. Санкт-Петербург:* Экстрапринт, с. 48-65.

Khlopachev, G. A. 2016. The images, symbols, and codes in Upper Palaeolithic: the archaeological collections from the Museum of Anthropology and Ethnography. In: Khlopachev, G. A. (Ed.). *The Upper Palaeolithic: images, symbols, codes.* Sankt-Petersburg: Extraprint, p. 48–65. (In Russian).

*Khlopachev 2018.* Хлопачев, Г. А. 2018. Опыт реконструкции плана и некоторые особенности структуры Юдиновского верхнепалеолитического поселения. *Записки Института истории материальной культуры РАН,* 17, с. 97-106.

Khlopachev, G. 2018. A reconstruction of the plan and some structural peculiarities of the Upper Palaeolithic settlement of Yudinovo. *Transactions of the Institute for the History of Material Culture,* 17, p. 97–106. (In Russian).

*Khlopachev 2019a.* Khlopachev, G. 2019. Le site Paléolithique supérieur de Yudinovo :résultats des recherches archéologiques des années 2004–2016. *L'anthropologie,* 123, p. 403–422.

*Khlopachev 2019b.* Хлопачев, Г. А. 2019. Юдиновская верхнепалеолитическая стоянка. В: Гаврилов, К. Н., Очередной, А. К., Желтова, М. Н. (ред.). *Культурная география палеолита Восточно-Европейской равнины: от микока до эпиграветта.* Москва: Институт археологии, с. 147-180.

Khlopachev, G. 2019. The Upper Palaeolithic site at Yudinovo. In: Gavrilov, K., Ocherednoi, A., Zsheltova, M. (Eds.). *The cultural geography of the Palaeolithic in the East-European plain from the Micoquian to the Epigravettian.* Moscow: Institute of Archaeology, p. 147–280. (In Russian).

*Khlopachev et al. 2013.* Хлопачев, Г. А., Грибченко, Ю. Н., Сапелко, Т. В. 2013. Палеолитическая стоянка Елисеевичи 1: результаты полевых исследований 2010-2011 гг. В: Чистов, Ю. К. (ред.). *Радловский сборник: Научные исследования и музейные проекты МАЭ РАН в 2012 г.* Санкт-Петербург: МАЭ РАН, с. 80-90.

Khlopachev, G., Gribchenko, Yu., Sapelko, T. 2013. The Palaeolithic site of Yeliseevichi I: the results of field investigations, 2010–2011. In: Chistov, Yu. (Ed.). *The Radlov's papers: The scientific investigations and museum projects of the Museum of Archaeology and Ethnography in 2012.* Saint-Petersburg: MAE RAS, p. 80–90. (In Russian).

*Khlopachev et al. 2017.* Хлопачев, Г. А., Грибченко, Ю. Н., Кулькова, М. Н., Сапелко, Т. В. 2017. Позднепалеолитическая стоянка Елисеевичи 1: новые данные о возрасте и длительности существования. *Stratum plus*, 1, с. 41-57.

Khlopachev, G., Gribchenko, Yu., Kulkova, M., Sapelko, T. 2017. The Yeliseebichi Upper Palaeolithic site: the new data concerning the age and duration of habitation. *Stratum plus,* 1, p. 44–57. (In Russian).

*Khlopachev, Gribchenko 2012.* Хлопачев, Г. А., Грибченко, Ю. Н. 2012. Возраст и этапы заселения Юдиновского верхнепалеолитического поселения. *Краткие сообщения Института археологии РАН,* 227, с. 134-143.

Khlopachev, G., Gribchenko, Yu. 2012. The age and stages of the inhabiting of Yudinovo Upper Palaeolithic settlement. *The short reports of the Institute of Archaeology,* 227, p. 136–146. (In Russian).

*Kierdorf 1993.* Kierdorf, U. 1993. Fork Formation and Other Signs of Osteophagia on Long Bone Swallowed by Red Deer Stag (Cervus elaphus). *International Journal of Osteoarchaeology 3,* p. 37–40.

*Kijashko, Khlopachev 2022.* Кияшко, П. В., Хлопачев, Г. А. 2022. Находки раковин моллюсков и остатков полихет с верхнепалеолитических стоянок Юдиново и Елисеевичи 1: таксономия, возможности палеогеографических и археологических реконструкций. *Camera Praehistorica,* 2 (9), с. 106-133.

Kijashko, P. V., Khlopachev, G. A. 2022. Fossil molluscan shells and polychaeta tubes from the Yudinovo and Eliseevichi Upper Palaeolithic settlements: taxonomy, possibilities of palaeogeographical and archaeological reconstructions. *Camera Praehistorica,* 2 (9), p. 106–133. (In Russian).

*Kirillova et al. 2016.* Kirillova, I.V., Argant, J., Lapteva, E.G., Korona, O.M., van der Plicht, J., Zinovyev, E.V. Kotov, A. A., Cherova, O. F., Fadeeva, E. O., Baturina, O. A., Kabilov, M. R., Shidlovskiy, F. K. & Zanina, O. G. 2016. The diet and environment of mammoths in North–East Russia reconstructed from the contents of their feces. *Quaternary International 406,* p. 147–161.

*Klein 1973.* Klein, R. G. 1973. *Ice-age hunters of the Ukraine.* Chicago–London: The University of Chicago Press.

*Kohn 2010.* Kohn, M. J. 2010. Carbon isotope compositions of terrestrial C3 plants as indicators of (paleo) ecology and (paleo)climate. *Proceedings of the National Academy of Sciences 107,* p. 19691–19695.

*Kolobova 2014.* Колобова, К. А. 2014. *Верхний палеолит западного Памиро-Тянь-Шаня.* Автореферат диссертации на соискание ученой степени доктора исторических наук. Новосибирск: ИАЭТ СО РАН.

Kolobova, K. A. 2014. *The Upper Palaeolithic of the western Pamir–Tian–Shan.* The issue of the dissertation of doctor habitus. Novosibirsk: Institute of Archaeology and Ethnography of the Siberian Branch of the RAS. (In Russian).

*Komar 2015.* Komar, M. 2015. Interprétation paléogéographique des données palynologiques du site du Paléolithique supérieur de Mezhyrich (Ukraine). *L'anthropologie,* 119, p. 473–486.

*Komar et al. 2003.* Komar, M. S, Kornietz, N. L., Nuzhnyi, D. Yu., Péan, S. 2003. Mezhirich Upper Palaeolithic site: the reconstruction of environmental conditions of the Late Pleistocene and human adaptation in the Middle Dnieper basin (Northern Ukraine). *The Stone Age of Ukraine,* 4, p. 262–277.

*Kononenko 2009.* Кононенко О.М. 2009. Вістря верхньопалеолітичної стоянки Радомишль I: техніко-типологічна характеристика. В: Васильев, С., Кулаковская, Л. (ред.). *С. Н. Бибиков и первобытная археология.* Санкт-Петербург: ИИМК, с. 165-173.

Kononenko, O. 2009. The points of the Upper Palaeolithic site Radomyshl I: techno–typological characteristici. In Vasiliev, S., Kulakovska, L. (Eds.). *Sergey Bibikov and Prehistoric Archaeology.* Sankt–Petersburg: IHMC, p. 165–173. (In Ukrainian).

*Kononenko 2015.* Кононенко, О. М. 2015. Крем'яні знаряддя верхньопалеолітичної стоянки Радомишль I: типологічна специфіка та її інтерпретація. *Археологія і давня історія України,* 3 (16), с. 35-64.

Kononenko, O. 2015. The stone tools of the Upper Palaeolithic site Radomyshl I: specificity and interpretation of the typology. *The Archaeology and Ancient History of Ukraine,* 3 (16), p. 35–64. (In Ukrainian).

*Kononenko 2021.* Kononenko, O. 2021. The Upper Palaeolithic site Radomyshl I (Ukraine): Another phenomenon of the Gravettian technocomplex? *Quaternary International,* 587–588, p. 251–276.

*Kosintsev et al. 2012.* Kosintsev, P. A., Lapteva, E. G., Korona, O. M. & Zanina, O. G. 2012. Living environments and diet of the Mongochen mammoth, Gydan Peninsula, Russia. *Quaternary International 276,* p. 253–268.

*Kozłowski et al. 2017.* Kozłowski, S. K., Terberger, T., Bobak, D., Orschiedt, J., & Połtowicz–Bobak, M. 2017. Eastern Borders of the Magdalenian 'à navettes'. Maszycka cave in Lesser Poland (southern Poland). In C. Bourdier, L. Chehmana, R. Malgarini et M. Połtowicz–Bobak (Eds.), *L'essor du Magdalénien. Aspects culturels, symboliques et techniques des faciès à Navettes et à Lussac–Angles.* Société préhistorique française, No. 8, p. 187–205.

*Krajcarz et al. 2016.* Krajcarz, M., Pacher, M., Krajcarz, M. T., Laughlan, L., Rabeder, G., Sabol, M., Wojtal, P. & Bocherens, H. 2016. Isotopic variability of cave bears ($\delta^{15}N$, $\delta^{13}C$) across Europe during MIS 3. *Quaternary Science Reviews 131,* p. 51–72.

*Krajcarz et al. 2018.* Krajcarz, M. T., Krajcarz, M. & Bocherens, H. 2018. Collagen-to collagen prey-predator isotopic enrichment ($\delta^{13}C$, $\delta^{15}N$) in terrestrial mammals – a case study of a subfossil red fox den. *Palaeogeography, Palaeoclimatology, Palaeoecology 490,* p. 563–570.

*Krotova 2003.* Кротова, О. О. 2003. Проблеми датування та періодизації пам'яток степової зони доби верхнього палеоліту. *Кам'яна доба України,* 4, с. 183-197.

Krotova, O. O. 2003. The problems of chronology and periodization of the Upper Palaeolithic sites in the steppe zone. *The Stone Age of Ukraine,* 4, p. 183–197. (In Ukrainian).

*Krotova 2013.* Кротова, О. О. 2013. *Пізньопалеолітичні мисливці Азово-Чорноморських степів.* Київ: Олег Філюк.

Krotova, O. O. 2013. *The Upper Palaeolithic hunters of Azov–Black Sea steppes.* Kyiv: Oleg Filiuk. (In Ukrainian).

*Krotova 2021a.* Кротова, А. А. 2021. Стоянка Ямы в круге памятников Костенковско-Виллендорфского культурного единства. В: Васильев, С. А. (ред.). *Верхний палеолит Европы: время культурных новаций.* Санкт-Петербург: ИИМК РАН, с. 104-107.

Krotova, A. A. 2021. Yamy site in the context of the Kostenki–Willendorf cultural entity. In: Vasiliev, S. A. (Ed.). *The Upper Palaeolithic of Europe: the time of the cultural innovations.* Sankt–Petersburg: Institute of the history of material culture RAS, p. 104–107. (In Russian).

*Krotova 2021b.* Кротова, О. О. 2021. Елементи індустрії мізинського типу у верхньому палеоліті Східної України. *Археологічні зошити з Пересопниці,* 8, с. 48-62.

Krotova, O. O. 2021. Elements of the Upper Palaeolithic Mizyn culture industry in Eastern Ukraine. *The archaeological papers from Peresopnitsa,* 8, p. 48–62. (In Ukrainian).

*Kuhn et al. 2001.* Kuhn, S. L., Stiner, M. C., Reese, D. S., Güleç, E. 2001. Ornaments of the earliest Upper Paleolithic: New insights from the Levant. *Proceedings of the National Academy of Sciences of the USA,* 98, p. 7641–7646.

*Kulakovska et al. 2021.* Kulakovska, L., Kononenko, O., Haesaerts, P., Pirson, S., Spry-Marqués, P., Bosch e, M. D., Popova, L., Popiuk, Y., Damblon, F., Usik, V., Nigst, Ph. R. 2021. The new Upper Palaeolithic site Korman' 9 in the Middle Dniester valley (Ukraine): Human occupation during the Last Glacial Maximum. *Quaternary International,* 587–588, p. 230–250. https://doi.org/10.1016/j.quaint.2021.02.021

*Lavrushin et al. 2010.* Лаврушин, Ю. А., Бессуднов, А. Н., Спиридонова, Е. А., Кураленко, Н. П., Холмовой, Г. В., Бессуднов, А. А. 2010. Дивногрье (Средний Дон): природные события времени финального палеолита. *Бюллетень комиссии по изучению четвертичного периода,* 70, с. 23-34.

Lavrushin, Yu. A., Bessudnov, A. N., Spiridonova, E. A., Kuralenko, N. P., Kholmovoi, G. V., Bessudnov, A. A. 2010. Divnogorie (Mid Don): the environmental events during the Final Palaeolithic. *Bulletin of Commission for the Study of the Quaternary,* 70, p. 23–34. (In Russian).

*Laws 1966.* Laws, R. M. 1966. Age criteria for the African elephant. *East African Wildlife Journal,* 4, p. 1–37.

*Laymann et al. 2007.* Laymann, C. A., Arrington, D. A., Montaña, C. G. & Post, D. M. 2007. Can stable isotope ratios provide for community-wide measures of trophic structure? *Ecology 88,* p. 42–48.

*Lee-Thorp et al. 1989.* Lee-Thorp, J. A., Sealy, J. C. & van der Merwe, N. J. 1989. Stable carbon isotope ratio differences between bone collagen and bone apatite, and their relationship to diet. *Journal of Archaeological Science 16,* p. 585–599.

*Lengyel et al. 2021.* Lengyel, G., Bárány, A., Béres, S., Cserpák, F., Gasparik, M., Major, I., Molnár, M., Nadachowski, A., Nemergut, A., Svoboda, J., Verpoorte, A., Wojtal, P., Wilczyński, J. 2021. The Epigravettian chronology and the human population of eastern Central Europe during MIS2. *Quaternary Science Reviews,* 271, p. 107–187. http://creativecommons.org/licenses/by-nc-nd/4.0/

*Levytsky 1949.* Левицький, І. Ф. 1949. Гонцівська палеолітична стоянка. *Палеоліт і неоліт України,* I/III, с. 198-237.

Levytsky, I. 1949. Gintsy Palaeolithic site. *The Palaeolithic and Neolithic of Ukraine,* I/III, p. 198–237. (In Ukrainian).

*Lisitsyn 2019.* Lisitsyn, S. N. 2019. The Eastern Frontier of the Gravettian in the Kostenki–Borshchevo Palaeolithic Locality, the Don Basin, Russia. *Vestnik of Saint Petersburg University.* History, 64 (2), p. 525–554. https://doi.org/10.21638/11701/spbu02.2019.208

*Lisitsyn 2021.* Lisitsyn, S. 2021. The revision of the Gravettian sequence in the Kostenki–Borshchevo locality in the river Don basin (Russia). In: Lengyel, G., Wilczyński, J., Sánchez de la Torre, M., Mangado, X., Fullola, J. M. (Eds.). *Studies on the Palaeolithic of Western Eurasia.* Oxford: Archaeopress, p. 134–158.

*Lisitsyn, Dudin 2019.* Лисицын, С. Н., Дудин, А. Е. 2019. Граветт / Эпиграветт в Костенковско-Борщевском районе на Дону: критерии разделения, культурная интерпретация и периодизация. *Camera Praehistorica,* 1 (2), с. 70-107.

Lisitsyn, S. N., Dudin, A. E. 2019. The Gravettian / Epigravettian in the Kostenki–Borshevo locality on the Don – the division criteria, cultural interpretation and periodisation. *Camera Praehistorica,* 1 (2), p. 70–107. (In Russian).

*Ložek 1964.* Ložek, V. 1964. *Quartärmollusken der Tschechoslowakei.* Rozpravy Ústredniho Ústavu Geologického 31. Praha: Nakladatelství Československé akademie věd.

*Lozovski, Lozovskaya 2014.* Lozovski, V., Lozovskaya, O. 2014. Analyse du débitage laminaire du site de Mezhyrich: habitations no 1, 2 et 3. *L'Anthropologie,* 118, p. 495–503.

*Lupenko 1983.* Лупенко, Е. Л. 1983. *Отчет о работе археологической экспедиции Ровенского краеведческого музея в 1982 г.* Науковий архів ІА НАНУ, ф. е., 1984/164. Київ: Інститут археології.

Lupenko, Ye. L. 1983. *The field report of the expedition of the Rivne Natural History Museum in 1982.* The scientific archive of the Institute of Archaeology, fund of the expeditions, 1984/164. Kyiv: Institute of Archaeology (In Russian).

*Maier 2015.* Maier, A. 2015. *The Central European Magdalenian. Regional diversity and internal variability.* Dordrecht; New York: Springer.

*Maier et al. 2020.* Maier, A., Lieberman, C., Pfeifer, S. 2020. Beyond the Alps and Tatra Mountains – the 20-14 ka Repopulation of the Northern Mid-latitudes as Inferred from Palimpsests Deciphered with Keys from Western and Central Europe. *Journal of Paleolithic Archaeology,* 3, p. 398–452. https://doi.org/10.1007/s41982-019-00045-1

*Maier et al. 2021.* Maier, A., Mayr, C., Peresani, M. (2021). The Last Glacial Maximum in Europe – State of the Art in Geoscience and Archaeology. *Quaternary International 581–582*, p. 1–6. https://doi.org/10.1016/j.quaint.2021.02.036

*Malikov et al. 2023.* Malikov, D. G., Svyatko, S. & Pyryaev, A. N. 2023. Paleoecology of the mammoth fauna of Southern Siberia during the last glacial period based on stable isotope data. *Quaternary International 674–675,* p. 49–61.

*Mania 1973.* Mania, D. 1973. *Paläökologie, Faunenentwicklung und Stratigraphie des Eiszeitalters im mittleren Elbe-Saalegebiet auf Grund von Molluskengesellschaften.* Geologie, 78/79. Berlin: Akademie-Verlag.

*Markova, Puzachenko 2022.* Markova, A. K., Puzachenko, A. Yu. 2022. The Palaeoenvironment of the Central Russian Plain during the end of the Valdai Glaciation based on small mammal data from the Late Palaeolithic site Byki 7 (Seim R. Basin). *Geography, environment, sustainability,* 15 (1), p. 102–111. https://doi.org/10.24057/2071-9388-2021-124

*Marks 1976.* Marks, A. E. 1976. Glossary. In: Marks, A. E. (Ed.). *Prehistory and paleoenvironments in the Central Negev, Israel, vol. 1.* Dallas: SMU Press, p. 371–383.

*Marquer et al. 2015.* Marquer, L., Lebreton, V., Otto, Th., Messager, E. 2015. Étude des macro-, méso- et micro-charbons du site épigravettien de Mezhyrich (Ukraine): données taphonomiques et anthracologiques. *L'anthropologie,* 119, p. 487–504.

*Matheus 1995.* Matheus, P. E. 1995. Diet and co-ecology of Pleistocene short-faced bears and brown bears in Eastern Beringia. *Quaternary Research 44,* p. 447–453.

*McKendrigk et al. 1980.* McKendrigk, J. D., Batzli, G. O., Everett, K. R. & Swanson, J. C. 1980. Some effects of mammalian herbivores and fertilization on tundra soils and vegetation. *Arctic and Alpine Research 12,* p. 565–578.

*McPherron, Dibble 2002.* McPherron, Sh. P., Dibble, H. L. 2002. *Using Computers in Archaeology: A Practical Guide.* New York: McGraw-Hill.

*Meng 2009.* Meng, S. 2009. Rezente zentralasiatische und fossile mitteleuropäische Faunen mit *Vallonia tenuilabris* (A. Braun, 1843). *Mollusca,* 27 (1), p. 45–66.

*Meng et al. 2021.* Meng, S., Vasyliev, P., Khoptynets, I., Tkach, V., Maier, A. 2021. On the present habitats and ecology of *Vertigo pseudosubstriata* Ložek, 1954 (Mollusca, Gastropoda, Vertiginidea) in Central Asia, its distribution history in Central and Eastern Europe. *Journal of Quaternary Science,* 36 (6), p. 1090–1100.

*Meng, Hoffmann 2009.* Meng, S., Hoffmann, M. H. 2009. *Pupilla loessica* Ložek 1954 (Gastropoda: Pulmonata: Pupillidae) – "A Living Fossil" in Central Asia? *Quaternary Science Journal,* 58 (1), p. 55.69.

*Metcalfe et al. 2013.* Metcalfe, J. Z., Longstaffe, F. J., Hodgins, G. 2013. Proboscideans and paleoenvironments of the Pleistocene Great Lakes: landscape, vegetation, and stable isotopes. *Quaternary Science Reviews 76,* p. 102–113.

*Minagawa & Wada 1984.* Minagawa, M. & Wada, E. 1984. Stepwise enrichment of $^{15}N$ along food chains: Further evidence and the relation between $\delta^{15}N$ and animal age. *Geochimica et Cosmochimica Acta 48,* p. 1135–1140.

*Mirchink 1929.* Мирчинк, Г. Ф. 1929. Геологические условия нахождения палеолитической стоянки в д. Тимоновке под г. Брянском. *Русский антропологический журнал,* XVIII, (1-2), с. 57-58.

Mirchink, G. F. 1929. The geological conditions of the Palaeolithic site in Timonovka village near Briansk city. *Journal Russe d'Anthropologie,* XVIII (1–2), p. 57–58. (In Russian).

*Mix et al. 2001.* Mix, A. C., Bard, E., & Schneider, R. 2001. Environmental processes of the ice age: land, oceans, glaciers (EPILOG). *Quaternary Science Reviews,* 20(4), p. 627–657.

*Mol, van Essen 1987.* Mol, D., van Essen, H. 1987. *De mammoet. Sporen uit de IJstijd.* 's-Gravenhage (BZZToH).

*Monigal 2002.* Monigal, K. 2002. *The Levantine Leptolithic: Blade production from the Lower Paleolithic to the dawn of the Upper Paleolithic.* PhD. thesis. Dedman College, Southern Methodist University, Dallas.

*Motuz 1987.* Мотуз, В. М. 1987. Наземные моллюски из четвертичных отложений стоянки Молодова 5. В: Иванова, И. К., Цейтлин, С. М. (ред.). *Многослойная палеолитическая стоянка Молодова V: люди каменного века и окружающая среда. К XII Конгрессу ИНКВА, Канада.* Москва: Наука, с. 162-167.

Motuz, V.M. (1987): The terrestrial molluscs from the site Moldova V. In: Ivanova, L. K., Tzeitlin, S. M. (Eds.). *The Multilayered Palaeolithic Site Moldova V: Stone Age Men and Their Environment. XII Congress of INQUA in Canada.* Moscow: Nauka, p. 162–167. (In Russian).

*Movius et al. 1968.* Movius, H. L., David, N. C., Bricker, H. M., Clay, R. B. 1968. The analysis of certain major classes of Upper Paleolithic tools. *American School of Prehistoric Research Bulletin,* 26, p. 1–58.

*Nadachowski et al. 2018.* Nadachowski, A., Lipecki, G., Baca, M., Żmihorski, M., Wilczyński, J. 2018. Impact of climate and humans on the range dynamics of the woolly mammoth (*Mammuthus primigenius*) in Europe during MIS 2. *Quaternary research,* 90 (3), p. 439–456. https://doi.org/10.1017/qua.2018.54

*Naito et al. 2016.* Naito, Y. I., Chikaraishi, Y., Drucker, D. G., Ohkouchi, N., Semal, P., Wißing, C. & Bocherens, H. 2016. Ecological niche of Neanderthals from Spy Cave revealed by nitrogen isotopes of individual amino acids in collagen. *Journal of Human Evolution 93,* p. 82–90.

*Naudinot et al. 2017.* Naudinot, N., Tomasso, A., Messager, E., Finsinger, W., Ruffaldi, P., Langlais, M. 2017. Between Atlantic and Mediterranean: Changes in technology during the Late Glacial in Western Europe and the climate hypothesis. *Quaternary International,* 428, p. 33–49.

*Naumenko, Matsui 2020.* Науменко, У. З., Мацуй, В. М. 2020. Карта викопних смол України. *Мінеральні ресурси України,* 4, с. 13-17. https://doi.org/10.31996/mru.2020.4.13-17

Naumenko, U., Matsui, V. 2020. Map of fossil resins of Ukraine. *The mineral resources of Ukraine,* 4, p. 13–17. (In Ukrainian). https://doi.org/10.31996/mru.2020.4.13-17

*Niţă et al. 2021.* Niţă, L., Anghelinu, M., Cordoș C. 2021. The shouldered points and the Gravettian of the Eastern Carpathian area: insights from Bistricioara–Lutărie III (Ceahlău Basin, Northeastern Romania). *Materiale şi cercetări arheologice,* S1, p. 291–311.

*Niţu et al. 2019.* Niţu, E–Ch., Cârciumaru, M., Nicolae, A., Cirstina, O., Lupu, Fl., Leu, M. 2019. Mobility and social identity in the Mid Upper Paleolithic: New personal ornaments from Poiana Cireşului (Piatra Neamţ, Romania). *PLoS ONE,* 14 (4), e214932. https://doi/org/10.1371/journal.pone.0214932

*Noiret 2009.* Noiret, P. 2009. *Le Paléolithique supérieur de Moldavie.* Liège, ERAUL, 121. Liège: Études et Recherches Archéologiques de l'Université de Liège.

*Nuzhnyi 1998.* Нужний, Д. Ю. 1998. Нові дані про пізній палеоліт Овруцького кряжу. *Археометрія та охорона історико-культурної спадщини,* 2, с. 72-90.

Nuzhnyi, D. Yu. 1998. The new data about the Upper Palaeolithic of the Ovruch Upland. *Archaeometry and the protection of historical and cultural heritage,* 2, p. 72–90. (In Ukrainian).

*Nuzhnyi 2003.* Нужний, Д. Ю. 2003. *Звіт про розкопки верхньопалеолітичної стоянки Бармаки на Рівненщині у 2002 році.* Науковий архів ІА НАНУ, ф. е., 2002/114. Київ: Інститут археології.

Nuzhnyi, D. Yu. 2003. *The field report about excavations of the Barmaky Upper Palaeolithic site in Rivne, 2002.* The scientific archive of the Institute of Archaeology, fund of the expeditions, 2002/114. Kyiv: Institute of Archaeology (In Ukrainian).

*Nuzhnyi 2006.* Nuzhnyi, D. 2006. The latest Epigravettian assemblages of the Middle Dnieper basin (Northern Ukraine). *Archaeologia Baltica,* 7, p. 58–93.

*Nuzhnyi 2008a.* Nuzhnyi, D. 2008. The Epigravettian variability of the middle Dnieper river basin. In: Kulakovska, L. (Ed.). *The investigations in prehistoric archaeology in Ukraine.* Kyiv: Korvin Press, p. 96–135.

*Nuzhnyi 2008b.* Нужний, Д. Ю. 2008. *Розвиток мікролітичної техніки в кам'яному віці: удосконалення зброї первісних мисливців.* Київ: КНТ.

Nuzhnyi, D. Yu. 2008. *The evolution of microlithic technology in Stone Age: the improvement of prehistoric hunters' weapon.* Kyiv: KNT. (In Ukrainian).

*Nuzhnyi 2009.* Nuzhnyi, D. 2009. The industrial variability of the eastern Gravettian assemblages of Ukraine. *Quartär,* 56, p. 159–174.

*Nuzhnyi 2015.* Нужний, Д. Ю. 2015. *Верхній палеоліт західної і північної України.* Київ: видавець Олег Філюк.

Nuzhnyi, D. Yu. 2015. *The Upper Paleolithic of Western and Northern Ukraine.* Kyiv: Oleh Filiuk. (In Ukrainian).

*Nuzhnyi et al. 2004.* Нужний, Д. Ю., Корнієць, Н. Л., Пеан, С. 2004. *Звіт про розкопки верхньопалеолітичних поселень Бармаки та Межиріч у 2004 році.* Науковий архів ІА НАНУ, ф. е., 2003/132. Київ: Інститут археології.

Nuzhnyi, D. Yu., Korniets, N. L., Pean, S. 2004. *The field report on excavations of Upper Palaeolithic sites Barmaky and Mezhyrich in 2003.* Kyiv: The scientific archive of the Institute of Archaeology, fund of the expeditions, 2004/132. (In Ukrainian).

*Nuzhnyi et al. 2005.* Нужний, Д. Ю., Корнієць, Н. Л., Пеан, С. 2005. *Звіт про розкопки верхньопалеолітичних поселень Бармаки та Межиріч у 2004 році.* Науковий архів ІА НАНУ, ф. е., 2004/194. Київ: Інститут археології.

Nuzhnyi, D. Yu., Korniets, N. L., Péan, S. 2005. *The field report about the excavations of Upper Palaeolithic sites Barmaky and Mezhyrich in 2004.* Kyiv: The scientific archive of the Institute of Archaeology, fund of the expeditions, 2004/194. (In Ukrainian).

*Nuzhnyi et al. 2006.* Нужний, Д. Ю., Корнієць, Н. Л., Пеан, С. 2006. *Звіт про розкопки верхньопалеолітичних поселень Бармаки та Межиріч у 2005 році.* Науковий архів ІА НАНУ, ф. е., 2005/133. Київ: Інститут археології.

Nuzhnyi, D. Yu., Korniets, N. L., Pean, S. 2006. *The field report about excavations of the Upper Palaeolithic sites Barmaky and Mezhyrich in 2005.* The scientific archive of the Institute of Archaeology, fund of the expeditions, 2005/133. Kyiv: Institute of Archaeology (In Ukrainian).

*Nuzhnyi et al. 2017.* Нужний, Д. Ю., Шидловський, П. С., Лизун, О. М. 2017. Семенівські верхньопалеолітичні стоянки в контексті епіграветy Середнього Подніпров'я. *Кам'яна доба України,* 17-18, с. 16-47.

Nuzhnyi, D., Shydlovsky, P., Lyzun, O. 2017. Upper Paleolithic sites Semenivka in the context of Epigravettian of the Middle Dnieper area. *The Stone Age of Ukraine,* 17–18, p. 16–47. (In Ukrainian).

*Nuzhnyi, Piasetsky 2003.* Нужний, Д. Ю., Пясецький, В. К. 2003. Крем'яний комплекс верхньопалеолітичної стоянки Бармаки на Рівненщині та проблема існування пам'яток мізинської індустрії на Волинській височині. *Кам'яна доба України,* 2, с. 58-74.

Nuzhnyi, D., Yu., Piasetsky, V. K. 2003. The flint assemblage of the Barmaky Upper Paleolithic site from Rivne city and the problem of the Mezin industry in the Volhynian upland. *The Stone Age of Ukraine,* 2, p. 58–74 (in Ukrainian).

*Nuzhnyi, Shydlovskyi 2015.* Nuzhnyi, D., Shydlovskyi, P. 2015. Variabilité de l'industrie lithique entre les structures de l'habitation no 1 de Mezhyrich, site du Paléolithique supérieur d'Ukraine. *L'anthropologie,* 119, p. 394–416.

*Nuzhnyi, Stupak 2001.* Нужный, Д. Ю., Ступак, Д. В. 2001. Поселенческие структуры весенне-летнего периода и сезонная адаптация епигравetских охотников на мамонта северной Украины. В: Манушина, Т., Вишневский, В., Лозовский, В., Лозовская, О. (ред.). *Каменный век европейских равнин.* Сергиев Посад: Подкова, с. 51-75.

Nuzhnyi, D. Yu., Stupak, D. V. 2001. The spring–summer settlement structures and seasonal adaptation of Epigravettian mammoth hunters of Northern Ukraine. In: Manushina, T., Vishnevsky, V., Lozovsky, V., Lozovskaya, O. (Eds.). *The Stone Age of the European plains.* Sergiev Posad: Podkova, p. 51–75. (In Russian).

*Olenkovsky 2008.* Оленковский, Н. П. 2008. *Эпиграветт Восточной Европы. Культурно-исторический аспект.* Херсон: Наддніпрянська правда.

Olenkovsky, N. P. 2008. *Epigravett of Eastern Europe. Cultural–historical aspect.* Kherson: Naddniprianska pravda. (In Russian).

*Olivier 1982.* Olivier, R. C. D. 1982 Ecology and behaviour of living elephants: bases for assumptions concerning the extinct woolly mammoths. In Hopkins, D. M., Matthews Jr., J. V., Schweger, C. E. & Young, S. B. (Eds.) *Paleoecology of Beringia.* Academic Press, New York, p. 291–305.

*Ostrovskyi, Grigoriev 1966.* Островский, М. И., Григорьев, Г. П. 1966. Липская палеолитическая культура. *Советская археология,* 4, с. 4-16.

Ostrovskyi, M. I., Grigoriev, G. P. 1966. Lipskaya Palaeolithic culture. *Soviet archaeology,* 4, p. 4–16. (In Russian).

*Pasda 2001.* Pasda, K. 2001. Zur Taphonomie von Rentieren (*Rangifer tarandus groenlandicus*) in der Tundra Westgrönlands. *Quartär 51/52,* p. 173–194.

*Pasda 2005.* Pasda, K. 2005. Some taphonomic investigations on reindeer (*Rangifer tarandus groenlandicus*) in West Greenland. In: T. O'Connor (Ed.). *Biosphere to Lithosphere: New studies in vertebrate taphonomy.* Oxford: Oxbow Books, p. 4–15.

*Pasda 2009.* Pasda, K. 2009. *Osteometry, osteological age and sex determination of the Sisimiut reindeer population (Rangifer tarandus groenlandicus).* BAR International Series 1947. Oxford.

*Pataki et al. 2003.* Pataki, D. E., Ehleringer, J. R., Flanagan, L. B., Yakir, D., Bowling, D. R., Still, C. J., Buchmann, N., Kaplan, J. O. & Berry, J. A. 2003. The application and interpretation of Keeling plots in terrestrial carbon cycle research. *Global Biogeochemical Cycles 17,* 1022, https://doi.org/10.1029/2001GB001850

*Péan 2015.* Péan, S. 2015. Mammouth et comportements de subsistance à l'Épigravettien : analyse archéozoologique du secteur de la fosse no 7 associée à l'habitation no 1 de Mezhyrich (Ukraine). *L'anthropologie,* 119, p. 417–463.

*Péan et al. 2015.* Péan, S., Nuzhnyi, D., Prat, S. 2015. Hommes et environnements au Paléolithique supérieur en Ukraine : introduction aux recherches interdisciplinaires menées sur le site de Mezhyrich. *L'anthropologie,* 119, p. 349–354.

*Pedersen et al. 2018.* Pedersen, J. B., Maier, A., & Riede, F. 2018. A punctuated model for the colonisation of the Late Glacial margins of northern Europe by Hamburgian hunter–gatherers. *Quartär 65,* p. 85–104.

*Peltier, Fairbanks 2006.* Peltier, W.R., Fairbanks, R.G., 2006. Global glacial ice volume and Last Glacial Maximum duration from an extended Barbados sea level record. *Quaternary Science Reviews 26,* p. 862–875.

*Peresani et al. 2019.* Peresani, M., Forte, M., Quaggiotto, E., Colonese, A. C., Romandini, M., Cilli, C., Giacobini, G. 2019. Marine and freshwater shell exploitation in the Early Upper Paleolithic: re-examination of the assemblages from Fumane Cave (NE Italy). *PaleoAnthropology,* p. 64–81. doi:10.4207//PA.2019.ART124

*Peterson & Fry 1987.* Peterson, B. J. & Fry, B. 1987. Stable Isotopes in Ecosystem Studies. *Annual review of ecology and systematics 18,* p. 293–320.

*Piasetsky 1997.* Пясецкий В. К. 1997. Начало раскопок позднепалеолитического поселения Ровно (Бармаки). *Российская археология,* 1, с. 151-162.
Piasetsky, V. K. 1997. The excavations of the Upper Paleolithic site Rovno (Barmaky). *Russian Archaeology,* 1, p. 151–162 (in Russian).

*Piasetsky 1999.* Пясецький, В. К. 1999. Палеоліт східної частини Волинської Височини. *Vita antiqua,* 2, с. 8-17.
Piasetsky, V. K. 1999. The Palaeolithic of the eastern part of the Volhynian upland. *Vita Antiqua,* 2, p. 8–17. (In Ukrainian).

*Piasetsky 2009.* Пясецький, В. К. 2009. *Палеоліт Волинської височини і Малого Полісся.* Рівне: Друк Волині.
Piasetsky, V. K. 2009. *The Palaeolithic of Volyhnian upland and Lower Polissia.* Rivne: Druk Volyni. (In Ukrainian).

*Piasetsky, Samoliuk 1990.* Пясецкий, В. К., Самолюк, В. А. 1990. *Отчет о раскопках позднепалеолитического поселения Ровно (Бармаки) за 1990 год*. Науковий архів ІА НАНУ, ф. е., 1990/116. Київ: Інститут археології.
Piasetsky, V. K., Samoliuk V. A. 1990. The field report about the excavations of the Upper Palaeolithic site Rovno (Barmaky) in 1990. *The scientific archive of the Institute of Archaeology, fund of the expeditions, 1990/116.* Kyiv: Institute of Archaeology (In Russian).

*Pidoplichko 1940.* Пидопличка, И. Г. 1940. Палеолитическая стоянка Чулатов I. *Советская археология,* 5, с. 65-80.
Pidoplichko, I. G. 1940. The Palaeolithic site of Chulativ I. *Soviet archaeology,* 5, p. 65–80. (In Russian).

*Pidoplichko 1969.* Пидопличко, И. Г. 1969. *Позднепалеолитические жилища из костей мамонта на Украине*. Киев: Наукова думка.
Pidoplichko, I. G. 1969. *The Upper Palaeolithic mammoth bone dwellings in Ukraine.* Kyiv: Naukova Dumka. (In Russian).

*Pidoplichko 1976.* Пидопличко, И. Г. 1976. *Межирические жилища из костей мамонта*. Киев: Наукова думка.
Pidoplichko, I. 1976. *The mammoth bone dwellings in Mezhyrich.* Kyiv: Naukova Dumka. (In Russian).

*Polikarpovich 1968.* Поликарпович, К. М. 1968. *Палеолит Верхнего Поднепровья.* Минск: Наука и техника.
Polikarpovich, K. M. 1968. *The Palaeolithic of the Upper Dnieper.* Minsk: Nauka i technika. (In Russian).

*Połtowicz-Bobak 2013.* Połtowicz-Bobak, M. 2013. *Wschodnia prowincja magdalenienu.* Rzeszów: Wydawnictwo Uniwersytetu Rzeszowskiego.

*Połtowicz-Bobak, Bobak 2020.* Połtowicz-Bobak, M., Bobak, D. 2020. Human settlement in Polish territory during the Last Glacial Maximum (ca 24,000–19,000 cal. BP): the calm before a new deal. *Acta Geographica Lodziensia,* 110, p. 21–31.

*Popiuk et al. 2021.* Popiuk, Y., Ridush, B., Solovey, T. 2021. Middle and Late Pleistocene terrestrial snails from the Middle Dniester area, Ukraine (based on Mykola Kunytsia's collections). *Geological Quarterly,* 65 (1), p. 6.

*Posth et al. 2023.* Posth, C., Yu, H., Ghalichi, A., Rougier, H., Crevecoeur, I., Huang, Y., Ringbauer, H., Rohrlach, A. B., Nagele, K., Villalba-Mouco,V., Radzeviciute, R., Ferraz, T., Stoessel, A., Tukhbatova, R., Drucker, Lari, M., Modi, A., Vai, S., Saupe, T., Scheib, Ch. L., Catalano, G., Pagani, L., Talamo, S., Fewlass, H., Klaric, L., Morala, A., Rue, M., Madelaine, S., Crepin, L., Caverne, J-B., Bocaege, E., Ricci, S., Boschin, F., Bayle, P., Maureille, B., Le Brun-Ricalens, F., Bordes, J-G., Oxilia, G., Bortolini, E., Bignon-Lau, O., Debout, G., Orliac, M., Zazzo, A., Sparacello, V., Starnini, E., Sineo, L., van der Plicht, J., Pecqueur, L., Merceron, G, Garcia, G, Leuvrey, J-M., Bay Garcia, C., Gomez-Olivencia, A., Połtowicz-Bobak, M., Bobak, D., Le Luyer, M., Storm, P., Hoffmann, C., Kabaciński, J., Filimonova, T., Shnaider, S., Berezina, N., Gonzalez-Rabanal, B., Gonzalez Morales, M. R., Marin-Arroyo, A. B., Lopez, B., Alonso-Llamazares, C., Ronchitelli, A., Polet, C., Jadin, I., Cauwe, N., Soler, J., Coromina, N., Rufi, I., Cottiaux, R., Clark, G., Straus, L. G., Julien, M-A., Renhart, S., Talaa, D., Benazzi, S., Romandini, M., Amkreutz, L., Bocherens, H., Wising, C., Villotte, S., de Pablo, J. F-L., Gomez-Puche, M., Esquembre-Bebia, M., Bodu, P., Smits, L., Souffi, B., Jankauskas, R., Kozakaitė, J., Cupillard, C. A., Benthien, H., Wehrberger, K., Schmitz, R. W., Feine, S. C., Schuler, T., Thevenet, C., Grigorescu, D., Luth, F., Kotula, A., Piezonka, H., Schopper, F., Svoboda, J., Sazelova, S., Chizhevsky, A., Khokhlov, A., Conard, N. J., Valentin, F., Harvati, K., Semal, P., Jungklaus, B., Suvorov, A., Schulting, R., Moiseyev, V., Mannermaa, K., Buzhilova, A., Terberger, T., Caramelli, D., Altena, E., Haak, W., Krause J. 2023. Palaeogenomics of Upper Palaeolithic to Neolithic European hunter-gatherers. *Nature,* 615 (7950), p. 117–126.

*Praslov, Ivanova 1982.* Праслов, Н. Д., Иванова, М. А. 1982. Костенки 21 (Гмелинская стоянка). В: Праслов, Н. Д., Рогачев, А. Н. (ред.). *Палеолит Костенковско-Борщевского района на Дону, 1879-1979.* Ленинград: Наука, с. 198-210.

Praslov, N. D., Ivanova, M. A. 1982. Kostenki 21 (Gmelin site). In: Praslov, N. D., Rogachev, A. N. (Eds.). *Paleolithic of Kostenki–Borshchevo Area on the River Don, 1879–1979. Results of field investigations.* Leningrad: Nauka, p. 198–210. (In Russian).

*Prisiazhniuk 2015.* Prisiazhniuk, V. 2015. Les mollusques du site paléolithique de Mezhyrich (Ukraine, Pléistocène supérieur). *L'anthropologie,* 119, p. 464–472.

*Pryor et al. 2020.* Pryor, A. J. E., Beresford-Jones, D. G., Dudin, A. E., Ikonnikova, E. M., Hoffecker, J. F., Gamble, C. 2020. The chronology and function of a new circular mammoth-bone structure at Kostenki 11. *Antiquity,* 94 (374), p. 323–341. https://doi.org/10.15184/aqy.2020.7

*Pryshchepa (Ed.) 2021.* Прищепа, Б. А. (ред.). 2021. *Археологічні зошити з Пересопниці, вип. 8. Матеріали науково-практичної конференції «Дослідження пам'яток кам'яної доби на території Волині».* Пересопниця-Рівне: ПП «Формат-А».

Pryshchepa, B. A. (Ed.). 2021. *Archaeological notebooks from Peresopnytsia, vol. 8. Materials of the scientific and practical conference «Research of Stone Age sites on the territory of Volhynia».* Peresopnytsia–Rivne: PP «Format-A». (In Ukrainian).

*Reimer et al. 2020.* Reimer, P.J., W.E.N. Austin., E. Bard., A. Bayliss., P.G. Blackwell., C. Bronk Ramsey., M. Butzin., H. Cheng., R.L. Edwards., M. Friedrich., P.M. Grootes., T.P. Guilderson., I. Hajdas., T.J. Heaton., A.G. Hogg., K.A. Hughen., B. Kromer., S.W. Manning., R. Muscheler., J.G. Palmer., C. Pearson., J. van der Plicht., R.W. Reimer., D.A. Richards., E.M. Scott., J.R. Southon., C.S.M. Turney., L. Wacker., F. Adolphi., U. Büntgen., M. Capano., S.M. Fahrni., A. Fogtmann-Schulz., R. Friedrich., P. Köhler., S. Kudsk., F. Miyake., J. Olsen., F. Reinig., M. Sakamoto., A. Sookdeo & Talamo, S. 2020. The IntCal20 Northern Hemisphere Radiocarbon Age Calibration Curve (0–55 cal kBP). *Radiocarbon 62,* p. 725–757.

*Reiss et al. 2023.* Reiss, L., Mayr, C., Pasda, K., Einwögerer, T., Händel, M., Lücke, A., Maier, A. & Wissel, H. 2023. Changing food webs before and during the Last Glacial Maximum based in stable isotopes of animal bone collagen from Lower Austria. *Journal of Quaternary Science 38,* p. 1337–1356.

*Reiss et al. 2025.* Reiss, L., Pasda, K., Mayr, C., Ludwig, P., Stiller, L., Chabai, V. & Maier, A. 2025. Food web reconstruction of Barmaky, the oldest post-LGM hunter-gatherer site in north-western Ukraine. *Boreas.* https://doi.org/10.1111/bor.70018.

*Reynolds et al. 2019.* Reynolds, N., Germonpré, M., Bessudnov, A. A., Sablin, M. V. 2019. The Late Gravettian Site of Kostënki 21 Layer III, Russia: a chronocultural reassessment based on a new interpretation of the significance of intra-site spatial patterning. *Journal of Paleolithic Archaeology,* 2, p. 160–210. https://doi.org/10.1007/s41982-018-0018-6

*Rivals et al. 2010.* Rivals, F., Mihlbachler, M. C., Solounias, N., Mol, D., Semprebon, G. M., de Vos, J. & Kalthoff, D. C. 2010. Palaeoecology of the Mammoth Steppe fauna from the late Pleistocene of the North Sea and Alaska: Separating species preferences from geographic influence in paleoecological dental wear analysis. *Palaeogeography, Palaeoclimatology, Palaeoecology 286,* p. 42–54.

*Rivals et al. 2012.* Rivals, F., Semprebon, G. & Lister, A. 2012. An examination of dietary diversity patterns in Pleistocene proboscideans (Mammuthus, Palaeoloxodon, and Mammut) from Europe and North America as revealed by dental microwear. *Quaternary International 255,* p. 188–195.

*Rivals et al. 2015.* Rivals, F., Mol, D., Lacombat, F., Lister, A. M. & Semprebon, G. M. 2015. Resource partitioning and niche separation between mammoths (*Mammuthus rumanus* and *Mammuthus meriodionalis*) and gomphotheres (Anancus arvernensis) in the Early Pleistocene of Europe. *Quaternary International 379,* p. 164–170.

*Rogachev, Anikovich 1982.* Рогачев, А. Н., Аникович, М. В. 1982. Костенки 4. В: Праслов, Н. Д., Рогачев, А. Н. (ред.). *Палеолит Костенковско-Борщевского района на Дону, 1879-1979.* Ленинград: Наука, с. 76-85.

Rogachev, A. N., Anikovich, M. V. 1982. Kostenki 4. In: Praslov, N. D., Rogachev, A. N. (Eds.). *Paleolithic of Kostenki–Borshchevo Area on the River Don, 1879–1979. Results of field investigations.* Leningrad: Nauka, p. 76–85. (In Russian.)

*Rogachev, Anikovich 1984.* Рогачев, А. Н., Аникович, М. В. 1984. Поздний палеолит Русской равнины и Крыма. В: Борисковский, П. И. (ред.). *Палеолит СССР. Археология СССР.* Москва: Наука, с. 162-271.

Rogachev, A. N., Anikovich, M. V. 1984. The Upper Palaeolithic of the USSR. In: Boryskovski, P. I. (ed). *The Palaeolithic of the USSR. The Archaeology of the USSR.* Moscow: Nauka, p. 161–271. (In Russian).

*Rogachev, Kudryashov 1982.* Рогачев, А. Н., Кудряшов, В. Е. 1982. Борщево 2. В: Праслов, Н. Д., Рогачев, А. Н. (ред.). *Палеолит Костенковско-Борщевского района на Дону, 1879-1979.* Ленинград: Наука, с. 211-216.

Rogachev, A. N., Kudryashov, V. E. 1982. Borshchevo 2. In: Praslov, N. D., Rogachev, A. N. (Eds.). *Palaeolithic of the Kostenki–Borshchevo area on the River Don, 1979–1989.* Leningrad: Nauka, p. 211–216. (In Russian).

*Rogachev, Popov 1982.* Рогачев, А. Н., Попов, В. В. 1982. Костенки 11 (Аносовка 2). В: Праслов, Н. Д., Рогачев, А. Н. (ред.). *Палеолит Костенковско-Борщевского района на Дону, 1879-1979.* Ленинград: Наука, с. 116-132.

Rogachev, A. N., Popov, V. V. 1982. Kostenki 11 (Anosovka). In: Praslov, N. D., Rogachev, A. N. (Eds.). *Palaeolithic of the Kostenki–Borshchevo area on the River Don, 1979–1989.* Leningrad: Nauka, p. 116–132. (In Russian).

*Rountrey et al. 2012.* Rountrey A. N., Fisher, D. C., Tikhonov, A. N., Kosintsev, P. A., Lazarev, P. A., Boeskorov, G. & Buigues, B. 2012. Early tooth development, gestation, and season of birth in mammoths. *Quaternary International 255,* p. 196–205.

*Rudenko 1959.* Руденко, А. С. 1959. Морские моллюски из Мезинской стоянки. *Краткие сообщения Института археологии АН УССР,* 8, с. 110-113.

Rudenko, A. S. 1959. The sea molluscs from the Mizyn site. *The short reports of the Institute of Archaeology, Academy of Sciences of the Ukrainian SSR,* 8, p. 110–113. (In Russian).

*Sablin 1997.* Саблин, М. В. 1997. Остатки млекопитающих из позднепалеолитического поселения Пушкари I. *Пушкаревский сборник,* I, с. 31-34.

Sablin, M. V. 1997. The mammalian remains from the Upper Palaeolithic settlement of Pushkari I. *Pushkari reports,* I, p. 31–34. (In Russian).

*Sablin 2014.* Саблин, М. В. 2014. Палеонтология стоянки Юдиново: новые факты, анализ, интерпретация. *Археологический альманах,* 31, с. 133-149.

Sablin, M. V. 2014. Palaeontology of the Yudinovo site: the new facts, analysis, interpretation. *Archaeological almanac,* 31, p. 133–149. (In Russian).

*Sablin, Khlopachev 2002.* Sablin, M. V., Khlopachev, G. A. 2002. The Earliest Ice Age Dogs: Evidence from Eliseevichi I. *Current Anthropology,* 43 (5), p. 795–799.

*Sapelko 2014.* Сапелко, Т. В. 2014. Палинология позднепалеолитических памятников Десны. *Археологический альманах,* 31, с. 117-132.

Sapelko, T. V. 2014. Palynology of Late Palaeolithic archaeological sites in the Desna River region. *Archaeological almanac,* 31, p. 117–32. (In Russian).

*Sapozhnikov 2003.* Сапожников, И. В. 2003. *Большая Аккаржа: хозяйство и культура позднего палеолита степной зоны.* Киев: Шлях.

Sapozhnikov, I. V. 2003. *Bolshaya Akkarzha: Upper Palaeolithic economy and culture of steppe Ukraine.* Kyiv: Shliakh. (In Russian).

*Savych 1975.* Савич, В. П. 1975. *Пізньопалеолітичне населення південно-західної Волині.* Київ: Наукова думка.

Savych, V. P. 1975. *The Late Palaeolithic population of south-western Volhynia.* Kyiv: Naukova dumka. (In Ukrainian).

*Sawicki 1927a.* Sawicki, L. 1927. Stanowiska młodszego paleolitu w Gródku na Wołyniu. *Ziemia,* 3, p. 36–42.

*Sawicki 1927b.* Sawicki, L. 1927. Szczątki człowieka paleolitycznego. *Ziemia,* 4, p. 59–60.

*Sawicki 1933.* Sawicki, L. 1933. *Z zagadnień prehistorji dyluwjalnej Wołynia.* Rocznika Wołyńskiego, 3. Równe.

*Schoeninger & DeNiro 1984.* Schoeninger, M. J. & DeNiro, M. J. 1984. Nitrogen and carbon isotopic composition of bone collagen from marine and terrestrial animals. *Geochimica et Cosmochimica Acta 48,* p. 625–639.

*Schwartz-Narbonne et al. 2015.* Schwartz-Narbonne, R., Longstaffe, F. J., Metcalfe, J. Z. & Zazula, G. 2015. Solving the woolly mammoth conundrum: amino acid $^{15}N$ enrichment suggests a distinct forage or habitat. *Scientific Reports 5,* 9791.

*Schwartz-Narbonne et al. 2019.* Schwartz-Narbonne, R., Longstaffe, F. J., Kardynal, K. J., Druckenmiller, P., Hobson, K. A., Jass, C. N., Metcalfe, J. Z. & Zazula, G. 2019. Reframing the mammoth steppe: insights from analysis of isotopic niches. *Quaternary Science Reviews 215,* p. 1–21.

*Sergin 1981.* Сергин, В. Я. 1981. Раскопки жилища на Гонцовском палеолитическом поселении. *Краткие сообщения Института археологии,* 165, с. 43-50.

Sergin, V. Ya. 1981. The excavation of the dwelling on the Gintsy Palaeolithic settlement. *Short reports of the Institute of Archaeology,* 165, p. 43–50. (In Russian).

*Sergin 2007.* Сергин, В. Я. 2007. Позднепалеолитические поселения и некоторые особенности природной среды. В: Жилин, М. Г. (ред.). *Своеобразие и особенности адаптации культур лесной зоны Северной Евразии в финальном плейстоцене — раннем голоцене.* Москва: ИА РАН, с. 5-32.

Sergin, V. Ya. 2007. The Upper Palaeolithic settlements and some peculiarities of environmental conditions. In: Zhylin, M. (Ed.). *Originality and specificity of the adaptation of the cultures of the forest zone of Northern Eurasia in the final Pleistocene – early Holocene.* Moscow: Institute of Archaeology RAS, p. 5–22. (In Russian).

*Sergin 2024.* Сергин, В. Я. 2024. *Гонцовское поселение.* Москва: ИА РАН.

Sergin, V. Ya. 2024. *The Gintsy settlement.* Moscow: Institute of Archaeology, Russian Academy of Sciences. (In Russian).

*Shovkoplias 1950.* Шовкопляс, І. Г. 1950. Супонєвська палеолітична стоянка. *Археологія,* IV, с. 177-183.

Shovkoplias, I. G. 1950. The Suponevo Palaeolithic site. *Arheologia,* IV, p. 177–183. (In Ukrainian).

*Shovkoplias 1951.* Шовкопляс, І. Г. 1951. Житла Супонєвської палеолітичної стоянки. *Археологія,* V, с. 127-142.

Shovkoplias, I. G. 1951. The dwellings of the Suponevo Palaeolithic site. *Arheologia,* V, p. 127–142. (In Ukrainian).

*Shovkoplias 1955.* Шовкопляс, И. Г. 1955. Добраничевская палеолитическая стоянка. *Краткие сообщения Института истории материальной культуры,* 59, с. 32-45.

Shovkoplias, I. G. 1955. The Dobranichivka Palaeolithic site. *The short reports of the Institute of the history of the material culture,* 59, p. 32–45. (In Russian).

*Shovkoplias 1959.* Шовкопляс, И. Г. 1959. Нижний горизонт Мезинской палеолитической стоянки. *Краткие сообщения Института археологии АН УССР,* 8, с. 92-103.

Shovkoplias, I. G. 1959. The lower horizon of the Mizyn Palaeolithic site. *The short reports of the Institute of Archaeology, Academy of Sciences of the Ukrainian SSR,* 8, p. 92–103. (In Russian).

*Shovkoplias 1965.* Шовкопляс, И. Г. 1965. *Мезинская стоянка.* Киев: Наукова думка.

Shovkoplias, I. G. 1965. *Mizyn site.* Kyiv: Naukova dumka. (In Russian).

*Shovkoplias 1972.* Шовкопляс, И. Г. 1972. Добраничевская стоянка на Киевщине (некоторые итоги исследования). *Материалы и исследования по археологии СССР,* 185, с. 177-188.

Shovkoplias, I. G. 1972. Dobranichivka site in Kyiv district. *Materials and investigations of archaeology in the USSR,* 185, p. 177–188. (In Russian).

*Shovkoplias 1992.* Шовкопляс, И. Г. 1992. Добраничевская позднепалеолитическая стоянка на Украине: исследование, экспонирование. *Краткие сообщения Института археологии РАН,* 206, с. 85-90.

Shovkoplias, I. G. 1992. Dobranichivka – the Upper Palaeolithic site in Ukraine: investigations, exposition. *The short reports of the Institute of Archaeology RAS,* 206, p. 85–90. (In Russian).

*Shydlovskyi 2005.* Shydlovskyi 2005. Шидловський, П. С. 2005. Вплив фізичного оточення на формування матеріальної культури пізньопалеолітичного населення Середнього Подніпров'я. В: Н. Гаврилюк (ред.). *Проблеми археології Середнього Подніпров'я: до 15-річчя заснування Фастівського державного краєзнавчого музею.* Київ-Фастів: ФДКМ, с. 31-39.

Shydlovskyi, P. S. 2005. The influence of environment on the formation of material culture of the Upper Palaeolithic hunters of the Middle Dnieper region. In: N. Gavrylyuk (Ed.). *Problems of archaeology of the Middle Dnipro region: on the 15th anniversary of the foundation of the Fastiv State Natural History Museum.* Kyiv–Fastiv: FDKM, p. 31–39. (In Ukrainian.).

*Shydlovskyi 2012.* Шидловський, П. 2012. Дослідження крем'яного інвентарю Кирилівської стоянки. *Вісник Київського національного університету імені Тараса Шевченка.* Історія, 112, с. 53-59.

Shydlovskyi, P. 2012. The studies of the flint collection of Kyrylivska site. *The Proceedings of the Kyiv National University named after Taras Shevchenko.* History, 112, p. 53–59. (In Ukrainian).

*Shydlovskyi et al. 2006.* Шидловський, П. С., Вєтров, Д. О., Васильєв, П. М., Біденко, Д. О. 2006. Дослідження палеолітичної стоянки Семенівка III в 2004-2005 рр. В: Н. Гаврилюк (ред.). *Археологічні дослідження в Україні 2004-2005 рр.* Київ-Запоріжжя: Дике поле, с. 381-385.

Shydlovskyi, P. S., Vetrov, D. O., Vasyliev, P. M., Bidenko, D. O. 2006. Research of the Semenivka III Palaeolithic site in 2004–2005. In: N. Gavriliuk (Ed.). *Archaeological research in Ukraine, 2004–2005.* Kyiv–Zaporizhya: Dyke pole, p. 381–385. (In Ukrainian).

*Shydlovskyi et al. 2019.* Shydlovskyi, P., Tsvirkun, O., Péan, S., Chymyrys, M., Mamchur, B. 2019. A new study of fourth dwelling from Mezhyrich Upper Palaeolithic campsite: the results of international summer school activity. *Vita Antiqua,* 11, p. 92–115.

*Shydlovskyi et al. 2022.* Shydlovskyi, P., Tsvirkun, O., Péan, S., Chymyrys, M. 2022. Spatial Distribution of Mezhyrichian Objects (Eastern Epigravettian): A Model of Seasonal Mobility. In: Sobkowiak-Tabaka, I., Diachenko, A., Wiśniewski, A. (Eds.). *Quantifying Stone Age Mobility. Quantitative Archaeology and Archaeological Modelling.* Cham: Springer International Publishing, p. 193–224.

*Shydlovskyi et al. 2023.* Шидловський П. С., Цвіркун О. І., Чимирис М. В. Проблеми радіовуглецевої хронології Межиріцького поселення мисливців на мамонтів. *Кам'яна доба України,* 22, с. 86-103.

Shydlovskyi, P., Tsvirkun, O., Chymyrys, M. 2023. Issues of radiocarbon chronology of the Mezhyrich mammoth hunters' settlement. *The Stone Age of Ukraine,* 22, p. 86–103. (In Ukrainian).

*Sinitsyn 2014.* Синицын, А. А. 2014. К проблеме культурной принадлежности Пушкарей 1. *Труды исторического факультета СПбГУ,* 18, с. 234-244.

Sinitsyn, A. A. 2014. Towards the problem of cultural definition of Pushkari I. *The papers of the Historical Department of Sankt-Petersburg State University,* 18, p. 234–244. (In Russian).

*Sinitsyn et al. 1997.* Синицын, А. А., Праслов, Н. Д., Свеженцев, Ю. С., Сулержицкий, Л. Д. 1997. Радиоуглеродная хронология верхнего палеолита Восточной Европы. Проблемы и перспективы. В: Синицын, А. А., Праслов, Н. Д. (ред.). *Радиоуглеродная хронология палеолита Восточной Европы и Северной Азии.* Санкт-Петербург: Академ Принт, с. 21-66.

Sinitsyn, A. A., Praslov, N. D., Svezhentsev, Yu. S. Sulerzhytsky, L. D. 1997. The radiocarbon chronology of the Upper Palaeolithic of Eastern Europe. Problems and perspectives. In: Sinitsyn, A., Praslov, N. (Eds.). *The radiocarbon chronology of the Palaeolithic of Eastern Europe and Northern Asia.* Sankt-Petersburg: Academ Print, p. 21–66. (In Russian).

*Sitlivy et al. 2012.* Sitlivy, V., Chabai, V., Anghelinu, M., Uthmeier, Th., Kels, H., Hilgers, A., Schmidt, Ch., Niţă, L., Bălteanu, I., Veselsky, A., Hauck, T. 2012. The earliest Aurignacian in Romania: New investigations at the open-air site of Românești-Dumbrăviţa I (Banat). *Quartär,* 59, p. 85–130.

*Soffer 1985.* Soffer, O. 1985. *The Upper Paleolithic of the Central Russian Plain.* Orlando: Academic Press.

*Soffer 1993.* Соффер, О. А. 1993. Экономика верхнего палеолита: продолжительность заселения стоянок на Русской равнине. *Российская археология,* 3, с. 5-17.

Soffer, O. A. 1993. The economy of the Upper Palaeolithic: the duration of site setting on the Russian Plane. *Russian Archaeology,* 3, p. 5–17. (In Russian).

*Soffer et al. 1997.* Soffer, O., Adovasio, J. M., Kornietz, N. L., Velichko, A. A., Gribchenko, Yu. N., Lenz, B. R., Suntsov, V. Yu. 1997. Cultural stratigraphy at Mezhirich, an Upper Palaeolithic site in Ukraine with multiple occupations. *Antiquity,* 71, p. 48–62.

*Sonnevile-Bordes, Perrot 1954-1956.* Sonnevile-Bordes, D. de et J. Perrot. 1954–1956. Lexique typologique du Paléolithique supérieur. *Bulletin de la Societé préhistorique francaise* (Paris), 51 (7) [1954], p. 327–335; 52 (1–2) [1955], p. 76–79; 53 (7–8) [1956], p. 408–412; 53 (9) [1956], p. 547–559.

*Stanko et al. 1989.* Станко, В. Н., Григорьева, Г. В., Швайко, Т. Н. 1989. *Позднепалеолитическое поселение Анетовка II.* Киев: Наукова думка.

Stanko, V. N., Grigorieva, G. V., Shvaiko, T. N. 1989. *The Upper Palaeolithic settlement Anetovka II.* Kyiv: Naukova dumka. (In Russian).

*Stevens & Hedges 2004.* Stevens, R. E. & Hedges, R. E. M. 2004. Carbon and nitrogen stable isotope analysis of northwest European horse bone and tooth collagen, 40,000 BP–present: palaeoclimatic interpretations. *Quaternary Science Reviews 23,* p. 977–991.

*Stevens et al. 2008.* Stevens, R. E., Jacobi, R., Street, M., Germonpré, M., Conard, N. J., Münzel, S. C. & Hedges R. E. M. 2008. Nitrogen isotope analyses of reindeer (*Rangifer tarandus*), 45,000 BP to 9,000 BP: palaeoenvironmental reconstructions. *Palaeogeography, Palaeoclimatology, Palaeoecology 262,* p. 32–45.

*Stewart et al. 2003.* Stewart, K.M., Bowyer, R. T., Kie, J., Dick, B. L. & Ben-David, M. 2003. Niche partitioning among mule deer, elk, and cattle: do stable isotopes reflect dietary niche? *ÉCOSCIENCE,* 10, p. 297–302.

*Stiner et al., 2013.* Stiner, M. C., Kuhn, S. L., Güleç, E. 2013. Early Upper Paleolithic shell beads at Üçagızlı Cave I (Turkey): Technology and the socioeconomic context of ornament life-histories. *Journal of Human Evolution,* 64, p. 380–398.

*Stratigraphy of the Ukrainian SSR 1975. Стратиграфія УРСР. Том. X. Неоген. 1975.* Київ: Наукова думка.

*The Stratigraphy of the Ukrainian SSR. Neogene. Tome X. 1975.* Kyiv: Naukova dumka. (In Ukrainian).

*Stupak 2009.* Ступак, Д. В. 2009. Кам'яні комплекси верхньопалеолітичної стоянки Бужанка 2. Варіанти використання сировини. *Археологический Альманах,* 20, с. 219-229.

Stupak, D. 2009. The stone complexes of the Upper Palaeolithic site Buzhanka 2. The variants of the raw material exploitation. *Archaeological Almanac,* 20, p. 219–229. (In Ukrainian).

*Stupak 2013.* Ступак, Д. В. 2013. Особливості використання кам'яної сировини населенням Середнього Подесення за доби верхнього палеоліту. *Археологія і давня історія України,* 10, с. 144-155.

Stupak, D. 2013. The peculiarities of the stone raw materials exploitation in the Middle Desna basin region. *Archaeology and Ancient History of Ukraine,* 10, p. 144–155. (In Ukrainian).

*Stupak 2014.* Stupak, D. 2014. Les assemblages lithiques du site épigravettien de Buzhanka 2 (Ukraine). *L'anthropologie,* 118, p. 538–553.

*Stupak et al. 2014.* Ступак, Д. В., Хлопачев, Г. А., Грибченко, Ю. М., Комар, М. С. 2014. Нова верхньопалеолітична стоянка Оболоння. *Археологічний Альманах,* 31, с. 9-30.

Stupak, D., Khlopachev, G., Gribchenko, Yu., Komar, M. 2014. The new Upper Palaeolithic site Obolonnya. *Archaeological Almanac,* 31, p. 9–30. (In Ukrainian).

*Sulerzhytsky 2004.* Сулержицкий, Л. Д. 2004. Время существования некоторых позднепалеолитических поселений по данным радиоуглеродного датирования костей мегафауны. *Российская археология,* 3, с. 103-112.

Sulerzhytsky, L. 2004. The age of some Upper Palaeolithic settlements on the base of radiocarbon datation of the megafauna's bones. *Russian Archaeology,* 3, p. 103–112. (In Russian).

*Sümegi et al. 2016.* Sümegi, P., Marković, S.B., Molnár, D., Sávai, S., Náfrádi, K., Szelepcsényi, Z., Novák, Z. 2016. Črvenka loess–paleosol sequence revisited: local and regional Quaternary biogeographical inferences of the southern Carpathian Basin. *Open Geosciences,* 8 (1), p. 390–404.

*Svensson et al. 2005.* Svensson, A. M., Andersen, K. K., Bigler, M., Clausen, H. B., Dahl-Jensen, D., Davies, S. M., Johnsen, S. J., Muscheler, R., Rasmussen, S. O., Röthlisberger, R., Steffensen, J. P., Vinther, B. M. 2006. The Greenland ice core chronology 2005, 15–42 ka. Part 2: comparison to other records. *Quaternary Science Reviews,* 25, p. 3258–3267.

*Svezhentsev 1993.* Svezhentsev, Yu. S. 1993. Radiocarbon chronology for the Upper Palaeolithic sites of the East European Plain. In: Soffer, O., Praslov, N. D. (Eds.). *From Kostenki to Clovis. Upper Paleolithic – Paleo–Indian Adaptations.* New–York; Londres: Plenum Press, p. 23–30.

*Svezhentsev, Popov, 1993.* Svezhentsev, Yu., Popov, S. 1993. Late Paleolithic Chronology of the East European Plain. *Radiocarbon,* 35 (3), p. 495–501.

*Sytnyk 2010.* Ситник, О. С. 2010. Липська пізньопалеолітична культура: аналіз та інтерпретація джерел. *Кам'яна доба,* 13, с. 113-137.

Sytnyk, O. S. 2010. Lyps'ka Palaeolithic culture: analysis and interpretation of sources. *The Stone Age of Ukraine,* 13, p. 113–137. (In Ukrainian).

*Szpak et al. 2010.* Szpak, P., Gröcke, D. R., Debruyne, R., MacPhee, R. D. E., Dale Guthrie, R., Froese, D., Zazula, G. D., Patterson, W. P. & Poinar, H. N. 2010. Regional differences in bone collagen $\delta^{13}C$ and $\delta^{15}N$ of Pleistocene mammoths: implications for paleoecology of the mammoth steppe. *Palaeogeography, Palaeoclimatology, Palaeoecology 286,* p. 88–96.

*Tarasov 1979.* Тарасов, Л. М. 1979. *Гагаринская стоянка и её место в палеолите Европы.* Ленинград: Наука.

Tarasov, L. M. 1979. *Gagarino site and its place in the European Palaeolithic.* Leningrad: Nauka. (In Russian).

*Tarriño et al. 2015.* Tarriño, A., Elorrieta, I., García–Rojas, M., 2015. Flint as raw material in prehistoric times: Cantabrian Mountains and Western Pyrenees data. *Quaternary International 364,* p. 94–108.

*Tátá et al. 2014.* Tátá, F., Cascalheira, J., Marreiros, J., Pereira, T., Bicho, N. 2014. Shell bead production in the Upper Paleolithic of Vale Boi (SW Portugal): an experimental perspective. *Journal of Archaeological Science,* 42, p. 29–41.

*Tieszen 1991.* Tieszen, L. L. 1991. Natural variations in the carbon isotope values of plants: implications for archaeology, ecology, and paleoecology. *Journal of Archaeological Science 18,* p. 227–248.

*Tixier 1974.* Tixier, J. 1974. Glossary for the description of stone tools with special reference to the Epipalaeolithic of the Maghreb. *Newsletter of lithic technology,* 1, 36 p.

*Tsvirkun, Shydlovskyi 2022.* Цвіркун, О. І., Шидловський, П. С. 2022. Техніко-типологічні особливості крем'яного комплексу 1-го ГПК Межиріцької стоянки. *Археологія і давня історія України,* 4 (45), с. 58-80.

Tsvirkun, O., Shydlovskyi, P. 2022. Technological and typological features of the household I lithic assemblage from Mezhyrich settlement. *Archaeology and Ancient History of Ukraine,* 4 (45), p. 58–80. (In Ukrainian).

*Tütken et al. 2007.* Tütken T., Furrer, H. & Vennemann T. W. 2007. Stable isotope compositions of mammoth teeth from Niederweningen, Switzerland: Implications for the Late Pleistocene climate, environment, and diet. *Quaternary International 164–165,* p. 139–150.

*Újvári et al. 2022.* Újvári, G., Klötzli, U., Stevens, T., Svensson, A., Ludwig, P., Vennemann, T., Gier, S., Horschinegg, M., Palcsu, L., Hippler, D., Kovács, J., Di Biagio, C., Formenti, P. 2022. Greenland Ice Core Record of Last Glacial Dust Sources and Atmospheric Circulation. *Journal of Geophysical Research: Atmospheres,* 127. https://insu.hal.science/insu-03839369v1

*van Geel et al. 2011.* van Geel, B., Fisher, D. C., Rountrey, A. N., van Arkel, J., Duivenvoorden, J. F., Nieman, A. M., van Reenen, G. B. A., Tikhonov, A. N., Buigues, B. & Gravendeel, B. 2011. Palaeo-environmental and dietary analysis of intestinal contents of a mammoth calf (Yamal Peninsula, northwest Siberia). *Quaternary Science Reviews 30,* p. 3935–3946.

*van Klinken 1999.* van Klinken, G. J. 1999. Bone collagen quality indicators for palaeodieatary and radiocarbon measurements. *Journal of Archaeological Science 26,* p. 687–695.

*Vanderklift & Ponsard 2003.* Vanderklift, M. A. & Ponsard, S. 2003. Sources of variation in consumer-diet $\delta^{15}N$ enrichment: a meta analysis. *Oecologia 136,* p. 169–182.

*Vasyliev 2014.* Васильев, П. М. 2014. Новые исследования верхнепалеолитической стоянки Погон (2011-2013). *Археологический Альманах,* 31, с. 31-50.

Vasyliev, P. 2014. The new investigations of the Upper Palaeolithic site Pogon (2011–2013). *Archaeological Almanac,* 31, p. 31–50. (In Russian).

*Vasyliev 2018.* Васильев, П. М. 2018. Погон. Возможности реконструкции и перспективы исследования. *Stratum plus,* 1, с. 285-304.

Vasyliev, P. 2018. Pogon. The potential reconstructions and prospects for future investigations. *Stratum plus,* 1, p. 285–304. (In Russian).

*Vasyliev 2019.* Васильєв, П. М. Мікролітичний комплекс пізнього гравету Північної України: на прикладі стоянок Пушкарі та Клюси. *Археологія і давня історія України,* 4 (33), с. 129-147.

Vasyliev, P. 2019. Microlithic complex of Late Gravettian of Northern Ukraine: on the example of Pushkari I and Kliusy sites. *The Archaeology and Ancient History of Ukraine,* 4 (33), p. 129–147. (In Ukrainian).

*Vasyliev et al. 2019.* Васильєв, П. М., Хоптинець, І.М., Ткач, В.В. 2019. *Звіт про розвідки на палеолітичних пам'ятках Рівненської області у 2018 році. Науковий архів ІА НАНУ, ф. е., 2019/74.* Київ: Інститут археології.

Vasyliev, P. M., Khoptynets, I. M., Tkach, V. V. 2019. *The report about the surveys of Palaeolithic sites in the Rivne district. The scientific archive of the Institute of Archaeology, fund of the expeditions, 2019/74.* Kyiv: Institute of Archaeology (In Ukrainian).

*Veklich 1982.* Веклич, М. Ф. 1982. *Палеоэтапность и стратотипы почвенных формаций верхнего кайнозоя.* Киев: Наукова думка.

Veklich, M. F. 1982. *Palaeostage and stratotypes of soil formations of the Upper Cainozoic.* Kyiv: Naukova dumka. (In Russian).

*Velichko et al. 1977.* Величко, А. А., Грехова, Л. В., Губонина, З. П. 1977. *Среда обитания первобытного человека Тимоновских стоянок.* Москва: Наука.

Velichko, A., Grekhova, L., Gubonina, Z. 1977. *The Early Man environment at the Timonovka sites.* Moscow: Nauka. (In Russian).

*Velichko et al. 1997.* Величко, А. А., Грехова, Л. В., Грибченко, Ю. Н., Куренкова, Е. И. 1997. *Первобытный человек в экстремальных условиях среды. Стоянка Елисеевичи.* Москва: Институт географии РАН.

Velichko, A., Grekhova, L., Gribchenko, Yu., Kurenkova, E. 1997. *The Early Man in the extreme environmental conditions. Yeliseevichi site.* Moscow: Institute of Geography. (In Russian).

*Velichko et al. 1999.* Величко, А. А., Грибченко, Ю. Н., Куренкова, Е. И., Новенко, Е. Ю. 1999. Геохронология палеолита Восточно-Европейской равнины. В: Грибченко, Ю. Н., Николаев, В. И. (ред.). *Ландшафто-климатические изменения, животный мир и человек в позднем плейстоцене и голоцене.* Москва: Институт географии РАН, с. 19-50.

Velichko, A., Gribchenko, Yu., Kurenkova, E., Novenko, E. 1999. Geochronology of the Palaeolithic of the Eastern European Plain. In: Gribchenko, Yu., Nikolaev, V. (Eds.). *The landscape and climate changes, animals and humans in the late Pleistocene and Holocene.* Moscow: Institute of Geography, p. 19–50. (In Russian).

*Velichko et al. 2009.* Величко, А. А., Писарева, В. В., Седов, С. Н., Синицын, А. А., Тимирева, С. Н. 2009. Палеогеография стоянки Костенки-14 (Маркина гора). *Археология, этнография и антропология Евразии,* 4 (40), с. 35-50.

Velichko, A. A., Pisareva, V. V., Sedov, S. N., Sinitsyn, A. A., Timireva, S. N. The paleogeography of Kostenki-14 (Markina gora) site. *Archaeology, ethnography and anthropology of Eurasia,* 4 (40), p. 35–50. (In Russian).

*Velichko, Gribchenko, Kurenkova 1997.* Velichko, A. A., Gribchenko, Yu. N., Kurenkova, E. I. 1997. Geoarchaeology of the Paleolithic in the East European Plain. *Anthropologie,* XXXV/2, p. 215–232.

*Vereshchagin & Baryshnikov 1982.* Vereshchagin, N. K. & Baryshnikov, G. F. 1982. Paleoecology of the mammoth fauna in Eurasian arctic. In: Hopkins, D. M., Matthews Jr., J. V., Schweger, C. E. & Young, S. B. (Eds.) *Paleoecology of Beringia.* Academic Press, New York, p. 267–279.

*Voevodsky 1929.* Воеводский, М. В. 1929. Тимоновская палеолитическая стоянка. *Русский антропологический журнал,* XVIII, (1-2), с. 59-70.
Voevodsky, M. V. 1929. The Timonovka Palaeolithic site. *Journal Russe d'Anthropologie,* XVIII (1-2), p. 59-70. (In Russian).

*Voevodsky 1941.* Воєводський, М. В. 1941. Результати робіт Деснянської експедиції 1936-1938 рр. *Палеоліт і неоліт України,* т. 1, с. 41-57.
Voevodsky, M. V. 1941. The results of the Desna expedition investigations, 1936–1938. *The Palaeolithic and Neolithic of Ukraine,* tome 1, p. 41–57. (In Ukrainian).

*Voevodsky 1952.* Воеводский, М. В. 1952. Палеолитическая стоянка Рабочий ров (Чулатово II). В: Плисецкий, М. С. (ред.). *Ископаемый человек и его культура на территории СССР.* Москва: Издательство МГУ, с. 101-132.
Voevodsky, M. V. 1952. The Palaeolithic site Rabochiy Rov (Chulativ II). In: Plisetcky, M. S. (Ed.). *The fossil humans and their culture in the territory of the USSR.* Moscow: State University, p. 101–132. (In Russian).

*von den Driesch 1976.* von den Driesch, A. 1976. *A guide to the measurement of animal bone from archaeological sites.* Peabody Museum Bulletin 1. Harvard: Peabody Museum of Archaeology and Ethnology.

*Weniger, Jöris 2008.* Weninger, B., Jöris, O., 2008. A 14C age calibration curve for the last 60ka: the Greenland–Hulu U/Th timescale and its impact on understanding the Middle to Upper Palaeolithic transition in Western Eurasia. In: Adler, D.S., Jöris, O. (Eds.), Setting the Record Straight: toward a Systematic Chronological Understanding of the Middle to Upper Palaeolithic Boundary in Eurasia. *Journal of Human Evolution,* vol. 55, p. 772–781.

*Whyte 2005.* Whyte, I. 2005. Loxodonta africana (Blumenbach1797) – African savanna elephant. In: John D. Skinner and Christian T. Chimimba (Hrsg.): *The Mammals of the Southern African Subregion.* Cambridge University Press, p. 51–59.

*Wiśniewski et al. 2017.* Wiśniewski, A., Połtowicz-Bobak, M., Bobak, D., Jary, Z., Moska, P. 2017. The Epigravettian and the Magdalenian in Poland: new chronological data and an old problem. *Geochronometria,* 44, p. 16–29.

*Wojtal 2020.* Wojtal, P., Svoboda, J., Roblíčkova, M. & Wilczyński, J. 2020. Carnivores in the everyday life of Gravettian hunter gatherers in Central Europe. *Journal of Anthropological Archaeology 59,* p. 101–171.

*Wooller et al. 2007.* Wooller, M., Zazula, G., Edwards, M., Froese, D.G., Boone, R.D., Parker, C. & Bennett, B. 2007. Stable carbon isotope compositions of eastern Beringian grasses and sedges: investigating their potential as paleoenvironmental indicators. *Arctic Antarctic and Alpine Research 39,* p. 318–333.

*Wooller et al. 2021.* Wooller, M. J., Bataille, C., Druckenmiller, P., Erickson, G. M., Groves, P., Haubenstock, N., Howe, T., Irrgeher, J., Mann, D., Moon, K., Potter, B. A., Prohaska, T., Rasic, J., Reuther, J., Shapiro, B., Spaleta, K. J. & Willis, A. D. 2021. Lifetime mobility of an Arctic woolly mammoth. *Science 373,* p. 806–808.

*Zaliznyak 2005.* Залізняк, Л. 2005. *Фінальний палеоліт і мезоліт континентальної України.* Київ: Шлях.
Zaliznyak, L. 2005. *The Late Palaeolithic and Mesolithic of continental Ukraine.* Kyiv: Slyakh. (In Ukrainian).

*Zaliznyak 2017.* Залізняк, Л. Л. 2017. Овруцький варіант епіграветy Східної Європи. *Археологія,* 1, с. 3-16.
Zaliznyak, L. L. 2017. The Ovruch variant of the Epigravettian of Eastern Europe. *Arheologia,* 1, p. 3–16. (In Ukrainian).

*Zaliznyak 2021.* Залізняк, Л. Л. 2021. Фінальний палеоліт Житомирського Полісся. *Археологія,* 3, с. 5-27.
Zaliznyak, L. L. 2021. The Late Palaeolithic of Zhytomyr Polissya. *Arheologia,* 3, p. 5–27. (In Ukrainian).

# CONTRIBUTORS


**Michael BRANDL**
**Austrian Archaeological Institute, Austrian Academy of Sciences**
Archaeological Sciences, Hollandstrasse 11–13, 1020 Vienna, Austria
Michael.Brandl@oeaw.ac.at

**Victor CHABAI**
**Institute of Archaeology, National Academy of Sciences of Ukraine**
12, Volodymyr Ivasiuk Avenue, 04210 Kyiv, Ukraine
v.p.chabai@gmail.com

**Diana DUDNYK**
**Institute of Archaeology, National Academy of Sciences of Ukraine**
12, Volodymyr Ivasiuk Avenue, 04210 Kyiv, Ukraine
di.dudn.k@gmail.com

**Volodymyr HRYTSENKO**
**National Museum of Natural History, National Academy of Sciences of Ukraine**
15, Bogdan Khmelnytsky Street, 01601 Kyiv, Ukraine
favosites@ukr.net

**Andreas MAIER**
**Institute of Prehistoric Archaeology, University of Cologne**
Bernhard-Feilchenfeld-Strasse 11, 50969 Cologne, Germany
a.maier@uni-koeln.de

**Christoph MAYR**
**Department of Geography and Geosciences, Institute for Geography**
Friedrich-Alexander-Universitat Erlangen-Nurnberg, Hartmannstr. 14, 91052 Erlangen, Germany
christoph.mayr@fau.de

**Stefan MENG**
**Institute of Geography and Geology, University of Greifswald**
Friedrich-Ludwig-Jahn Str. 17A, 17487 Greifswald, Germany
stefan.meng@uni-greifswald.de

**Kerstin PASDA**
**Institute of Prehistoric Archaeology, Friedrich-Alexander-Universitat Erlangen-Nurnberg**
Kochstrase 4/18, 91540 Erlangen, Germany
k.pasda@mail.de

**Lilian REISS**
**Muséum National d'Histoire Naturelle**
57 Rue Cuvier, 75005 Paris, France
lilian.reiss@posteo.de

**Dmytro STUPAK**
**Institute of Archaeology, National Academy of Sciences of Ukraine**
12, Volodymyr Ivasiuk Avenue, 04210 Kyiv, Ukraine
stupak17@ukr.net

**Andrei VESELSKY**
**Institute of Archaeology, National Academy of Sciences of Ukraine**
12, Volodymyr Ivasiuk Avenue, 04210 Kyiv, Ukraine
veselsky@i.ua